DEVELOPMENTS IN PRECAMBRIAN GEOLOGY 8

DVISORY EDITOR B.F. WINDLEY

PRECAMBRIAN CONTINENTAL CRUST AND ITS ECONOMIC RESOURCES

S.M. NAQVI (EDITOR)

ELSEVIER

Developments in Precambrian Geology 8

PRECAMBRIAN CONTINENTAL CRUST AND ITS ECONOMIC RESOURCES

DEVELOPMENTS IN PRECAMBRIAN GEOLOGY
Advisory Editor B.F. Windley

Further titles in this series

1. B.F. WINDLEY and S.M. NAQVI (editors)
   Archaean Geochemistry
2. D.R. HUNTER (Editor)
   Precambrian of the Southern Hemisphere
3. K.C. CONDIE
   Archean Greenstone Belts
4. A. KRONER (Editor)
   Precambrian Plate Tectonics
5. Y.P. MEL'NIK
   Precambrian Banded Iron-formations. Physicochemical Conditions of Formation
6. A.F. TRENDALL and R.C. MORRIS (Editors)
   Iron-Formation: Facts and Problems
7. B. NAGY, R. WEBER, J.C. GUERRERO and M. SCHIDLOWSKI (Editors)
   Developments and Interactions of the Precambrian Atmosphere, Lithosphere and Biosphere

DEVELOPMENTS IN PRECAMBRIAN GEOLOGY 8

PRECAMBRIAN CONTINENTAL CRUST AND ITS ECONOMIC RESOURCES

Edited by

S.M. NAQVI

National Geophysical Research Institute, Hyderabad, India

ELSEVIER, Amsterdam — Oxford — New York — Tokyo 1990

ELSEVIER SCIENCE PUBLISHERS B.V.
Sara Burgerhartstraat 25
P.O. Box 211, 1000 AE Amsterdam, The Netherlands

Distributors for the United States and Canada:

ELSEVIER SCIENCE PUBLISHING COMPANY INC.
655, Avenue of the Americas
New York, NY 10010, U.S.A.

ISBN 0-444-88310-X

This book is printed on acid-free paper.

Printed in The Netherlands

DR.B.P. RADHAKRISHNA--AN APPRECIATION

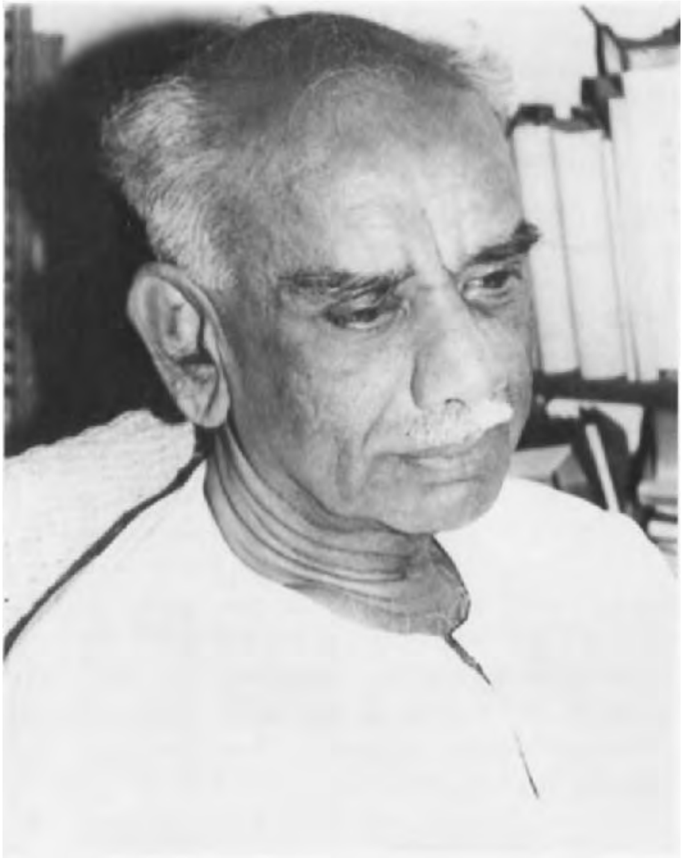

Dr. Bangalore Puttaiya Radhakrishna is among the leading contributors who have profoundly influenced the field of Precambrian geology of India. In the more than five decades of his career, one finds in him a rare and venerable blend of the different and successive aspects of basic research and its application to societal needs of teaching and of the guidance and promotion of research and developmental activities. The manifoldness of his contribution may be realised from the fact that any one of these activities could occupy a full lifetime work.

During his early career he worked actively with Sri B. Rama Rao and Prof. C.S. Pichamuthu, two stalwarts of the Archaean geology of India; it was thus natural that he started with detailed field mapping of the complex geology of the Dharwar region and made significant contributions to our knowledge and understanding of the Archaean geology of South India. Among his pioneering works are studies of the origin of Closepet Granite, a Late-Archaean potassium-rich granite which he proved to consist of multiple intrusives of several varieties rather than a single body, and of the Dharwar schistose rock formations. His other important contributions are a revision of Dharwar stratigraphy, recognition of older and younger greenstone belts in the Dharwar Craton, revival of the concept of polyphase Peninsular gneisses being basement for the younger Dharwar Schist belts and studies of the crustal evolution and mineralization episodes in the Precambrian of India. He has championed the concept of a Proterozoic mobile belt around the stable cratonic nuclei of Dharwar, Bhandara and Bundelkahnd. His keen interest in and fascination for the variety and grandeur of the landforms of scenic Mysore led him to a geo-tectonic study of the plateau, wherein he established intermittent uplift of the Peninsular region since the Jurassic. From the drainage pattern on its eastern and western parts, he showed clearly that vertical block movements have taken place during Tertiary and Recent times. Dr.Radhakrishna was among the first to have recognised the significance of well-preserved Archaean terrains, such as in the South Indian shield, and to build up and test models of crust formation since the earliest geological eras. It is largely owing to his relentless efforts and encouragement that today the Peninsular shield of India is considered as one of the best-studied Precambrian terrains of the world. For his academic contributions, the Geological Society of India awarded him The Mysore Geologists Association's Gold Medal.

Dr. Radhakrishna believes that among the main tasks of a geologist is to find resources for the various needs of mankind and hence, during the course of his professional career his major interest was naturally directed towards the exploration and exploitation of the mineral and groundwater resources of Karnataka. Owing to his deep commitment to the nation's economic growth, he was entrusted with the additional responsibility of being Managing Director of the Board of Mineral Development of the Karnataka and Chitradurga Copper Corporation. He was responsible for starting several state mining ventures to exploit chromite, iron, manganese, copper, bauxite and clay deposits. It is a measure of his contribution that today Dr.Radhakrishna's name is associated with almost every mineral industry in Karnataka. In tune with the scales of the socio-economic structure of India and his belief in the philosophy that 'Small is Beautiful', he has been able successfully to guide profitable exploitation by small-scale mining. He explored and reopened base-metal deposits at Chitradurga and within a year a plant with a capacity of 250 tonnes per day was commissioned.

Although making drinking water available to all its population has been adopted as the major mission of technology in India since 1986, it was Dr. Radhakrishna's foresight that created a ground--water cell in the Department of Mines and Geology of the Karnataka state as early as 1964. This cell has been playing a key role in harnessing the groundwater resources in this region. His emphasis on investigations of deep fissures and fractures within the crystalline complexes as sources of groundwater paid rich dividends and established this approach as a standard practice for surveys in hard-rock terrains. If today drinking water is available in most of the villages in Karnataka State, this is thanks to the vision, commitment and pioneering lead given by Dr. Radhakrishna. For his contributions to the mineral industry, he was honoured with the National Mineral Award and also the state award of Rajyothsava Prashasti.

He was among the first in the country to recognise the crucial role which geophysics and geochemistry play in deepening our understanding of the geological processes and manifestations. I had first-hand experience of how he actively supported geophysical mapping when the National Geophysical Research Institute developed the first indigenous capabilities for airborne magnetometer investigations by his sponsoring of surveys over some of the mineralized segments of the western Dharwar province in Karnataka. The extensive geochemical and geochronological coverage of the Dharwar Craton by the National Geophysical Research Institute and scientists of other organizations in India has been always encouraged and supported by him.

Dr. Radhakrishna has enthused, moulded and guided more than one generation of Indian geologists in undertaking investigations associated with the Dharwar terrane. Almost every Indian and foreign scientist who has taken interest in working on the Precambrian rocks of India, especially those of the Dharwar Craton, has had the benefit of his valuable insights and advice. He has led a number of promising young workers to the frontiers of Precambrian geology and provided them with all possible academic help.

Dr. Radhakrishna has repeatedly focussed attention on the outstanding problems of the Precambrian terranes of India and has promoted international collaborative efforts to solve the fundamental problems connected with Archaean crustal evolution. Indeed he may be considered as one of the leading earth-science promotors in the world. This comes to him naturally because of his conspicuously quiet and selfless dedication to the cause of geological study. As one of the founders of the Geological Society of India, he first laid down a strong foundation as its Secretary and later took over the editing of its Journal in the year 1968. He has been carrying out this responsibility with meticulous care and has sustained it over a remarkably long period. Soon, the Journal, which was being published twice a year, became a quarterly and then a monthly. In fact, it is the only earth-science journal from India to have found a place amongst the internationally recognized earth-science publications and the esteem that it enjoys today in the earth-science community all over the world is entirely due to his ceaseless efforts. He has been the moving spirit behind and instrumental in bringing out twelve special memoirs of the Geological Society of India, which focus on studies of specific and main aspects of Indian geology. In this series, some of the major geological and tectonic units, such as the Deccan Traps, Aravalli, the Precambrian rocks of Eastern and Southern India, etc., have been taken up as the theme, and these volumes contain extremely valuable state-of-art reference material for researchers all over the world. The new information and insight contained therein about the various rock units of the Indian continental lithosphere are indeed much needed in synthesizing global views of the geological processes. The community of earth scientists owes a lot to Dr. Radhakrishna for this valuable service. It is measure of his selfless service to the cause of geological studies and it finds expression in his own words:'No other work has given me greater satisfaction and sense of fulfillment than the work I have been able to do for the society'.

Dr. Radhakrishna has over a hundred papers published in various journals to his credit. In recognition of his scientific contribution and the role he has played in the dissemination of knowledge, the Geological Society of London has conferred upon him an Honorary Fellowship. He has been elected Fellow of many other learned societies, including the Indian Academy of Sciences and the Indian National Science Academy.

Dr. Radhakrishna's interests go beyond geology, into the fields of ancient metallurgy in India, philosophy, Karnatak music, etc. A saintly person with a total Gandhian approach, he radiates an aura of distinguished scholarship coupled with exceptional simplicity. He is a true Karmayogi in the sense of Bhagwat Gita, indeed a saintly intellectual among worldly people.

It has been a privilege to know Dr. Radhakrishna and a pleasure to work with him on several projects of mutual interest. He has been a guide, friend and philosopher to me during my efforts in applying and refining various geophysical and geochemical techniques to delineate the structure and dynamics of the crust and lithosphere below the Indian sub-continent, while orienting the National Geophysical Research Institute for this purpose. It is immensely gratifying to see that this volume is being brought out by earth scientists from all over the world to commemorate the 70th birthday of one of the leading lights of our branch of science and I join them in wishing him "jivem shradha satat"; many more years of creative endeavour and satisfaction.

April, 1989 Hari Narain

This Page Intentionally Left Blank

PREFACE

During the past two years, the compilation and preparation of this volume to commemorate the seventieth birthday of Dr.B.P. Radhakrishna, my mentor, has been the greatest pleasure and satisfying work for me. Dr.Radhakrishna has contributed immensely to the understanding of Precambrian rocks during the last forty years. He has explored and mapped these rocks and provided a basic framework of knowledge on which his students could work with more sophisticated tools. It was the great desire of his students, friends, co-workers and admirers that a volume in his honour should be brought out to mark his selfless and dedicated service to the field of the earth sciences. Through his work and efforts, the Dharwar Craton of India is now as well known to earth scientists as those of Swaziland or Pilbara. Dr.Radhakrishna has devoted his entire life to the study of Precambrian rocks; therefore, it is befitting that the present volume is devoted to studies related to the Precambrian continental crust and its economic resources.

Since 1964, the time when the Upper Mantle Project was started, the Precambrian continental crust has been studied in considerable detail in many areas. Multidisciplinary studies with modern tools and techniques have been used at increasing levels of accuracy. The Precambrian continental crust has been subjected to several thermal events and multiple episodes of deformation. These events have obliterated the scenario produced by early events and present-day efforts are directed to evaluating the cause-effect processes of each event. How far back the known geological processes of the Phanerozoic can be extended into the Precambrian is one of the main questions before us. The present volume provides some more data and interpretations towards finding the answer to some of these questions.

The book contains 30 contributions resulting from researches on almost all the important Precambrian terranes. They are distributed in five chapters, namely, (1) Concepts and Models, (2) Archaean Cratons and Shields, (3) Precambrian Mobile Belts, (4) Proterozoic Basins, Rifts and the Himalaya, and (5) Economic Resources. Our aim has been to present a high-quality scientific book befitting the occasion of the seventieth birthday of Dr.B.P.

Radhakrishna. I am happy that most of papers included here provide new data and information. Due to limitations on the size of the book, some papers were drastically reduced in length and some could not be included.

I am extremely grateful to the contributors from all over the world for their spontaneous response and cooperation in bringing out this volume in its present form. I am deeply indebted to Dr. Hari Narain for his guidance and advice at each and every step during the progress of the book. I wish to express my gratitude to Prof. B. Chadwick, Prof. R.M. Shakelton, Prof. K.C. Condie, Prof. K. Naha, Prof. R.K. Verma, Prof. A.B. Roy, Prof. R.S. Sharma, Prof. Richard W. Ojakangas, Prof. J.A. Donaldson, Prof. A.K. Saha, Prof. A.S. Janardhan, Prof. S.K. Sen, Dr. R. Srinivasan, Dr.U. Raval, Dr.M. Ramakrishnan, Dr. K. Gopalan, Dr.A.G. Menon and other friends for critically reviewing the manuscripts. I am thankful to Prof. V.K. Gaur, Director, NGRI for providing facilities and permitting me to bring out this volume. Camera-ready copy of the manuscripts has been prepared by K.V. Anjaiah and Mrs. Nancy Rajan. I am immensely indebted to Dr.R. Srinivasan and Dr.S. Nirmal Charan, without whose help and persistent efforts it would not have been possible to publish this volume in its present form. Dr. S.M. Hussain, Dr. Y.J. Bhaskara Rao and Mr. B. Udai Raj have assisted in various ways in the preparation of the manuscript. Students, co-workers and admirers of Dr. Radhakrishna express their profound thanks to the editor-in-chief, Prof. Brian F. Windley and the publishers of the Elsevier book series on Developments in Precambrian Geology, for recommending and publishing this volume.

S.M.Naqvi

CONTRIBUTORS

C.R. Anhaeusser, Economic Geology Research Unit, University of Witwatersrand, 1 Jan Smuts Avenue, Johannesburg 2001, South Africa.

P.W.U. Appel, The Geological Survey of Greenland, Oster Voldgade 10, DK-1350, Copenhagen, Denmark.

D.M. Banerjee, Department of Geology, Delhi University, New Delhi, India.

P.K. Banerjee, Geological Survey of India, Marine Wing, Ratnakar Building, 4-Chowringhee Lane, Calcutta, India.

S. Bhattacharji, Department of Geology, Brooklyn College, New York, U.S.A.

M.K. Bose, Department of Geology, Presidency College, Calcutta, India.

K.C. Condie, Department of Geosciences, New Mexico Institute of Mining and Technology, Socorro, New Mexico, U.S.A

M. Deb, Department of Geology, University of Delhi, New Delhi, India.

T.C. Devaraju, Department of Studies in Geology, Karnatak University, Dharwar, India.

V.Divakara Rao, National Geophysical Research Institute, Uppal Road, Hyderabad, India.

V.V. Fed'kin, Institute of Experimental Mineralogy, USSR Academy of Sciences, Chernogolvka, Moscow district, U.S.S.R.

J. Foden, Bureau of Mineral Resources, Geology and Geophysics, P.O.Box 378, Canberra City, ACT 2601, Canberra, Australia.

W.S. Fyfe, Department of Geology, University of Western Ontario, London, Ontario N6A 5B7, Canada.

A.Y. Glikson, Bureau of Mineral Resources, Geology and Geophysics, P.O.Box 378, Canberra City, ACT 2601, Canberra, Australia.

P.K. Govil, National Geophysical Research Institute, Uppal Road, Hyderabad, India.

Hari Narain, National Geophysical Research Institute, Uppal Raod, Hyderabad, India.

S.D. Khanadali, Department of Studies in Geology, Karnatak University, Dharwar, India.

K. Laajoki, Department of Geology, University of Oulu, Linnanmaa, SF-90570, Oulu, Finland.

C. Leelanandam, Department of Geology, Osmania University, Hyderabad, India.

D.C. Mishra, National Geophysical Research Institute, Uppal Road, Hyderabad, India.

D. Mukhopadhyay, Department of Applied Geology, Indian School of Mines, Dhanbad, India.

K. Naha, Department of Geology and Geophysics, Indian Institute of Technology, Kharagpur, India.

S. M. Naqvi, National Geophysical Research Institute, Uppal Road, Hyderabad, India.

R.C. Newton, Department of Geological Sciences, The University of Chicago, Chicago, U.S.A.

T.H.C. Nutt, University of Rhodesia, Box M.P. 167, Mount Pleasant, Harare, Zimbabwe.

R.W. Ojakangas, Department of Geology, University of Minnesota, Duluth, Minnesota, U.S.A.

N. Rajshekhar, Department of Geology, Veerasaiva College, Bellary, India.

P. Rama Rao, National Geophysical Research Institute, Uppal Road, Hyderabad, India.

R.U.M. Rao, National Geophysical Research Institute, Uppal Road, Hyderabad, India.

U. Raval, National Geophysical Research Institute, Uppal Road, Hyderabad, India.

A.B. Roy, Department of Geology, University of Rajasthan, Udaipur, India.

G.R. Reddy, Bhabha Atomic Research Centre, Trombay, Bombay, India.

J.J.W. Rogers, Department of Geology, University of North Carolina, Chapel Hill, NC 27514, U.S.A.

A.K. Saha, Department of Geology, Presidency College, Calcutta, India.

Sun Dazhong, Tianjin Institute of Geology and Mineral Resources, Chinese Academy of Geological Sciences, Tianjin, China.

M. Schidlowski, Max-Planck Institute fur Chemie, Saarstrasse 23, Mainz D-6500, Federal Republic of Germany.

R.S. Sharma, Department of Geology, Banaras Hindu University, Varanasi, India.

M. Shukla, Birbal Sahni Institute of Paleobotany, 53, University Road, Lucknow, India.

Lu Songnain, Tianjin Institute of Geology and Mineral Resources, Chinese Academy of Geological Sciences, Tianjin, China.

C. Srikantappa, Department of Geology, Manasa Gangotri, Mysore, India.

R. Srinivasan, National Geophysical Research Institute, Uppal Road, Hyderabad, India.

G. Subba Rao, Department of Studies in Geology, Karnatak University, Dharwar, India.

M.V. Subba Rao, National Geophysical Research Institute, Uppal Road, Hyderabad, India.

T.J. Sugden, Department of Geology, University of Leicester, Leicester, U.K.

M. Thompson, Department of Geology and Applied Geochemistry, Imperial College of Science and Technology, London, SW72 BP, England.

K.S. Valdiya, Department of Geology, Nainital University, Nainital, India

B.S. Venkatachala, Birbal Sahni Institute of Paleobotany, 53, University Road, Lucknow, India.

J.N. Walsh, Department of Geology, Royal Holloway and Bedford New College, University of London, Egham Hill, Surrey TW 20 OEY, U.K.

J.F. Wilson, University of Rhodesia, P.O. Box. MP. 167, Mount Pleasant, Harare, Zimbabwe.

B.F. Windley, Department of Geology, University of Leicester, Leicester, LE17 RH, U.K.

D.J. Wronkiewicz, Department of Geosciences, New Mexico Institute of Mining and Technology, Socorro, New Mexico, U.S.A.

V.K. Yadav, Birbal Sahni Institute of Paleobotany, 53, University Road, Lucknow, India.

CONTENTS

CHAPTER 3. PRECAMBRIAN MOBILE BELTS

CHAPTER 4. PRECAMBRIAN BASINS, RIFTS AND THE HIMALAYA

CHAPTER 5. ECONOMIC RESOURCES

This Page Intentionally Left Blank

REFLECTIONS ON THE ARCHAEAN

W.S. FYFE

ABSTRACT

Understanding the history of Earth involves the understanding of all energy sources and heat transport processes. The early hot Earth models appear to be well established and geology appears to support models of a high degree of early turbulence. It is clear that the surface environment and atmospheric composition has been moderated by life processes throughout all Earth history.

INTRODUCTION

As earth scientists, we have several major roles to play in human society. We must describe the materials which form the accessible regions of the planet and provide those materials which man needs for his changing technologies. We must understand the way the environment for life works, how it changes slowly or catastrophically, its sensitivity. Such data and the records of recent change, must provide the data needed for intelligent management and sustainable development. But we also have the even greater philosophical task of understanding how our planet has evolved over its entire history and how this evolution has influenced the development of life itself. It is this knowledge that perhaps teaches us about the sensitivity and limits of our planet and is needed to teach us how we must respect the system which allowed our development. This realization is behind the magnificent opening statement of the recent Bruntland report (1987).

"In the middle of the 20th century, we saw our planet from space for the first time. Historians may eventually find that this vision had a greater impact on thought than did the Copernican revolution of the 16th century, which upset the human self-image by revealing that the Earth is not the centre of the universe. From space, we see a small and fragile ball dominated not by human activity and edifice but by a pattern of clouds, oceans, greenery, and soils. Humanity's inability to fit its doings into that pattern is changing planetary systems, fundamentally. Many such changes are accompanied by life-threatening hazards. This new reality, from which there is no escape, must be recognized - and managed".

Today, we have truly amazing powers of observation. From space, we can see our planet and observe processes as never before. But we can also see other planets in our solar system. I have no doubt that the results which will come from the soon to be launched mission to Mars will be simply fantastic (McKenna-Lawlor, 1988). Observations from this greater sample of planets has already had a vast impact on our models of Earth.

While we can observe on large scales, our powers of observation on the microscale have also increased to the point that we can study most earth processes at the atomic-molecular level. And with the power of the modern computer, the new developments in geophysics, seismic tomography (Dziewonski and Woodhouse, 1987), deep electric sounding and the like, now allow us to study "real time" geology as never before.

In building models of evolution of our planet, we have much higher constraints and we must never forget that the understanding of the present processes must lead us to better understand the processes of the past, such a philosophy was beautifully stated by Lyell in 1872.

"Geology is the science which investigates the successive changes that have taken place in organic and inorganic kingdoms of nature. By those researches into the state of the earth and its inhabitants at former periods, we require a more perfect knowledge of its present condition, and more comprehensive views concerning the laws now governing its animate and inanimate productions."

FORCING

Perhaps all change in a system is related to changes in the power supply of the system under study. Our colleagues in Physics might tend to use the word forcing, *the measurable and determinable influences that lead to motions*. For the Earth there are two major forcing processes. We must understand the history of the Sun and the Sun-Earth orbital history. We still know remarkably little about this topic but as our Sun has evolved it is certain that the fluxes of radiation and particles have not remained constant. For example, it is possible that the early Sun provided less radiation in the visible but much more radiation in the ultraviolet region of the spectrum (see Holland, 1984).

The other great forcing process comes from the energy sources of the interior of the Earth. Today we consider that most of this energy comes from the decay of the radionuclides of U-Th-K. There is also the potential source of energy from the latent heat of crystallization of the liquid outer core which must tend to thermostat the temperature of the core-mantle boundary (cf. an ice-liquid water system at 0^{o} C). And in the past a vast energy source came from the energy of gravitational accumulation of the planet, separation of the core, and other highly variable energy sources from more frequent meteorite, and comet, collisions. Studies from other planets and particularly the Moon and Mars have shown us that the outer layers of planets passed through a largely molten state, confirming the ideas that Francis Birch of Harvard proposed in his famous paper of 1965.

Ultimately, it is the understanding of change in the power sources and the cooling mechanisms that are required to understand the record in the ancient fragments we study in the Archaean.

THE COOLING PROCESS AT PRESENT

Any hot object cools by two dominant processes, heat conduction through the material and convection involving coupled mass and heat transport. From the study of convection, we know that convective transport is related to two main parameters of a system, the scale (mass-thickness, etc.) and the temperature gradient (see Turcotte and Schubert, 1982; Elder, 1968, 1987). Convection can be described by two main parameters, the adiabatic gradient and the Rayleigh number. The adiabatic gradient sets the limit; if it is not exceeded, there will be no convection. If exceeded, the Rayleigh number will tell us about the vigour of convection. The parameters of the Rayleigh number tell us that size and grad T are of enormous importance. In fact, huge T gradients are quite impossible in a system like Earth because vigorous convection will simply sweep the energy to the surface too rapidly. Convection depends on scale or thickness to a power function in the range 3-5, depending on the distribution of heat sources.

If a body is convecting, the surface temperature gradients will indicate the vigour and patterns of convection. The near surface gradients will be irregular. For the modern Earth, these patterns are now clear. We have giant convection cells which sweep energy into the ocean ridge systems where heat flow is high. The descending cells are associated with the great trench systems and low heat flow regions. Such patterns are reflected in the records of volcanism and metamorphic patterns.

On the modern Earth we see other patterns of heat-mass transport. We have the hot spot regions (e.g. the Hawaiian Islands) which represent turbulence or noise superposed on the overall large systems. These appear to have deep source regions and some believe that processes near the core-mantle boundary are of great significance (Courtillot and Besse, 1987). There is also subduction related volcanism where the deep injection of H_2O into warm overlying mantle lowers the mantle viscosity (water-weakening in rock volcanics) and leads to mantle convection. Hot spots and the subduction related processes account for about 10% of the overall convective transport of energy with about 90% being focussed on the ridges.

For the present Earth, heat is removed almost equally by conduction through the lithosphere and convection into highly focussed volcanic belts. We know that as the Earth cools (cf.the Moon or Mars) eventually conduction will dominate. For the early more energetic Earth, convection must have dominated.

Over the past two decades we have discovered another most important process involved in the cooling mechanisms of Earth. The major convective processes move hot materials (plumes) to the near surface. Pressure release on the viscous rising plumes can lead to melting and rapid melt separation (Turcotte and Schubert, 1982). The typical surface product is basalt, the low melting fraction of typical mantle. This material and its derivatives form the new crust at a truly remarkable rate (100 Ma ± to form over 60% of the planet's surface). Most of the process occurs in submarine environments and as cool basalt liquid (density 2.7) crystallizes to solid (density 3.0) a porous cracked medium must result and if water is present, fluid convection must occur and carry away the heat. Straus and Schubert (1977) showed that the adiabatic gradient for convection in porous medium is very low (about 1^0C/km) and such convection can occur in almost all permeable crust. Thus a large part of the ridge cooling is water cooling. At ridges this produces about 100 km^3 of hot sea water annually or it processes the entire ocean mass in a few million years. It is a process of fundamental importance to heat transport, ore genesis and even the nutrient supply to the oceanic biosphere. In ridge environments almost half the heat introduced is passed on to the hydrosphere. The same processes will cool any high level volcanic rock (or intrusive) which invades the hydrosphere or deep groundwater systems. We now know that deep fluid convection occurs in all ocean floor systems (even sub-sediment) which have been studied. And now, the same deep cells are being found on the continents and involve deep groundwater flow. *We live on a water cooled planet!* Perhaps as much as half the internal energy is carried to the surface by water circulation.

RECYCLING

There have been other fundamental observations very recently. Gilluly (1971) suggested that sediments must be recycled into the mantle. He was concerned with the lack of sediments in relation to known erosion rates. There has been a long debate as to whether or not sediments are subducted on a significant scale.

Molnar and Gray (1979) looked at the pure physics of convective dragging and subduction of continental material. They concluded that if thin continental crust was coupled to its mantle, physics did not preclude subduction. Fyfe (1982) was impressed by the lack of pelagic sediment equivalents in blue schist terraines.

But there is nothing like observation! First studies of the lithosphere while it bends into trenches showed the formation of massive horst and graben structures with sediments trapped in the grabens. Such observations led to the Hilde-Uyeda (1983) "buzz-saw" model of subduction. Such structures are common in all trench environments as revealed by side-scan sonar techniques.

The very recent observations in the Japan trench, the Kaiko project, have finally settled all arguments (Lallemont et al., 1986). In this trench system almost all deep sea sediments are carried back towards the mantle (how far we know not). Even Japan is being tectonically eroded (Uyeda, 1983). And finally, studies of the systematics of short lived ^{10}Be in andesites is revealing that much of the marine surface must be recycled (Carnegie Institution, 1986). Continents are not just created - they can be destroyed as suggested long ago by Gilbert (1893).

Such modern observations must be built into our models of the past. We must consider the types of cooling processes, the possibilities of massive recycling. We also know that modern plate tectonics is related to the formation of most of our resources from metals to soils.

EARLY COOLING PROCESSES

Present models of rapid planetary accretion imply that at an early stage in the history of our planet, the combined influences of gravitational heating and the presence of a range of short lived isotopes, must have liberated enough energy to cause a high degree of melting. Magma oceans could have surrounded the early Earth. Core formation would be fast. In such an Earth the combined operation of the thickness and grad T terms of the Rayleigh number would have led to very vigorous convection and most of the early heat would have been dissipated by rapid overturn of the surface.

For Earth, with a partially molten outer shell, atmospheric gases and in particular H_2O-CO_2 (with traces of HCl-HF, N_2, Ar) would have been at much higher levels than today. The excess energy from Earth sources would have been rapidly radiated into space through a hot Venus-type atmosphere.

Why have we not continued in the Venus model? The problem is extremely complex and as yet not really understood (Kasting et al., 1988; Broecker, 1985). It is even possible that much of our volatiles were accumulated late by comet collisions. But it is certain that the carbon dioxide cycle which regulates our present system (at least before man chose to burn fossil carbon) is a complex interactive geosphere-biosphere system.

THE FIRST RAIN

Given a high water content in the early atmosphere, rain would begin to fall well above $100^{\circ}C$. But with the beginning of precipitation solid crust of multi-km thickness would form rapidly over the entire globe. The first crust could well have had almost mantle composition. The acid gases and CO_2 in the atmosphere would be rapidly cleaned out by salt-carbonate equilibria but CO_2

levels would have been much higher. The solid crust would form on liquid upper mantle and be almost synchronously subducted.

As the instant liquid water cooling of the surface acts new chemical separation processes would occur rapidly. Even with a thin mafic crust, silica stripping would be rapid and cover the protoplanet with chert. We know that at present the rate of SiO_2 transport associated with ridge cooling is massive (see Fyfe and Lonsdale, 1981). Pre-4 billion, this rate would have been at least an order of magnitude faster. At this stage a serpentine, peridotite, chert crust would float; the chance of preservation of light materials becomes possible. The salt solutions contained in the proto oceans would also cause interesting new phases to form, phases like hornblende and phlogopite. Mixing the silica and the new array of minerals with volatiles into the still liquid upper mantle would rapidly begin to produce new types of magmas, even those like tonalite. Once a light siliceous, hydrated outer shell formed dense mantle magmas would underplate such crust and floating of plagioclase could produce a massive anorthositic underplate as with the moon. What must be stressed is that water cooling plus density selection of magmas would produce a complex crust and lithosphere rapidly.

At a previous meeting on the formation of continental crust (Fyfe, 1980) I raised the question as to how fast a magma ocean covered with a light partly anorthositic crust would solidify totally. I still think that this question is not well answered. The eruption of komatiites throughout the entire Archaean period indicates much higher temperatures in the mantle and more turbulence than at present. Given such temperatures and higher Rayleigh numbers, convection would be more chaotic or turbulent. It is interesting to speculate that the Archaean-Proterozoic break might well represent the time when the presence of mantle melts on a large scale ceased. A small drop in the temperature gradient and increase in lithospheric thickness and viscosity would have a very large influence on convective style. Even more recently it has been suggested (Hale, 1987) that the state of the core may have had an influence on this situation with the initiation of core crystallization adding a deep internal control on the system.

LIFE

It is now clear that evidence is present for the existence of microorganisms to the limit of the geologic record. It is also clear that there was probably a complex array of microorganisms (Walsh and Lowe 1985). The interactions of life and the environment has recently been reviewed by Veizer (1987) and Holland (1984).

We know well, that for the present Earth the biomass has an enormous influence on our atmosphere and aquatic environments. We also know that sedimentary environments are highly variable on many scales (e.g. the floor of the Black Sea or the Pacific Ocean, oxygen rich and anoxic lakes, etc.). There are bacteria (Segerer, et al., 1985) which can modify their biosynthetic pathways to cope with drastic change in the local environment.

Given more volcanism on the early Earth, more black smokers, etc., and more rapid fluctuations, and possibly dramatic differences in atmospheric circulation patterns (were there features like the Himalayas?), one might expect great local variability. The feature which impresses me, is that overall, while there may be differences in scale, the array of early Earth materials is not very different from that of the present (Bridgwater and Fyfe, 1974). The high degree of instability in the early Earth may easily account for the dominance of the most robust simple systems of life, the microorganisms. As more refined data and more extensive observations are produced the evidence for similarity tends to increase and now it seems for example, that the world's greatest iron formation (T. Krogh, N. Muchado, D. Lindenmayer, pers. comm., 1988) of Carajas, Brazil, may be Archaean and not Proterozoic and such deposits may be biological (Holm, 1987).

THE ARCHAEAN AND ORE DEPOSITS

Those of us who work or live on continents tend to think of the Archaean crust as being very rich in mineral deposits. But on reflection it becomes clear that this is hardly true. By far the bulk of materials needed by man are derived from much younger rocks. In part this is simply a question of the available preserved sample of rocks of different ages. But I think that more fundamentally it reflects the change in the varieties of environments which have led to a much greater degree of geochemical variation in the present.

If the early crust of the Earth was dominantly submarine, sedimentary processes would be less important. If early volcanism was dominantly mafic to ultramafic, and submarine, only a limited array of processes and hydrothermal solutions were available.

The Archaean was a superb time for the formation of massive sulphides (Cu, Zn) but while the frequency is high the scale is small compared to the modern plutonic-sedimentary environments (cf. modern ocean ridges and the porphyry copper environment and the dolomite-Pb-Zn-Ag connection). Metamorphic gradients were highly suitable for lode gold (Fyfe, 1986) but not for alluvial or lateritic deposits. There were no great carbon deposits and little tin or uranium (there was simply too much ^{235}U to allow concentration on some of the modern scales). On modern Earth there tends to be a micro-environment capable of concentrating almost any element. The Archaean was simply too turbulent and fluids were dominated by seawater.

CONCLUSION

Some years ago Hargraves (1976) and Fyfe (1978) discussed the possibility of an early globe covered with light hydrated and siliceous materials. Given more chaotic convection patterns, a necessity of the early energetics, a global hot spot model was suggested to explain the structure of the preserved sample. Perhaps it is still a model with some merit. There is little doubt that the Earth was hotter and convection must have been more turbulent. Hargraves' (1986) suggestion of a higher frequency of eruptive sites with essentially a mini-plate model of the early Earth perhaps summarizes much of the present thought.

It is great pleasure to contribute to this volume in honour of the great Indian Earth Scientist, Dr.B.P.Radhakrishna who devoted so much of his life to the study of the ancient rocks of India.

REFERENCES

Birch, F., 1965. Speculations on the earth's thermal history. Geol. Soc. Am. Bull., 76: 133-154.

Bridgwater, D. and Fyfe, W.S., 1974. The pre-3 b.y. crust:fact-fiction-fantasy. Geosci. Canada, 1: 9-11.

Broecker, W.S., 1985. How to build a habitable planet. Eldigio Press Palisades, New York, 291pp.

Brundtland, G.H., 1987. Our common future. The World Commission on Environment and Development. Oxford University Press, 383pp.

Carnegie Institution Washington., 1986. Year Book 85: pp.76-84.

Courtillot, U. and Besse, J., 1987. Magnetic field reversals, polar wander and core-mantle coupling. Science, 237: 1140-1147.

Dziewonski, A.M. and Woodhouse, J.H., 1987. Global images of the Earth's interior. Science, 236: 37-48.

Elder, J.W., 1968. Convection - the key to dynamic geology. Sci. Prog., 56: 1-33.

Elder, J.W., 1987. The structure of the planets. Academic Press, 210pp.

Fyfe, W.S. 1978. The evolution of the Earth's crust: modern plate tectonics to ancient hot spot tectonics? Chem. Geol., 23: 89-114.

Fyfe, W.S. 1980. Crust formation and destruction, In: D.W.Strangway (Editor), The continental crust and its mineral deposits. Geol. Canada, Special Paper 20: pp.77-88.

Fyfe, W.S. 1982. Andesites - product of geosphere mixing.In: R.S. Thorpe (Editor), Andesites. John Wiley and Sons, pp.663-668.

Fyfe, W.S., 1986. The transport and deposition of gold. In: L.A.Clark (Editor), Gold in the Western Shield. CIM Spec. Vol., 38: pp.663-668.

Fyfe, W.S. and Lonsdale, P., 1981. Ocean floor hydrothermal activity In: C.Emiliani, (Editor), The oceanic lithosphere, John Wiley, pp. 589-638.

Gilbert, G.K., 1893. Continental problems. Geol. Soc. Am. Bull., 41: 179-190.

Gilluly, J., 1971. Plate tectonics and magmatic evolution. Geol. Soc. Am. Bull., 82: 2387-2396.

Hale, C.J., 1987. Paleomagnetic data suggest link between the Archaean-Proterozoic boundary and inner-core nucleation. Nature, 329: 233-236.

Hargraves, R.B., 1976. Precambrian geologic history. Science, 193: 363-371.

Hargraves, R.B., 1986. Faster spreading or greater ridge length in the Archaean? Geology, 14: 750-752.

Hilde, T.W.C. and Uyeda, S., 1983. Convergence and subduction. Tectonophysics, 99: 85-400.

Holland, H.D., 1984. The chemical evolution of the atmosphere and Oceans. Princeton University Press, 582pp.

Holm, N.G., 1987. Possible biological origin of banded iron-formations from hydrothermal solutions. Origins of life, 17: 229-250.

Kasting, J.F., Toon, D.W. and Pollack, J.B., 1988. How climate evolved on the terrestrial planets. Sci. American, 258(2): 90-97.

Lallemont, S., Lallemand, S., Jolivet, L. and Huchon, P., 1986. Kaiko: L' exploration des fosses du Japon. La Recherche, 182: 1344-1357.

Lyell, Sir Charles, 1872. Principles of Geology, 1: 671pp.

McKenna-Lawlor, S.M.P., 1988. Mission to Mars and its Moons. New Scientist, 3 March, 54-57.

Molnar, P. and Gray, D., 1979. Subduction of continental lithosphere: some constraints and uncertainties. Geology, 7: 58-63.

Segerer, A., Stetter, K.O. and Klink, F., 1985. Two contrary modes of chemolithotrophy in the same archaebacterium. Nature, 313: 787-790.

Straus, J.M. and Schubert, G., 1977. Thermal convection in a porous medium: effect of temperature- and pressure-dependent thermodynamics and transport properties. J. Geophys. Res., 82: 325-333.

Turcotte, D.L. and Schubert, G., 1982. Geodynamics. John Wiley and Sons, 450pp.

Uyeda, S., 1983. Comparative subductology. Episodes: 19-24.

Viezer, J., 1987. The earth and its life: geologic record of interactions and controls, In: J.M.Robson (Editor), Origin and evolution of the Universe: evidence of design? McGill Univ. Press, pp.167-194.

Walsh, M.M. and Lowe, D.R., 1985. Filamentous microfossils from the 3,500-Myr-old Onverwacht Group, Barberton Mountain Land, South Africa. Nature, 314: 530-532.

THE NATURE OF THE ORTHOPYROXENE ISOGRAD IN PRECAMBRIAN HIGH-GRADE TERRAINS

ROBERT C. NEWTON

ABSTRACT

The principal modes of generation of orthopyroxene in the ancient granulite facies terrains correspond to the several ways of large-scale crustal desiccation:

1. *Pre-metamorphic drying.* The heat of shallow rift-graben plutons preconditioned the Adirondack terrain of New York to very dry metamorphism during subsequent orogenesis. Much of the orthopyroxene is of relict igneous origin. Metamorphic orthopyroxene is sparse, the orthopyroxene isograd poorly defined, and the terrain predominantly non-charnockitic.

2. *High-pressure subsolidus dehydration.* Reduction of H_2O activity by infiltration of CO_2-rich fluids during late Archaean metamorphism of southern India generated a well-defined orthopyroxene isograd by breakdown of hornblende in felsic gneisses. CO_2 action was first concentrated in deformational channelways, which later coalesced to produce massive charnockite as a wave of fluids rose in the crust. Anatectic melting occurred at high crustal levels of the amphibolite facies but was inhibited by low H_2O pressures in the granulite zone. Large-scale fluid transfer accomplished Rb depletion, K-metasomatism and high oxidation states and left ubiquitous high-density CO_2-rich fluid inclusions in granulites.

3. *Anatectic desiccation.* Absorption of H_2O into anatectic melts caused biotite breakdown to orthopyroxene in the Namaqualand terrain of South Africa. Orthopyroxene in acid gneiss is patchily distributed; a discrete isograd has not been identified. Shear localization of leucosomes suggests that low-$P(H_2O)$ fluids initially triggered partial melting. The granitic liquid was not extensive enough to segregate but eventually froze in place, releasing the H_2O. Rehydration of orthopyroxene was incomplete, perhaps for kinetic reasons.

Regional orthopyroxene isograd relations may also be those of retrogression, as in the Limpopo Belt of southern Africa, where a fossil horizon exists of rehydration to ferromagnesian amphibole. The widespread presence of orthoamphibole in acid gneisses probably records the former extent of orthopyroxene development during the prograde cycle.

More than one of the above processes may have operated on a given terrain to influence the resulting patterns of orthopyroxene distribution, and their combined effects may be difficult to decipher. In particular, siliceous melts and low- H_2O fluids may have commonly cooperated in various ways, as yet poorly understood, in producing the Precambrian granulite facies terrains.

INTRODUCTION

Importance of granulite facies terrains

Regionally distributed granulite facies rocks record processes which operated on extensive areas of the deep continental crust. It has been suggested that the typical lower crust is closely similar to the large Precambrian granulite facies terrains, such as the Adirondack Highlands (Sack,1980), Enderby Land, Antarctica (Ellis, 1980), and the Pikwitonei Domain of the Superior Province in Manitoba (Fountain and Salisbury, 1981). Orthopyroxene- and garnet-bearing intermediate rocks have densities and seismic velocities suitable for lower crustal rocks, and some rocks from the highest-grade terrains have extremely low levels of large-ion lithophile elements (LILE), including the radioactive heat producers U,K and Th (Heier, 1973). Low heat production is an essential feature of models of the deeper portions of the shield areas, where heat flow is very low.

One of the outstanding results of field work is that rocks of surficial origin, including sediments, volcanics and evaporites, are present in all granulite facies areas. Therefore, at least parts of all exposed high-grade terrains went through upper crustal cycles before becoming parts of the deeper crust. This fact implies that, if the high-grade terrains are indeed representative of the deep continental crust, some processes of deep burial and thermal processing of surficial materials have been important in building the crust over geologic time.

Orthopyroxene isograds

Of special interest in the study of ancient crustal processes are the regional orthopyroxene isograds. The appearance of the definitive granulite facies mineral orthopyroxene, especially in felsic and intermediate quartzofeldspathic gneisses, may be considered to mark a fossilized boundary between the upper crust and lower crust. This critical horizon is exposed in many terrains, principally in the Precambrian Shield areas. Amphibolite facies to granulite facies transitions have been reported from the Kapuskasing (Percival, 1983) and Pikwitonei (Hubregtse, 1980) areas of the Superior Province of Canada, the Western Grenville (Wynne-Edwards, 1972) and Adirondack (Wiener et al., 1984) areas of southern Canada and northern New York, the Rogaland (Kars et al., 1980) and Bamble (Touret, 1971) terrains of Norway, the Inari (Hormann et al., 1980), and West Uusimaa (Schreurs, 1984) areas of Finland, the Limpopo (Van Reenen et al., 1988) and Namaqualand (Waters and Whales, 1984) areas of southern Africa, the Broken Hill area of southern Australia (Phillips and Wall, 1981), the Jimperding Belt of western Australia (Gee, 1979) and the southern Karnataka and northern Tamil Nadu areas of India (Subramaniam, 1967; Raith et al., 1982).

Orthopyroxene appears in metabasic lithologies nearly at the same place in prograde successions as in felsic gneisses, though an orthopyroxene isograd in basic rocks may occur at slightly lower grade, as in Adirondacks (Buddington, 1963) and Bamble (Field et al., 1980). Other lithologies such as metapelites and calc-silicates, do not produce orthopyroxene. While characteristic and sometimes quantitatively important, these lithologies are not diagnostic of the granulite facies in their assemblages and will not be considered in detail here.

Origins of the isograds

It has been established by many calculations on model orthopyroxene-producing reactions in rock systems, that attendant H_2O pressures must have been quite low, probably less than 0.4 of the rock pressures (Phillips, 1980; Valley et al., 1983; Hansen et al., 1984; Bhattacharya and Sen, 1986). Thus, the various ways in which orthopyroxene could be produced in granulite facies metamorphism correspond largely to the possible mechanisms of large-scale crustal desiccation. The major conceptual mechanisms are:

1) Primary igneous processes. Voluminous mantle-derived intermediate magmas could have precipitated orthopyroxene at deep levels, thus freezing into the granulite facies, while rest magmas progressively richer in H_2O may have risen to higher levels, eventually to freeze into the amphibolite facies (Drury, 1980). In this hypothesis, granulite facies metamorphism is closely related to crustal accretion.

2) Pre-metamorphic desiccation. This has been suggested to have been of importance in the Adirondack terrain. Shallow anorogenic anorthosite and related plutons baked out their supracrustal cover rocks in a rift-graben, over a period of 150-300 million years prior to the Grenville orogeny (McLelland and Husain, 1986). Orthopyroxene in the Adirondacks might thus be at least partly relictic from a pre-orogenic stage, either as primary igneous pyroxene or in pyroxene hornfels aureoles.

3) Partial melting of quartzofeldspathic rocks, as by vapor-absent biotite-quartz reactions, with absorption of H_2O into acid melts, leaving an orthopyroxene-bearing restite assemblage. This mechanism has been identified as the major process producing orthopyroxene in the Namaqualand, South Africa, terrain (Waters and Whales, 1984), in the Broken Hill terrain of southern Australia (Philips, 1980) and as a general principle (Powell, 1983; Crawford and Hollister, 1986).

4) Streaming of low-$P(H_2O)$ volatiles, most plausibly CO_2, through the crust during metamorphism. Janardhan et al., (1979; 1982) postulated this on the basis of field evidence for deformation-aided charnockitic alteration in acid gneisses at the orthopyroxene isograd in southern India. The implied orthopyroxene-producing reactions are thus subsolidus dehydration reactions of biotite and amphibole at reduced H_2O pressures.

5) Escape of H_2O through fractures at decreased $P(H_2O)$ during metamorphism. This mechanism was proposed to explain the deformation-related patchy distribution of charnockite in biotite-garnet paragneisses of southern Kerala, India by Srikantappa et al., (1985).

Each of these suggested mechanisms would be expected to yield different kinds of orthopyroxene isograds having features diagnostic of their diverse origins.

In addition to relictic and prograde orthopyroxene isograds, relations of orthopyroxene-bearing terrains with surrounding regions may be those of retrogression, as inferred by Van Reenen (1986) for the Southern Marginal Zone of the Limpopo Belt. A mappable isogradic boundary relates orthopyroxene to retrogressive magnesian amphibole, anthophyllite or gedrite, in acid gneisses. Apparently similar regional replacement of orthopyroxene by orthoamphibole exists also in the early Archaean gneisses of central Labrador (Collerson and Bridgwater, 1979).

The present paper discusses the phenomena of the reported occurrences and inferences about isogradic reactions. All of the conceived mechanisms are feasible in different high-grade terrains, and orthopyroxene isograds of more than one type may occur in a single terrain. This could confuse the interpretation of the metamorphism, unless the different orthopyroxene-producing or orthopyroxene-consuming events are carefully distinguished.

REACTION MECHANISMS

Pressure-temperature-H_2O activity model

Figure 1 is a temperature-pressure-H_2O activity model illustrating the major reactions which form orthopyroxene "O". Its hydrate precursor, "H", could be biotite or amphibole. The subparallel lines of the diagram are univariant equilibrium curves in planes of constant H_2O activity, varying from unit activity, where a vapor phase is pure H_2O, to very low activities, where a vapor phase is dominantly anhydrous or may be lacking. Univariant plane curves of the same type together form a surface, one of which is a subsolidus dehydration surface, labelled (L) for liquid absent, which corresponds to the generalized reaction H = O + vapor. Others are a minimum melting surface at high H_2O activities, labelled (O) for orthopyroxene absent, and the surface of a high-temperature melting reaction lacking the hydrate, labelled (H). The top side of the model is a plane of constant pressure containing traces of the divariant surfaces. The heavy line formed by the intersection of the surfaces is the univariant space curve of the H_2O-deficient melting reaction. It emanates from a low-pressure invariant point, I_o, at unit H_2O activity, and is the locus of all isobaric invariant points I_p, at reduced H_2O activity. In a system where H_2O is the only volatile component, the reaction is vapor-absent. If H_2O activity is lowered by the presence of another volatile, such as CO_2, there may be a vapor phase, but the univariant space curve may nearly coincide with that of the vapor-absent curve in the pure H_2O system because of low solubility of the other volatile component in the silicate melt. The general model of Figure 1 is illustrated by the experimentally determined examples which follow.

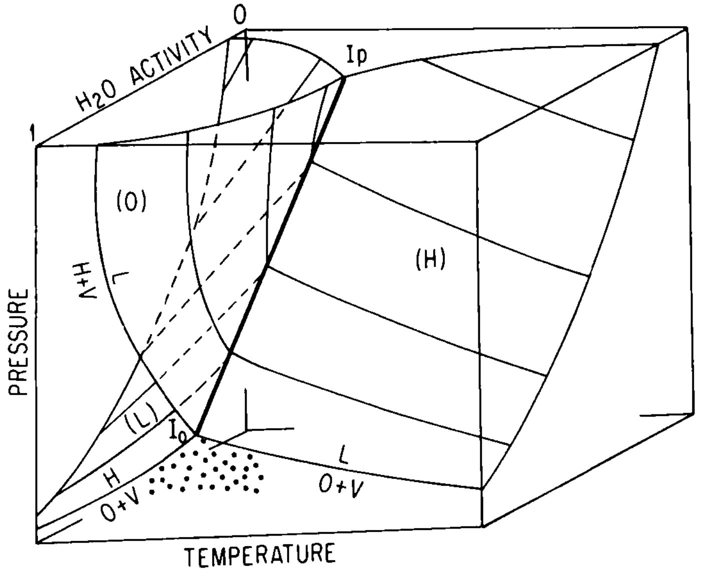

Figure 1. Temperature-pressure-H_2O model of dehydration and melting reactions in a generic system of a mafic hydrate (amphibole or biotite), orthopyroxene, feldspar and quartz. The three divariant surfaces are labelled as follows: (O) = orthopyroxene-absent reaction: (L) =liquid-absent reaction, and (H) = hydrate-absent reaction. The stippled area at low pressures is the region where a H_2O-rich vapor could coexist with orthopyroxene.

Subsolidus dehydration reactions

Figure 2 shows experimental subsolidus dehydration and melting curves for biotite and hornblende in reaction with quartz. Biotite is represented by phlogopite, $KAlMg_3Si_3O_{10}(OH)_2$.Contours of constant H_2O activity are shown. It is seen that the proposed orthopyroxene isograd reaction:

A) biotite + quartz = orthopyroxene + K-feldspar + H_2O

must be attended by H_2O activities less than about 0.3 for granulite facies metamorphism at typical conditions near 5 kbar and 700^o-800^oC, as in southern Kerala, India (Ravindra Kumar et al., 1985) and southern Finland (Schreurs, 1984). The vapor-absent melting curve puts an upper limit of about 830^o for subsolidus dehydration at 5 kbar in the model system. Similar information is forthcoming from the hornblende-quartz reaction:

B) hornblende + quartz = orthopyroxene + Clinopyroxene + plagioclase + H_2O

according to the calculations of Wells (1979) for the Buksefjorden (SW Greenland) area. Wells' calculations were based on the experimental diagram of Choudhuri and Winkler (1967), which remains the only available work on hornblende close enough to natural systems for interpretation of the granulite facies. If regional anatectic melting was not the principal cause of reduced H_2O activity, the above reactions must have been driven either by influx of anhydrous volatiles or by opening of brittle fractures which would allow H_2O to escape at reduced pressure. The former possibility is supported in the Buksefjorden, S. Finland and S. India areas by the occurrence of ubiquitous dense CO_2 inclusions in metamorphic minerals. The latter hypothesis was suggested by Srikantappa et al., (1985) for the biotite to orthopyroxene reaction in southern Kerala. This concept has been termed "fissure equilibrium" when applied to some kinds of shallow metamorphism (Thompson, 1955). It seems less likely to be important in granulite facies metamorphism, in view of the high ductility of rocks at elevated pressures and temperatures, especially in the presence of a mineralizing fluid.

Dehydration-melting reactions

Absorption of H_2O into anatectic melts with reduction of H_2O activity as melting proceeds is one of the most commonly-proposed mechanisms for formation of orthopyroxene and the granulite facies in general (Powell, 1983; Crawford and Hollister, 1986). Waters (1988) put forth the reaction:

C) biotite + quartz(+plagioclase)=liquid + orthopyroxene (+K-feldspar)

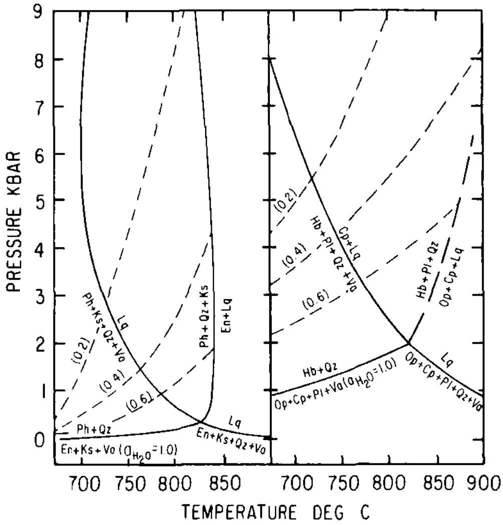

Figure 2. Experimental subsolidus dehydration and melting equilibria for phlogopite (Peterson and Newton, 1987) and hornblende in a mafic system (Wells, 1979). Dashed lines are contours of constant H_2O activity on the subsolidus reaction surface, calculated by Hansen et al. (1984) for phlogopite and Wells (1979) for hornblende, based on the experimental work of Choudhuri and Winkler (1967). The vapor-saturated hornblende solidus is modelled by the basalt-H_2O solidus of Lambert and Wyllie (1972).

to explain the sporadic appearance of orthopyroxene in the highest-grade portion of the Namaqualand, South Africa, terrain. This reaction requires substantially reduced H_2O activity to proceed. The reaction could be vapor-absent, as written, or there may be small amounts of a pore fluid, dominated by a volatile such as CO_2 as melting proceeds.

Progressive decrease of H_2O activity with progressive anatexis leading to the appearance of orthopyroxene can be modelled with reference to Figure 1. Figure 3 shows an isobaric section from the block model, after Waters (1988). It is supposed that there is initially a small amount of pore fluid. Increasing temperature produces a small amount of partial melting at point "a". If the amount of biotite is large compared to the amount of pore fluid, the further course of melting will be constrained to follow the isobaric univariant solidus(O), along path A, and H_2O activity

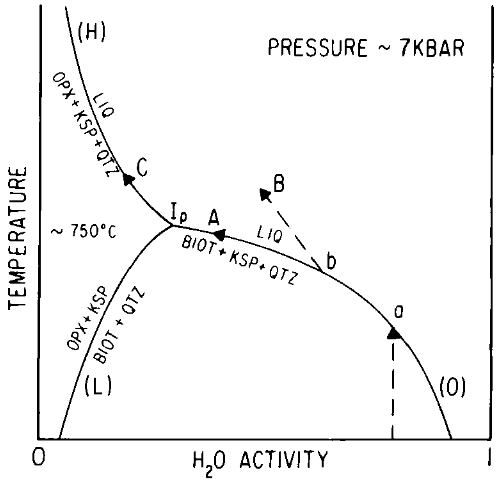

Figure 3. Isobaric section of Fig. 1, for biotite, illustrating decrease of H_2O activity in partial melting. Possible paths of temperature increase, (A, B and C) depend on the initial amounts of pore fluid and biotite.

will steadily decrease until orthopyroxene appears at the isobaric invariant point, I_p. It could well happen that the system has become vapor-absent by this time: all of the small amount of initial pore fluid may have been dissolved into the melt. If, however, the amount of biotite in the rocks is small, it could become exhausted in reaction (O) at some point "b", before orthopyroxene appears. The H_2O activity-temperature function is now divariant and departs from the solidus, as along path B.

The amount of anatectic melt generated is roughly the same as the amount of biotite consumed, since biotite supplies the H_2O needed for melting. For biotite-rich rocks, the invariant point acts somewhat as a thermal brake, in that large quantities of heat must be supplied before further temperature increase is possible. In many terrains partial melting leading to orthopyroxene formation did not exhaust all of the biotite, which can be stabilized to somewhat higher temperature by increasing TiO_2 content (Schreurs, 1984). If all biotite is used up in melting, at I_p, further temperature rise is possible and decrease of H_2O pressure will be buffered to the melting equilibrium (H), along path C. Large degrees (probably >30%) of melting would be needed for an anatectic melt to segregate into small plutons and rise some distance in the crust (Wickham, 1987). Such charnockitic magmas would probably lack biotite among their liquidus phases. Possible examples of diapiric charnockite plutons occur in southern Norway, where zoned granites and syenites show continuous gradation from biotite-absent charnockite with CO_2-rich fluid inclusions to biotite granite with H_2O-rich fluid inclusions (Madsen, 1977); the localities of these plutons in the amphibolite facies part of the Bamble terrain locally defy the regional orthopyroxene isograd(Touret, 1971).

Premetamorphic desiccation

Another idea for regional distribution of orthopyroxene in gneissic terrains is that the orthopyroxene gneisses are cumulates precipitated directly in early crustal accretion. As applied by Drury (1980) to the granulite facies-amphibolite facies boundary in the Outer Hebrides, voluminous mantle-derived tonalitic magmas differentiated into early pyroxene-plagioclase-enriched cumulates with positive Eu anomalies, and H_2O-enriched rest magmas eventually rose into the upper levels of the crust to form amphibolite facies gneisses with negative Eu anomalies. The hypothesis of juvenile crust-forming magmas "freezing into" the granulite facies has been put forth also for the Scourie terrain (Holland and Lambert, 1975) and the Bamble terrain (Field et al., 1980). A variant of this idea, which assigns an important role to streaming of CO_2 released from deep-crustal intermediate melts on freezing, was put forth by Wells (1979) for the SW Greenland terrain, Lamb et al. (1986) for the Bamble terrain, and Frost and Frost (1987) for the Archaean Wind River terrain.

An unmodified theory of primary crustal accretion of gneiss precursors freezing directly into the granulite facies at deep crustal levels and differentiating to the amphibolite facies at shallower depths is fraught with many problems. These include ubiquitous involvement of supracrustal rocks, implying an upper-crustal pre-granulite history, the inability of purely igneous processes to fractionate Rb from K (Lamb et al., 1986), and the fact that amphibole tonalite grading downward into pyroxene tonalite has never been recorded in deeply dissected Phanerozoic batholith suites. On the contrary, orthopyroxene-bearing rocks are invariably the most shallow facies of granitic intrusions, as in the Cloudy Pass Batholith of Washington State

(Grant, 1969) and the Cheviot Granite of northern England (Haslam, 1986).

Premetamorphic regional desiccation of surficial sequences by baking out around large mafic or anorthositic intrusions has been suggested as the major reason for the dryness of the Adirondack Mountains terrain (McLelland and Husain, 1986), by analogy with the pyroxene-hornfels aureole of the Nain Complex, central Labrador (Berg, 1977), where some of the dryest metamorphic rocks known, including metasediments with osumilite, are found around the margins of the anorthosite body. Regional geobarometry shows that the anorthosite was emplaced in a rift graben at maximum depths of 6-10 km and that the supracrustal country rocks were H_2O-rich and in the low greenschist facies before contact metamorphism.

The appearance of orthopyroxene resulting from plutonic crystallization at very low pressures, or from regional desiccation by shallow contact metamorphism around plutons prior to regional metamorphism, corresponds to the stippled area in Figure 1 in the low pressure field of anhydrous mafic silicates plus vapor. Subsequent regional metamorphism at high pressures of a terrain thoroughly dried out by shallow plutonism would preserve the igneous orthopyroxene and the pyroxene-hornfels aureoles.

Regional retrogressive relations

A regional boundary between granulite facies and amphibolite facies may correspond to large-scale retrogression. This relationship could result either from late metamorphic influx of H_2O or from a subsequent metamorphism, or simply from cooling at nearly constant H_2O activity. Refreezing of anatectic melts with release of H_2O could produce retrogressive alteration of pyroxene to hydrous minerals. Retrogressive biotite or amphibole can sometimes be detected by replacement textures or by lower F and/or Ti contents than the primary hydrates (Janardhan et al., 1982).

Ferromagnesian amphibole retrogressive after orthopyroxene in acid gneisses has been reported many times (Austrheim and Robins, 1981; Collerson and Bridgwater, 1979; Srikantappa et al., 1986; Janardhan et al., 1982; Van Reenen, 1986). To the author's knowledge, ferromagnesian amphibole has never been reported as a precursor to orthopyroxene in prograde metamorphism of acid gneisses, and it may be suspected that this mineral is a nearly infallible indicator of retrogression from the granulite facies. The simple reaction involved is:

D) orthopyroxene + quartz + vapor = ferromagnesian amphibole.

This reaction may be a kinetically-favored metastable reaction in rocks of calc-alkaline chemistry, as indicated by secondary hornblende development subsequent to orthoamphibole (Collerson and Bridgwater, 1979).

Figure 4 shows a possible isobaric, subsolidus temperature-H_2O activity cycle, based on Fig. 1, which produces orthopyroxene from calcic amphibole breakdown. Decrease of H_2O activity might be caused by influx of CO_2 with increasing temperatures, as suggested by the ascending portion of the heavy line. When amphibole becomes unstable at point a, H_2O activity may temporarily increase as H_2O is delivered to the vapor. At point b, amphibole is exhausted and H_2O activity begins to decrease again. Relaxation from peak metamorphic conditions may begin when heating and CO_2 inlux abate, at point c. Cooling without further change in the ambient vapor phase may bring the rocks back into the stability field of hornblende, but, if hornblende is suppressed, perhaps by failure of the fluids to mobilize large rock volumes, local

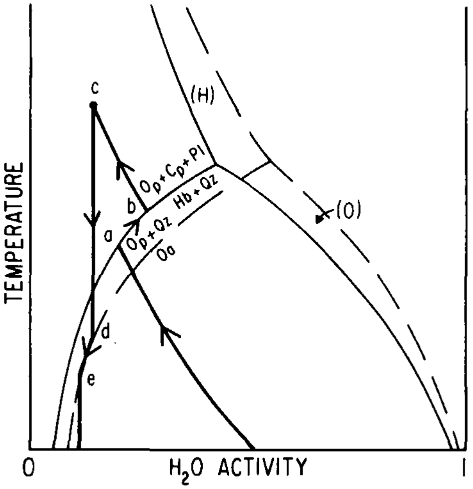

Figure 4. Possible isobaric subsolidus T-a(H_2O) paths for prograde CO_2 influx (ascending path) and retrograde cooling at constant pore fluid composition with metastable inversion of orthopyroxene to orthoamphibole (descending path).

alteration of orthopyroxene may produce orthoamphibole by reaction D) at point d. Further cooling then will cause further depletion of H_2O in the vapor phase until the retrogressive reaction ends, either because all orthopyroxene is converted or for kinetic reasons. Late-metamorphic very CO_2-rich fluid inclusions could have been produced by depletion of pore fluids in H_2O by orthoamphibole formation. In this scenario, rehydration may proceed at even lower H_2O activity than earlier dehydration. Van Reenen (1986) estimated that $P(H_2O)$ was only about 0.2 times P(total)during the retrogressive formation of orthoamphibole after orthopyroxene in the Limpopo Belt.

TERRAINS ILLUSTRATIVE OF THE PROPOSED PROCESSES

Southern India-Low-H_2O volatile streaming

Figure 5 shows the geology of the orthopyroxene isograd in the vicinity of the southern Closepet Granite, southern Karnataka, South India. The three principal rock types are dominant tonalitic to granodioritic light-gray hornblende-biotite gneiss ("Peninsular Gneiss"), dark orthopyroxene-bearing charnockitic gneiss, and pink leucogranite, of palingenetic and metasomatic origin (Radhakrishna, 1956). Minor lithologies include metabasic

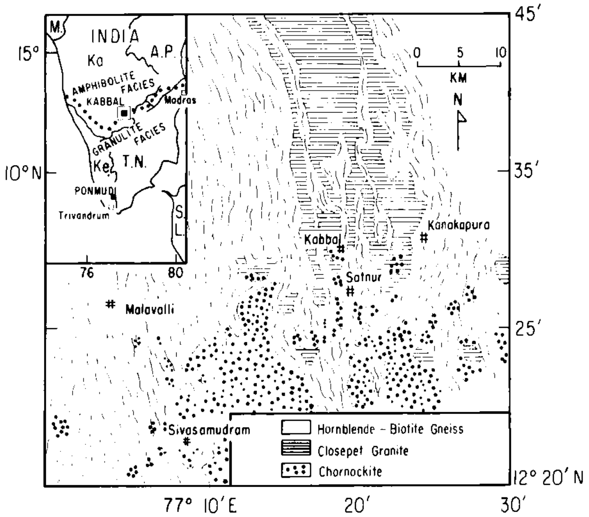

Figure 5. Relations of amphibole-biotite gneiss ("Peninsular Gneiss"), charnockite and Closepet Granite at the orthopyroxene isograd in southern Karnataka, India. Geology compiled from Suryanarayana (1960), Devaraju and Sadashivaiah (1969), Mahabaleswar and Naganna (1981), Mahabaleswar et al., (1986). Regional orthopyroxene isograd (inset) from Subramaniam (1967).

and metasedimentary enclaves. The following general observations are outstanding:

1) There is a narrow transitional interval between Peninsular Gneiss in the north to massive charnockite in the south in which both rock types coexist in close association. In especially good exposures, like the rock quarry at Kabbal, Karnataka (Pichamuthu, 1960; Friend, 1981) charnockitic alteration of migmatitic gneiss occupies shear veins, fold hinges and other deformation features, suggestive of alteration by channelized fluids. Although the gray gneiss is migmatitic, the diffuse and near-isochemical nature of the charnockitic alteration makes it seem doubtful that melting reactions are directly related to orthopyroxene production. A further observation in favor of low-P(H_2O) volatile streaming is that charnockitic veins contain large quantities of high-density CO_2-rich fluid inclusions in quartz and feldspar, whereas the adjacent unaltered gray gneiss wall rock contains practically none (Hansen et al., 1984).

2) The terrain immediately to the south of the transitional zone of mixed facies rocks is a monotonously charnockitic massif, the Biligirirangan (BR) Hills. Other similar massifs, the Nilgiri Hills and Shevaroy Hills, lie to the south of a narrow mixed facies terrain along the orthopyroxene isograd. The dominant quartzofeldspathic gneisses in these massifs contain orthopyroxene and lack hornblende. Biotite is generally stable throughout. Metasedimentary units are present throughout the massif terrains. Paleopressures increase from about 5 kbar at the northern edge of the transition zone to 7.5 kbar at the southern edge (Hansen et al., 1984). Paleotemperatures are about $750^{\circ}C$ across this interval.

3) The southward trending Closepet granite becomes segmented and phases out almost exactly at the latitude where charnockite appears. Linear trends in the Peninsular Gneiss, as observed on the ground and in Landsat images, are continuous into the charnockitic terrain. Therefore, charnockite can be considered in some way a continuation of or counterpart of the Closepet Granite in the deeper crust. Charnockite and granite formation are very closely related in time of emplacement in their overlap region (Friend, 1981).

The isograd relations in southern India are those of a progressive overprint of the granulite facies on the pre-existing amphibolite facies gneisses. The main orthopyroxene-producing reaction in gray gneiss involves disappearance of hornblende. Almost simultaneously, metabasic enclaves develop orthopyroxene. Hornblende remains a stable mineral in some mafic parageneses. A decrease of H_2O pressure across the transition zone is indicated as the decisive factor in the onset of granulite assemblages. Large-scale granite formation took place mainly at metamorphic conditions below orthopyroxene grade, perhaps because of influx of H_2O and K_2O expelled from deeper levels of the crust.

Further south, deep within the granulite facies terrain, another kind of partial charnockitic mottling of acid gneisses has been reported from several widely-separated localities (Holt and Wightman, 1983; Ravindra Kumar et al., 1985; Srikantappa et al., 1985). These localities involve paragneisses, mostly graphite-bearing, interlayered with garnet-sillimanite metapelites (khondalites) and minor calc-silicates and marbles. Occasional quartzofeldspathic rocks of calc-alkaline compositions are always charnockitic: primary hornblende does not occur in acid gneisses. The southern mixed facies gneisses give petrographic evidence of the biotite breakdown reaction, with evidence for the participation also of garnet. This is a higher-grade reaction than that of hornblende breakdown, indicating higher temperature, lower pressure, or lower H_2O pressure, than at the regional orthopyroxene isograd, where biotite and quartz are still stable together.

The sequence of prograde orthopyroxene-producing reactions was diagrammed by Hansen et al., (1987) with the projection of Froese (1978). The coordinates are A (= Al_2O_3-Na_2O-K_2O-CaO), F (=FeO-Fe_2O_3-TiO_2) and M(=MgO). The projection is thus from quartz, K-feldspar, ilmenite, magnetite, and a plagioclase of fixed composition. As shown in Figure 6, in the lowest grade, or "Peninsular Gneiss" facies, orthopyroxene is not stable. Gray gneiss, metabasite and metapelite assemblages are represented. Hornblende and biotite react at the orthopyroxene isograd to produce the lowest granulite facies, or "Kabbal Facies". At still higher grade, within the charnockitic terrain, biotite and garnet react to produce orthopyroxene in metasedimentary gneisses, ushering in the "Ponmudi Facies", named for a mixed-facies quarry

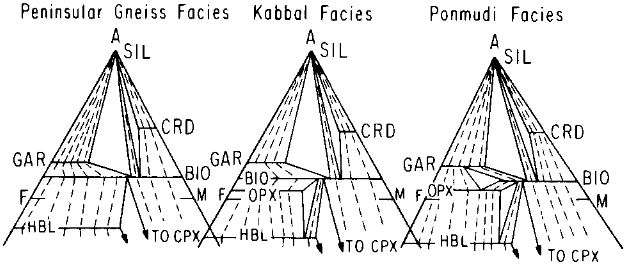

Figure 6. Froese (1978) projection of quartzofeldspathic gneisses in S. India, after Hansen et al., (1987). The three facies types are separated by two orthopyroxene-producing isograd reactions, one involving the hornblende-biotite reaction, and the other the biotite-garnet reaction (E and F of text).

north of Trivandrum (Fig.5) showing incipient biotite-garnet-quartz reaction in graphitic gneisses (Ravindra Kumar et al., 1985).

Numerous chemical studies of gray gneisses and incipient charnockitic alteration at the orthopyroxene isograd have

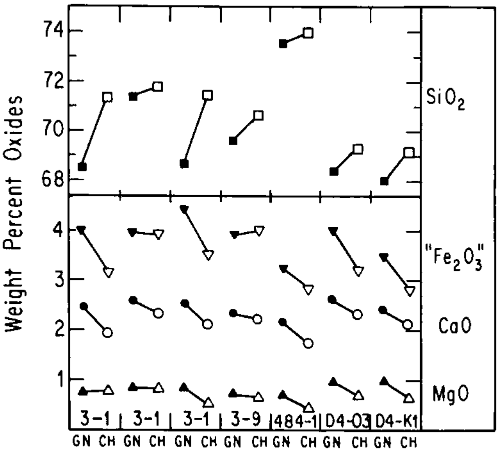

Figure 7. Oxide wt. percentages in "close-pair" analyses of charnockitic veins(CH) and host migmatitic gneiss (GN) at the orthopyroxene isograd in southern Karnataka and in the northern Central Highlands of Sri Lanka (D4). The analyses show a consistent pattern of decrease of CaO, MgO and FeO and increase of SiO_2, indicating that the orthopyroxene-forming reaction was an open-system or metasomatic reaction. Data from Hansen et al., (1987).

concluded that the charnockitic metamorphism is nearly isochemical (Janardhan et al., 1982; Condie et al., 1982; Weaver and Tarney, 1983). However, detailed comparison of the Kabbal quarry charnockitic veins and immediately-adjacent host gray gneiss (Stahle et al., 1987; Hansen et al., 1987) have revealed subtle chemical changes, including slight decrease of CaO, FeO and MgO and increase of SiO_2 of charnockite relative to protolith (Fig. 7). It is not clear whether significant change in alkalis is involved in charnockitization. The former study reported a slight increase in Rb, whereas the latter study reported a slight decrease in Rb and a definite decrease of Y. Thus, the orthopyroxene isograd in gray gneiss is an open system reaction in southern India.

A logical framework for a metasomatic reaction is conservation of an inert component, usually taken to be Al_2O_3 (Ferry, 1984). The whole-rock analyses, mineral analyses and point-count data of adjacent charnockite and gray gneiss samples of Hansen et al., (1987) on the Kabbal rocks leads to the following reaction among hornblende, biotite, quartz, magnetite, plagioclase, K-feldspar, orthopyroxene, ilmenite and vapor at fixed Al_2O_3. The hornblende formula is based on 23 oxygens and that of biotite on 11 oxygens:

E) HBL+1.30 BIOT+1.24 QTZ+0.82 MT+(4.23 SiO_2+0.38 Na_2O) (added from vapor) = 1.49 PLAG(AN21) + 1.43 KSP+3.67 OPX+0.57 ILM+2.30 (H_2O+F) + 0.41 O_2 + (1.44 CaO + 2.12 FeO + 0.58 MgO) (removed in vapor)

The deduced reaction is predominantly that of hornblende breakdown, with the participation of about half as much biotite by mass as hornblende. Interestingly, the open system reaction proceeded at nearly constant mass.

A similar analysis may be applied to the orthopyroxene-producing reaction by biotite breakdown in the southern Kerala paragneisses. The point-count and analytic data indicate that a reaction closed to major element transport is feasible.

F) BIOT + 0.99 GAR + 2.37 QTZ = 0.21 ANOR + 0.89 KSP + 2.53 OPX + 0.31 ILM + (H_2O + F)

If a metasomatic reaction with fixed Al_2O_3 is considered, the point count and analytic data are equally well satisfied, and the coefficients of the orthopyroxene-producing reaction are not materially different. Thus, an open-system reaction is not demanded, but not excluded.

The deduction of an open-system reaction for the regional orthopyroxene isograd in southern Karnataka is consistent with the concept of CO_2 streaming as a cause of granulite facies metamorphism. The amount of CO_2 to cause subsolidus breakdown of amphibole at $P(H_2O) \leq 0.3P(rock)$ is at least three times the amount of H_2O in the rock in the form of amphibole. At the low porosity conditions of the deep crust, no significant regional dehydration could be accomplished without pervasive infiltration of CO_2 from a large source. This source has not yet been identified conclusively. Possible sources include a degassing mantle below the site of metamorphism (Sheraton et al., 1973), exsolution of CO_2 from a basaltic crustal underplate (Touret, 1971), decarbonation of limestone deeply buried by thrusting (Glassley, 1983), and deep-crustal CO_2 inclusions in minerals, purged in younger metamorphism (Stahle et al., 1987). The first two mechanisms have the advantage of a built-in source of heat as well as low-H_2O volatiles. Harris et al., (1982) postulated that heat transported into the South India crust by mantle-derived CO_2 was an important heat factor in the high-grade metamorphism. It is possible that CO_2 from carbonates buried to mantle depths by underthrusting could have been an important agency of heat transfer. Deep crustal intrusions as a source of heat for granulite facies metamorphism have been suggested often (cf. Sandiford and Powell, 1986).

Massive CO_2 streaming has been suggested as a primary cause of metamorphism in the Bamble, South Norway, terrain (Touret, 1971) and the West Uusimaa, South Finland, area (Schreurs, 1984; Schreurs and Westra, 1986). In the former area, a metamorphic progression exists similar to that of southern India, with several mappable prograde isograds, including the disappearance of muscovite, the appearance of cordierite and the appearance of orthopyroxene. The highest metamorphic grade occurs in the area around Tromoy Island on the Skagerrak coast, where felsic and intermediate rocks extremely depleted in LILE occur. According to the geothermometry and geobarometry of Lamb et al., (1986) P-T conditions were essentially constant across the Bamble terrain: the major metamorphic determinant was decrease of $P(H_2O)$ southwards. Fluid inclusions in metamorphic minerals change from dominantly aqueous in the amphibolite facies in the north to dominantly carbonic in the granulite facies in the south.

The West Uusimaa area is a prograde terrain containing an extremely discrete orthopyroxene isograd. Orthopyroxene appears in quartzofeldspathic rocks over a narrow ground interval, less than 5 km wide, independent of lithology and structure, in a linear zone 120 km long. Paleotemperatures, as determined by garnet-biotite thermometry, jump from 650°C to 750°C in this zone. Paleopressures are constant at about 4 kbar over the zone, and fluid inclusions generally change from aqueous to carbonic as grade increases. Schreurs and Westra (1986) invoked a large deep-crustal basic intrusion underneath the granulite-facies portion of their terrain to provide heat and CO_2-rich fluids.

In summary, the streaming through the crust of copious CO_2-rich vapors seems demonstrated as a primary cause of some granulite facies metamorphic terrains. These are generally older Precambrian, the youngest terrain so implicated being the Bamble terrain (1550 Ma). Some of the phenomena of LILE depletion in some granulite facies terrains may be dependent on volatile streaming processes, since several groups have found that extreme Rb depletion is not predictable by igneous fractionation or partial melt extraction (Okeke et al., 1983; Smalley et al., 1983).

The Namaqualand, South Africa terrain - Dehydration melting

Drying out of a granulite-facies terrain may result from absorption of H_2O into anatectic melts. Granitic liquids may segregate and move upward, leaving desiccated and LILE-depleted granulite residues (Fyfe, 1973; Nesbitt, 1980). CO_2-rich fluid inclusions in granulites have been explained as residual pore fluids remaining after anatectic extraction of H_2O (Crawford and Hollister, 1986). The most extensive analysis of this granulite-forming mechanism is that of Waters and Whales (1984) and Waters (1988) with reference to the Namaqualand granulite facies terrain of South Africa. The granulite facies there is heralded by the appearance of garnet and K-feldspar in leucosome segregations in pelitic rocks, best interpreted as resulting from a melting reaction of the type of C), with garnet instead of orthopyroxene as the mafic restite mineral.

Several features of this progressive metamorphic terrain which are quite remarkable may be listed:

1) The regional assemblage spinel-quartz is developed by decomposition of cordierite at the highest grades. This assemblage is quite rare, having been reported previously from SW Norway (Kars et al., 1980). The association betokens high temperatures and relatively low pressures, probably below 5 kbar (Seifert and Schumacher, 1986).

2) Amphibolite lenses have margins which have been converted to two-pyroxene granulite (Waters, 1988). These occurrences coincide with the development of garnet-bearing leucosomes in the dominant quartzofeldspathic gneisses. Waters (1988) suggested that absorption of H_2O into partial melts set up chemical potential gradients which caused H_2O to migrate from the metabasites into the leucosomes. A problem exists in that H_2O could not have been present at high activity in a vapor phase. Perhaps a static CO_2-rich pore fluid acted as a bridge for H_2O.

3) Orthopyroxene in acid gneisses never becomes pervasive, but is distributed in discrete leucosomes, even at the highest grades encountered, though its amount becomes progressively greater. There is no marked orthopyroxene isograd for gneisses and the metamorphism does not lead to a charnockitic massif terrain like those of southern India. The orthopyroxene-bearing segregations often occur in thin deformation zones, like shear bands, perhaps similar to those at the orthopyroxene isograd in southern India.

A problem exists in the ultimate removal of H_2O from the terrain. The classic desiccation concept is coalescence and removal upward of the H_2O-bearing granitic melts (Fyfe, 1973; Lowman, 1984). However, modern analyses of melt segregation (Wickham, 1987) indicate that granite bodies of sizes capable of bouyant rise cannot accumulate until melting amounts to as much as 30-40% of the entire terrain. In addition, the Namaqualand orthopyroxene-bearing leucosomes are almost isochemical with their host rocks, indicating retention of in situ partial melts.

Back-reaction of garnet and orthopyroxene to biotite is very limited in Namaqualand granulites, and does not account for more than a small fraction of the H_2O which must have been absorbed into the melt segregations. Three methods of removal of the H_2O upon eventual freezing of the melts were suggested by Waters (1988). These are: a) rapid removal of H_2O with failure to react for kinetic reasons, b) armoring of the garnet and orthopyroxene grains by quartz and feldspar, and c) effective channelization of the H_2O upon release from the melt pockets so that its subsequent contact with orthopyroxene and garnet would have been minimal.

Partial melting dehydration is the preferred general mechanism of Crawford and Hollister (1986) for producing granulite-facies terrains, and has been suggested for numerous areas, including the Adirondack Mountains (Stoddard, 1980), the Scourie (Scotland) area (Lowman, 1984) and the Arunta Block granulites of central Australia (Warren, 1983). Some authors envision a combined role of acid melt formation and volatile action. Thus, Waters(1988) suggested that volatiles with reduced H_2O activity migrating along shear bands in Namaqualand may have triggered the first partial melting. Frost and Frost (1987) described pyroxene granulite selvedges on charnockitic dikes in amphibolite in the Wind River, Wyoming, terrain, and suggested that acid melts could perform both desiccation of host rocks by H_2O absorption and extended dehydration by concomitant release of CO_2.

The Adirondack Mountains Pre-metamorphic desiccation.

The Adirondacks Mountain area of New York state is a very dry high-grade terrain of late Proterozoic(~ 1000 Ma) age (Fig.8). Evidence against pervasive volatile streaming as an important agency in this granulite facies metamorphism lies in the preservation of strong local gradients in oxygen isotopes in skarns around plutonic bodies (Valley and O'Neil, 1984), in small scale H_2O and CO_2 fugacity contrasts apparently buffered by local assemblages (Valley et al., 1983), by reduced, Fe-rich pyroxenes and oxide minerals, which militates against the influence of a voluminous oxidizing CO_2 phase (Lamb and Valley, 1984), and by general lack of pervasive metasomatism, with preservation of relict textures.

The dryness of the Adirondack Highlands assemblages was ascribed by McLelland and Husain(1986) to baking out at shallow depths of the metasediment-rich terrain by shallow plutons, including the Marcy anorthosite. If the pressures were only 2-3 kbar, dehydration reactions could have occurred in many assemblages without widespread melting. These pressures are much less than the peak pressures of 6-8 kbar yielded by geobarometry (Bohlen et al., 1985). Initial dryness and peak metamorphic temperatures (700^{o}-800^{o}C) below the dry anatectic range also limited widespread development of pyroxene in regional gneisses by dehydration melting.

Figure 8 shows the major lithologies of the Adirondack dome. Paleotemperatures increase from about 650^{o}C in the northwest ("Lowlands") to a maximum near 800^{o} C centered on the anorthosite massif in the eastern or '"Highlands" part of the area, and paleopressures increase somewhat from 6 to 7.5 kbar over this interval (Bohlen et al., 1985). The paleotemperature and paleopressure distributions most likely result from post-metamorphic

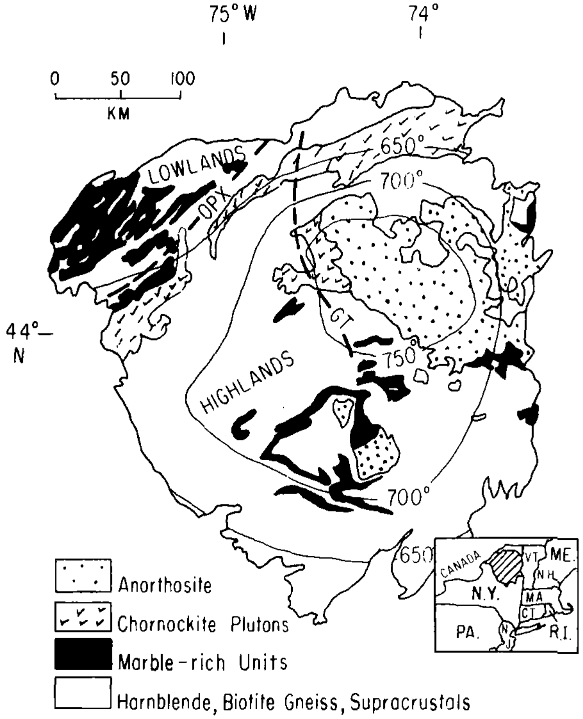

Figure 8. Lithology, isograds and paleo-isotherms in the Adirondack Highlands of New York, from Bohlen and Essene (1977), McLelland and Isachsen (1986), Bohlen et al. (1985), Buddington (1963) and Stoddard (1980).

rebound, since the anorthosite intrusion predates metamorphism by about 300 Ma (Ashwal and Wooden, 1983), and therefore would not have contributed directly to metamorphic heat.

A diffuse orthopyroxene isograd exists in the northwest sector, as shown in Figure 8. Orthopyroxene in metabasic rocks may appear at somewhat lower grade than in felsic rocks. The isograd for felsic rocks encloses the outcrops of the large charnockitic quartz syenite complexes, the Diana and the Stark, whose pyroxene is probably of igneous, rather than metamorphic, origin. The common interstitial textural association of orthopyroxene containing coarse exsolution lamellae of augite on (001) implies inversion from igneous pigeonite (Bohlen and Essene, 1978). Some pyroxene megacrysts from charnockites and anorthosites preserve evidence of pyroxene immiscibility at igneous temperatures near $1100^{\circ}C$ (Bohlen and Essene, 1978). It is not clear whether orthopyroxene formed from pigeonite simply in premetamorphic cooling from igneous temperatures or during the later metamorphic event. Metamorphic pyroxene in felsic rocks is rare in the Adirondack Highlands, as evidenced by the large proportion of non-charnockitic hornblende granite.

McLelland et al., (1988) have demonstrated the existence of metamorphic orthopyroxene replacing biotite in felsic rocks in several widely-scattered localities in the central Adirondacks. These localities show dark charnockitic gneiss, with orthopyroxene grown across foliation, in zones within a meter or two of the contacts of marble units. The darkened rocks contain high-pressure CO_2 inclusions in quartz (density ~ 1.02 gm/cm^3); this type of fluid inclusion is rare in Adirondack rocks. The very local distribution of CO_2-induced charnockite formation in the Adirondacks, despite the large amount of marble in the supracrustal assemblage, casts doubt on the hypothesis that crustal stratigraphic limestone can be an important source of CO_2 for high-grade regional metamorphism in the Adirondacks, as advocated by Glassley (1983) for the Norder Stromfjord area of Greenland.

A very diffuse isograd for the appearance of garnet in felsic rocks in the Adirondack Highlands has been presented by several authors, including deWaard(1965) and Buddington (1963). The latter version is shown in Figure 8. Much of the garnet occurs as very fine granules at grain boundaries of pyroxene and plagioclase in quartz syenites and anorthosites. The incipient nature of the garnet-forming reaction indicates very limited diffusion, in general accord with the dryness of the terrain and lack of evidence for pervasive volatile fluxes.

The Limpopo Belt - Retrogressive orthopyroxene isograd

The Limpopo Belt of southern Africa (Fig.9) furnishes one of the most intriguing high-grade terrains. The region consists of three provinces (Van Reenen et al., 1988). The Southern Marginal Zone comprises the northern edge of the Archaean Kaapvaal Craton. In this zone, the cratonal granitoid-greenstone association experiences a metamorphic gradient from greenschist facies in the south to granulite facies, including orthopyroxene in basic and acid rocks in the northernmost Kaapvaal Craton. Individual volcanic-sedimentary basins ("greenstone belts") can be traced into the granulite facies area, where they become greatly segmented and attenuated. The northernmost edge of the Kaapvaal

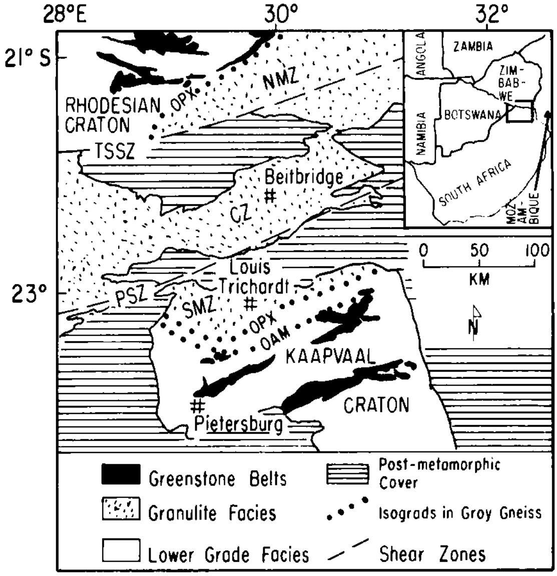

Figure 9. The Limpopo high-grade belt of southern Africa, from Van Reenen et al., 1988, Symbols:NMZ = Northern Marginal Zone(Rhodesian Craton); SMZ = Southern Marginal Zone (Kaapvaal Craton); CZ = Central Zone (dominantly granulite facies supracrustals); TSSZ = Tuli Sabi Shear zone; PSZ = Palala Shear Zone; OPX marks regional orthopyroxene amphibole isograd; OAM marks regional orthoamphibole isograd. The former is interpreted as a retrogressive isograd and the latter as a fossil prograde orthopyroxene isograd.

Craton is marked by the Palala Shear Zone, a profound linear mylonitized zone which records both left-lateral transcurrent and sub-vertical movements of large magnitude during post-Archaean times. The Central Zone of the Limpopo terrain features a variegated metasedimentary sequence, mostly of granulite grade, of the continental platform or shelf type, with abundant pelites, carbonates, quartzites, and a large gabbroic anorthosite complex, the Messina Suite. Quartzofeldspathic gneisses crop out among the metasediments, and may be in part an older basement and in part are intrusive. Still farther north across the Tuli Sabi Shear Zone,the Rhodesian Craton emerges as the Northern Marginal Zone, which has not been mapped in as great detail, but which is probably nearly a mirror image of the Southern Marginal Zone. Isograds of the appearance of orthopyroxene and ferromagnesian amphibole in gray gneiss have been mapped in the Southern Marginal Zone by Van Reenen et al., (1988). They interpreted the orthopyroxene-orthoamphibole isograd as a retrogressive feature,

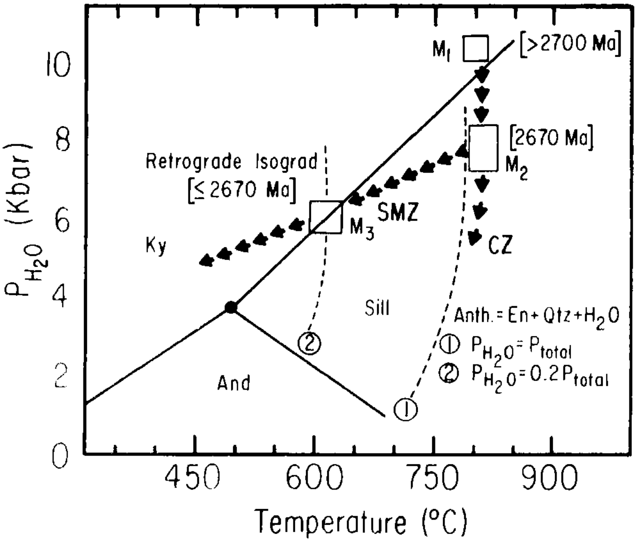

Figure 10. P-T uplift paths from peak conditions in late Archaean metamorphism of the Limpopo Belt, after Van Reenen et al. (1987). Paths are constrained by geothermometry and geobarometry of discrete metamorphic assemblages labelled "M". M_3 denotes the retrogressive orthopyroxene to orthoamphibole event in the Southern Marginal Zone (SMZ). The P-T path of the Central Zone (CZ) is more nearly isothermal, suggesting faster uplift. Age relations of M_1, M_2 and M_3 given in millions of years (Ma). Abbreviations: Anth = anthophyllite; En = enstatite; Qtz = Quartz; Ky = kyanite; Sill = sillimanite; And = andalusite.

marking arrested replacement of orthopyroxene by magnesian amphibole (anthophyllite and gedrite) based on textural evidence. The retrogressive reaction is similar to D). An analogous retrogressive reaction affects cordierite of metapelites of the Southern Marginal Zone, in which the reaction:

G) cordierite + H_2O = orthoamphibole + kyanite + quartz

is inferred from incipient alteration along cleavage cracks and grain boundaries of cordierite.

Magnesian amphibole-orthopyroxene relations in P-T-H_2O activity space may be modeled from experimental work on anthophyllite, following Van Reenen (1986). Figure 10 shows a continous P-T path of metamorphism in the Southern Marginal zone which could have converted early-formed (M1) orthopyroxene to magnesian amphibole during the uplift cycle, starting in the field of kyanite, and traversing the sillimanite field over a period of at least 30 Ma. Cordierite-bearing coronas around garnet were formed at reduced pressure during the nearly isothermal uplift (M2). Secondary kyanite in the retrogressive assemblage after cordierite constrains the P-T path in cooling from the granulite facies to a relatively high pressure trend. If the process of reaction G) at M3 is attributed to cooling from late Archaean granulite facies metamorphism, the H_2O activity (approximately the molar fraction of H_2O in a fluid phase) must have been approximately 0.2, based on calculations of anthophyllite stability.

An interpretation of the retrograde magnesian amphibole isograd in gray gneisses in the Southern Marginal Zone was offered by Van Reenen et al., (1988). The metamorphic gradient on the Southern Marginal Zone cratonal border presumably represents, for the most part, an arrested pattern of isothermal surfaces and H_2O activity contours that were ascending in the crust during the prograde cycle. The orthoamphibole isograd thus represents the farthest penetration of the appearance of orthopyroxene upwards and into the cratonal interior when metamorphism reached its greatest extent. As the orthopyroxene isogradic surface retreated downward in the crust during the cooling cycle, it left a wake of orthoamphibole, as diagrammed in Figure 4. The orthoamphibole may be to some extent metastable, in that the fluid activity may have been very local, affecting isolated orthopyroxene crystals without producing a general remobilization of the entire rock.

The retrogressive career of the Limpopo Central Zone is of great interest. Geothermometry and geobarometry of cordierite, orthopyroxene and plagioclase coronas around garnet (Harris and Holland, 1984) and of sapphirine and kornerupine after gedrite (Windley et al., 1984) indicate rapid ascent from deep-seated conditions. The contrasting P-T trajectories of the Central Zone and the Southern Marginal Zone are explicable in terms of a symmetrical compressional orogen, as a platform basin was caught between massive cratonal blocks, with rapid bouyant uplift in the center and slower, more oblique ascent on the margins.

SUMMARY

The common factor in the several modes of regional orthopyroxene production which have been discussed here is dryness. Reduced water activity could have been effected by initial dryness, absorption of H_2O into anatectic melts, and purging with carbonic fluids. Reduced fluid pressure in open channels is a less probable mechanism. There are likely to be characteristic differences in the granulite facies terrains produced by each of the desiccation mechanisms. Initial dryness may result in an indefinite orthopyroxene isograd: the distribution of original igneous pyroxene may survive through high-grade metamorphism, with occurrences in characteristic sites such as plutonic aureoles. The rarity of dense CO_2 inclusions, the preserved low oxidation states and the lack of LILE depletion are also consonant with vapor-deficient metamorphism in the Adirondacks. Absorption of H_2O into partial melts leaving orthopyroxene restites might result in sporadic occurrence of orthopyroxene in neosome patches, as in Namaqualand, rather than monotonous pyroxene gneisses, unless wholesale evacuation of large amounts of melted country rock was achieved. It is not likely that most granulite terrains are the basified residues of massive outmelting. Pervasive upwards streaming of low-H_2O volatiles seems to be the only mechanism capable of producing the charnockitic massif terrains. An arrested wave or front of such fluids would account for a discrete regional orthopyroxene isograd in acid gneisses.

Retrogressive alteration of orthopyroxene to ferromagnesian amphibole can result in a fairly discrete isograd, as in the Limpopo Belt. This could be accomplished in the waning stages of metamorphism by a decrease of temperature and/or an increase of H_2O activity. The latter circumstance could arise in several ways, including simple cooling at constant pressure and pore-fluid composition, late influx of H_2O exsolved from freezing anatectic melts, or secular change in the character of underthrusted volatiles.

It is quite possible that more than one of the above drying mechanisms could have operated jointly. Many interesting suggestions have been presented whereby CO_2-rich fluids could have operated jointly with magmas with mutual enhancement of their effects. CO_2-rich fluids moving along deformation surfaces could have triggered partial melting in the Namaqualand terrain, with further decrease of H_2O activity as the amount of melt increased (Waters, 1988). A CO_2-rich pore fluid would seem to have been necessary in that region to produce a low-H_2O bridge between acid melt patches and dehydrating amphibolites. Acid melts could have served as vectors of CO_2 transport through the crust, with absorption of H_2O and release of CO_2 as the melts depressurized (Frost and Frost, 1987). Underplating of the crust by basic magmas (Schreurs and Westra, 1986) could have been a source of heat and CO_2-rich solutions, and mid-crustal injection of tonalitic magmas could have performed the same functions (Wells, 1979). The carbonic fluid itself could have been a potent mechanism of heat transfer which could have produced anatectic melting (Harris et al., 1982). The exact ways in which fluids and melts could have conspired to create granulite facies terrains, including the features of LILE depletion and metasomatic charnockite formation, remain as major problems of granulite facies metamorphism.

ACKNOWLEDGEMENTS

The author benefited from discussions and communications with J.M. ferry, C.R.L.Friend, B.R.Frost, W.E. Glassley, J.A. Grant, E.C.Hansen, J.M. McLelland, M.Raith, J.W. Valley, D.D.Van Reenen and D.J. Waters. The author's research is supported by a U.S. National Science Foundation grant, number EAR-8411192. This paper is largely an outgrowth of the author's experience in southern India, which was financed by U.S. National Science Foundation grants EAR-8219248 and INT-8219140.

REFERENCES

Ashwal, L.D. and Wooden, J.L., 1983. Sr and Nd Isotope geochronogy, geologic history and origin of the Adirondack Anorthosite. Geochim. Cosmochim. Acta, 47: 1875-1886.
Austrheim, H. and Robins, B., 1981. Reactions involving hydration of orthopyroxene in anorthosite gabbro. Lithos, 14: 275-282.
Berg, J.H. 1977. Regional geobarometry in the contact aureoles of the anorthositic Nain Complex, Labrador. J. Petrol., 18: 399-430.
Bhattacharya, A. and Sen, S.K., 1986. Granulite metamorphism, fluid buffering, and dehydration melting in the Madras charnockites and metapelites. J. Petrol., 27: 1119-1141.
Bohlen, S.R. and Essene, E.J., 1977. Feldspar and oxide thermometry of granulites in the Adirondack Highland. Contr. Min. Pet., 62: 153-169.
Bohlen, S.R. and Essene, E.J., 1978. Igneous pyroxenes from metamorphosed anorthosite massifs. Contr. Min. Pet., 65: 433-442.
Bohlen, S.R., Valley, J.W. and Essene, E.J., 1985. Metamorphism in the Adirondacks. 1. Petrology, Pressure and Temperature. J. Petrol., 26: 971-992.
Buddington, A.F., 1963. Isograds and the role of H_2O in metamorphic facies of orthogneisses of the northwest Adirondack area, New York. Geol. Soc. Amer. Bull., 74: 155-1182.
Choudhuri, A. and Winkler, H.G.F., 1967. Anthophyllit und Hornblende in einegen Metamorphosen Reaktionen. Contr. Min. Pet., 14: 293-315.
Collerson, K.D. and Bridgwater, D., 1979. Metamorphic development of early Archaean tonalitic and trondhjemitic gneisses: Saglek area, Labrador. In: F., Barker, (Editor), Trondhjemites, Dacites and Related rocks. Amsterdam, Elsevier, pp.205-273.
Condie, K.C., Allen, P. and Narayana, B.L., 1982. Geochemistry of the Archaean low-to high-grade transition zone, southern India. Contr. Min. Pet., 81: 157-167.
Crawford, M.L. and Hollister, L.S., 1986. Metamorphic fluids: the evidence from fluid inclusions. In: J.M. Walther, and B.J. Wood, (Editors), Advances in Physical Geochemistry, New York, Springer-Verlag.
Devaraju, T.C. and Sadashivaiah, M.S., 1969. The charnockites of Satnur-Halaguru area, Mysore State. Ind. Mineral., 10: 67-88.
deWaard, D., 1965. The occurrence of garnet in the granulite-facies terrane of Adirondack Highlands. J. Petrol., 6: 165-191.
Drury, S.A., 1980. Lewisian pyroxene gneisses from Barra and the geochemistry of Archaean lower crust. Scott. J. Geol., 16: 199-207.
Ellis, D.J., 1980. Osumilite-sapphirine-quartz granulites from Enderby Land, Antarctica: P-T conditions of metamorphism, implications for garnet-cordierite equilibria and evolution of the deep crust. Contr. Min. Pet., 74: 201-210.
Ferry, J.M., 1984. A biotite isograd in south-central Maine, USA: Mineral Reactions, fluid transfer, and heat transfer. J. Petrol., 25: 871-893.

Field, D., Drury, S.A. and Cooper, D.C., 1980. Rare-earth and LIL element fractionation in high-grade charnockitic gneisses, south Norway. Lithos, 13: 182-289.

Fountain, D.M. and Salisbury, M.H., 1981. Exposed cross-sections through the continental crust: implicaions for crustal structure, petrology and evolution. Earth Plan. Sci. Lett., 56: 263-277.

Friend, C.R.L., 1981. The timing of charnockite and granite formation in relation to influx of CO_2 at Kabbaldurga, Karnataka, South India. Nature, 294: 550-552.

Froese, E., 1978. The graphical representation of mineral assemblages in biotite-bearing granulites. Curr. Res., part A., Geol. Surv. Can., Pap. 78-1A: 323-325.

Frost, B.R. and Frost, C.D., 1987. CO_2, melts and granulite metamorphism. Nature 327, 503-506.

Fyfe, W.S., 1973. The generation of batholiths. Tectonophysics, 17: 273-283.

Gee, R.D., 1979. Structure and tectonic style of the Western Australian Shield. Tectonophysics, 58: 327-369.

Glassley, W.E., 1983. Deep crustal carbonates as CO_2 fluid sources: evidence from metasomatic reaction zones. Contr. Min. Pet., 84: 15-24.

Grant, A.B., 1969. Chemical and physical controls for base metal deposition in the Cascade Range of Washington. Wash. Div. of Mines and Geol. Bull., 58: 1-107.

Hansen, E.C., Janardhan, A.S., Newton, R.C., Prame, W.K.B.N. and Ravindra Kumar, G.R., 1987. Arrested charnockite formation in southern India and Sri Lanka. Contr. Min. Pet., 96: 225-244.

Hansen, E.C., Newton, R.C. and Janardhan, A.S., 1984. Fluid inclusions in rocks from the amphibolite-facies gneiss to charnockite progression in southern Karnataka, India: Direct evidence concerning the fluids of granulite metamorphism. J. Meta. Geol., 2: 249-264.

Harris, N.B.W. and Holland, T.J.B., 1984. The significance of cordierite-hypersthene assemblages from the Beitbridge region of the Central Limpopo Belt; evidence for rapid decompression in the Archaean? Amer. Mineral., 69: 1036-1049.

Harris, N.B.W., Holt, R.W. and Drury, S.A., 1982. Geobarometry, geothermometry, and late Archaean geotherms from the granulite facies terrain of South India. J. Geol., 90: 509-528.

Haslam, H.W., 1986. Pyroxenes and coexisting minerals in the Cheviot granite J. Petrol., 50: 671-674.

Heier, K.S., 1973. Geochemistry of granulite facies rocks and problems of their origin. Phil Trans. R. Soc. Lond., A273: 429-442.

Holland, J.G. and Lambert, R.St.J., 1975. The chemistry and origin of the Lewisian Gneisses of the Scottish Mainland: the Scourie and Inver Assemblages and sub-crustal accretion Precamb. Res., 2: 161-188.

Holt, R.W. and Wightman, R.T., 1983. A crustal transition zone in the Archaean granulite facies terrain of South India. J. Geol. Soc. Lond., 140: 651-656.

Hormann, P.K., Raith, M., Raase, P. Ackermand, D. and Seifert, F. 1980. The granulite complex of Finnish Lapland: Petrology and metamorphic conditions in the Ivalojoki-Inarijarvi area. Geol. Surv. Finland, Bull., 308: 1-95.

Hubregtse, J.J.M.W., 1980. The Archaean Pikwitonei granulite domian and its position at the margin of the northwestern Superior Province (Central Manitoba). Manitoba Geol. Surv., Pap., GP80-3: 1-16.

Janardhan, A.S., Newton, R.C. and Hansen, E.C., 1982. The transformation of amphibolite facies gneiss to charnockite in southern Karnataka and northern Tamil Nadu, India. Contr. Min Pet., 79: 130-149.

Janardhan, A.S., Newton, R.C. and Smith, J.V., 1979. Ancient crustal metamorphism at low P(H_2O): charnockite formation at Kabbaldurga, south India. Nature, 278: 511-514.

Kars, H., Jansen, J.B.H., Tobi, A.C. and Poorter, R.P.E., 1980. The metapelitic rocks of the polymetamorphic Precambrian of Rogaland, SW Norway. Contr. Min. Pet., 74: 235-244.

Lamb, R.C., Smalley, P.C. and Field, D., 1986. P-T conditions for the Arendal granulites, southern Norway: implications for the roles of P, T and CO_2 in deep crustal LILE - depletion. J. Meta Geol., 4: 143-160.

Lamb, W. and Valley, J.W., 1984. Metamorphism of reduced granulites in low -CO_2 vapour-free environment. Nature, 312: 56-58.

Lambert, I.B. and Wyllie, P.J., 1972. Melting of gabbro (quartz eclogite) with excess of water to 35 kilobars, with geological applications. J. Geol., 80: 693-708.

Lowman, P.D., Jr., 1984. Formation of the earliest continental crust: inferences from the Scourian Complex of northwest Scotland and geophysical models of the lower continental crust. Precamb. Res., 24: 199-215.

Madsen, J.K., 1977. Fluid inclusions in the Kleivan granite, South Norway, 1: Microthermometry. Amer., J. Sci., 277: 673-696.

Mahabaleswar, B. and Naganna, C., 1981. Geothermometry of Karnataka charnockites. Bull. Mineral, 104: 848-855.

Mahabaleswar, B., Vasant Kumar, I.R. and Friend, C.R.L., 1986. Geochemistry of the Archaean gneiss complex and associated rocks of the Kanakapura area, Karnataka, South India. J. Geol. Soc. India, 27: 282-297.

McLelland, J.M.,Hunt, W.M. and Hansen, E.C., 1988. The relationship between metamorphic charnockite and marble near Speculator, central Adirondack Mountains, New York. J. Geol., (in press).

McLelland, J.M. and Husain, J., 1986. Nature and timing of anatexis in the eastern and southern Adirondack Highlands. J. Geol., 94: 17-26.

McLelland, J.M. and Isachsen, Y.M., 1986. Synthesis of geology of the Adirondack Mountains, New York, and their tectonic setting within the southeastern Grenville Province. Geol. Assoc. Canada Spec. Pap., 31: 75-94.

Nesbitt, H.W., 1980. Genesis of the New Quebec and Adirondack granulites: evidence for their production by partial melting. Contr. Min. Pet., 72: 303-310.

Okeke, P.O., Borley, G.D. and Watson, J., 1983. A geochemical study of Lewisian metasedimentary granulites and gneisses in the Scourie-Laxford area of the north-west Scotland. Min. Mag., 47: 1-10.

Percival, J.A., 1983. High-grade metamorphism in the Chapleau-Foleyet Area, Ontario. Amer. Mineral., 68: 667-686.

Peterson, J.W. and Newton, R.C., 1987. Reversed biotite + quartz melting reactions. EOS, 68: 451.

Phillips, G.N., 1980. Water activity changes across an amphibolite-granulite facies transition, Broken Hill, Australia. Contr. Min. Pet., 75: 377-386.

Phillips, G.N. and Waal, V.J., 1981. Evaluation of prograde regional metamorphic conditions: their implications for the heat source and water activity during metamorphism in the Willyama Complex, Broken Hill, Australia. Bull. Mineral., 104: 801-810

Pichamuthu, C.S., 1960. Charnockite in the making. Nature, 188: 135-136.

Powell, R., 1983. Processes in granulite-facies metamorphism. In: M.P. Atherton, and C.C. Gribble, (Editors). Migmatites, Melting and Metamorphism. Nantwich (UK). Shiva, pp.127-139.

Radhakrishna, B.P., 1956. The Closepet Granite of Mysore State, India. Bangalore: Mysore Geol. Assoc. Spec. Publ., 110pp.

Raith, M., Raase, P., Ackermand, D. and Lal, R.K., 1982. Regional geothermobarometry in the granulite facies terrain of South India. Trans. Roy. Soc. Edinburgh, Earth Sci., 73: 221-244.

Ravindra Kumar, G.R., Srikantappa, C. and Hansen, E.C., 1985. Charnockite formation at Ponmudi in South India. Nature, 313: 207-209.

Sack, R.O., 1980. Adirondack mafic granulites and a model lower crust. Geol. Soc. Amer. Bull., 91: 89-93.

Sandiford, M. and Powell, R., 1986. Deep crustal metamorphism during continental extension: modern and ancient examples. Earth Plan. Sci. Lett., 79: 151-158.

Schreurs, J., 1984. The amphibolite-granulite facies transition in West-Uusimaa, S.W. Finland. A fluid inclusion study. J. Meta. Geol., 2: 327-342.

Schreurs,J. and Westra, L., 1986. Cordierite-orthopyroxene rocks: the granulite facies equivalents of the Orijarvi cordierite-anthophyllite rocks in West Uusimaa, southwest Finland. Lithos., 18: 215-228.

Seifert, F.A. and Schumacher, J.C., 1986. Cordierite-spinel quartz assemblages: a potential geobarometer. Bull. Geol. Soc. Finland, 58: 95-108.

Sheraton, J.W., Skinner, A.C. and Tarney, J., 1973. The geochemistry of the Scourian gneisses of the Assynt district. In: R.G. Park, and J. Tarney, (Editors). The Early Precambrian rocks of Scotland and Related Rocks of Greenland. Univ. Keele, pp.13-30.

Smalley, P.C., Field, D., Lamb, R.C. and Clough, P.W.L., 1983. Rare earth, Th-Hf-Ta and large-ion lithophile element variation in metabasalts from the Proterozoic amphibolite-granulite transition zone at Arendal, South Norway. Earth Plan. Sci. Lett., 63: 446-458.

Srikantappa, C., Raith, M., Ashamanjari, K.G. and Ackermand, D., 1986. Pyroxenites and gabbroic rocks from the Nilgiri granulite terrane, southern India. Ind. Mineral., 27: 62-83.

Srikantappa, C., Raith, M. and Spiering, B., 1985. Progressive charnockitization of a leptynite-khondalite suite in southern Kerala, India evidence for formation of charnockites through decrease in fluid pressure? J.Geol. Soc. India, 26: 849-872.

Stahle, H.J., Raith, M., Hoernes, S. and Delfs, A., 1987. Element mobility during incipient granulite formation at Kabbaldurga, southern India. J. Petrol., 28: 803-834.

Stoddard, E.F., 1980. Metamorphic conditions at the northern end of the northwest Adirondack Lowlands. Geol. Soc. Amer. Bull., 91: 97-100.

Subramaniam, A.P., 1967. Charnockites and granulites of southern India: a review. Dan. Geol. Foren., 17: 473-493.

Suryanarayana, K.V., 1960. The Closepet granite and associated rocks. Ind. Mineral., 1: 86-100.

Thompson, J.B., 1955. The thermodynamic basis for the mineral facies concept. Amer. J. Sci., 253: 65-103.

Touret, J., 1971. Le facies granulite en Norwege Meridionale. Lithos, 4: 239-249;423-436.

Valley, J.W., McLelland, J., Essene, E.J. and Lamb, W., 1983. Metamorphic fluids in the deep crust: evidence from the Adirondacks. Nature, 301: 226-228.

Valley, J.W. and O'Neil, J.R., 1984. Fluid heterogeneity during granulite facies metamorphism in the Adirondacks: stable isotope evidence. Contr. Min. Pet., 85: 158-173.

Van Reenen, D.D., 1986. Hydration of cordierite and hypersthene and a description of the retrograde orthoamphibole isograd in the Limpopo belt, South Africa. Amer. Mineral., 71: 900-915.

Van Reenen, D.D., Roering, C., Smit, C.A., Barton, J.M. and Van Schalwyk, J.F., 1988. The high grade margin of the northern Kaapvaal Craton, South Africa. J. Geol., (in press).

Warren, R.G., 1983. Metamorphic and tectonic evolution of granulites, Arunta Block, central Australia. Nature, 305: 300-303.

Waters, D.J., 1988. Partial melting and the formation of granulite facies assemblages in Namaqualand, South Africa. J. Meta. Geol., (in press)

Waters, D.J. and Whales, C.J., 1984. Dehydration melting and the granulite transition in metapelites from southern Namaqualand, S. Africa. Contr. Min. Pet., 88: 269-275.

Weaver, B.L. and Tarney, J., 1983. Elemental depletion in Archaean granulite-facies rocks. In: M.P. Atherton, and C.C. Gribble, (Editors). Migmatites, Melting and Metamorphism. Nantwich (UK): Shiva, pp.250-263.

Wells, P.R.A., 1979. Chemical and thermal evolution of Archaean sialic crust, southern West Greenland. J. Petrol., 20: 187-226.

Wickham, S.M., 1987. The segregation and emplacement of granitic magmas. J. Geol. Soc. London, 144: 281-297.

Wiener, R.W., McLelland, J.M., Isachsen, Y.W. and Hall, L.M., 1984. Stratigraphy and structural geology of the Adirondack Mountains, New York: Review and synthesis. In: M.J. Bartholomew, (Editor). The Grenville Event in the Appalachians and Related Topics. Geol. Soc. Am. Spec., Pap., 194: 55pp.

Windley, B.F., Ackermand, D. and Herd, R.K., 1984. Sapphirine/kornerupine-bearing rocks and crustal uplift history of the Limpopo Belt, southern Africa. Contr. Min. Pet., 86: 342-358.

Wynne-Edwards, H.R., 1972. The Grenville Province. Geol. Assoc. Canada Spec. Pap., 11: 263-324.

This Page Intentionally Left Blank

A THERMAL MODEL FOR THE EVOLUTION OF THE PRECAMBRIAN SINGHBHUM IRON ORE BASIN OF THE INDIAN SHIELD

S.BHATTACHARJI AND A.K.SAHA

ABSTRACT

The Archaean iron ore basin of Singhbhum-Keonjhar in eastern India evolved between 3.8 and 2.9 Ga. The basin is characterized by approximately 7.5 km of volcanogenic and meta-sedimentary materials, mafic and felsic lavas, tuffs and mafic-ultramafic intrusions. It also shows poly-phase deformation with superposed folding and post depositional granite intrusions. The analysis of a thermal model in basin subsidence which incorporates the effects of increased crustal density by igneous intrusions and emplacements and elastic flexuring during gravitational loading is presented. Punctuated thermal pulses from the mantle or crust-mantle boundary can account for the 5 to 7.8 km subsidence of the Singhbhum Basin crust. An estimation of radial stress at the base of the Singhbhum iron ore basin is presented to show its significance in the development of fractures and fault or lineament openings which can provide passages for the migration of mafic and felsic lavas and tuffs inside the basin. The importance of thermal events in the evolution of Archaean iron ore basins on the eastern Indian shield is documented.

INTRODUCTION

The evolution of Archaean sedimentary basins is an unresolved problem of geodynamics. Repeated thermal and tectonic events, poly-phase deformation with intense flexuring and faulting, and diagenesis of sediments and their metamorphism are common features of many Archaean basins. These and post-depositional deformation and igenous activities often make it difficult to establish the controlling factors in basin subsidence and its evolutionary processes.

GEOLOGIC SETTING

The Archean iron ore basin of Western Singhbhum - Keonjhar in eastern India, modelling of the evolution of which has been attempted, forms a part of the Singhbhum-Orissa iron ore craton. The evolution of this craton started over 3.8 Ga ago, the

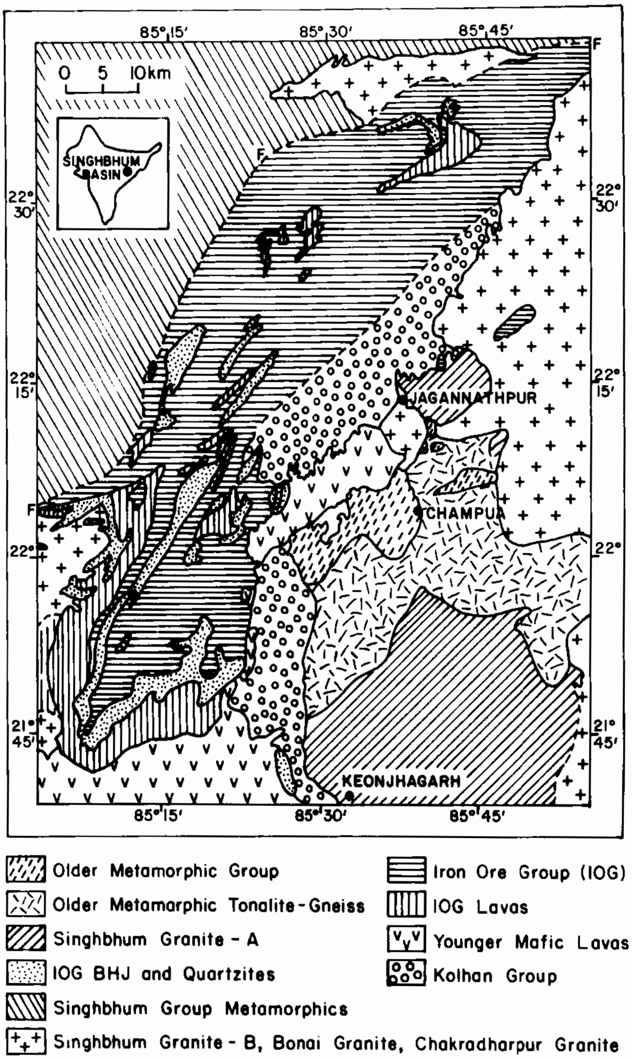

Figure 1. Generalized geological map of a part of the Singhbhum-Orissa iron ore craton showing the geological framework of the Archaean iron ore basin.

major part of its evolution, however, was completed by 2.9 Ga (Sarkar and Saha, 1977, 1983; Saha and Ray, 1984; Saha, et al., in press). This NNE-SSW iron ore basin is 140 km long and is 50 km wide at the widest part (Fig. 1). The basin is occupied by the Iron Ore Group of rocks, overlain in places by the younger sub-horizontal Kolhan Group of sediments and a group of younger mafic lavas (Jagannathpur lavas). The generalized geological succession of the Iron Ore Group (IOG) is as follows:

5. Mafic-ultramafic intrusions
4. Tuffaceous shale, slate and phyllite with local manganiferous shale, dolomite and mafic lava.
3. Banded haematite jasper (BHJ) with iron ore, chert and quartzite.
2. Phyllitic shale with interbedded ferruginous chert, acid intermediate tuffs.
1. Local mafic lavas.

The rocks of the basin are folded into a north-plunging synclinorium with an overturned western limb, the plunge being of the order of 5° - 10°. Superposed on these folds are a set of east-west trending folds, open in the south and southerly overturned in the north (Sarkar and Saha, 1962). Although the thicknesses of the individual members are highly variable, the total stratigraphic thickness of the Iron Ore Group in the basin is estimated to be about 7.5 km.

The proportion of mafic lavas varies from 3 to 10 percent from the southern to the northern ends of the basin. Shales, slates, phyllites and tuffs constitute 70 to 75 percent, while BHJ and quartzites vary approximately between 5 and 20 percent from the northern to southern ends of the basin. Alteration of the BHJ close to the ground surface has given rise to iron-ore deposits which do not generally extend over 50 m below the surface.

The basement of the basin is made up of the Older Metamorphic Group (OMG): ortho- and para-amphibolites, metapelites and quartzites, which are intruded by the OMG tonalite-gneiss (ca.3.8 Ga)and the Singhbhum Granite (SBG-A, ca.3.3Ga) (Saha et al., in press). The eastern part of the basin is truncated in places by a later phase of the Singhbhum Granite (Ca. 3.1Ga). Thus the IOG rocks of the basin were deposited and folded in between 3.3 and 3.1 Ga. Recent gravity studies (Verma, 1985 and Fig.2) show that at present the basin is shallower at the southern end and has a maximum depth of 7.60 km in the central part.

On unfolding the major folds in the basin and also considering the subsequent erosion of the rocks of the basin and parts that have been covered under the Copper Belt thrust zone in the north

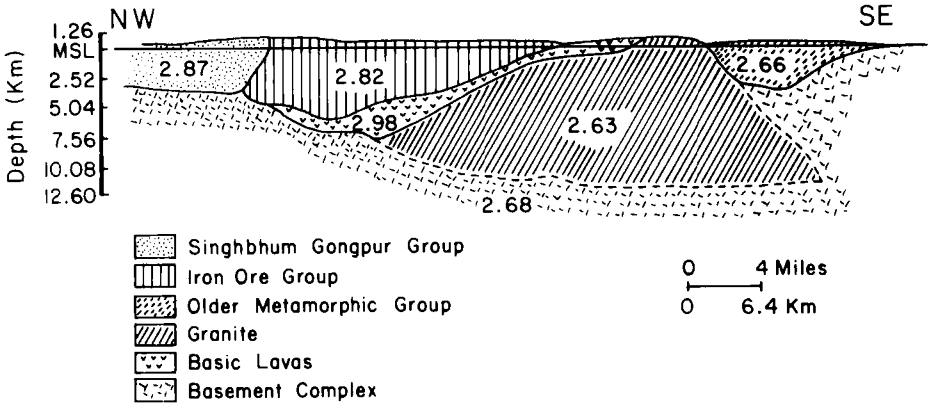

Figure 2. Geological structure of the Singhbhum Iron Ore Basin and adjacent region, density, and the depth of the basin from gravity studies. (modified after Verma, 1985).

(Sarkar and Saha, 1983), the original length of the basin is estimated at 150-160 km and the original width at about 80 km. The maximum depth of the basin may have been of the order of 10 km.

The above-mentioned characteristics of the Iron Ore Basin indicate that several factors, individually or collectively, may have been important in basin subsidence. Among them, important controlling factors may be: (1)thermal heating and crustal subsidence during cooling of thermal pulses (igneous intrusions); (2) elastic flexuring during isostatic subsidence of the basin crust by loading of sedimentary, metamorphic and igneous formations and (3) crustal flexuring by tectonic deformation.

The geological evidence of the occurrence of acid and mafic volcanics with sedimentary deposition (and ultramfic intrusions at the northern part of the basin) signal the importance of thermal pulses and crustal loading in basin development. Based on these evidences, we examine a thermal model (Haxby et al. 1976) in basin subsidence which incorporated the effects of increased density of the crust due to igneous intrusion(s) as well as metamorphism, and elastic flexuring during loading.

THERMAL MODEL OF BASIN EVOLUTION

The time/space evolution of a basin can be associated with the thermal decay of a heat pulse originated at some depth in the upper mantle. The basic assumption in the thermal model is that a thermal pulse of suitable strength and dimension (i.e., partial melt) intrudes into the crust from the upper mantle and transforms into denser mass during cooling. This produces an axisymmetric load on the crust which, in turn, produces elastic flexuring of the crust and initiates basin formation.

Theoretical background

The maximum displacement (W_o) at the center of a disc-shaped load on an elastic crust can be expressed by:

$$Wo= \frac{Po}{(\rho m-\rho s)g}\left[1+\frac{a}{\alpha}\ker\frac{a}{\alpha}\right] \quad . \qquad ......(1)$$

Here ρo, $_m$, $_s$, g, a and α are the load, the density of the mantle rocks, the density of sediments, acceleration due to gravity, length (radius) of the disc load and a flexural parameter (Brotchie and Silvester, 1969; Haxby et al., 1976).

The flexural parameter (α) is expressed by:

$$\alpha = \left[\frac{D}{(\rho m-\rho s)g}\right]^{1/4} \quad . \qquad ......(2)$$

Here the flexural rigidity (D) of the crust is given by:

$$D= \frac{Eh^3}{\left[12(1-\nu^2)\right]} \quad , \qquad ......(3)$$

where E, h and ν are modulus of elasticity, the thickness of the elastic zone of the lithosphere, and Poisson's ratio respectively. The values for various constants appearing in (1), (2) and (3) are given in Table 1. Using these constants, one can determine the flexural rigidity (D) and the flexural parameter (α) of the elastic zone of the Archaean lithosphere of the Indian Shield under the Singhbhum iron ore basin.

APPLICATION OF THE THERMAL MODEL TO THE SINGHBHUM IRON ORE BASIN

Based on the geological evidence cited earlier, we assume that thermal (mantle) perturbation and thermal pulses in the Singhbhum crust are primarily responsible for the initiation of the iron ore basin.

Elastic thickness of the Singhbhum crust

For the estimation of the Singhbhum Basin's crustal subsidence during thermal cooling and loading, we first estimate the thickness (h) of the elastic zone of the Singhbhum crust by using a non-linear law given by Kirby (1977) and discussed by Singh (1981) and Bhattacharji and Singh (1984). Using available heat-flow data for the northern Indian Shield in the Singhbhum region (Rao et al, 1976) and, using shear-flow profiles from olivine rheology (Singh, 1981; Bhattacharji and Singh, 1984), we obtain the estimated thickness of Singhbhum basement crust to be 31 km. This estimated thickness is consistent with deep seismic sounding data available for the Indian Shield, and the estimation of the thickness of the Archaean crust of Singhbhum, based on an Archaean geothermal gradient by Saha et al., (1984).

TABLE 1.
Flexural parameters

Constants	Values
E (dyne cm^{-2})	6.10^{11}
	0.28 or 0.25 (for brittle crust)
m (g cm^{-3})	3.30
s (g cm^{-3})	2.50 (sediments)
s (g cm^{-3})	2.82 (Iron Ore Group rocks)
	2.98 (mafic lavas)
g (cm 8^{-2})	10^3

Estimation of crustal subsidence

Using the estimated thickness of the Singhbhum basement crust (h) and constants E and (Table 1), we obtain the flexural rigidity (D) and flexural parameter (α) from equations (3) and (2), respectively. We get:

D = 1.6 X 10 dyne cm, and

α = 75 km (for ρ_s = 2.75 g cm^{-3})

However, when we take the average density of Iron Ore Group rocks ^{s} = 2.90 g cm^{-3} and mafic lavas, ^{s} = 3.0g cm^{-3}, we get:

α = 80 km

Using various estimates of the length (radius) of the sedimentary and igneous load (a) inferred from the geometry of the Iron Ore Basin, we obtain values of a/α. We have taken two estimates (maximum and minimum) of the approximate length by unfolding the major folds in the basin.

a = 150 km, and

a = 80 km.

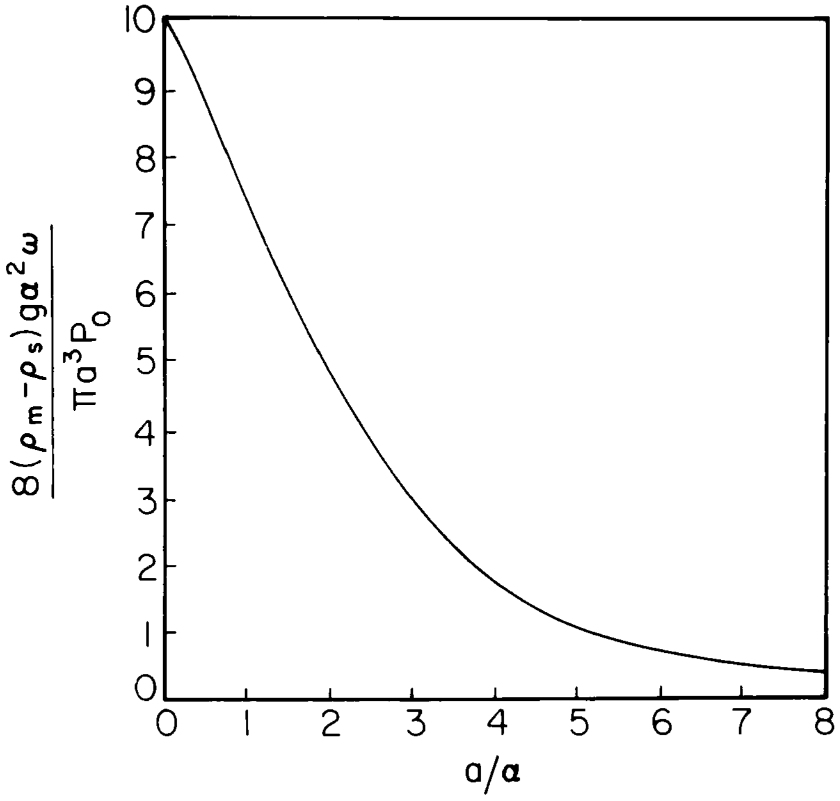

Figure 3. Maximum subsidence (W_0) of an elastic crust (lithosphere) vs. a/α for a disc load. (after Bhattacharji and Singh, 1984).

Thus we obtain

$a/\alpha = 2$ (for $\alpha = 75$km), and
$a/\alpha = 1$ (for $\alpha = 80$km).

These values of a/α , and Figure 3 would yield a relationship between maximum displacement (subsidence, W_o) and the load (Po) due to the Iron Ore Group of rocks in the basin.

Using Figure 3 and for $a/\alpha = 2$, and $a/\alpha = 1$, we get the total subsidence of the Singhbhum Basin due to the elastic flexuring of the Singhbhum crust,

$W_o = 5.0$ km and
$W_o = 7.8$ km, respectively.

These estimates of maximum subsidence are consistent with the stratigraphical thickness of rocks and the maximum depth at the central region along a NW-SE profile of the basin (Verma, 1985; Fig.2).

ESTIMATION OF THE DEPTH (d) AND STRENGTH (T_1, °C) OF THE HEAT SOURCE CAUSING BASIN SUBSIDENCE

Case (1) For $a/\alpha = 2$, we get:

$$Po = 6.37 \times 10^3 Wo.$$

Having obtained Po, we can proceed to relate it to the depth (d, km) and the strength (T_1°C) of the heat source which can produce a basin subsidence of 5 - 7.5 km. The relation of Po and T_1 and d is given by:

$$P_o = \rho m \ \beta g d T_1, \qquad \text{......(4)}$$

where ρm, β , g, d and T_1 are the average density of the upper mantle rocks, coefficient of thermal expansion, depth of thermal pulse (perturbation), and the temperature excess of the heat source. Taking $\beta = 4 \times 10^{-5}/^oC$, and using various constants (Table 1) and estimates of the parameters, we get:

$$d \times T_1 = 4.77 \times 10^3 \ W_o.$$

TABLE 2.

Required thermal strength (T_1) and the vertical height (d) of a thermal pulse for maximum basin subsidence (W_0)=5-10km for the Singhbhum Iron Ore Basin.

A. Iron Ore Group rocks including mafic lavas; basin dimension (a)=150 km

d, km for T_1°C 300°	 500°	 800°	W_0, km
79	48	30	5.0
95	57	36	6.0
110	67	42	7.0
119	71	45	7.5
127	76	48	8.0
143	86	54	9.0
159	95	60	10.0

B. Mafic lavas; basin dimensions (a)=150km

51	31	19	5.0
62	37	23	6.0
72	43	27	7.0
77	46	29	7.5
82	50	31	8.0
93	56	35	9.0
102	62	38	10.0

C. Iron Ore group rocks including mafic lavas; basin dimension (a) = 80km

38	22	14	5.0
46	27	17	6.0
53	31	20	7.0
57	34	21	7.5
60	36	23	8.0
68	40	25	9.0
76	45	28	10.0

For the Iron Ore Basin of depths W_o=5 km and 7.5 km and T_1=800oC, we get:

d = 30 km, and
d = 45 km, respectively.

For $T_1 = 500^oC$, we get

d = 48 km (required for 5 km subsidence), and
d = 72 km (for 7.5 km subsidence).

Table 2A shows estimates of d, and T_1 for depth of subsidence of 5-10 km of the Singhbhum crust by elastic flexuring. A variety of combinations of d and T_1 would yield maximum deflections of 5-7.5 km in the central region of the iron ore basin.

We now estimate the depth of the heat source for the mafic lavas emplaced in the iron ore basin which are capable of producing various crustal subsidence on thermal cooling. For an average density of mafic lavas, ρs = 3.0g cm^{-3} and D = $1.6x10^{30}$ dyne cm of the Singhbhum crust, we get: α =85 km

Thus, for Case (i) for a/α = 1.76, we get:

Po = $4.07 \times 10^2\ W_o$ and
$dxT_1 = 3.10 \times 10^3\ W_o$.

Table 2B shows estimates of d and T_i for various basin depths (W_o). These estimates indicate that in areas of emplacement of higher density mafic lavas in the basin, maximum crustal subsidence of the basin would result from a much reduced depth of the heat source. The heat source causing such basin subsidence is either in the crust or in the crust - mantle region.

Case (ii): for a/α = 1 (i.e, basin radius of 80km) we get:

Po = $3.0x10^2\ W_o$ and
$dxT_1 = 2.27x10^3\ W_o$.

Table 2C gives various estimates of d for W_o = 5 to 10km, and T_1 = 300^oC, 500^oC and 800^oC, respectively.

ESTIMATION OF RADIAL STRESS (σr) AT THE BASE OF THE BASIN

In order to determine whether flexuring of the Singhbhum basement crust during loading could produce fractures at the base of the basin and give rise to the emplacement of magmas and lava flows in the basin, we estimate the radial stress (σr) below the center of the disc load in the basin. Following Lambeck and Nakiboglu (1980), the maximum radial stress

$$(\sigma r \text{ max}) = \frac{3D\ Po(1+\nu)}{h^2(\rho m-\rho s)g\alpha^2} \cdot a/\alpha \text{ kel } \quad a/\alpha. \qquad \text{......(5)}$$

This expression is plotted in Figure 4. For the Singhbhum Iron Ore Basin, for an average thickness of 5 km, and for $a/\alpha = 2$(i.e, 150km length) and Poisson's ratio $\nu = 0.25$ (brittle crust), we get:

$(\sigma r \text{ max}) = 3.07\text{kb}$.

This radial stress is sufficiently high to cause fracturing of the Singhbhum basement crust of granites. During the loading and flexuring of the basement crust, the radial stress (σr) in areas of maximum deflection at the base of the basin is tensile and deviatoric. This deviatoric tensile stress can readily exceed the tensile strength of the basement crust during flexuring and produce extensional fractures. These fractures then provide passages for the migration of mafic lavas and volcanics in the basin. At this higher magnitude of tensile stress, lineaments and deep fractures in the thermally weakened Singhbhum crust can also open up and facilitate migration of mafic and ultramafic materials inside the basin and adjacent areas thereof during its subsidence. This can produce further loading, variable subsidence and tilting of the basin floor.

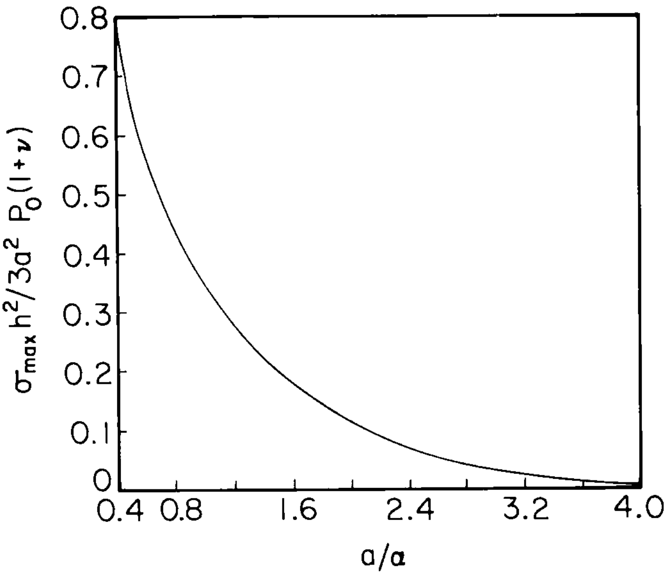

Figure 4. Maximum radial stress (σr max) vs. a/α for disc load. (after Bhattacharji and Singh, 1984).

CONCLUDING REMARKS

This analysis shows that thermal events may have been of paramount importance in the development of the Precambrian Singhbhum Iron Ore Basin. The thermal model used in the analysis can adequately explain the 5.0 to 7.5 km depths of the basin recorded in stratigraphical thickness, and in the thickness estimated from the gravity studies.

The thermal (igneous) sources for basin subsidence appear to be in the crust-mantle boundary or in the upper mantle. In areas of thick mafic lavas, subsidence in the order of 5 km can also result from a crustal heat (magma) source.

Estimated temperature excess(es) of the heat pulses in the order of 300^o - 800^oC provide the requisite (thermal) subsidences of the basin floor. Estimated radial stress of approximately 3.1 kb at the base of the 5 km thick iron ore basin is tensile and deviatoric, especially in areas of maximum flexuring. This magnitude of stress is considerably higher than the tensile strengths of granites and gneisses of the Singhbhum basement crust. Such a high radial stress during the iron ore basin's development can produce extensional fractures at its base. They in turn, provide passages for the migration of the partial melts inside the basin. This tensile radial stress can also open up deep fractures and lineaments of the basement crust of the basin at different stages of basin flexuring. This may produce magma (or lava flows) in the basin, additional basin subsidence and differential tilting of the basin floor. The variable thickness of the Iron Ore Basin may result from them.

REFERENCES

Bhattacharji, S. and Singh, R.N., 1984. Thermo-mechanical structure of the southern part of the Indian Shield and its relevance to Precambrian basin evolution. Tectonophysics, 105: 103-120.

Brotchie, J.F. and Silvester, R., 1969. Crustal flexure. J.Geophys. Res., 74: 5240-5252.

Haxby, W.F., Turcotte, D.L., and Bird, J.M., 1976. Thermal and mechanical evolution of the Michigan Basin. Tectonophysics, 36: 57-75.

Kirby, S.H., 1977. State of stress in the lithosphere: inference from the flow laws of olivine. Pure and Appl. Geophys., 115: 245-258.

Lambeck, K. and Nakiboglu, S.M., 1980. Seamount loading and stress in the ocean lithosphere. J.Geophys. Res., 85: 6403-6418.

Rao, R.U.M., Rao, G.V. and Narain, H., 1976. Radioactive heat generation and heat flow in the Indian region. Earth Planet. Sci. Lett., 30: 57-64.

Saha, A.K. and Ray, S.L. 1984. The structural and geochemical evolution of the Singhbhum Granite batholithic complexes. Tectonophysics, 105: pp.163-176.

Saha, A.K. Ghosh, A., Dasgupta, D., Mukopadhyay, K., and Ray, S.L., 1984. Studies on crustal evolution of the Singhbhum-Orissa Iron-Ore Craton. In: A.K. Saha (Editor), Crustal Evolution and Metallogenesis in selected areas of the Indian Shield. Ind. Soc. Earth Sci., Monograph volume, pp.1-74.

Saha, A.K., Ray, S.L., and Sarkar, S.N., 1987. Early history of the earth: evidence from the Eastern Indian Shield. Mem. Geol. Soc. India, 8: 13-38.

Sarkar, S.N. and Saha, A.K., 1962. A revision of the Precambrian stratigraphy and tectonics of Singhbhum and adjacent areas. Quart. J. Geol. Min. Met. Soc. India, 34: 97-136.

Sarkar, S.N. and Saha, A.K., 1977. The present status of the Precambrian stratigraphy, tectonics and geochronology of Singhbhum-Keonjhar-Mayurbhanj region, Eastern India, Ind. J. Earth Sci., S.Ray volume, pp.37-65.

Sarkar, S.N. and Saha, A.K., 1983. Structure and tectonics of the Singhbhum-Orissa Iron-ore craton, eastern India. In: S.Sinha-Roy (Editor), Recent Researches in Geology, 10, Hindustan Publishing Corporation (India), pp.1-25.

Singh, R.N., 1981. On the state of stress in the northern part of the Indian Shield. In: H.K.Gupta and F.M. Delany (Editors), Zagros, Hindukush, Himalaya Geodynamics Evolution. Am.Geophys. Union. Washington, D.C., and Geol. Soc. Am., Boulder, Colo., pp.307-312.

Verma, R.K. 1985. Analysis of gravity field over Singhbhum and the adjoining areas. In: Verma, R.K. Gravity field, seismicity and tectonics of the Indian Peninsula and the Himalaya, Allied Publishers, New Delhi (India), 91-107.

A NEW LOOK AT THE ARCHAEAN-PROTEROZOIC BOUNDARY SEDIMENTS AND THE TECTONIC SETTING CONSTRAINT

KENT C. CONDIE AND DAVID J. WRONKIEWICZ

ABSTRACT

To identify meaningful geochemical changes in sediments across the Archaean-Proterozoic (A-P) boundary (at 2500 Ma), it is necessary to compare sediments from similar lithologic associa- tions to minimize the effect of tectonic setting. This study evaluates data for pelites from quartzite-pelite (QP) and greenstone (GR) associations. Of the compositional differences believed to occur in GR and QP pelites across the A-P boundary, decreases in Ni and Cr are the only well-documented examples. Higher Cr and Ni in Archaean pelites may be due to 1) intense chemical weathering of komatiite in the sediment source or 2) scavenging of Ni-Cr by clay-size particles from seawater that is enriched in these elements by hydrothermal leaching of komatiite at ocean ridges.

Relatively small decreases in Eu/Eu* and increases in La/Sc and Th/Sc in GR pelites occur across the A-P boundary and similar changes are allowed but not demanded by results from QP pelites. La/Yb ratios in QP pelites are relatively constant and Th/U ratios are variable through time. Based on limited data, early Archaean QP pelites are more like post-Archaean than late-Archaean QP pelites. Changes in element ratios in GR pelites at the A-P boundary probably reflect a greater proportion of granite in arc systems after 2500 Ma, which in turn, may be caused by a greater importance of fractional crystallization. Variable and high CIA values of some Archaean QP pelites may reflect variable and locally intense chemical weathering. Pelites from Precambrian cratonic basins typically exhibit increases in light REE, HFSE, La/Sc and Th/Sc and decreases in Eu/Eu* and Ti/Zr with increasng stratigraphic level; these changes probably reflect progressive erosion of deeper crustal levels containing greater proportions of granite.

Compared to GR associations, QP associations may be under-represented in the Archaean geologic record due to selective

burial or erosion at collisional plate boundaries and selective preservation of GR associations as a result of widespread tonalitic underplating. Continental growth rates should not be inferred from trace-element distributions in pelites.

INTRODUCTION

Numerous studies have proposed compositional changes in sediments across the Archaean-Proterozoic (A-P) boundary (2500 Ma) and have interpreted these changes in terms of changing patterns in the evolution of the crust, atmosphere or oceans (Van Moort, 1973; Veizer, 1973; Schwab, 1978; Taylor and McLennan, 1981a; McLennan, 1982). In most instances, sediment averages are compared on both sides of the A-P boundary and no distinctions are made between sediments from different tectonic settings. Ignoring tectonic setting, however, may lead to ambiguous results considering the differences in sediment compositions and proportions in different tectonic settings (Ronov et al., 1965; Dickinson,, 1971; Ronov et al., 1972; Condie, 1982; Bhatia and Crook, 1986). Calculations of the average composition of sediments of any age depends upon the relative proportions of chemical analyses available of sediments from different tectonic settings. To identify meaningful geochemical differences between sediment averages of different ages necessitates accurately weighting averages for each age according to the distribution of tectonic settings of that age. The same problem exists if one compares averages ot specific lithologies, such as average shales from different tectonic settings. For instance, if an average shale of one age, comprised chiefly of samples from volcanic arcs, is compared to an average shale of another age that includes samples chiefly from cratons, compositional differences between the two averages may reflect differences in tectonic setting and not secular changes in crustal or atmospheric composition. Because most published average sediment analyses ignore the effect of tectonic setting (see for instance McLennan, 1982), the significance of these analyses is uncertain, and the interpretation of crustal or atmospheric evolution based on such data may be completely misleading.

The accurate identification of ancient tectonic settings (especially in the Archaean) is a subject of disagreement and discussion among geologists. One possible approach that minimizes the effect of tectonic setting on ancient sediment compositions is to compare sediments from similar lithologic associations. Dickinson (1971) was the first to show formally that modern plate settings are characterized by specific rock associations. These associations can be recognized in the geologic record at least as far back as the early Proterozoic (Condie, 1982) and probably into the Archaean. For example, greenstone associations (characterized by dominance of submarine volcanics and graywackes) and quartzite-pelite associations (comprised chiefly of quartzites and shales± carbonates) are recognized from the present back to about 3500 Ma (Condie and Boryta, 1988). Although caution must be exercised in assigning specific modern tectonic settings to these ancient lithologic associations, provenance differences between tectonic settings can be minimized by comparing sediments from similar lithologic associations.

This study addresses only pelites from greenstone and quartzite-pelite associations (GR and QP pelites, respectively) and graywackes from greenstone associations. Because we do not know the relative proportions of these lithologic associations with geologic time, average sediment compositions are calculated individually for each association and not for a mixture of associations. Geochemical results are compiled from published papers and from unpublished results of the authors and their associates. At each geographic location, statistical parameters are calculated and mean values plotted on Figures 1-6. Means and standard deviations of selected element concentrations and ratios are summarized as a function of age in Tables 1 and 2 and references are given in Appendix I.

SiO_2/Al_2O_3 AND K_2O/Na_2O RATIOS

Among the geochemical parameters for which secular changes have been proposed in clastic terrigenous sediments are the SiO_2/Al_2O_3 and K_2O/Na_2O ratios (Ronov and Migdisov, 1971; Veizer, 1973; Engel et al. 1974; Schwab, 1978). An alleged increase in both of these ratios across the A-P boundary has been interpreted in terms of evolutionary changes in the composition of upper continental crust. However, when the distribution of data from pelites and graywackes is considered separately, secular trends are not apparent within either group except perhaps for K_2O/Na_2O ratios in

Table 1.
Geochemical Characteristics of Pelites of Various Ages

	QP Associations				GR Associations		
Age (Ma)	≥3500	2500-3500	1500-2500	≤1500	≥3500	2500-3500	1500-2500
SiO_2/Al_2O_3	3.6±0.4	3.9±1.2	4.1±0.2	3.8±0.5	4.5±0.5 (3.5±0.3)[1]	3.6±0.5	4.0±0.6
K_2O/Na_2O	3.0±1.0	9.4±2.0 (4.0±5.5)[8]	4.6±3.0	4.5±1.0	5.4±1.5 (2.4±1.2)[2]	2.4±1.0	2.2±1.1
CIA	73±5	73±7	69±3	72±5	72±3	70±5	69±4
La/Yb	14±4	13±4	12±4	13±3	14±6	10±1	10±3
Eu/Eu*	0.69±0.05	0.70±0.07	0.65±0.12	0.63±0.07	0.88±0.04	0.94±0.11	0.75±0.06
La/Sc	2.2±0.4	1.7±0.4	2.4±1.0	2.4±0.4	1.5±0.5 (2.1±0.3)[4]	1.0±0.5 (0.75±0.41)[5]	1.7±0.3
Th/Sc	0.77±0.22	0.45±0.25	0.96±0.41	0.90±0.10	0.53±0.14 (0.71±0.10)[4]	0.28±0.05 (0.22±0.02)[5]	0.48±0.12
Th/U	4.8±1.0	3.8±1.0	4.0±0.5	4.6±0.7	4.6±0.6	3.7±0.4	3.2±0.8
Cr (ppm)	325±12	578±200 (350±31)[6]	89±20	106±25	526±35	554±73 (323±65)[6]	129±17
Ni (ppm)	148±17	272±140 (130±24)[6]	36±8	53±8	223±44	285±25 (135±19)[6]	55±7
n	8	128	87-103	>20[7]	23-31	12-17	11-27
N	1	4	7	>10[7]	3	5	4

Given are mean values and one standard deviation of the mean; [1]excluding Holenarsipur [2]excluding Pilbara; [3]excluding Pongola and including only Booysens and KB shales from Witwatersrand; [4]excluding Isua; [5]excluding Whim Creek; [6]excluding southern Africa sites; [7]based in part on composites (like NASC) representing many sample sites. QP, quartzite-pelite association; GR, greenstone association; CIA = $[Al_2O_3/CaO^* + Na_2O + K_2O] \times 100$, using non-carbonate and non-phosphate CaO and oxides as molecular values (Nesbitt and Young, 1982). Eu*, Eu value interpolated on chondrite-normalized plot; n, number of samples; N, number of supracrustal sequences.

graywackes (Fig.1; Table 1 and 2). Pelites (both GR and QP) exhibit a slight inverse covariance between these ratios and have high K_2O/Na_2O ratios (>1) compared to graywackes. Unlike pelites, graywackes show rather constant SiO_2/Al_2O_3 ratios (0.45). The inverse relationship of the pelite element ratios probably reflects variations in the amount of K-bearing clay minerals in the original sediments. Variable K_2O/Na_2O ratios, yet approximately constant SiO_2/Al_2O_3 ratios in graywackes may be due to variations in feldspar content and feldspar composition. Mean values of the K_2O/Na_2O ratio in graywackes decrease with age (Table 2). Because of the large standard deviations in each age category, however, it is not clear if this trend is real. If it is, it may reflect a decreasing proportion of granite and rhyolite in graywacke sources with time.

Secular changes in SiO_2/Al_2O_3 and K_2O/Na_2O ratios in average fine-grained sediments proposed by earlier investigators appear to result from a tectonic setting bias. Almost all of the analyses of Archaean clastic sediments used by these investigators are graywackes and pelites from GR associations, while the post-Archaean clastic sediments are chiefly from QP associations.

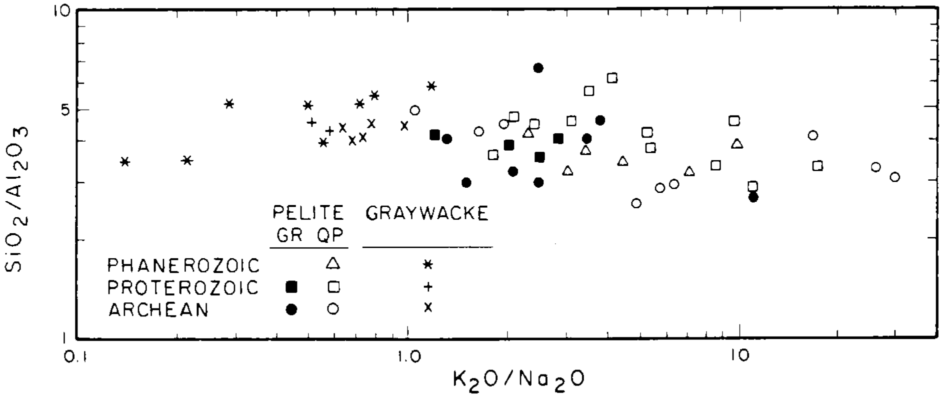

Figure 1. SiO_2/Al_2O_3-K_2O/Na_2O diagram showing the distribution of average compositions of graywackes and pelites from greenstone (GR) and quartzite-pelte (dQP) associations of various ages. Each point in this and subsequent figures represents a mean value of two or more samples from a specific supracrustal sequence, group or formation. For sequences that vary in composition with stratigraphic level, more than one mean value may be plotted.

Hence, proposed differences in the average values of SiO_2/Al_2O_3 and K_2O/Na_2O ratios across the A-P boundary probably reflect provenance differences between the two lithologic associations and not changes in continental evolution as advocated by some investigators (Engel et al., 1974).

RARE EARTHS Th, U, Sc, AND Co

Taylor and McLennan (1983,a,b; 1983; 1985) have proposed that significant changes occur in the distribution of REE, Th and U in fine-grained sediments across the A-P boundary. Among the proposed changes are decreases in Eu/Eu* and increases in La/Yb, Th/Sc, La/Sc and Th/U ratios. These changes have been interpreted to reflect changes in the compositions of the upper continental crust and in the growth rate of continents. Archaean clastic sediments, in particular, have been characterized by an absence of chondrite-normalized negative Eu anomalies. Gibbs et al. (1986) have questioned the interpretation of some of these geochemical variations, suggesting that they reflect differences in tectonic setting rather than crustal compositions.

In general, GR pelites have less pronounced Eu anomalies (higher Eu/Eu* values) than QP pelites (Table 1; Fig. 2). Both groups show a decrease in mean Eu/Eu* across the A-P boundary although the standard deviations completely overlap in the QP populations. The decrease in Eu/Eu* in both pelite groups is considerably less than the decrease proposed by Taylor and McLennan (1985, Table 5.2) between Archaean and post-Archaean pelites (0.99 to 0.65) and statistically may not be real in the QP

Table 2.

Geochemical Characteristics of Greenstone Graywackes of Various ages

	2500-3500 Ma	1500-2500 Ma	≤1500 Ma
SiO_2/Al_2O_3	4.5±0.3	4.4±1.0	4.6±0.5
K_2O/Na_2O	0.68±0.31	0.55±0.23	0.40±0.50
CIA	55±3	55±4	53±5
La/Yb	16±3	15±5	14±4
Eu/Eu*	0.97±0.05	0.95±0.04	1.0±0.03
La/Sc	1.8±0.2	1.9±0.3	1.9±0.4
Th/Sc	0.5±0.3	0.6±0.2	0.6±0.3
Th/U	3.7±0.2	3.4±0.4	3.5±0.3
Cr (ppm)	181±30	175±19	76±10
Ni (ppm)	89±20	63±10	32±9
n	15-79	5-25	10-83
N	5	2	8-15

See footnote of Table 1 for explanation.

pelites. It is noteworthy in this respect that Eu anomalies in early Archaean QP pelites from the Belt Bridge Complex are similar to those in post-Archaean QP pelites. Although increases in mean values of La/Sc and Th/Sc ratios are observed across the A-P boundary in both pelite populations, only those in the GR group are statistically valid. The scatter in Th/U ratio remains rather constant in QP pelites and may decrease in GR pelites across the A-P boundary. As with Eu anomalies, early Archaean QP pelites are

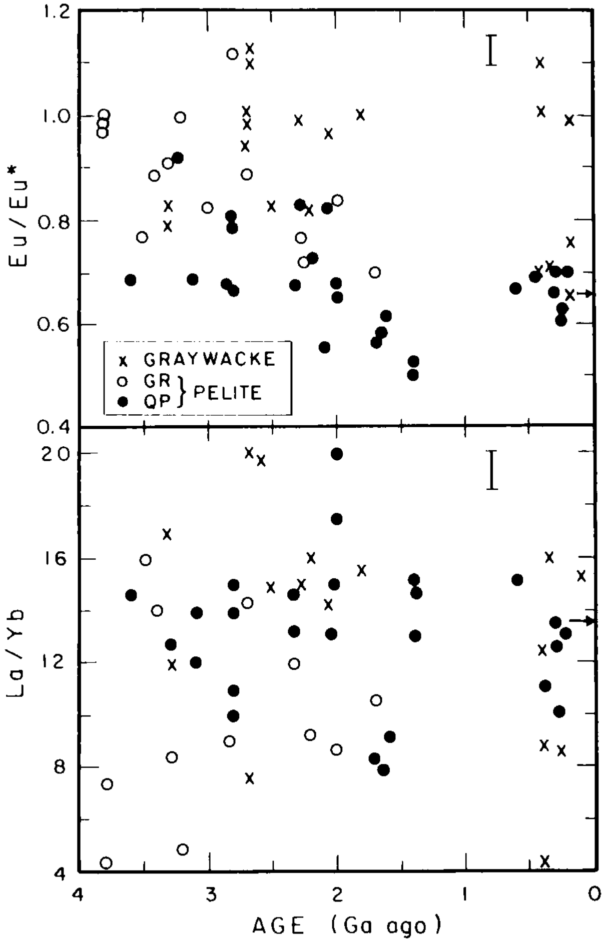

Figure 2. Distribution of Eu/Eu* and La/Yb ratios with age in average greenstone graywackes and in pelites from greenstone (GR) and quartzite-pelite (QP) associations. Arrows indicate average compositions of the upper continental crust from Taylor and McLennan (1985). Vertical is average error for mean values.

more like post-Archaean than late Archaean QP pelites in terms of La/Sc, Th/Sc and Th/U ratios (Figs. 3-4; Table 1). No changes in the La/Yb ratios (or LREE/HREE ratio) are apparent in either pelite group across the A-P boundary or this ratio remains relatively constant in the QP group through time. The La/Yb ratio in GR pelites may decrease between the early and late Archaean if pelites from the three early Archaean localities are representative. Although fewer data are available for graywackes, none of the element ratios appears to change significantly with age (Table 2; Figs. 2-4).

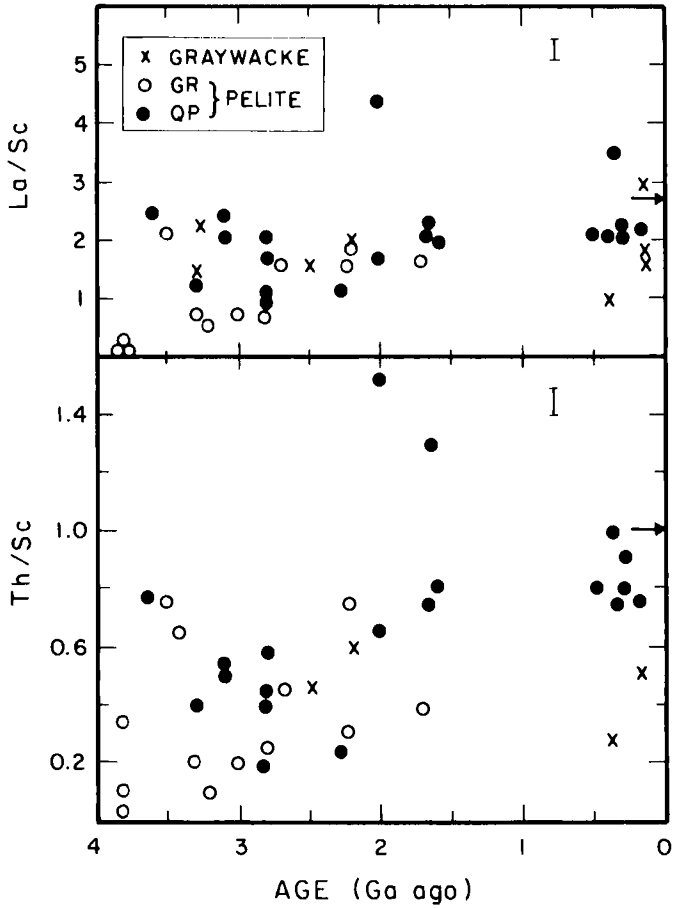

Figure 3. Distribution of La/Sc and Th/Sc ratios with age in average greenstone graywackes and in pelites from greenstone (GR) and quartzite-pelite (QP) associations. Other information as given in Fig. 2.

Differences between GR and QP pelites are particularly evident in terms of La-Th-Sc and Th-Hf-Co distributions (Fig.5). Proterozoic QP pelites are similar to Phanerozoic shales and support the conclusions of Taylor and McLennan (1985) that the composition of the average Proterozoic upper continental crust is similar to the present upper crust. Archaean QP pelites are relatively enriched in Sc and Co, a feature that may reflect a greater proportion of mafic rocks exposed to erosion in Archaean continental crust. GR pelites differ from most QP pelites by their relatively large enrichments in Sc and Co, a feature that probably reflects penecontemporaneous mafic volcanic sources.

Available geochemical data from QP pelites allow but do not demand changes in Eu/Eu*, La/Sc and Th/Sc ratios across the A-P boundary. Changes in these three ratios in GR peliets across the A-P boundary, however, appear to be real. The large differences in Eu/Eu*, La/Yb, Th/U, La/Sc and Th/Sc ratios in pelites proposed to occur across the A-P bondary by Taylor and McLennan (1985) probably relfect a tectonic setting bias. Their Archaean average pelites are strongly weighted by GR pelites, whereas their post-Archaean average pelites are almost exclusively QP pelites. Perhaps the most intriguing question to emerge from the data we have compiled and evaluated is whether early Archaean QP pelites (as represented by the Belt Bridge Complex) are more like post-Archaean than late Archaean QP pelites. This question can only be more fully evaluated if more early Archaean QP pelites are found and analyzed.

NI AND CR

The high Ni and Cr contents of Archaean relative to post-Archaean pelites has been recognized by many investigators (Naqvi and Hussain, 1972; Naqvi, 1983; McLennan et al., 1983a,b; Laskowski and Kroner, 1985; Taylor and McLennan, 1985; Wronkiewicz and Condie, 1987; 1988) and is confirmed by the results of this study. Ni and Cr contents of GR and QP pelites of the same age are similar (Fig.6; Table 1). A dramatic decrease in both of these elements occurs in pelites in crossing the A-P boundary. Ratios of these elements to neighbouring compatible elements (such as Ni/Co and Cr/V) also decrease, as pointed out by Taylor and McLennan (1985). A small decrease in the concentration of Ni and Cr in graywackes may also occur across the A-P boundary followed by a

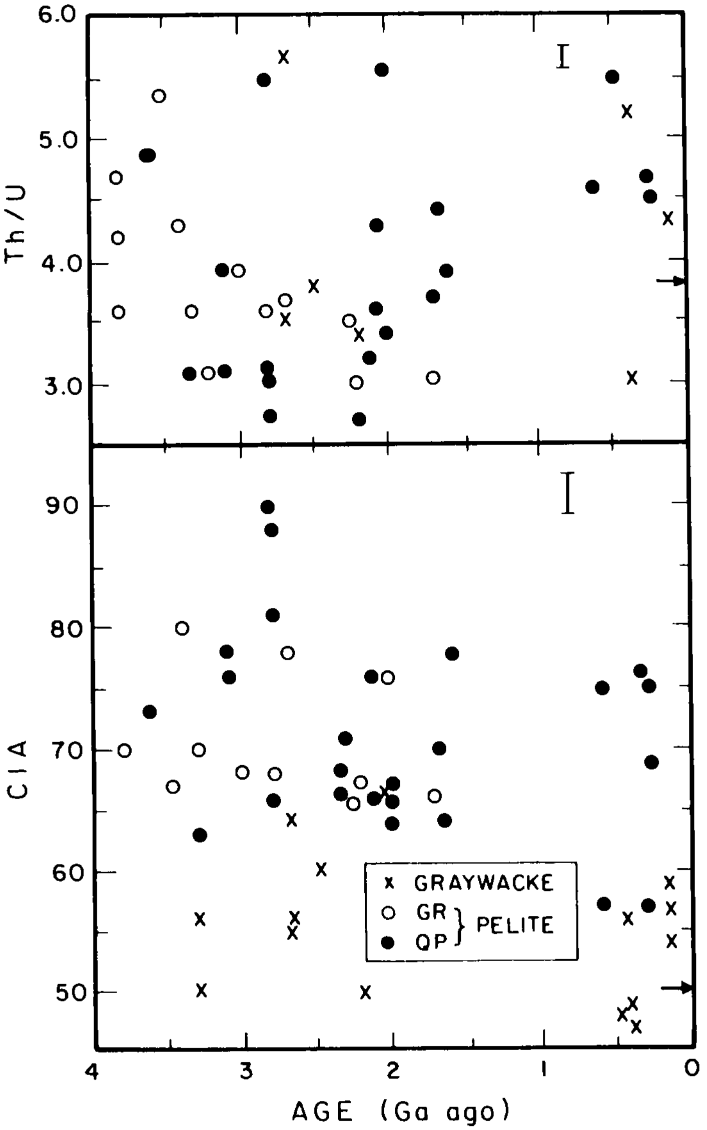

Figure 4. Distribution of Th/U ratio and CIA with age in average greenstone graywackes and in shales from greenstone (GR) and quartzite-pelite (QP) associations. Other information as given in Fig. 2.

significant decrease in graywackes younger than 1500 Ma (Table 2).

Several explanations are possible for the relative enrichment of Ni and Cr in Archaean pelites. Most investigators suggest that the presence of komatiites in Archaean source areas accounts for

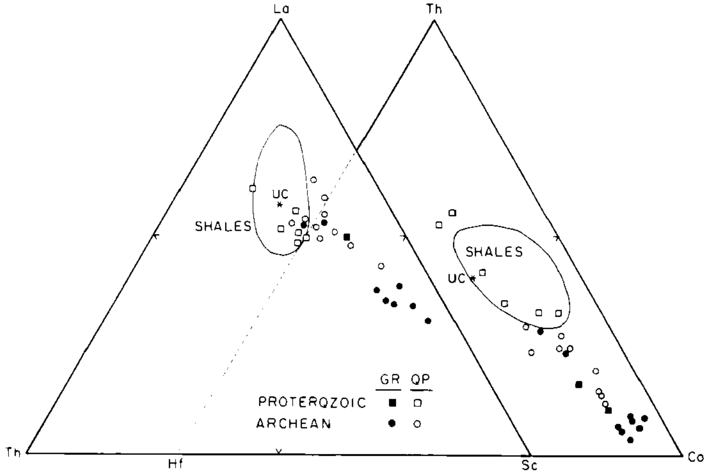

Figure 5. La-Th-Sc and Th-Hf-Co diagrams showing distribution of average pelite compositions from greenstone and quartzite-pelite associations. UC, upper continental crust and field of Phanerozoic shales from Taylor and McLennan (1985).

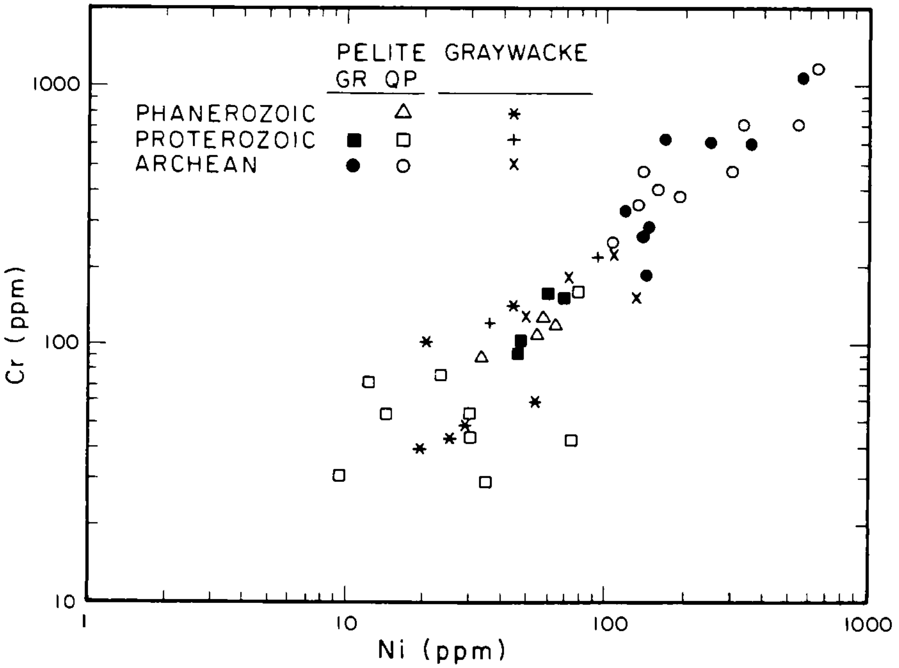

Figure 6. Distribution of Cr and Ni with age in average greenstone graywackes and in pelites from greenstone (GR) and quartzite-pelite (QP) associations.

higher Ni and Cr in derivative sediments (Laskowski and Kroner, 1985; Wronkiewicz and Condie, 1987). However, in some instances, it is not possible to obtain a mass balance when Mg and various compatible trace elements (Sc,V,Co,Ti) are considered (McLennan et al., 1983a,b). It is difficult or impossible to obtain approximate mass balances for such elements for many of the pelite data points shown in Figure 6, even when unrealistically high proportions (up to 50 percent) of komatiite are assumed in the sources. One possible explanation of this problem is to invoke intense chemical weathering of komatiites in pelite source regions. This weathering not only decouples such elements as Mg, V and Ti from Cr-Ni, but also concentrates large amounts of Ni and Cr in residual clays (Esson, 1983). Thus, a relatively small proportion of highly weathered komatiite in sediment source areas could supply significant quantities of Ni and Cr into a sedimentary basin (Wronkiewicz and Condie, 1988). The fact that Archaean Gr as well as QP pelites, exhibits significant Ni-Cr enrichment, however, presents a problem for the weathering model. This is because GR pelites are often integral members of graywacke turbidite successions that are derived in large part from active

Table 3.
Stratigraphic Geochemical Changes of QP Pelites in Cratonic Basins.

Basin	Pongola[2]		Witwatersrand[1]			Huronian[4]		Pine Creek[3]		Belt[5]	
Age (Ma)	3100		2800			2300		2000		1400	
	L	U	L	M	U	L	U	L	U	L	U
Zr (ppm)	185	240	94	120	201	169	284	95	166	85	134
La (ppm)	39	47	16	24	50	33	41	34	42	27	35
Ni (ppm)	135	158	300	627	523	78	14	52	12	36	30
Eu/Eu^*	0.69	0.68	0.79	0.81	0.67	0.83	0.68	0.84	0.56	0.55	0.52
La/Yb	12	14	11	10	14	13	15	20	18	15	15
La/Sc	2.1	2.4	1.2	0.94	2.1			1.7	4.4		
Th/Sc	0.51	0.53	0.29	0.19	0.42			0.66	1.7		
Ti/Zr	29	23	26	34	26	27	8	48	13	23	18
CIA	76	78	90	81	88	68	66	76	66		

Values given are means; blanks reflect data not available. L, lower; M, middle; U, upper, Refs. 1, Wronkiewicz and Condie (1987); 2, Wronkiewicz and Condie (1988); 3, Taylor and McLennan (1983); Ewers et al., (1985); 4, McLennan et al., (1979); 5, Schieber (1986).

volcanic sources not subjected to intense weathering. The fact that Archaean graywackes show only a small amount of Cr-Ni enrichment, yet associated Gr pelites show significant enrichment suggests the ultimate cause of Ni-Cr enrichment may involve a grain-size effect.

Another possibility that could concentrate Ni-Cr preferentially in fine-grained particles is the scavenging of these elements by clay-sized particles from seawater. This would require a greater concentration of these elements in the oceans than found today. A possible source for increased input of Ni and Cr into the sea is from hydrothermal leaching of oceanic crust in a manner similar to that proposed to occur at modern ocean ridges (Thompson, 1983). The probable importance of submarine volcanism and an oceanic crust comprised largely of komatiite in the Archaean (Arndt, 1983) are consistent with such a model. A komatiitic crust would provide a large, continuously replenished source for Ni and Cr. These elements could be leached from komatiites by hydrothermal waters at ocean ridges and enter the Archaean oceans. If this mechanism is to explain the high Cr and Ni contents in Archaean QP pelites, it also necessitates a relatively short ocean mixing time in the Archaean compared to the residence times of Cr and Ni in sea water, in order for these elements to be transported into shallow cratonic basins where QP associations are deposited.

WEATHERING INDICES

The Chemical Index of Alteration (CIA) has been proposed as a measure of the intensity of chemical weathering in clastic sediment source areas (Nesbitt and Young, 1982). As expected, graywackes exhibit relatively low CIA values (~55) indicating only slight chemical weathering, and graywacke CIA values as a function of time are rather constant (Fig. 4; Table 2). It is noteworthy that both Gr and QP pelites have similar mean CIA values (~70) which are also rather constant with time (Table 1). However, Archaean QP pelites exhibit a large range in CIA with values up to 90 in samples from the Witwatersrand Supergroup in South Africa (Wronkiewicz and Condie, 1987) (Fig. 4) These rocks also have low contents of Ca, Sr and Na. The variable, and occasionally high CIA values and low Ca, Sr and Na in Archaean QP pelites may reflect more variable and locally intense chemical weathering than is characteristic of most post-Archaean QP sources. The higher

CIA values in GR pelites than in associated graywackes (70 versus 55) are probably caused by mineral fractionation during sediment transport. The finer sediments contain greater proportions of clays and thus have higher Al_2O_3 contents (and CIA values) than the coarser sediments.

CRATONIC BASIN EVOLUTION

Geochemical data are available from pelites at different stratigraphic levels within several Precambrian cratonic basins. Despite significant age differences in the basins, several compositional trends are consistently observed between lower and upper stratigraphic levels (Table 3). All show upward increases in HFSE and light REE and decreases in the Ti/Zr (except for Witwatersrand) and Eu/Eu* ratios. La/Yb, La/Sc and Th/Sc ratios generally increase or are approximately constant with stratigraphic level. These changes probably reflect progressive uplift and erosion of source areas exposing more granite with time. The increases in Zr and other HFSE and the decrease in the Ti/Zr ratio may reflect increasing contributions of zircon and other minor resistate phases from the source granites. The fact that the La/Yb ratio does not decrease with increasing zircon content may indicate that REE are largely concentrated in clay minerals (Wronkiewicz and Condie, 1988). The decreasing Eu/Eu* values at higher stratigraphic levels probably reflect intracrustal melting as a major source for the granites being unroofed, as originally suggested by McLennan et al., (1979).

Pelites from the three Proterozoic basins show decreasing Ni (also Cr, Co) with increasing stratigraphic height, while pelites from the two Archaean basins increase in Ni upwards (Table 3). The trends in the Proterozoic basins are consistent with increasing proportions of granite in the sources with time, while the Archaean basins seem to suggest more komatiite-basalt input with time. CIA values are relatively constant within the Pongola and Huronian basins, suggesting that climatic conditions did not significantly change with time.

DISCUSSION

It appears that some of the compositional changes proposed to occur in clastic terrigenous sediments across the A-P boundary result from the comparison of sediment averages that include, in the Archaean, chiefly Gr sediments and in the post-Archaean, chiefly QP sediments. When only QP sediments are compared, the differences between early and late Archaean pelites may be as pronounced as those between late Archaean and post-Archaen pelites. The only well-documented changes in clastic sediment composition at the A-P boundary are decreases in Cr and Ni in pelites. Average sediment compositions that are calculated without a tectonic setting (lithologic associations) weighting factor must be considered suspect and apparent differences between such average sediments of different ages should not be interpreted in terms of crustal or atmosphere-ocean evolution.

Data suggest that REE distributions and ratios such as La/Sc, Th/Sc, Th/U, Eu/Eu* and La/Yb in post-Archaean QP pelites can be used to characterize the average composition of the upper continental crust (Taylor and McLennan, 1981a,b;1985) (Figs.1-4). It is very doubtful, however, whether average Archaean sediments, which include mainly graywackes and pelites from GR associations, can be used in a similar way to estimate the composition of Archaean upper continental crust. Most provenance studies of clastic sediments from Archaean Gr successions indicate that sediments are derived generally from local, volcanic-dominated sources (Ayres; 1983; Ojakangas, 1985). Evidence is continuing to accumulate to suggest that Proterozoic and most late Archaean GR successions developed in arc-like volcanic belts and that derivative sediments are largely reworked volcaniclastic debris (Ayres et al., 1985; Condie, 1982; 1986a). Furthermore, recent geochemical studies of early Archaean GR sediments from Isua (3800 Ma) and southern India (>3400 Ma) indicate considerably more diversity than has been found in late Archaean GR sediments (Naqvi et al., 1983; McLennan et al., 1984; Boak and Dymek, 1987).

Geochemical data from Archaean QP pelites are on the whole similar to those of post-Archaean QP pelites and suggest that cratons were in existence by 3500 Ma (Gibbs et al., 1986; Condie and Boryta, 1988). These early cratons may have differed from post-Archaean cratons in containing small amounts of komatiite that was exposed to weathering and erosion. The presence of a larger proportion of crustal-derived granites in post-Archaean cratons is perhaps allowed but not demanded by element ratios in QP pelites. If greenstones form in arc systems, which seems likely (Condie, 1988), element ratios in GR pelites suggest an increase in the amount of granite (relative to tonalite) in post-Archaean relative to Archaean arc systems. Because arc systems represent juvenile additions to the continental crust (even oceanic arcs eventually collide and accrete to continents), it is unlikely that arc granites represent intracrustal melts of older rocks. The negative Eu anomalies in these rocks may have developed by fractional crystallization (Condie et al., 1985). Why granites should be more important in post-Archaean than in Archaean arcs is not entirely clear. REE distributions and experimental data suggest that the source of tonalite and andesite production in arcs shifted from the descending slab (batch melting of hydrous mafic rock) to fractional crystallization of basaltic magma after the end of the Archaean (Martin, 1986; Condie, 1988). Perhaps the greater importance of fractional crystallization after 2500 Ma is also responsible for a greater proportion of granites being produced in post-Archaean arcs. Since arc systems eventually become part of continents, the less pronounced geochemical changes in QP than in GR pelites across the A-P boundary may reflect a relatively minor contribution from accreted arcs to cratonic sediments. It is probably not possible to use trace element distributions to support one model or another for continental growth rate as proposed by Taylor and McLennan (1981a; 1985).

Although a considerably greater number of chemical analyses are available for GR than for QP Archaean pelites, this sample distribution may not reflect the relative importances of the GR and QP tectonic settings on the earth at that time. Taylor et al., (1986) suggest that the proportion of Archaean arc-like environment may have been underestimated relative to cratonic environment. However, in terms of plate tectonics, just the opposite may be true. Archaean QP successions comprise a very small proportion of known Archaean supracrustal rocks, and are chiefly found in Archaean high-grade terranes (Condie, 1981). Because such successions may have been deposited in small cratonic basins on leading edges of colliding continental plates, they may be underrepresented in the geologic record. Many of them may have been buried at great depths during collision and have not as yet been exposed by uplift and erosion, while others may have been rapdily uplifted and destroyed by erosion. On the other hand, Archaean greenstone succcessions may be overrepresented in the geologic record. Most of these successions owe their preservation to extensive underplating with tonalite (and granodiorite) (Condie, 1986b). Production of large volumes of tonalite, especially in the late Archaean and probably along convergent plate margins (Martin, 1986; Condie, 1988), may have resulted in a preservational bias for GR successions.

REFERENCES

Arndt, N.T., 1983. Role of a thin, komatiite-rich oceanic crust in the Archaean plate-tectonic process. Geology, 11: 372-375.

Ayres, L.D., 1983. Bimodal volcanism in Archaean greenstone belts exemplified by graywacke composition, Lake Superior Park, Ontario. Canadian J. Earth Sci., 20: 1168-1194.

Ayers, L.D., Thurston, P.C., Card, K.D. and Weber, W. (Editors), 1985. Evolution of Archaean supracrustal sequences. Geol. Assoc. Canada, Spec., Paper, 28.

Bavinton, D.A. and Taylor, S.R., 1980. REE geochemistry of Archaean metasedimentary rocks from Kambalda, Western Australia. Geochim, Cosmochim. Acta, 44: 639-648.

Bhatia, M.R. and Crook, K.A.W., 1986. Trace element characteristics of graywackes and tectonic setting discrimination of sedimentary basins. Contr. Min. Pet., 92: 181-193.

Boak. J.L. and Dymek, R.F., 1987. A systematic chemical stratigraphy for clastic metasedimentary and metavolcanic rocks from the 3800 Ma Isua supracrustal belt, West Greenland. (ms. in prep.)

Cameron, E.M. and Garrels, R.M., 1980. Geochemical compositions of some Precambrian shales from the Canadian Shield. Chem. Geol., 28: 181-197.

Condie, K.C., 1967. Geochemistry of early Precambrian graywackes from Wyoming. Geochim. Cosmochim. Acta, 31: 2135-2149.

Condie, K.C., 1981. Archaean Greenstone Belts: Elsevier, Amsterdam, 434pp.

Condie, K.C., 1982. Early and Middle Proterozoic supracrustal successions and their tectonic settings. Am. J. Sci., 282: 341-357.

Condie, K.C., 1986a. Geochemistry and tectonic setting of early Proterozoic supracrustal rocks in the southwestern United States. J. Geol., 94: 845-864.

Condie, K.C., 1986b. Origin and early growth rate of continents. Precamb. Res., 32: 261-278.

Condie, K.C., 1988. Geochemical changes in basalts and andesites across the Archaean-Proterozoic boundary: Identification and significance. Lithos, (in press).

Condie, K.C. and Boryta, M., 1988. Geochemistry of the Beit Bridge Complex, Limpopo belt, South Africa: Implications for crustal evolution in Southern Africa: Contr. Min. Pet. (in press).

Condie, K.C. and Budding, A.J. 1979. Geology and geochemistry of Precambrian rocks, Central and south-central New Mexico, New Nexico Bureau of Mines and Mineral Resources, Memoir, 35: 58.

Condie, K.C., Macke, J.E. and Reimer, T.O., 1970. Petrology and geochemistry of early Precambrian graywackes from the Fig Tree Group, South Africa. Geol. Soc. America Bull., 81: 2759-2776.

Condie, K.C. and Snansieng, S., 1971. Petrology and geochemistry of the Duzel and Gazelle Formations, northern California. J. Sed. Pet., 41: 741-751.

Condie, K.C., Viljoen, M.J. and Kable, E.J.B., 1977. Effects of alteration on element distributions in Archaean tholeiites from the Barberton greenstone belt, South Africa. Contr. Min. Pet., 64; 75-89.

Condie, K.C., Bowling, G.P. and Allen, P. 1985. Missing Eu anomaly and Archaean high-grade granites. Geology, 13: 633-636.

Danchin, R.V., 1967. Cr and Ni in the Fig Tree shale from South Africa. Science, 158: 261-262.

Dickinson, W.R., 1971. Plate tectonics in geologic history. Science, 174: 107-113.

Engel, A.E.J., Itson, A.P., Engel, C.G., Stickney, D.M. and Cray, E.J., Jr. 1974. Crustal evolution and global tectonics: a petrogenetic view. Geol. Soc. America Bull., 85: 843-858.

Eriksson, K.A. and Soegaard, K., 1985. The petrography and geochemistry of Archaean and Early Proterozoic sediments: implication for crustal compositions and surface processes. Geol. Survey Finland Bull., 331: 7-32.

Esson, J., 1983. Geochemistry of a nickeliferous laterite profile, Liberdale, Brazil. Geol. Soc. London, Spec. Publ. No. 11: 91-98.

Ewers, G.R., Needham, R.S., Stuart-Smith, P.G. and Crick, I.H., 1985. Geochemistrty of the low-grade early Proterozoic sedimentary sequence in the Pine Creek geosyncline, Northern Australia. Australian. J. Earth Sci., 32: 137-154.

Gibbs, A.K., Montgomery, C.W., O'Day, P.A. and Erslev, E.A., 1986. The Archaean-Proterozoic transition evidence from the geochemistry of metasedimentary rocks of Guyana and Montana. Geochim. Cosmochim. Acta, 50: 2125-2141.

Gromet, L.P., Dymek, R.F., Haskin, L.A. and Korotev, R.L., 1984. The North American shale composite: its compilation, major and trace element characteristics. Geochim. Cosmochim. Acta, 48: 2469-2482.

Haskin, L.A., Wildeman, T.R., Frey, F.A., Collins, K.A., Keedy, C.R. and Haskin, M.A., 1966. Rare earths in sediments. J. Geophys. Res. 71: 6091-6105.

Jenner, G.A., Fryer, B.J. and McLennan, S.M., 1981. Geochemistry of the Archaean Yellowknife Supergroup. Geochim. Cosmochim. Acta, 45: 1111-1129

Jones, W.B., 1985. Chemical analyses of Bosumtwi Crater target rocks compared with Ivory Coast tektites. Geochim. Cosmochim. Acta, 49: 2569-2576.

Laskowski, N. and Kroner, A., 1985. Geochemical characteristics of Archaean and Proterozoic to Paleozoic fine-grained sediments from southern Africa and significance for the evolution of the continental crust. Geol. Rundschau, 74: 1-9

Martin, H., 1986. Effect of steeper Archaean geotherm gradients on geochemistry of subducton-zone magmas. Geology, 14: 753-756.

McLennan, S.M., 1982. On the geochemical evolution of sedimentary rocks. Chem. Geol., 37: 335-350.

McLennan, S.M., Fryer, B.J. and Young, G.M., 1979. REE in Huronian sedimentary rocks: composition and evolution of the post-Kenoran upper crust. Geochim. Cosmochim. Acta, 43: 375-388.

McLennan, S.M. and Taylor,. S.R., 1980. Th and U in sedimentary rocks: crustal evolution and sedimentary recyling. Nature, 285: 621-624.

McLennan, S.M., Taylor, S.R. and Eriksson, K.A. 1983a. Geochemistry of Archaean shales from the Pilbara Supergroup, W. Australia. Geochim. Cosmochim. Acta, 47: 1211-1222.

McLennan, S.M., Taylor, S.R. and Kroner, A., 1983b. Geochemical evolution of Archaean shales from South Africa, I. The Swaziland and Pongola Supergroups: Precamb. Res., 22: 93-124.

McLennan, S.M., Taylor, S.R. and McGregor, V.R., 1984. Geochemistry of Archaean measedimentary rocks from West Greenland, Geochim. Cosmochim. Acta, 48: 1-13.

Nance, W.B. and Taylor,S.R. 1976. REE patterns and crustal evolution-I. Australian post-Archaean sedimentary rocks. Geochim. Cosmochim. Acta, 40: 1539-1551.

Nance, W.B. and Taylor, S.R., 1977. REE patterns and crustal evolution-II. Archaean sedimentary rocks from Kalgloorlie, Australia. Geochim. Cosmochim. Acta, 41: 225-231.

Naqvi, S.M. 1983. Early Precambrian clastic metasediments of Dharwar greenstone belt, Implications to Sial-Sima transformation processes. In: Precambrian of South India (Ed. S.M.Naqvi and J.J.W.Rogers) Geol. Soc. India Mem., 4: 220-236.

Naqvi, S.M and Hussain, S.M. 1972. Petrochemistry of some early Precambrian metasediments from the central part of the Chitradurga schist belt, Mysore, India. Chem. Geol., 10: 109-135.

Naqvi, S.M., Condie, K.C., and Allen, P., 1983. Geochemistry of some unusual Early Archaean sediments from Dharwar craton, India. Precamb. Res., 22: 125-147.

Nesbitt, H.W. and Young G.M., 1982. Early Proterozoic climates and plate motions inferred from major element chemistry of lutites. Nature, 299: 715-717.

Ojakangas, R.W., 1985. Review of Archaean clastic sedimentation, Canadian Shield: major felsic volcanic contributions to turbidite and alluvial fan-fluvial facies associations. Geol. Assoc. Canada. Spec. Paper, 28: 23-47.

Ondrick, C.W. and Griffiths. J.C., 1969. Frequency distribution of elements in Rensslaer graywacke, Troy, New York. Geol. Soc. America Bull., 80: 509-518.

Pettijohn, F.J., 1963. Chemical composition of sandstones-excluding carbonate and volcanic sands. U.S. Geol. Survey, Professinal Paper, 440-S.

Rogers, J.J.W., Condie, K.C. and Mahan, S., 1970. Significance of Th, U, and K in some early Precambrian graywacke from Wyoming and Minnesota. Chem. Geol., 5: 207-213.

Ronov, A.B., Girin, Y.P., Kazakov, G.A. and Ilyukhin, M.N., 1965. Comparative geochemistry of geosynclinal and platform sedimentary rocks. Geochem. International, 2: 692-708.

Ronov, A.B. and Migdisov, A.A. 1971. Geochemical history of the crystalline basement and the sedimentary cover of the Russian and North American platforms. Sedimentology, 16: 137-185.

Ronov, A.B, Balashov, Y.A., Girin, Y.P., Bratishko, R.K. and Kazakov, G.A. 1972. Trends in REE distribution in the sedimentary shell and in the earth's crust: Geochem. International, 9:987-1015.

Schieber, J., 1986. Stratigraphic control of REE pattern types in mid-Proterozoic sediments of the Belt Supergroup, Montana, Chem. Geol., 54: 135-148.

Shaw, D.M., 1956. Geochemistry of pelitic rocks. Part III: Major elements and general geochemistry. Geol. Soc. America Bull., 67: 919-934.

Schwab, F.L., 1978. Secular trends in the composition of sedimentary rock assemblages Archaean through Phanerozoic time. Geology, 6: 532-536.

Taylor, S.R. and McLennan,S.M. 1981a. The composition and evolution of the continental crust: REE evidence from sedimentary rocks. Phil. Trans. Royal Soc. London, 301A: 381-399.

Taylor, S.R. and McLennan, S.M., 1981b. The REE evidence in Precambrian sedimentary rocks: Implications for crustal evolution, In: A. Kroner (Editor), Precambrian Plate Tectonics, Elsevier, Amsterdam, pp.527-548.

Taylor, S.R., and McLennan, S.M., 1983. Geochemistry of early Proterozoic sedimentary rocks and the Archaean/Proterozoic boundary. Geol. Soc. America, Special Paper 161: 119-129.

Taylor, S.R. and McLennan, S.M., 1985. The Continental Crust: Its composition and Evolution. Blackwell Scientific Publications, Oxford, U.K., 312pp.

Taylor, S.R., Rudwick, R.L., McLennan, S.M. and Eriksson, K.A., 1986. REE patterns in Archaean high-grade metasediments and their tectonic significance. Geochim. Cosmochim. Acta, 50: 2267-2279.

Thompson, G., 1983. Basalt-seawater interaction. In: Rona, P.A., Bostrom, K., Laubier, L., and Smith, K.L., Jr., (Editors), Hydrothermal Processes at Seafloor Spreading Centers. Plenum, New York, 225-265.

Van Moort, J.C., 1973. The magnesium and calcium contents of sediments, especially pelites, as a function of age and degree of metamorphism. Chem. Geol., 12: 1-37.

Veizer, J., 1973. Sedimentation in geologic history: recycling vs. evolution or recyling with evolution. Contr. Min. Pet., 38: 261-278.

Weber, J.N., 1960. Geochemistry of graywackes and shales. Science, 131: 664-665.

Weber, J.N. and Middleton, G.V., 1961. Geochemistry of the turbidites of the Normanskill and Charny Formations-I. Geochim. Cosmochim. Acta, 22:200-243.

Whetten, J.T., 1966. Sediments from the lower Columbia River and origin of graywacke. Science, 152: 1057-1058.

Wildeman, T.R., and Condie, K.C. 1973. REE in Archaean graywacke from Wyoming and from the Fig Tree Group, South Africa. Geochim. Cosmochim. Acta, 33: 483-492.

Wronkiewicz, D.J. and Condie, 1987. Geochemistry of Archaean shales from the Witwatersrand Supergroup, South Africa: source-area weathering, provenance and tectonic setting. Geochim. Cosmochim. Acta, 51: 2401-2416.

Wronkiewicz, D.J. and Condie, K.C., 1988. Geochemistry and provenance of shales from the Pongola Supergroup, South Africa. Geochim. Cosmochim. Acta. (in press)

APPENDIX 1
PELITE AND GRAYWACKE REFERENCES

PELITES

≥3500 Ma

1. Belt Bridge Complex
South Africa (QP)
Condie and Boryta
(1988)

2. Pilbara,W.Australia(GR)
(Gorge Creek Group)
McLennan et al.(1983a)

3. Isua, W.Greenland (GR)
McLennan et al. (1984)
Boak and Dymek (1987)

4. Holenarsipur, India (GR)
Naqvi et al. (1983)
Condie, (1987)
unpub. data

2500-3500 Ma

1. Moodies Group, South Africa (QP)
McLennan et al. (1983b)
Condie, (1987) unpub. data

2. Beartooth Mtns., Wyoming (QP)
Gibbs et al. (1986)

3. Witwatersrand Supergroup,South
Africa (QP)
Wronkiewicz and Condie (1987)

4. Pongola Supergroup, South Africa
(GR)
Wronkiewicz and Condie (1988)

5. Fig Tree Group, South Africa(GR)
Danchin (1967)
Condie et al. (1970)
Wildeman and Condie (1973)
McLennan et al. (1983b)

6. Kalgoorlie, W.Australia (GR)
Nance and Taylor (1977)

7. Pilbara, W.Australia (Whim Creek
Group) (GR)
McLennan et al. (1983a)

8. Bababudan Group,India (GR)
Condie, K.C. (1987), unpub.data

9. Malene supracrustals,W.Greenland
(GR)
McLennan et al. (1984)

PELITES (CONTINUED)

1500-2500 Ma

1. Roraima Group, Brazil(QP)
Gibbs et al. (1986)

2. San Andres Mtns.
New Mexico
Condie, K.C. and Alford,D.
(1987) unpub. data

3. Huronian Supergroup,
Canada (QP)
McLennan et al. (1979)

4. Mt. Isa Group, Australia
(QP)
Nance and Taylor (1976)

5. Amadeus basin, Australia
(QP)
Nance and Taylor (1976)

6. Pine Creek Geosyncline,
Australia (QP)
Taylor and McLennan (1983)
Ewers et al. (1985)

7. Manzano Mnts., New Mexico (QP)
Condie, and Budding (1979)
Condie, K.C. (1987)
unpub. data

8. Ranibennur Group, India (GR)
Condie, K.C. (1987) unpub.
data

9. Barama-Mazaruni Supergroup
Guyana (GR)
Gibbs et al. (1986)

10. Birimian System, Ivory Coast
(GR)
Jones (1985)

11. Mazatzal Mountains, Arizona (GR)
Condie, K.C., (1987) unpub. data

≥1500 Ma

1. Slate Circle Shale (Silurian)(QP)
Nance and Taylor (1976)

2. Littleton Formation (QP)
Shaw (1956)

3. Belt Supergroup, Montana (QP)
Schieber (1986)

4. Nam Group, South Africa (QP)
McLennan et al. (1983b)
Laskowski and Kroner (1985)

5. Miscellaneous Phanerozoic (QP)
Ronov et al. (1965)
Ronov and Migdisov (1971)
Ronov et al. (1972)
Cameron and Garrels (1980)
Gromet et al. (1984)
Taylor and McLennan (1985)

GRAYWACKES

2500-3500 Ma

1. Kambalda, W.Australia (GR)
   Bavinton and Taylor (1980)

2. Yellowknife Supergroup, Canada (GR)
   Jenner et al. (1981)

3. South Pass, Wyoming (GR)
   Condie, (1967)
   Rogers et al. (1970)
   Wildeman and Condie, (1973)

4. Fig Tree Group (Sheba and Belview Road Fms.) (GR)
   Condie et al. (1970)
   Wildeman and Condie (1973)

5. Chitradurga Group, India (GR)
   Condie, (1987), unpub. data

1500-2500 Ma

1. Birimian System, Ivory Coast (GR)
   Jones (1985)

2. Ranibennur Group, India (GR)
   Condie, (1987), unpub. data

≥1500 Ma

1. Baldwin Fm., Australia (GR)
   Nance and Taylor (1977)

2. Gazelle Fm., California (GR)
   Condie and Snansieng (1971)

3. Miscellaneous Phanerozoic (GR)
   Weber (1960)
   Weber and Middleton (1961)
   Pettijohn (1963)
   Haskin et al. (1966)
   Whetten (1966)
   Ondrick and Griffiths (1969)
   Taylor and McLennan (1985)
   Condie, (1987), unpub. data

This Page Intentionally Left Blank

PHYSICO-CHEMICAL CONDITIONS OF METAMORPHISM OF THE ANCIENT FOLD-BELT COMPLEXES

V.V.FED'KIN

ABSTRACT

Detailed studies on the compositions of coexisting minerals, their zoning, composition of inclusions and mutual grain contacts enable application of the chemical inhomogeneity of the rock-forming minerals as an indicator of physico-chemical data on mineral stability and permit of deducing the system of consistent mineralogical geothermometers, geobarometers and geohydrometers. Taking all these into account, one can follow the evolution of physico-chemical conditions of metamorphism (T.P, composition and regime of volatile components during the crystal growth of rock-forming minerals such as garnet, staurolite, cordierite, etc.

Based on these data, regularities regarding the evolution of metamorphic processes in ancient shield complexes and fold belts have been deduced. The ancient geothermal gradients are somewhat inconsistent with one another at different stages of fold-belt formation. In the younger fold systems, they correspond to higher pressures during early stages of the geosynclinal regime and to higher temperatures and relatively lower pressures at its final stages.

Inversions of P-T conditions at different levels correspond to different metamorphic stages. In the more ancient and rigid fold belt bases, a discontinuous shift of the retrograde P-T path towards lower pressures is observed. In the metapelite fold-belt complex, a_{H20} decreases from 0.9 to 0.3 with increasing P and T_1, whereas in the granulite complexes a_{H20} is constant and equals 0.2. Partial CO_2 pressure at the amphibolite to granulite facies transition varies between 0.3 - 0.6 kbar.

INTRODUCTION

Advances in microprobe techniques have contributed greatly to studies on the compositions of coexisting rock-forming minerals. Detailed experimental and theoretical studies on mineral equilibria help to deduce precise and consistent mineralogical geothermometers and geobarometers, as well as activity coefficients of volatile components. Taking all these into account, one can follow the evolution of physico-chemical conditions of metamorphism during the formation of the ancient complexes. This study aims to relate the major regularities of metamorphic processes to geodynamic pecularities of the development of certain regions of the earth's crust. The author and his coworkers have been engaged in research on this problem for many years (Fed'kin, 1982a,b; 1986a,b; Fed'kin et al., 1983; Perchuk et al., 1985; Perchuk, 1986; Perchuk and Fed'kin, 1986; Pokrovskii et al., 1986). Studies on the metamorphic complexes of the Precambrian and Phanerozoic fold regions show that the parameters of mineral formation (temperature, pressure, H_2O and CO_2 regimes) are closely interrelated to the ancient geothermal gradient and geotectonic conditions of a region. The methods used here for the petrological investigation make it possible to reproduce the evolution of thermodynamic conditions of metamorphism and help in solving some geodynamic problems.

METHODS OF STUDY

According to Korzhinskii's (1973) principle of local mosaic equilibrium, our study was based on the assumption that at different stages of geological events, as the large mineral grains grow, either cores of the developing phases or their rims are in equilibrium. The same applies to mutual grain contacts and inclusions in minerals. In this case, chemical inhomogeneity of rock-forming silicates (garnet, biotite, staurolite, cordierite etc.) is indicative of the physico-chemical conditions of formation of certain zones and inclusions. Using the diffusion and/or growth mineral zoning as an indicator, changes in the thermodynamic parameters of metamorphism were first traced from Turkestan complexes of South Tien-Shan. Similar views were put forth by Perchuk (1983,1986), Perchuk et al., (1983,1984 and 1985); Lavrent'eva (1983); Fed'kin et al., (1983); Fed'kin and Danilovich (1986) Fed'kin, (1986a,b); Perchuk and Fed'kin (1986).

To estimate the P-T equilibrium conditions for mineral assemblages of metapelitic complexes, we have used the following experimentally determined geothermometers and geobarometers.

1. The Bi-Gr-geothermometer studied experimentally by Lavrent'eva and Perchuk (1981) with Aranovich's correction for the

Ca-content of Gr

$$RT\ln K_D^{Bi-Gr} + 5.9687T - 7391.64 - 0.07551P = 0. \qquad \ldots\ldots(1)$$

2. The Cor-Gr geothermometer

$$RT\ln K_D^{Gr-Cor} + 2.668T - 6134 - 0.03535P = 0 \qquad \ldots\ldots(2)$$

and the Cor-Gr geobarometer for assemblages Q + Gr + Cor+Al_2SiO_5

$$RT\ln K_{Mg}^{Gr-Cor} -1201 - 3.62T + 0.45213P = 0 \qquad \ldots\ldots(3)$$

3. The Sta-Gr geothermometer

$$RT\ln K_D^{Sta-Gr} + 7.7051T - 7041.1 = 0 \qquad \ldots\ldots(4)$$

and the Sta-Gr geobarometer (Fig.1) for Sta+Gr+Bi + Mu + Al_2SiO_5+Q paragenesis (Fed'kin, 1975). The analogous expressions for Bi-cor and Bi-Sta pairs may be inferred from combination of the equations (1), (2) and (1), (4) :

$$Rt\ln K_D^{Bi-Cor} + 3.031T - 1252 - 0.04\ P = 0 \qquad \ldots\ldots(5)$$

$$RT\ln K_D^{Bi-Sta} + 2.0064T - 350.54 - 0.0755P = 0. \qquad \ldots\ldots(6)$$

The entropy changes of the exchange equilibria in these pairs are very slight and the accuracy of the geothermometers (5) and (6) permits one to use them as tentative ones. The minerals Bi, Cor, and Sta have great ability to exchange their composition and the Bi-Cor and Bi-Sta thermometers can function sensibly only in case when the real mineral compositions are not far from the equilibrium ones. Nevertheless, they can provide us with further information on equilibrium relations in the assemblages containing these minerals.

---

*Symbols: And-andalusite, Bi-biotite, Ca-calcite, Chl-chlorite, Cor-cordierite, Dol-dolomite, Fib-fibrolite, For-forsterite, Fsp-feldspar, Gr-garnet, Ky-kyanite, Mu-muscovite, Pl-plagioclase, Q-quartz, Sil-sillimanite, Sta-staurolite, Tur-tourmaline, Woll-wollastonite, R-universal gas constant (1.987 cal.grad. mol) T-temperature°, K, p-pressure, bar; $K_D^{A-B} = X_{Mg}/(1-X_{Mg})\ /\ X_{Mg}/(1-X_{Mg})$ distribution coefficient, $K^{-A-B} = X_{Mg}^{A}/X_{Mg}^{B}$ Partition coefficient of Mg between phases A and B; X_{Mg} = Mg/(Mg+Fe+Mn).

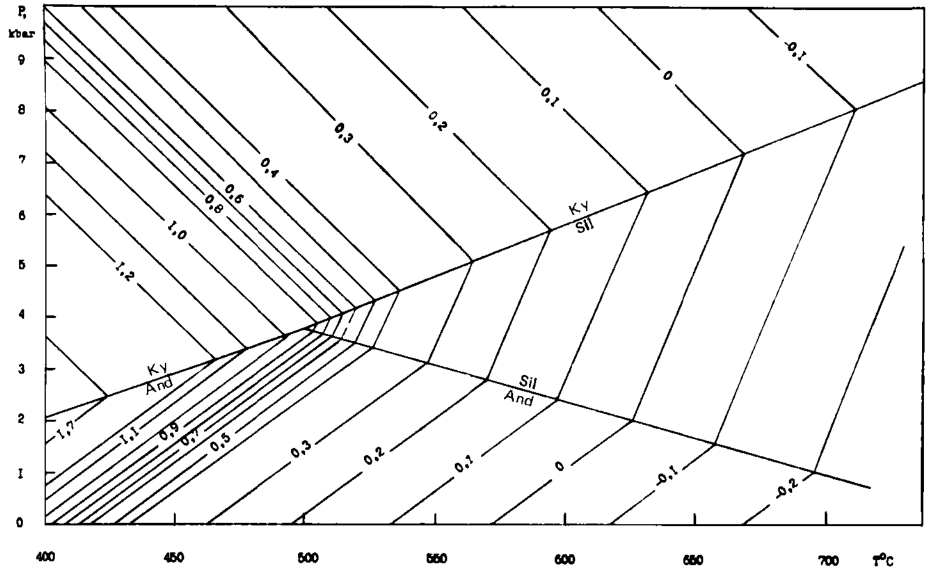

Figure 1. Staurolite-garnet geobarometer for Sta + Gr + Bi + Mu + Al_2O_3 SiO_2 + Q parageneses; the figures are lnk $= X_{Mg}^{Sta} / X_{Mg}^{Gr}$.

4. Three internally consistent geobarometers are as follows:
Q + Gr + Bi + Al_2SiO_5 + Pl; Q + Gr + Bi + Mu + Al_2SiO_5 ;
Q + Gr + Bi + Mu + Pl

(Aranovich, 1983). The activity composition relationships for garnet and plagioclase are given according to Aranovich (1983).

In this paper, mineral equilibria in staurolite-garnet-biotite schists from the Borsh series, North Pamirs (Sample 332a) are considered. Besides Sta, Gr, Bi, Mu, Pl and Q, other minerals in the rock are as follows: secondary Chl developed after Bi, pseudomorphic andalusite after kyanite, as well as small amounts of accessory apatite, magnetite, ilmenite, and zircon. There is no

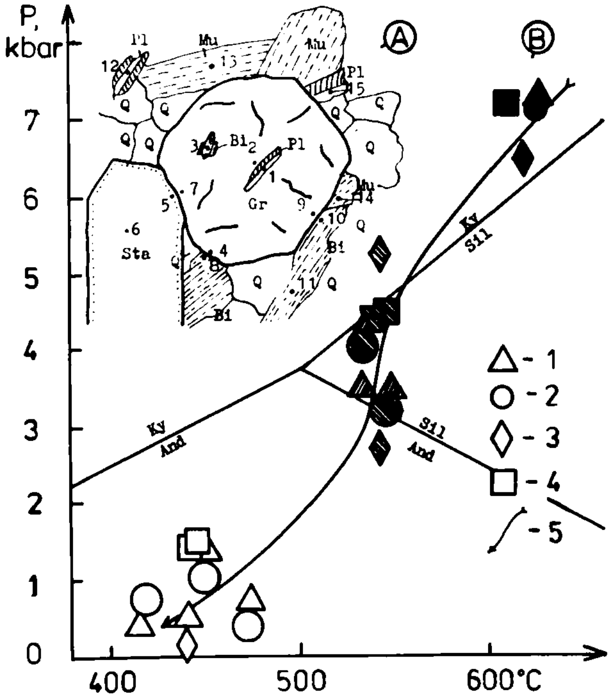

Figure 2. The mineral interrelations in the specimen No.332a (A), and P-T conditions of their formations (B). The point numbers correspond to the numbers of analyses (Table 1). 1-4 - geothermobarometers: Bi-Gr-Pl-Al$_2$SiO$_5$ (1), Bi-Gr-Mu-Pl (2), Bi-Gr-Mu-Al$_2$SiO$_5$ (3), Sta-Gr-Bi-Mu-Al$_2$SiO$_5$ (4); 5 - P-T evolution trend. Full symbols-core, open rim, striped symbols-rim-core combinations.

Table 1.

Microprobe analyses of minerals from the specimen No 332a (North Pamirs)

Analyses Nos.	1	2	3	4	5	6	7	8	9	10	11	12	13	14	15
Mineral	Pl_i	Gr_c	Bi_i	Gr_r	Sta_r	Sta_c	Gr_r	Bi_r	Gr_r	Bi_r	Bi_c	Pl_c	Mu_c	Mu_r	Pl_c
SiO_2	65.41	37.31	33.62	36.90	27.81	26.98	37.48	34.95	37.67	35.46	36.62	63.63	47.20	46.25	61.38
TiO_2	-	-	-	0.05	0.02	-	0.06	1.47	-	-	1.69	0.16	0.41	0.74	0.03
Al_2O_3	22.11	21.50	18.53	19.15	53.36	53.38	21.14	19.89	20.13	24.09	19.72	21.85	36.49	35.72	24.03
FeO	0.15	37.32	26.07	32.00	12.11	14.04	30.50	20.58	36.98	24.28	16.83	0.17	0.77	0.75	0.22
MgO	0.01	2.55	8.85	1.83	1.65	1.05	3.01	11.21	1.69	8.61	11.48	-	0.42	0.67	0.09
MnO	-	1.31	0.37	8.89	1.13	0.40	5.75	0.33	1.34	0.29	-	-	0.01	-	0.09
CaO	1.57	0.62	0.19	1.19	0.12	-	1.40	-	1.35	-	-	4.47	-	-	5.68
Na_2O	10.42	-	-	0.04	0.07	-	0.18	0.76	-	-	0.72	9.65	1.39	1.34	8.26
K_2O	0.24	-	5.68	-	0.34	-	0.08	6.54	-	4.06	9.28	0.34	9.06	9.16	0.07
Total	99.91	100.61	93.31	100.05	96.61	95.85	99.60	95.73	99.16	96.79	96.34	100.27	95.75	94.63	99.85
Cations to 8(Pl), 11(Bi,Mu), 12(Gr), and 23,5(Sta) oxygen atoms without the hydrogen															
Si	2.875	2.996	2.658	3.032	3.986	3.914	3.018	2.626	3.076	2.609	2.714	2.818	3.092	3.073	2.731
Ti	-	-	-	0.003	0.002	-	0.004	0.083	-	-	0.094	0.005	0.020	0.037	0.001
Al	1.146	2.035	1.727	1.854	9.015	9.128	2.006	1.762	1.937	2.089	1.722	1.140	2.817	2.798	6.260
Fe	0.006	2.506	1.724	2.198	1.452	1.703	2.054	1.293	2.525	1.494	1.043	0.006	0.042	0.042	0.008
Mg	0.001	0.305	1.043	0.224	0.352	0.227	0.361	1.255	0.206	0.944	1.268	-	0.041	0.066	0.006
Mn	-	0.089	0.025	0.619	0.137	0.049	0.392	0.021	0.093	0.018	-	-	0.001	-	0.003
Ca	0.074	0.053	0.016	0.105	0.018	-	0.121	-	0.118	-	-	0.212	-	-	0.271
Na	0.888	-	-	0.006	0.019	-	0.028	0.111	-	-	0.103	0.829	0.176	0.173	0.712
K	0.013	-	0.573	-	0.062	-	0.008	0.627	-	0.381	0.877	0.019	0.757	0.776	0.004
Total	5.003	7.986	7.765	8.041	15.043	15.021	7.993	7.779	7.955	7.536	7.821	5.030	6.946	6.965	4.996
The mineral composition parameters															
X_{Mg}	-	0.103	0.327	0.071	0.180	0.115	0.123	0.413	0.070	0.295	0.446	-	-	-	-
X_{Fe}	-	0.848	0.540	0.699	-	-	0.701	0.425	0.858	0.474	0.367	-	-	-	-
X_{Ca}	0.076	0.018	-	0.033	-	-	0.041	-	0.040	-	-	0.200	-	-	0.274
$X_{Al}{}^{VI}$	-	-	-	-	-	-	-	-	-	-	-	-	0.948	0.928	-

Abbreviations: c - core, r - rim, i - inclusion, X_{Mg}^{Sta}= Mg/(Mg+Fe), X_{Mg}^{Gr}/Σ(VIII), X_{Mg}^{Bi}=Mg/Σ(VI),

X_{Ca}^{Gr}=Ca/Σ(VIII), X_{Ca}^{Pl}=Ca/(Ca+K+Na), X_{Fe}^{Bi}=Fe/Σ(VI, X_{Fe}^{Gr}=Fe/Σ(VIII), X_{Al}^{Mu}=Al^{VI}/Σ(VI).

Table 2.

P-T conditions of formation of some mineral associations in the specimen No.332a (North Pamirs)

Geothermobarometers	BGPA		BGMA		BGMP		SGBM	
Association	T°C	P,kbar	T°C	P,kbar	T°C	P,kbar	T°C	P,kbar
$Gr_2Bi_3Pl_1Mu_{13}Sta_6$	627	7.30	620	6.40	626	7.14	610	7.2
$Gr_9Bi_{10}Pl_{12}Mu_{14}Sta_6$	534	3.99	536	4.26	534	4.06	528	4.4
$Gr_7Bi_{11}Pl_{15}Mu_{14}Sta_5$	549	3.49	543	2.76	547	3.27	546	4.5
$Gr_4Bi_8Pl_{15}Mu_{14}Sta_5$	474	0.71	464	0.55	471	0.34	445	1.5
$Gr_9Bi_{11}Pl_{15}Mu_{14}Sta_5$	415	0.38	-	-	418	0.74	443	1.55
$Gr_4Bi_{11}Pl_{12}$	441	0.48	-	-	-	-	-	-
$Gr_9Bi_8Pl_{15}Mu_{13}$	451	1.40	442	0.05	449	1.00	-	-

Note: The mineral figures correspond to the numbers of analyses (Table 1).

reaction between the major rock-forming minerals Sta, Gr, Bi, Mu, Pl within the rock. Hence, the changes in physico-chemical conditions of their crystallization are reflected only by the alteration of large-grain composition from core to rims.

The mineral interrelations in the thin section of 332a and the points where the microprobe analyses (Table 1) have been obtained for coexisting phases are shown in Fig. 2a. The thermodynamic parameters (T and P) of the inner, intermediate, and outer zones of the equilibrium garnet staurolite-biotite were compared. These data are summarized in Table 2 and shown in Fig. 2B together with the proposed equilibrium conditions between the core of one mineral and the rim of another. The geothermometers and geobarometers we used were consistent within an accuracy of (±20°C,± 0.7kbar) respectively. The highest parameters of mineral formation were obtained at the contacts between garnet central zones and Bi and Pl inclusions, whereas the lowest ones were at the contacts between the grain borders. Sometimes, the Bi composition along its cleavage has been changed more intensively then along its cross-section. In such grains, reverse zoning has been observed. In this case, P-T conditions of the equilibrium Gr-Bi may differ by 100°C and 3.5-4.0 kbar (Table 2, analyses 2,3), Gr composition at the grain rim remaining almost unchanged (Table 1, analyses 4, 9). This is due to the fact that minerals show different sensitivities to changes in chemical compositions under variable thermodynamic conditions. Staurolite, garnet, and feldspar are highly sensitive to any changes in external parameters, although they are rather inert to the changes in their compositions. The high capacity of Gr for recrystallization and continuous growth of outer zones appears to protect inner zones from the chemical effects. Bi and Pl are the most sensitive to any changes in T and P and their compositions are thus modified with variation in these parameters. They commonly occur as new generations of different composition in the groundmass and as a rule are indicative of the latest, low-temperature rock reconstructions. Thus, microprobe analysis recognized small grains of a newly grown plagioclase containing 2-4 mole per cent of anorthite (sample 332a). This Pl displays unrealistically high P values (above 10-15kbar) irrespective of Gr composition, whereas Pl_{20-27} grains in contact, together with either Bi-Gr or Sta-Gr geothermometers, agree well in pressure estimations (Table 2).

In the light of the foregoing, microprobe analyses were carried out on the minerals of metamorphic rocks of the ancient fold-belt systems. Particular attention was paid to the study of compositions of silicate minerals at mutual grain contacts and in the inclusions. With this approach it may be assumed that the composition of coexisting phases is indicative of the changes in physico-chemical conditions of metamorphism at different stages of the formation of a given complex. Therefore a point referring to the different mineral zones may be grouped into an evolutionary trend of P-T parameters on the P-T diagram.

RESULTS AND DISCUSSION

Thermobarometric calculations based on the microprobe analytical data on coexisting minerals allow estimation of the physico-chemical conditions of the formation of the ancient metamorphic complexes which form a fold belt of the Phanerozoic geostructures (Fig. 3). In many cases we succeeded in recognizing the regularities of the evolution of P-T conditions at the prograde and retrograde metamorphic stages and figured out separate periods of metamorphism. The metamorphic P-T parameters obtained for the core and rim mineral compositions are indicative of certain periods in the geological history of the region. But

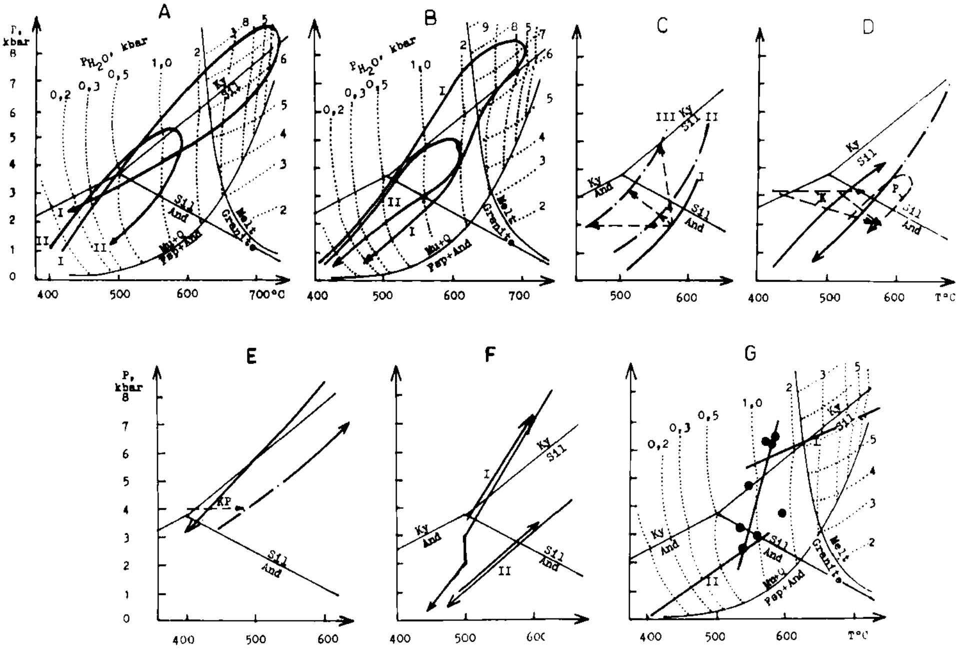

Figure 3. P-T trends of metamorphism of the ancient fold-belt complexes: A-the Belopotok suite, Ukrainian Carpathians; B-The Karakchatau Mountain complex, Uzbekistan; C-The Kasan complex, the Middle Tien-Shan; D-The Male Carpaty crystalline complex (CSSR); E-The Povazsky Inoves-crystalline complex (CSSR); F-The Borshit series, North Pamirs; G - The Turkestan complex, Sokh river basin, South Tien-Shan, and P-T conditions of formation Mu+Q+Fsp+Al_2SiO_5 paragenesis. Triple point of Al_2SiO_5 polymorphs. The line of the Mu +Q stability is calculated according to Robie et al. (1978), the granite melt curve after Perchuk and Fed'kin (1976). Dotted lines are these equilibria for different P_{H_2O}(kbar). Dashed lines are P-T trends after K-Korikovskii et al. (1985), Perchuk et al. (1986), KP-Korikovskii and Putis (1986). Dotted-dashed lines are the proposed trends based on our preliminary data.

the relation between these periods, which consist of gradually changing conditions of mineral formation (P-T trends), is often difficult to determine. We aim at further P-T investigations, but what we attempt at present is to group conventionally the points obtained in the different parts of zoned crystals, inclusions, and at the phase contacts into a P-T trend. The metamorphic complexes under investigation were the most ancient ones, which were high grade metamorphosed. They form part of the fold-belt system surrounding Precambrian median massifs or constitute the basement for the fold-belt. Unlike the Precambrian shield, these complexes display distinct traces of both prograde and retrograde stages (Fig. 3A, B, D, E). In most cases, the retrograde branch of the trend is characterised by higher temperatures than the prograde one. However, some complexes, such as Povazsky Inovec (Czechoslovakia) show the reverse relations. The samples from the Borshit series (North Pamirs) have a complex mineral zoning (Fed'kin, 1982b ; Fed'kin et al., 1983). This is evidence for repeated variations in metamorphic parameters and the metamorphic path. On the other hand, some samples from the Borshit series show traces of uneven shift of geothermal gradient during the course of development of the region and evolution of metamorphic conditions. This phenomenon is typical of the bases of ancient fold-block or ridges of an ancient foundation which underwent tectonic crushing and differential ascent of some blocks. The Turkestan complex of South Tien-Shan is a convincing example of such a geological phenomenon. Based on the thermodynamic parameters obtained for the complex central zone in the Sokh river basin, the following two stages of deep-seated mineral formation can be distinguished: (I)high-pressure stage at $T = 540-700^{o}C$ and $P = 5.7 - 7.0$ kbar. (II)low-pressure stage at $T = 410-570^{o}C$ and $P = 0.2-3.9$ kbar (Fig.3-6). A sharp ascent of the Sokh river block and the resulting decompression and degassing of the complex took place between these two stages under nearly isothermal conditions (Fed'kin, 1982a, 1986). What is noteworthy here is the observation of the shift of geothermal gradient towards higher temperatures (at $P_{const.}$) or lower pressures (at $T_{const.}$) in the ancient fold bases. The same applies to the relatively folded surroundings of median massifs and shields. In the latter, one or several metamorphic cycles were recognized using the method of physico-chemical petrology (Fig. 3A, 3B). Thus, in the ancient

Belopotoc suite (Uzbekistan), the transition of P-T mineral-formation conditions from prograde to retrograde occurs at 2 levels: at T = 700-730°C and P = 8.5 - 9.0 kbar, and at T = 580-610°C and P = 5.0-5.4 kbar. These levels correspond to the different stages of metamorphism. It is also likely that there were more stages, but their traces have dissappeared, due to later more intensive metamorphic processes.

ESTIMATION OF FLUID REGIME

During metamorphism in most of the ancient fold-belt complexes, the behaviour of H_2O and CO_2 regimes can be estimated by either water and carbonate-mineral equilibria or the beginning of granitic eutectic melting under conditions of variable water activity. Q-Mu schists are widespread in the above-mentioned Belopotoc suite, but they do not contain Fsp+Sill assemblage, nor do they show traces of melting and migmatization. Comparing these data with the P-T evolution trends of physico-chemical conditions of the Belopotoc suite metamorphism (Fig. 3A), one can come to the conclusion that in the rocks of the above-mentioned complex, partial water pressure P_{H_2O} is 5-6 kbar at the maximum metamorphic level (T=650-700°C, P=7.5-8.5 kbar). Lower H_2O pressures would cause Mu dehydration, whereas higher ones would give rise to granitic eutectic melting at the same P-T parameters. Similar relationships were observed in the metapelites of the Karakchatau Mountain complex (Fig. 3B). At the peak of the first metamorphic stage (700°C, 8.5 kbar), P_{H2O} was determined to be 4.5-6 kbar, whereas at the second stage $P_{H_2O} \geqslant 2.0$ kbar. The monovariant assemblage Mu + Q + Fsp + Al_2SiO_5, was formed in the rocks of the Turkestan complex within a narrow temperature range 530-570°C at $P_{H2O}=0.8-1.4$ kbar (Fig. 3G). P-T conditions of these parageneses were estimated by Bi-Gr and Cor-Gr geothermometers. In this complex, partial CO_2 pressure was calculated from the equilibria Cc + Q=Wol+CO_2 (0.2-0.6 kbar) and Dol + Q = Cc + For + CO_2 (0.5 kbar).

The analysis of metamorphic fluid regimes showed that H_2O and CO_2 behaviour in the Phanerozoic fold-belt regions differed markedly from that in Precambrian shields (Aranovich etal., 1987). In the zonal complexes of the ancient fold-belts, H_2O acti vity was seen to decrease from 0.9 to 0.3 with increasing pressure, whereas in granulites, constant H_2O of about 0.2 (Fig. 4) attended a distinct P-T trend in the evolution of metamorphic

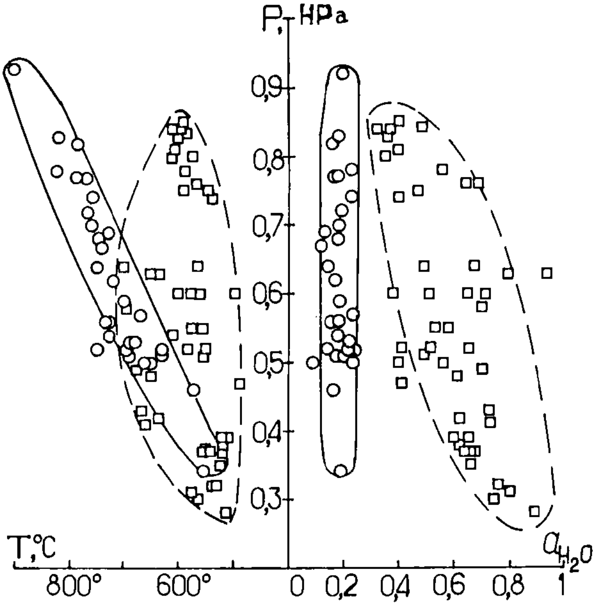

Figure 4. P-T (left) and P- α_{H2O} (right) correlations for granulites (circles) and for zonal metamorphic complexes (squares).

conditions. Taking into account the effect of increasing rock porosity at a high metamorphic level, as well as the salting-out effect, one can interpret these peculiarities and construct a model of essentially water composition of metamorphic fluid which is close to the ratio of volatiles in the present-day lithosphere (Aranovich et al., 1987). According to this model, the partial CO_2 pressures of metamorphism of fold-belt complexes did not exceed 0.3-0.6 kbar.

Based on the microprobe data obtained and the interpretation in terms of P-T conditions, the following inferences may be drawn:

1. The development of metamorphic processes in all the fold-belt regions proceeds with an attendant time-shift of the isothermal gradient towards lower pressures (or elevated temperatures) and rarely in the reverse direction.

2. In relatively rigid geostructures exposed to tectonic transformation or crushing, changes in geothermal environment (shift of geotherms) are for the most part uneven and are specific to the tectonic environment of a region. This is connected with the interchange of relatively quiet periods and long-term

geothermal endurance with periods of complex sharp ascent.

3. The methods of physico-chemical petrology enable us to recognize the cyclicity of metamorphic processes and to follow their evolution at the prograde and retrograde stages. These features are best manifested both in the plastic fold systems surrounding medial massifs and in the basement of fold structures (belts) of Alpine type.

4. In the ancient fold-belt complexes, water activity during the course of metamorphism decreases from 0.9 to 0.3 with increasing pressure. Contrary to this, in the shields a constant water activity H_2O = 0.2 has been estimated. Partial CO_2 pressures of the metamorphic transition from amphibolitic to granulitic facies vary within 0.3 and 0.6 kbar.

ACKNOWLEDGEMENTS

The author is grateful to Dr. L.Ya.Aranovich, Institute of Experimental Mineralogy, USSR Academy of Sciences, for review of the manuscript and his helpful remarks. The author thanks T.Kazachenko and L.V. Khudyakova for their help during preparation of the paper.

REFERENCES

Aranovich, L.Ya., 1983. Biotite-garnet equilibria in metapelites. I. Thermodynamics of solid solutions and mineral reactions. In: Contributions to Physico-chemical Petrology, v.11,"Nauka" Press, Moscow (in Russian), pp.112-127.

Aranovich, L.Ya and Podlesskii, K.K., 1983. The cordierite-garnet-sillimanite-quartz equilibrium: experiments and applications. In: S.K. Saxena (Editor), Kinetics and Equilibrium in Mineral Reactions. Springer-Verlag, New York, pp.173-198.

Aranovich, L.Ya., Shmulovich, K.I. and Fed'kin, V.V. 1987. H_2O and CO_2 activity at metamorphism: estimations and possible evolution mechanism. In: Contribution to Physico-chemical Petrology, v.19, "Nauka" Press, Moscow (in Russian) (in press).

Fed'kin, V.V., 1975. Staurolite - composition, properties, parageneses, formation conditions, "Nauka" Press, Moscow, (in Russian), 272p.

Fed'kin, V.V. 1982a. Nonequilibrium mineral assemblages as indicators of the metamorphic evolution of aluminosilicate complexes. In: Geology of the metamorphic complexes, Sverdlovsk (in Russian), pp.63-71.

Fed'kin, V.V. 1982b. Evolution of metamorphism of the oldest metamorphc rock masses in the North Pamirs. Dokl. Akad. Nauk SSSR. (in Russian), 268(1): 175-180.

Fed'kin, V.V. 1986a. Chemical inhomogeneity in minerals and evolution of metamorphism. In morphology and phase equilibria of minerals - IMA 1982, Sofia, pp.323-332.

Fed'kin, V.V. 1986b. Geothermobarometry of the metapelitic complexes and the problem of metamorphic evolution. In: Experiments for solution of actual geological problems. "Nauka" Press, Moscow (in Russian), pp.183-200.

Fed'kin, V.V., Ghirnis, A.V. and Yakovleva, L.Yu. 1983. Thermodynamic conditions of formation of the oldest metamorphic rock masses in the North Pamirs. In: Contributions to Physico-chemical Petrology, "Nauka" Press, Moscow (in Russian), 11: pp.320-366.

Fed'kin, V.V. and Danilovich, Yu.R. 1986. Thermodynamic regime of the metamorphism of the Pre-Mesozoic rocks of the Rakhov mountains. Dokl. Adad. Nauk SSSR,(in Russian) (261)3: 191-196.

Korikovskii, S.P. and Putis, M. 1986. Metamorphic zoning and diaphthoresis in the Povazsky Inovec crystalline complex. Geol. Zbor. Geol. Carpath. (Bratislava), (in Russian), 37: 115-136.

Korikovskii, S.P., Cambel, B., Baronikhin, V.A. Putis, M. Miklosh, Ya.1985. Phase equilibria and geothermometry of the metapelitic hornfelses around the Modra granite massif. Geol. Zbor. Geol. Carpath., (Bratislava) (in Russian), 36(1): 51-74.

Korzhinskii, D.S., 1973. Theoretical foundations for mineral paragenesis analyses. "Nauka" Press, Moscow, (in Russian), 288.

Lavrent'eva, I.V., 1983. On the regression metamorphic stage of the Khanka rocks (Primorie). Mineralogical Journal (Kiev), (in Russian), 5: 65-76.

Lvarent'eva, I.V., Perchuk, L.L. 1981. Phase correspondence in the system biotite-garnet, Experimental data. Dokl. Akad. Nauk, SSSR, (in Russian), 260: 731-734.

Perchuk, L.L., 1983. Thermodynamic aspects of metamorphism. In: Zonal and polymetamorphic complexes, "Nauka" Press, Moscow (in Russian), pp.134-140.

Perchuk, L.L., 1986. Evolution of metamorphism. In: Experiments for solution of actual geological problems, "Nauka" Press Moscow (in Russian), pp.304-346.

Perchuk, L.L., Aranovich, L.Ya., Podlesskii, K.K., Lavrent'eva, I, Gerasimov, V.Yu., Fed'kin, V.V., Kitsul, V.I., Karsakov, L.P. and Berdnikov, N.V. 1985. Precambrian granulites of the Aldan shield, eastern Siberia, USSR, Jour. Metam. Geol., 3: 265-310.

Perchuk, L.L., Lavrent'eva, I.V., Aranovich, L.Ya. and Podlesskii, K.K., 1983. Biotite-garnet-cordierite equilibria and evolution of metamorphism, "Nauka" Press, Moscow (in Russian), 197pp.

Perchuk, L.L., Lavrent'eva, I.V., Kotelnikov, A.R. and Petric, I. 1984. Correlation of the thermodynamic regimes of metamorphism in the complexes of the Main Caucasus Range and the Western Carpathians. Geol. Zbor. Geol. Carpath. (Bratislava), (in Russian), 35: 105-155.

Perchuk, L.L. and Fed'kin, V.V., 1976. The temperature and Fluid regime of origin of granitoids. In: Thermodynamic regime of metamorphism, "Nauka" Press, Leningrad (in Russian), 97-105.

Perchuk, L.L., Fed'kin, V.V. 1986. P-T evolution of regional metamorphism. Geology and Geophysics (Novosibirsk), (in Russian), 65-69.

Pokrovskii, A.V., Fed'kin, V.V., Kuselman, A.R. 1986. Thermodynamic regime and formation conditions of the Karakchatau metamorphic complex (South Nuratau, West Uzbekistan). Uzbek Geological Journal, (2) (in Russian), 3-12.

Robie, R.A., Hemingway, B.S., Fisher, J.R. 1978. Thermodynamic properties of minerals and related substances at 298, 15K and 1 bar (10^5 Pascals) pressure and at high temperature. US. Govt. Printing Office, Washington, 456pp.

ON THE ELECTRICAL STRUCTURE BENEATH THE SOUTH INDIAN SHIELD AND ITS THERMOTECTONIC SIGNIFICANCE

U. RAVAL

ABSTRACT

The large-scale electrical texture of the greenstone-granite and gneiss-granulite terranes in the peninsular Indian shield is studied on the basis of existing magnetovariational and laboratory measurements. The spatial changes of the variation field are examined in terms of N-S and E-W orientations. The former are broadly correlated with the shear zones and metamorphic transition zones of the shield and the E-W disposition is indicative of an eastward gradient. The sea-land interface and younger sedimentary cover severely inhibit separation of possible intracontinental sources near the eastern and southern margins. Some numerical simulations are presented for a quantitative appreciation of the gradual and/or abrupt metamorphic gradations, as well as variations in the disposition of the mid-crustal conductive layer. For the latter, the crustal sections inferred on the basis of DSS (viz. Kavali-Udipi) imply the possibility of highly conducting zones at mid (Lower) crustal and upper-mantle depths on the eastern side of the Proterozoic Cuddapah Basin. Over the Eastern Ghat Mobile Belt (EGMB), a remarkable superposition of various geophysical parameters seems to exist. In the absence of the MT coverage, Adam's (1976) empirical relations have been utilized to estimate from the available heat-flow measurements, the expected depth ranges of the conducting zones at the intracrustal (ICL), asthenospheric (HCL) and upper-mantle (UCL) levels. Supportive evidence, viz., seismicity, gravity, magnetic and teleseismic P-wave travel-time residuals are presented and discussed in detail. The need for deep electrical probing experiments to evaluate (i) geotectonic correlations of the anomalies on finer scales and (ii) the possibility of a conductive feature parallel to the Eastern Ghat as suggested here from this study is emphasized.

INTRODUCTION

The realization that the electrical conductivity distribution provides an independent and complementary parameter (Schmucker, 1973; Tozer, 1981; Gough, 1986) to constrain crust and upper-mantle structures has led to increased activity in the electrical probing of the Precambrian shields (Jones 1981, 1987; Hjelt, 1984 and references therein). The significance of the electrical conductivity is attributable to (1) a large range of

Table 1.
A classification of Precambrian shields on the basis of inferred upper and lower crustal parameters.

Category	Region	P (gm/cm^3)	(S/m)	V_p (Km/s)	V_s (Km/s)	Poisson's ratio	Type
Normal	(C,M,A)-C U.U.		10^{-3}-10^{-4}	6.6	3.18	0.25	I
Intermediate	N-SC (S,G,Ch)-C N-SW;S-NO	3.11	100-300	6.8-7.3	4.1	0.25	II
Low	SE-AF;SE-GC; E-AF;SE-G C	3.11	10-50	6.8	3.4-3.7	0.30	III
South Indian Shield	Ch(po)	2.90*	2.63×10^{-8}+	6.33@to 6.64			
	S(S)	2.72	4.57×10^{-9}	5.50 to 6.2			
	G(Hy)	2.66	5.89×10^{-8}	5.83 to 6.5			
	G	2.66	10^{-8}	6.05 to 6.5			

(C,M,A)-C: Central, Manitoba, Alberta in Canada; U.U: Ukraine in USSR; N-SC: North Scotland; (S,G, Ch) - Superior, Grenville, Churchill Provinces in Canada; N-SW: North Sweden; S-NO: South Norway; SE-AF: Southeast African Shield; SE-GC: Southeast-Grenville in Canada; C(Po): Charnockite (Porthimud); S(S): Syenite (Sivamalai); G(Hy): Granite (Hyderabad); G: Granite. * surface values; (+ at 300°C; @ range obtained) from laboratory studies. (Lastavickova et al., 1988).

resistivity values of 10+6 to 10 (ohm-m) found up to the upper-mantle depths. Such high contrasts in some situations lead to better lateral resolutions than those of offered even by the seismic method and (2) its strong dependence on temperature and fluid content (including porosity, salinity and interconnectivity), which can play a crucial role in constraining the thermal and rheological profiles.

Detection of possible highly conductive layers at the lower (or mid) crustal levels in many parts of the world and the often found correlation with strong seismic reflectors (Jones, 1987) provides an impetus for coincident deep electrical and seismic probings and to delineate the electrical structure, especially below, terrains of variable metamorphic grades such as in the south Indian shield (SIS). Using the results of deep electrical and seismic probings from various shields, Jones (1981) has suggested some rules-of-thumb and a classification (Table 1) on the basis of inferred lower crustal (LC) structures in these areas. The primary interest of such studies is thus to decipher the conducting zone at the intracrustal level (ICL) and electrical asthenosphere (HCL). The candidates for the former include highly porous, interconnected layers with water contents of up to ~2% graphite, hydrated minerals, hydrous serpentinized rocks, deep faults, etc. Shankland and Ander (1983) and Jones (1987) have discussed these in detail and relate the electrical conductivity to grade of metamorphism, fluid fluxes and tectonic deformations within the old stable platform. The conductivity of the HCL, mostly due to fractional melting, is regarded as thermally induced near the litho-asthenospheric interface (Shankland and Waff, 1977; Jones, 1982; Tarits, 1986). The presence of carbon may also cause high conductivity (Duba and Shankland, 1987). Generally, the asthenosphere is deeper under continents than beneath oceans, but near the continental margins (or transition) a complex overlapping of the subterranean conductive zones may occur. The electrical structure beneath the SIS hence becomes particularly interesting owing to the following :-

- In the western and eastern parts of the Dharwar cratons (Fig. 1a) of the northern block of the shield (Naqvi and Rogers, 1987), one may expect a mid (or lower) crustal (LC) conductor as characterized by the 'normal' or Type I electrical structure in Table 1 above. The DSS study along the Kavali- Udipi profile (Kaila etal., 1979) does reveal strongly reflecting horizons at midcrustal depths and the heat flow (Gupta et al. 1987) and teleseismic P-wave travel time residuals (SriNagesh et al. 1989) corroborate the normal nature of this part of the SIS. It will be interesting to characterize the different blocks of the SIS on the basis of electrical zoning of their lower crusts as has been done for the Canadian and other shield regions (Jones, 1981).

* Recently Burke (1983) has suggested that the Closepet granite may be an old 'Andean' type feature. This calls for a comparison between the electrical signatures of this 'plate tectonic relic' with its present-day counterpart (Schmucker et al., 1964; Schwarz et al., 1984).

* The grade of metamorphism varies from greenstone through amphibolite to granulite facies. This may give rise to undulations/deformations of the intracrustal layers, depending upon the intensity of the stress and P-T regimes. The resulting shears between blocks of different rheology are a consequence of the deeper thermomechanical process responsible for the block uplift (20-25 km.) which appears to have caused the exposures of deep crust in the SIS. It thus provides us with an opportunity to analyse whether the high electrical conductivity at lower crustal levels is due to composition or caused by the intrinsic P-T regime at deeper levels. The problem is similar to that across the Kapuskasing zone (KSZ) of the central Canadian Shield (Woods and Allard, 1986; Kurtz et al., 1986). The intermittent existence of stable supracrustals within the southern granulite terrane (Drury et al., 1984) makes the distribution of possible midcrustal conductors more complicated although tectonically interesting.

* The disposition of the Proterozoic units, particularly the Eastern Ghat Mobile Belt (EGMB), with reference to the Archaean craton in the SIS seems anologous to the similar juxtapositioning of the Limpopo mobile belt and the Kapvaal craton and that on eastern side of the Canadian shield. In the South-African shield a change from a high-resistivity upper crust (10^4ohm-m) under the craton to moderate resistivity (~500 ohm) within the mobile belts is reported (Vanzijl, 1977) and in the case of the

Canadian region, Jones (1981) has presented characteristic transitions in the electrical conductivity from "normal" to "intermediate" to "low" types, as one moves from the central part to the eastern mobile belts (Edwards et al., 1980).

* Activity coeval with the Pan African and later events in the SIS (Hansen et al., 1985; Nair and Vidyadharan, 1982) suggest the possibility of a thin fold-belt similar to the one in the southern cape mobile belt of Africa. Such linear belts have revealed coincident electrical and static magnetic anomalies most probably caused by hydrous serpentinized basalts lying over a mobile belt due to past subductions of the oceanic crust (De Beer and Gough, 1980).

* Deep-seated faults/fractures within the SIS (Grady, 1971; Katz, 1978 Hari Narain and Subrahmanyam., 1986) may also contribute to electrical conductivity due to fluid content and heat flow. In addition there is also the possibility of reactivation of the old weak (rift)- zones (De Beer et al., 1975).

* Development of a nascent subduction (Sykes, 1978) and/or plausible transformation over the geological time-scale of the passive 'Indian margin' into an 'active' one- as has been conceived for the transition of the Atlantic to Andean type margin (Dewey, 1969). These factors will significantly modify the electrical structure near the margin.

* Recently Burke (1983) and Stein et al. (1987) have argued that the tractional forces due to the Himalayan-collision and geometries of plate boundaries and plate-push from the south appreciably affect the stress and thermal regimes of the Indian Shield. In view of this, the Proterozoic Mobile Belts (PMB) may perhaps act as 'rheological waveguides' constrained by interspersed stable Archaean cratons. Alternatively, possible interaction between the old Precambrian platform with the present-day tectonics becomes worth deciphering.

Towards an understanding of the above factors, knowledge of the electrical conductivity distribution beneath the SIS could provide an independent informational parameter to complement other geophysical data sets. However, except for the Indo-Australian magnetometric array study (Srivastava and Habiba Abbas, 1980; Srivastava et al., 1984) not many measurements are as yet available. The investigations following this geomagnetic depth sounding (GDS) experiment, have been primarily concerned with the channelling of currents (Thakur et al., 1986; Thakur, 1983; Ramaswamy et al., 1985; Mareschel et al., 1987), except for those by Srivastava et al., (1982) and Nityananda and Jayakumar (1981). In this study an attempt is made to reexamine the g.m. variation fields and search for possible large-scale correlations, particularly in the light of the points listed above.

ON ELECTRICAL SIGNATURES

G.M. Variation Field

The magnetometer array experiment (Thakur, 1983) provides the database for the observations discussed here. Fig. 1b shows the location of array stations on the geological and tectonic map of the area. The centrally situated and minimally disturbed Hyderabad station, in the northern part of the SIS, has been assumed a normal station for the sake of comparison.

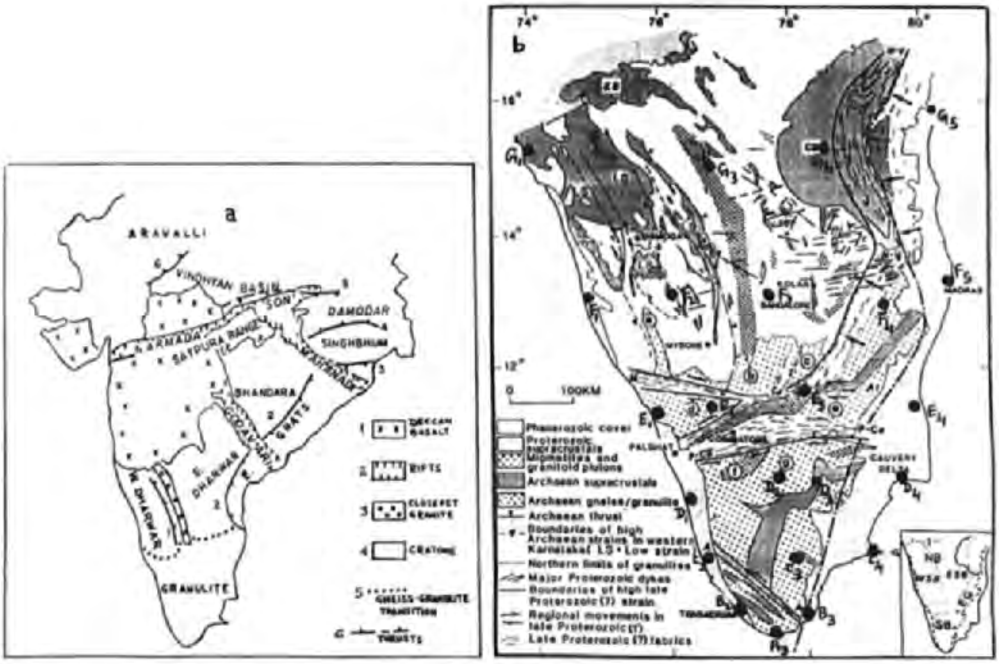

Figure 1. The South Indian Shield (SIS) and location of the magnetometer array stations.

Fig. 2a presents the spatial variations, in N-S orientation of the Fourier transform anomalies (FTA) and the variation field. The FTA are given for different periods (T=37 to 108 minutes). Near the Palghat-Tiruchi, line which is a major shear zone, a positive maximum is seen on the eastern side, perhaps controlled by the Annamalainagar station. The pattern of this eastern profile is similar for all periods. The change from positive to negative side takes place near the metamorphic transition (~13-14^{o}N). For the central and western profiles, the anomaly points are few owing to sparsity of FTA in these regions. In the case of the Sq.(H) variation also a southward increase is seen, with values along east (with respect to the SIS) remaining consistently above those along the western side. The southward increase and differences between the eastern, western and central profiles for the Z-component are given in Fig. 2b. The figure also

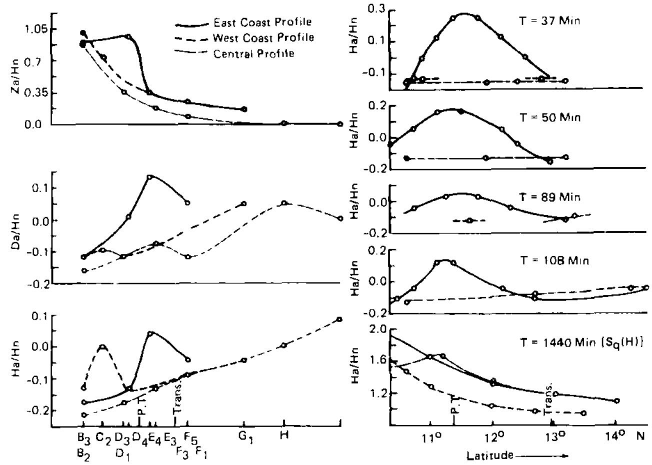

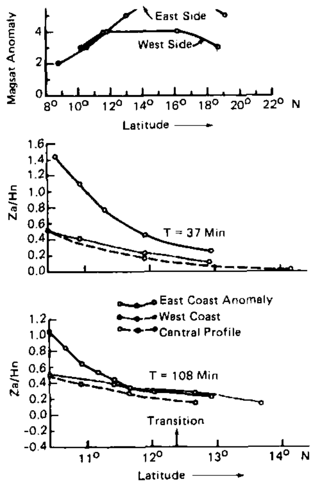

Figure 2a. The latitudinal (N-S) variation of (a) the relative geomagnetic field variations along the east, west and central profiles (on the left hand side) and (b) Fourier transform (F-T) anomalies of the horizontal (H) component for different periods (on the right). The abbreviations : P-T; CG; F; TZ respectively denote the Palghat-Tiruchi line, Closepet Granite, major faults and the transition (metamorphic) zone.

Figure 2b. Latitudinal (N-S) variation of the F-T anomalies of the vertical (Z) component for two periods along the east (E) west (W) and central (C) profiles. The top figure represents the magsat anomalies along the E & W margins.

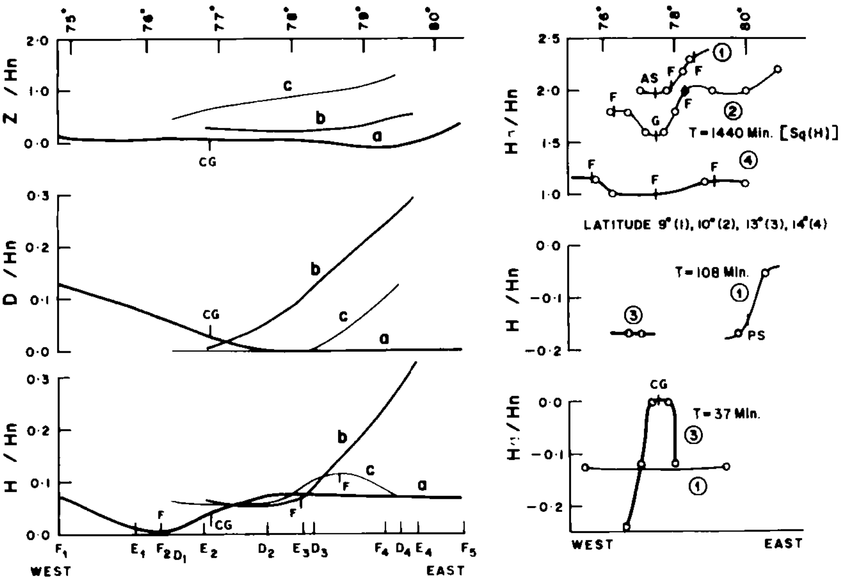

Figure 3. Longitudinal (E-W) variation of the (a) relative variation field (left) and (b) F-T anomalies for different periods.

gives long-wavelength changes in the static magnetic anomalies (Mishra, 1986). The spatial changes of the relative variation fields (Fig. 2a) also show a southward increase. For the D-component, the central profile is undulatory with gradient changes near Salem, Bangalore and Hyderabad and the H-profile depicts a steady negative increase with a perturbation near a major fault.

In Fig.3, which gives the E-W spatial changes, one notices that the amplitude of the variation fields (VF) for both H and D elements differs on either side of the Palghat-Tiruchi line and shows a southward increase. At different latitudes, the VF on the eastern side is greater. However, this difference between the E & W decreases southward, as may be expected from the peninsular geometry of the SIS. Near some major geological tectonic features, gradient changes could be seen. On the right-hand side of this diagram (Fig. 3) anomalies are given for different periods. At T=37 min, and 13^{O}N, a significant signature near the Closepet Granite is seen. The low in Sq.(H) at $\sim 10^{O}$N may be attributed to a subsurface intrusion and/or a deeper Moho. At T=108 min a relatively sharp change near the SE coastline (Palk-Strait effect) could also be seen.

Two points emerge: (a) there seems to be a significant variation in electrical signature as one passes from W to E and it will be valuable to decipher quantitatively how much of it could be attributed to differences in the ocean-continent transitions on either side and how much to the continental lithosphere; and (b) the Dharwar Craton and its roots, particularly the western block, has remained relatively undisturbed since its formation (~3.3 Ga ago); this is also supported by heat flow and a recent teleseismic study (SriNagesh et al. 1989). This region may be taken to represent the normal and stable platform and datasets over it may be used to standardize the geophysical signatures in other shield areas of the Indian subcontinent.

Induction Arrows

These also provide useful information regarding the subsurface conductivity distribution (Parkinson, 1959) and they are shown in Fig. 4 along the E, C and W profiles. The diagram also gives the changes caused in their azimuths and amplitudes due to variation in the period. The latter are often correlated with different source (or electric current) depths. Whereas the anisotropy or the nonuniform part of the change might have been caused locally,

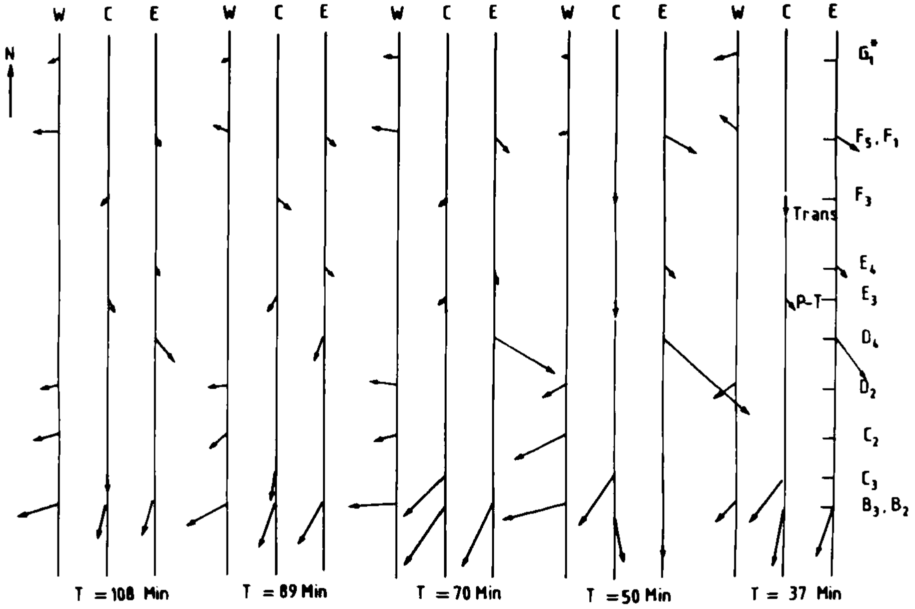

Figure 4. Multiperiod induction vectors along the E, W and C profiles.

over a regional scale one finds that the induction arrows on the W-side are transverse to the coast and those on the E-side are of relatively higher magnitude and are oriented in a SSE direction. Near the southern tip of the SIS, both merge into a SSW-NNE orientation which almost overlaps with the direction of motion of the Indian plate. Most of the deep continental faults are oriented NE-SW or transverse to these (Grady, 1971; Katz, 1978; Srinivasan and Sreenivas, 1977) and the anomalous stations of the induction field appear to lie over or in close proximity to these faults.

It appears to be of special interest to note that the orientations of the induction vectors near the coast conform closely with that of the first azimuth of the station anomalies over the Indian continent (Dziewonski and Anderson, 1983) and seem to correlate with the geometry and movement of the plate. Alternatively, they might be linked with the anisotropies in the thermal, rheological and electrical nature of the litho-asthenospheric system.

Numerical Models

Following Larsen (1975), single-station, long period data have been inverted (Sastry et al., 1990) to obtain a 1-D model up to upper-mantle depths below a region close to Hyderabad. This study has delineated conductors at lower-crustal, asthenosphere and upper-mantle transition levels. Multi-period induction responses, computed respectively for each conducting layer and for combined sections, are given in Figs. 5d and 5a-2. Although, in principle, the various period ranges are sensitive to different conductive depths, in practice it is difficult to achieve a spectral resolution owing to poor S/N ratios and masking effects.

The juxtapositioning of low-and high-grade terrains is marked by shears, uplifts and/or oblique over-thrusting, apart from some local exceptions, which distort the mega-layers in the crust. To estimate how undulations of a mid-crustal conductive layer will affect the induction response, some representative models of the metamorphic transitions are numerically simulated (Fig. 5 a,b & c). These 2-D models give the apparent resistivity variation across a deep fault separating the two regions of a bimodal metamorphic terrain. In one case, the conductivity is assumed to depend on the composition and hence the exposed deep crustal section is taken to be moderately conducting (Fig. 5a). In the

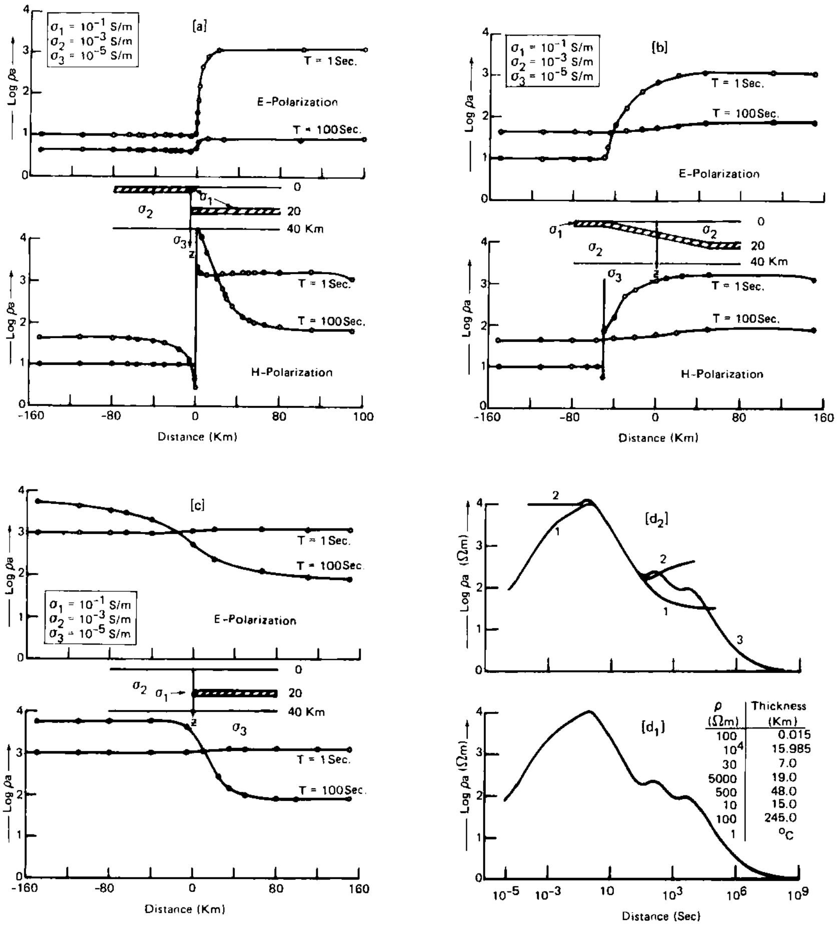

Figure 5. The apparent resistivity obtained numerically for various possible transition models. (A) sudden (fault) (B) gradual (Shear) and (C) partly present intracrustal layer (D1): 1-D layered model inferred at Hyderabad, (D2): component system of the 1-D model.

other case, the high electrical conductivity at the mid (or low) crustal level is attributed to the P-T regime at LC depths and thus the exposed section is assumed to be resistive (Fig. 5c). The third model represents the case where the transition (or uplift) is characterised by a gently dipping shear rather than a steep fault (Fig. 5b). These numerical results show the behaviour of the apparent resistivity expected along profiles from the Dharwar greenstone terrane to either the southern granulite zone or the EGMB. However in reality, possible remobilization of the EGMB and the intermittent presence of stable supracrustals in the southern granulite part may complicate the problem.

Laboratory Data

The dependence of electrical conductivity on temperature, fluidity, porosity/interconnectivity and salinity has motivated laboratory determinations thereof, under appropriate P-T conditions, on some representative rock samples of the SIS (Lastavickova et al., 1987). These data are, however, few and need to be augmented to examine (i) conductivity variations across metamorphic transitions and (ii) whether the conductivity is from deep crustal exposures or due to the P-T regime or composition. A wide spectrum of age groups available in the SIS allows study of the relationship between the electrical conductivity and age for the continental lithosphere. Table 2a gives conductivities of some representative rocks of the SIS, at 0.5 Gpa and 300°C which correspond to a depth of ~20 km. The Indian basalts are found to be more conductive than the average. Although SIS rocks, being older, exhibit relatively low conductivities, at high temperatures (between say 300 and 700°C) a steep rise in electrical conductivity is measured for the Porthimund charnockites and Sivamalai syenites. From measurements of compressional-wave velocities (Vp) over some rock samples, the following relation is obtained using a linear regression model

$$\log \rho \,(\mathrm{Ohm\text{-}m}) = A + B\, V_p\, (\mathrm{kms}^{-1}).$$

The influence of dehydration on the electrical conductivity-temperature relationship has also been analysed employing a temperature cycle (Sharma et al.1986) and it is seen that between 715 and 875°C serpentine shows an anomalous behaviour wherein its dehydration commences and is completed. Assuming anhydrous conditions below 10 km, a crustal electrical-conductivity profile was derived (see Table 2b) by Sharma et al. (1986) under the granite (G) and Peninsular gneiss (P) rocks.

Lower-Crustal (LCL), Asthenospheric (HCL) and Upper-Mantle conductors (UCL)

Adams (1976) has proposed empirical relations which connect the depths of the three possible major electrical layers and heat flow, and has discussed their significance (Adams, 1980). In Fig. (6) approximate estimates of these conductive layers under the SIS are presented from the available heat-flow measurements.

Table 2A.

Variation of electrical conductivity of some representative rocks of the SIS with P & T.

Rock type	Density (Kg/m^3)	V_p(m/s)	Conductivity (S/m) 0.5 Gpa 300°C	500°C
Granite (Hyderabad AP)	2660	6400	5.8×10^{-8}	9.2×10^{-7}
Granite (Hyderabad AP)	2660	6510	1.0×10^{-8}	2.5×10^{-6}
Charnockite (Porthimund TN)	2901	6640	2.6×10^{-8}	8.3×10^{-6}
Syenite (Sivamalai TN)	2718	6204	4.6×10^{-9}	1.5×10^{-6}

(Adopted from Lastavickova et al., Studia Geophysica et geodetica, in press)

Table 2B.

Conductivity profile up to Moho

Depth	Greenstone Log (ohm^{-1} cm^{-1})	Peninsular Gneisses Log (ohm^{-1} cm^{-1})
5	-	-
10	-	-10.35
15	-10.5	-10.05
20	-10.3	- 9.1
25	- 7.1	- 6.6
35	- 6.55	- 5.65
38	- 6.3	- 5.4

(Adopted from S.R. Sharma et al., 1986)

Electrical signatures and other g.p. parameters

As mentioned earlier, the paucity of deep electrical soundings in the SIS prevents, at present, a more quantitative and finer resolution of the electrical structure. Constrained by this, we have indicated above only some broad and large-scale trends. In the following, we discuss other available information for further elaboration.

HEAT FLOW

Owing to a close linkage between electrical and thermal states, the suggestion that the crust-mantle interface below the Indian Shield is hotter than its counterparts elsewhere (Rao and Jessop, 1974;Singh and Negi,1982) assumes special significance. One of the

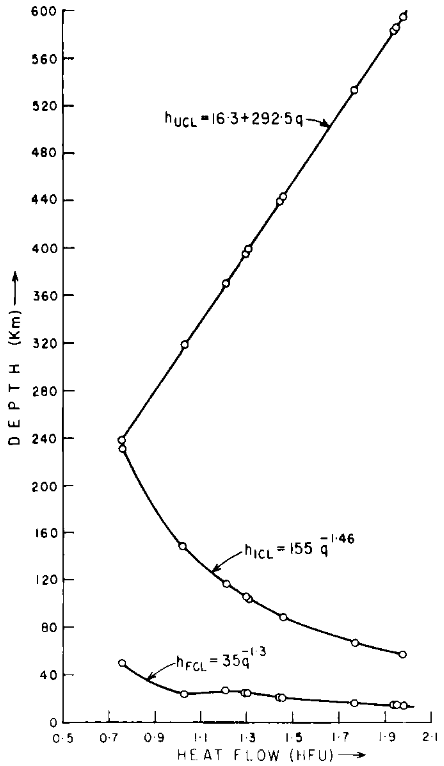

Figure 6. The ICL, HCL & UCL depths derived from Adam's empirical relations.

reasons for this could be the relatively large shear heating due to faster movement of the Indian Plate. A thermal anomaly generated near the litho-asthenospheric boundary (at about 100 km. depth) following jumps in the plate velocity (Froidevaux and Souriau, 1978) may reach the base of the crust in ~30-40 Ma. presuming only the heat conduction. Possible secondary convections and hydrothermal circulation may further enhance the rate of heat transport, particularly in the mobile belts and associated active zones. Thus, along the NE-SW orientation the Indian Plate might be relatively hotter, less viscous and electrically conductive. This inference seems to be supported by the orientation of the induction vectors and first azimuth direction of station anomalies near the coast (Dzeiwonski and Anderson, 1983), a geoidal low and teleseismic P-wave travel time residual studies. The collision in the north and plate push from the other sides may also give rise to stress-induced thermal regimes. While discussing the relatively hotter Moho below the Indian Shield, it may be pertinent to point out that the data considered in these suggestions belong to a mobile belt environment and not strictly to cold stable cratonic parts like western Dharwar,Bundelkhand and the Bhandara nuclei.This mobile belt (Radhakrishna and Naqvi, 1986) appears to form an intercratonic rheological wave guide and therefore within it a higher heat flow may result due to periodic remobilizations, including those during the last 200 Ma.

MAGNETICS

This aspect is connected with the heat flow and thermal gradient through depth of the curie-point isotherm. Table 3 gives the magnetic susceptibility of some representative rocks of the SIS (Subramanyam and Verma, 1982). Negi et al. (1987) have used heat-flow values to obtain expected depths of the magnetic and thermal lithospheric boundaries on the basis of the curie point of magnetite and the solidus of the upper-mantle rocks. From this,also the difference in the variation of these parameters on the eastern and western sides may be noted. A similar pattern is obtained from the Magsat anomalies over the SIS and their interpretation (Mishra, 1986), as seen above from the top diagram of Fig. 2a. The E-W aeromagnetic profiles (Fig. 8) on the eastern side of the Cuddapah Basin also exhibit a prominent magnetic anomaly which appears to have a N-S linear orientation and to be controlled by a regional high. Magnetic trends are also seen in

Table 3.

Magnetic susceptiblity of SIS rocks

Rock types	Range (K x 10^{-6} SI)
Granites	226- 38,956
Dolerites	892- 99,274
Granodiorites	226- 28,274
Archaean schists	226- 87,964
Amphibolites	666-103,672
Granulite facies gneisses	440- 13,823
Biotite gneisses	138- 10,317
Charnockites	
Acid	226- 53,407
Intermediate	226- 85,451
Basic	226-113,097
Ultrabasic	452-157,079
Khondalites	226- 7,401

Adopted from C. Subrahmanyam and R.K. Verma (1981).

the Tamil Nadu region and an intense NNW-directed feature along the Kerala coast (Ramachandran et al., 1986 and Suryanarayana and Bhan, 1985). From these magnetic features and recent reports (Hansen et al., 1985; Nair and Vidhyadharan, 1982) of formations coeval with the Pan-African thermal event, the possibility arises of younger (<1000 Ma.) fold belts similar to that near the southern cape of Africa. This may be of particular significance in view of the superposition of Bettie magnetic and SCCB conductive anomalies (De Beer et al., 1980) wherein it has been suggested that alteration of the oceanic crust near the continent-ocean transition or underneath the fold belts could give rise to such an overlap of magnetic and conductive anomalies.

GRAVITY

There are three main gravity features in the SIS. Their tectonic significance and possible relation with electrical signatures are examined. The first one is a long-wavelength regional low (Verma, 1985) which appears to correlate with suggestions of relatively high heat flow, uplift, low viscosity and high conductivity. It may imply that the depth of the asthenosphere, particularly in the EGMB and southern granulite part, could be shallower. On a local scale, a second characteristic anomaly is observed, across the transition from normal to exposed deep crustal sections (Verma, 1985) similar to the one reported over the Kapuskasing Structural Zone (KSZ) in the Canadian Shield (Fountain and Salisbury, 1981; Percival and Card, 1985). Mishra (in this volume), has quantitatively analysed this feature across the Palghat-Tiruchi (P-T) line and attributes the major gravity low south of the Palghat to thickening of the Moho. It is interesting to note that this gravity low coincides with the low in Sq. (H). The latter has been interpreted earlier in terms of a subsurface intrusion (Srivastava et al., 1982). The degree and gradient in g.m. variation fields and the low Sq.(H) may be caused by either granitic batholiths or Moho undulation. However, the long-period nature of the Sq. favours a deeper source. The third and an important gravity high lies over the EGMB (Kaila and Bhatia, 1981). It has been correlated with a linear anorthositic emplacement all along the EGMB continuing south (Fig. 7a), implying mantle upwelling. Rejuvenation of this zone, may be responsible for the observed heat flow and other attendant

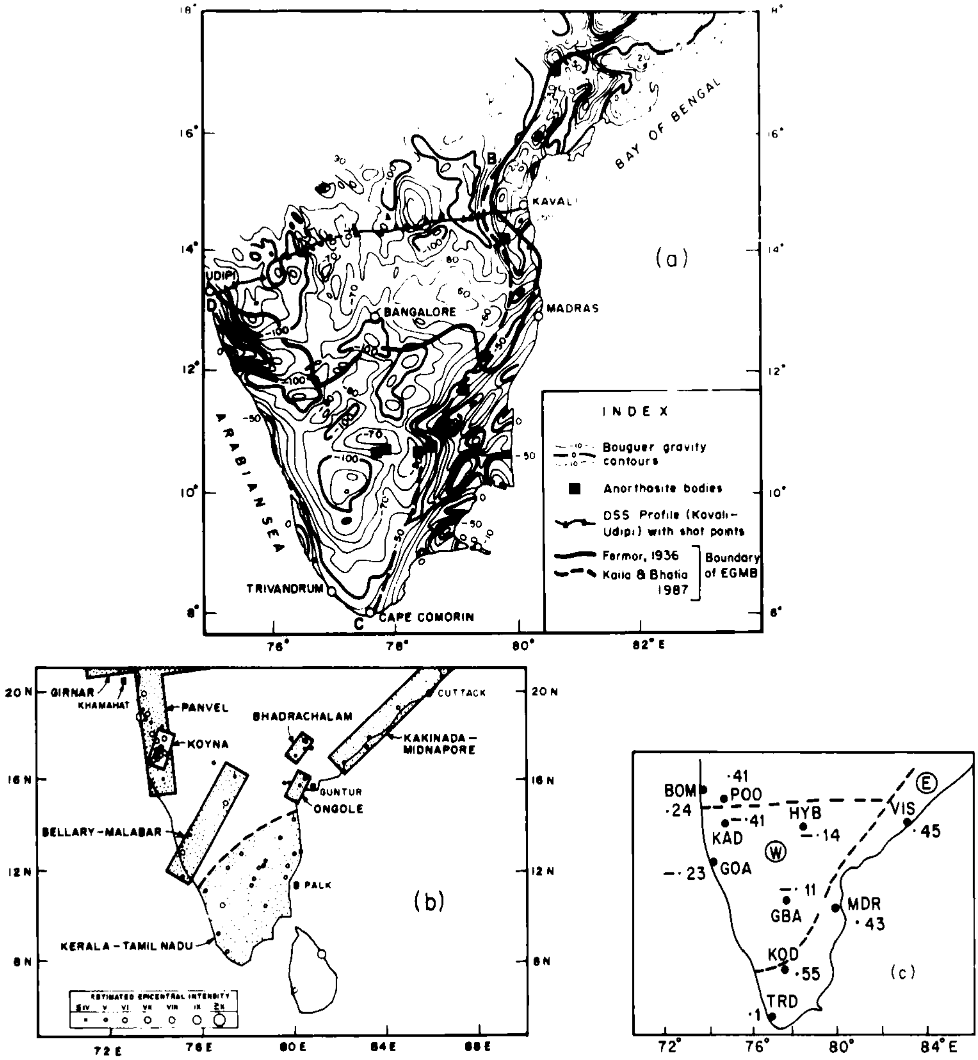

Figure 7. (a) The gravity field and anorthosite formation below 16^{0} N (b) the seismicity zones and (C) values of P-wave travel time residuals, over the SIS.

characteristics of the region. Alternatively, sensitivity of the EGMB and southern granulite part to the Pan-African event (~580 Ma.); Gondwana activity (~225 Ma.) and updoming (Burke and Dewey, 1973), plate separations on the eastern and western sides of the Indian plate and a flood-basaltic event (~65 Ma.) deserve closer examination. Recently, dykes coeval with the Deccan Trap activity have been confirmed (Anil Kumar et al., 1988) within this stable Archaean-Proterozoic shield.

SEISMICITY AND TELESEISMIC SIGNATURES

The first of these parameters, associated with the rheology of the lithosphere, may be connected with the electrical conductivity through the fluid-content, porosity, and P-T regime (Ranalli and Murphy, 1987) and hence their correlation assumes significance in the SIS. Grady (1971) has shown that most earthquake epicentres lie close to NE-trending deep faults in the Peninsular shield and Chandra (1977) has proposed a NNW-trending zone (Fig. 7) of seismic activity containing these faults, the EGMB and its southwest extension (See Fig.1b). The available focal depths in this region are 12 km. (17.5^{O}N, 73.7^{O}E-Koyna) and 33 km. (17.9^{O}N, 80.6^{O}E - Godavari). The focal depth below the EGMB may be indicative of the brittle-ductile transition within the crust and hence it is interesting to note that these depths lie close to a zone of reflectors (conductors?) as seen in the DSS section under the region (Fig. 8). Recently, SriNagesh et al. (1989) have analysed the teleseismic P-wave travel time residuals. The study shows that beneath the EGMB and southern granulite part of the SIS anomalous positive residuals (low velocity) are estimated in contrast to the western Dharwar region which is characterized by negative values (Fig. 7). This observation conforms with other g.p. indications discussed above.

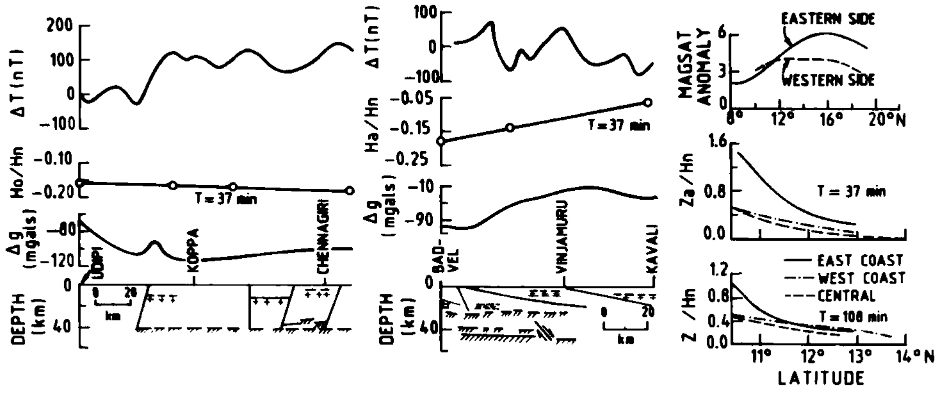

Figure 8. The structural sections near the east and west coast inferred from DSS studies. The gravity, aeromagnetic and geomagnetic field variations over these parts are also shown.

Seismic Structure below the E and W coasts

The crustal sections inferred on the basis of the DSS studies by Kaila et al. (1979) also clearly show the differences in the structures below the E and W coasts, as seen in Fig.8 (gravity, aeromagnetic and geomagnetic variations), which also gives a few other geophysical magneto-variational profiles in the region but not over same latitude on the western side; a feature revealed by the DSS section under the EGMB is the juxtapositioning of a midcrustal reflector and the indication of a mantle disturbance (upwelling or thrusting). From studies made elsewhere, both these factors could be linked with significant electrical signatures which may partly be responsible for the observed g.m. variation field and its gradient noted above. Separation of the contributions to the induction field from the juxtaposed midcrustal reflector and possibly a conductive asthenosphere is indeed a formidable signal-extraction problem, owing to the presence of younger sediments, deep faults and associated hydrothermal circulations, and the proximity of the coastline. It may thus be worthwhile to measure the g.m. variation field on the seaward side (Filloux, 1980; Tarits, 1986) and in corresponding regions of Antarctica (Crawford, 1974).

SUMMARY AND CONCLUSIONS

An attempt has been made to present a discussion of only the broad and long-wavelength electrical signatures over the peninsular part of the Indian Shield, constrained by the sparsity of station-density and of laboratory measurements and the absence of MTS, which severely inhibit finer resolutions at present. The representative numerical models provide the variations of resistivity expected on regional and local scales. A comparison of different geophysical, geological and tectonic signatures indicates that:

* The metamorphic transitions, shear zones, and deep faults (or old sutures) seem to correlate with changes in the g.m. variation fields. Electrical probing may help in tracing the possible rejuvenation of old and hidden weak zones in the SIS, during the Gondwanan and later activities (De Beer and Gough, 1980).
* Some of the anomalous stations lie close to deep seated continental faults as seen on the Landsat imagery.

* With respect to g.m. variation fields, the western Dharwar craton appears to be relatively undisturbed, in conformity with results of heat-flow and teleseismic studies.

* While the DSS is suggestive of a midcrustal layer and upper-mantle upwell beneath the EGMB, the heat-flow values support undulations of the mega-crustal layers.

* Different geophysical and tectonic signatures are seen to overlap remarkably over the EGMB. It may be worthwhile to find out if the same is true over various continuations of mobile belts over the Indian Shield (Radhakrishna and Naqvi, 1986). The linear trend, along the eastern margin near 80°E and the continent to ocean transition are sub-parallel to the 85°E and 90°E ridges. The signatures of activity along these might bear some relation to possible secondary convection in this region (Haxby and Weissel, 1986; Cazenave et al., 1987).

* A correspondence of particular significance is observed between the induction vectors and the first azimuth of the station anomalies near the margins, both seem related to geodynamics of the Indian Plate.

In conclusion, the study has attempted to bring out the significance of probing the electrical structures of this important segment of the continental crust-mantle, particularly with regard to the fact that within the SIS, Archaean supracrustals and Proterozoic mobile belts rest over one of the most active litho-asthenospheric systems of the present Wilson cycle and from this there clearly follows an urgent need for a focussed GDS and MTS in the region.

ACKNOWLEDGEMENTS

The author is grateful to M/S. K. Veeraswamy and R.B. Singh for their help in the computational work. Permission of the Director, NGRI to publish is thankfully acknowledged. The author has greatly benefitted from many fruitful discussions on the SIS, with Drs. S.M.Naqvi,D.C.Misra,N.K.Thakur and R.Srinivasan. Mrs.Nancy Rajan and Mr.C.Manohar have patiently assisted in the typing and drafting work respectively.

REFERENCES

Adam, A., 1976. Quantitative connections between regional heat flow and the depth of conductive layers in the earth's crust and upper mantle, Acta Geodaet. Geophys. et Montanist Acd. Sci. Hungary, 11: 503-509.

Adam, A., 1980. The change of electrical structure between an orogenic and an ancient tectonic area (Carpathians and Russian platform). J. Geomag. Geoelectr., 32: 1-46.

Anil Kumar., Bhaskar Rao., Y.J., Padmakumari., Dayal., A.M. and Gopalan. K., 1988. Late cretaceous mafic dyke in the Dharwar Craton. Proc. Ind. Acad. Sci. (Earth and Plant. Science), 97, 1: 107-114.

Burke, K., 1983. Is the Kapuskasing structure the site of a cryptic suture? (Abstract) A Lunar and Planetary Institute Workshop. Ottawa, Ontario, Canada: 20-23.

Burke, K. and Dewey, J.F., 1973. An outline of Precambrian plate movement. In: D.Tarling and S.K. Runcorn (Editors), Implications of continental drift to the earth sciences, 2, 1035, Academic Press, New York, 1035pp.

Cazenave, A., Monnereau, M. and Gilbert, D., 1987. Seasat gravity undulations in the Central Indian Ocean, Phys. Earth Planet. Interiors, 48: 130-141.

Chandra, U., 1977. Earthquakes of Peninsular India-A seismotectonic study. Bull. Seism. Soc. Amer., 67: 1387-1413.

Crawford, A.R., 1974. Indo-Australia, Gondwanaland and the distortion of a granulite belt. Tectonophysics, 22: 141-157.

De Beer, J.H., Gough, D.I. and Van zijl, J.S.V., 1975. An electrical conductivity anomaly and rifting in Southern Africa, Nature, 255: 678-680.

De Beer, J.H. and Gough, D.I., 1980. Conductive structures in southernmost Africa: a magnetometer array study. Geophys. J.R. Astr. Soc., 63: 479-495.

Dewey, J.F., 1969. Continental Margins: A model for conversion of Atlantic type to Andean type. Earth Planet. Sci. Lett. (3) 6: 189-197.

Drury, S.A., Harris, N.B.W., Holt, R.W., Reeves-Smith, G.J. and Wightman, R.T., 1984. Precambrian tectonics and crustal evolution in South India, J. Geol., 92: 3-20.

Duba, A.G. and Shankland, T.J., 1987. Analyzing electromagnetic Induction data: suggestions from laboratory measurements. Pure Appl. Geophys., 125: 285-289.

Dzeiwonski, A.M. and Anderson, D.L., 1983. Travel times and station corrections for P-waves at teleseismic distances. J. Geophys. Res., 88, B4: 3295-3314.

Edwards, R.N., Bailey, R.C. and Garland., G.D. 1980. Crustal and upper mantle electrical conductivity studies with natural and artificial sources. In: D.W. Strangway (Editor), The earth's crust and its mineral deposits, J.T. Wilson Symposium, University of Toronto, Geol. Assoc. Can. Spec. Publ., 20: pp.255-271.

Filloux, J.H., 1980. Magnetotelluric soundings over the north east Pacific may reveal spatial dependence of depth and conductance of the asthenosphere. Earth Planet Sci. Lett., 46: 244-252.

Fountain, D.M., and Salisbury, M.H. 1981. Exposed cross-section through the continental crust: implications for crustal structure, petrology and evolution. Earth Planet Sci. Lett., 56: 263-277.

Froidevaux, C. and Souriau, M., 1978. Thermo-mechanical models of lithosphere and asthenosphere: Can a change in plate velocity induce magmatic activity? Phil. Trans. R. Soc. Lond., A288: 387-392.

Gough, D.I., 1986. Magnetotelluric evidence for subduction of sea floor sediments. Nature, 321: 566.

Grady, J.C. 1971. Deep main faults of South India. J. Geol. Soc. India, 12: 56-62.

Gupta, M.L., Sharma, S.R., Sundar, A. and Singh, S.B., 1987. Geothermal studies in the Hyderabad granitic region and the crustal thermal structure of the Southern Indian Shield. Tectonophysics, 140: 257-264.

Hansen, E.C., Hickman, N.H., Grant, H.K. and Newton, R.C., 1985. Pan-African age of "Peninsular Gneiss" near Madurai, S. India (Abst.) EOS., 66: 419-420.

Hari Narain and Subrahmanyam, C., 1986. Precambrian tectonics of the South Indian shield inferred from Geophysical data. J. Geol., 94: 187-198.

Haxby, W.F and Weissel, J.K. Evidence for small-real mantle convention from Seasat Altimeter Data. J. Geophy. Res., 91(B3): 3507-3520.

Hjelt, S.E., 1984. Deep electromagnetic studies of the Baltic shield. J. Geophys., 55: 144-152.

Jones, A.G., 1981. On a type classification of lower crustal layers under Precambrian regions. J. Geophys. 49: 226-233.

Jones, A.G., 1982. On the electrical crust - mantle structure in Fennoscandia : No Moho, and the asthenosphere revealed ? Geophys. J.R. Astron. Soc., 68: 371-388.

Jones, A.G., 1987. MT and reflection: an essential combination. Geophys. J.R. Astr. Soc., 89: 7-18.

Kaila, K.L., Roy Chowdhury, K., Reddy, P.R., Krishna, V.G., Hari Narain, Subbotin, S.I., Sollogub, V.B., Chekunov, A.V., Kharetchko, G.E., Lazarenko, M.A. and Ilchenko, T.V., 1979. Crustal structure along Kavali-Udipi profile in the Indian peninsular shield from Deep Seismic Sounding. J. Geol. Soc. India, 20: 307-333.

Kaila, K.L. and Bhatia, S.C., 1981. Gravity study along the Kavali-Udipi deep seismic sounding profile in the Indian Peninsular shield: some inferences about the origin of anorthosites and the Eastern Ghats Orogeny. Tectonophysics, 79: 129-143.

Katz, M.B., 1978. Tectonic evolution of the Archaean granulite facies belt of Sri Lanka-South India, J. Geol. Soc. India, 19: 185-205.

Kurtz, R.D., Nisbett, E.R., Craven, S.A. and Stevens, R., 1987. MT study of the Archaean Kapuskasing zone (KSZ). Symp. No. GA 1.5-p56, (abs.), V.2 (IAVCEI, IAGA) IUGG87 XIX Gen. Assembly, Vancouver, Canada, Aug 9-22: 465pp.

Kurtz, R.D., De Laurier, J.M. and Gupta, J.C., 1986. A magnetotelluric sounding across Vancouver Island detects the subducting Juan de Fuca Plate, Nature, 321: 596-599.

Larsen, J.C., 1975. Low frequency (0.1-6.0 cpd) electromagnetic study of deep mantle electrical conductivity beneath the Hawaiian Islands. Geophys. J.R. Astr. Soc., 43: 17-46.

Lastavickova, M., Ramana, Y.V. and Gogte, B.S., 1987. Comparison of electric and elastic parameters of Precambrian Indian rocks. Stud. Geophy. et Geodetic., (in press).

Mareschal, M., Vasseur, G., Srivastava, B.J. and Singh, R.N., 1987. Induction models of southern India and the effect of off-shore geology. Phys. Earth Planet. Interior, 45: 137-148.

Mishra, D.C., 1986. Satellite magnetic map and tectonic correlation. J. Geol. Soc. India, 28: 501-503.

Nair, M.M. and Vidhyadharan, K.T., 1982. Rapakivi granite of Ezhimala complex and its significance. J. Geol. Soc. India 23: 46-51.

Naqvi, S.M. and Rogers, J.J.W., 1987. Precambrian Geology of India, Oxford Univ. Press, 223pp.

Negi, J.G., Agarwal, P.K. and Pandey, O.P., 1987. Large variation of curie depth and lithospheric thickness beneath the Indian subcontinent and a case for magnetothermometry, Geophys. J.R. Astr. Soc., 88: 763-775.

Nityananda, N. and Jayakumar., 1981. Proposed relation between anomalous geomagnetic variations and the tectonic history of South India, Phys. Earth Planet. Interior, 27: 223-228.

Parkinson, W.D., 1959. Directions of rapid geomagnetic fluctuations: Geophys. J. Astr. Soc., 2: 1-14.

Percival, J.A. and Card, K.D., 1983. Archean crust as revealed in the Kapuskasing uplift, Superior province, Canada. Geology, 11: 323-326.

Radhakrishna, B.P. and Naqvi, S.M., 1986. Precambrian continental crust of India and its evolution. J. Geol., 94: 145-166.

Ramachandran, T.V. Misra, A. and Misra, R.S., 1986. Geological evaluation of absolute total intensity Aeromagnetic data of Tamil Nadu. J. Assoc. Expl. Geophys., 7: 151-162.

Ramaswamy, V., Agarwal, A.K. and Singh, B.P., 1985. A three-dimensional numerical model study of electromagnetic induction around the Indian Peninsula and Sri Lanka island. Phys. Earth Planet. Interior, 39, 52-61.

Ranalli, G. and Murphy, D.C., 1987. Rheological stratification of the lithosphere. Tectonophysics, 132: 281-295.

Rao, R.U.M. and Jessop, A.M., 1975. A comparison of the thermal characters of shields. Can. J. Earth Sci., 12: 347-360.

Sastry, T.S., Prasad, S.N., Srivastava, B.J. and Someswara Rao, M., 1990. Vertical electrical profile at Chhautuppal (Hyderabad) in Peninsular India. Phys. Earth Planet. Int. Lett. Sec. (in press).

Schmucker, U., 1973. Regional induction studies : a review of methods and results. Phys. Earth Planet. Interior, 7: 365-378.

Schmucker, U., Hartmann, O., Giesecke, A.A. Jr., Casaverde, M., and Forbush, S.E., 1964. Electrical conductivity anomaly in the earth's crust in Peru. Carnegie. Inst. Washington Yr. book, 63: 354-362.

Schwarz, G., Haak, V., Martinez, E. and Bannister, J., 1984. The electrical conductivity of the Andean crust in northern Chile and Southern Bolivia as inferred from magnetotelluric measurements. J. Geophys., 55: 169-178.

Shankland, T.J. and Waff, H.S., 1977. Partial melting and electrical conductivity anomalies in the upper mantle. J.Geophys. Res., 82: 5409-5417.

Shankland, T.J. and Ander, M.E., 1983. Electrical conductivity, temperatures and fluids in the lower crust. J. Geophys. Res., 88: 9475-9484.

Sharma, S.R., Gupta, M.L. and Mahesh, P.S., 1986. Electrical, conductivity of rocks and elevated temperatures and the electrical conductivity model of the earth's crust of the Southern Indian Shield, Proc. of the Seminar on "Crustal Dynamics" Indian Geophys. Union, Hyderabad, 99-106.

Singh, R.N. and Negi, J.G. 1982. High Moho temperature in the Indian Shield. Tectonophysics, 82: 299-306.

SriNagesh, D., Rai, S.S., Ramesh, D.S., Gaur, V.K. and Rao, C.V.R. 1989: Evidence for thick continental roots beneeth South Indian Shield: Geophys. Res. Lett. 16: 1055-1058.

Srinivasan, R. and Sreenivas, B.L., 1977. Some new geological features from the Landsat imagery of Karnataka, J. Geol. Soc.India, 18: 589-597.

Srivastava, B.J. and Habiba Abbas., 1980. An interpretation of the induction arrows at Indian stations. J. Geomag. Geoelectr., 32 (Supp. I), pp. SI 187-Sl 196.

Srivastava, B.J., Prasad, S.N., Singh, B.P., Arora, B.R., Thakur, N.K. and Mahashabde, M.V., 1982. Induction Anomalies in geomagnetic Sq. in Peninsular India, Geophys. Res. Lett., 9: 1135-1138.

Srivastava, B.J., Singh, B.P. Lilley, F.E.M., 1984. Magnetometer array studies in India and the lithosphere: In: S.M. Naqvi, H.K. Gupta and S. Balakrishna (Editors), Lithosphere: Structure, Dyanmics and Evolution, Tectonophysics, 105: pp.355-371.

Stein, S., Cloetingh, S., Wiens, D.A. and Wortel, R., 1987. Why does near ridge extensional seismicity occur primarily in the Indian Ocean ? Earth Planet. Sci. Lett., 82: 107-113.

Subrahmanyam, C. and Verma, R.K., 1982. A gravity interpretation of the Dharwar greenstone gneiss granite terrain in the southern Indian shield and its geological implications: Tectonophysics, 84: 225-245.

Surayanarayana, M. and Bhan, S.K. 1985. Aeromagnetic survey over parts of Kerala and the adjoining offshore region, India. Geophy. Res. Bull., 23: 105-114.

Sykes, L.R., 1970. Seimicity of the Indian Ocean nascent island arc between Ceylon and Australia. J. Geophys. Res., 75: 504pp.

Tarits, P., 1986. Conductivity and fluids in the oceanic upper mantle. Phys. Earth Planet. Interior, 42: 215-226.

Thakur, N.K., 1983. Some studies of crust and upper mantle by Geomagnetic deep sounding. Ph.D. thesis (unpublished) submitted to University of Bombay, 171pp.

Thakur, N.K. Mahashabde, M.V., Arora, B.R., Singh, B.P., Srivastava, B.J. and Prasad, S.N., 1986. Geomagnetic variation anomalies in Peninsular India. Geophys. J.R. Astr. Soc., 86: 839-854.

Tozer, D.C., 1981. The mechanical and electrical properties of earth's asthenosphere. Phys. Earth Planet. Interior, 25: 280-296.

Vanzijil, J.S.V., 1977. Electrical studies of the Deep Crust in various tectonic provinces of Southern Africa. Amer. Geophys. Union, Monograph, 20: 470-500.

Verma, R.K., 1985. Gravity field, seismicity and tectonics of the Indian peninsula and the Himalayas. SESL, Reidel Publ. Co. Dordrecht, Holland, 213 pp.

Woods, D.V. and Allard, M., 1986. Reconnaissance electromagnetic induction study of the Kapuskasing structural zone: implications for lower crustal conductivity. Phys. Earth Planet. Interior, 42: 135-142.

Yuen, D.A. and Fleitout, L., 1985. Thinning of the Lithosphere by small-scale convective destabilization. Nature, 313: 125-128.

PRECAMBRIAN CRUSTAL EVOLUTION AND METALLOGENY OF SOUTHERN AFRICA

CARL R. ANHAEUSSER

ABSTRACT

Southern Africa offers a unique insight into many aspects of Precambrian geology, crustal evolution, and metallogeny. The earliest recorded events date back to approximately 3800-3500 Ma ago when vast areas of primordial crust developed following the complex interaction of sial and sima. Episodic introduction of granitic magmas assisted in the destruction of extensive volcanic or greenstone terranes, and this process, involving cratonization, led to the creation of microcontinental masses, including the Rhodesian and Kaapvaal crustal fragments, and high metamorphic grade structural provinces, as exemplified by the Limpopo Belt straddling the Zimbabwe-South African border.

Intracratonic volcanism and sedimentation commenced during Late Archaean times, leading to the sequential development of interior basins which increased progressively in size from approximately 3000 Ma to 1800 Ma ago. During this time intracontinental magmatism led to the emplacement of large mafic and ultramafic layered bodies and smaller alkalic intrusions of carbonatite and kimberlite. In addition, tectonic activity, probably linked to the dynamo-thermal events occurring in the adjacent high-grade metamorphic mobile belts, or to some Proterozoic plate motion, produced structural features in the cratons on a hitherto underemphasized scale.

Whilst the eastern half of the subcontinent experienced relative inactivity during the period 1800-300 Ma the emphasis of continued continental growth switched to the western regions where, from 2000 Ma to Late Proterozoic times, orogenic activity led firstly, to the development of the Namaqualand Metamorphic Complex and, later, to the Damara orogenic belt of South West Africa/Namibia.

The metallogeny of southern Africa is inextricably interwoven with the stages of crustal evolution and continental development. Mineralization is linked to metallogenic provinces and is also

shown to be genetically related to host rock evolution and the superimposed influence of igneous intrusion, metamorphism, and structural disturbance.

Southern Africa is one of the world's great storehouses of minerals and metals and the resources of the region are highlighted with the aid of tabulated data on mineral reserves.

INTRODUCTION

Southern Africa, defined as that region of the African subcontinent extending southwards from the Angolan border with South West Africa/Namibia in the west, to the Zambezi River and Central Mozambique in the east, contains some of the world's great metallogenic provinces, and is the world's principal producer of precious metals and minerals, including gold, platinum metals and gem diamonds. The region is, furthermore, well endowed with ferrous metals, base metals, and non-metallic mineral resources important, not only to the overall economy of the southern African countries concerned, but as strategic mineral resources to the Western World (Van Rensburg and Pretorius, 1977).

Prior to the Mesozoic fragmentation of Gondwana, southern Africa formed a part of a major landmass incorporating the remainder of the African continent as well as India, Australia, Antarctica and South America. Whilst it can be shown that the various continental masses making up Gondwanaland evolved along broadly similar geologic paths, the southern African region has preserved a number of unique geological features, particularly in the time span extending back in history from the Early Proterozoic to the Early Archaean (1600-3800 Ma), that sets the region apart as one of the great repositories of metals and minerals on the surface of the earth.

Whilst much is now known of the geology of the African subcontinent, including the economic mineral occurrences, there are still many unanswered questions regarding the evolutionary aspects of the crust and the intracratonic volcano-sedimentary cover sequences developed throughout the region. In addition, genetic aspects of the mineralized provinces are, in many instances, no nearer a solution despite years of detailed study of surface and underground mine exposures as well as drillcore.

Many attempts have also been made to synthesize the evolution of crustal domains or "provinces" throughout southern Africa and, up until recently, this had to be approached without the aid of sophisticated geophysical techniques such as gravity and electrical resistivity soundings as well as seismic profiling methods. Furthermore, the chronology of events in diverse and complex geological terrains is often equivocal and constraints imposed by isotopic and palaeomagnetic results have fostered ongoing interpretative debates. However, with due allowance being made for the above mentioned shortcomings, the broad framework of crustal evolution in southern Africa appears to have been reasonably well established (Tankard et al., 1982) and is only likely to deviate where increased geophysical detail becomes available.

Space limitations preclude a comprehensive review of current thoughts on crustal development in southern Africa, but in this contribution an attempt will be made to highlight some of the major events that have influenced the geological development of the subcontinent. As the metallogeny of the region has been inextricably linked, both spatially and temporally, to the geological evolution of southern Africa this aspect will be briefly reviewed.

GEOLOGICAL OVERVIEW OF SOUTHERN AFRICA

Geologically, southern Africa is divisible into a variety of tectono-stratigraphic domains, which include the Rhodesian and Kaapvaal "cratons" or "crustal blocks" of the southern African shield, and the flanking, generally high-grade metamorphic terranes, variously termed "mobile belts", or "structural provinces" (Anhaeusser et al.,1969; Tankard et al., 1982). Whilst definitions may vary, preference in this paper is afforded the scheme adopted by Anhaeusser and Button (1976) and Pretorius and Maske (1976), which depicts southern Africa as possessing two older (>2500 Ma) cratonic domains on the eastern half of the subcontinent and two younger (<2500 Ma) cratonic domains on the western half (Fig. 1). These four crustal blocks, the presence of which is supported by an analysis of the regional gravity field over southern Africa (Hunter and Pretorius, 1981), represent segments of the African subcontinent variously influenced by crust-forming processes, but which stabilized relative to the intervening orogenic tracts now occupied by complex tectono-

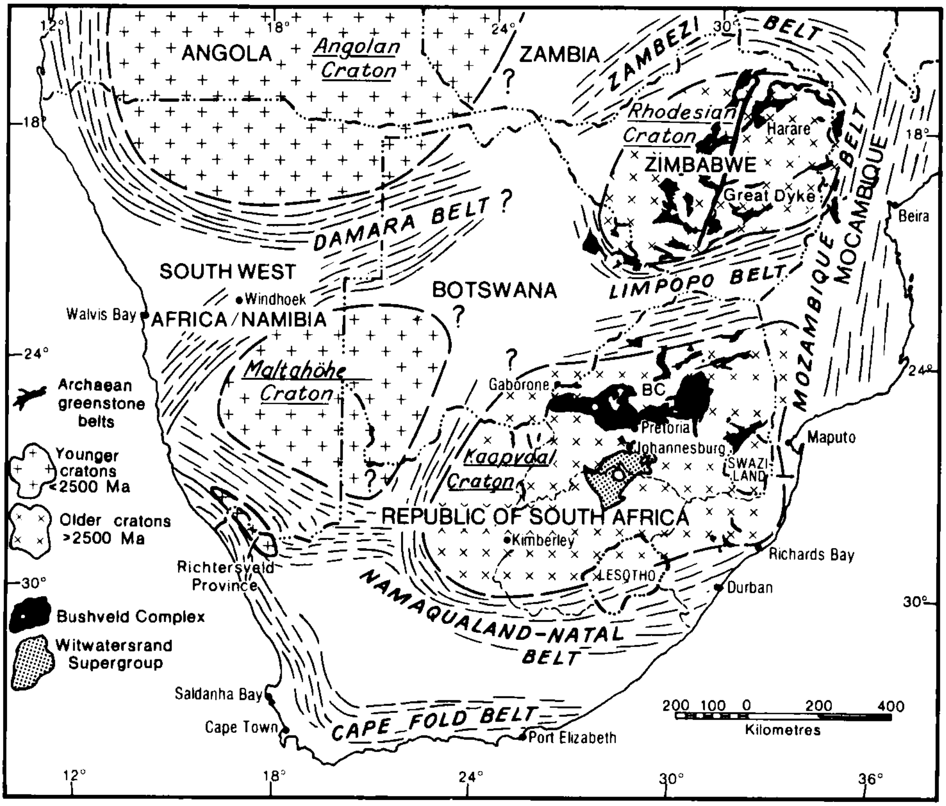

Figure 1. Map showing the main crustal provinces and better known geological features in southern Africa, including the Archaean greenstone belts, the Great Dyke, the Bushveld Complex, and the Witwatersrand Basin (After Anhaeusser and Button, 1976 and Pretorius and Maske, 1976).

thermal mobile belt regimes. However, should any impression have been created that the cratonic nuclei, coupled with their intracratonic volcano-sedimentary cover sequences, endured only as passive geological domains while the mobile belt regimes experienced ongoing dynamo-thermal activity, then this notion can be conclusively dispelled by an examination of the events that affected the southern African region.

A sequence of chronologically well-defined evolutionary stages of crustal development have been recognized for the Precambrian rocks of southern Africa, the more significant of which are summarized in the following sections.

EARLY ARCHAEAN CRUSTAL DEVELOPMENT

The Kaapvaal and Rhodesian cratons, separated by the Limpopo Belt, constitute Archaean crystalline basement areas that can be traced back in time to approximately 3800 Ma (Barton et al., 1983). The complex nature and protracted history of Archaean geology in southern Africa, and elsewhere in the world, has led to the formulation of numerous models which attempt to address the multitude of issues relating to the growth and development of the ancient crust. Comprehensive reviews have thus been provided which attempt to examine aspects of granite-greenstone and high-grade metamorphic mobile belt evolution (Goodwin, 1968; Anhaeusser et al., 1969; Anhaeusser, 1973a; Windley, 1976, 1977; McCall, 1977; Tarling, 1978; Glikson, 1979; Condie, 1981; Kroner, 1981, 1985; Kroner and Greiling, 1984; Nisbet, 1987; Cloud, 1988). Views are divided as to whether Archaean granite-greenstone terranes evolved in subduction-related magmatic arc or marginal basin settings, or whether they formed in intracontinental rift settings, the latter view implying the existence of primitive pre-greenstone sialic crust. Because of the sound arguments offered by the two schools, and also bearing in mind the considerable age variations reported from Archaean terranes, support for both standpoints may have validity.

In southern Africa it has been proposed that the earliest recognizable greenstone successions, made up essentially of komatiites and basaltic komatiites, represent relics of a once extensive primitive simatic crust (Anhaeusser, 1973a). In support of this view it can be demonstrated that mafic and ultramfic xenoliths occur prolifically in all the ancient granitic, gneissic, and migmatitic terranes.

Furthermore, the generation of tonalite-trondhjemite gneisses from mafic-ultramafic precursors has been demonstrated by Glikson and Jahn (1985) who suggested the Archaean granite-greenstone terranes were produced by a process of "sima-to-sial transformation". However, a recently reported age of 3644 ± 4 Ma for gneisses in Swaziland exceeds current estimates for the age of the nearby Barberton greenstone belt (Compston and Kroner, 1988) thereby fostering the evolutionary debate with the suggestion that at least some sialic crust existed in the area prior to the greenstones. Such a relationship can best be demonstrated on the

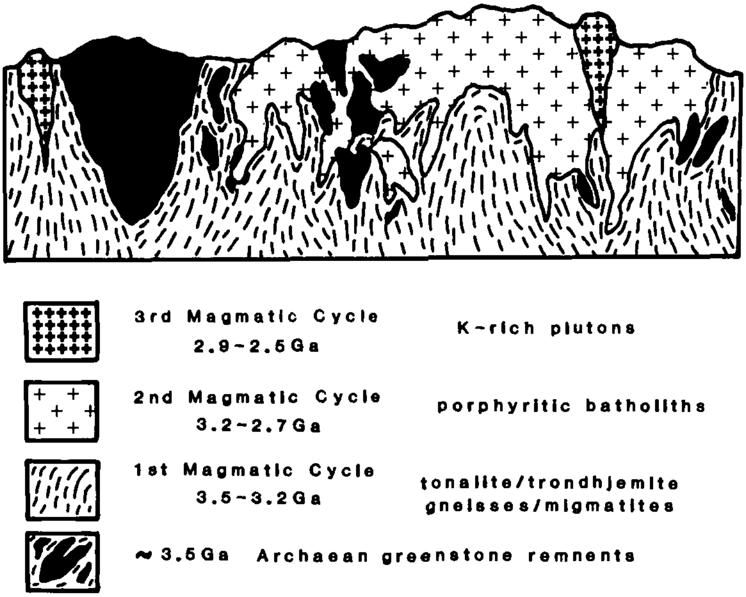

Figure 2. Schematic section through the Archaean granite-greenstone crust in the Barberton Mountain Land region of the eastern Kaapvaal Craton showing the threefold "magmatic cycle" subdivision of the granitic rocks in the area (Adapted after Anhaeusser and Robb, 1981 and Robb et al., 1983).

Rhodesian Craton where "younger" greenstones (3000-2700 Ma) rest on "older" (3500 Ma) granite-greenstone basement (Wilson, 1979; Foster and Wilson, 1984), thereby providing support for the view that at least some greenstone belts may have formed in intracratonic rift settings during the Late Archaean.

Much of the crystalline basement of southern Africa formed prior to 3000 Ma ago and, once again, because of the nature and complexity of this terrane there are widely divergent views on the evolution of the granitic crust (Anhaeusser, 1973a, 1981; Hunter, 1974a; Condie and Hunter, 1976; Glikson, 1979; Anhaeusser and Wilson, 1981; Tankard et al., 1982; Robb and Anhaeusser, 1983; Robb et al., 1983; Wilson, 1979).

Based on studies of the well-exposed granitic terrane in the eastern and central sectors of the Kaapvaal Craton (Anhaeusser, 1973b, 1983; Anhaeusser and Robb, 1980, 1981) a three-fold subdivision of the Archaean granites was proposed, each "magmatic cycle" reflecting stages in the formation and genetic evolution of the sialic crust of this region in particular, but also of areas further afield, including Zimbabwe (Fig. 2).

The early stages of Archaean proto-cratonization are thought to have been accomplished by the generation of primitive tonalitic and trondhjemitic magmas and complex migmatites following the melting of an ensimatic source (Green and Ringwood, 1968; Lambert and Wyllie, 1972; Arth and Hanson, 1975). The dominant processes of cratonization developed during the second magmatic stage when enormous volumes of K-rich magma were emplaced into the earlier-formed greenstones and Na-rich gneisses, such that by 3000 Ma ago sheet-like batholithic massifs had developed on a crust approaching 35 km in thickness (Robb et al., 1983).

The third magmatic stage coincided with the intrusion of essentially post-tectonic plutons of divergent compositions emplaced between 2800 and 2500 Ma ago and found in widely dispersed regions on both the Kaapvaal and Rhodesian cratons (Hunter, 1974b; Wilson, 1979; Barton, 1983a) as well as in the southern and northern marginal zones of the Limpopo Belt (Barton and Key, 1981).

THE ARCHAEAN-PROTEROZOIC LIMPOPO OROGEN

The Limpopo Belt situated between the Rhodesian and Kaapvaal cratons (Fig. 1) remains an enigmatic problem in any synthesis of the crustal evolution of southern Africa. Simply stated the Limpopo structural province can be subdivided into three zones, a Central zone bordered more or less symmetrically by two marginal zones. Both the Northern Marginal Zone, which abuts the southern edge of the Rhodesian Craton, and the Southern Marginal zone, flanking the northern edge of the Kaapvaal Craton, appear to be transitional with the adjacent cratons, their "boundaries" being defined metamorphically by the recognition of orthopyroxene and orthoamphibole isograds (Van Reenen and Du Toit, 1977; Robertson et al., 1981) and by gradational increases in the degree of deformation (Coward et al., 1976; Du Toit and Van Reenen, 1977; Barton and Key, 1981; Robertson et al., 1981; Tankard et al., 1982).

The early suggestion that the Limpopo mobile belt represented reworked cratonic material, with or without infolded supracrustal rocks, and that the initiation of these belts was triggered by huge transcurrent dislocation and a high heat flow related to

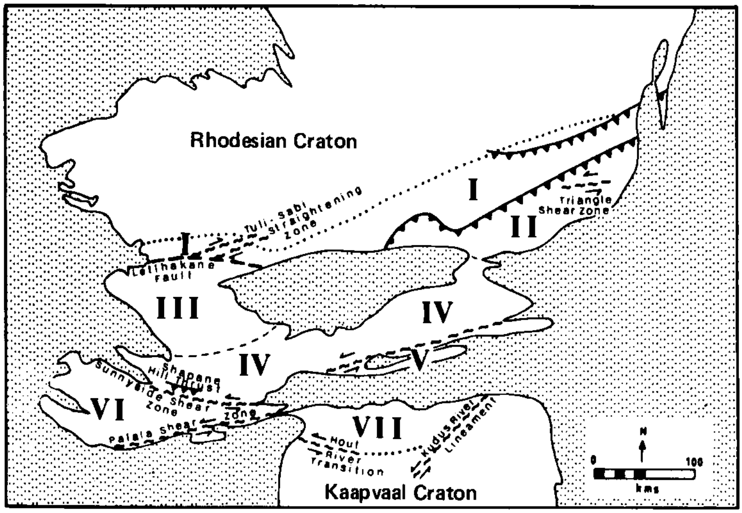

DOMAIN	Structural Zone	DOMAIN	Structural Zone
I	NORTHERN MARGINAL	V	SOUTHERN MARGINAL
II	NORTHERN MARGINAL	VI	SOUTHERN MARGINAL
III	CENTRAL	VII	SOUTHERN MARGINAL
IV	CENTRAL		

ORTHOPYROXENE ISOGRAD

GRADATIONAL CONTACT

SHEAR ZONE (with sense of movement)

THRUST ZONE (teeth in upper plate)

FAULT ZONE

▨ COVER

Figure 3. Simplified map showing the seven tectono-stratigraphic domains of the Limpopo Belt (After Watkeys, 1983).

mantle sources (Anhaeusser et al., 1969) was abandoned following the discovery of the ~3800 Ma Sand River gneisses in the Central zone by Barton et al. (1983) - rocks considerably older than any yet found on the adjacent low metamorphic grade cratons. Ongoing investigations have indicated further that, far from being a simple linear zone, the Limpopo Belt comprises seven tectono-stratigraphic domains (Fig. 3) separated by contacts that include wide ductile shear zones, wide dextral and sinistral shear and straightening zones, thrusts, and ultramylonitized shear zones. Each domain possesses its own internal stratigraphic, structural, and metamorphic history (Watkeys, 1983). Whilst there is some degree of consensus that the marginal zones consist of significant proportions of reworked continental crust related to the adjacent cratons, there is not the same unanimity concerning the origin and nature of the pre-3000 Ma geological events recorded within the Central Zone. This has led to widespread speculation involving plate tectonic modelling, coupled with the suggestion that the Central Zone may be a segment of allocthonous crust genetically unrelated to those comprising the marginal zones (Barton and Key, 1981; Barton, 1983b). But for the older ages reported in the Central Zone the need may not have arisen to go beyond the view that the entire Limpopo structural province represents reworked intracratonic crust, along the lines initially suggested by Anhaeusser et al., (1969). Apart from the assumption that plate tectonic processes operated in the Archaean there remains a pressing need, using other isotopic dating techniques, to verify the ~3790 Ma Rb-Sr whole rock ages reported by Barton et al., (1983). Just how reliable the Rb-Sr method remains for dating gneisses that were subjected to polyphase metamorphism, including granulite facies conditions, is open to debate. Whatever the views may be there is no doubt that the Limpopo Belt was involved in multiple structural, metamorphic, and igneous intrusive events developed episodically over a protracted period extending from Early Archaean (~3800 Ma) to Early Proterozoic (~2000 Ma) times. Precisely what influence these events had on the neighbouring cratons remains obscure, but if the Limpopo Belt was an orogenic zone it must undoubtedly have contributed greatly as a source terrane for intracratonic sedimentation initiated approximately 3000 Ma ago.

LATE ARCHAEAN - EARLY PROTEROZOIC SUPRACRUSTAL DEVELOPMENT

The ancient basement discussed previously, was buried beneath a Late Archaean-Early Proterozoic succession of volcano-sedimentary basins Fig. 4) represented by rocks of the Pongola, Dominion, Witwatersrand, Ventersdorp, Transvaal-Griqualand West, and Waterberg-Umkondo sequences (Button et al., 1981; Tankard et al.,1982). The detritus contributing to the sequential evolution of the volcano-sedimentary basins was derived from both intracratonic as well as from external sources, such as the neighbouring orogenic mobile belt terranes. Sediments may also have been derived from sources further afield if a Gondwana-like supercontinent existed during Late Archaean-Early Proterozoic times.

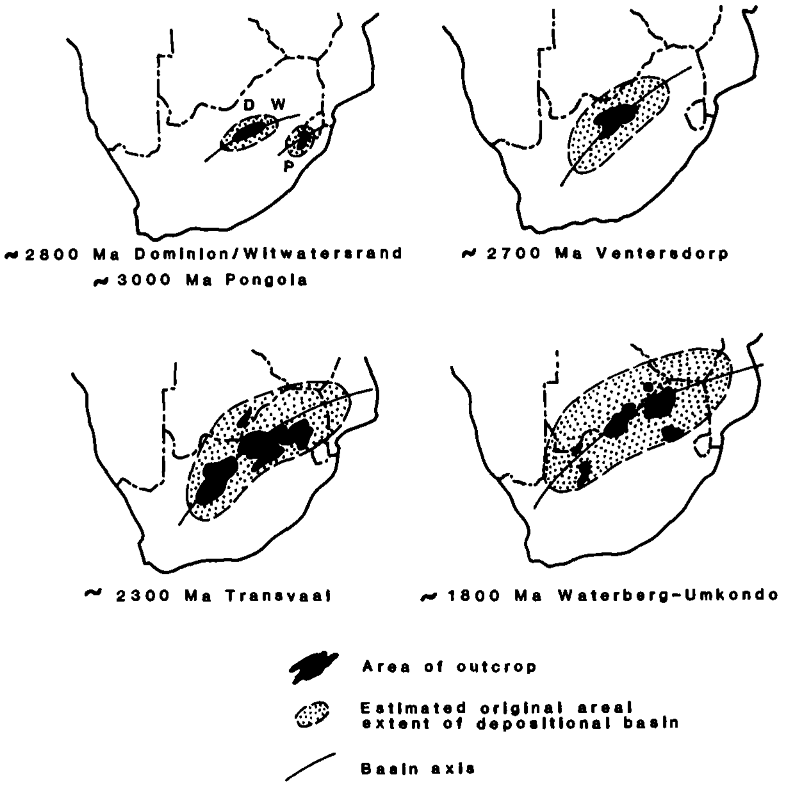
D
W
P
~2800 Ma Dominion/Witwatersrand
~3000 Ma Pongola
~ 2700 Ma Ventersdorp
~ 2300 Ma Transvaal
~ 1800 Ma Waterberg-Umkondo
Area of outcrop
Estimated original areal extent of depositional basin
Basin axis

Figure 4 Schematic diagrams showing the distribution of intracratonic volcano-sedimentary basins on the Kaapvaal and Rhodesian cratons from Late Archaean to Early Proterozoic times (Modified after Anhaeusser, 1973a).

The intracratonic volcano-sedimentary basins that developed on the Kaapvaal Craton between 3000-1800 Ma show a progressive size increase corresponding with a concomitant decrease in age of the basins from southeast to northwest. In addition there is a consistent northeast orientation of the basin axes which migrated to the northwest across the Kaapvaal Craton (Anhaeusser, 1973a). The largest of these basins, which formed approximately 1800 Ma ago, led to the accumulation of the extensive Matsap-Waterberg-Soutpansberg-Umkondo sequences dominated by red bed sediments - an event which coincided on a global scale with the advent of an oxygenated atmosphere (Cloud, 1976).

The development of each basin was accompanied by basic volcanism, providing an almost continuous record of the nature of the mantle beneath the Kaapvaal Craton for over 1200 Ma. Myers et al. (1987) demonstrated that these volcanic rocks show quantitatively similar trace element patterns reflecting either some fundamental process occurring with each volcanic event and/or a single source region that supplied all of these melts. This remarkable degree of mantle homogeneity beneath the crust of southern Africa was also noted by Anhaeusser (1976a) who showed that magmas containing anomalous quantities of chrome were emplaced episodically into the region over a time span of 1500 Ma.

PLUTONIC ACTIVITY ON THE KAAPVAAL AND RHODESIAN CRATONS

Granitic intrusions

Plutonic events in the cratonic areas, involving granitic rocks, largely ceased after 2700 Ma with only minor intrusions being emplaced in Swaziland, and some granitic activity being associated with the Kanye Volcanic Group in Botswana (Gaberone granite, 2590 Ma) and the Bushveld Complex (Bushveld granite 2010 Ma) (Button et al., 1981; Vermaak and Von Gruenewaldt, 1986).

Basic and ultrabasic intrusions

The Archaean crystalline basement and, in places, the Late Archaean-Early Proterozoic volcano-sedimentary cover, was also invaded sporadically by massive intrusions (Fig. 5) of basic and ultrabasic magma (Anhaeusser, 1987), including (a) the emplacement of the Mashaba Ultramafic Suite (2800-3000 Ma) and the Great Dyke (~2500 Ma) in Zimbabwe (Wilson, 1979), (b) the 3150 Ma Messina Layered Intrusion emplaced into the Central Zone of the Limpopo Belt (Barton et al., 1979), (c) the Usushwana and Rooiwater complexes (2780 Ma and >2650 Ma, respectively), emplaced into the eastern sector of the Kaapvaal Craton (Davies et al., 1970; Vearncombe et al., 1987), (d) the Bushveld Complex (2050 Ma) emplaced in the central Kaapvaal Craton (Vermaak and Von Gruenewaldt, 1986),and (e) the Molopo Farms Complex (2050 Ma), straddling the border between eastern Botswana and South Africa (Gould and Rathbone, 1985).

Alkaline and alkaline/ultrabasic intrusions

Further major magmatic activity occurred on the eastern half of the subcontinent also in the form of sporadic intrusions of a remarkable spectrum of alkalic and alkaline/ultrabasic rocks ranging from lamprophyres through cartbonatite and alkaline complexes to kimberlites and related rocks (Verwoerd, 1967; Ferguson, 1973; Bristow, 1985). The ages of these intrusions vary from 2600 Ma for lamprophyres intruded into the Limpopo Belt (Watkeys and Armstrong, 1985); 2050 Ma for the Phalaborwa Complex (Fig. 5) intruded into the eastern part of the Kaapvaal Craton (Eriksson, 1984); kimberlites emplaced into the central and western parts of the Kaapvaal Craton between 1400-1600 Ma

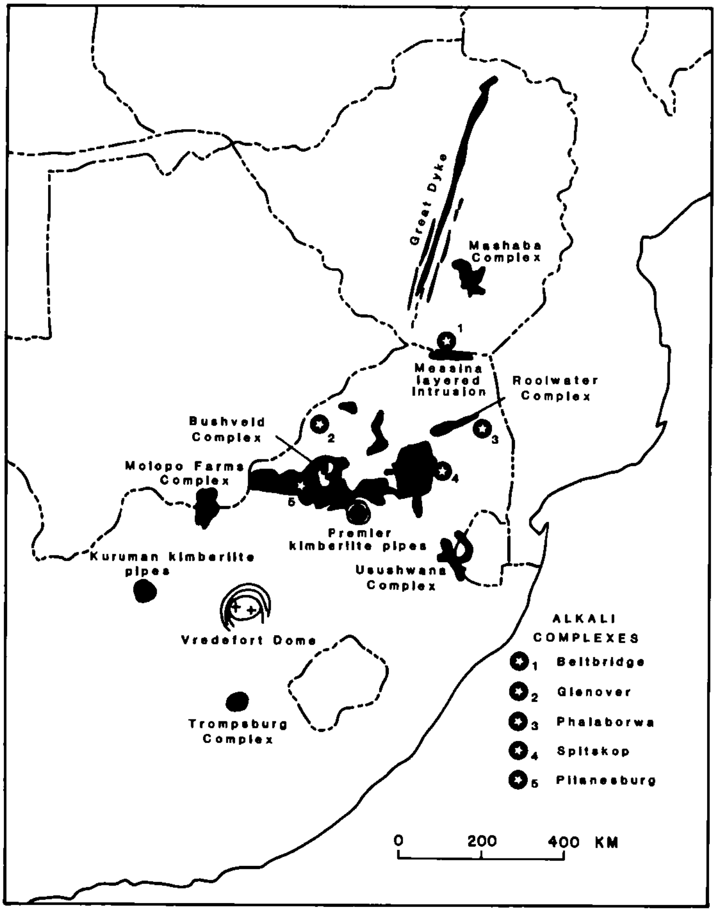

Figure 5 Simplified map of the eastern half of the African sub-continent showing the distribution of some of the more important mafic, ultramafic, alkalic and kimberlitic complexes of Archaean and Proterozoic age, as well as the location of the Vredefort ring structure.

(Kramers, 1979; Bristow et al., 1986); and additional carbonatite and alkaline complexes, like Pilanesberg (Fig.5), intruded into the central Kaapvaal Craton at about 1200-1400 Ma (Ferguson, 1973; Harmer, 1985; Lurie, 1986).

The extent of the alkalic magmatic activity on the Kaapvaal Craton in the time-span 1200-1400 Ma has not been fully determined because younger cover obscures numerous shield volcanoes formed by multi-phase eruptions of magma possessing basalt-trachyte as well as variolitic trachyte lineage (Frick and Walraven, 1985).

KAAPVAAL INTRACRATONIC TECTONISM

The cratons have generally been perceived as stable crustal nuclei that, for prolonged periods following their formation, were tectonically inactive parts of the earth's crust. Events documented on the Kaapvaal Craton must, however, seriously question the validity of this impression. Apart from the major upheavals that must have accompanied the emplacement of the large layered igneous intrusions, including the 500 km long Great Dyke and the Bushveld Complex, which is 67000 km^2 in areal extent, other significant intracratonic events include the domical upwarping of numerous areas of granitic basement. On the Kaapvaal Craton a "grid pattern" of domes and intervening basins was first recognized by Brock and Pretorius (1964). One of these structures, the Vredefort Dome, occupies a central position in the craton (Fig. 5) and is distinguished by a 17 km-wide collar of steeply dipping and overturned sedimentary and volcanic rocks of the Witwatersrand, Ventersdorp, and Transvaal successions surrounding a 36 km diameter core of Archaean granitic basement. An outer rim synclinorium of upper Transvaal strata 20-30 km wide completes the structure (Simpson, 1978). Data consistent with the view that approximately 14 km of ~3800-2800 Ma Archaean crust may have been "turned up on edge" in the centre of this structure, thereby revealing mafic and felsic granulites derived from supracrustal rocks that had been profoundly reconstituted in the middle crust, were reported by Hart et al., (1981a,b). The scale of the Vredefort structure, which was updomed ~2000 Ma ago, defines an intracratonic event of immense magnitude, the likes of which appear to be unequalled elsewhere on Earth. This uniqueness has prompted much debate as to the origin of the Vredefort ring structure with views being divided between supporters of its formation by endogenous processes as opposed to it representing an astrobleme formed by the impact of a cosmic body, as suggested initially by Dietz (1961).

Further evidence of intracratonic deformation on a scale hitherto unsuspected is emerging from detailed structural and seismic reflection investigations in the principal gold producing areas of the Witwatersrand Basin. Much of this information remains unpublished in view of the competitive nature of the gold mining industry, but accounts by Roering (1984), McCarthy et al., (1986) and Tweedie (1986), among others, leave little doubt that the Witwatersrand, Ventersdorp, and Transvaal successions in the central Kaapvaal Craton have been subjected to deformation of a magnitude previously not anticipated. This is manifest in entire sequences being overfolded, duplicated by imbricate thrust faulting, sheared and mylonitized, subjected to large-scale wrench faulting, cleavage development, and folding on a variety of scales, as well as to faulting resulting in horst and graben development.

THE GREAT 1800-300 Ma HIATUS

With the exception, in northwestern Zimbabwe, of the deposition of the Piriwiri, Deweras, and Lomagundi groups of sediments, believed to be of Middle Proterozoic age (~1500 Ma), and discounting the unknown extent of the alkali igneous and volcanic activity on the Kaapvaal Craton referred to earlier, a major hiatus ensued in the regions underlain by Archaean and Early Proterozoic basement and platformal sequences on the eastern half of the African subcontinent. This hiatus, extending from approximately 1500-1800 Ma until Karoo times (Late Palaeozoic-Early Mesozoic), influenced both the Kaapvaal and Rhodesian cratons suggesting that these regions were essentially neutral geological terranes for over 1500 Ma. Erosion in this region appears to have been minimal, thereby ensuring the preservation of one of the most complete geologic records of Archaean and Early Proterozoic rocks on earth.

PROTEROZOIC OROGENS AND CRATONIZATION

(a) The Namaqua-Natal structural provinces

In contrast to the "relative geological inertness" of the Rhodesian and Kaapvaal cratons on the eastern half of southern

Africa during the period 1800 to 300 Ma some of the flanking mobile belts were exceptionally active regions. During the period 1200-900 Ma, for example, the eastern or Natal sector of the Namaqua-Natal mobile belt (Fig. 1) underwent its main tectonothermal activity leading, ultimately, to the allochthonous Natal

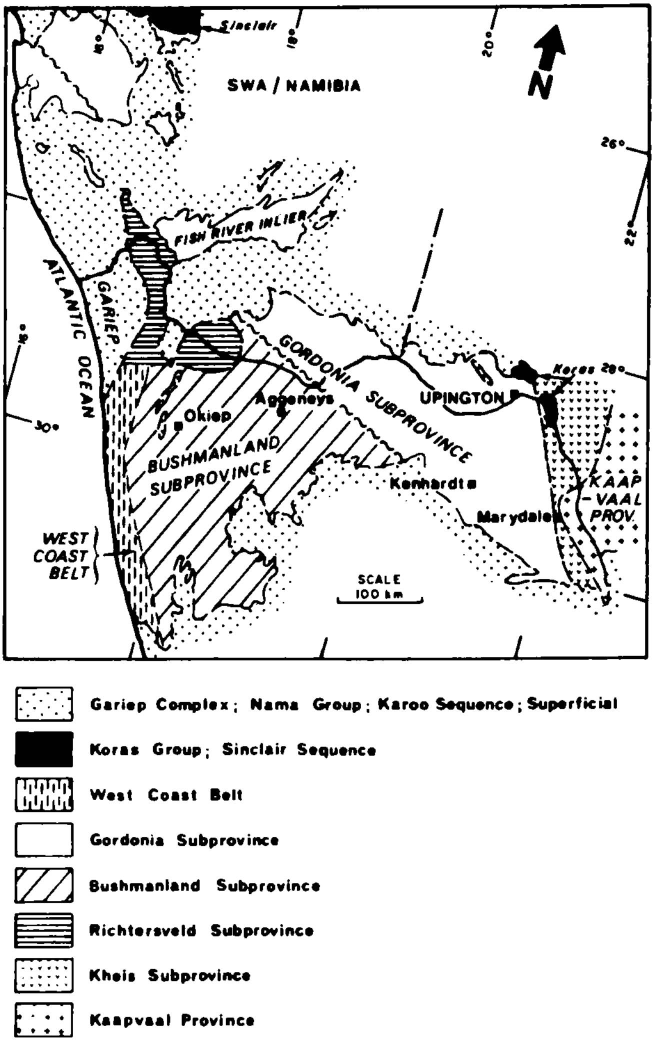

Figure 6. Tectonic subdivisions of the Namaqualand Metamorphic complex (After Joubert, 1986b).

structural province being thrust northwards onto a foreland represented by the southeastern margin of the Kaapvaal Craton (Matthews, 1972, 1981).

On the western half of southern Africa a microcontinent, comprising the Richtersveld Subprovince which originated during a major crust-producing event some 2000 to 1730 Ma ago (Reid, 1982), together with the approximately 1600 Ma old Bushmanland Subprovince, were accreted to the African subcontinent as a unit approximately 1400 to 1200 Ma ago (Joubert, 1986a,b). The region, comprising the Namaqualand Metamorphic Complex (Joubert, 1981, 1986a, b; Botha, 1983) (Fig. 6), consists of a polyphase deformed and metamorphosed gneissic terrane formed from numerous sedimentary and volcanic rocks, intruded by a variety of granitic as well as mafic and ultramafic rock types. The collision zone, which includes the Gordonia Subprovince, is marked by a major northwest-trending strike-slip orogen segmented by shears and sutures, the latter occupied by numerous bodies of mafic and ultramafic rock. The Gordonia Subprovince, in turn, abuts against the Kheis Subprovince which skirts the Kaapvaal Craton and represents a transi-

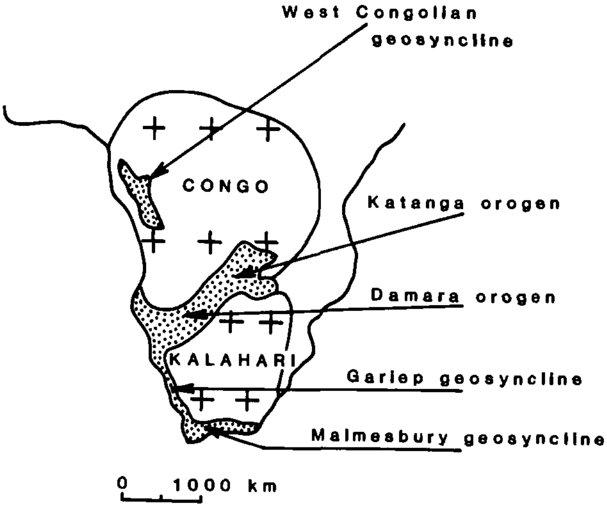

Figure 7. Schematic map showing the extent of the Late Proterozoic Congo and Kalahari cratons and (Pan-African orogenic zones in southern Africa (Adapted from Clifford, 1970; Kroner, 1977, and Martin and Porada, 1977).

tional zone between relatively undeformed Archaean and Early Proterozoic rocks and intensely deformed and metamorphosed assemblages of the Namaqualand Metamorphic Complex (Vajner, 1974).

Tectonism of the Namaqua structural province subsided between 1200-1000 Ma and the gneissic terrane acted as a basement to volcano-sedimentary successions of the Karas and Sinclair groups in eastern Namaqualand and southern South West Africa/Namibia, respectively. By this stage Late Proterozoic cratonization processes had fused the Namaqua-Natal structural provinces to the Kaapvaal-Rhodesian crustal segments, resulting in an aggregate craton known as the Kalahari Craton or Kalahari Province (Clifford, 1970; Tankard et al., 1982). This coincided with the similar development of the aggregated Congo Craton in Central Africa (Fig. 7) that followed the Kibaran orogeny approximately 1100 Ma ago, and which incorporated the Angolan Craton straddling the border between Angola and South West Africa/Namibia (Fig. 1).

(b) Pan-African orogenesis

The Late Proterozoic cratonization episode was succeeded by the onset of Pan-African geosynclinal development and subsequent tectonism which affected widespread areas on the western half of the African subcontinent (Fig. 7) and adjoining areas of South America (Kroner, 1977; Martin and Porada, 1977a,b; Tankard et al., 1982; Miller, 1983a,b). These include (a) the coastal and intracratonic, northeast-trending branches of the Damara orogen in South West Africa/Namibia, as well as the adjacent platformal sequences developed on the Angolan and Maltahohe cratons (Fig. 1), (b) the Gariep geosyncline along the west coast straddling the South West Africa/Namibia -South Africa border, and (c) the Malmesbury geosyncline sweeping around the southwestern and southern coast of South Africa beneath the cover of Lower Palaeozoic sediments that constitute the Cape Fold Belt (Tankard et al., 1982).

The Damara episode was initiated 1000-900 Ma ago and followed a protracted history of intracratonic rifting trending north-northwest, northeast, and south away from a triple junction that constituted part of the tectonic regime responsible for the commencement of the opening up of the South Atlantic ocean approximately 840 Ma ago. The Damara orogen underwent a continuous evolution involving rifting, spreading, spreading reversal, subduction, continental convergence, doming, thrusting and several stages of syn- and post-tectonic granite emplacement and metamorphism - the tectono-thermal history of which, as outlined by Miller (1983b), began to subside 500-450 Ma ago.

METALLOGENY

Having initially provided a geological overview of southern Africa there remains the task of highlighting this region's vast and diverse mineral occurrences. Because of the importance of minerals and mining in the economy of southern Africa the mineral provinces have been well documented and reviewed in the past by numerous authors (Haughton, 1964; Anhaeusser, 1976a, b, c; Anhaeusser and Button, 1976; Coetzee, 1976; Pretorius, 1976a, b). A large amount of additional geological and related information pertaining to many of the important ore deposits of the region is also available in a recently published set of two volumes entitled Mineral Deposits of Southern Africa (Anhaeusser and Maske, 1986).

The nature and distribution of mineral deposits in southern Africa was examined by Sohnge (1986) in relation to the tectonic and chronological framework broadly outlined earlier in this paper. A number of mineral provinces and subprovinces were defined that emphasized the link between the types of ore deposits generated in different environments and the advance of crustal evolution through successive geological eras. The concept of mineral provinces provides explorationists with a framework within which mineralization may be associated with specific lithologic types or geologic events. These together are usually of a regional nature and might also involve magmatism, structural deformation, or metamorphism.

The most important mineral occurrences of southern Africa, shown chronologically in Fig.8, can also be categorized genetically (Anhaeusser, 1987b), again emphasizing the geological environment, but placing importance on the link between mineralization, host rock evolution and the influence of superimposed ore forming processes.

Syngenetic, stratiform mineral deposits

Deposits of this type include the stratiform, stratabound, non-magmatic deposits such as the important gold-uranium occurrences associated with placer-type sedimentation in the intracratonic

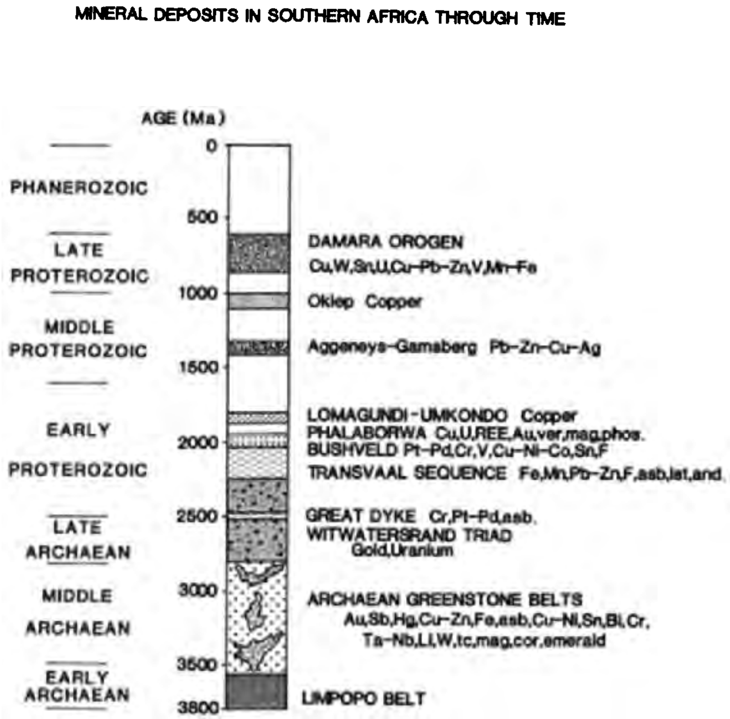
MINERAL DEPOSITS IN SOUTHERN AFRICA THROUGH TIME
AGE (Ma)
0
500
1000
1500
2000
2500
3000
3500
3800
PHANEROZOIC
LATE PROTEROZOIC
MIDDLE PROTEROZOIC
EARLY PROTEROZOIC
LATE ARCHAEAN
MIDDLE ARCHAEAN
EARLY ARCHAEAN
DAMARA OROGEN
Cu,W,Sn,U,Cu-Pb-Zn,V,Mn-Fe
Okiep Copper
Aggeneys-Gamsberg Pb-Zn-Cu-Ag
LOMAGUNDI-UMKONDO Copper
PHALABORWA Cu,U,REE,Au,ver,mag,phos.
BUSHVELD Pt-Pd,Cr,V,Cu-Ni-Co,Sn,F
TRANSVAAL SEQUENCE Fe,Mn,Pb-Zn,F,asb,lat,and.
GREAT DYKE Cr,Pt-Pd,asb.
WITWATERSRAND TRIAD
Gold,Uranium
ARCHAEAN GREENSTONE BELTS
Au,Sb,Hg,Cu-Zn,Fe,asb,Cu-Ni,Sn,Bi,Cr,
Ta-Nb,Li,W,tc,mag,cor,emerald
LIMPOPO BELT

Figure 8. Diagram illustrating the chrono-stratigraphic distribution and nature of mineralization in southern Africa (After Anhaeusser, 1987).

Pongola, Witwatersrand Triad (Dominion Reef, Witwatersrand, Ventersdorp), and Transvaal basins. Also in this category are the vast iron, manganese, and asbestos occurrences in the Transvaal Sequence, the copper occurrences of the Lomagundi/Umkondo and Klein Aub/Doornpoort formations of Zimbabwe and South West Africa/Namibia, respectively, as well as the extensive lead, zinc, copper, and silver deposits like those found in the Bushmanland Sequence near Aggeneys and Gamsberg in Namaqualand (Anhaeusser and Button, 1976; Pretorius, 1976a; Tankard et al., 1982; Beukes, 1986; Joubert, 1986b; Killick, 1986; Newham, 1986).

The second variety of stratiform deposits includes those having a magmatic origin and being associated with major layered igneous intrusions. These include the Mashaba Complex and Great Dyke in Zimbabwe and the Bushveld, Rooiwater, and Usushwana complexes on the Kaapvaal Craton. These intrusions are major sources of chromite, titaniferous - and vanadium-bearing magnetite, the platinum-palladium group of metals, and important quantities of copper, nickel, cobalt, and gold produced as by-products to the platinum extraction (Anhaeusser, 1976a; Wilson, 1979; Vermaak and Von Gruenewaldt, 1986; Vearncombe et al., 1987).

Epigenetic mineral deposits

Deposits in this category occur in a variety of geological settings in southern Africa and are often produced as a result of the concentration and redistribution of metals by magmatic hydrothermal or epithermal systems accompanying igneous intrusions. Important in this group of deposits are the numerous gold occurrences located in the Archaean greenstone belts of Zimbabwe and the eastern Kaapvaal Craton (e.g. the Barberton area), and in Early Proterozoic Transvaal sediments (e.g. the Pilgrim's Rest-Sabie region). Major deposits of tin and fluorite associated with the granitic rocks of the Bushveld Complex are also epigenetic in character (Anhaeusser, 1976a,b; Anhaeusser and Button, 1976; Foster and Wilson, 1984; Vermaak and Von Gruenewaldt, 1986).

Mineralization associated with volcanism

The southern African stratigraphic record displays numerous episodes of volcanism, the nature of which varies significantly from the Early Archaean greenstone terranes where komatiites and basaltic komatiites predominate to the Proterozoic where flood basalts are extensively developed in the intracratonic basins and calc-alkaline volcanic suites occur in the orogenic belts. Basalts akin to ocean-ridge tholeiites occur in the Late Proterozoic Damara orogen.

On the Rhodesia Craton numerous Archaean nickel-copper deposits are found associated with ultramafic to mafic volcanic and plutonic rocks and important antimony-gold occurrences, also associated with altered (sheared and carbonated) komatiites, are mined in the Murchison greenstone belt located on the eastern side of the Kaapvaal Craton. Mineral occurrences associated with Archaean intermediate to felsic volcanic rocks include small deposits of antimony, gold, mercury, copper-zinc-lead, tungsten, barite, and massive pyrite-pyrrhotite (Anhaeusser and Viljoen, 1986).

No significant mineralization has yet been ascribed to the intracratonic flood basalts although minor showings of copper have been linked to the mafic lavas in the Waterberg Sequence. It has also been speculated that auriferous exhalites accompanied, or were closely followed by, the andesitic-basaltic volcanism of the Dominion Group and may have contributed to an endogenous origin for some of the gold in the Witwatersrand Basin (Hutchinson and Viljoen, 1988).

Important deposits of copper-zinc, with minor lead, are found in the Early to Late Proterozoic volcanic sequences developed on the western half of the African subcontinent in the Namaqualand Metamorphic Complex and in the Damara orogen in South West Africa/Namibia (Joubert, 1981, 1986b; Miller, 1983b; Killick, 1986).

Mineralization associated with granitic intrusions and metamorphosed terranes

Deposits that may be categorized under this heading occur scattered throughout southern Africa, but are best represented by the pegmatite belts developed in sectors of the Archaean granitic terrane of the Rhodesian and Kaapvaal cratons, and in the orogenic zones of Namaqualand and in the central parts of the Damara orogen. Important deposits of tin, tungsten, tantalum, niobium, lithium, mica, bismuth, beryllium, emeralds, corundum as well as uranium are found in these rocks (Anhaeusser, 1976a; Anhaeusser and Viljoen, 1986; Joubert, 1986b; Killick, 1986; Richards, 1986; Sohnge, 1986).

Some Archaean gold, tungsten, and tin deposits have been linked with intrusive granitic stocks and small plutons and, in southern South West Africa/Namibia, porphyry copper-molybdenum mineralization associated with calc-alkaline volcanic and plutonic rocks of Early Proterozoic age were described by Minnitt (1986) and Viljoen et al. (1986).

Metamorphism has been responsible for the development of important refractory mineral deposits, such as the extensive andalusite occurrences found in the aureole surrounding the Bushveld Complex, and the sillimanite, kyanite, and graphite deposits found in the high-grade metamorphic mobile belts (Anhaeusser, 1976a; Hammerbeck, 1986). An unusual and rare, but extremely important gold deposit, producing 1.5t of gold per annum and representing 10 per cent of Zimbabwe's gold output, is also located in high-grade metamorphic rocks situated in the North Marginal Zone of the Limpopo Belt (Bohmke and Varndell, 1986).

Mineralization associated with carbonatites and alkaline rocks (including kimberlites)

A number of important intrusive carbonatite and alkaline complexes occur throughout southern Africa (Verwoerd, 1967). Two of these occurrences to have received notoriety include the 2050 Ma Phalaborwa Complex situated near the eastern margin of the Kaapvaal Craton and the ~1200 Ma Premier kimberlite pipe, located towards the centre of the craton. Few mines, if any, elsewhere in southern Africa and perhaps in the world, can match Phalaborwa for the variety of its products and potentially extractable metals. The principal commodity produced at the mine is copper, with apatite, vermiculite, magnetite, sulphuric acid, zirconia, uranium, nickel, silver, gold, and platinum group elements either mined separately (as with the apatite and vermiculite) or as by-products. Potentially extractable metals include thorium, aluminium, potassium, and rare earth elements. Numerous other phosphate deposits in the form of apatite-rich carbonatites occur throughout southern Africa, with some carbonatites also showing economically potential deposits of niobium, titanium, strontium, hafnium, fluorite, barite, soda, limestone, and the semiprecious stone, sodalite (Verwoerd, 1986).

Although most of southern Africa's kimberlitic diamond deposits are of Late Cretaceous age, a few occurrences of Middle Proterozoic age are known, including the Premier diamond mine which still has the distinction of having produced the largest diamond ever found on earth (the 3025 carat Cullinan diamond). Green diamonds, the colour apparently produced by radiation damage to the diamond structure, have been found in ~2700 Ma Witwatersrand conglomerates (Young, 1917), suggesting that some kimberlitic intrusions may have been emplaced into the Kaapvaal Craton during Late Archaean times.

MINERAL RESOURCES

No single mineral resource inventory exists for the entire southern African region, but several attempts at compiling information pertinent to the mineral reserves of the Republic of South Africa have been produced (Coetzee, 1976; Pretorius, 1976b;

Van Rensburg and Pretorius, 1977; Von Gruenewaldt, 1976; Vermaak, 1979; Minerals Bureau of South Africa, 1986). Recent articles reviewing the precious, base, and ferrous metal resources, as well as the non-metallic mineral resources of the subcontinent include those of De Villiers et al. (1987), Forsyth (1987), Hammerbeck (1987), and Malan (1987).

Tables I-IV provide some indication of the reserves of selected metals and minerals available in southern Africa and a guide to the world ranking occupied by the various commodities. Although the mineral deposits are regionally well dispersed throughout the subcontinent there are concentrations of metals and minerals in clearly defined mineral provinces (as indicated by Sohnge, 1986).

TABLE I.
Southern African reserves of precious metals

Commodity	Reserves		World (%)	World Rank
Diamonds*	594	Mcar.	39.0	1
Gold	20467	t	50.8	1
Platinum Group Metals	31250	t	81.4	1
Silver#	9500	t	2.5	7

*Diamonds of gem and industrial quality mostly derived from pipes and alluvial sources younger than Precambrian,

Mcar = millions of carats; t = metric ton.

# Silver recovered as a by-product of gold and lead mining (after Minerals Bureau of South Africa, 1986)

The impact of this concentration was high-lighted by Pretorius (1976b) who provided tabulated data showing the distribution, quantity, and value of mineral commodities in the different geologic environments and as a function of their chronostratigraphic position. Despite being seemingly outdated the data nevertheless still reflect the main features pertaining to mineral availability and production in southern Africa. In South Africa alone, over 73% of the value of minerals ever produced has been derived from the Late Archaean-Early Proterozoic volcano-sedimentary basins with approximately 68% of the value stemming from the gold-silver-uranium production in the Witwatersrand Basin. The Bushveld Complex with its platinum group metals, nickel, chrome, vanadium, and tin, contributed 6% of the total value- a figure that now probably exceeds 10% following the expansion of mining (particularly platinum mining) over the past decade. The sedimentary successions of the Transvaal-Griqualand West sequences accounted for 5.5% of the value, with manganese, iron, asbestos, gold, limestone, and fluorite being the main commodities exploited. As an indication of the significance of the Phalaborwa Complex as a supplier of minerals almost 2% by

TABLE II.
World production of ferromanganese and ferrochrome alloys in 1984.

Alloys of ferromanganese		Alloys of ferrochrome	
Country	Production (kt)	Country	Production (t)
Japan	718	RSA	889 881
Norway	480	Japan	324 000
RSA	381	Zimbabwe	220 300
France	359	Sweden	145 000
FRG	309	Brazil	132 300
Brazil	285	FRG	70 000
Mexico	203	USA	59 200
India	168	Turkey	59 200
Spain	155	Finland	58 644
Italy	124	Italy	49 942
Canada	116	India	31 504
Australia	106	France	20 000
Belgium	95	Greece	20 000
UK	75	Spain	14 000
Yugoslavia	67	Norway	11 000
Portugal	65	Mexico	7 000
USA	60		
Korea	59		
Other ME*	39		
Total ME	3 864	Total ME	2 771 171
USSR	1 832	USSR	432 000
China	490	China	120 000
Poland	135	Poland	47 000
Romania	128	Czechoslovakia	29 000
Czechoslovakia	100	GDR	21 000
Other CPE⁺	100		
Total World	6649	Total World	2771 171

* ME : Market economies Kt = Kiloton (t x 10^3)
⁺ CPE : Centrally planned economies t = metric ton
RSA : Republic of South Africa
(after Minerals Bureau of South Africa, 1986 and Hammerbeck, 1987)

value of South Africa's mineral production stems from this source alone, with copper, phosphates, and vermiculite being the principal money earners.

Ferrous metals have become increasingly important in southern Africa (Hammerbeck, 1987), the region being the dominant world supplier of chromium from Archaean greenstone belt sources and layered ultramafic complexes in Zimbabwe (Mashaba, Great Dyke) and the Bushveld Complex in South Africa (Vermaak, 1979). Manganese, from extensive deposits in the Transvaal-Griqualand West succession, and vanadium from the Bushveld Complex, by far eclipse anything else known in the world. Southern Africa's resources of high-grade iron ores, although not large by world standards, are nevertheless substantial, and other commodities necessary to sustain a high-technology ferrous alloy, super alloy, and special steels industry, including nickel, cobalt, tungsten, silicon molybdenum, niobium-tantalum, titanium, zirconium, and rare earths, are in favourable supply. Table II shows the position of South Africa and Zimbabwe relative to the rest of the world in the production of ferrous metals.

The value of non-metallic minerals, while being relatively modest compared to that derived from the precious and ferrous metals, is nevertheless considerable. Resources of some selected non-metallic commodities are substantial, ranking highly by comparison with the rest of the world (Table III).

TABLE III.
South African reserves of selected non-metallic minerals

Commodity	Reserves (Mt)	World (%)	World Rank
Alumino - silicates	51.6	37.7	1
Asbestos (crocidolite,amosite, chrysotile)	7.8	5.8	4
Fluorspar	31.0	9.5	4
Phosphate (rock)	2310.0	6.9	3
Vermiculite	73.0	40.1	2

Mt = megaton (t x 10^3)
(after Minerals Bureau of South Africa, 1986)

As outlined by Forsyth (1987), the golden era of base metal exploration dawned in the early 1960's. Up until this time copper was the dominant commodity in this category, being mined from Early Proterozoic Lomagundi-Umkondo sediments in Zimbabwe, and from Middle Proterozoic basic bodies intruded into the Okiep copper district of the Namaqualand Metamorphic Complex (Joubert, 1986b). In addition, important copper-lead-zinc production stemmed from the remarkable Tsumeb ore pipe found in dolomites on the northern shelf of the Damara orogen in South West Africa/Namibia (Killick, 1986). Also, some tin production was derived from pegmatites occurring in the Archaean, Namaqualand, and Damaran granitoids, as well as in the Bushveld granites and associated sediments, and copper-nickel was obtained as a by-product of platinum mining in the Bushveld Complex.

Subsequently, numerous base metal discoveries ensued in a variety of settings, but principally in the high-grade metamorphic terranes such as the Limpopo Belt (Selebi-Phikwe, copper-nickel), the Namaqualand Metamorphic Complex (Prieska, copper-zinc; Aggeneys, lead-zinc-silver-copper; Gamsberg, zinc; Rosh Pinah, zinc) and the Damara orogen (Matchless, Otjihase, Oamites; copper-zinc-silver-lead).

TABLE IV.
Southern African reserves of metallic minerals

	Reserves	World	
Commodity		(%)	Rank
Antimony *	254 kt	5.5	4
Beryllium *	24 kt	3.3	7
Chromium (ore)	3953 Mt	91.3	1
Cobalt *	32 kt	0.5	10
Copper *	6 mt	1.2	11
Iron^{+}	5987 Mt	6.7	5
Lead $^{\#}$	5 Mt	3.9	5
Manganese (ore)	12700 Mt	78.5	1
Nickel $^{\sigma}$	6649 kt	7.7	6
Titanium $^{@}$	31 Mt	12.8	3
Uranium $^{\theta}$	n/a	15.0	2
Vanadium *	7800 kt	47.1	1
Zinc *	15 Mt	5.4	4
Zirconium *	6.9 Mt	17.7	3

* contained metal ; + estimated iron content ; σ sulphide ore;
θ U_3O_8;n/a not available for disclosure;
Mt = megaton (6 x 10^6); kt= kiloton (t x 10^3)
(after Minerals Bureau of South Africa, 1986)

On the cratons the Archaean greenstone belts yielded significant deposits of nickel-copper (e.g. Shangani, Trojan, Empress) and antimony-gold (Murchison), and Phalaborwa began copper and phosphate production in 1966. In recent years interesting lead-zinc deposits have been found in Early Proterozoic dolomites of the Transvaal-Griqualand West sequence (Pering, Bushy Park, Leeubosch) (Beukes, 1986). Table IV provides some indication of the metallic mineral reserves of South Africa.

Overall, southern Africa is lacking in few metals and minerals, has substantial reserves to sustain a mining industry well into the 21st century, and should remain a dominant supplier of a wide range of mineral commodities and specialized mineral products for a long time into the future.

CONCLUDING REMARKS

The African subcontinent must remain one of the most singularly unique geological regions on earth. Despite its relatively small areal extent of approximately 3,447,000 km^2 it can boast a wide range of tectono-stratigraphic domains ranging in age from Archaean to Late Proterozoic, as well as still younger Phanerozoic environments not discussed in this contribution. The region has contributed substantially to a general understanding of geological processes and responses (be they igneous, sedimentary, volcanic, or metamorphic) because a number of exceptional geological features were able to withstand the ravages of time. Included among these outstanding geological terranes are: (a) the classically symmetrical Limpopo Belt wedged between the Kaapvaal and Rhodesian cratons, (b) numerous granite-greenstone tracts, but specifically the Barberton Mountain Land and the Belingwe region of southern Zimbabwe, (c) the series of intracratonic volcano-sedimentary basins developed on the Kaapvaal Craton, in particular the units making up the Witwatersrand Triad, (d) the Great Dyke of Zimbabwe, (e) the Bushveld Complex on the Kaapvaal Craton, (f) the Vredefort ring structure, (g) the Phalaborwa carbonatite complex, (h) the Early to Middle Proterozoic Namaqualand-Natal tectono-metamorphic domain accreted onto the earlier formed Kaapvaal Craton, and (i) the Late Proterozoic Damara orogen flanked by platformal sequences deposited on younger cratonic basement.

Southern Africa can also boast a number of unique mineral provinces and deposits, most of which have no counterparts elsewhere in the world. Such a list would include (a) the Witwaterstrand gold (silver)-uranium province, (b) the Bushveld Complex with its platinum-chrome-vanadium occurrences, (c) the Kalahari manganese field in the Early Proterozoic Transvaal-Griqualand West sequence, (d) the unique copper-phosphate-vermiculite deposits associated with the Phalaborwa Complex, (e) the Shurugwi/Great Dyke/Mashaba high-grade chrome occurrences in south-central Zimbabwe, (f) the Late Proterozoic Tsumeb lead-copper-zinc-silver deposit in South West Africa/Namibia, and (g) the Rossing uranium deposit developed in pegmatitic alaskites intruded during the waning stages of evolution of the central Damara orogen.

ACKNOWLEDGEMENTS

The writer would like to thank Mrs. Lorna Tyler for typing the manuscript and Mr.N.A. de N.C. Gomes for assisting with the illustrations.

REFERENCES

Anhaeusser, C.R., 1973a. The evolution of the early Precambrian crust of southern Africa. Phil. Trans. R. Soc. Lond., A.273 : 359-388.

Anhaeusser, C.R., 1973b. The geology and geochemistry of the Archaean granites and gneisses of the Johannesburg-Pretoria dome. Spec. Publ. Geol. Soc. S. Afr., 3: 361-385.

Anhaeusser, C.R., 1976a. Archaean metallogeny in Southern Africa. Econ. Geol., 71: 16-43.

Anhaeusser, C.R., 1976b. The nature and distribution of Archaean gold mineralization in southern Africa. Minerals Sci. Engng., 8: 46-84.

Anhaeusser, C.R., 1976c. The nature of chrysotile asbestos occurrences in Southern Africa: a review. Econ. Geol., 71: 96-116.

Anhaeusser, C.R., 1981. Geotectonic evolution of the Archaean successions in the Barberton Mountain Land, South Africa. In: A.Kroner (Editor), Precambrian Plate Tectonics, Developments in Precambrian Geology 4, Elsevier, Amsterdam, pp.137-160.

Anhaeusser, C.R. (Editor), 1983. Contributions to the Geology of the Barberton Mountain Land. Spec. Publ. Geol. Soc. S. Afr., 9, 223pp.

Anhaeusser, C.R., 1987a. The nature and geotectonic setting of Archaean and Early Proterozoic layered intrusions in southern Africa: a review. Progr. with Abstr. Indaba on the Tectonic setting of Layered Intrusives, Univ. Pretoria: 1-4.

Anhaeusser, C.R., 1987b. Geological overview of Southern Africa's mineral resources. S. Afr. J. Sci., 83: 268-270.

Anhaeusser, C.R. and Button, A., 1976. A review of southern African stratiform ore deposits - their position in time and space. In: K.H. Wolf (Editor), Handbook of Strata-Bound and Stratiform Ore Deposits. Vol.5 Regional Studies. Elsevier, Amsterdam, pp.257-319.

Anhaeusser, C.R. and Maske, S. (Editors), 1986. Mineral Deposits of Southern Africa, I and II. Geol. Sco. S. Afr., Johannesburg, 2335pp.

Anhaeusser, C.R., Mason, R., Viljoen, M.J. and Viljoen, R.P., 1969. A reappraisal of some aspects of Precambrian shield geology. Bull. Geol. Soc. Amer., 80: 2175-2200.

Anhaeusser, C.R. and Robb, L.J., 1980. Regional and detailed field and geochemical studies of Archaean trondhjemitic gneisses, migmatites and greenstone xenoliths in the southern part of the Barberton Mountain Land, South Africa. Precamb. Res., 11: 373-397.

Anhaeusser, C.R. and Robb, L.J., 1981. Magmatic cycles and the evolution of the Archaean granitic crust in the eastern Transvaal and Swaziland. Spec. Publ. Geol. Soc. Aust., 7 : 457-467.

Anhaeusser, C.R. and Viljoen, M.J., 1986. Archaean metallogeny of Southern Africa. In: C.R. Anhaeusser and S. Maske (Editors), Mineral Deposits of Southern Africa, I. Geol. Soc. S. Afr., Johannesburg: 33-42.

Anhaeusser, C.R. and Wilson, J.F. 1981. Chapter 8: The granitic-gneiss Greenstone Shield. In: D.R.Hunter (Editor), Precambrian of the Southern Hemisphere. Developments in Precambrian Geology 2, Elsevier, Amsterdam, pp.423-499.

Arth, J.G. and Hanson, G.N., 1975. Geochemistry and origin of the early Precambrian crust of northeastern Minnesota. Geochim. Cosmochim. Acta, 39: 325-362.

Barton, J.M. Jr., 1983a. Isotopic constraints on possible tectonic models for crustal evolution in the Barberton granite-greenstone terrane, southern Africa. Spec. Publ. Geol. Soc. S. Afr., 9: 73-79.

Barton, J. M. Jr., 1983b. Our understanding of the Limpopo Belt - a summary with proposals for future research. Spec. Publ. Geol. Soc. S. Afr., 8: 191-203.

Barton, J.M. Jr., Fripp, R.E.P., Horrocks, P. and McLean, N., 1979. The geology, age, and tectonic setting of the Messina Layered Intrusion, Limpopo Mobile Belt, southern Africa. Amer. J.Sci., 279: 1108-1134.

Barton, J.M. Jr. and Key, R.M., 1981. The tectonic development of the Limpopo Mobile Belt and the evolution of the Archaean cratons of southern Africa. In: A. Kroner (Editor), Precambrian Plate Tectonics. Developments in Precambrian Geology 4, Elsevier, Amsterdam, pp.185-212.

Barton, J.M. Jr., Ryan, B. and Fripp, R.E.P., 1983. Rb-Sr and U-Th-Pb isotopic studies of the Sand River Gneisses, Central Zone, Limpopo Mobile Belt. Spec. Publ. Geol. Soc. S.Afr., 8: 9-18.

Buekes, N.J., 1986. The Transvaal Sequence in Griqualand West. In: C.R. Anhaeusser and S. Maske (Editors), Mineral Deposits of Southern Africa, I. Geol. Soc. S. Afrc., Johannesburg, pp.819-828.

Bohmke, F.C. and Varndell, B.J., 1986. Gold in granulites at Renco Mine, Zimbabwe. In: C.R. Anhaeusser and S. Maske (Editors), Mineral Deposits of Southern Africa, I. Geol. Soc. S. Afr., Johannesburg, pp.221-230.

Botha, B.J.V. (Editor), 1983. Namaqualand Metamorphic Complex. Spec. Publ. Geol. Soc. S. Afr., 10: 198.

Bristow, J.W., 1985. Preface to Special Issue entitled: "Alkaline and alkaline-ultrabasic rocks and their xenoliths". Trans. Geol. Soc. S. Afr., 88: (iii)-(v).

Bristow, J.W., Smith, C.B., Allsopp, H.L., Shee, S.R. and Skinner, E.M.W., 1986. Setting, geochronology and geochemical characteristics of 1600 m.y. kimberlites and related rocks from the Kuruman Province, South Africa. Ext. Abstr. Fourth Int. Kimberlite Conference, Perth. Abstr. Geol. Soc. Aust., 16 : 112-114.

Brock, B.B. and Pretorius, D.A. 1964. Rand Basin sedimentation and tectonics. In: S.H. Haughton (Editor), The Geology of Some Ore Deposits in Southern Africa, I. Geol. Soc. S. Afr., Johannesburg, pp.549-599.

Button, A., Pretorius, D.A., Jansen, H., Stocklmayer, V., Hunter, D.R., Wilson, J.F., Wilson, A.H., Vermaak, C.F., Lee, C.A. and Stagman, J.G., 1981. Chapter 9: The Cratonic Environment. In: D.R. Hunter (Editor), Precambrian of the Southern Hemisphere. Developments in Precambrian Geology 2, Elsevier, Amsterdam, pp.501-639.

Clifford, T.N., 1970. The structural framework of Africa. In: T.N. Clifford and I. Gass (Editors), African Magmatism and Tectonics. Oliver & Boyd, Edinburgh, pp.1-26.

Cloud, P., 1976. Major features of crustal evolution. A.L. du Toit Memorial Lecture No.14, Annex. Trans. Geol. Soc. S. Afr., 79: 32.

Cloud, P., 1988. Oasis in Space. Earth History from the Beginning. W.W. Norton & Company, New York: 508pp.

Coetzee, C.B. (Editor), 1976. Mineral Resources of the Republic of South Africa. Handbook. Geol. Surv. S. Afr., 7: 462pp.

Compston, W. and Kroner, A., 1988. Multiple zircon growth within early Archaean tonalitic gneiss from the Ancient Gneiss Complex, Swaziland. Earth Planet. Sci. Lett., 87: 13-28.

Condie, K.C. 1981. Archaean Greenstone Belts. Elsevier, Amsterdam, 434pp.

Condie, K.C. and Hunter, D.R., 1976. Trace element geochemistry of Archaean granitic rocks from the Barberton region, South Africa. Earth. Planet. Sci. Lett., 29: 389-400.

Coward, M.P., James, R.P. and Wright, L., 1976. Northern margin of the Limpopo Mobile Belt. Bull. Geol. Soc. Amer., 87: 601-611.

Davies, R.D., Allsopp, H.L., Erlank, A.J. and Manton, W.I., 1970. Sr-isotopic studies on various layered mafic intrusions in southern Africa. Spec. Publ. Geol. Soc. S. Afr., 1: 576-593.

De Villiers, J.S., Lee, C.A. and Killick, A.M., 1987. Precious metal resources of Southern Africa. S. Afr. J. Sci., 83: 270-273.

Dietz, R.S., 1961. Vredefort ring structure : meteorite impact scar? J. Geol. , 69: 499-516.

Du Toit, M.C. and Van Reenen, D.D., 1977. The southern margin of the Limpopo Mobile Belt, northern Transvaal, with special reference to metamorphism and structure. Bull. Geol. Surv. Botswana, 12: 83-97.

Eriksson, S.C., 1984. Age of carbonatite and phosphorite magmatism of the Phalaborwa Complex (South Africa). Isotope Geoscience, 2: 291-299.

Ferguson, J., 1973. The Pilanesberg alkaline province, southern Africa. Trans. Geol. Soc. S. Afr., 76: 249-270.

Forsyth, M.B., 1987. Base metal resources of Southern Africa. S. Afr. J. Sci., 83: 281-283.

Foster, R.P. and Wilson, J.F., 1984. Geological setting of Archaean gold deposits in Zimbabwe. In: R.P. Foster (Editor), Gold'82: The Geology, Geochemistry and Genesis of Gold Deposits. Spec. Publ. Geol. Soc. Zimbabwe, A.A. Balkema, Rotterdam, pp.521-551.

Frick, C. and Walraven, F., 1985. The petrology and geochemistry of the pre-Karoo Elandskraal volcano, South Africa. Trans. Geol. Soc. S. Afr., 88: 225-243.

Glikson, A.Y., 1979. Early Precambrian tonalite-trondhjemite sialic nuclei. Earth Sci. Rev., 15: 1-73.

Glikson, A.Y. and Jahn, B.M., 1985. REE and LIL elements, eastern Kaapvaal shield, South Africa : evidence of crustal evolution by 3-stage melting. Spec. Pap. Geol. Soc. Can., 28: 303-324.

Goodwin, A.M., 1968. Evolution of the Canadian shield. Proc. Geol. Assoc. Can., 19: 1-14.

Gould, D. and Rathbone, P.A., 1985. The geological structure of the Molopo Farms project area. In: D.G. Hutchins and A.P. Lynam (Editors), The Proceedings of a Seminar on the Mineral Exploration of the Kalahari, October, 1983. Bull. Geol. Surv. Botswana, 29: pp.160-186.

Green, T.H. and Ringwood, A.E., 1968. Genesis of the calc-alkaline igneous rock suite. Contr. Min. Pet., 18: 105-162.

Hammerbeck, E.C.I., 1986. Andalusite in the metamorphic aureole of the Bushveld Complex. In: C.R. Anhaeusser and S. Maske (Editors), Mineral Deposits of Southern Africa, I . Geol. Soc. S. Afr. Johannesburg, pp.993-1004.

Hammerbeck, E.C.I., 1987. Ferrous metals : mainstay of Southern Africa's industrial development. S. Afr. J. Sci., 83 : 277-280.

Harmer, R.E., 1985. Rb-Sr isotopic study of units of the Pienaars River Alkaline Complex, north of Pretoria, South Africa. Trans. Geol. Soc. S. Afr. 88: 215-223.

Hart, R.J., Nicolaysen, L.O. and Gale, N.H., 1981a. Radioelement concentrations in the deep profile through Precambrian basement of the Vredefort structure. J. Geophys. Res., 86, B 11: 10639-10652.

Hart, R.J., Welke, H.J. and Nicolaysen, L.O., 1981b. Geochronology of the deep profile through Archaean basement at Vredefort, with implications for early crustal evolution. J. Geophys. Res., 86, B 11: 10663-10680.

Haughton, S.H. (Editor), 1964. The Geology of some Ore Deposits in Southern Africa, Vols. I and II. Geol. Soc. S. Afr., Johannesburg: 625 and 739.

Hunter, D.R., 1974a. Crustal development in the Kaapvaal craton, I. The Archaean. Precamb. Res., 1: 259-294.

Hunter, D.R., 1974b. Crustal development in the Kaapvaal craton. II. The Proterozoic. Precamb. Res. 1: 295-326.

Hunter, D.R. and Pretorius, D.A., 1981. Chapter 7 : Structural Framework. In: D.R. Hunter (Editor), Precambrian of the Southern Hemisphere. Development in Precambrian Geology 2, Elsevier, Amsterdam, pp.397-422.

Hutchinson, R.W. and Viljoen, R.P., 1988. Re-evaluation of gold source in Witwatersrand ores. S. Afrc. J. Geol., 91: (in press).

Joubert, P., 1981. The Namaqualand Metamorphic Complex. In: D.R. Hunter (Editor), Precambrian of the Southern Hemisphere. Developments in Precambrian Geology 2, Elsevier, Amsterdam, pp.671-705.

Joubert, P., 1986a. Namaqualand - a model of Proterozoic accretion? Trans. Geol. Soc. S. Afr. , 89: 79-96.

Joubert, P., 1986b. The Namaqualand Metamorphic Complex - a summary. In: C.R. Anhaeusser and S.Maske (Editors), Mineral Deposits of Southern Africa, I. Geol. Soc. S. Afr., Johannesburg, pp.1395-1420.

Killick, A.M., 1986. A review of the economic geology of northern South West Africa/Namibia. In: C.R. Anhaeusser and S. Maske

(Editors), Mineral Deposits of Southern Africa, II. Geol. Soc. S. Afr., Johannesburg, pp.1709-1717.

Kramers, J.D., 1979. Lead, uranium, strontium, rubidium, and potassium in inclusion bearing diamonds and mantle derived xenoliths from southern Africa. Earth Planet. Sci. Lett., 43: 58-70.

Kroner, A., 1977. Precambrian mobile belts of southern and eastern Africa - ancient sutures or sites of ensialic mobility? A case for crustal evolution towards plate tectonics. Tectonophysics, 40: 101-135.

Kroner, A., 1981. Precambrian plate tectonics. In: A.Kroner (Editor), Precambrian Plate Tectonics. Developments in Precambrian Geology 4, Elsevier, Amsterdam, pp.57-90.

Kroner, A., 1985. Evolution of the Archaean continental crust. Ann. Rev. Earth Planet. Sci., 13: 49-74.

Kroner, A. and Greiling, R. (Editors), 1984. Precambrian Tectonics Illustrated. E. Schweizerbart'sche Verlagsbuchhandlung, Stuttgart, 419pp.

Lambert, I.B. and Wyllie, P.J., 1972. Melting of gabbro (quartz eclogite) with excess water to 35 kilobars, with geological applications. J.Geol., 80: 693-708.

Lurie, J., 1986. Mineralization of the Pilanesberg alkaline complex. In: C.R. Anhaeusser and S. Maske (Editors), Mineral Deposits of Southern Africa, II. Geol. Soc. S. Afr., Johannesburg, pp.2215-2228.

Malan, W.W., 1987. Non-metallic mineral resources of South Africa. S.Afr. J.Sci., 83: 274-277.

Martin, H. and Porada, H., 1977a. The intracratonic branch of the Damara orogen in South West Africa. Part I. Discussion of geodynamic models. Precamb. Res., 5: 311-338.

Martin, H. and Porada, H., 1977b. The intracratonic branch of the Damara orogen in South West Africa. Part II. Discussion of relationships with the Pan African mobile belt system. Precamb. Res., 5: 339-357.

Matthews, P.E., 1972. Possible Precambrian obduction and plate tectonics in south eastern Africa. Nature, 240: 37-39.

Matthews, P.E., 1981. Eastern or Natal sector of the Namaqua-Natal mobile belt in southern Africa. In: D.R. Hunter (Editor), Precambrian of the Southern Hemisphere. Developments in Precambrian Geology, 2, Elsevier, Amsterdam, pp.705-715.

McCall, G.J.H., 1977. The Archaean-Search for the Beginning. Dowden, Hutchinson & Ross, Pennsylvania, 505pp.

McCarthy, T.S., Charlesworth, E.G. and Stanistreet, I.G., 1986. Post-Transvaal structural features of the northern portion of the Witwatersrand Basin. Trans. Geol. Soc. S. Afr., 89: 311-323.

Miller, R. McG. (Editor), 1983a. Evolution of the Damara Orogen of South West Africa/Namibia. Spec. Publ. Geol. Soc. S. Afr., 11: 515pp.

Miller, R. McG., 1983b. The Pan-African Damara Orogen of South West Africa/Namibia. Spec. Publ. Geo. Soc. S. Afr., 11: 431-515.

Minerals Bureau of South Africa, 1986. South Africa's Mineral Industry, 1985, 224pp.

Minnitt, R.C.A. 1986. Porphyry copper-molybdenum mineralization at Haib River, South West Africa/Namibia. In: C.R.Anhaeusser and S.Maske (Editors), Mineral Deposits of Southern Africa. Geol. Soc. S. Afr., Johannesburg, pp.1567-1585.

Myers, R.E., Cawthorn, R.G., McCarthy, T.S. and Anhaeusser,C.R., 1987. Fundamental uniformity in the trace element patterns of the volcanics of the Kaapvaal Craton from 3000 to 2100 Ma: evidence for the lithospheric origin of these continental tholeiites. In: T.C. Pharaoh, R.D. Beckinsale and D.Rickard (Editors), Geochemistry and Mineralization of Proterozoic Volcanic Suites. Spec. Publ. Geol. Soc. Lond., 33, Blackwell, London, pp.315-325.

Newham, W.D.N. (Compiler F. Mendelsohn), 1986. The Lomagundi and Sabi metallogenic provinces of Zimbabwe. In: C.R.Anhaeusser and S.Maske (Editors), Mineral Deposits of Southern Africa, II. Geol. Soc. S.Afr., Johannesburg, pp.1351-1394.

Nisbet, E.G., 1987. The Young Earth: an Introduction to Archaean Geology. Allen & Unwin, London, 402pp.

Pretorius, D.A., 1976a. The nature of the Witwatersrand gold-uranium deposits. In: K.H.Wolf (Editor), Handbook of Strata-bound and Stratiform Ore Deposits, II. Regional Studies and Specific Deposits, Elsevier, Amsterdam, 7, pp.29-88.

Pretorius, D.A., 1976b. The stratigraphic, geochronologic, ore-type, and geologic-environment sources of mineral wealth in the Republic of South Africa. Econ. Geol., 71: 5-15.

Pretorius, D.A. and Maske, S., 1976. Preface to an issue devoted to mineral deposits in southern Africa. Econ. Geol., 71: 1-4.

Reid, D.L., 1982. Age relationships within the Vioolsdrif batholith, lower Orange River region. II. A two stage emplascement history and the extent of Kibaran overprinting. Trans.Geol. Soc. S. Afr., 85: 105-110.

Richards, T.E., 1986. Geological characteristics of rare-metal pegmatites of the Uis type in the Damara orogen, South West Africa/Namibia. In: C.R. Anhaeusser and S. Maske (Editors), Mineral Deposits of Southern Africa, II. Geol. Soc. S. Afr., Johannesburg, pp.1845-1862.

Robb, L.J. and Anhaeusser, C.R., 1983. Chemical and petrogenetic characteristics of Archaean tonalite-trondhjemite gneiss plutons in the Barberton Mountain Land. Spec. Publ. Geol. Soc. S.Afr., 9: 103-116.

Robb, L.J., Anhaeusser, C.R. and Van Nierop, D.A., 1983. The recognition of the Nelspruit batholith north of the Barberton greenstone belt and its significance in terms of Archaean crustal evolution. Spec. Publ. Geol. Soc. S.Afr., 9: 117-130.

Robertson, I.D.M., Du Toit, M.C., Joubert, P., Matthews, P.E., Lockett, N.H., Mendelsohn, F., Broderick, T.J., Bloomfield, K. and Mason, R., 1981. Chapter 10: Mobile Belts. In: D.R.Hunter (Editor), Precambrian of the Southern Hemisphere, Developments in Precambrian Geology 2, Elsevier, Amsterdam, pp.641-802.

Roering, C., 1984. The Witwatersrand Supergroup at Swartkops : a reexamination of the structural geology. Trans. Geol. Soc. S. Afr., 87: 87-99.

Simpson, C., 1978. The structure of the rim synclinorium of the Vredefort Dome. Trans. Geol. Soc. S.Afr., 81: 115-121.

Sohnge, A.P.G., 1986. Mineral provinces of Southern Africa. In: C.R. Anhaeusser and S. Maske (Editors), Mineral Deposits of Southern Africa, I. Geol. Soc. S.Afr., Johannesburg, pp.1-23.

Tankard, A.J., Jackson, M.P.A., Eriksson, K.A., Hobday, D.K., Hunter, D.R. and Minter, W.E.L., 1982. Crustal Evolution of Southern Africa. 3.8 Billion Years of Earth History. Springer-Verlag, New York: 523pp.

Tarling, D.H. (Editor), 1978. Evolution of the Earth's Crust. Academic Press, London, 443pp.

Tweedie, K.A.M., 1986. The discovery and exploration of Beisa and Beatrix gold and uranium mines in the southern extension of the Weltom Goldfield. In: C.R. Anhaeusser and S.Maske (Editors), Mineral Deposits of Southern Africa. Geol.Soc. S.Afr., Johannesburg, pp.541-547.

Vajner, V., 1974. Crustal evolution of the Namaqua mobile belt and its foreland in parts of the northern Cape. Bull. Precambrian Res. Unit, Univ. Cape Town, 15: 1-15.

Van Reenen, D.D. and Du Toit, M.C., 1977. Mineral reactions and the timing of metamorphic events in the Limpopo Metamorphic Complex south of the Soutpansberg. Bull. Geol. Surv. Botswana, 12: 107-127.

Van Rensburg, W.C.J. and Pretroius, D.A., 1977. South Africa's Strategic Minerals - Pieces on a Continental Chess Board. Valiant Publishers, Johannesburg, 156.

Vearncombe, J.R., Barton, J.M. Jr. and Walsh, K.L., 1987. The Rooiwater Complex and associated rocks, Murchison granitoid-greenstone terrane, Kaapvaal Craton. S.Afr. J.Geol., 90: 361-377.

Vermaak, C.F., 1979. The global status of the South African minerals economy and data summaries of its key commodities. Rev. Pap. Geol. Soc. S.Afr., 1: 57pp.

Vermaak, C.F. and Von Gruenewaldt, G., 1986. Introduction to the Bushveld Complex. In: C.R. Anhaeusser and S. Maske (Editors), Mineral Deposits of Southern Africa, II. Geol. Soc. S.Afr., Johannesburg, pp.1021-1029.

Verwoerd, W.J., 1967. The carbonatites of South Africa and South West Africa, Handbook Geol. Surv. S.Afr., 6: 452.

Verwoerd, W.J., 1986. Mineral deposits associated with carbonatites and alkaline rocks. In: C.R.Anhaeusser and S.Maske (Editors), Mineral Deposits of Southern Africa, II. Geol. Soc. S.Afr., Johannesburg, pp.2173-2191.

Viljoen, R.P., Minnitt, R.C.A., and Viljoen, M.J., 1986. Porphyry copper molybdenum mineralization at the Lorelei, South West Africa/Namibia. In: C.R. Anhaeusser and S.Maske (Editors), Mineral Deposits of Southern Africa, 11. Geol. Soc. S.Afr., Johannesburg, pp.1559-1565.

Von Gruenewaldt, G., 1976. An evaluation of the mineral resources of the Bushveld Complex. Res. Rep. Institute for Geological Research on the Bushveld Complex, Univ. Pretoria, 3: 28pp.

Watkeys, M.K., 1983. Brief explanatory notes on the provisional geological map of the Limpopo Belt and environs. Spec. Publ. Geol. Soc. S.Afr., 8: 5-8.

Watkeys, M.K. and Armstrong, R.A., 1985. The importance of being alkaline deformed Late Archaean lamprophyric dykes, Central Zone, Limpopo Belt. Trans. Geol. Soc. S. Afr., 88: 195-206.

Wilson, J.F., 1979. A preliminary reappraisal of the Rhodesian Basement Complex. Spec. Publ. Geol. Soc. S. Afr., 5: 1-23.

Windley, B.F., 1976. The Early History of the Earth. John Wiley & Sons, London, 619pp.

Windley, B.F., 1977. The Evolving Continents. John Wiley & Sons, London, 385pp.

Young, R.B., 1917. The Banket. A Study of the Auriferous Conglomerates of the Witwatersrand and the Associated Rocks. Gurney & Jackson, London, 125pp.

STRUCTURAL STYLES IN THE PRECAMBRIAN METAMORPHIC TERRANES OF PENINSULAR INDIA: A SYNTHESIS*

K. NAHA AND D. MUKHOPADHYAY

ABSTRACT

Structural features are known in reasonable detail for three Precambrian metamorphic terranes of Peninsular India, namely, Karnataka in South India, Rajasthan in Western India, and Bihar-Orissa in Eastern India. All the rock groups of the Early Precambrian Dharwar tectonic province of Karnataka -- the supposed Sargur and Dharwar supracrustal belts, the Peninsular Gneiss and the granulite--have been involved in the same style and sequence of superposed deformations. The folds of the first set are isoclinal with attenuated limbs and thickened hinges. These, together with their axial planar cleavage, have been affected in selected sectors by near-coaxial upright folds of varying tightness. On these structures a set of open folds has been overprinted. Superposition of folds of three sets has resulted in interference patterns of different types from the scale of hand specimen to map. This structural unity runs counter to any suggestion of two groups of supracrustal rocks now separated by an angular unconformity. Migmatization synkinematic with the first folding in a large part of the Peninsular Gneiss also argues against the gneiss, as *we see it now*, being the basement for the supracrustal rocks. Evidence has been adduced from relict structures in enclaves in the Peninsuar Gneiss for one episode of deformation prior to the first decipherable folding in the supracrustal rocks. The NNW extension of the supracrustal belts is due to the north-northwesterly strike of axial planes of folds of two systems.

The NNE to NE extension of the supracrustal Aravalli and Delhi belts of Rajasthan in Western India is also a reflection of the strikes of axial planes of folds of two generations, whose axes have a nearly orthogonal relation. W- to WNW-trending reclined

---

*Presented at the IASPEI regional assembly in Hyderabad, India, in 1984 isoclinal folds of the first generation, which are ubiquitous in the Aravalli Group, are absent in the rocks of the Delhi Group. Structures of the three later generations are, however, common to both the groups. These are the upright folds on N- to NNE-trending axes, overprinted by gravity-induced conjugate folds, which are in turn followed by upright conjugate folds indicating longitudinal shortening. The Banded Gneissic Complex, considered by Heron to be the basement, comprises granites and gneisses of different ages -- some older lying below the Aravalli Group, and some others representing the migmatized Aravalli rocks. Similarity in structural style and sequence of even the undoubtedly older gneisses with those in the Aravalli rocks suggests remobilization of the basement during the first deformation in the Aravalli Group.

In the eastern part of the Indian shield, several distinct tectonic provinces can be recognized, but their interrelation remains obscure. The Older Metamorphic Group of supracrustal rocks and the intrusive tonalitic gneisses show the same sequence of superposed folding, with NE-plunging early folds overprinted by folds plunging SE. The Singhbhum Granite body is a composite batholith with several independent plutons showing swirling patterns of primary foliation. The dominantly chemogenic and volcaniclastic sedimentary rocks of the Iron Ore province are folded into an overturned synclinorium with NNE-plunging axis. Coaxial refolding followed by EW warping are the manifestations of later deformational phases. The North and East Singhbhum province comprises the metaflysch sequence of the Chakradharpur-Tatanagar-Ghatsila belt, the long linear zone of Dalma metavolcanics, and the northern belt of metasediments. The most pervasive planar structure here is an EW-striking schistosity axial planar to large-scale folds of nearly EW axial trend, with northerly axial trend in some sectors. These structures apparently continue northward to the Chhotanagpur Gneiss terrane, where the structural details are imperfectly known. The southern boundary of the Northern and Eastern Singhbhum province is marked by a belt of cataclasis and mylonitization -- the Singhbhum shear zone -- whose tectonic significance is a matter of debate.

INTRODUCTION

The structural synthesis on a regional scale of the Precambrian metamorphic terranes of Peninsular India started with Holmes' famous paper of 1949, where he used orogenic trends and their intersections to divide the structural provinces of the peninsular Precambrian tract (Fig. 1). But as pointed out by Naha (1964), uncritical acceptance of "orogenic trends" for correlating Precambrian tectonic provinces led to a number of erroneous inferences. The "orogenic trends", which have been used in India following the suggestion of Holmes (1949) and Krishnan (1960), are either orographic features or strikes of secondary foliation in the metamorphic rocks. Barring special orientations of folds, neither the orographic trends (which are usually parallel to the formational boundaries) nor the strikes of foliation (which are generally parallel to the axial planes of the dominant set of

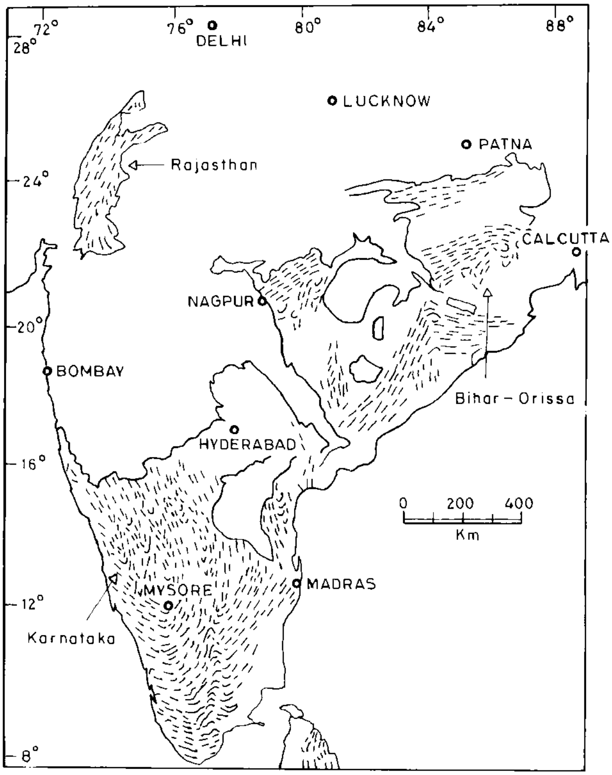

Figure 1. "Trend lines" in the Precambrian metamorphic terranes of India (after Krishnan, 1960); locations of the three terranes discussed are shown.

folds) represent the trends of reginal fold axes. Furthermore, it has become increasingly apparent that superposed deformations are the rule rather than the exception in the Precambrian metamorphic terranes of Peninsular India; and the application of orogenic trends with their intersecting relations is fraught with difficulties in these terranes.

Structural features are known in reasonable detail for three Precambrian metamorphic terranes of Peninsular India, viz, Karnataka in South India, Rajasthan in Western India, and Bihar-Orissa in Eastern India (Fig. 1). All these three tectonic provinces show certain common features. (1) They provide evidence of structural overprinting in either some parts or the whole of the terrane. (2) They have basement gneisses overlain at places by conglomerates, which in turn are followed by metasedimentary and meta-igneous rocks. (3) In Karnataka and Rajasthan, in particular, the following features are seen: (a) The basement gneisses show structures indentical in style and sequence with those in the metamorphic rocks. (b) Small to large enclaves of metasedimentary and meta-igneous rocks, which may or may not belong to the rock groups framing the gneisses, are present (c) Demonstrable evidence of supposedly younger metamorphic rocks having been migmatized by some components of the "basement" gneisses indicates that the latter contain rocks of more than one generation. (d) Folds in the gneisses, accordant with the earliest decipherable isoclinal folds in the metasediments, point to ductile deformation in the basement gneisses during the earlier stage of folding. (e) Rare structures of pre-F_1 phase occurring as relicts, either in the small enclaves within the gneisses or in the quartzo-feldspathic layers themselves, provide the only clue, in addition to the basal conglomerates, regarding the basement nature of the gneisses.

In the third tectonic province of Bihar-Orissa in Eastern India, the structural relations between the Older Metamorphic Group and the Singhbhum Granite are not so clear . A synopsis of the major structural characteristics of the three tectonic provinces follows.

KARNATAKA

Five linear belts of metasedimentary and meta-igneous rocks occurring in gneissic country were termed " the Dharwar System" in 1886 by Foote (Rama Rao, 1940; Pichamuthu, 1967). The gneissic complex with a host of small enclaves was termed 'the Fundamental Gneiss' in the belief that this group forms the basement on which the rocks of the Dharwar Group occur unconformably (Fig. 2). The five belts of Dharwar schists were supposed to occur in synclinal cores, the anticlinal portions having been occupied by the basement gneiss. These gneisses were subsequently named 'the Peninsular Gneiss' and were considered by Smeeth in 1916 (See Pichamuthu, 1967) to be younger than the rocks of the Dharwar Group, intruding them at a number of places. The dominant NNW trend of the five Dharwar schist belts was thought to represent the 'Dharwar orogenic tend'. A general increase in metamorphic grade as one moves southward also led to the inference by Pichamuthu that the overall structure of the rocks of the Dharwar Group is an anticlinorium plunging toward NNW.

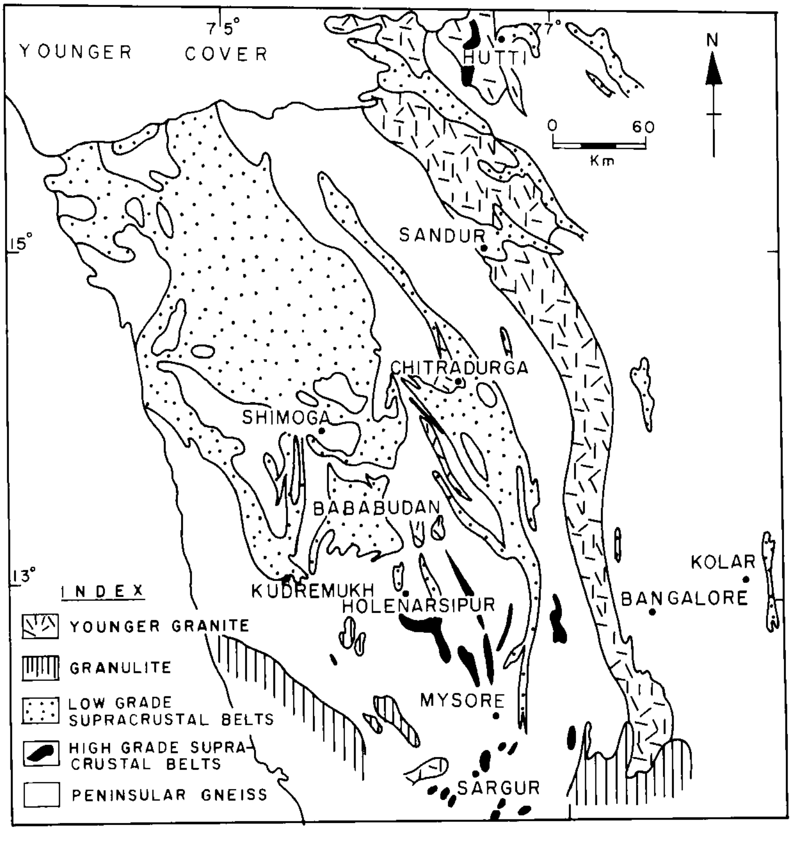

Figure 2. Geological map of Karnataka showing the distribution of different tectono-metamorphic units.

This simple structure suggested for the supracrustal rocks of Karnataka has, however, been belied by studies during the last decade (Naqvi, 1973; Chadwick et al., 1978; Janardhan et al., 1979; Mukhopadhyay and Ghosh, 1981; Naha and Chatterjee, 1982; Ghosh and Sengupta, 1985; Naha et al., 1986; see Mukhopadhyay, 1986 for an exhaustive review and references). Structures of three generations in hand specimen and outcrop are common in all the supracrustal rocks -- banded ferruginous quartzite, quartzite, mica schist and chlorite schist, marble and calc-silicate rocks. Structures of the first generation comprise isoclinal folds on stratification (DhF_1) having long limbs and thickened hinges, with an axial planar cleavage. At a number of places these folds are recumbent to reclined, with fold axes plunging gently westward. The DhF_1 folds have been affected locally by near-coaxial upright folding (DhF_{1a}) during the second phase; these two sets of folds may represent structures formed at different stages of progressive deformation. Structures of the third generation (DhF_2) consist of upright folds with varying tightness, with the axial planes striking between NNW and NNE. The DhF_{1a} folds have affected the axial planes of the DhF_1 folds with the fold axes remaining nearly constant. As a result, the DhF_1 folds change from recumbent/reclined through inclined, to upright

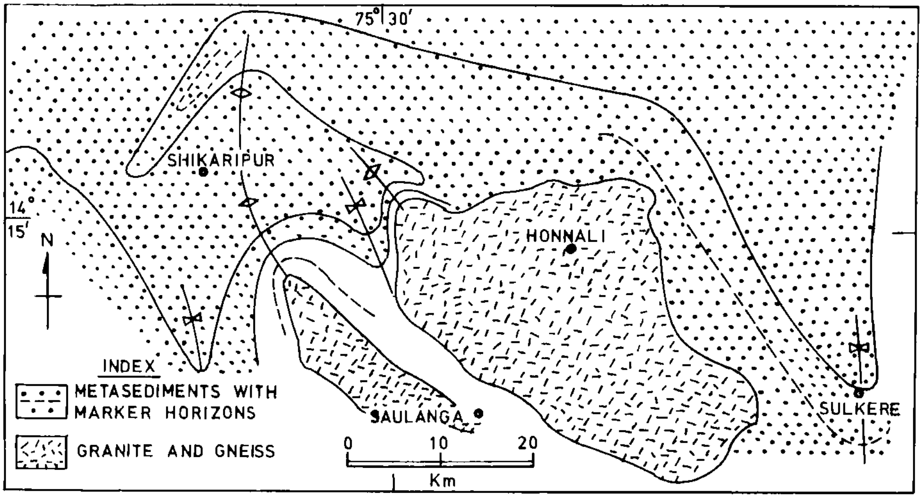

Figure 3. Map of a part of the Shimoga schist belt showing the pattern of refolding; DhF_2 axial traces shown (after Mukhopadhyay, 1986, Fig. 5).

attitude, even within a few metres at some places. By contrast, DhF_2 folding has caused a reorientation of both axes and axial planes of the folds of the first two phases. Superposition of folds of three generations has resulted in fold interference of all the three types of Ramsay (1967) in different scales.

This sequence of superposed deformations lends a new meaning to the map pattern of the supracrustal rocks in different parts of Karnataka. In a number of instances, it can be demonstrated that the terminations of the metasedimentary bands northward or southward represent the hinges of isoclinal DhF_1 folds of large scale (e.g. Bababudan; Gadag and Dodguni in the Chitradurga belt; Shikaripur in the Shimoga belt - Fig. 3; Kolar - Fig. 4A). In some other instances these terminations represent hinges of folds of a later generation, as proved by the reorientation of the axial planes of the DhF_1 folds of smaller scale around the terminations (e.g., Chitradurga arc; Shikaripur -Fig. 3 ; Kudremukh - Fig. 4B).

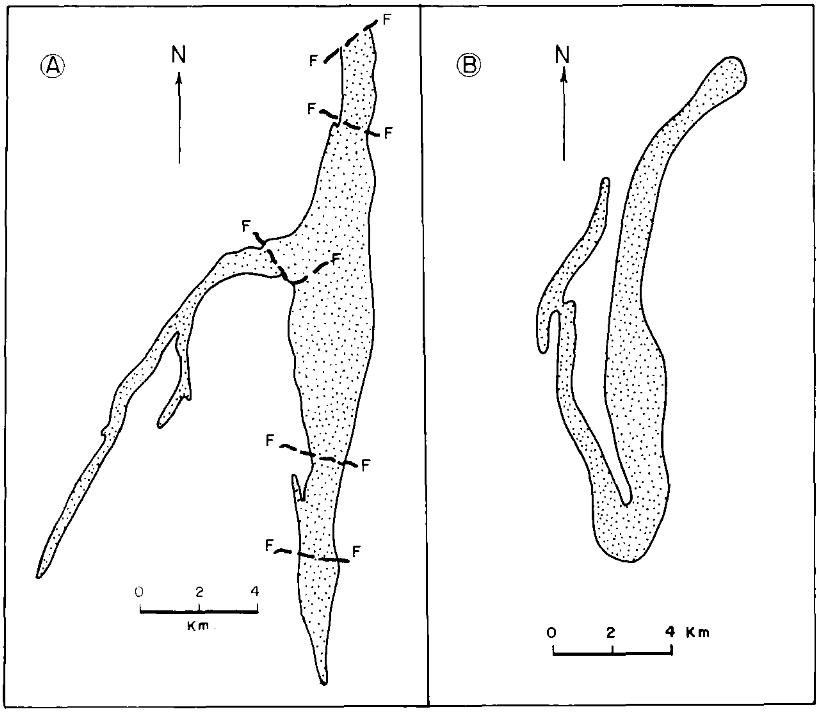

Figure 4. Map patterns showing refolding around (A) Kolar (after Viswanatha in Swami Nath and Ramakrishnan, 1981) and (B) Kudremukh (after Iyengar, 1912).

The variation in the map pattern of the supracrustal belts in different parts is primarily due to the interlimb angle of the later folds. Where the later folds are open, the map patterns seen near Bababudan and Shikaripur result. By contrast, the pattern seen around Kolar in the east and Kudremukh in the west (Fig. 4) is a consequence of later folds becoming very tight to isoclinal. Therefore, the NNW-trending formational boundaries in a number of instances conceal folds of different generations and divergent axes, and do not represent a unique 'Dharwar orogenic trend'.

The sequence of superposed folding seen in small to large scales can be demonstrated in all the supracrustal rocks of different metamorphic grades, whether occurring as small enclaves within Peninsular Gneiss or as large, linear belts (Naha et al., 1986). Thus, the same sequence is seen in the Chitradurga, the Shimoga, the Bababudan and the Kudremukh schist belts among the lower grade supracrustal rocks. In the higher metamorphic grades also the same sequence of multiple deformations in seen in the Holenarsipur schist belt, the Kunigal schist belt and the Sargur schist belt. The same sequence is duplicated even in the granulite terrane. The Manjarabad charnockite band west of Holenarsipur shows a southerly termination of a fold of later-generation, the axial planes of isoclinal first folds having a nearly EW strike in that sector (Naha et al., 1986).

The same style and sequence of multiple deformations are demonstrable in the Peninsular Gneiss also. The isoclinal folds (DhF_1), the near-coaxial open folds (DhF_{1a}) and the upright DhF_2 folds with axial planes striking nearly NS are observed in the Peinsular Gneiss also. Over a large tract, these composite gneisses have been formed by migmatization of meta-igneous and metasedimentary rocks. Quartzofeldspathic veins transforming the amphibolites (and possibly pyroxene granulites), hornblende-biotite gneiss and biotite gneiss are isoclinally folded or boudinaged, depending on whether they are at a high or low angle to the foliation of the palaeosomes. Boudinage structures and buckle folds in the basic enclaves and the invading veins indicate that migmatization and DhF_1 folding were broadly coeval (Naha et al., 1986). Some granitic gneisses of supposedly pre-Dharwar age (e.g., Sirankatte Gneiss) have evolved synkinematically with the DhF_1 deformation and have been affected by subsequent movements.

However, in a large number of outcrops of Peninsular Gneiss, small enclaves of amphibolite, and granodioritic to dioritic gneiss in some instances, show a folding, a secondary S-plane and migmatitic layering athwart the banding in the gneissic host, towards which they are drawn into parallelism (Naha et al., 1986). These provide tangible evidence of a pre-DhF_1 deformation, metamorphism and migmatization in the Peninsular Gneiss. Pebbles of gneisses and hornblende schists in conglomerates at different levels of the Dharwar sequence also furnish indirect evidence of a pre-Dharwar deformation, metamorphism and migmatization. But the presence of these features only in small scale, and the main migmatization synkinematic with the isoclinal DhF_1 folding in the Peninsular gneiss, suggest that the gneissic complex, as we see it now, represents an extensively remobilized basement. Indirect support for this conclusion comes from Rb-Sr dates of Peninsular gneisses, showing ages around 3300 Ma., 3000 Ma. and 2600 Ma. (Radhakrishna, 1983). This suggests that the Peninsular Gneiss represents an omnibus group comprising gneisses evolved at different times.

RAJASTHAN

To a large extent, the relation between the supracrustal rocks of the Aravalli Group (with which the overlying Raialo Formation is now lumped) and the Banded Gneissic Complex (BGC) is comparable to that obtained between the Peninsular Gneiss and the Dharwar Group in Karnataka. The rocks of the Aravalli Group throughout central and southern Rajasthan (Fig. 5) show evidence of superposed deformations from the scales of map to microsections (Naha et al., 1966; Roy et al., 1971; see Naha and Halyburton, 1974, 1977, Roy et al., 1984, and Sharma and Roy, 1986, for references). The first deformation is marked by isoclinal folds on bedding with attenuated limbs and thickened hinges, and an axial planar cleavage. These AF_1 folds are reclined over a large area, plunging toward W and WNW in the Nathdwara-Udaipur region (Fig. 6). But the axial trends turn gradually through WSW-SW-SSW to S southeast of Udaipur toward Salumbar (Fig. 5), along the border of the BGC, possibly due to the shape of the sedimentational trough. The AF_1 isoclinal folds are involved in near-coaxial

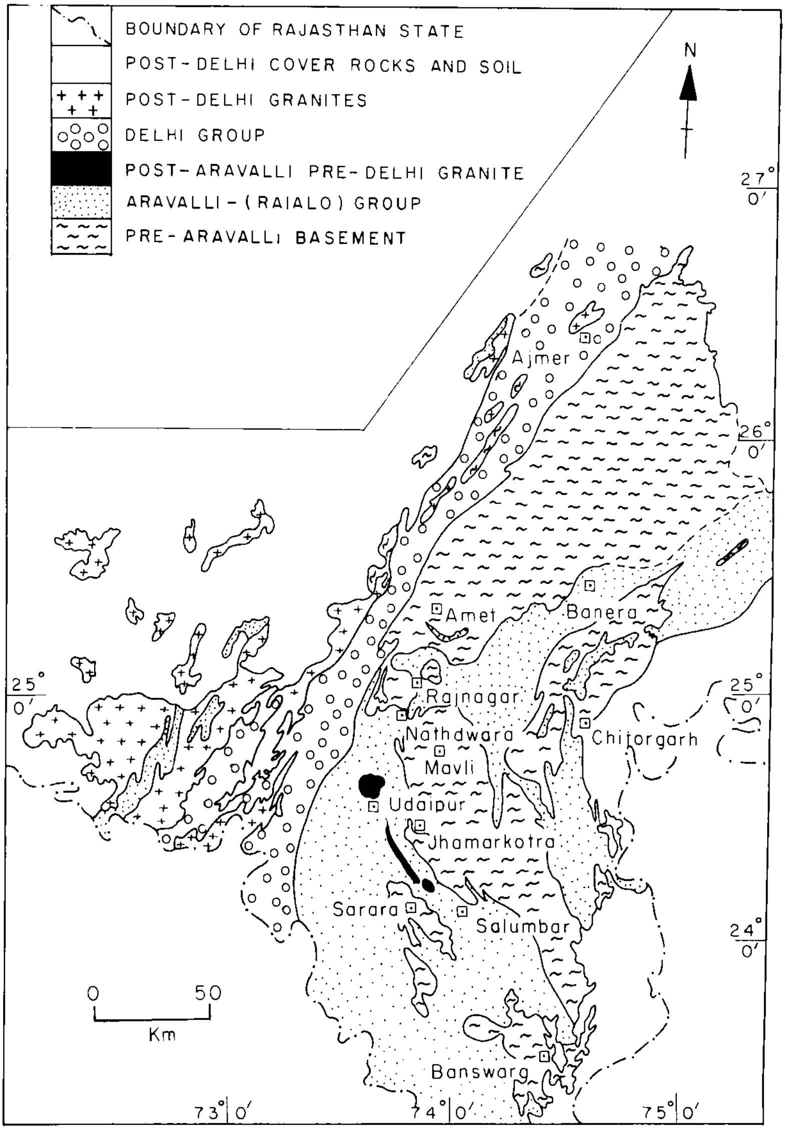

Figure 5. Simplified geological map of south-central and southern Rajasthan (modified after the Geological and Mineral Map of Rajasthan, 1st ed., 1969, Geological Survey of India).

upright folding (AF_{1a}), because of which the AF_1 folds change from reclined through inclined to upright attitudes. The early folds have been affected extensively by very open to isoclinal AF_2 folds with axial planes striking N to NNE. Depending on the angular relation betwen the strikes of axial planes of the AF_1 and AF_2 folds, different patterns of fold interference have

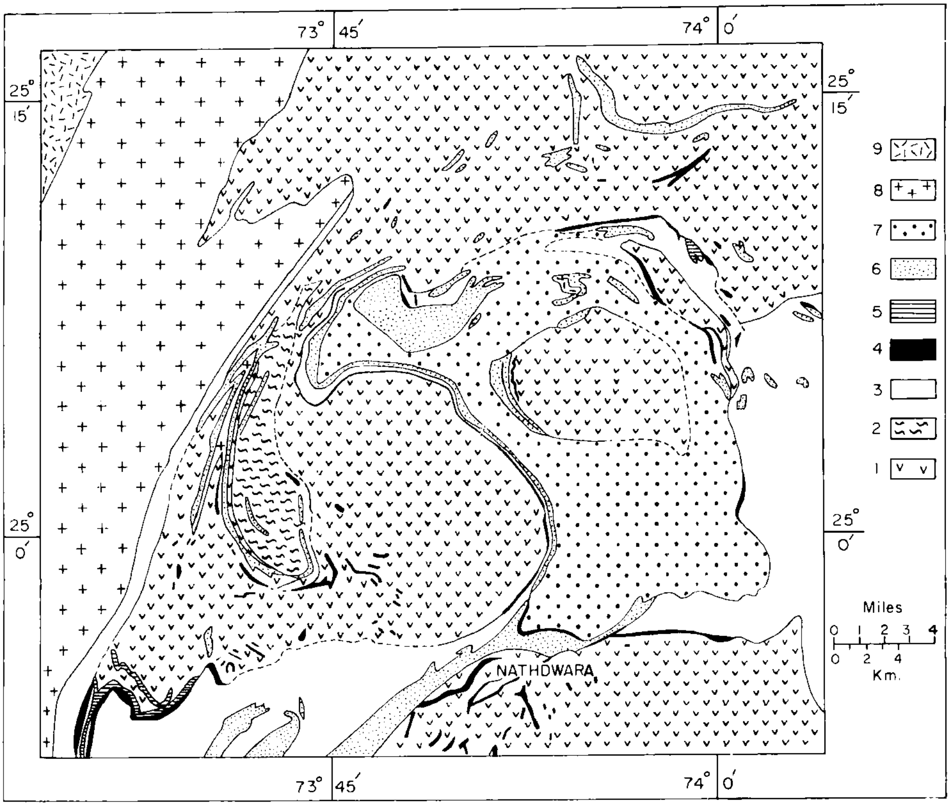

Figure 6. Geological map of the 'hammer-head syncline' and 'hook syncline' region between Ajmer and Udaipur in central Rajasthan (after Heron, 1953). 1= Pre-Aravalli gneisses and schists; 2= Pre-Aravalli granite; 3= Aravalli phyllite and biotite schist ; 4= Aravalli quartzite; 5= Aravalli limestone;6 = Raialo marble; 7= Raialo garnet-biotite schist; 8= Delhi metasedimentary rocks; 9= Post-Delhi granite.

resulted. From the distribution of AF_1 lineations involved in AF_2 folds caused by flexural-slip, it has been demonstrated that the AF_1 folds had initially a gentle plunge towards W, between Nathdwara and Udaipur (Naha and Halyburton, 1977). The apparently simple map pattern of the supracrustal rocks with northward and southward closing folds, therefore, conceals folds of two generations. As already mentioned, the reclined AF_1 folds have their axial planes striking between NNW and EW in the Salumbar area southeast of Udaipur. This variation is considered to be the effect of the resistant basement represented by BGC.

Structures of two later generations (AF$_3$ and AF$_4$) have been noted in mesoscopic scale. The AF$_3$ structures are either recumbent folds with NE-SW trend, or a set of conjugate reclined folds with axial planes dipping gently NE and SW. The structures of AF$_4$ generation are upright conjugate folds and kink bands with axial planes striking NNE-SSW and EW.

The Banded Gneissic Complex was considered by Heron (1953) to be the basement on which the rocks of the Aravalli Group were deposited with an erosional unconformity, represented by conglomerate horizons. However, in a major part of central and southern Rajasthan, the BGC is a migmatitic gneiss with metamorphic palaeosomes in various stages of transformation. The enclaves are in many instances similar in mineral composition, texture and structure to the rocks of the Aravalli Group bordering the gneissic complex. All the structures present in the rocks of the Aravalli Group match in their entirety with those in the BGC in style, orientation and sequence (Fig. 7). This similarity in structures is noticed in the high-grade enclaves within the BGC also. Structural and textural features indicate that the migmatization in the BGC was broadly synkinematic with the AF$_1$ folding in the rocks of the Aravalli Group. These features, coupled with the fact that a number of conglomerate horizons have a tectonic rather than stratigrphic significance, indicate that the BGC over a sizeable tract represents migmatized portions of

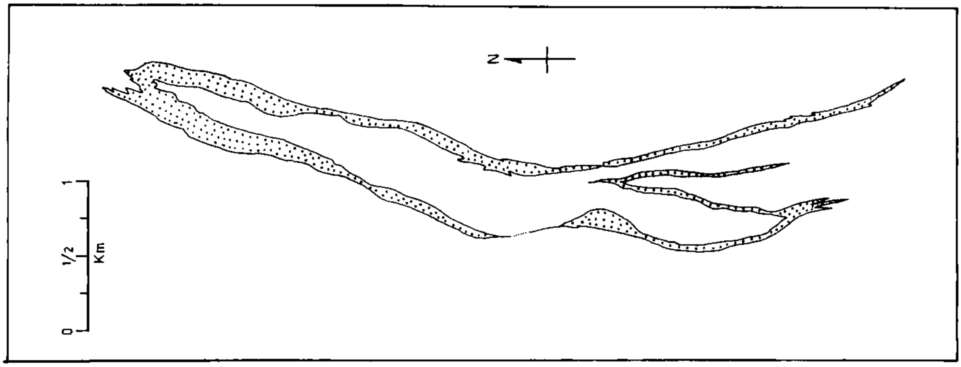

Figure 7. Refolded fold traced by a quartzite band within the Banded Gneissic Complex in the 'hook syncline', in the west central part of Fig. 6.

the Aravalli Group. However, undoubted conglomerate with pebbles, cobbles and boulders of granite gneiss, amphibolite and other components of the BGC at the base of the Aravalli Group near Salumbar indicates that the BGC does represent the Precambrian basement at some places. A rare pre-AF_1 fabric overprinted by AF_1 structures in BGC near Salumbar (Mohanty and Naha, 1986) strengthens the case for a basement gneiss. We are, therefore, justified in concluding that the BGC represents a basement which has been remobilized extensively, so that the BGC-Aravalli contact in its present state is a migmatite front and/or a tectonic contact in certain sectors. Wide variation in radiometric dates (Rb-Sr) from 3000 Ma. to 2000 Ma. in the BGC of Heron (Choudhary et al., 1984) finds a rational explantion in this scheme of a remobilized basement.

The rocks of the Delhi Group form the core of the Aravalli Mountain Chain (Fig. 5), extending from Delhi to north Gujarat. Heron considered the Delhi-Aravalli contact to be an angular unconformity, but as pointed out by Sen (1970), there is hardly any area where an angular unconformity is demonstrable. However, the special geometry of superposed folding in the Aravalli and the Delhi groups has helped in establishing the presence of an angular unconformity between the two (Naha et al., 1984). The rocks of the Delhi Group from widely separated areas such as Khetri in northwestern Rajasthan and Todgarh in central Rajasthan (as well as other areas - see Gangopadhyay, 1972, and Sharma and Roy, 1986 for references) show the same style and sequence of superposed deformations, although the orientations are slightly different. The DF_1 folds are isoclinal, recumbent or gently plunging reclined folds with a NW or SE trend in central Rajasthan, and a NS trend in the Khetri belt. They have been affected by upright, coaxial DF_2 folds which range from open to isoclinal style. Structures of the DF_3 and DF_4 generations, identical with the AF_3 and AF_4 structures, respectively, are seen in mesoscopic scale only. The absence of the westerly trending AF_1 structures in the rocks of the Delhi Group (Naha et al., 1966; Mukhopadhyay and Dasgupta, 1978), the increase in the intensity of the AF_2 deformation in the Aravalli rocks near the contact with the rocks of the Delhi Group, and the fairly constant orientation of the axes of the upright DF_2 folds in contrast with those of the upright AF_2 folds, suggest that there is an angular unconformity between the rocks of the Delhi and the Aravalli Groups.

BIHAR - ORISSA

The Precambrian terrane of Bihar-Orissa comprises four distinct geological provinces-the Archaean nucleus made up of the Singhbhum Granite and the Older Metamorphic Group (OMG), the Iron Ore provinces, the Proterozoic mobile belt of northern and eastern Singhbhum, and the Chhotanagpur Gneiss tract (Fig. 8). The interrelation of these provinces is, however, far from clear.

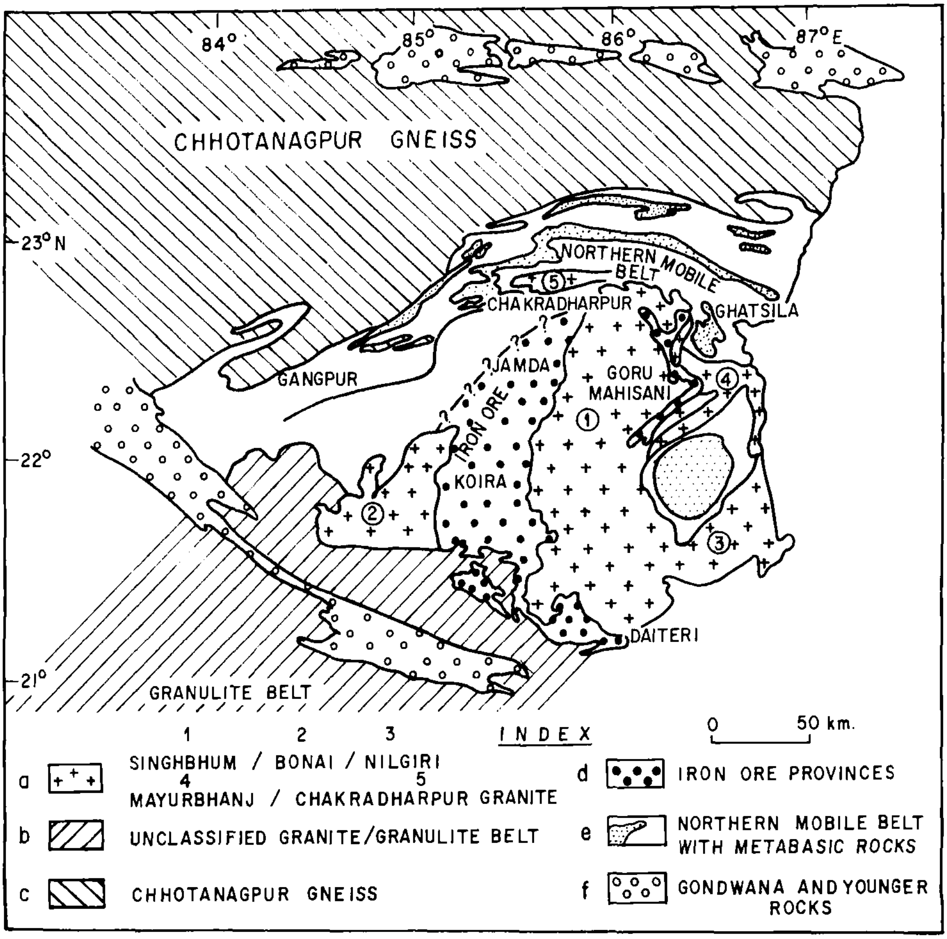

Figure 8. Generalized geological map of the eastern Indian shield in Bihar-Orissa.

Archaean nucleus

In its general aspect, the Singhbhum Granite resembles the Peninsular Gneiss of Karnataka and the Banded Gneissic Complex of Rajasthan. Here also, the higher grade supracrustal rocks forming the Older Metamorphic Group occur within the Singhbhum Granite as enclaves varying in size from a few square metres to hundreds of square kilometres. Within the granite occur the oldest gneisses, the Older Metamorphic Tonalite Gneiss. The structural elements in the OMG are, however, oriented oblique to those within the adjacent supracrustal envelope forming the Iron Ore province. The Older Metamorphic Group in the type area has the axial planes of the folds of the first generation striking NW and axes plunging NE. These have been affected by folds plunging toward SE (Sarkar and Saha, 1983).

The supposedly primary foliation within the granitic rocks shows swirling patterns, which led Saha (1972) to identify at least twelve different intrusive bodies, domical or sheet-like in shape. But it may be mentioned that doubt has been cast on the primary origin of such foliation, from studies in other parts of the world (Berger and Pitcher, 1970). Granitic rocks of proven diverse ages within the Singhbhum Granite massif (e.g., Mayurbhanj Granite, which may be as late as Middle Proterozoic - Saha et al., 1977), however, suggest remobilization of the basement during later orogenesis.

Iron Ore provinces

Banded Iron Formation (BIF), along with other metasedimentary and metavolcanic rocks, occurs in the western, eastern and southern flanks of the Singhbhum Granite massif. The most spectacular development of BIF is in the Jamda-Koira valley to the west, where its outcrop defines a major horseshoe-shaped syncline. Plunge variation of the main syncline and transverse folding are regarded by Sarkar and Saha (1983) to be synchronous with the main folding. However, within BIF near Malangtoli south of Jamda, Chatterjee and Mukherji (1981) have described three sets of folds whose interference has resulted in type 1 and type 2 patterns of Ramsay. In the eastern BIF basin of Gorumahishani, the strikes of the axial planes of the dominant folds are nearly NS, almost parallel to the elongation of the belt. The Gorumahishani belt represents either a pinched-in synclinal cusp within the basement (cf, Ramsay, 1967) or a faulted graben. Significantly, this belt is parallel to one set of regional fractures within the Singhbhum Granite. In the Tomka-Daiteri basin to the south, the regional folds have their axial planes striking EW. Thus, the axial traces of the regional folds within the different Iron Ore basins curve round the Singhbhum Granite, suggesting that the folds in the supracrustal envelope were moulded around the rigid basement block.

Proterozoic mobile belt of north and east Singhbhum

Sandwiched between the Singhbhum Granite to the south and the Chhotanagpur Gneiss to the north, this mobile belt, comprising a

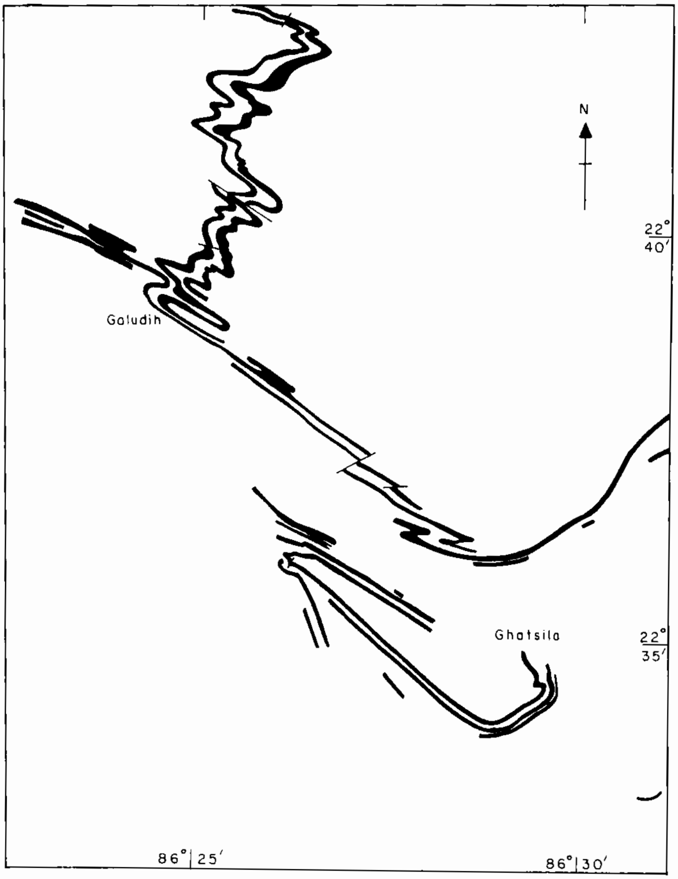

Figure 9. Quartzite bands in the Ghatsila-Galudih area showing upright folds with ESE axial trend, and axial depression near Ghatsila (after Naha, 1965).

metaflysch-metavolcanic sequence trends broadly EW. In the eastern part of the belt around Galudih-Ghatsila (Figs. 8,9), a series of upright and rarely reclined folds plunge gently toward E to ESE, ending in an axial depression near Ghatsila (Naha, 1965). Upright and locally reclined folds with NE plunge northeast of Ghatsila (Fig. 10; Mukhopadhyay and Sengupta, 1971) may represent the folds of the Galudih-Ghatsila sector reoriented by structural overprinting. In western Singhbhum, a series of large-scale folds with axial planes striking EW was regarded by Bhattacharyya (1983) as structures of second generation; the folds of the first phase with their axial planes striking EW have NS trending axes. Mappable folds with axial planes striking EW and axes plunging northward are present west and south of Chakradharpur (Mukhopadhyay, 1984). They have an axial planar schistosity identical in orientation with that in the Galudih-Ghatsila sector, but the relationship betwen the major folds in eastern and western Singhbhum is obscure.

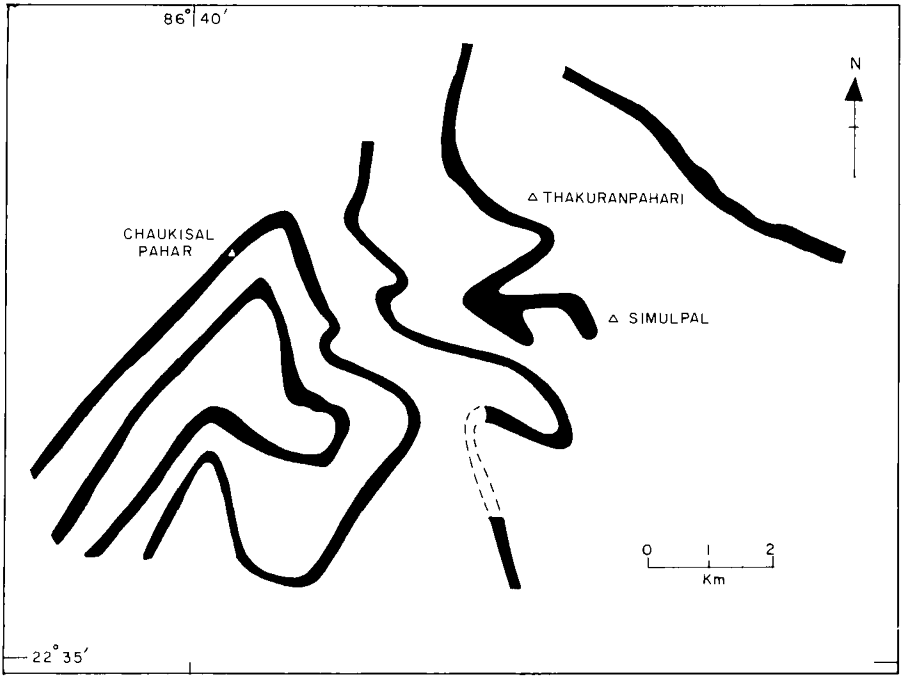

Figure 10. Quartzite bands showing refolded reclined folds plunging NE near Simulpal, northeast of Ghatsila (modified after Mukhopadhyay and Sengupta, 1971, Fig. 5).

Near the southern boundary of the mobile belt close to the Singhbhum Granite craton, a narrow zone of mylonitic rocks with down-dip-stretching lineation defines a ductile shear zone- the Singhbhum shear zone. The reclined attitude of the early folds within the shear zone is probably due to rotation of the fold axes toward the direction of stretching attendant to the simple shear movement. The shear zone perhaps came into existence early in the deformational history, but movement continued up to the late stages of orogenesis.

The structural relation between the northern mobile belt and the Iron Ore provinces is uncertain because of scanty information about the structure of the transition zone. Sarkar and Saha (1977, 1983) consider the northern mobile belt to be younger, cutting across the structural grain of the older Archaean nucleus and the Iron Ore provinces. However, neither structural nor radiometric data provide unequivocal evidence of superposition, and the possibility of the two provinces representing contemporaneous but different tectonic settings cannot be ruled out (Sarkar and Chakraborti, 1982).

In westerly continuation of the north Singhbhum mobile belt, there occurs the Gangpur Group, where folds of three generations have been reported by Chaudhuri and his co-workers (Chaudhuri and Pal, 1983). Isoclinal reclined folds with easterly plunge have been involved in coaxial upright folding, followed by upright folds with axial planes striking NS.

CHOTANAGPUR GNEISS TERRANE

This region is composed of granitic gneisses, intrusive rocks of different ages, and both high-and low-grade supracrustal belts. Our knowledge about this terrane is too fragmentary to arrive at a regional synthesis. However, it seems reasonable to consider this zone to be a medley of remobilized Archaean basement, Proterozoic granite plutons, and supracrustal belts of diverse ages and varied tectono-metamorphic settings.

DISCUSSION

A comparison of the structural history of the Precambrian metamorphic terranes of Karnataka and Rajasthan in particular shows some striking similarities. (1) The supposed basement in these two regions is made up of composite gneisses formed by migmatization of pre-existing rocks. (2) Rare relict fabric in the gneissic complex, overprinted by structures of the first generation in the supracrustal rocks, provides incontrovertible evidence of a basement antedating the first deformation in the schistose rocks. The presence of conglomerate of undoubted sedimentary origin in some places at the gneiss-schist contact strengthens this inference (3) The palaeosomes of different dimensions within the migmatites are similar in mineral composition, texture and structure to those in the supracrustal rocks bordering the migmatites. Even where the supracrustal enclaves are of higher metamorphic grade ("Sargur Group" in Karnataka and "Bhilwara Group" in Rajasthan), the structural similarity with the gneissic host and supracrustal belts bordering the migmatites is retained. (4) The migmatitic gneisses have been involved in the same style and sequence of superposed deformations affecting the supracrustal rocks. (5) The interface between the gneisses and the supracrustal rocks is a migmatitic and/or tectonic contact over a large area. (6) Wide variations in Rb-Sr dates in different parts of the Banded Gneissic Complex and the Peninsular Gneiss also reinforce the case for the gneissic complex in its present state being a reactivated basement.

There is considerable uncertainty regarding the interrelation among the four tectonic units in the Bihar-Orissa Precambrian belt in eastern India. The Singhbhum Granite massif is an undoubted basement block within which occur some metamorphic enclaves in various stages of transformation. Evidence of remobilisation is discernible in parts of this basement also. It is flanked in the south, west and north by banded iron formations which show evidence of superposed folding. North of the basement in eastern and northern Singhbhum there occurs a metaflysch-metavolcanic sequence forming the Proterozoic mobile belt. This belt, which is bounded to the south by a ductile shear zone, also shows structural overprinting; but the relationship between this belt and the Iron Ore Provinces is not clear. Finally, north of this mobile belt there occurs the Chhotanagpur Gneiss, information about which is meagre. This gneissic terrane comprises granites and gneisses, as well as metasedimentary and meta-igneous rocks of varied ages and different tectonic settings.

ACKNOWLEDGEMENTS

The authors are indebted to Dr. S.Mohanty of the Indian School of Mines, Dhanbad, and Prof. Asoke Mookherjee of the Indian Institute of Technology, Kharagpur, for critically reading the manuscript. One of the authors (KN) is grateful to the Jawaharlal Nehru Memorial Fund for financial support.

REFERENCES

Berger, A.R. and Pitcher, W.S., 1970. Structures in granitic rocks :a commentary and a critique of granite tectonics. Proc. Geol. Assoc. London, 81: 441-461.

Bhattacharyya, D.S., 1983. Tectonic evolution of northwest Singhbhum, In: Recent Researches in Geology, 10: 74-80.

Chadwick, B., Ramakrishnan, M., Viswantha, M.N. and Murthy, V.S., 1978. Structural studies in the Archaean Sargur and Dharwar supracrustal rocks of the Karnataka craton, J.Geol. Soc. India, 19: 531-549.

Chatterjee, A.K. and Mukherji, P., 1981. The structural setup of a part of the Malangtoli iron deposits, Orissa, J. Geol. Soc. India, 22: 121-130.

Chaudhary, A.K., Gopalan, K. and Sastry, C.A., 1984. Present status of the geochronology of the Precambrian rocks of Rajasthan. Tectonophysics, 105: 131-140.

Chaudhuri, A.K. and Pal., A.B., 1983. Three phases of folding with macroscopic axial plane folding in the Gangpur Group in eastern India, In: Recent Researches in Geology, 10: 110-119.

Gangopadhyay, P.K., 1972. Structure and tectonics of the Alwar region of NE India, with special reference to Precambrian stratigraphy. Proc. 24th Int. Geol. Congress: 118-124.

Ghosh, S.K. and Sengupta, S., 1985. Superposed folding and shearing in the western quartzite of Kolar Gold Field: Ind. J. Earth Sci., 12: 1-8.

Heron, A.M., 1953. The geology of central Rajputana. Mem. Geol. Surv. India. 79: 1-389.

Holmes, A., 1949. The age of uraninite and monazite from the post-Delhi pegmatites of Rajputana. Geol. Mag., 86: 288-302.

Iyenger, P.S., 1912. The geology of Kudremukh and Gangamula regions, Kadur district, Rec. Mysore Geol. Dept., 12: 45-70.

Janardhan, A.S., Ramachandra, H.M. and Ravindra Kumar, G.R., 1979. Structural history of the Sargur supracrustals and associated gneisses southwest of Mysore, Karnataka, J.Geol. Soc. India, 20: 61-72.

Krishnan, M.S., 1960. Geology of India and Burma, 4th ed.,Higginbothams, Madras, 604.

Mohanty, S. and Naha, K., 1986. Stratigraphic relations of the Precambrian rocks in the Salumbar area, southeastern Rajasthan, J. Geol. Soc. India, 27: 479-493.

Mukhopadhyay, D., 1984. The Singhbhum shear zone and its place in the evolution of the Precambrian mobile belt of North Singhbhum. Proc. Seminar on "Crustal evolution of the Indian shield and its bearing on metallogeny", Ind. J. Earth Sci., 205-212.

Mukhopadhyay, D., 1986. Structural pattern in the Dharwar craton, J. Geol. 94: 167-186.

Mukhopadhyay,D and Dasgupta, S., 1978. Delhi pre-Delhi relations near Badnor, central Rajasthan. Ind. J. Earth Sci., 5: 183-190.

Mukhopadhyay, D. and Ghosh, D., 1981. A tectono-stratigraphic model of the Chitradurga schist belt, Karnataka. J.Geol. Soc. India, 22: 22-31.

Mukhopadhyay, D. and Sengupta, S., 1971. Structural geometry and the time relation of metamorphic recrystallization to deformation in the Precambrian rocks near Simulpal, Eastern India. Geol. Soc. Am. Bull., 82: 2251-2260.

Naha, K., 1964. A critique of "orogenic trends" in Archaean correlation in India. Tectonophysics, 1: 431-438.

Naha, K., 1965.Metamorphism in relation to stratigraphy, structure and movements in part of east Singhbhum, eastern India. Quart. J.Geol. Mining Met. Soc. India. 37: 41-85.

Naha, K., Chaudhuri, A.K. and Bhattacharyya, A.C., 1966. Superposed folding in the Older Precambrian rocks around Sangat, central Rajasthan, India. Neues Jahrb. Geol. Palaeontol. Abh. 126: 205-231.

Naha, K., and Chatterjee, A.K., 1982. Axial plane folding in the Bababudan Hill Ranges of Karnataka, Ind. J.Earth Sci., 9: 37-43.

Naha, K. and Halyburton, R.V., 1974. Early Precambrian stratigraphy of central and southern Rajasthan, India. Precambrian Res., 1: 55-73.

Naha, K. and Halyburton, R.V., 1977. Structural pattern and strain history of a superposed fold system in the Precambrian of central Rajasthan, India, parts I and II. Precamb. Res., 4: 39-111.

Naha, K., Mukhopadhyay, D.K., Mohanty, R., Mitra, S.K. and Biswal, T.K., 1984. Significance of contrast in the early stages of the structural history of the Delhi and the pre-Delhi rock groups in the Proterozoic of Rajasthan, western India. Tectonophysics, 105: 193-206.

Naha, K., Srinivasan,R. and Naqvi, S.M. 1986. Structural unity in the Early Precambrian Dharwar tectonic province, Peninsular India. Quart. J. Geol. Mining Met. Soc. India, 58: 219-243.

Naqvi, S.M., 1973. Geological structure and aeromagnetic and gravity anomalies in the central part of the Chitradurga schist belt, Mysore, India. Geol. Soc. Am. Bull., 84: 1721-1732.

Pichamuthu, C.S., 1967. The Precambrians of India, In Rankama, K., ed., The Geological systems-- The Precambrian. Wiley, New York, 3: 1-96.

Radhakrishna, B.P., 1983. Archaean granite-greenstone terrain of the South Indian Shield, In: S.M. Naqvi, and J.J.W. Rogers (Editors), Precambrian of South India. Mem. Geol. Soc. India, 4: pp.1-46.

Rama Rao, B., 1940. The Archaean complex of Mysore. Mysore Geol. Dept. Bull., 17: 1-101.

Ramsay, J.G., 1967. Folding and fracturing of rocks. McGraw-Hill, New York, N.Y., 568.

Roy, A.B., Paliwal, B.S. and Goel. O.P., 1971. Superposed folding in the Aravalli rocks of the type area around Udaipur, Rajasthan, J. Geol. Soc. India, 12: 342-348.

Roy, A.B., Paliwal, B.S. and Bejarnia, B.R., 1984. The Aravalli rocks: an evolutionary model and metallogenetic trends. Proc. Seminar on "Crustal evolution of the Indian shield and its bearing on metallogeny", Ind. J. Earth. Sci., 73-83.

Saha, A.K., 1972. The petrogenetic and structural evolution of the Singhbhum Granitic Complex, eastern India. Proc. 24th Int. Geol. Congress: 147-155.

Saha, A.K., Bose, R.N., Ghosh, S.N. and Roy, A., 1977. Petrology and emplacement of Mayurbhanj Granite batholith, eastern India. Bull. Geol. Mining Met. Soc. India, 49: 1-34.

Sarkar, A.N. and Chakraborti, D.K., 1982. One orogenic belt or two? : a structural reinterpretation supported by Landsat data products of the Precambrian metamorphics of Singhbhum, eastern India. Photogrammetria 37: 185-201.

Sarkar, S.N. and Saha, A.K., 1977. The present status of the Precambrian stratigraphy, tectonics and geochronology of Singhbhum-Keonjhar-Mayurbhanj region, eastern India. Ind. J. Earth Sci., S. Ray v. 37-65.

Sarkar, S.N. and Saha, A.K., 1983. Structure and tectonics of the Singhbhum-Orissa Iron Ore craton, eastern India, In: Recent Researches in Geology, 10: 1-25.

Sen, S., 1970. Some problems of Precambrian geology of central and southern Aravalli Range, Rajasthan, J. Geol. Soc. Ind. 11: 217-231.

Sharma, R.S. and Roy, A.B., 1986. Evolution of Precambrian lithosphere: western India, In: The Indian Lithosphere: 1-14, INSA, New Delhi,

Swami Nath, J. and Ramakrishnan M., eds. 1981. Early Precambrian supracrustals of southern Karnataka, Mem. Geol. Surv. India, 112: 1-350.

ARCHAEAN SEDIMENTATION, CANADIAN SHIELD

RICHARD W. OJAKANGAS

ABSTRACT

The resedimented (turbidite) facies association dominates the Archaean rock assemblages of the volcanic-sedimentary (greenstone) belts of the Canadian Shield. The alluvial-fan braided-fluvial facies association is widespread but of secondary importance. Both facies associations contain an abundance of felsic volcanic detritus, and in many greenstone belts, it is the dominant material. Rapid resedimentation of pyroclastic sediment from felsic centers seems to have been common. Plutonic detritus may have had either a synvolcanic or a granitic cratonic provenance.

Major gneissic subprovinces consist largely of paragneisses whose protoliths may have had a volcanic parentage similar to the sediments of the greenstone belts.

The original total volume of erupted felsic volcanic material, if the large amounts in the metasedimentary rocks of the greenstone belts and in the paragneisses of the gneiss subprovinces are included, may have been an order of magnitude greater than the volume of felsic volcanic rocks exposed today. The total volume of felsic volcanic material may have been greater than the total volume of intermediate-mafic volcanic material.

Numerous quartzarenite and carbonate occurrences have been described, indicating that at least several portions of the Canadian Shield were tectonically stable as early as 2980 Ma.

INTRODUCTION

The Canadian Shield includes two major Archaean provinces, the large Superior Province and the much smaller Slave Province (Fig.1). Volcanic-sedimentary (greenstone) belts are abundant, with more than 30 delineated in the Superior Province. In the superior province the greenstone belts and associated granitic plutons have been grouped into broad volcanic granite subprovinces (e.g. Goodwin,1968) which alternate with broad gneiss-granite subprovinces (Fig. 2). An excellent recent overview of the geology of the Canadian Shield is one by Ayres and Thurston (1985).

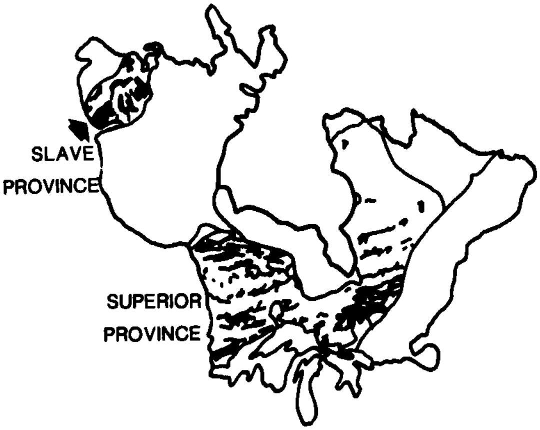

Figure 1. Map of Canadian Shield showing Superior and Slave Provinces. Archean volcanic-sedimentary belts are black. After Baragar and McGlynn (1976). From Ojakangas (1985), by permission of the Geological Association of Canada.

Most of the volcanic-sedimentary sequences are about 2700 to 2750 Ma old. The oldest published date on volcanic rocks is 3013 Ma from the North Spirit Lake area (Nunes and Wood, 1980). Gneissic rocks have been dated at about 3000 Ma in the English River Subprovince (Krogh et al., 1976) and elsewhere as well. Four areas of older gneisses, most of which are older than 3500 Ma, occur near the edges of the Canadian Shield in the Minnesota River Valley of Minnesota, in northern Michigan in Montana, and in Labrador; none of these terranes have been suggested as source areas for sediment of the greenstone belts.

The individual greenstone belts include thick mafic to felsic volcanic accumulations, with associated sedimentary rock sequences which generally occur near the tops of volcanic cycles. Estimates of the total thicknesses of the volcanic and sedimentary rocks are on the order of tens of thousands of metres. They have generally been subjected to only greenschist grade metamorphism, and their sedimentary structures, primary textures and mineralogies are commonly well-preserved (Figs. 3 and 4).

The gneiss-granite subprovinces, such as the Quetico and English River Subprovinces of Figure 2, which consist of paragneisses and minor orthogneisses, have been termed metasedimentary

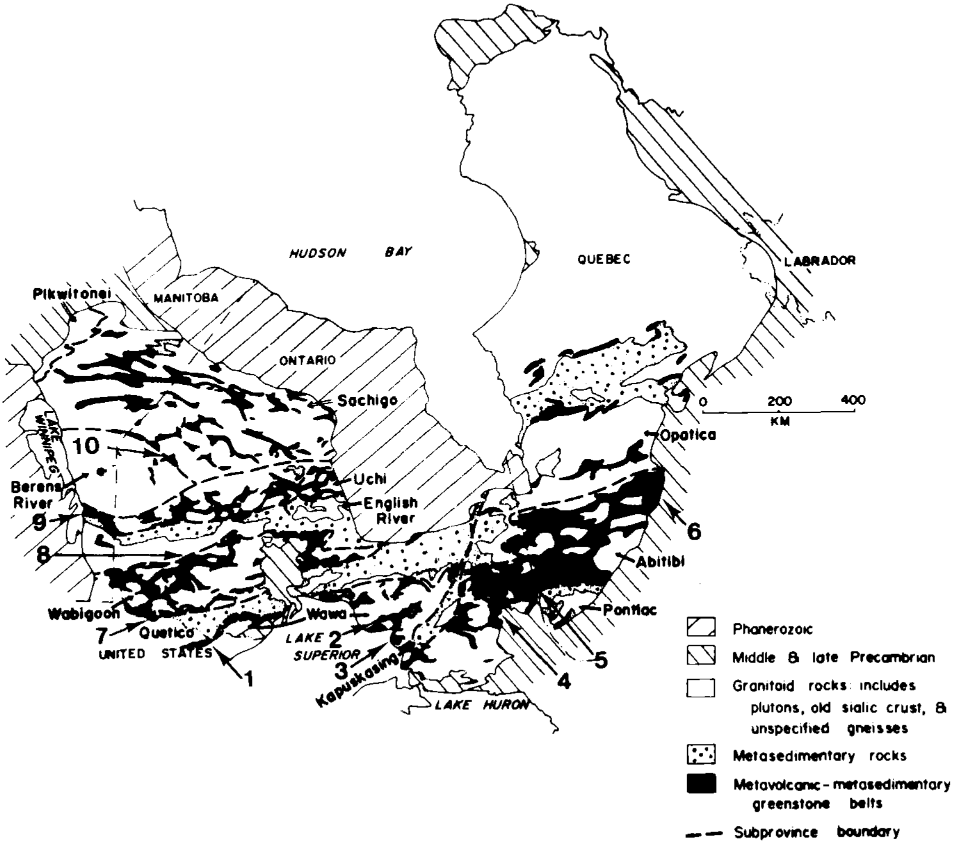

Figure 2. Map of Superior Province showing volcanic-sedimentary subprovinces of volcanic-sedimentary rocks (greenstone belts) and granitic rocks, and gneiss subprovinces of metasedimentary rocks (stippled). Some of the greenstone belts mentioned in the text are marked by numbers, as follows: 1= Vermilion district, northeastern Minnesota; 2= Michipicoten (Wawa); 3= Gamitagama (Lake Superior Park); 4= Kirkland Lake; 5= Rouyn-Noranda; 6= Chibougamau; 7= Rainy Lake; 8= Sioux Lookout; 9= Rice Lake - Gem Lake - Bee Lake; 10= North Spirit Lake. Map after Ayres and Cerny (1982). From Ojakangas (1985), by permission of the Geological Association of Canada.

belts (e.g., Pettijohn., 1972; Goodwin, 1968). In contrast to the regional low metamorphic grade of the greenstone belts, the rocks of the gneiss belts have commonly been metamorphosed to amphibolite facies. Primary bedding may be preserved, but original textures and mineralogy have been obscured by recrystallization (Fig. 5).

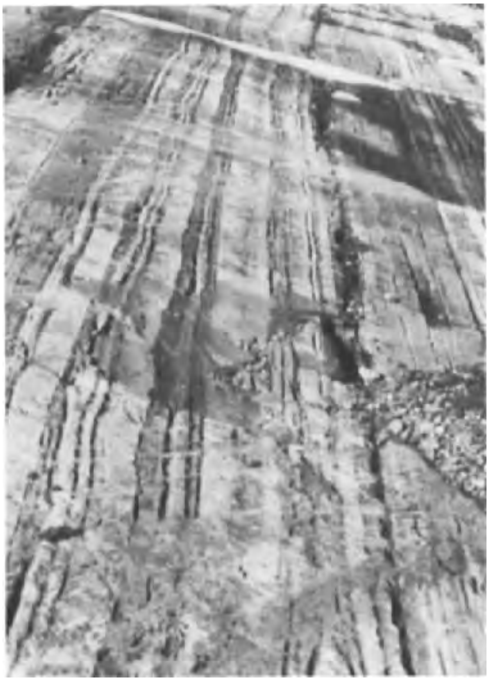

Figure 3. Alternating graywacke beds (weathered white) and mudstone beds (black), Vermilion District, Minnesota. Tops to left. Hammer at centre indicates scale.

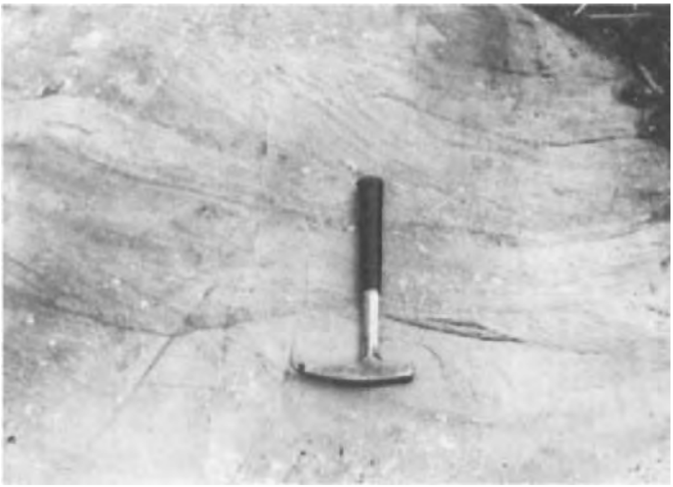

Figure 4. Cross-bedded sandstone near Wawa, Ontario.

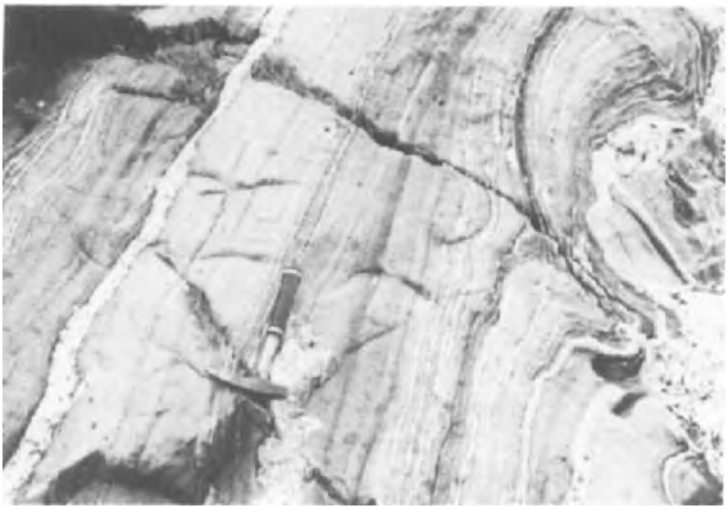

Figure 5. Paragneiss of probable graywacke-mudstone parentage at Ear Falls in the northern supracrustal domain of the English River Subprovince, Ontario.

Most of the shield rocks have been affected by at least two folding events. Faults, both dip-slip and strike-slip, commonly are parallel to the trends of rock units, thereby complicating correlations between fault blocks.

In this review, emphasis will be on the sedimentary rocks within the greenstone belts. Original sedimentary rock names will be used, even though all the rocks have been metamorphosed. Pyroclastic rocks, although commonly associated with the sedimentary units, will not be discussed here. The metasedimentary rocks of the gneiss-granite subprovinces, which are now gneisses, will be referred to only briefly.

Most thorough studies of clastic sedimentary rock units have two major objectives: interpretation of the environments of deposition, and determination of the provenance of the sediments. Both rely heavily upon paleogeographic data, including paleocurrent analyses, and conversely, provide valuable information for paleogeographic reconstructions.

Recent reviews of Archaean sedimentation include those by Pettijohn (1970, 1972), Lowe (1980,1982), Condie (1981, p.131-170) and Ojakangas (1985). More than 200 references are cited in the latter review.

SEDIMENTATION

In general, two major sedimentary facies associations characterize Archaean sedimentary rocks of the Canadian Shield (Ojakangas, 1985). The resedimented (turbidite) facies association is dominant, whereas the alluvial fan-fluvial facies association, although widespread, is volumetrically much less important. Other facies, including pelagic and shelf, constitute a minor part of the sedimentary rock column.

The Resedimented (Turbidite) Facies Association

This facies consists mainly of graywacke beds (commonly graded) intercalated with mudstones and siltstones (Fig. 3). These graywacke-mudstone sequences commonly contain some conglomerates that are either graded or massive and lack cross-bedding; they are generally matrix-supported with a sand-silt-clay matrix and range from unsorted to inversely-normally graded to normally-graded to graded-laminated types. The conglomerates fit Walker's (1975) model of deposition in channels on proximal portions of submarine fans, whereas the graywacke sequences may have been deposited on suprafan lobes and in midfan to distal fan areas. Most workers have related the resedimented facies association to deposition on submarine fans, but resedimentation by turbidity currents should also have been possible along the ramps or slopes of explosive felsic volcanic centres, many of which may have been islands. Final deposition would have been either at the base of the slope or farther basinward on basin plains. The siltstones may constitute distal or lateral edges of individual turbidite deposits, or may be products of normal bottom currents. The intercalated mudstones (now slates) are the result of hemipelagic or pelagic sedimentation.

The Alluvial Fan - Fluvial Facies Association

This facies includes conglomerates (generally clast-supported), sandstones with medium- to large-scale cross-bedding (Fig.4), and minor siltstone and mudstone. Sedimentary structures include dewatering features, mudcracks, and ripple marks. The deposits fit models for alluvial fans and braided streams. Minor associated lake and aeolian sediments have also been reported.

Pelagic Facies Association

This facies association (Dimroth et al., 1982a) is difficult to map separately except where it comprises discrete units of black graphitic shale, iron-formation, and chert in the volcanic-sedimentary sequences. The distal parts of the resedimented (turbidite) facies association commonly grade outward into this facies which was presumably deposited in relatively deep water on fans or basin plains where only fine clastic deposition and chemical precipitation occurred. The greatest volume of pelagic sediment probably occurs in the resedimented facies association as mud interbeds between graywacke turbidite beds, but this component is not commonly defined as part of the pelagic association.

Banded iron-formation (BIF), here including ferruginous and non-ferruginous chert, has long been recognized as a minor but important rock type in Archaean volcanic-sedimentary belts, and has been called Algoma-type iron-formation (Gross, 1965). A volcanogenic exhalative origin is generally assumed for this rock type because of its close association with volcanic rocks. Some iron-formations are quite large; one in the Vermilion District of Minnesota is more than 40 km long and is about 100 m thick. In most greenstone belts, some thin beds of iron oxide-chert iron-formation occur between turbidite beds or in the Bouma E interval, indicating that this type is akin to pelagic muds, raining down into deeper water environments from the top of the water column where it formed. Whereas all of the iron formations probably accumulated below wave base in deep water, not all did; a close association with stromatolites at Atikokan (Steeprock) in northwestern Ontario suggests deposition there in shallow water.

Shelf Facies

This facies consists mainly of quartz arenites and carbonates, four of them stromatolite-bearing. Several minor occurrences and one large occurrence were known by the early 1980's, as summarized by Ojakangas (1985). Since that review was completed, there have been several exciting new discoveries of quartz arenite units, including supermature quartz arenites, within the greenstone belts. In the Sachigo Subprovince (Figure 2), within an area of 500 km by 300 km, each of the eight greenstone belts contains quartzite units (e.g., Donaldson and

DeKemp, 1987; personal communication, P.C. Thurston, 1987). New occurrences have also been described from the Slave Province (Covello et al., 1987) and from an area east of the southern part of Hudson Bay (Roscoe and Donaldson, in press).

The new quartz arenite occurrences range from single beds to units as thick as 1500 m, and are associated with iron-formation, argillaceous rocks, and shallow to subaerial felsic volcanic sequences (personal communication, P.C. Thurston, 1987). Several are intercalated with mafic to ultramafic flows, implying a tensional regime and deep fracturing of a stable crustal area upon which quartz arenite was produced by a combination of weathering, aeolian processes on the vegetationless surface, and reworking in shallow water. This tectonic setting is not uncommon in the Proterozoic and Archaean, and is remarkably similar to that of the Bababudan Group quartzites of the Dharwar Craton in southern India, as described by Srinivasan and Ojakangas (1986).

Sedimentary structures include probable planar cross-bed sets as thick as 2 m (comparable in scale to that described by Schau and Henderson in 1983 in the northwestern Churchill Province near the Slave Province), planar lamination, and hummocky cross-stratification which is indicative of storm activity in shallow water.

Slightly rounded zircons from a quartzite that unconformably overlies a volcanic sequence dated at 2980 Ma also date at 2980 Ma; other zircons from other quartzite units date at 3023 Ma (personal communication, P.C. Thurston, 1987). Therefore, at least parts of the Canadian Shield experienced stability by 2980 Ma.

PALEOCURRENTS AND PALEOGEOGRAPHY

Paleogeographic reconstructions are objectives of most sedimentological studies, but paleocurrent studies are commonly difficult in Archaean rocks because of metamorphism and deformation. Sole marks in Archaean turbidite sequences are rarely observed because mudstones are welded to the soles of the graywacke turbidite beds. The small-scale cross-bedding of the Bouma C intervals of graded turbidite beds may be obscured by cleavage, recrystallization, and shearing. Even where paleocurrent indicators are measureable, deformation (and especially multiple deformation) may make relationships between outcrops problematic. Nevertheless, paleocurrent studies have been accomplished in both the resedimented (turbidite) facies association and in the alluvial fan-fluvial facies association at several localities of Archaean rocks. Changes in pebble size, facies changes, and lithology have also been used with some success in paleogeographic studies.

COMPOSITIONS OF SEDIMENTARY ROCKS

Mineralogical Composition

The original mineralogical composition of Archaean clay-, silt- and sand-sized grains may be obscured by recrystallization during metamorphism, by cataclasis during deformation, and by diagenesis during burial in thick piles of sediment. Except for the volumetrically minor quartz arenites, Archaean clastic sedimentary rocks are immature, both mineralogically and texturally. The graywackes of the resedimented facies association and the sandstones of the alluvial fan - fluvial facies association contain an abundance of felsic volcanic detritus, and can be termed volcanogenic graywackes and sandstones.

Major components are: (1) rock fragments of fine-grained, felsic volcanic material, some porphyritic, (2) unit sodic plagioclase grains, and (3) unit quartz grains, a few of which contain embayments of felsic volcanic groundmass, all clearly indicating a volcanic origin. Also present at some localities are intermediate-mafic volcanic fragments, quartz-plagioclase plutonic rock fragments, composite quartz grains of several quartz crystals (of plutonic origin?), and minor chert and slaty fragments. What was probably original clayey matrix has been transformed into micaceous matrix, and original fine-grained to glassy volcanic grains have been recrystallized to a fine-grained matrix of quartz and feldspar. K-feldspar is generally lacking.

Several petrographic problems are encountered by workers in Archaean sedimentary rocks, including: (1) distinguishing felsic volcanic rock fragments from matrix, especially in recrystallized or cataclasized rocks; (2) distinguishing epiclastic volcanic rock fragments derived from the erosion of crystallized volcanic rocks or lithified volcaniclastic rocks from volcaniclastic detritus derived from unconsolidated pyroclastic accumulations; (3) distinguishing unit quartz grains and unit plagioclase grains of volcanic origin from such grains of plutonic origin; (4) distinguishing the commonly untwinned or poorly twinned plagioclase from orthoclase, and (5) distinguishing felsic volcanic rock fragments from chert. The latter two problems can be handled by staining thin-sections or thin-section peels for feldspars. The first listed problem is of greatest concern, because the inability to recognize felsic volcanic rock fragments, classifying them instead as fine-grained matrix, may totally obscure a dominant felsic volcanic origin. In addition, rock fragments commonly are flattened and squeezed and become part of the matrix during diagenesis (i.e., deep burial) and thereby the apparent relative abundance of quartz in the framework grains increases (McLennan, 1984). The second listed problem is of importance in the interpretation of the environmental and tectonic setting of the greenstone belts, as discussed later.

Compositions of graywackes from five different greenstone belts are listed in Table I, although petrographic data from the literature are difficult to compare because of differences in

Table 1.
Petrography of Graywackes

	Vermilion District Minnesota (Ojakangas 1972b) (N = 13)	Lake Superior Park Ontario (Ayres, 1983) (N = 7)	Minnitaki Lake Ontario (Walker & Pettijohn, 1971) (N = 4)	Yellowknife Supergroup Dist. of MacKenzie (Henderson, 1975a) (N = 9)	North Spirit Ontario (Donaldson & Jackson, 1965) (N = 6)
Quartz	5	20	21	25	64
Plagioclase	25	26	15	13	4
K-feldspar	tr	tr	--	--	2
Rock Fragments					
Felsic volcanic	26	11	19	8	--
Intermediate mafic volcanic	6	tr	tr	3	--
Sedimentary	--	tr	--	6	--
Plutonic, felsic	1	tr	tr	1	
Matrix	25	43	43	37	30

operational definitions of different workers and because of varying amounts of deformation and metamorphism. The greywackes of Vermilion District and Lake Superior Park are interpreted as being dominantly volcanic in origin, the Minnitaki Lake and Yellowknife graywackes are inferred to have both volcanic and plutonic sources, and the North Spirit Lake graywackes are interpreted as having largely plutonic, and perhaps recycled sedimentary sources. Volcanogenic graywackes have been reported in many greenstone belts.

Similarly, the sandstones of the alluvial fan - fluvial facies association commonly contain an abundance of felsic volcanic detritus.

The lack of K-feldspar and the abundance of Na-rich plagioclase may be a reflection of the predominance of tonalites and trondhjemites and the lack of K-feldspar-bearing granites which were not common until late in the history of greenstone belts (e.g., Taylor and McLennan, 1985,p. 135 and 215), and which intruded the sedimentary-volcanic sequences rather than providing sediment to them.

CHEMICAL COMPOSITION

Granodiorite and tonalite have long been suggested as likely source rocks of graywackes, irrespective of age (e.g., Condie, 1967; Pettijohn, 1972). However, chemical techniques cannot distinguish a plutonic provenance from a volcanic provenance (e.g., Taylor and McLennan, 1985,p. 139). A detailed geochemical appraisal of Archaean sedimentary rocks is given by Taylor and McLennan (1985), and only a few aspects will be elaborated upon here.

Plots of K_2O/Na_2O(e.g., Condie, 1981, p. 147; McLennan, 1984; Ojakangas, 1985) may help to clarify the weathering-sedimentary differentiation histories of the sedimentary rocks, as well as providing clues to the nature of the source rocks. On such plots, the average granodiorite and the average Precambrian crust are quite similar, but the average rhyodacite, dacite, tonalite, diorite, and andesite are closer to the average Archaean graywacke than is granodiorite. Coupled with the abundance of felsic volcanic detritus noted in petrographic studies, it is reasonable to propose that the chemistry of the Archaean graywackes strongly reflects that parentage. The same type of plots for Archaean argillites and slates (originally mudstones) show an enrichment in potassium relative to the graywackes (e.g., Ojakangas, 1985); this has traditionally been explained as the result of the albitization of the graywackes during diagenesis (e.g., Pettijohn, 1972). It may also be possible that the relatively higher Na contents of the graywackes are the direct result of plagioclase-bearing source rocks, with the higher K-contents of the finer-grained rocks due to K-metasomatism during the recrystallization of the original clay minerals to micas.

Plots of K_2O/Na_2O for schists and paragneisses of the gneissic subprovinces, which resemble the plots for the graywackes and slates, are suggestive of graywacke-slate protoliths.

The argillites and slates also have more iron and magnesium than do associated graywackes; this may represent the weathering of mafic rocks in the source areas (Condie, 1981, p. 140; McLennan, 1984; Sawyer, 1986). Although locally important in graywackes, mafic sand-sized and coarser grains are generally minor or absent, probably due to weathering in the source areas.

The CIA (chemical index of alteration) proposed by Nesbitt and Young (1982) as a guide to weathering is useful in the study of graywackes and associated mudstones. The index is as follows: $CIA=[Al_2O_3/(Al_2O_3 + CaO + Na_2O + K_2O)] \times 100$, using molar proportions, with corrections made for Ca not bound in silicates. If CIA values are low (less than about 55), this indicates little weathering of the material; higher values indicate some weathering; and very high values of about 78 - 87 have been observed in the highly weathered Amazon River and Amazon Fan muds (Kronberg et al., 1986). Bailes (1982) and Ojakangas (1986) used the CIA to ascertain whether volcanogenic detritus of Lower Proterozoic graywacke-mudstones was epiclastic or more directly derived from volcanic centres. Sawyer (1986) utilized CIA values in a study of metasediments of the Quetico belt; he calculated values of less than 58, and interpreted this to mean a general lack of chemical weathering. CIA calculations from his data, yield indices of 54 for the average acid volcanics of the proposed source areas and 50 for the average of acid plutons.

CIA values calculated for rocks of the Vermilion District of Minnesota are as follows: for 4 dacite porphyries, about 48; for

3 dacitic pyroclastic units, 48; for 18 graywackes, about 50; for 11 slates, about 51; and for one biotite schist, about 51. No corrections were made for Ca because carbonate modes and CO_2 percentages were not available and because the Ca that may have come from the weathering of the more easily weathered mafic volcanics may have been absorbed onto original clay minerals which are now recrystallized matrix, thereby making such corrections inaccurate. However, samples with high Ca contents relative to the other comparable rock types were omitted from these calculations on the assumption that carbonate minerals were present. Obviously, a more rigorous study of CIA values is desirable. However, the CIA values do suggest minimal weathering of the dominant felsic volcanic source rocks of the Vermilion District.

SOURCE ROCKS

The abundance of felsic volcanic rock fragments in the Archaean sediments, plus the presence of some intermediate-mafic volcanic fragments, indicates an important volcanic contribution to the majority of the graywacke sequences. There is also abundant evidence to indicate the contemporaneity of sedimentation and volcanism, including interbedded tuffs in graywacke sequences and the lateral gradation of pyroclastic or volcaniclastic units into graywacke units (e.g., Ojakangas, 1972a, 1972b; Ayres, 1977). It seems likely that the rapid erosion of pyroclastic volcanic detritus was the origin of much of the felsic volcanic material in the sediments. Ayres (1983) and Thurston et al., (1985) suggested that various sorting mechanisms, including eruption, weathering, and hydraulic factors during transportation may have concentrated volcanic quartz, thereby resulting in quartz-rich sands. This could be a partial explanation for the quartz budget problem which has been discussed by several workers including Pettijohn (1970, 1972), who emphasized the necessity of a plutonic or cratonic source because of the difficulty of deriving much quartz from the weathering of porphyritic flows.

Certainly cratonic basement rocks could have been local sources of sediment as well, based on the ages of the granitic and gneissic rocks cited in the introduction. Perhaps the best documented cratonic source for graywackes is in the Slave Province where the graywacke sequence rests on granitic basement (Henderson, 1981). However, unconformable relationships of sediments on basement rocks are uncommon; Baragar and McGlynn (1976) documented only six such occurrences on the shield, including the one just cited in the Slave Province. Many past workers have cited the presence of granitic clasts in conglomerates as evidence for derivation from granitic basement. However, synvolcanic plutons have been shown to be the sources of the clasts in several localities, including the Vermilion District of Minnesota where an unconformity with conglomerate resting upon tonalite is shown to be *within* the greenstone belt rather than beneath it (Ojakangas, 1972a, 1972b, 1985). That tonalite batholith intruded the older part of the volcanic sediment succession and shed sediment into the younger part while volcanism was apparently continuing nearby. In other greenstone belts, the contemporaneity of plutons and volcanic rocks has been verified by radiometric evidence (e.g., Blackburn et al., 1985).

Determination of the protoliths of the quartzofeldspathic gneisses of the gneissic subprovinces is difficult (Ojakangas, 1985). Chemical rather than mineralogical data must be utilized, and sedimentary, volcanic, or plutonic sources could all have been protoliths based upon the chemistry. Yet, most workers have preferred sedimentary protoliths. For example, a sedimentary protolith for some Minnesota gneisses in the Quetico Subprovince (Fig. 2) is suggested by the gradation between graywacke-slate units and biotite gneisses. It has also been suggested that the Vermilion granitic complex of the Quetico Subprovince may have been produced by melting, under upper amphibolite to granulite facies conditions, of older, short-lived volcanogenic (dacitic and basaltic) graywacke (Arth and Hanson, 1975).

SUMMARY AND DISCUSSION

The two common environments of deposition are shown in Figure 6. The dominant resedimented (turbidite) facies is interpreted to be marine, deposited below wave base, because of both the great thicknesses (thousands of metres) and the lengths (ie., lateral extent) of the belts. Deposition on submarine fans is generally indicated, with conglomerates localized in channels, but deposition on the flanks or ramps of volcanic edifices is also deemed important. Less common are the sandstones and conglomerates of the alluvial fan - braided fluvial facies, with attributes of deposition in those settings.

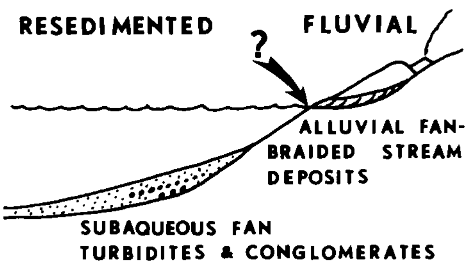
RESEDIMENTED
?
FLUVIAL
ALLUVIAL FAN-BRAIDED STREAM DEPOSITS
SUBAQUEOUS FAN TURBIDITES & CONGLOMERATES

Figure 6. Summary model showing the environments of deposition of Archaean sediments. Most Archaean sediments were moved from land or near shore and resedimented by turbidity currents and associated mechanisms in relatively deep water on or near subaqueous fans; these are the graywackes and associated poorly sorted conglomerates. A less important environment of deposition was on land, usually on volcanic land masses, as alluvial fan and braided stream deposits. The question mark and arrow refer to the marked lack of known intervening shelf deposits.

Although these two environments are diagrammatically shown adjacent to each other, their lateral relationships are generally obscure because of faulting and folding and the two-dimensional nature of the outcrop belts. Shelf deposits between the subaerial and submarine facies are uncommon, but have been identified locally, as in the Chibougamau area of Quebec (Dimroth et al., 1982b). (The quartz arenites and carbonates, while shelf deposits, are not located at such junctures, and probably generally represent an unrelated facies). Nevertheless, the lateral equivalency of these two main facies has been proposed in several areas, as for example, in the Abitibi belt, of Figure 2 (Dimroth and Rocheleau, 1979). The application of Walther's Law indicates the lateral equivalency of these two main facies. The thick resedimented facies, the result of major subsidence, is the most likely facies to be preserved. The subaerial alluvial fan braided fluvial facies was more likely to be eroded than preserved. In a few places, turbidite sequences overlie fluvial sequences, suggesting rapid subsidence and hence rapid burial and preservation (e.g., Turner and Walker, 1973; Hyde, 1980).

The provenance question can be simply stated: cratonic or volcanic? Generally, both types of terranes provided sediment, so

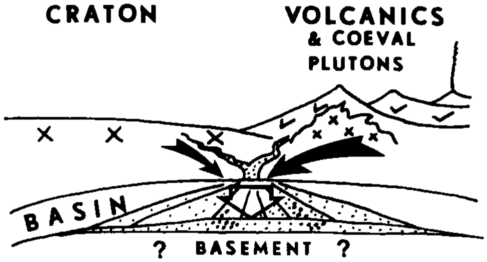

Figure 7. Summary model showing the sources of Archaean sediment. Most came from felsic volcanic centres while some from associated high-level coeval felsic plutons. A smaller volume of sediment was eroded from cratonic sources. The model also shows the relative importance of the fluvial and subaqueous fan environments depicted in Figure 6. Little is known about the basement upon which the resedimented association was deposited.

the question becomes one of their relative importance. It is not simply a matter of the recognition of fine-grained volcanic detritus versus coarser-grained plutonic detritus, for both synvolcanic (coeval) plutons and granitic cratons provided plutonic detritus. The interpretation is made here, as in an earlier review (Ojakangas, 1985) that volcanic and coeval plutonic sources commonly dominated over cratonic sources, as illustrated diagrammatically in Figure 7.

The quartzose North Spirit Lake graywackes (Table I), while probably largely derived from plutonics (cratonic?) have at least a partial source from pre-existing quartz arenites (Donaldson and Jackson, 1965; Donaldson and Ojakangas, 1977).

The presence of cratonic detritus in graywackes of some belts, such as in the Yellowknife Supergroup of the Slave Province, may mean the locus of deposition was near the edge of the basin. In contrast, felsic volcanogenic detritus, including detritus from rapidly unroofed synvolcanic plutons as in the Vermilion District of Minnesota (Ojakangas, 1972a; 1972b), may indicate that the locus of deposition was in a more central location within the basin. However, dimensions of the individual depositional basins and their original boundaries are largely unknown, as the greenstone belt rocks are erosional remnants with adjacent younger granitic complexes in intrusive and fault contact.

The ratio of mafic to felsic volcanic rocks in greenstone belts of the Canadian Shield has generally been estimated at a low 10 to 15 percent (e.g., Pettijohn, 1972; Goodwin, 1977a, 1977b). (Andesites are apparently low in volume; several older reports may have overestimated andesite by not taking into account silicification of basalts). A bimodal igneous suite is well-established with calc-alkaline felsics and basalts and tholeiitic basalts represented in different sequences (Thurston et al., 1985). While the *present* volume of felsic volcanics (largely dacites) within greenstone belts is indeed low, the *original* volume was probably much larger. The volume of felsic detritus now residing in the sedimentary rocks of the greenstone belts is very large (e.g., Ayres, 1983). If the volume now in the gneissic belts as schist and paragneiss is added, and if it is considered that some granitic batholiths may be the products of the melting of volcanogenic graywackes at crustal depths (e.g., Arth and Hanson, 1975; Southwick, 1979), the volume becomes equal to or greater than that of mafic-intermediate volcanic rocks (Ojakangas, 1985).

The tectonic settings of the greenstone belts are somewhat difficult to assess. Although there are similarities with modern and Phanerozoic volcanic arcs (e.g., Condie, 1981), some major differences such as the greater abundance of andesites in the younger arcs (McLennan, 1984) also exist, and make tectonic comparisons tenuous. McLennan (1984) has shown that petrography cannot simply be used to determine an Archaean tectonic setting as has been done with Phanerozoic rocks by Crook (1974), Maynard et al., (1982), and Dickinson et al., (1983). Similarly, tectonic settings based on chemical data, as done by Bhatia (1983) for the Phanerozoic, may not be comparable. Nevertheless, a tectonic setting involving volcanic arcs of some sort is clearly indicated for all of the greenstone belts, and the sandstones generally plot in the magmatic arc portion of the Dickinson et al., (1983) triangle.

The overall tectonic framework of the greenstone belts has been the subject of much discussion (eg., Windley, 1984, p.59-65; Young, 1978; Ayres and Thurston, 1985; Blackburn et al., 1985). The major question is the role of plate tectonics. Because the Archaean crust was thinner and hotter than younger crust, plate tectonics of Archaean time may have involved smaller, thinner plates moving shorter distances (Windley, 1981, 1984). A plate tectonic model then requires that the depositional basins be designated as magmatic arc, fore-arc, or continental margin.

Extension (rifting) has been proposed by Windley (1981) Henderson (1981) and Ayers and Thurston (1985). Rifting, sagging, and sagduction has been proposed (Goodwin and Smith, 1980; Goodwin,1981), with the sagging at least partly due to the weight of the volcanoes and the uplifting of volcanic chains along growth faults (Dimroth et al., 1982a). A more conventional downwarping model was proposed by Baragar and McGlynn (1976).

Goodwin and West (1974) proposed that the gneiss belts were foreland basins in which graywacke sedimentation occurred. Goodwin (1981) further stated that many of the paragneisses represent tubidite facies deposited in medial portions of troughs, and that large volumes of epiclastic detritus demand major sialic plutonic crustal sources. The northern portion of the English River Subprovince may have been a long trough between two quasi-contemporaneous, island-arc volcanic complexes (Breaks et al., 1978). Blackburn (1982) suggested that epiclastic sediment was shed northward and southward from the Wabigoon Subprovince (Fig. 2), perhaps across growth faults, into the adjacent gneissic subprovinces.

The overall setting has been favourably compared to a back-arc marginal basin for the greenstone belts, with the main arc of plutonic batholiths representing the high-grade gneissic complexes (Windley,1984, p.63)

With plate tectonics becoming accepted for the Archaean, more detailed mineralogical and chemical comparisons should be made. The differences between the Recent-Phanerozoic rock record and that of the Archaean, such as differences in the volumes of andesites and K-rich granites, must be taken into account. The recent advances in U-Pb radiometric dating of zircons, with dates obtainable on single crystals, make a more detailed approach possible. For example, more dating of zircons from graywackes, cross-bedded sandstones, and clasts of conglomerates would pinpoint source rocks. Dating of zircons from tuffs interbedded with sediments would determine the ages of continuing contemporaneous volcanism and sedimentation. Zircons from coeval plutons would help distinguish the source of plutonic detritus in the sedimentary column. The dating of zircons from graywackes and from the late-stage K-rich granites could help to distinguish between older and younger graywacke sequences.

CONCLUSIONS

1) Archaean sedimentary rocks of the Canadian Shield, both those in the volcanic-sedimentary (greenstone) belts and the metasedimentary gneissic subprovinces, are dominated by the resedimented (turbidite) facies association of graywacke and mudstone. Deposition occurred in relatively deep water on subaqueous (probably submarine) fans and on the ramps of volcanic edifices.

2) The alluvial fan - fluvial facies association is widespread but subordinate to the resedimented facies, and consists largely of cross-bedded sandstone and conglomerate (commonly clast-supported).

3) The above two facies associations commonly occur in close proximity, but generally without intervening shelf-type facies. This suggests tectonic instability, as does relatively common stratigraphic juxtaposition of the resedimented facies upon the alluvial fan - fluvial facies.

4) Felsic volcanic detritus is abundant in both the resedimented and the alluvial fan - fluvial facies associations of the greenstone belts and in the paragneisses of the gneiss subprovinces. Although part of the sediment may have been epiclastic, the rapid reworking of unconsolidated pyroclastic material on the slopes of volcanic edifices was undoubtedly very important. Low CIA values calculated for the graywackes and mudstones, similar to those calculated for felsic volcanic dykes and pyroclastics, indicate that little weathering of the detritus occurred, a finding compatible with a more direct sediment source from pyroclastic piles rather than from the weathering and erosion of consolidated or crystallized volcanic material.

5) Felsic plutonic detritus, generally subordinate to the volcanic detritus, may have been derived from either cratonic sources or from coeval, subvolcanic plutons.

6) Chemical data generally reinforce the petrographic data. Combined, they are suggestive of dacitic rather than granodioritic sources. Moderately high Fe and Mg contents indicate a partial

derivation from weathered mafic material.

7) The original volume of the felsic material (largely the particulate products of explosive eruptions) including that portion now residing in the sedimentary rocks of both the greenstone belts and the gneiss subprovinces, plus an unknown portion that may have been partially melted to form the magmas that resulted in granitic batholiths late in the evolution of the greenstone belts,may have been an order of magnitude greater than the volume of felsic volcanic rocks still present as volcanic rocks in the greenstone belts. This total volume of felsic volcanics may have been equal to or greater than the volume of mafic volcanics.

8) The recent discovery and mapping of numerous quartz arenite units indicates that several portions of the Canadian Shield were stable as early as 2980 Ma. This stability may have preceded the widespread volcanism that formed most of the greenstone belts. The sequence of events on the Canadian Shield is now more comparable to the history of the Dharwar craton in Southern India, as described by Radhakrishna (1983), Srinivasan and Sreenivas (1968), and Srinivasan and Ojakangas (1986) than was previously supposed.

9) The sedimentational history is compatible with a plate tectonics model.

REFERENCES

Arth, J.G. and Hanson, G.N, 1975. Geochemistry and Origin of the Early Precambrian Crust of Northeastern Minnesota: Geochim., Cosmochim, Acta. 39: 325-362.

Ayres, L.D. 1977. Importance of Stratigraphy in Early Precambrian Volcanic Terranes: Cyclic Volcanism at Setting Net Lake, Northwestern Ontario: In: W.R.A. Baragar, L.C. Coleman, and J.M. Hall (Editors), Volcanic Regimes in Canada, Geological Association of Canada Spec. Paper 16, pp.243-264.

Ayres, L.D. 1983. Bimodal Volcanism in Archaean Greenstone Belts, as exemplified by Graywacke Composition, Lake Superior Park, Ontario: Canadian J. Earth Sci. 20: 1168-1194.

Ayres, L.D. and Cerny, 1982. Metallogeny of Granitoid Rocks in the Canadian Shield: Can. Mineral., 20: 439-536.

Ayres, L.D., and Thurston, P.C., 1985. Archaean supracrustal sequences in the Canadian Shield: An overview. In: L.D. Ayres, P.C. Thurston, K.D. Card, K.D and W. Weber (Editors), Evolution of Archaean Supracrustal Sequences, Geol. Assoc. Canada Spec. Paper 28, pp.343-380.

Bailes, A.H., 1982. Origin of early Proterozoic volcaniclastic turbidites, south margin of the Kisseynew sedimentary gneiss belt, File Lake, Manitoba: Precamb. Res., 12: 197-225.

Baragar, W.R.A. and McGlynn, J.C., 1976. Early Archaean Basement on the Canadian Shield: A Review of the Evidence: Geol. Surv. Canada Paper, 76-14: 21.

Bhatia, M.R., 1983. Plate tectonics and geochemical composition of sandstones. J. Geol., 91: 611-627.

Blackburn, C.E., 1982. Evolution of Volcanic-Sedimentary Sequences, Western Wabigoon Subprovince, N.W. Ontario (Abs.), Geol. Assoc. Canada Program with Abstracts, 7: 39pp.

Blackburn, C.E., Bond, W.D., Breaks, F.W., Davis, D.W., Edwards, G.R. Poulsen, K.H., Trowell, N.F., and Wood, J., 1985. Evolution of Archaean volcanic-sedimentary sequences of the western Wabigoon Subprovince and its margins: A review: In: L.D Ayres, P.C. Thurston, K.D. Card and W. Weber (Editors), Evolution of Archaean Supracrustal sequences: Geol. Assoc. Canada Spec. Paper, 28, pp.89-116.

Breaks, F.W., Bond, W.D., and Stone D. 1978. Preliminary Geological Synthesis of the English River Subprovince: Ontario Geol. Surv. Misc. Paper 72 ; 55.

Condie, K.C., 1967. Composition of the Ancient North American Crust: Science, 155: 1013-1015.

Condie, K.C., 1981. Archaean Greenstone Belts: Elsevier Scientific Publishing Co., Amsterdam, 434pp.

Covello, L., Roscoe, S.M., Donaldson, J.A., Roach, D., and Fyson, W.K., 1987. Mafic-quartz arenite association in Precambrian terranes: an Archaean example from the Slave Province (abs.): Geol. Assoc. Canada Program with Abstracts, Yellowknife '87: 20pp.

Crook, K.A.W., 1974. Lithogenesis and geotectonics: the significance of compositional variations in flysch arenites (greywackes): In: R.H. Dott, and R.H.Shaver (Editors), Modern and Ancient Geosynclinal Sedimentation. Society of Economic Paleontologists and Mineralogists Spec. Publ., 19: pp.304-310.

Dickinson, W.R., Beard, L.S., Brakenridge, G.R., Erjavec, J.L., Ferguson, R.C., Inman, K.F., Knepp, R.A., Lindberg, F.A. and Ryberg, P.T., 1983. Provenance of North American Phanerozoic sandstones in relation to tectonic setting. Geological Soc. Amer. Bull., 94: 222-235.

Dimroth, E., Imreh, L., Rocheleau, M., and Goulet, N., 1982a. Evolution of the South-Central Part of the Archaean Abitibi Belt, Quebec, Part I: Stratigraphy and Paleogeographic Model. Canadian J. Earth Sci., 19: 1729-1758.

Dimroth, E., Muller, W., Archer, P., Gobeil, A. and Alland, G.O., 1982b. Evidence for Extensive Shallow Marine Sedimentation in the Chibougamau Area, Quebec. Geol. Surv. Canada, Paper 82-1A: 29-36.

Dimroth, E. and Rocheleau, M., 1979. Volcanology and Sedimentology of Rouyn-Noranda Area. Geol. Assoc. Canada Annual Meeting, Field Trip A-1, Universite Laval, Quebec, pp.151-193.

Donaldson, J.A. and DeKemp, E., 1987. The komatiite-quartz arenite association in Precambrian terranes: An Archaean example from the Superior Province (abst.). Geol. Assoc. Canada Program with Abstracts, Yellowknife '87, 37pp.

Donaldson, J.A. and Jackson, G.D., 1965. Archaean Sedimentary Rocks of the North Spirit Lake Area, Northwestern Ontario. Canadian J. Earth Sci., 2: 622-647.

Donaldson, J.A. and Ojakangas, R.W., 1977. Orthoquartzite Pebbles in Archaean Conglomerate, North Spirit Lake, Northwestern Ontario. Canadian J. Earth Sci., 14: 1980-1990.

Goodwin, A.M., 1968. Archaean Protocontinental Growth and Early Crustal History of the Canadian Shield. Int. Geol. Cong. 23rd Session Proceedings, 1, pp.69-89.

Goodwin, A.M., 1977a. Archaean Basin-Craton Complexes and the Growth of Precambrian Shields. Canadian J. Earth Sci., 14: 2737-2759.

Goodwin, A.M., 1977b. Archaean volcanism in Superior Province, Canadian Shield: In: W.R.A. Baragar, L.C. Coleman and J.M. Hall (Editors), Volcanic Regimes in Canada, Geol. Assoc. Canada, Spec. Paper 16, pp.205-242.

Goodwin, A.M., 1981. Archaean Plates and Greenstone Belts. In: A. Kroner (Editor), Precambrian Plate Tectonics, Elsevier, Amsterdam, pp.105-135.

Goodwin, A.M. and Smith, I.E.M., 1980. Chemical discontinuities in Archaean metavolcanic terrains and the development of Archaean crust. Precamb. Res., 10: 301-311.

Goodwin, A.M., and West, G.F., 1974. The Superior Geotraverse Project. Geosci. Canada, 1, pp.21-29.

Gross, G.A., 1965. Geology of Iron Deposits in Canada - General Geology and Evaluation of Iron Deposits. Geol. Surv. Canada, Report 22, 1, 181pp.

Henderson, J.B., 1975. Sedimentology of the Archaean Yellowknife Supergroup at Yellowknife, District of Mackenzie. Geol. Surv. Canada, Bull., 246: 62pp.

Henderson, J.B., 1981. Archaean Basin Evolution in the Slave Province, Canada: In: A. Kroner (Editor), Precambrian Plate Tectonics, Elsevier, Amsterdam, pp.213-235.

Hyde, R.S., 1980. Sedimentary Facies in the Archaean Timiskaming Group and Their Tectonic Implications, Abitibi Greenstone belt, Northeastern Ontario, Canada. Precamb. Res., 12: 161-195.

Krogh, T.E., Harris, N.B.W., and Davis, G.L., 1976. Archaean Rocks from the Eastern Lac Seul Region of the English River Gneiss Belt, Northwestern Ontario, part 2. Geochronology: Canadian J. Earth Sci., 13: 1212-1215.

Kronberg, B.I., Nesbitt, H.W., and Lam, W.W., 1986. Upper Pleistocene Amazon deep-sea fan muds reflect intense chemical weathering of their mountainous source lands. Chem. Geol., 54: 283-294.

Lowe, D.R., 1980 Archaean Sedimentation. Annual Review of Earth and Planetary Sciences, 8: 145-167.

Lowe, D.R., 1982. Comparative Sedimentology of the Principal Volcanic Sequences of Archaean Greenstone Belts in South Africa, Western Australia, and Canada. Implications for Crustal Evolution. Precamb. Res., 17: 1-29.

Maynard, J.B., Valloni, R. and Yu, H., 1982. Composition of modern deep-sea sands from arc-related basins. In: J.K. Leggett (Editor), Trench-Forearc Sedimentation: Geol. Soc. London Special Publication, 10: pp.551-561.

McLennan, S.M., 1984. Petrological characteristics of Archaean graywackes: J. Sed. Petr., 54: 889-898.

Nesbitt, H.W. and Young, G.M. 1982. Early Proterozoic climate and plate motions inferred from major element chemistry of lutites: Nature, 299: 715-717.

Nunes, P.D., and Wood, J., 1980. Geochronology of the North Spirit Lake Area, District of Kenora-Progress Report. In: E.G. Pye (Editor), Summary of Geochronology Studies, 1977-1979, Ontario Geol. Surv. Misc. Paper, 92, pp.7-14.

Ojakangas, R.W., 1972a. Archaean Volcanogenic Graywackes of the Vermilion District, Northeastern Minnesota. Geol. Soc. America Bull., 85: 429-442.

Ojakangas, R.W. 1972b. Graywackes and Related Rocks of the Knife Lake Group and Lake Vermilion Formation, Vermilion District. In: P.K. Sims and G.B. Morey (Editors), Geology of Minnesota. A Centennial Volume, Minnesota Geol. Surv., pp.82-90.

Ojakangas, R.W., 1985. Review of Archaean clastic sedimentation, Canadian Shield: Major felsic volcanic contributions to turbidite and alluvial fan-fluvial facies associations. In: L.D. Ayres, P.C. Thurston, K.D. Card and W. Weber (Editors), Evolution of Archaean Supracrustal Sequences, Geol. Assoc. Canada Spec., Paper, 28, pp.23-47.

Ojakangas, R.W., 1986. An early Proterozoic metagraywacke-slate turbidite sequence: The Tampere Schist Belt, southwestern Finland. Bull. Geol. Soc. Finland, 58: 241-261.

Pettijohn, F.J., 1970. The Canadian Shield, a Status Report, 1970: In: A.J. Baer (Editor), Symposium on Basins and Geosynclines of the Canadian Shield, Geol. Surv. Canada Paper, 70-40, pp.239-265.

Pettijohn, F.J., 1972. The Archaean of the Canadian Shield: A Resume. Geol. Soc. America Memoir 135: 131-149.

Radhakrishna, B.P., 1983. Archaean granite-greenstone terrain of the South Indian Shield. In: S.M. Naqvi and J.J.W. Rogers (Editors), Precambrian of South India, Geol. Soc. India, Mem., 4, pp.1-46.

Roscoe, S.M., and Donaldson, J.A., (in press). Uraniferous pyritic quartz-pebble conglomerate and layered ultramafic intrusions in a sequence of quartzite, carbonate, iron-formation, and basalt of probable Archaean age at Lac Sakami, Quebec. Geol. Surv. Canada Report of Activities, 1987.

Sawyer, E.W., 1986. The influence of source rock type, chemical weathering and sorting on the geochemistry of clastic sediments from the Quetico metasedimentary belt, Superior Province, Canada. Chem. Geol., 55: 77-95.

Schau, M., and Henderson, J.B., 1983. Archaean Chemical Weathering at Three Localities on the Canadian Shield: Precamb. Res., 20: 189-224.

Southwick, D.L., 1979. The Vermilion granitic complex, northern Minnesota. Minnesota Geol. Surv. Guidebook, 10: 1-11.

Srinivasan, R. and Ojakangas, R.W., 1986. Sedimentology of quartz-pebble conglomerates and quartzites of the Archaean Bababudan Group, Dharwar Craton, South India. Evidence for early crustal stability: J. Geol., 94: 199-214.

Srinivasan, R., and Sreenivas, B.L., 1968. Sedimentation and tectonics in Dharwars (Archaeans), Mysore State, India. The Indian Mineralogist, 9: 47-58.

Taylor, S.R. and McLennan, S.M., 1985. The Continental Crust: its Composition and Evolution. Blackwell Scientific Publications, Oxford, 312pp.

Thurston, P.C., Ayres, L.D., Edwards, G.R., Gelinas, I, Ludden, J.N., and Verpacist, P., 1985. Archaean bimodal volcanism: In L.D. Ayres, P.C. Thurston, K.D. Card and W. Weber (Editors), Evolution of Archaean Supracrustal Sequences. Geol. Assoc. Canada Spec. Paper 28, pp.7-22.

Turner, C.C., and Walker, R.G., 1973. Sedimentology, Stratigraphy and Crustal Evolution of the Archaean Greenstone Belt Near Sioux Lookout, Ontario: Canadian J. Earth Sci., 10: 817-845.

Walker, R.G., 1975. Generalized Facies Models for Resedimented Conglomerates of Turbidite Association. Geol. Soc. America Bull., 86: 737-748.
Walker, R.G., and Pettijohn, F.J., 1971. Archaean Sedimentation: Analysis of the Minnitaki Basin, Northwestern Ontario. Geol. Soc. America Bull., 82: 2099-2130.
Windley, B.F., 1981. Precambrian Rocks in the Light of the Plate-Tectonic Concept. In: A.Kroner (Editor), Precambrian Plate Tectonics, Elsevier, Amsterdam, pp.1-20.
Windley, B.F., 1984. The Evolving Continents (2nd Edition). John Wiley and Sons, New York, pp.1-399.
Young, G.M., 1978. Some aspects of the evolution of the Archaean crust. Geosci., Canada, 5: 140-149.

TRACE AND RARE EARTH ELEMENT GEOCHEMISTRY AND ORIGIN OF THE CLOSEPET GRANITE,DHARWAR CRATON, INDIA

V. DIVAKARA RAO, P. RAMA RAO, M.V. SUBBA RAO, P.K. GOVIL, R.U.M. RAO, J.N. WALSH, M. THOMPSON AND G.R. REDDY

ABSTRACT

Late Archaean - Early Proterozoic K-rich granitic activity of the type Closepet, Bellary and Hospet in the Dharwar Craton and similar coeval granites of the Singhbhum and Bundelkhand have contributed substantially to the crustal growth and stabilization in the Indian Shield.

The 2.5 Ga. old Closepet Granite of the Dharwar Craton is a composite granite of two major phases, the pink and grey and a minor phase of mafic granite, with transitional as well as sharp boundaries between major phases. Overall compositions of various phases show the adamellite-quartz monzonite character of the granite. ΣREE, chondrite-normalised REE, and Ce_N/Yb_N and La_N/Yb_N ratios in different phases suggest that the major pink and grey phases are CR-type granites (crustal remelting source) while the minor mafic granite is of MM type (mixed source, metamorphic, metasomatic). The relative abundances of LREE and HREE in pink and grey granites support a common source of felsic nature, while a mixed mafic and felsic source can be suggested for the mafic phase from the negative Eu anomaly, relatively low Ce_N/Yb_N and moderate La_N/Yb_N ratios, the LREE/HREE ratio and the overall composition. Large scatter observed in some of the large ion lithophile (LIL) and other mobile elements and the scatter in K/Rb, Ca/Sr and Th/U ratios in these different phases suggest that syn- or post-granite emplacement/metasomatic processes have played a substantial role in the redistribution of these elements during or after the emplacement of the granite.

Major, trace and REE data and the field relations between the different phases in the Closepet Granite suggest that this composite granite is a palingenetic and anatectic product of the basement gneisses.

INTRODUCTION

Late Archaean to Early Proterozoic K-rich granitic activity has played a major role in crust forming and stabilization events in the Indian Shield (Divakara Rao and Rama Rao, 1982; Divakara Rao, 1985). This activity followed the early Archaean Na-rich tonalitic/trondhjemitic granite/gneiss formation. There appears to be no major granitic event of regional importance after the K-rich granites were involved in crust forming processes.

The Closepet Granite in Karnataka (Fig. 1) is one of the largest and most important units of this K-rich phase, with coeval granites occurring at Hyderabad, Molakalamuru, Bellary, Hospet, Singhbhum and Bundelkhand. These early Proterozoic granites occur amidst Na-rich tonalites/trondhjemites that form the basement throughout the shield. These basement gneisses are of three

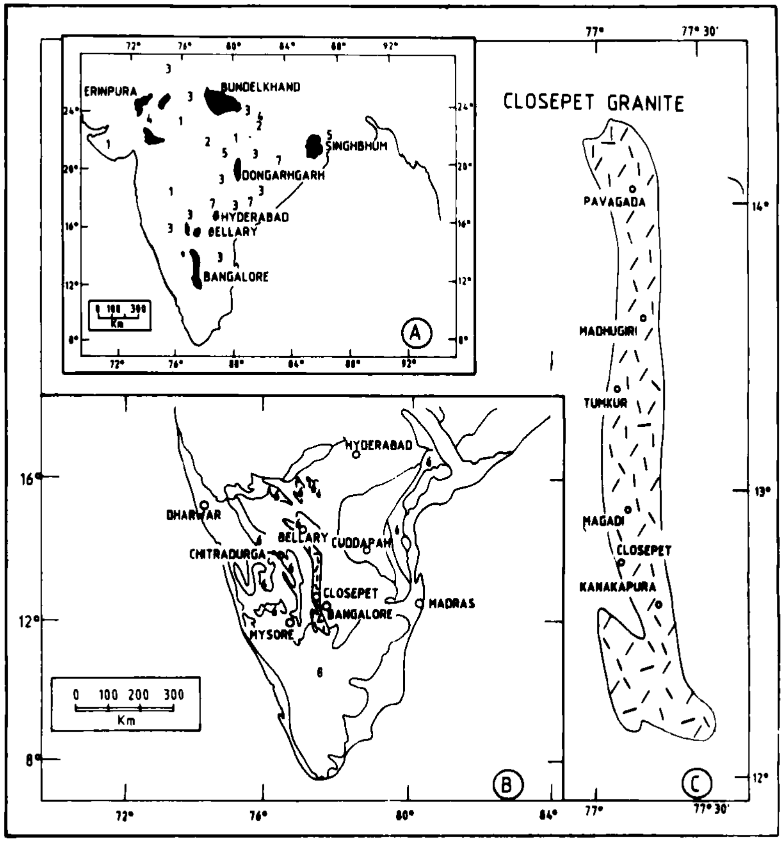

Figure 1. Generalised geological map of South India showing the location of the Closepet and other coeval granites.

phases, the first mafic phase post-dating the greenstone belts such as Holenarsipur, Krishnarajpet and their equivalents. The second, slightly more feldspathic phase pre-dates the secondary greenstone belts such as Chitradurga, Shimoga and Bababudan. A third phase, that is not very common but can be detected, post-dates the secondary greenstones (Divakara Rao et al., 1983; Naqvi et al., 1983).

The granitic rocks around Arasikere, Chitradurga, Hosadurga and Shimoga are probably contemporaneous with or partly older than the Closepet Granite (Divakara Rao et al., 1972 a, b). Post-Closepet granitic activity, though present, is less abundant and of sporadic nature, limited to small lenses like those at Chamundi, Chipurupalli, Rajam, Kanigiri, Tirunelveli, Tiruchirapalli (most of these latter granites date around 800-1000 Ma. old, Dhanaraju et al., 1983).

The origin of the K-rich granites (including the Closepet) is still controversial; magmatic, metasomatic and anatectic modes of origin have been suggested and supported. Available geochemical and mineralogical data on these granites are not conclusive in either supporting or contradicting any of these above models.

THE CLOSEPET GRANITE COMPLEX

The first detailed field, mineralogical and chemical description of the 200 km long, 20 km wide Closepet Granite was by Radhakrishna (1956). It extends from Kanakapura in the south to Bellary in the north (Fig. 1) with similar (coeval) granites occurring further north up to Hospet and Hyderabad with patches of older gneisses in between. In many places the western margin of the granite appears to have been faulted. Lenses of supracrustals of banded haematite quartzite and fuchsite quartzite occur at places in the Closepet Granite. The foliation of the granite is NNW-SSE with the feldspar porphyroblasts and the mafic minerals aligning in the same direction throughout the body (the regional trend of the Dharwar formations). The Closepet Granite is a composite body and consists of three different phases, grey, pink and mafic, the former two (pink and grey) being porphyritic, containing porphyroblasts of K-feldspar, a few millimeters to a few centimeters in length, while the mafic phase is usually equigranular. Pink and grey phases have sharp and/or gradational contact with each other. The occurrence of one phase in the other as lenses is common.

TABLE 1.

MAJOR AND TRACE ELEMENT CONCENTRATIONS

PINK GRANITES

Wt.%	CG78	CG115	CG142	CG162	CG210	CG221	CG223	CG227	CG229	CG232	CG233	CG237
SiO_2	67.09	70.21	72.56	69.71	63.99	70.12	71.70	70.24	74.30	70.42	68.09	71.06
TiO_2	0.56	0.25	0.12	0.26	0.74	0.47	0.42	0.38	0.13	0.30	0.80	0.34
Al_2O_3	15.25	14.28	14.21	18.41	15.73	15.02	15.01	16.00	13.12	15.85	14.44	15.36
Fe_2O_3	1.61	0.72	0.54	1.07	2.38	1.87	0.80	0.82	0.35	0.15	2.17	0.85
FeO	1.88	1.12	0.48	1.00	2.96	1.68	0.80	1.52	0.44	1.68	1.92	1.16
CaO	2.78	2.23	1.10	1.72	3.61	1.67	1.68	2.05	1.25	1.71	2.62	1.93
MgO	1.30	1.05	0.90	0.47	1.50	1.18	1.05	1.10	0.92	1.03	1.43	1.09
Na_2O	3.82	3.82	3.67	3.50	4.12	4.14	3.78	3.99	3.57	3.91	3.92	3.97
K_2O	5.01	4.59	6.21	3.74	2.26	3.32	5.22	4.33	5.63	5.00	3.06	4.03
P_2O_5	0.31	0.13	0.05	0.07	0.41	0.17	0.11	0.14	0.07	0.11	0.14	0.12
MnO	0.07	0.04	0.02	0.02	0.12	0.04	0.03	0.04	0.02	0.03	0.08	0.04
LOI	0.83	0.52	0.87	0.57	2.00	1.08	0.45	0.93	0.33	0.22	0.48	0.56
TOTAL	100.51	98.96	100.73	100.54	99.82	100.76	101.05	101.54	100.13	100.41	99.15	100.51
ppm												
Zr	231	236	163	-	307	224	166	230	73	210	204	236
Y	69	12	43	-	65	45	19	16	32	11	18	25
Rb	116	92	162	52	114	63	132	123	100	90	129	123
Sr	528	407	237	500	352	301	387	244	245	290	288	276
Ba	902	1059	359	910	500	761	909	733	964	841	612	531
Cr	13	16	9	4	19	10	3	11	15	18	22	16
Ni	3	3	1	5	4	-	-	3	-	-	5	-
K/Rb	358	371	318	596	164	436	328	292	467	461	197	271
K/Ba	46.12	34.00	143.45	34.06	37.40	36.13	47.63	48.98	48.44	49.35	41.50	62.90
Ca/Sr	37.50	39.15	32.91	24.60	73.29	39.53	31.00	59.83	35.92	42.06	64.93	50.00

PINK GRANITES

Wt.%	CG249	CG251	CG255	CG260	CG264	CG314	Min.	Max.	Avg.	SD
SiO_2	71.31	71.61	70.05	71.09	71.06	62.62	63.99	74.30	69.84	2.94
TiO_2	0.39	0.25	0.54	0.33	0.27	0.82	0.12	0.82	0.41	0.21
Al_2O_3	15.50	15.15	15.20	15.11	15.32	19.40	13.12	19.40	15.46	1.43
Fe_2O_3	1.02	1.04	2.17	0.73	0.98	0.75	0.15	2.38	1.11	0.65
FeO	1.24	0.76	1.28	1.12	1.08	0.96	0.44	2.96	1.28	0.60
CaO	2.26	1.64	2.82	1.99	1.79	2.94	1.10	3.61	2.09	0.64
MgO	1.10	1.01	1.24	1.04	1.06	1.17	0.47	1.50	1.09	0.22
Na_2O	4.07	3.75	3.96	3.89	3.79	3.64	3.50	4.12	3.85	0.18
K_2O	3.03	4.75	3.11	4.51	4.77	4.58	2.26	6.21	4.29	1.03
P_2O_5	0.14	0.13	0.21	0.14	0.14	0.05	0.05	0.41	0.15	0.09
MnO	0.03	0.03	0.07	0.03	0.04	0.08	0.02	0.08	0.05	0.03
LOI	0.28	0.46	0.58	0.23	0.42	0.25	0.22	2.00	0.61	0.43
TOTAL	100.37	100.58	101.23	100.21	100.72	97.26	-	-	-	-
ppm										
Zr	232	182	218	172	158	-	73	307	203	5.12
Y	45	36	27	13	40	-	11	69	32.25	18.06
Rb	145	118	111	103	116	114	52	162	111.28	26.23
Sr	293	408	526	211	332	187	187	528	334	105.25
Ba	633	1009	736	809	713	660	359	1059	758	187.73
Cr	16	13	15	16	9	2	2	22	12.61	5.58
Ni	-	2	3	-	1	1	1	5	2.82	-
K/Rb	173	334	232	363	341	333	164	596	335.28	110
K/Ba	39.65	39.04	35.05	46.23	55.54	57.58	34.00	143.45	50.17	24.74
Ca/Sr	54.95	28.68	38.21	67.30	38.55	47.05	28.68	73.29	44.74	14.07

GREY GRANITES

Wt.%	CG82	CG130	CG200	CG222	CG226	CG228	CG235	CG236	CG241	CG242	CG243	CG244
SiO_2	67.71	66.15	70.12	70.16	71.25	70.25	71.11	70.35	70.00	70.54	71.33	72.48
TiO_2	0.31	0.32	0.24	0.37	0.33	0.34	0.28	0.37	0.35	0.28	0.31	0.21
Al_2O_3	17.43	20.71	19.07	15.01	15.05	15.46	15.73	15.01	15.31	15.61	15.27	14.64
Fe_2O_3	1.73	1.44	1.37	1.18	0.78	0.63	0.01	1.12	1.18	0.74	0.67	0.61
FeO	-	0.84	-	1.44	1.36	1.40	1.92	1.44	1.48	1.12	1.20	0.72
CaO	1.29	1.86	1.36	1.98	2.14	1.97	1.92	2.38	2.31	1.81	1.97	1.35
MgO	3.67	0.45	0.23	1.13	1.05	1.05	1.02	1.17	1.16	1.03	1.06	0.95
Na_2O	3.50	3.77	3.37	3.83	4.00	3.94	4.05	3.95	3.91	3.92	3.97	3.76
K_2O	4.34	4.34	4.22	5.02	3.68	4.44	3.77	4.16	4.00	4.73	3.84	5.12
P_2O_5	0.08	0.10	0.04	0.18	0.13	0.13	0.11	0.17	0.15	0.11	0.11	0.09
MnO	0.02	0.04	0.02	0.04	0.03	0.03	0.03	0.05	0.05	0.03	0.03	0.03
LOI	-	0.34	-	1.20	1.20	0.64	0.38	0.32	0.51	0.77	0.85	0.49
TOTAL	100.08	100.36	100.04	101.54	101.00	100.28	100.33	100.49	100.41	100.69	100.61	100.45
ppm												
Zr	-	-	-	381	269	235	232	288	207	228	196	170
Y	-	-	-	10	54	18	55	45	21	41	26	27
Rb	84	120	134	94	107	141	131	161	88	121	93	94
Sr	210	410	210	472	256	322	301	397	420	328	301	293
Ba	650	720	590	1042	645	940	640	876	709	869	685	686
Cr	3	2	4	8	15	13	7	11	16	6	18	7
Ni	4	5	5	-	3	-	1	3	2	3	2	1
K/Rb	261	300	261	442	285	261	239	214	377	324	343	452
K/Ba	55.38	50.00	59.32	39.92	47.28	39.15	48.91	39.38	46.83	45.10	14.59	61.95
Ca/Sr	43.81	32.44	46.19	29.87	59.77	43.79	45.51	42.82	39.29	39.33	46.84	32.76

GREY GRANITES

Wt.%	CG245	CG247	CG248	CG252	CG253	CG261	CG321	Min.	Max.	Avg.	SD
SiO_2	70.20	70.62	71.93	71.50	70.60	66.81	70.93	66.15	72.48	70.21	1.63
TiO_2	0.28	0.29	0.18	0.28	0.23	0.49	0.17	0.17	0.49	0.30	0.07
Al_2O_3	13.25	15.71	14.50	14.55	15.81	15.56	17.75	13.25	20.71	15.86	1.74
Fe_2O_3	0.82	0.75	0.52	0.80	0.44	0.33	0.88	0.01	1.44	0.84	0.41
FeO	1.16	1.08	0.76	1.00	1.00	3.16	0.72	0.72	3.16	1.28	0.58
CaO	1.91	1.77	1.78	2.21	1.64	1.92	1.11	1.11	2.38	1.82	0.35
MgO	1.03	1.03	0.95	1.10	1.02	1.09	0.29	0.23	3.67	1.08	0.69
Na_2O	3.69	3.97	3.79	3.93	3.91	3.79	3.23	3.23	4.05	3.80	0.22
K_2O	5.03	4.07	5.08	3.52	4.57	6.02	4.82	3.52	6.02	4.46	0.62
P_2O_5	0.11	0.11	0.07	0.10	0.08	0.28	0.04	0.04	0.28	0.11	0.05
MnO	0.04	0.04	0.03	0.03	0.02	0.06	0.03	0.02	0.06	0.03	0.01
LOI	0.75	0.40	0.59	0.59	0.28	0.28	0.39	0.28	1.20	0.59	0.29
TOTAL	98.27	99.84	100.18	99.61	99.60	99.79	100.36	-	-	-	-
ppm											
Zr	172	213	131	188	138	518	-	131	518	237.73	99.54
Y	36	39	33	40	23	35	-	10	55	33.53	12.84
Rb	131	102	121	106	137	120	143	84	161	117.26	21.51
Sr	303	346	210	241	238	336	210	210	472	305.47	77.58
Ba	864	807	764	560	676	1158	730	560	1158	769	156.17
Cr	20	9	11	10	10	5	3	2	20	9.36	5.22
Ni	2	3	-	-	-	4	3	1	5	3	1.27
K/Rb	318	331	348	275	277	416	280	214	452	316	67.19
K/Ba	48.26	41.88	55.10	52.14	56.06	43.09	54.79	14.59	61.95	47.32	0.42
Ca/Sr	44.88	36.42	60.48	65.56	49.15	40.77	37.62	29.87	65.56	46.14	9.87

MAFIC GRANITES

Wt.%	CG220	CG234	CG246	CG308	11	93	94	Min.	Max.	Avg.	SD
SiO_2	68.04	69.03	70.76	67.03	65.20	60.05	71.70	60.05	71.70	67.40	3.91
TiO_2	0.53	0.54	0.21	0.93	0.71	0.25	0.24	0.21	0.93	0.49	0.37
Al_2O_3	16.16	15.03	15.20	13.82	15.67	21.70	14.88	13.82	21.70	16.06	2.59
Fe_2O_3	1.28	1.70	0.59	1.67	2.35	3.05	0.01	0.01	3.05	1.52	1.02
FeO	1.84	1.60	1.00	2.96	2.28	2.16	1.20	1.00	2.96	1.86	0.67
CaO	1.96	2.49	1.34	2.97	3.28	4.06	1.82	1.34	4.06	2.56	0.94
MgO	1.16	1.23	1.00	1.26	1.61	1.76	0.43	0.43	1.76	1.21	0.43
Na_2O	3.90	3.87	3.85	3.73	4.04	4.99	3.62	3.62	4.99	4.00	0.46
K_2O	4.84	4.24	5.42	5.12	3.91	1.47	4.67	1.47	5.42	4.24	1.32
P_2O_5	0.20	0.28	0.10	0.50	0.36	0.21	0.08	0.10	0.50	0.25	0.15
MnO	0.04	0.06	0.03	0.07	0.09	0.09	0.02	0.02	0.09	0.06	0.03
LOI	0.71	1.07	0.28	0.37	0.46	0.49	0.37	0.28	1.07	0.54	0.27
TOTAL	100.66	101.14	99.78	100.43	99.96	100.28	99.04	-	-	-	-
p											
Zr	500	307	167	610	75	-	94	75	610	292.16	222.04
Y	67	32	62	148	46	-	4	4	148	59.83	48.81
Rb	103	145	223	153	-	37	-	37	223	132.20	68.47
Sr	328	398	105	470	757	400	450	105	757	415.42	193.82
Ba	1521	766	381	1225	962	135	863	135	1521	836.14	472.66
Cr	16	15	11	12	32	15	29	11	32	18.57	8.38
Ni	7	1	-	2	22	15	10	2	22	9.5	8.01
K/Rb	390	243	202	278	365	330	356	202	390	309.14	69.66
K/Ba	26.42	45.95	118.11	34.69	32.22	90.37	42.87	26.42	118.11	55.80	34.65
Ca/Sr	78.65	44.72	91.43	45.10	31.34	72.50	27.69	27.69	91.43	55.92	24.81

Predominant minerals in the major pink and grey phases are quartz, K-feldspar, plagioclase, perthite and microcline with sporadic to abundant myrmekitic growth. Biotite and hornblende are the accessories. The mafic phase is characterised by higher amounts of hornblende and biotite. K-metasomatism resulting in microcline formation is a common phenomenon in the granite, being more notable in the major phases than in the mafic phase. Zircon, allanite, apatite and sphene are common accessories in all the phases.

CHEMISTRY OF THE GRANITE

The pink and grey granite phases are similar in whole rock as well as mineral compositions and exhibit scatter in SiO_2 and K_2O content with little variation in other major oxides (Table 1). K-feldspar, plagioclase and biotite in both types have remarkably similar compositions (Table 2) while their composition in the mafic granite is different.

The granite as a whole ranges in composition from quartz-monzonite to granodiorite (Fig. 2). It appears to have been unevenly enriched in K (post-formational metasomatism) while Rb exhibits depletion resulting in substantial variation in K/Rb

TABLE 2.

AVERAGE MINERAL COMPOSITIONS OF THE GRANITIC ROCKS

	PLAGIOCLASE		K-FELDSPAR			BIOTITE		
	Pink granite	Grey granite	Pink granite	Grey granite	Mafic granite	Pink granite	Grey granite	Mafic granite
SiO_2	64.09	63.08	63.72	63.51	63.31	36.16	36.71	37.52
TiO_2	0.02	0.02	0.01	0.01	0.04	3.04	3.33	2.66
Al_2O_3	22.07	23.00	18.44	18.64	18.56	16.23	15.70	15.89
FeO^*	0.07	0.06	0.04	0.04	0.03	19.99	19.90	17.43
MnO	0.07	0.01	0.04	0.03	0.05	0.33	0.30	0.27
MgO	-	-	-	-	0.03	9.70	10.62	11.91
CaO	2.74	4.02	-	-	-	0.02	0.03	-
Na_2O	9.85	9.17	0.75	0.49	0.48	0.07	0.04	0.03
K_2O	0.30	0.25	16.57	16.80	16.67	12.19	10.01	10.43
Cr_2O_3	0.04	0.01	0.02	0.02	-	0.02	0.05	-
BaO	0.05	0.03	0.32	0.33	0.46	0.15	0.13	0.10

* Total iron as FeO

TABLE 3.

Th AND U CONCENTRATIONS

PINK GRANITES

	CG7	CG9	CG15	CG21	CG45	CG67	CG70	CG79	CG91	CG96	CG102	CG114	CG117	CG118
Th	10.4	0.08	10.2	11.9	10.0	5.7	8.3	18.4	11.8	4.9	1.1	8.8	11.3	11.4
U	0.6	0.3	0.4	0.5	0.5	0.7	0.9	0.9	0.7	0.4	0.4	0.8	0.8	1.3
Th/U	17.33	2.67	25.50	23.80	20.00	8.14	9.22	20.44	16.86	12.25	2.75	11.0	14.12	8.77

	CG163	CG166	CG178	CG192	CG201	CG204	CG207	CG213	CG214	CG223	CG231	CG245	CG313
Th	10.4	17.7	15.8	14.0	25.6	27.2	14.1	7.0	2.7	10.1	10.3	16.8	33.6
U	0.5	1.0	1.7	1.3	1.2	1.4	1.1	0.5	0.2	1.1	0.5	0.8	1.8
Th/U	20.80	17.70	9.29	10.77	21.33	19.43	12.82	14.00	13.50	9.18	20.60	21.00	18.67

GREY GRANITES												MAFIC GRANITES	
	CG5	CG12	CG75	CG82	CG101	CG132	CG144	CG155	CG200	CG217	CG248	CG23	CG43
U	5.3	12.9	16.8	12.7	14.7	24.5	18.7	19.0	25.8	30.4	40.1	18.1	0.5
Th	0.6	0.6	0.4	1.0	0.7	2.3	0.7	1.1	1.0	1.0	1.1	0.6	0.2
Th/U	8.83	21.50	42.00	12.70	21.00	10.65	26.71	17.27	25.80	30.40	36.45	30.17	2.50

ratios in the different phases (Fig. 3), often more than crustal averages. Ba, Sr, Th and Zr also show uneven distributions, due to depletion at places and enrichment at others. Between Th and U, the former shows random enrichment (with U being at normal level) resulting in scatter of Th/U ratio (Table 3, Fig. 4). This part of the shield was earlier described as a "Th-rich province" (Divakara Rao et al., 1972 a,b). The abundance and distribution of rare-earth elements (REE) in the major phases (pink and grey) are similar, with the LREE/HREE fractionation being low, and ΣREE being less. The mafic phase has more ΣREE with a moderate to significant negative Eu anomaly and variable Ce_N/Yb_N ratio.

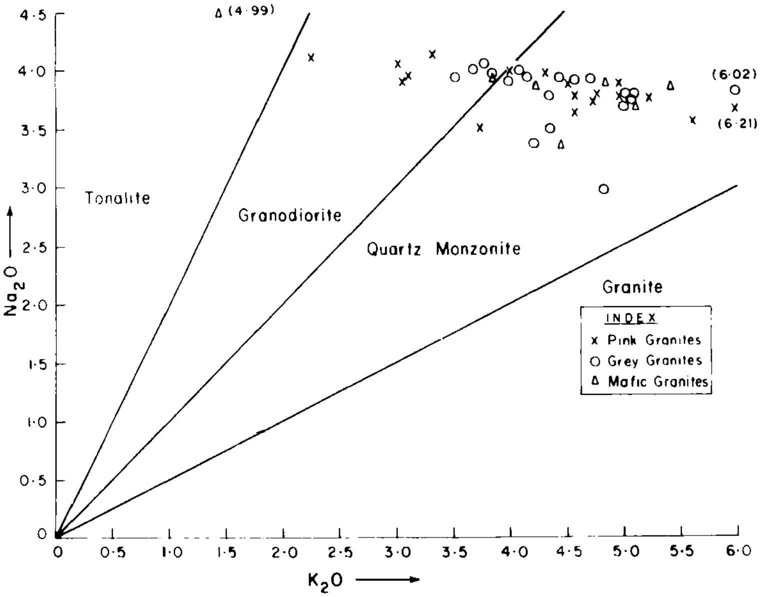

Figure 2. Na_2O vs. K_2O diagram of the Closepet Granite depicting its granodioritic to quartz-monzonitic nature.

ORIGIN OF THE CLOSEPET GRANITE

Major and trace elemental abundances, especially alkalies, in the various phases of the Closepet Granite suggest the quartz monzonite-granodiorite nature of this pluton (Fig. 2). The scatter and uneven distribution of K,Na and Rb and the ratios Na/K and K/Rb suggest syn-or post-formational metasomatic enrichment of these elements, especially K. The abundance of myrmekite and microcline, the latter forming at the expense of plagioclase,

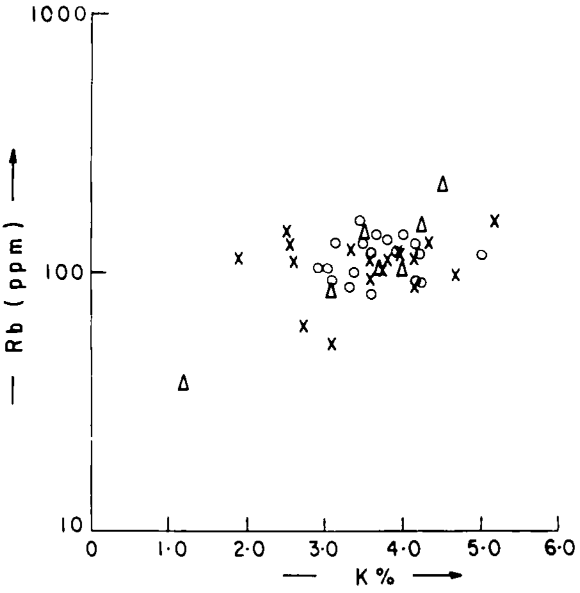

Figure 3. Relationship of K with Rb in the Closepet Granite Complex.

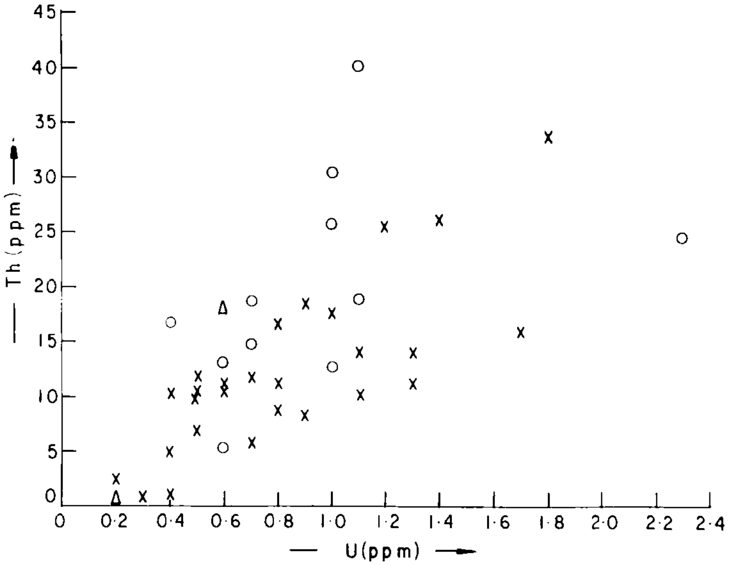

Figure 4. Diagram showing the relation between of Th and U in the Closepet Granite.

TABLE 4.

RARE-EARTH ELEMENT CONCENTRATIONS

GREY GRANITES

REE (ppm)	CG46	CG144	CG226	CG254	CG130	CG200	Avg.
La	96.89	93.52	45.83	33.00	37.28	43.86	58.39
Ce	168.00	169.00	84.00	60.00	66.17	73.02	103.36
Pr	-	-	-	-	8.80	8.58	8.69
Nd	-	-	-	-	27.26	27.29	27.27
Sm	11.26	7.97	4.03	2.29	4.05	4.06	5.61
Eu	2.04	1.54	0.77	0.65	1.28	0.94	1.20
Gd	-	-	-	-	2.65	2.44	2.54
Dy	-	-	-	-	1.95	1.31	1.63
Ho	-	-	-	-	0.40	0.25	0.33
Er	-	-	-	-	1.34	0.89	1.11
Tb	1.08	0.50	0.49	0.30	-	-	0.59
Yb	3.66	1.40	1.12	0.85	1.05	0.51	1.43
Lu	0.30	0.15	0.40	0.40	0.18	0.09	0.39
REE*	283.33	274.08	136.64	97.34	152.41	163.24	184.49
Ce_N/Yb_N	11.76	30.89	19.18	18.07	15.94	36.69	22.08
La_N/Lu_N	29.36	56.68	11.80	8.50	20.92	51.11	29.72
La_N/Yb_N	17.64	44.56	27.28	25.91	23.54	57.88	32.80
REE (N)	162.68	157.42	78.33	56.23	46.92	50.25	92.03
LREE/HREE	54.79	131.94	66.59	61.47	18.96	28.57	60.84

REE* = Total REE   REE (N) = Chondrite-Normalised REE

PINK GRANITES

REE (ppm)	CG67	CG138	CG227	CG255	CG115	CG264	Avg.
La	41.47	70.33	32.09	96.31	73.30	39.33	58.80
Ce	78.00	146.00	115.00	186.00	125.68	72.12	120.46
Pr	-	-	-	-	13.74	9.69	11.71
Nd	-	-	-	-	44.38	34.66	39.52
Sm	5.25	11.68	3.62	6.66	5.65	7.23	6.68
Eu	1.50	2.01	0.79	0.86	1.24	1.45	1.31
Gd	-	-	-	-	3.42	5.87	4.64
Dy	-	-	-	-	2.09	5.00	3.54
Ho	-	-	-	-	0.41	0.94	0.67
Er	-	-	-	-	1.45	2.67	2.06
Tb	0.56	1.16	0.53	1.12	-	-	0.84
Yb	1.94	3.30	0.80	2.00	0.85	1.89	1.79
Lu	0.22	0.40	0.40	0.40	0.13	0.26	0.62
REE*	128.94	234.88	153.23	293.35	272.34	181.11	210.96
Ce_N/Yb_N	10.29	11.31	36.73	23.79	37.25	9.69	21.51
La_N/Lu_N	17.14	15.98	8.26	24.80	56.95	15.28	23.06
La_N/Yb_N	14.26	14.21	26.71	32.10	56.94	13.86	26.34
REE (N)	74.06	134.91	88.30	169.29	83.84	55.76	101.02
LREE/HREE	45.85	46.92	87.11	54.93	31.47	9.80	46.01

MAFIC GRANITES

REE (ppm)	CG64	CG175	CG234	CG262	CG93	CG246	Avg.
La	151.00	35.43	99.48	186.00	46.75	97.95	102.76
Ce	291.00	65.00	192.00	390.00	97.41	184.59	203.33
Pr	-	-	-	-	13.52	19.83	16.67
Nd	-	-	-	-	52.25	74.79	63.57
Sm	21.00	11.32	12.89	26.67	10.90	13.65	16.07
Eu	4.98	2.12	1.96	3.67	1.95	0.60	2.54
Gd	-	-	-	-	8.80	9.77	9.28
Dy	-	-	-	-	7.33	6.29	6.81
Ho	-	-	-	-	1.37	1.12	1.24
Er	-	-	-	-	4.04	3.35	3.69
Tb	1.44	1.62	1.40	2.92	-	-	1.84
Yb	3.42	5.96	4.34	4.94	3.25	2.15	4.01
Lu	0.48	0.76	0.40	0.40	0.44	0.31	0.46
REE*	473.32	122.21	312.47	614.60	248.11	414.40	364.18
Ce_N/Yb_N	21.77	2.78	11.32	20.11	7.61	21.77	14.24
La_N/Lu_N	28.59	4.23	22.58	42.28	10.90	32.61	23.48
La_N/Yb_N	29.44	3.96	15.28	25.11	9.57	30.28	18.94
REE (N)	271.86	70.19	179.47	353.01	76.38	127.58	179.75
LREE/HREE	86.70	13.39	49.57	72.97	8.75	17.00	41.39

coupled with variation in K_2O from 3% to 8% in both pink and grey phases supports this late-stage K-enrichment. Discrepancies observable in the Th/U ratios and Th - U concentrations are due to uneven enrichment of Th with no change in U. Th shows enrichment not only in this younger Closepet Granite but also in the granulites that are in continuation with granite towards the South (Biligirirangan) and in the Eastern Ghat granulites that are quite remote from the Closepet. Both Th and K are high in the Eastern Ghat granulites, unusual for a granulite terrain (Divakara Rao, 1982; Subba Rao, 1986). The whole-rock and mineral compositional similarity between pink and grey phases of the granite (Tables 1 and 2), the distribution and scatter of K/Rb and Th/U and similar petrological characters suggest similar modes of origin for both the phases, probably from a single source. It is observed in the field that pink colouration of the feldspar advances as a front towards grey with patches of partial to fully pink coloured feldspars. This indicates that colouration of feldspars is

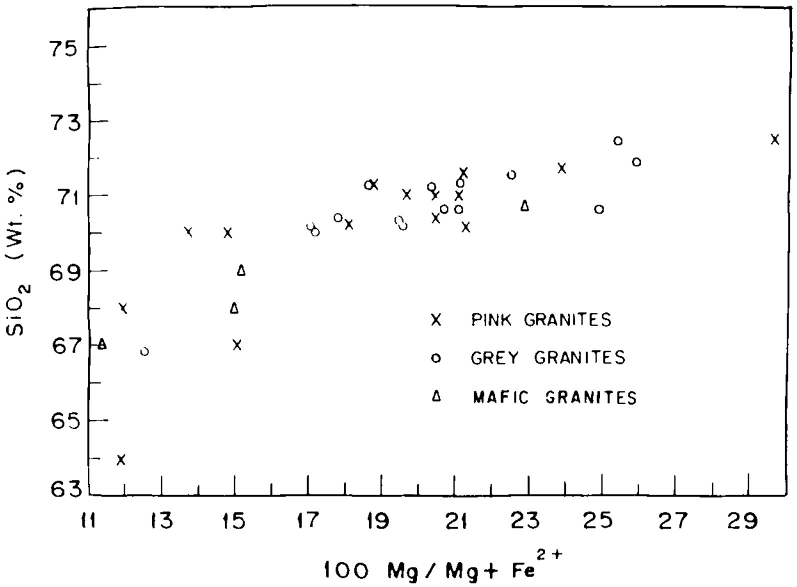

Figure 5. Figure showing the relationship of SiO_2 with Mg number in the Closepet Granite.

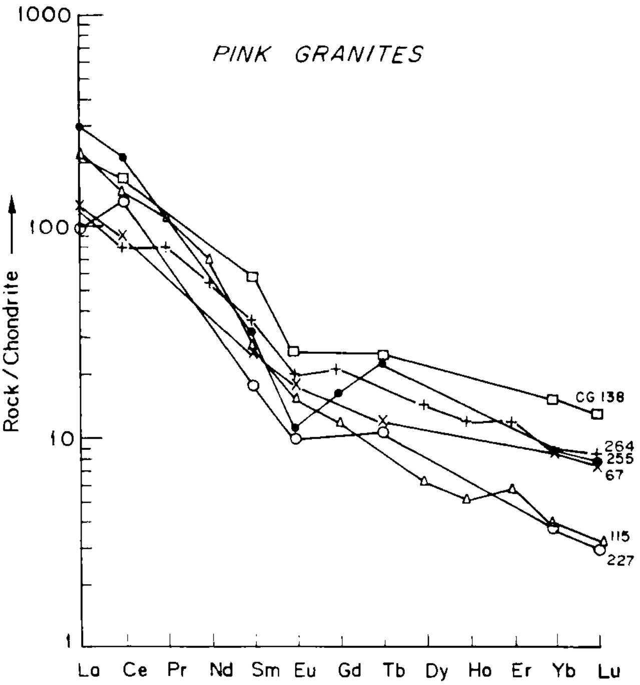

Figure 6. Chondrite-normalised REE patterns of the pink granites.

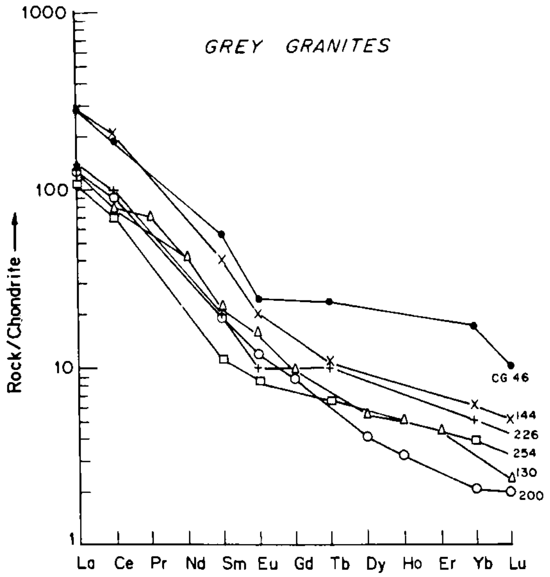

Figure 7. Chondrite-normalised REE patterns of the grey granites.

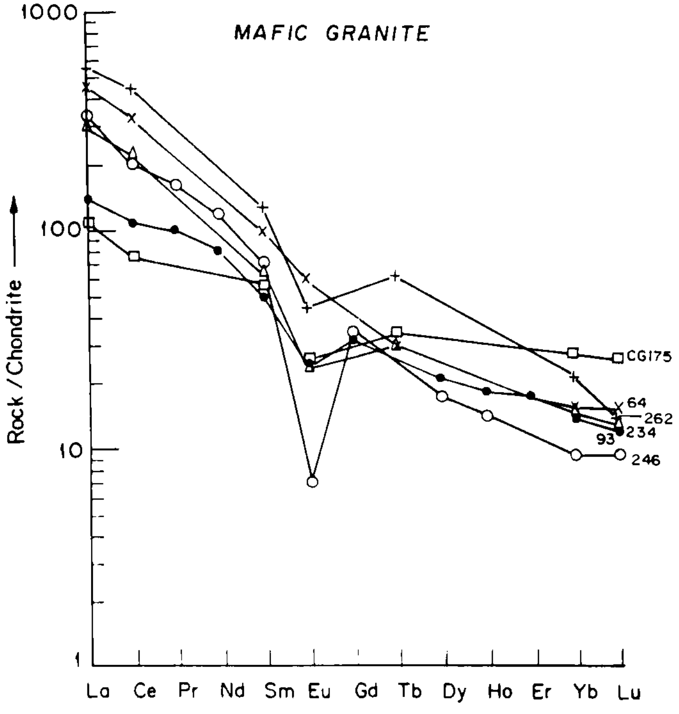

Figure 8. Chondrite-normalised REE patterns of the mafic granites.

probably a syn-or post-formational phenomenon and is not dependent on the original composition and origin of the granite. Experimental heating of the feldspar to higher temperatures (Divakara Rao et al., 1987) indicated that the pink colouration disappears totally at around 1000^{0} C; however, if the grains are heated to lower temperatures, the colour reappears on cooling. This suggests that the pink colouration is temperature controlled and is probably not genetically related to the granite. For identifying the mode of origin, the Closepet Granite can be considered as a two-phase rock, a K-rich porphyritic (both pink and grey) phase and a mafic-rich phase. Lack of evidence of fractionation in major oxides, especially between SiO_2 and Mg (Fig. 5), negates a magmatic origin for this granite. The scattered distribution of major and trace elements such as Mg, Fe, Ba, Sr and Rb, the lack of a linear relation between major elements and Mg, scatter in the distribution of K, Rb, Th and U, and their K/Rb and Th/U ratios and the similarity in total REE in the two phases suggest that these are CR-type granites and their protolith is of sedimentary nature (paragneisses).

Initial Sr isotopic ratios in the Closepet Granite range from 0.7050 for adamellite to 0.711 for granodiorites (Dhanaraju et al., 1983) which are in the range of CR-type to MM-type granites (Chaoqun, 1985). There is also an age gap of 250-300 Ma. between the adamellite and granodiorite, suggesting that the granite must have formed in phases or pulses, a characteristic feature of CR--type granites.

Rare-earth elemental abundances in the three different phases of the Closepet Granite (Figs. 6, 7 and 8) are sympathetic to the major- and trace-element chemistry in that the pink and grey phases have similar ΣREE and LREE/HREE, while the mafic phase has more ΣREE than the above two. Both ΣLREE and ΣHREE concentrations are similar in the major phases, while the mafic phase contains higher ΣHREE as well as ΣLREE, resulting in higher total REE. This is contrary to the expectation as mafic rocks usually have less total HREE. Ce_N/Yb_N and La_N/Yb_N ratios are high in the grey phase and low in pink phase, compared to the mafic phase, suggesting that the pink phase is probably either a late phase or reflects inhomogeneities in parent material. There is a large scatter in the LREE/HREE ratio in different phases from 9.80 to

87.11 in the pink (average: 46.01), 18.96 to 131.00 in the grey (average: 60.84) and 8.75 to 86.00 in mafic (average: 41.39) phases. Similar scatter is observed throughout the granite (74.0 ± 24.1 and 58.0 ± 16.0 reported earlier for the granite, Jayaram et al., 1983). This large variation in LREE/HREE ratio supports the heterogeneity of the source and an anatectic and palingenetic origin, rather than a magmatic origin, for the granite. The transitional-type granitoids usually have LREE around 155 ppm, which is significantly lower than that of the crustal-type granites (Jili and Jiayuan, 1985). Higher HREE in the mafic phase compared to the other two phases suggests that the parent material for the phase probably is a biotite-allanite-rich xenolith in the basement while the pink and grey phases are the palingenetic products from comparatively felsic-rich gneisses.

On the basis of major-and trace-elemental geochemistry, Divakara Rao et al., (1972 a, b) suggested a two-stage anatectic and palingenetic mode of origin for the Closepet Granite from the pre-existing para-gneisses. They attributed the scatter in elements like Th, U, K and Rb to metasomatic enrichment. Friend (1983,1984) has also arrived at a similar conclusion for the formation of the Closepet Granite (palingenesis and anatexis of Peninsular Gneisses) while describing the structures and textures of its southern parts. He suggested that the gneissic enclaves found as patches within the granite and their migmatitic equivalents are the source for this granite. From the whole-rock composition, Dhanaraju et al., (1983) have suggested an S-type nature for this granite.

In the classical petrogenetic sense, the formation of a granite can be described by magmatic differentiation of basic magma or by anatexis of older crust. There is also a third model of granite formation, by assimilation (i.e., combined crustal assimilation and fractional crystallization Taylor and McLennan, 1980; De Paolo, 1981; James, 1981) or perhaps magma mixing of a basic melt and an anatectic melt (Gray, 1984).

The major, minor, trace and REE abundances in the different phases of the Closepet Granite support a mixed source for its origin, more of a continental crustal source. The occurrence of cordierite and patches of supracrustals at places in the granite substantiates the crustal source which, following palingenesis and anatexis, has resulted in the formation of this granite.

Though major and trace elemental abundances suggest a crustal source for the mafic phase also, LREE/HREE and ΣREE indicate that this phase must have formed by anatexis and palingenesis of gneissic basement with a mafic xenolith, rich in biotite and/or allanite.

Geochemical and geological evidence available at present on the various phases of the Closepet Granite thus support a crustal remelting origin from the pre-existing gneisses rather than a magmatic origin.

AKNOWLEDGEMENTS

The authors are grateful to the Director, the National Geophysical Research Institute, Hyderabad for his encouragement and for permission to publish the paper. Dr.S.M.Naqvi and Dr. B.L.Narayana are thankfully acknowledged for their constructive suggestions. Mrs.Nancy Rajan is thanked for typing the manuscript.

REFERENCES

Chaoqun, Y., 1985. On Specialisation of granitoids of different genetic types in south China. In : Wu Liren et al (Editors), The crust - the significance of granites gneisses in the lithosphere. Theophrastus Publications, S.A., Athens, Greece. pp.365-387.

De Paolo, D.J., 1981. Neodymium isotopes in the Colorado Front-Range and crust-mantle evolution in the Proterozoic. Nature, 292: 193-196.

Dhanaraju, R., Varma, H.M., Padmanabhan, N. and Mahadevan, T.M., 1983. I-type and S-type classification of the Precambrian granitoids of southern India and its possible relevance to mineral exploration. In : S.M. Naqvi and J.J.W. Rogers (Editors), Precambrian of South India. Geol. Soc. India, Mem., 4: pp.389-400.

Divakara Rao, V., Aswathanarayana, U. and Qureshy, M.N., 1972a. Petrochemical studies in parts of the Closepet granite pluton, Mysore State. J. Geol. Soc. India, 13: 1-12.

Divakara Rao, V., Aswathanarayana, U. and Qureshy, M.N., 1972b. Trace element geochemistry of parts of Closepet granite. Mysore State, India. Mineral. Mag., 38: 678-686.

Divakara Rao, V., 1982. Importance and implications of the Eastern Ghats granulite belt in the early crustal evolution of the Indian shield. Proc. "Workshop on Geoscientific aspects of Eastern Ghats". Nov. 21-27, 1982. Andhra University, Visakhapatnam.

Divakara Rao, V., 1985. Polyphase granites of the Indian shield and lithosphere evolution. In : Wu Liren et al (Editors), The crust - the significance of granites - gneisses in the lithosphere. Theophrastus Publications, S.A., Athens, Greece, pp.147-168.

Divakara Rao, V. and Rama Rao, P., 1982. Granitic activity and crustal growth in the Indian shield. Precamb. Res., 16: 257-271.

Divakara Rao, V., Rama Rao, P., Govil, P.K. and Balaram, V., 1983. Geology and geochemistry of the Krishnarajpet schist belt, a greenstone belt of the Dharwar craton, India. In : S.M. Naqvi and J.J.W. Rogers (Editors), Precambrian of South India, Geol. Soc. India, Mem., 4: pp.293-308.

Divakara Rao, V., Rama Rao, P. and Subba Rao, M.V. (1987) Terminal report on the first phase of the Project"Geochemical and isotopic studies on acid plutonic rocks and evolution of continental lithosphere". National Geophys. Res. Inst., Hyderabad, (unpublished).

Friend, C.R.L., 1983. The link between charnockite formation and granite production: evidence from Kabbaldurga, Karnataka, southern India. In: M.P. Atherton and C.D. Gribble (Editors), Migmatites, Melting and Metamorphism; Shiva Publ., Cheshire, U.K., pp.264-276.

Friend, C.R.L., 1984. The origins of the Closepet granites and the implications for the crustal evolution of southern Karnataka. J. Geol. Soc. India, 25: 73-84.

Gray, C.M., 1984. An isotopic mixing model for the origin of granitic rocks in south-eastern Australia. Earth Planet. Sci. Lett., 70: 47-60.

James, D.E., 1981. The combined use of oxygen and radiogenic isotopes as indicators of crustal contamination. Annual Reviews of Earth and Planet. Sci., 9: 311-344.

Jayaram, S., Venkatasubramanian, V.S. and Radhakrishna, B.P., 1983. Geochronology and trace element distribution in some tonalitic and granitic gneisses of Dharwar craton. In: S.M.Naqvi and J.J.W. Rogers (Editors), Precambrian of South India. Geol. Soc. India, Mem., 4: pp.377-388.

Jili, S. and Jiayuan, L., 1985. REE geochemical characteristics of the two types of granitoids in Jiangxi province and their metallogenic implication. In: Wu Liren et al. (Editors), The crust-the significance of granites gneisses in the lithosphere. Theophrastus Publ., S.A. Athens, Greece, pp.345-364.

Naqvi, S.M. and 13 others 1983. Geochemistry of gneisses from Hassan district and adjoining areas, Karnataka, India. In: S.M. Naqvi and J.J.W. Rogers (Editors), Precambrian of South India. Geol. Soc. India, Mem., 4: pp.401-416.

Radhakrishna, B.P., 1956. The Closepet granite of Mysore State, India. Mysore Geologists Association, Bangalore, 110pp.

Subba Rao, M.V., 1986. Geochemistry, origin and evolution of granulitic rocks around Araku in the Eastern Ghats of Visakhapatnam district, Andhra Pradesh, India. Ph.D. Thesis, Andhra University, Visakhapatnam (Unpublished), 150pp.

Taylor, S.R. and McLennan, M. 1980. Evidence from rare earth elements for the chemical composition of the Archaean crust. In: J.E. Glover and D.I. Groves (Editors), Archaean Geology. Geol. Soc. Australia Spl. Publ., 7: pp.255-262.

COMPARISON OF THE INDIAN AND NUBIAN-ARABIAN SHIELDS

JOHN J.W. ROGERS

ABSTRACT

The Indian (IND) and Nubian-Arabian (NAS) shields have a similar outcrop area but are otherwise quite different. Precambrian rocks of IND evolved over a period of nearly 3000 Ma., whereas virtually all of the rocks of the NAS were formed between 1000 and 500 Ma. ago. Lithologic suites of the NAS are principally volcanic/sedimentary subduction complexes and calc alkaline batholiths, and most of the older suites of the shield formed in or near intra-oceanic arcs. The earliest rocks of the IND are mantle-derived tonalitic-trondhjemitic gneisses and mafic/ultramafic volcanic/sedimentary belts. Recognizable belts of compressional deformation characterize the middle Proterozoic of IND, and some of them resulted in production of large granulite-facies terrains. The IND does not generally contain identifiable volcanic/sedimentary or calc-alkaline subduction suites, and if subduction occurred in the older IND, it produced a different assemblage of rocks. Ophiolite/melange suture zones are easily recognized in the NAS, but possible sutures in the IND must be inferred from thrust faults separating different lithologic terrains. Both IND and NAS are similar in their later tectonic development, including: production of alkali granites; subsidence of thick, partly deformed basins on recently formed crust; and ultimate development of platformal cover sequences of clastic sediments.

The greater depth of exposure of the IND, containing exposed granulite, does not explain the lithologic difference from the NAS. Both seismic and gravity data indicate that the NAS contains denser, more mafic rocks than the IND at all levels throughout the crust. It is possible that future, post-stabilization processes will change the composition of the NAS to that of the IND, but the hypothesis is not testable with present data.

INTRODUCTION

This paper compares the general features of the Indian (IND) and Nubian-Arabian (NAS) shields, emphasizing both the similarities and contrast in their development. The NAS consists of a Nubian part, west of the present Red Sea, and an Arabian part, to the east.

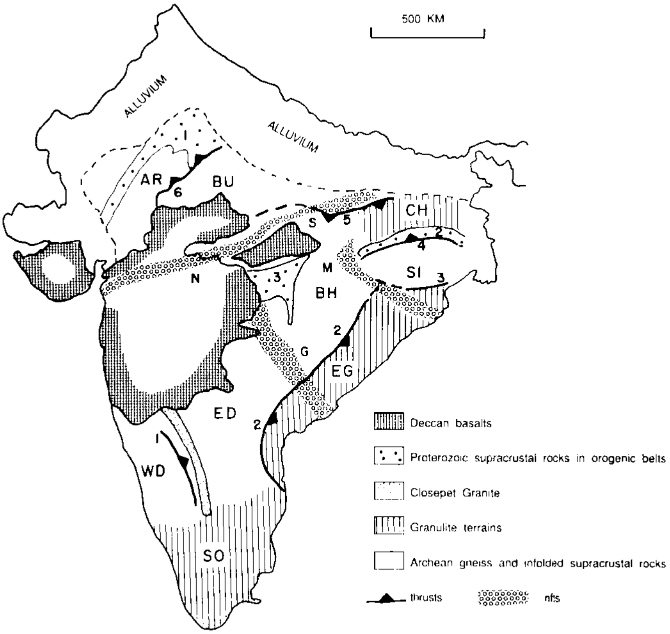

Figure 1. Generalized map of the Indian shield. The mapped Precambrian suites correspond broadly to the suites listed in Table 1, although some of the rocks counted for Table 1 cannot be shown at the scale of this figure. The nomenclature of the various areas and suites corresponds to maps in Naqvi and Rogers, (1987). Symbols used for Proterozoic supracrustal rocks in orogenic belts include; 1 - Delhi Supergroup; 2 - Singhbhum orogenic belt; and 3 - Sausar, Sakoli, and Dongargarh suites of the Bhandara craton. Granulite terrains include: CH - Chotanagpur; EG - Eastern Ghats; and SO - Southern granulite terrain, separated from the Dharwar craton (ED and WD) by a non-tectonic transition zone. Archaean gneissic terrains with infolded supracrustal rocks include: AR - Aravalli; BU - Bundelkhand; SI - Singhbhum; BH - Bhandara; ED - Eastern Dharwar; WD - Western Dharwar. Rift valleys include; N - Narmada; S - Son; M - Mahanadi; and G - Godavari. Major thrusts include: 1 - unnamed thrust in Western Dhrwar craton, 2 - Eastern Ghats front (numbered at two places); 3 - Sukinda; 4 - Singhbhum (Copper Belt); 5 - thrust south of Son valley; and 6 - Great Boundary fault. The map does not show platformal sedimentary (cover) sequences, principally middle to late Proterozoic but possibly ranging from the late Archaean to the lower Paleozoic.

Both the Indian (Fig. 1) and Nubian-Arabian shields (Fig. 2) are fragments of larger terrains. The Indian shield rifted from Gondwanaland, and an unknown extent has been subducted under the Himalayas. The Nubian-Arabian shield apparently has an exposed western border against older rocks in North Africa, although the exact location of the contact is controversial (Ries et al.,1985; Vail, 1985; Kroner et al., 1987a, 1987b). Precambrian

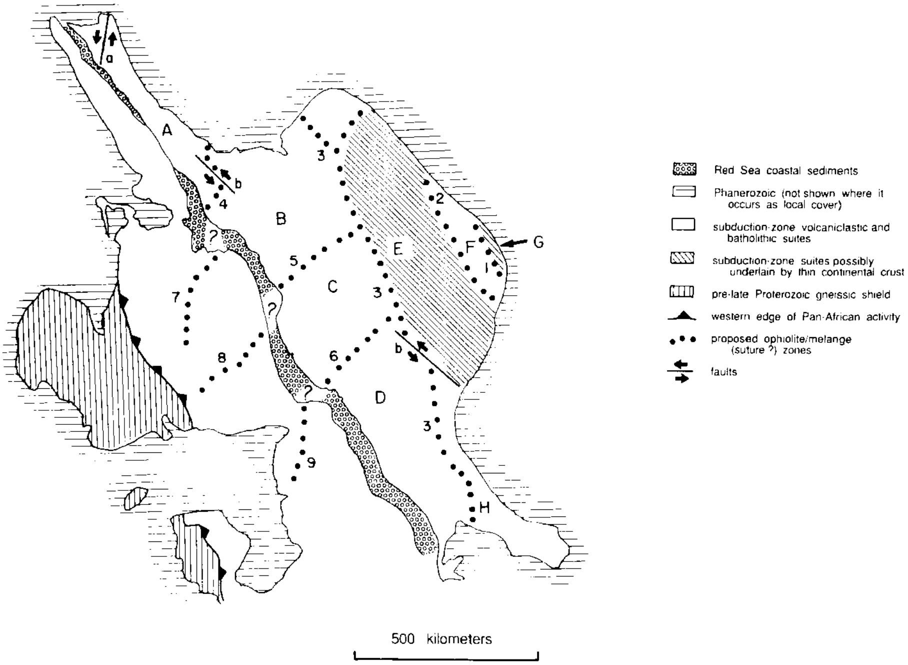
a
A
b
4
B
?
3
2
G
F
1
E
5
C
3
7
?
8
6
b
?
D
3
9
H
▩ Red Sea coastal sediments
▤ Phanerozoic (not shown where it occurs as local cover)
☐ subduction-zone volcaniclastic and batholithic suites
▨ subduction-zone suites possibly underlain by thin continental crust
▥ pre-late Proterozoic gneissic shield
▲ western edge of Pan-African activity
• • • proposed ophiolite/melange (suture ?) zones
⇄ faults
500 kilometers

Figure 2. Generalized map of Nubian-Arabian shield. The Red Sea has been closed by removal of 105 km left-lateral displacement along the Aqaba-Dead Sea shear zone and 6 degrees of counterclockwise rotation of Africa. The Arabian shield is shown in its present north-south orientation. Major suture zones are named following the terminology of Johnson et al. (1987) for the Arabian shield and Vail (1985) for the Nubian shield; symbols are: 1 - Ar Rayn; 2 - Haliban; 3 - Nabitah (numbered at three places) ; 4 - Yanbu; 5 - Bir Umq; 6 - Afaf; 7 - Sol Hamid; 8 - Nakasib; 9 - Baraka. Possible correlations of the shear zones across the Red Sea are shown by question marks. The major terrains of the Arabian shield are named following the terminology of Johnson et al. (1987); symbols are: A - Midyan; B - Hijaz; C - Jiddah/Taif; D - Asir; E - Afif; F - Ad Dawadimi; G - Ar Rayn; H - Nabalah/ Najran, Fault "a" shows the present location of the Tertiary Aqaba-Dead Sea left-lateral shear zone; fault "b" is shown as two of the many segments of the left-lateral Najd fault system of late Proterozoic age. Volcanic and sedimentary suites in successor basins and crustal downwarp basins (terminology of Johnson et al., 1987) are not shown.

outcrops in northeastern Africa extend south to the Ethiopian plateau basalts, but the southern areas have been explored only in reconnaissance (e.g., see Mohr, 1979), and they may be an extension of the Mozambique belt that occupies much of the eastern seaboard of Africa. The northern and eastern sides of the Nubian-Arabian shield are covered by thick Phanerozoic sedimentary sequences. Remarkably, both the Indian and Nubian-Arabian shields have nearly the same area of present surface exposure, approximately one million sq. km.

The geophysical properties of the Indian and Nubian-Arabian shields show significant differences, despite the fact that MOHO depths are 35 to 40 km in both shields. A deep seismic survey by Kaila et al, (1979) across the Dharwar craton (ED and WD in Fig. 1) of the Indian shield yielded average velocity variations shown in Fig. 3. These velocities are consistent with measurements from teleseismic data (summarized in Chapter 1 of Naqvi and Rogers, 1987). Unfortunately, the profile did not extend into the granulite terrain (SO in Fig. 1), and possible geophysical differences between it and the Dharwar craton have not been determined.

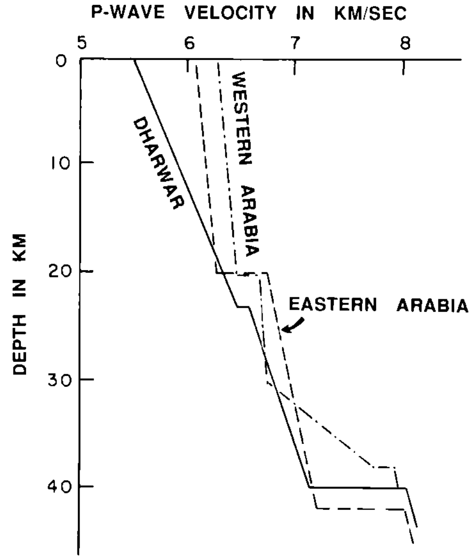

Figure 3. Comparison of P-wave velocities in: the Dharwar craton of the Indian shield; eastern part of the Nubian-Arabian shield (Afif terrain); and western part of the Arabian portion of the Nubian-Arabian shield. Indian data from Kaila et al. (1979); Arabian data from Mooney et al. (1985) and Gettings et al. (1986).

A refraction survey across the Arabian portion of the Nubian-Arabian shield (Fig. 2) produced different velocity profiles in the Afif region, possibly underlain by a thin old crust, and in the more mafic western parts of the shield (Fig. 3; Mooney et al., 1985; Gettings et al., 1986). Particularly in the west, the NAS shows higher velocities (higher crustal densities) throughout the entire thickness of the shield down to the MOHO. These high velocities confirm geologic observations (discussed below) that the western part of the NAS consists almost wholly of late Proterozoic, subduction-generated, supracrustal and batholithic suites formed originally on oceanic crust.

Gravity data (Bowin et al., 1981) confirm the seismic data for the Indian and Nubian-Arabian shields. On average, the NAS shows free-air anomalies in the range of 0 to +25 mgal in western Arabia and the Nubian part of the shield. Free-air gravity anomalies in the IND are in the range of 0 to -20 mgal for most of the unrifted parts of the shield, with the granulite area (SO in Fig. 1) showing anomalies of approximately -25 to -50 mgal. Thus, both seismic and gravity data indicate a denser crust in much of the Nubian-Arabian shield than in the Indian shield.

Average depths of erosion obviously vary enormously in the shields. In the Nubian-Arabian shield, however, the maximum metamorphic grade of any rock suite is amphibolite facies, mostly in the area of major batholiths. A large proportion of the NAS rocks in their shield are in greenschist facies. Greenschist--facies rocks occur in the Indian shield but they are primarily in cover suites not shown in Fig. 1. Conversely, large areas of the IND contain granulite-facies rocks, in some of which equilibration pressures of 6 to 10 kb have been measured (summary in Naqvi and Rogers, 1987). Thus, exposure depths in the Indian shield are probably in the range of 5 to 25 km, whereas most rocks exposed in the Nubian-Arabian shield probably were never buried deeper than 10 to 15 km.

The most striking difference between the Indian and Nubian-Arabian shields is the range of ages of formation. The Indian shield contains abundant areas of Archaean gneisses and associated, generally high-grade, supracrustal rocks (Radhakrishna and Naqvi, 1986), and ages as high as 3400 Ma. are widely distributed (summary in Naqvi and Rogers, 1987). Platformal cover sequences, deformed only on some margins, began to form over broad areas of the shield in the middle Proterozoic, and limited evidence on the ages of orogenic activity and rifting indicates that the Indian shield had become a unified, relatively stable, block by about 1500 Ma. ago. Conversely, the Nubian-Arabian shield shows largely indirect Pb and Nd isotopic evidence for rocks as old as Archaean or early Proterozoic (Stacey and Stoeser, 1983; Stacey and Hedge, 1984). Rocks of this age apparently occur at depth in the eastern part of the shield, and one exposed body in the Afif terrain has an age of 1600 to 1700 Ma. (Stacey and Hedge, 1984). All measured ages in the Nubian-Arabian shield west of the Afif terrain are in the range of 1000 to 500 Ma., both for supracrustal and batholithic suites (Jackson and Ramsay, 1980; Marzouki et al., 1982; Klemenic, 1985; Stern and Hedge, 1985; Stoeser and Camp, 1985). Undeformed cover sediments began to form in the early Phanerozoic in the NAS.

The abundances of various major rock suites in the Indian and Nubian-Arabian shields are summarized in Table 1. Each shield is discussed briefly below before further comparison is made.

LITHOLOGIES IN THE INDIAN SHIELD

The major lithologic suites of the Indian shield are identified in Fig. 1 and Table 1. An extensive bibliography for the following discussion was provided by Naqvi and Rogers (1987), and only a few summary papers are cited here.

Old Archaean gneissic complexes, commonly with intricately infolded mafic supracrustal suites, have been recognized in at least four parts of the Indian shield - the Dharwar craton (Pichamuthu and Srinivasan, 1983; Radhakrishna 1983); the Singhbhum nucleus (Sarkar, 1982); parts of the Aravalli-Delhi area (Naha and Roy, 1983; Sen, 1983); and probably the Bundelkhand area (Sharma, 1983). In addition, it seems likely that the Bhandara region contains an extensive Archaean craton (Radhakrishna and Naqvi, 1986). The gneisses are commonly in amphibolite facies and consist of the typical tonalite-trondhjemite ("gray gneiss") suite found in many shields. Most of them appear originally to have been mantle-derived magmatic rocks.

The supracrustal suites infolded with the gneisses are mostly mafic to ultramafic, consisting of komatiites to basalts, quartz-poor metasediments, some silicic volcanic rocks (forming a bimodal igneous assemblage), and minor chert, carbonate and other sediments. These assemblages have ages from at least 3,400 Ma. to later in the Archaean. An exception to the mafic composition is shown by the Aravalli Supergroup of the Aravalli area, which is siliceous, phosphatic, and at least partly platformal (Roy and Paliwal, 1981). The Aravalli suite is included in this category because of its intimate intermingling with the Banded Gneissic Complex.

Three broad areas of granulite-facies rocks are shown on Figure 1. All of them contain a mixture of high-grade suites (charnockites, khondalites, mafic granulites, etc.) and lower--grade suites, primarily in amphibolite facies. Both prograde and retrograde relationships have been shown between these facies (e.g., Janardhan et al., 1982; Chacko et al., 1987). The dominant composition of the areas is silicic, with mafic rocks forming less than 10% of the assemblages. The southern granulite area is commonly regarded as an extension of the Dharwar craton, differing largely in level of exposure, and the contact between the Dharwar craton and the granulite area is a gradational zone without tectonic discontinuity formed about 2500 Ma. ago (Pichamuthu, 1960; Gopalakrishna et al., 1986). The Eastern Ghats is a broad region lithologically similar to the southern granulites but separated from amphibolite-facies Archaean rocks on the west by a major thrust (the Eastern Ghats front; Crookshank, 1938; Kaila and Bhatia, 1981). The poorly known Chotanagpur terrain (Ghose, 1983) also contains abundant granulite-facies rocks and is separated on the south from the Singhbhum nucleus by the Singhbhum mobile belt and associated thrusts. Movement on both the Eastern Ghats front and the Singhbhum thrust appears to have occurred in the middle Proterozoic (summary in Rogers, 1986), and the metamorphism in these two terrains may have corresponding ages (see summary of geochronologic information for the Eastern Ghats in Chapter 5 of Naqvi and Rogers, 1987). The granulite terrains contain numerous anorthositic suites, which are apparently related to the granulite metamorphism.

Highly deformed suites of early to middle Proterozoic rocks occur in at least three places. Rocks of the Singhbhum mobile belt are a typical flysch (geosynclinal) suite compressed between the Chotanagpur area and Singhbhum nucleus (Sarkar, 1982); ophiolites have been proposed to occur as part of the melange in the belt. The Delhi suite, which may extend into the late Proterozoic, contains a more platformal sedimentary assemblage (Sant et al., 1980; Singh, 1982). Deformation may have been related to movement on the Great Boundary fault and formation of granulitic rocks in other parts of the Aravalli belt. Several suites of mostly platformal sediments in the Bhandara area have been deformed and metamorphosed, particularly along the Satpura trend south of the Narmada and Son rifts (Narayanaswamy et al., 1963).

Identifiable batholithic suites showing calcalkaline trends from gabbro to granite apparently are scarce in the Indian shield. Late Archaean/early Proterozoic potassic granites, generally without cogenetic mafic rocks, are common in several areas, particularly in the eastern part of the Dharwar craton (Closepet and related suites). The middle Proterozoic thrusting (subduction related?) does not seem to have produced calc alkaline batholiths.

Platformal sediments (not shown in Fig. 1) began to form at numerous places in the shield as the underlying basements became relatively stable (e.g., Chanda and Bhattacharyya, 1982; Srivastava et al., 1983; Meijerink et al., 1984). These suites consist primarily of fluvial to shallow-water clastic sediments and carbonates; those suites as old as middle Proterozoic have minor basaltic flows near their base. Some suites may be as young as lower Palaeozoic. The late Archaean Dharwar sedimentary assemblages of the Western Dharwar craton (Naqvi, 1985, and references cited therein) are somewhat arbitrarily included in this sedimentary suite. The Dharwar basins apparently range over an age of several hundred Ma., and some are intensely compressed, but the suite as a whole does not appear to have been part of a major orogenic belt.

LITHOLOGIES IN THE NUBIAN-ARABIAN SHIELD

Rock types in the Nubian-Arabian shield are summarized in Figure 2 and Table 1. Many of them are different from rocks in the Indian shield and the last section of this paper discusses the significance of this difference.

The major lithologic assemblage in both the Arabian and Nubian parts of the shield consists of volcanic and sedimentary rocks associated with the development of intra-oceanic island arcs. Older suites, with ages in the range of 900 to 700 Ma., commonly contain bimodal volcanic assemblages (basalt-rhyolite or spilite-keratophyre), and younger suites tend to contain calc alkaline volcanic assemblages (Stern, 1981; Roobol et al., 1983). Associated sedimentary rocks formed in a variety of settings, including marginal basin, fore-arc basin, back-arc basin, etc. (Camp, 1984; Clark, 1985; Stoeser and Camp, 1985; Johnson et al., 1987; Kroner et al., 1987a). Melange and other suites of accretionary prisms are also common (Al Shanti and Gass, 1983; Ries et al., 1983). In the central part of the Nubian-Arabian shield the arc suites formed on oceanic crust and show some tendency to become younger towards the northwest, indicating progressive accretion in that direction (Jackson and Ramsay, 1980; Stoeser and Camp, 1985). Much of the subduction apparently was directed downward toward the southeast. Volcanic/sedimentary assemblages do not appear to be significantly different in the Afif area, possibly underlain by thin continental sial, from those in the western part of Arabia, formed on oceanic crust. Subduction zones in the Afif area, however, were apparently oriented north-south.

In addition to volcaniclastic suites, some sedimentary assemblages near the western edge of the shield appear to have been deposited as continental-margin sediments by erosion of older rocks to the west (Kroner et al., 1987a). Old zircons in some Egyptian suites (Dixon, 1981) probably also were derived from this terrain.

Calc-alkaline batholiths constitute a major part of the Nubian-Arabian shield (Neary et al., 1976; Dixon, 1981; Marzouki et al., 1982; Jackson et al., 1984; Jackson, 1986; Stoeser, 1986). Older suites, close to 900 Ma. old, are generally more mafic (with tonalites and diorites) than younger suites, which consist mainly of granodiorites, adamellites, and granites formed closer to 700 Ma. ago. The batholithic suites are associated with the northwestward building of the island-arc terrain and also with closure along the north-south suture zones in the eastern part of the shield.

The suture zones shown in Figure 2 are intensely deformed belts that probably have undergone shearing in a variety of directions. Rock suites along the zones include melanges of dominantly oceanic rocks, some of which are ophiolites or fragments of ophiolites (Frisch and Al Shanti, 1977; Al Shanti and Gass, 1983; Ries et al., 1983; Coleman, 1984; Kroner, 1985; Stoeser and Camp, 1985). Correlation of several of these zones has been proposed across the present Red Sea, giving a coherence to both the Nubian and Arabian parts of the shield (Stoeser and Camp, 1985; Vail, 1985).

A suite of alkali-rich granites (including the alkali feldspar granite of Stoeser, 1986) is broadly distributed throughout the Nubian-Arabian shield. These rocks form separate plutons, do not have significant amounts of cogenetic mafic rocks, are undeformed, and appear to represent magmatic activity at the time of stabilization of the shield, about 600 to 550 Ma. ago (Rogers et al., 1978; Greenberg, 1981; Stern and Hedge, 1985).

Near the end of major compressive activity in the Nubian-Arabian shield, several areas accumulated thick sequences consisting predominantly of sedimentary with some volcanic rocks. These areas are categorized as successor basins, formed above suture zones, or basins of crustal downwarp that extended over broad areas (Johnson et al., 1987). These suites show some compressive deformation and may be transitional between the older subduction-zone assemblages and younger, Phanerozoic cover sequences.

The late Precambrian Najd fault system is primarily strike-slip (Moore, 1979; Stern, 1985). Stern et al. (1984) proposed that the NAS underwent significant extension related to strike-slip movement. The alkali granites of Egypt are associated with volcanic and sedimentary suites that may be rift related, and dike swarms are abundant at numerous places in the shield. Nevertheless, identifiable rift valleys of Najd age have not been found, and many writers describe the evolution of the Nubian-Arabian shield solely as a result of compressional movements (e.g., Shackleton, 1986).

Relatively undeformed platform sequences began to cover the NAS about 600 to 500 Ma. ago, possibly slightly older in the eastern part of the shield (McClure, 1980; Dabbagh and Rogers, 1983). These rocks are predominantly fluvial and shallow-water clastic sediments. Apparently the shield was rapidly uplifted and eroded near the beginning of the Phanerozoic, permitting sediments to form on terrain at the depth of alkali-granite emplacement shortly after the magmatism and shield stabilization.

The Nubian-Arabian shield does not contain any major areas of gneiss or granulite development. Local suites identified as gneiss apparently formed from supracrustal rocks at slightly higher grades of metamorphism than was typical of most of the shields, and a few granulite-facies rocks are associated with high-temperature contact zones around plutons.

DISCUSSION

The principal comparisons of the Indian and Nubian-Arabian shields are shown in Tables 1 to 3.

The comparison of abundances of rock suites in the two shields (Table 1) is clearly affected by somewhat arbitrary decisions about the assignment of individual rock types to the various groups. This problem is particularly acute for the Indian shield where many rocks do not have easily identified Phanerozoic analogues. As discussed previously, two uncertain assignments concern Archaean supracrustal suites. One problem is the Aravalli Supergroup of the Aravalli-Delhi belt, which is here placed in the category of mafic supracrustal suites infolded into gneiss despite its platformal lithology; the placement is based on its association with deformed gneisses. The second problem is the late Archaean Dharwar schist belts, which are here regarded as platformal cover sequences despite the intricate deformation of some belts and the possibility that one may represent a suture zone (Naqvi,1985). Possibly both the Aravalli and Dharwar suites are equivalent in the Indian shield to the sedimentary and minor volcanic assemblages of successor basins above suture zones and other crustal downwarp basins that have been proposed in the Nubian-Arabian shield (Johnson et al., 1987).

Abundances of rocks in the Indian shield were obtained by point counting maps of individual cratons in Naqvi and Rogers (1987). The following identifications were used:

1. Gneiss signifies rocks that are mostly Archaean and have a tonalitic to trondhjemitic composition. The category includes: undesignated sialic suites of the Singhbhum nucleus; the Banded

TABLE 1

Average abundances of rock suites in the Indian (IND) and Nubian-Arabian (NAS) shields.

IND	
Gneiss (mostly tonalite/trondhjemite)	41%
Granulite terrain (and associated anorthosite, etc.)	30
Archaean mafic supracrustal rocks infolded with gneiss	7
Archaean/early Proterozoic granite (Post-tectonic, potassic, alkali feldspar granite is approximately 1/3 of total)	11
Supracrustal rocks of early to middle Proterozoic orogenic belts	10

NAS	
Supracrustal volcanic and sedimentary suites	44%
Calc alkaline plutonic rocks	46
Post-tectonic, potassic, alkali feldspar granites	7
Gneiss (in the Nubian part of the NAS)	3

Gneissic Complex of the Aravalli-Delhi belt; 1/2 of the Bundelkhand area, presumed to be continuous under Vindhyan cover; and mapped gneissic terrains in the Bhandara and Dharwar cratons, assumed to be continuous under cover of late Dharwar supracrustal rocks and the Cuddapah basin.

2. Granulite terrains include all rocks in areas that contain significant amounts of charnockite, khondalite, mafic granulite, anorthosite, and related suites. This figure includes lower grade (commonly amphibolite-facies) rocks interdistributed with the granulites. The areas designated include: the Chotanagpur area; the Eastern Ghats; and the granulite terrain of southern India south of the Dharwar craton.

3. Supracrustal rocks infolded into Archaean gneisses include: the Older Metamorphic and Iron Ore suites of the Singhbhum nucleus; the Aravalli Supergroup of the Aravalli-Delhi belt; the Sukma, Bengpal, and Bailadila suites of the Bhandara craton; and the older ("Sargur") suites of the Western and Eastern Dharwar cratons. The problems of placement of the Aravalli Supergroup and schists of the late Archaean Dharwar belts of the Western Dharwar craton are discussed in the text.

4. Archaean/Early Proterozoic granites include: the major granite bodies of the Singhbhum nucleus (Singhbhum, Mayurbhanj,

Nilgiri, and Bonai); an estimate of the amount of granite in the Aravalli-Delhi belt older than the Erinpura and related suites; 1/2 of the Bundelkhand terrain, which was assumed to include the area overlain by the Vindhyan suite; the Dongargarh granite of the Bhandara area; and the Closepet and related potassic granites of the Eastern Dharwar craton.

5. Supracrustal rocks of Proterozoic mobile belts include: rocks of the Singhbhum mobile belt; the Delhi Supergroup of the Aravalli-Delhi belt; and the Sausar, Sakoli, and Dongargarh suites of the Bhandara craton.

Abundances of rocks in the Nubian-Arabian shield are a weighted average. Rocks in the Arabian shield (weighting of two) include alkali feldspar granites, calc-alkaline plutonic suites (all plutonic suites except alkali-feldspar granites and alkaline rocks), and supracrustal suites (from Stoesser, 1986). Rocks in the Nubian shield (weighting of one) are based on the tabulation of Rogers (1978) for Egypt. The Nubian shield includes: alkali--feldspar granites (alkali granites); calc-alkaline plutonic suites calc-alkaline rocks plus 1/2 of rocks mapped as "gabbro-diorite"); supracrustal suites (volcanic/sedimentary assemblages plus 1/2 of rocks mapped as gabbro-diorite); and gneiss.

Despite detailed problems of assignment of rock suites in Table 1, the differences between the two shields are so large that it is obvious that they are composed of different lithologic assemblages. The major distinctions are summarized in Table 2. Clearly the Indian shield is dominated by gneiss, mostly of tonalite-trondhjemite composition, whereas the Nubian-Arabian shield has very little gneiss and certainly no large terrains of orthogneiss. Granulite-facies rocks occur only in the Indian shield. Calc-alkaline batholiths are recognizable only in the Nubian-Arabian shield. No lithologic suites in the Indian shield can be shown to be subduction related because of their similarity to modern island-arc or continental-margin assemblages (with the possible exception of the Singhbhum belt; Fig. 1). If rocks in the Indian shield were formed by subduction, then conditions in the Archaean were sufficiently different from the present that the igneous and sedimentary products of a subduction environment were very different.

TABLE 2.
Comparison of the Indian (IND) and Nubian-Arabian (NAS) shields

	IND	NAS
Gneiss	abundant	rare; local
Calc alkaline volcanic suites	rare	abundant subduction-zone suites (both calc alkaline and primitive bimodal)
Calc alkaline batholiths	not identified	abundant
Ophiolites	rare or absent	abundant in melanges
Granulite and associated rocks (anorthosite, etc.)	abundant	absent
Sutures	probable but unproved	clearly present
Crustal density	low	high

Despite the differences in rock types, the generalized histories of the Indian and Nubian-Arabian sheilds are remarkably similar (Table 3). The oldest rocks in most of the Nubian-Arabian shield were formed in an oceanic environment as the volcanic/ sedimentary assemblages of intra-oceanic island arcs. Similarly, the oldest rocks in the Indian shield were mantle derived, either meta-igneous rocks with initial isotopic ratios characteristic of the mantle or metasediments derived from a mafic/ultramafic source. The Nubian-Arabian shield has clearly been assembled by suturing different blocks together, although it is likely that the blocks were not formed very far from each other. Although suturing is more problematical in the Indian shield, it seems likely that at least some disparate blocks were brought together about 1500 Ma. ago (Rogers, 1986); earlier (Archaean) sutures have also been proposed (Naqvi, 1985; Krogstad et al., 1986). Because the two shields are approximately the same size, and contain five to ten separate blocks depending on the method of counting, the individual terrains in the two shields have about the same average size (100,000 sq. km). Both shields contain late- to post-orogenic potassic granites, although their abundance seems to be higher in the Nubian-Arabian shield. Both shields contain early sedimentary (and minor volcanic) cover sequences that

TABLE 3A.

Diagramatic history of the Indian shield (IND)

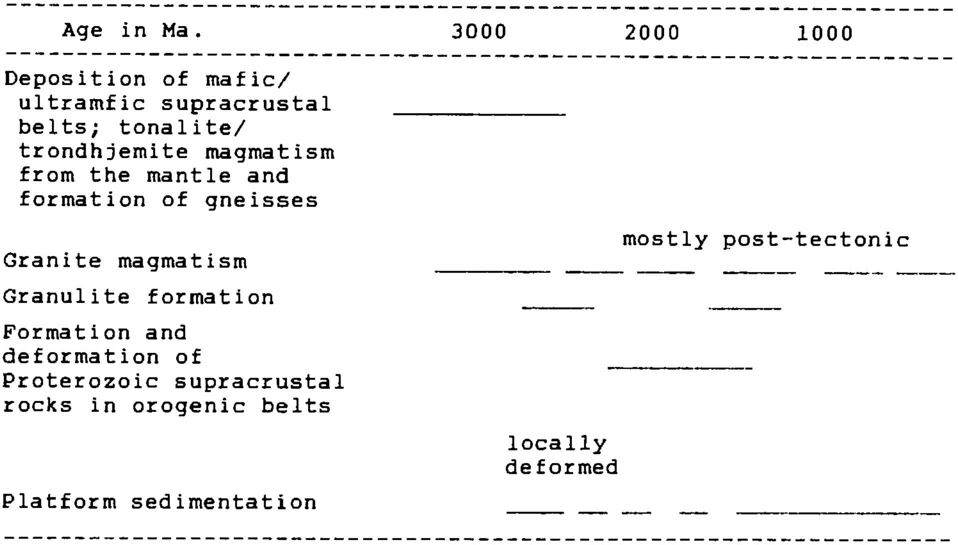

Age in Ma.	3000	2000	1000
Deposition of mafic/ ultramfic supracrustal belts; tonalite/ trondhjemite magmatism from the mantle and formation of gneisses			
Granite magmatism		mostly post-tectonic	
Granulite formation			
Formation and deformation of Proterozoic supracrustal rocks in orogenic belts			
Platform sedimentation	locally deformed		

TABLE 3B.

Diagrammatic history of Nubian-Arabian shield (NAS)

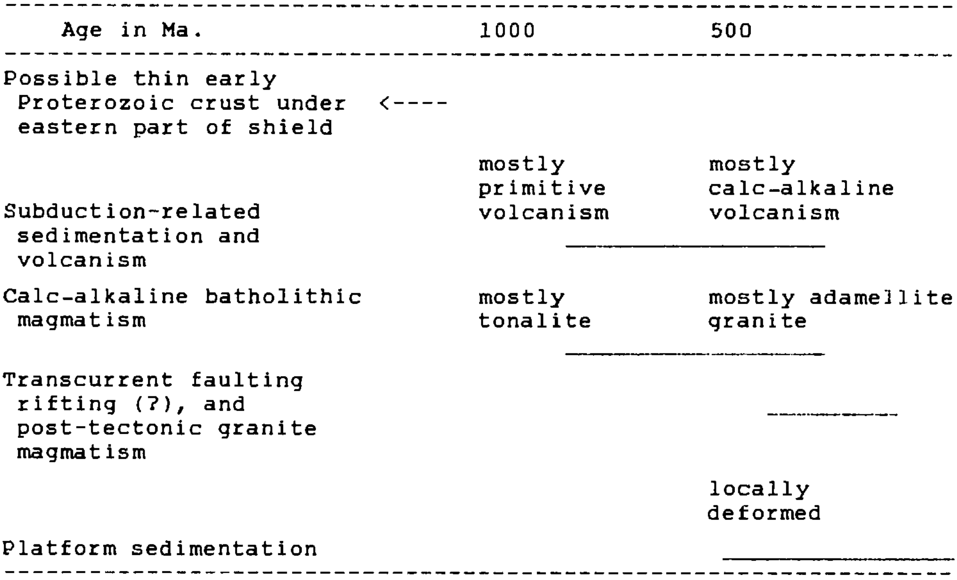

Age in Ma.	1000	500
Possible thin early Proterozoic crust under eastern part of shield <----		
Subduction-related sedimentation and volcanism	mostly primitive volcanism	mostly calc-alkaline volcanism
Calc-alkaline batholithic magmatism	mostly tonalite	mostly adamellite granite
Transcurrent faulting rifting (?), and post-tectonic granite magmatism		
Platform sedimentation		locally deformed

have undergone at least local deformation. Both shields ultimately became stable platforms and permitted deposition of extensive clastic suites that are either undeformed or deformed only locally. In short, both shields evolved by a similar sequence of events from an oceanic terrain to a crust of typical continental thickness, although the western Nubian-Arabian shield crust appears to be more mafic than the crust of the Indian shield.

An important question is whether the Indian and Nubian-Arabian shields really are lithologically different, despite their broadly similar histories, or whether they simply appear to be different because of erosional exposure to greater depth in the Indian shield. That is, if the Nubian-Arabian shield was eroded another 5 to 10 km, locally exposing granulite-facies rocks, would it be the same as the Indian shield? There is no compelling reason why the Indian shield should have been eroded more than the Nubian-Arabian shield. For example, the Nubian-Arabian shield is not so young that it could not have been eroded sufficiently to expose granulite-facies rocks. Nevertheless, the Indian shield generally does show higher-pressure assemblages than the Nubian-Arabian shield, and the possibility that this difference controls the differences in lithologies must be considered.

Three lines of evidence indicate that the differences between the Indian and Nubian-Arabian shields are caused by lithologic differences rather than by difference in exposure. One is that the entire thickness of the NAS crust (at least in the western part shows higher P-wave velocities than the Indian crust, and the indicated higher density is verified by higher free-air gravity values. Thus, the entire Nubian-Arabian shield is probably more mafic than the Indian shield. A second line of evidence is that calc-alkaline batholithic suites (gabbro to granite) should appear at the level of exposure in the Indian shield if they had formed there; their absence indicates lack of production rather than removal by erosion of upper-level rocks. A third line of evidence is that greenschist-facies supracrustal suites in the Indian shield do not contain the calc-alkaline volcanic rocks found in the Nubian-Arabian shield island-arc suites, a difference not related to level of erosion.

If the Nubian-Arabian shield would not become similar to the Indian shield through further erosion, would it become similar through time? That is, would further development of mostly silicic, gneissic, rocks in the Nubian-Arabian shield convert it to the lithology of the Indian shield? This question cannot be answered with any certainity. Some of the gneissic suites in the Indian shield were originally magmas emplaced at very low pressures of equilibration, and production of similar suites in the now-stable Nubian-Arabian shield does not seem likely in the future. Conversely, "maturing" and uplift of shields has been proposed on the basis of sedimentary assemblages formed on and around shield areas after they became stable to further compressive deformation (Rogers et al., 1984). It is possible that the Nubian-Arabian shield will continue to undergo transformation to a more sialic crust during the next few hundred million years. The accuracy of this paper cannot be ascertained until that time.

ACKNOWLEDGEMENTS

Work in India was supported by two grants from the National Science Foundation: a Special Foreign Currency Grant (INT78-17128), administered by S.M.Naqvi, and a grant in U.S. and Indian currency (EAR79-05723), administered by the writer. Work in the Nubian-Arabian shield was supported: in Egypt by a grant (OIP75-07943) from the National Science Foundation to the University of South Carolina; and in Saudi Arabia by funds made available by Riyadh University to visit students in the field. I have received help from numerous people during these programs and would particularly like to thank E.J. Callahan, T. Chacko, M.E. Dabbagh, J.K. Greenberg, S.M. Hussain, S.H.Jafri, J.R. Monrad, S.M. Naqvi, H. Narain, R.C. Newton, R. Ressetar, and P.T. Stroh.

REFERENCES

Al Shanti, A.M., and Gass, I.G., 1983. The upper Proterozoic ophiolite melange zones of the easternmost Arabian shield. J. Geol. Soc. London, 140: 867-876.

Bowin, C., Warsi, W., and Milligan, J., 1981. Free-air gravity anomaly map of the world. Geol. Soc. Am., 2 sheets.

Camp, V.E., 1984. Island arcs and their role in the evolution of the western Arabian shield. Geol. Soc. Am. Bull., 95: 913-921.

Chacko, T., Ravindra Kumar, G.R., and Newton, R.C., 1987. Metamorphic P-T conditions of the Kerala (South India) khondalite belt: a granulite-facies supracrustal terrain. J. Geol., 95: 343-358.

Chanda, S.K., and Bhattacharyya, A., 1982. Vindhyan sedimentation and paleogeography. In: K.S. Valdiya, S.B. Bhatia, and V.K.

Gaur (Editors), Geology of Vindhyanchal. Hindustan Publ. Co., New Delhi, pp.88-101.

Clark, M.D., 1985. Late Proterozoic crustal evolution of the Midyan region, northwestern Saudi Arabia. Geology, 13: 611-615.

Coleman, R., 1984. Ophiolites and the tectonic evolution of the Arabian Peninsular. In: I.G. Gass, S.J. Lippard, and A.W. Shelton (Editors), Ophiolites and Oceanic Lithosphere. Geol. Soc. London, Spec. Publ. 13, pp.359-366.

Crookshank, H., 1938. The western margin of the Eastern Ghats in southern Jeypore. Geol. Surv. India Records, 73: 398-434.

Dabbagh, M.E., and Rogers, J.J.W., 1983. Depositional environments and tectonic significance of the Wajid Sandstone of southern Saudi Arabia. J. Afr. Earth Sci., 1: 47-57.

Dixon, T.H., 1981. Age and chemical characteristics of some pre-Pan-African rocks in the Egyptian shield. Precamb. Res., 14: 119-133.

Frisch, W., and Al Shanti, A.M., 1977. Ophiolite belts and the collision of island arcs in the Arabian shield. Tectonophysics, 43: 293-306.

Gettings, M.E., Blank, Jr., H.R., Mooney, W.D., and Healey, J.H., 1986. Crustal structure of southwestern Saudi Arabia. J. Geophys. Res., 91: 6491-6512.

Ghose, N.C., 1983. Geology, tectonics and evolution of the Chotanagpur granite-gneiss complex, eastern India. Recent Res. Geol., 10: 211-247.

Gopalakrishna, D., Hansen, E.C., Janardhan, A.S., and Newton, R.C., 1986. The southern high-grade margin of the Dharwar craton. J. Geol., 94: 247-260.

Greenberg, J.K., 1981. Characteristics and origin of Egyptian Younger Granites. Geol. Soc. Am. Bull., 92 : Part I, 224-232; Part II, 749-840.

Jackson, N.J., 1986. Petrogenesis and evolution of Arabian felsic plutonic rocks. J.Afr. Earth Sci., 4: 47-59.

Jackson, N.J., and Ramsay, C.R., 1980. Time-space relationships of Upper Precambrian volcanic and sedimentary units in the central Arabian shield. J. Geol. Soc. London, 137: 617-628.

Jackson, N.J., Walsh, J.N., and Pegram, E., 1984. Geology, geochemistry and petrogenesis of late Precambrian granitoids in the central Hijaz region of the Arabian shield. Contr. Min. Pet., 87: 205-219.

Janardhan, A.S., Newton, R.C., and Hansen, E.C., 1982. The transformation of amphibolite facies gneiss to charnockite in southern Karnataka and northern Tamil Nadu, India. Contr. Min. Pet., 79: 130-149.

Johnson, P.R., Scheibner, E., and Smith, E.A., 1987. Basement fragments, accreted tectonostratigraphic terranes, and overlap sequences: elements in the tectonic evolution of the Arabian shield. In: Terrane Accretion and Orogenic Belts. Am. Geophys. Un. Geodynamics Series, 19: pp.323-343.

Kaila, K.L., and Bhatia, S.C., 1981. Gravity study along the Kavali-Udipi deep seismic sounding profile in the Indian Peninsular shield: some inferences about the origin of anorthosites and the Eastern Ghats orogeny. Tectonophysics, 79: 129-143.

Kaila, K.L., Roy Chowdhury, K., Reddy, P.R., Krishna, V.G., Narain H., Subbotin, S.I., Sologub, V.B., Chekhunov, A.B., Kharechko, G.B., Lazarenko, M.A., and Ilchenko, T.V.B., 1979. Crustal structure along the Kavali-Udipi profile in the Indian peninsular shield from deep seismic sounding. J. Geol. Soc. India, 20: 307-333.

Klemenic, P.M., 1985. New geochronological data on volcanic rocks from northeast Sudan and their implication for crustal evolution. Precamb. Res., 30: 263-276.

Krogstad, F.J., Hanson, G.N., and Rajamani, V., 1986. U-Pb zircon and sphene ages of discrete, juxtaposed late Archaean terranes, S. India (abst.). EOS (Trans. Am. Geopys. Un.), 67: 400.

Kroner, A., 1985. Ophiolites and the evolution of tectonic boundaries in the late Proterozoic Arabian-Nubian shield of northeast Africa and Arabia. Precamb. Res., 27: 277-300.

Kroner, A., Greiling, R., Reischmann, T., Hussein, I.M., Stern, R.J., Durr, S., Kruger, J., and Zimmer, M., 1987a. Pan-African crustal evolution in the Nubian segment of northeast Africa. In: A. Kroner (Editor), Proterozoic Lithospheric Evolution. Am. Geophys. Union. Geodynamics Series, 17: pp.235-257.

Kroner, A., Stern, R.J., Dawoud, A.S., Compston, W., and Reischmann, T., 1987b. The Pan-African continental margin in northeastern Africa : evidence from a geochronological study of granulites at Sabaloka, Sudan. Earth Planet. Sci. Lett. 85: 91-104.

Marzouki, F.M.H., Jackson, N.J., Ramsay, C.R., and Darbyshire, D.P.F., 1982. Composition, age and origin of two Proterozoic diorite-tonalite complexes in the Arabian shield, Precamb. Res., 19: 31-50.

McClure, H.A., 1980. Permian-Carboniferous glaciation in the Arabian peninsula. Geol. Soc. Am. Bull., 91 : part I, 707-712.

Meijerink, A.M.J., Rao, D.P., and Rupke, J., 1984. Stratigraphic and structural development of the Precambrian Cuddapah basin, S.E. India. Precamb. Res., 26: 57-104.

Mohr, P., 1979. Lithology and structure of the Precambrian rocks of Eritrea. In: S.A. Tahoun (Editor), Evolution and Mineralization of the Arabian-Nubian Shield, v.2. Pergamon Press, Oxford, pp.7-16.

Mooney, W.D., Gettings, M.E., Blank, Jr., H.R., and Healy, J.H., 1985. Saudi Arabian seismic refraction profile: a travel time interpretation of crustal and upper mantle structure. Tectonophysics, 111: 173-246.

Moore, J.M., 1979. Tectonics of the Najd transcurrent fault system, Saudi Arabia. J. Geol. Soc. London, 136: 441-454.

Naha, K., and Roy, A.B., 1983. The geology of the Precambrian basement in Rajasthan, western India. Precamb. Res., 19 : 217-223.

Naqvi, S.M., 1985. Chitradurga schist belt - an Archaean suture (?). J. Geol. Soc. India, 26: 511-525.

Naqvi, S.M., and Rogers, J.J.W., (Editors)., 1987. Precambrian Geology of India. Oxford Univ. Press, New York, 223pp.

Narayanaswamy, S., Chakravarty, S.C., Vemban, N.A., Shukla, K.D., Subramanyam, M.R., Venkatesh, V., Rao, G.V., Anandalwar, M.A., and Nagarajaiah, R.A., 1963. The geology and manganese ore deposits of the manganese belt in Madhya Pradesh and adjoining parts of Maharashtra; Part I, general introduction. Geol. Surv. India. Bull., Ser., A. : No. 22, 2-69.

Neary, C.R., Gass, I.G., and Cavanagh, B.J., 1976. Granitic association of northeastern Sudan. Geol. Soc. Am. Bull., 87: 1501-1512.

Pichamuthu, C.S., 1960. Charnockite in the making. Nature, 188: 135-136.

Pichamuthu, C.S., and Srinivasan, R., 1983. A billion-year history of the Dharwar craton (3200 to 2100 m.y. ago). In: S.M. Naqvi and J.J.W. Rogers (Editors), Precambrian of South India. Geol. Soc. India. Mem., 4: pp.121-142.

Radhakrishna, B.P., 1983. Archaean granite-greenstone terrain of the South Indian shield. In: S.M. Naqvi, and J.J.W. Rogers (Editors), Precambrian of South India. Geol. Soc. India. Mem., 4: pp.1-46.

Radhakrishna, B.P., and Naqvi, S.M., 1986. Precambrian continental crust of India and its evolution. J. Geol., 94: 145-166.

Ries, A.C., Shackleton, R.M., Graham, R.H., and Fitches, W.R., 1983. Pan-African structures, ophiolites and melange in the Eastern Desert of Egypt : a traverse at 26°N. J. Geol. Soc. London, 140: 75-95.

Ries, A.C., Shackleton, R.M., and Dawoud, A.S., 1985. Geochronology, geochemistry and tectonics of NE Bayuda desert, N Sudan : implications for the western margin of the late Proterozoic fold belt of NE Africa. Precamb. Res., 30 : 43-62.

Rogers, J.J.W., 1978. Inferred composition of early Archean crust and variation in crustal composition through time. In: B.F. Windley and S.M. Naqvi (Editors), Archaean Geochemistry. Developments in Precambrian Geology, v.1, Elsevier, Amsterdam, pp.25-39.

Rogers, J.J.W., 1986. The Dharwar craton and the assembly of peninsular India. J. Geol., 94: 129-144.

Rogers, J.J.W., Ghuma, M.A., Nagy, R.M., Greenberg, J.K., and Fullagar, P.D., 1978. Plutonism in Pan-African belts and the geological evolution of northeastern Africa. Earth Planet. Sci. Lett., 39: 109-117.

Rogers, J.J.W., Dabbagh, M.E., Olszewski Jr., W.E., Gaudette, H.E., Greenberg, J.K., and Brown, B.A., 1984. Early post-stabilization sedimentation and later growth of shields. Geology, 12: 607-609.

Roobol, M.J., Ramsay, C.R., Jackson, N.J., and Darbyshire, D.P.F. 1983. Late Proterozoic lavas of the central Arabian shield - evolution of an ancient volcanic arc system. J. Geol. Soc. London, 140: 185-202.

Roy, A.B., and Paliwal, B.S., 1981. Evolution of lower Proterozoic epicontinental sediments: stromatolite-bearing Aravalli rocks of Udaipur, Rajasthan, India. Precamb. Res., 14: 49-74.

Sant, V.N., Srikantan, B., Sharma, S.B., Ravindra, R., Siddiqui, M.A., Bakliwal, P.C., Joshi, S.M., Basu, S.K., Saha, A.K., Bhat, M.L., Datta, A.K., Sinha, P.N., and Chattopadhyay, N., 1980. Geology and mineral resources of Alwar District, Rajasthan, Geol. Surv. India Mem., 110: 118pp.

Sarkar, A.N., 1982. Precambrian tectonic evolution of eastern India: a model of converging microplates. Tectonophysics, 86 : 363-397.

Sen, S., 1983. Stratigraphy of the crystalline Precambrians of central and northern Rajasthan: a review. Recent Res. Geol., 10: 26-39.

Shackleton, R.M., 1986. Precambrian collision tectonics in Africa. In: M.P. Coward and A.C. Ries (Editors), Collision Tectonics. Geol. Soc. London, Spec. Publ. 19, pp.329-349.

Sharma, R.P., 1983. Structure and tectonics of the Bundelkhand complex, central India. Recent Res. Geol. 10: 198-210.

Singh, S.P., 1982. Stratigraphy of the Delhi Supergroup in the Bayana sub-basin, northeastern Rajasthan. Geol. Surv. India Records, 112: pt7, 46-62.

Srivastava, B.N., Rana, M.S., and Verma, M.K., 1983. Geology and hydrocarbon prospects of the Vindhyan basin. Petroleum Asia J., 1: 179-189.

Stacey, J.S., and Hedge, C.E., 1984. Geochronologic and isotopic evidence for early Proterozoic crust in the eastern Arabian shield. Geology, 12: 310-313.

Stacey, J.S., and Stoeser, D.B., 1983. Distribution of oceanic and continental leads in the Arbaian-Nubian shield. Contr. Min. Pet., 84: 91-105.

Stern, R.J., 1981. Petrogenesis and tectonic setting of late Precambrian ensimatic volcanic rocks, central Eastern Desert of Egypt. Precamb. Res., 16: 195-230.

Stern, R.J., 1985. The Najd fault system, Saudi Arabia and Egypt: a late Precambrian rift-related transform system? Tectonics, 4: 497-511.

Stern, R.J., and Hedge, C.E., 1985. Geochronologic and isotopic constraints on late Precambrian crustal evolution in the Eastern Desert of Egypt. Am. J. Sci., 285: 97-127.

Stern, R.J., Gottfried, D., and Hedge, C.E., 1984. Late Precambrian rifting and crustal evolution in the Northeastern Desert of Egypt. Geology, 12: 168-172.

Stoeser, D.B., 1986. Distribution and tectonic setting of plutonic rocks of the Arabian shield. J. Afr. Earth Sci., 4: 21-46.

Stoeser, D.B., and Camp, V.E., 1985. Pan-African microplate accretion of the Arabian shield. Geol. Soc. Am. Bull., 96: 817-826.

Vail, J.R., 1985. Pan-African (late Precambrian) tectonic terrains and the reconstruction of the Arabian-Nubian shield. Geology, 13: 839-842.

SOME DISTINCTIVE TRENDS IN THE EVOLUTION OF THE EARLY PRECAMBRIAN (ARCHAEAN) DHARWAR CRATON, SOUTH INDIA

R. SRINIVASAN AND S.M.NAQVI

ABSTRACT

The early Precambrian (Archaean) Dharwar sequence in south India provides evidence for a distinct trend of evolution which differs from trends exhibited in many other early Precambrian regions of the world. The supracrustal rock associations preserved in the Dharwar schist belts suggest the evolution of the depositional environment from a stable to a mobile regime. Layered igneous complexes, mature to supermature quartz-pebble conglomerates and quartzites deposited on platforms, ortho-quartzite-carbonate shelf assemblages and deposition of persistent beds of iron and manganese formations which serve as stratigraphic markers --- all these developed in the lower sections of the Dharwar supracrustal sequence may be cited as evidence for early stability. The mobile regime which can be shown on sedimentological grounds to have succeeded the stable regime witnessed accumulation of turbidite greywackes in a volcanically active environment. The tectonic environment of sedimentation and magmatism in the supracrustal belts seems to have evolved from a rifted continental margin, through a stable shelf to a geosynclinal type of setting. Sialic crustal differentiation about 3400 Ma. ago may have been responsible for the early stable conditions.

The supracrustal rocks show evidence of three phases of deformation (DF_1 to DF_3). A structural unity is evident amongst the supracrustal sequence, the Peninsular Gneiss and granulites of the Dharwar tectonic province. This structural unity suggests the evolution of the Peninsular Gneiss and granulites synkinematically with the deformation of the Dharwar supracrustal sequence. There is a wide spread of ages from 3400 Ma. to 2600 Ma. in the Dharwar craton. The structural unity amongst rocks developed over such a wide range of ages implies long-term stability of the stress regimes in the Archaean lithosphere.

Dharwar schist belts are a rich repository of iron, manganese, and limestone deposits, indicating substantial biological activity during the early Precambrian times. Stromatolites and $\delta^{13}C$ values for carbon in graphitic schists and preservation of syngenetic cyanobacterial microfossils have been recognised in widely separated regions in the Dharwar schist belts. The morphological diversity as exhibited by Dharwar stromatolites are rare in pre-Riphean sequences.

The foregoing observations indicate that, as compared to other Archaean terranes, the Archaean Dharwar craton appears to have more evolved characteristics.

EARLY PRECAMBRIAN CRUSTAL EVOLUTION - GENERAL STATEMENT

Studies carried out in different parts of the world have shown that greenstone belts evolved through most of the Precambrian, largely in the Archaean and some others in the Proterozoic (Windley, 1984a). Knoll (1984) classified the Archaean greenstone belts as belonging to two principal age groups (3.5 to 3.4 Ga and 2.9 to 2.6 Ga). Lowe (1985) identified three groups of greenstone belts-pre-3 Ga, post-3 Ga and those that evolved on late Archaean cratons formed from early Archaean greenstone belts. The characteristics of the greenstone belts of each of these groups and the evolutionary paths in them are different (Lowe, 1980; 1985). Variable characters noted by him in greenstone belts of different age groups, could be attributed to the different degrees of development of continental crust prior to their formation. Complex temporal and spatial relations characterise the greenstone belts with respect to granitic and gneissic rocks which surround them (Percival and Card, 1985). Greenstone belts invaded by gneisses as well as those resting on them have been found to co-exist in individual shields (Bickle, 1984). In fact, such a relation led to the distinction of older and younger greenstone belts (Glikson, 1976; Naqvi, 1976; Radhakrishna, 1976). In spite of such a distinction, a continuous history of tectonic evolution over a period of nearly a billion years is coming to be recognised in many Archaean terranes (Tankard et al., 1982; Watson, 1983; Naqvi, 1981; Pichamuthu and Srinivasan, 1983; Hunter et al., 1985; Naha et al., 1986). The importance of tectonic compression and transpression in the Archaean, as opposed to the earlier views on vertical tectonics, is being realised (Ramsay, 1963; Drury et al., 1984; deWit and Ashawal, 1985; Huddleston et al., 1985 Bauer et al., 1985) and that some form of plate tectonics was in operation in the Archaean is considered more plausible (Kroner, 1982; Bickle, 1984; Windley, 1984b; deWit and Ashwal, 1985; Naqvi, 1985; Hansen et al., 1988).

The relation between greenstone-granite province and gneiss-granulite provinces also shows variations. A transitional prograde relationship characterises some provinces such as, for example in parts of South India (Pichamuthu,1951; Shackleton, 1976; Janardhan et al., 1982; Condie et al., 1982; Raase et al., 1986). A structural unity between low-grade granite-greenstone and high-grade gneiss-granulite terranes has been documented (Bauer et al., 1985; Naha et al., 1986). However, an event of folding and metamorphism which may have pre-dated the deformation in greenstone belts has been picked up in some gneisses (Hunter et al., 1985; Naha et al., 1986; 1988) Coeval development of greenstone and gneiss-granulite terranes in two separate tectonic blocks also has been documented, for example, in the Rhodesian craton and Limpopo belt (see Tankard et al., 1982) and possibly the Dharwar craton of S. India and the Eastern Ghat mobile belt. Granulite metamorphism of greenstone-belt assemblages has been known from Greenland and the Baltic shield (Windley, 1984b).

Biological signatures in the form of stromatolites and microbiota, as well as stable isotopic fractionation which needs biological intervention, have now been well recorded from rocks younger than 3.5 - 3.6 Ga (see Schopf, 1983). The role of cyanobacteria during the early part of the Earth's history in building up the oxygen content, initially in the earth's hydrosphere and later in the atmosphere, is being investigated and the relation of this transition to the deposition of such unique deposits in the Precambrian as BIF, BMF and carbonate rocks is a subject of intensive study (See for example, Cloud, 1976; Schopf, 1983). The antiquity of this event controlled by biological activity in a given region is a subject matter of great interest. The Archaean is an eon, therefore, of diverse geological settings and evolutionary characteristics (Windley, 1984b). Such a wide variety of geological relations today makes it necessary to develop evolutionary concepts applicable to individual areas/regions, not necessarily applicable on a global scale.

In this paper a critical evaluation of our understanding of the early Precambrian crustal evolution of south India, which seems to have some unique characteristics compared to many other Archaean terranes of the world, is presented. These include (i) evidence of early crustal stability and evolution of the greenstone belt terranes from a stable to an unstable regime, (ii) structural unity for a large part of the stratigraphic column composed of supracrustal rocks, gneisses and granulites implying long-term stability of stress regimes in the Archaean lithosphere, and, (iii) substantial biological activity that promoted large-scale deposition of BIF, BMF and carbonate rocks not observed in other Archaean terranes.

GENERALISED SUCCESSION FOR THE EARLY PRECAMBRIAN DHARWAR SEQUENCE OF SOUTH INDIA

The early Precambrian terrane of South India, like many other shields, is composed of schist belts (referred to as greenstone belts in other regions), gneisses, granitoids, and granulites

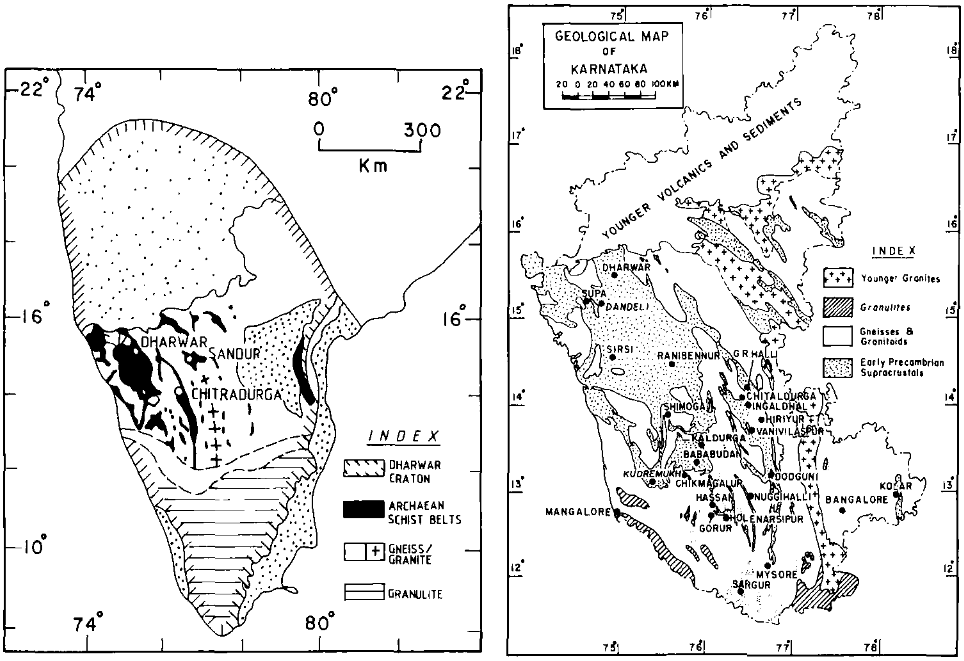

Figure 1a. Map of the Dharwar Craton showing Archaean schist belts, gneiss and granulite terrane.
1b. Geological map of Karnataka, type area for the early Precambrian of South India.

TABLE 1: GENERALISED SUCCESSION OF THE SUPRACRUSTAL ROCKS IN THE EARLY PRECAMBRIAN SCHIST BELTS OF SOUTH INDIA

Ga		
2.5 2.6	POLYMICTIC CONGLOMERATES AND GREYWACKES; METABASALTS, ANDESITES, DACITES AND RHYOLITES; BANDED IRON FORMATION.	CHITRADURGA AND GADAG AREAS OF CHITRADURGA SCHIST BELT; PARTS OF CENTRAL PORTION OF DHARWAR–SHIMOGA BELT.
2.7 2.8	QUARTZ–ARENITE/ARKOSE, METAPELITE, CARBONATE (Limestone and dolomite), BANDED MANGANESE AND IRON FORMATION WITH SOME MAFIC SILLS.	WESTERN MARGIN OF CHITRADURGA SCHIST BELT (low–grade metamorphosed) EASTERN MARGIN (high–grade metamorphosed) SOUTHERN AND WESTERN PART OF DHARWAR–SHIMOGA SCHIST BELT.
2.9 3.0	QUARTZ PEBBLE CONGLOMERATES, QUARTZ ARENITES, METABASALTIC AND RHYODACITIC LAVA FLOWS, GRAPHITIC SCHISTS AND BANDED IRON FORMATION.	BABABUDAN SCHIST BELT; KUDREMUKH–KODACHARI AREA OF WESTERN GHAT SCHIST BELT.
3.1 3.2 3.3 3.4	LAYERED ULTRAMAFIC–MAFIC COMPLEXES (deformed) ASSOCIATED WITH MINOR AMOUNTS OF QUARTZITES (detrital as well as chemogenic), HIGH Al–Mg SCHISTS.	NUGGIHALLI AND HOLENARASIPUR SCHIST BELTS.

(Fig.1). The supracrustal sequence designated as the Dharwar super group is known to be older than 2600 Ma. (Taylor et al., 1984). This sequence has been variously classified by different authors (Naqvi, 1981; Swami Nath and Ramakrishnan, 1981; Pichamuthu and Srinivasan, 1983; Radhakrishna and Naqvi, 1986). Neglecting the differences in regard to the nomenclature and position of the stratigraphic breaks, the supracrustal succesion may be summarised as in Table 1.

EVIDENCE FOR EARLY STABILITY OF THE CRUST

A review of Archaean sedimentation by Lowe (1980) has shown the evolution of greenstone belts from an essentially mobile volcanic phase at the base to one of stability at the top.

In contrast to this trend of development found in greenstone belts of many other parts of the world (South Africa, Australia, Canada, see Lowe, 1982) the early Precambrian schist belts of S.India show evidence for comparatively stable crustal conditions during the early stages of evolution.

Three lines of evidence suggest this relative stability:

1. Development of layered igneous complexes in the lowermost part of the stratigraphic sequence,
2. Deposition of mature to supermature quartz-pebble conglomerates and quartzites in the lower part, and
3. Orthoquartzite-carbonate facies assemblages again in the lower to middle part of the sequence (see Table. 1)

Layered igneous complex

Although layered igneous complexes with chromite are known from Archaean greenstone belts (Condie, 1981), economic concentrations of chrome spinel in layered igneous complexes are rare in Archaean terranes outside gneiss-granulite provinces. The ultramafic-mafic complex of the Nuggihalli schist belt of South India and the Selukwe greenstone belt of Zimbabwe are significant exceptions in this respect. The Nuggihalli belt is considered to constitute an older greenstone belt sequence (Naqvi, 1976), the Nuggihalli schist belt is a linear schist belt, about 50 km long with an

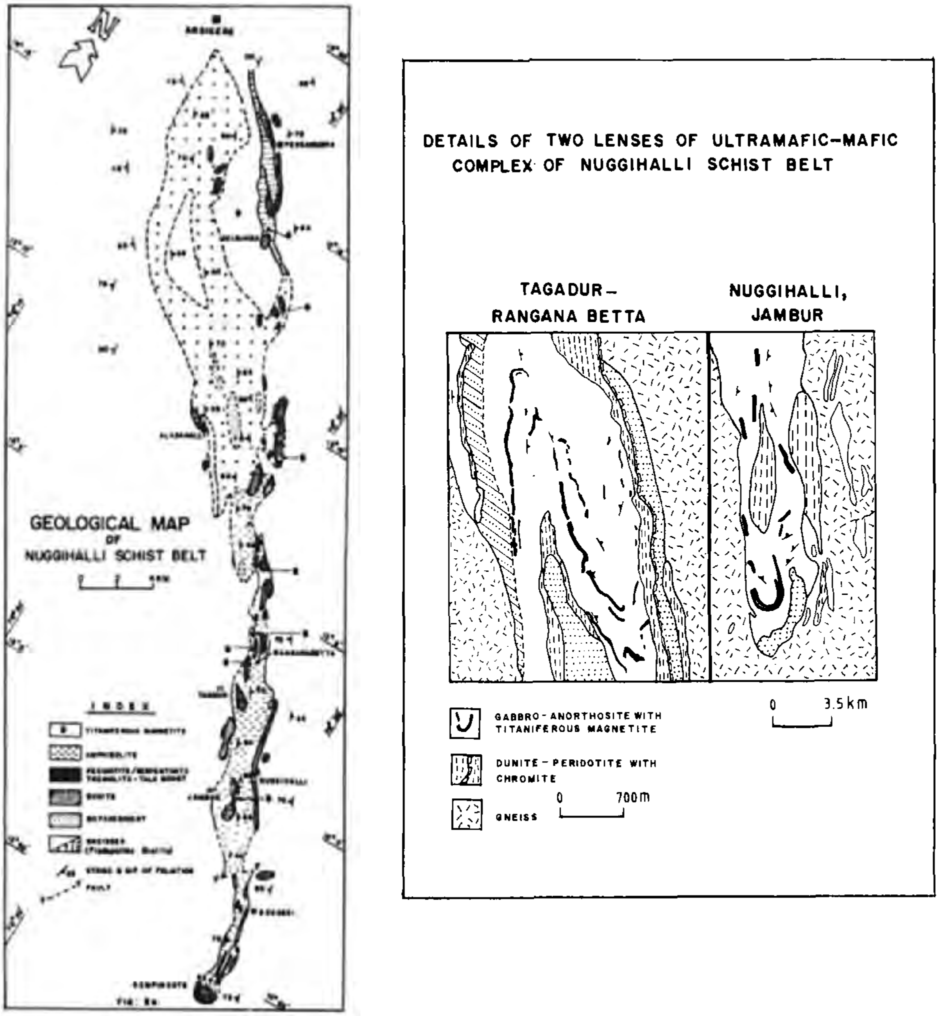
GEOLOGICAL MAP
OF
NUGGIHALLI SCHIST BELT
INDEX
DETAILS OF TWO LENSES OF ULTRAMAFIC-MAFIC COMPLEX OF NUGGIHALLI SCHIST BELT
TAGADUR-RANGANA BETTA
NUGGIHALLI, JAMBUR
GABBRO-ANORTHOSITE WITH TITANIFEROUS MAGNETITE
DUNITE-PERIDOTITE WITH CHROMITE
GNEISS
0 700m
0 3.5km

Figure 2a. Gelogical map of the Nuggihalli schist belt. Showing lensoidal bodies of ultramafic rocks. 2b. In detail each of the ultramafic lenses are actually highly deformed originally layered bodies.

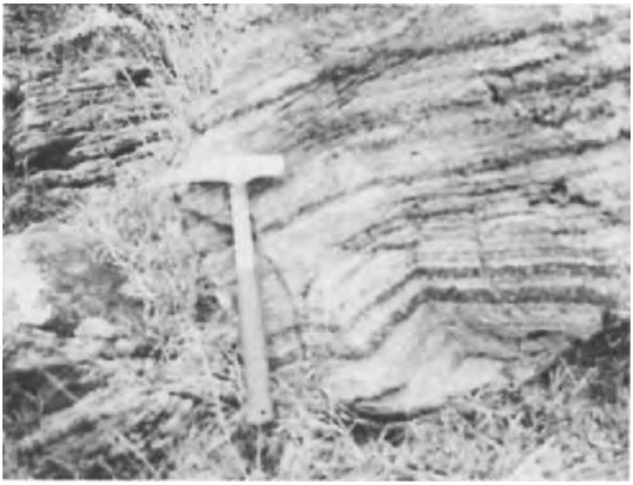

Figure 3. Centimetre to millimeter scale layering in Chromitite.

average width of outcrop of about 1 km; the maximum width is about 3 km near the village of Nuggihalli (Fig.2). Ultramafic-mafic rocks occur in the belt as lensoidal bodies amidst amphibolites. Large-scale geological mapping of individual lenses, shows that they are highly deformed, originally layered bodies now occurring as floating hinges. Two examples of such layered bodies from near Ranganabetta and Jambur are shown in Fig.2. Although the igneous complex is strongly deformed by folding, the layered character can be reconstructed as composed of (i) a highly serpentinized dunite-peridotite zone associated with chromite layers which is followed upward by (ii) a gabbro-anorthosite zone which consists of titaniferrous magnetite bands. Millimetre to centimetre scale layering of chromite and serpentinized peridotite can be seen (Fig.3). Cyclic layering of gabbro, gabbroic anorthosite and titaniferous magnetite is also clearly seen in drill cores (see Vasudev and Srinivasan, 1979). Chrome spinels are generally euhedral, and cumulus textures characterise the dunite, pyroxenite, and chromitites (Fig.4). The chemical composition of chrome spinels as determined by electron-microprobe analysis shows that they are iron-rich chrome spinels, comparable in composition to those of layered complexes (Fig.5). An iron enrichment trend similar to the Skaergaard trend is exhibited by the ultramafic-mafic complex on the FMA diagram (Pichamuthu and

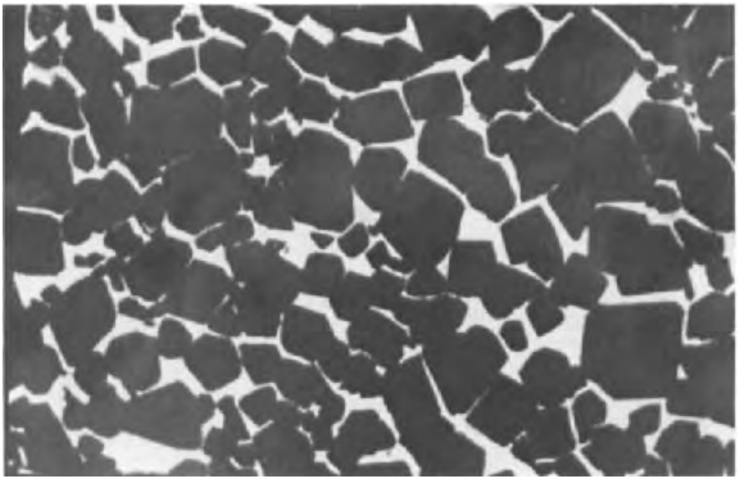

Figure 4. Cumulus texture of chromite, showing euhedral chromite crystals.

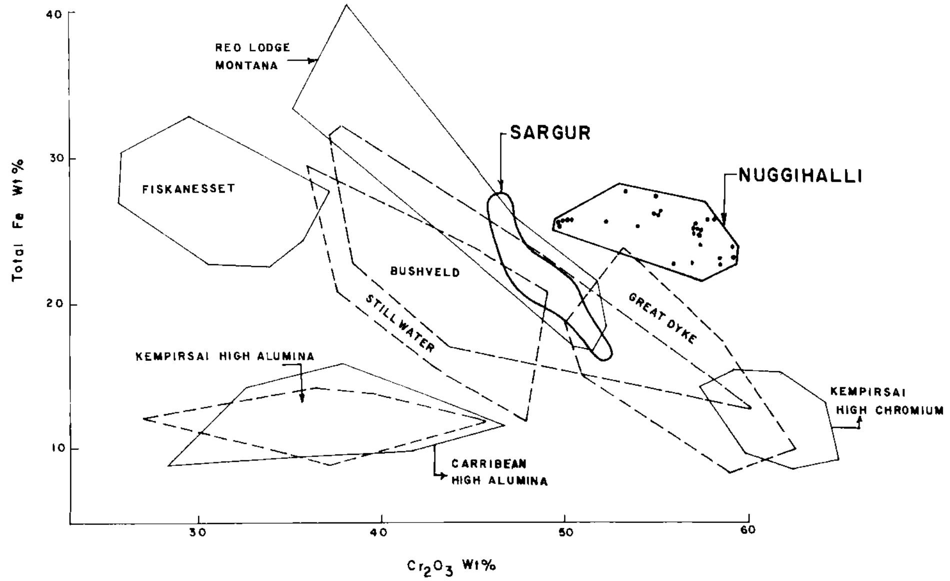

Figure 5. Total Fe vs Cr_2O_3 plot for chrome spinels of the Nuggihalli schist belt, showing their iron-rich nature as in the case of stratiform complexes.

Srinivasan, 1983). Layered igneous complexes constitute shallow level emplacements in stable tectonic environments (Jackson and Thayer, 1972). Stable crustal conditions are, therefore, indicated in the early part of the Precambrian earth's history of South India.

Quartz-pebble conglomerates and quartz arenites

Quartz-pebble conglomerates and quartz arenites form characteristic sedimentary members in the lower part of the Dharwar sequence designated by Swami Nath and Ramakrishnan (1981) as the Bababudan Group. Sedimentological studies on these rock formations (Srinivasan and Ojakangas, 1986) show that the quartz pebble conglomerate and quartzites together constitute about 25 to 50% of the nearly 2000 m thick Bababudan Group, the remaining part of the Group being composed of sub-aerial volcanic rocks, graphitic schists and banded iron-formations. The conglomerates are generally clast supported and the quartzites show well-developed trough-type cross-bedding. Rare instances of herring-bone-type cross-beds have been noted. Aeolian as well as fluvial ripple marks have been observed. The rocks are mineralogically mature and the textural maturity varies from submature to mature. Microcline has been observed as detritus, although rarely. Rounded zircons dominate the non-opaque heavy-mineral suite, denoting an extensive history of abrasion. Palaeocurrent plots and variance calculations for cross-bed orientation data, suggest that these mature sediments were deposited in braided fluvial plains on a peniplaned basement. Transition into shallow marine environments has also been suggested (Chadwick et al., 1985). The source terrane was probably a low-lying, deeply weathered surface, composed of granitoid and gneissic rocks upon which wind abrasion of quartz sand was an important process. The stable platform on which the sediment was accumulating appears to have been repeatedly rifted as indicated by the mafic to felsic lavas that are interbedded with these sediments. The strong strike persistence of the beds of banded iron-formation at the top of the Bababudan Group, however, indicates continued relatively stable conditions right up to the close of the Bababudan sedimentation cycle.

Orthoquartzite-carbonate assemblage

An orthoquartzite-carbonate facies has long been known to imply a stable environment of sedimentation. Such an assemblage is characteristic of the sequence found in the lower section of the Dharwar Supergroup which has been designated as the Dodguni Subgroup by Pichamuthu and Srinivasan (1983) or the Vanivilas Formation by Swami Nath and Ramakrishnan (1981). The assemblage consists of quartz arenites, metapelites, cherty dolomites, limestones and banded ferruginous manganese formations. Volcanic rocks are subordinate in the sequence. Cross-bedding shows a bimodal and bipolar nature, variance for cross-bed orientation is greater than 6000, as in the case of shallow offshore marine sedimentary rocks (Srinivasan and Ojakangas, 1986). An intertidal environment appears appropriate for these sandstones. The associated carbonate rocks show the development of stromatolites, corroborating a shallow-water marine environment (Srinivasan et al., 1988). Accumulation of manganese formation has been well documented from the shelf regions by Varentsov (1964). These manganese formations along with the associated carbonate rocks, serve as a stratigraphic marker horizon being strongly persistent along strike for hundreds of kilometers (see Pichamuthu, 1951) and therefore, they imply a good deal of stability in the environment during their accumulation.

The layered ultramafic-mafic complex of the Nuggihalli schist belt (older greenstone belt), the mature quartz-pebble conglomerates and quartzites of the Bababudan Group, and the orthoquartzite-carbonate sedimentation in the Vanivilas Formation indicate stable crustal conditions during the early stages of accumulation of the Dharwar supracrustal rocks.

Late-stage mobility

The early stable conditions reflected in the Dharwar sequence give way to the mobile conditions in the upper part. The metasediments and metavolcanics of the upper part of the sequence constitute the Chitradurga Group of Swami Nath and Ramakrishnan (1981). The metasedimentary rocks of the Chitradurga Group are represented by polymictic, disrupted framework conglomerates. The matrix supporting the clasts is either muds or sands, the latter no different from the graywackes into which the conglomerates grade (Ojakangas et al., 1988). The polymictic conglomerates resemble olisthostromes at the base (close to the source) but show well-organised bedding towards the upper part. Although cross--bedding is rarely observed, graded bedding is the most common sedimentary structure. Alternate pebbly and non-pebbly beds are noted. The graywackes are associated with conglomerates. The latter occur interbedded with them or generally underlie the main graywacke sequence. Preliminary sedimentological studies on the graywackes have been carried out by Ojakangas et al. (1988) and the geochemistry has been investigated by Naqvi et al. (1988). Sedimentological studies show that the graywackes are coarser near the conglomerate beds, as for example near the western margin of the Chitradurga schist belt or the southern part of the Dharwar-Shimoga belt. They are fine grained farther away, as for example in the central and northern parts of the Dharwar Shimoga belt. Alternate sand and mud packs characterise the graywackes. Thicknesses of the graywacke beds are highly variable. In some sections the beds are more than 5 m thick, elsewhere they are thin bedded and the laminae are measurable in millimeters. Graded bedding is the most common sedimentary structure; other structural features noted are partially or completly developed Bouma cycles, parting lineation, slump and flame structures.

The distribution of the polymictic conglomerates and graywackes, their mutual association characteristics, and the sedimentary structures suggest that they were deposited by turbidity currents (Srinivasan and Sreenivas, 1968; Naqvi et al., 1978; 1988). The turbidity currents carried and deposited sediments which were derived, not only from the pre-existing exposed gneissic crust, but also from the supracrustal rocks of the lower part of the Dharwar sequence described earlier. Supply from a general southerly direction, into a canyon-fan system in the northern part has been indicated by sedimentalogical studies (Ojakangas et al., 1988). The contribution of detritus from contemporaneous volcanism in the Dharwar sedimentary basins to the graywacke deposits also appears to be significant. Volcanic detritus appears to be especially abundant in the northern part of the Dharwar- Shimoga and Chitradurga schist belts (Naqvi et al., 1988; Ojakangas et al., 1988). A dynamic mobile environment with contemporaneous volcanism is indicated by the turbidite graywackes, in the upper part of the Dharwar sequence. This interpretation is also supported by the nonpersistent behaviour of the beds of banded iron-formation interbedded with the graywackes.

Trend of evolution of the Dharwar sedimentary basins

The foregoing description of sedimentation in the Dharwar schist belts, therefore, clearly points to the evolution of the Dharwar sedimentary basin from a condition of stability to one of instability, a trend unlike in most Archaean greenstone-belt depositories. However, this trend is not unlike that some Proterozoic sedimentary basins such as for example in the Coronation Geosyncline (Srinivasan and Ojakangas, 1986; Ramakrishnan, 1987) which evolved from a rifted basin through a shelf margin to a geosynclinal environment of back-arc type (Hoffman, 1973; Condie, 1982).

Cause of early stability

The cause of early stability in the south Indian early Precambrian seems to be the early sialic crustal differentiation. Preliminary geochronological studies in the region show that a tonalite-trondhjemite crust was formed in this terrane between 3.3

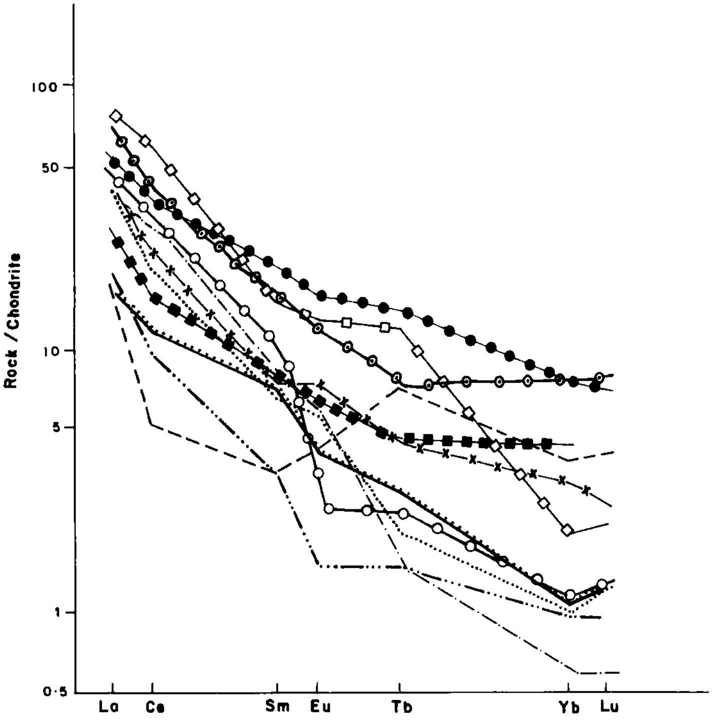

Figure 6. Chondrite-normalised REE patterns for gneiss pebbles in Kaldurga conglomerate. Steep fractionated pattern and derivation of gneisses from a mafic source with garnet and hornblende residue is indicated.

and 3.5 Ga ago (Beckinsale et al., 1980; Dhoundial et al., 1987). The bulk of the supracrustal accumulation constituting the Dharwar schist belts post-dated this event. Although Naqvi (1976) has expressed the opinion that some older schist belts such as Holenarsipur, Nuggihalli, and Sargur could be older than 3.4 Ga, unequivocal 3.4 Ga or older ages for the supracrustal rocks of these schist belts are yet to be obtained. However, it must be noted that the 3.3 to 3.4 Ga tonalite-trondhjemite gneisses which are found as pebbles in the polymictic conglomerates are characterised by REE patterns (Fig.6) which indicate metabasaltic amphibolite as the probable source rock, partial melting of which gave rise to tonalite-trondhjemite gneisses (Srinivasan, 1985). The initial Sr isotope ratios of 0.700 to 0.701 (Beckinsale et al., 1980; Venkatasubramanian and Narayanaswamy, 1974; Dhoundial et al., 1987) for the early tonalites and trondhjemites suggest that the parent basalt had a short crustal residence time.

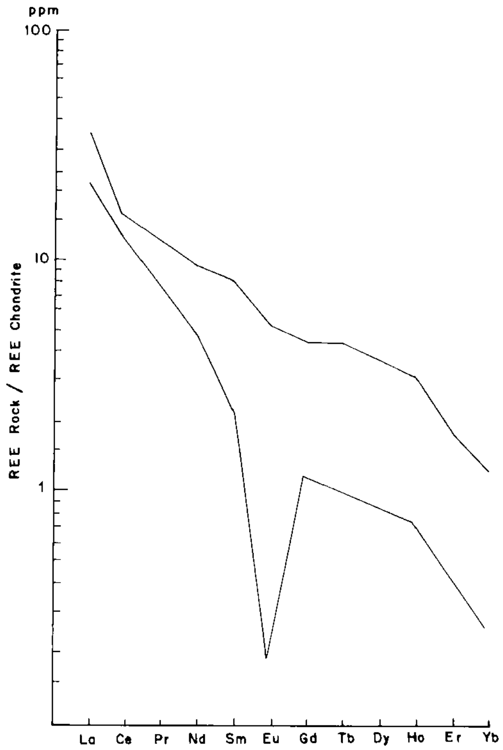

Figure 7. Chondrite-normalised REE patterns for Archaean Greywackes of the Dharwar-Shimoga Schist Belt, showing negative Eu anomaly.

Yet another evidence for the prevalence of an upper granitoid crust prior to the deposition of the Dharwar sediments comes from the REE composition of the sand packs of the graywackes of the southern part of the Shimoga and northwestern part of the Chitradurga schist belts. A negative Eu anomaly is evident in some of these graywackes of the Chitradurga Group (Fig.7). Naqvi et al., (1988) have observed pronounced negative europium anomalies in the mud packs of Dharwar graywackes.

LONG-TERM STABILITY OF STRESS REGIMES IN THE LITHOSPHERE

From the available geochronological data it is evident that the early Precambrian supracrustal sequence in South India evolved in the time span between 3.4 and 2.6 Ga ago, approximately over a period of 800 Ma. The structural patterns in this terrane have recently been reviewed by Mukhopadhyay (1986) and have been described by Naha and Mukhopadhyay (this volume). One of the significant features of this region is the remarkable structural unity observed in the early Precambrian terrane (Naha et al., 1986).

The structures in all the schist belts, in gneisses and granulites are identical in style, sequence and orientation. The earliest structure recognisable in all the schist belts is represented by isoclinal folds with attenuated limbs and thickened hinges. This deformation which may be designated as DF_1 was accompanied by metamorphism ranging from greenschist to amphibolite facies in the schist belts and development of penetrative schistosity. The axial planes of these early folds and the related schistosity have been involved in near co-axial refolding (DF_{1a}). Absence of evidence of development of new mineral fabric during DF_{1a} suggests that this deformation may be continuous with DF_1 deformation. DF_{1a} folds have variable degrees of tightness and their superposition on DF_1 folds accounts for the hook-shaped patterns of the schist belts. A set of upright open DF_2-folds with their axes and axial planes at high angles to the folds of earlier generation affect the earlier folds. A new cleavage has been superposed parallel to the axial planes of these folds. Metamorphism up to amphibolite facies accompanied this deformation also. Interference patterns producing characteristic dome-and- basin structures have been produced on all scales due to superposition of these open folds on the DF_1 and DF_{1a} folds.

Structures in gneisses completely match the structures in the supracrustal belts. Ductile deformation is characteristic in a major part of the gneissic terrain. The gneisses are generally migmatitic and the palaeosomes (consisting of infra- as well as supracrustal rocks) show evidence of changing ductility as migmatization accompanying deformation affected them, indicating synkinematic evolution of the gneisses with reference to the deformation of the supracrustal belts. It is however, important to note that there are some small relicts of amphibolites and migmatitic gneisses which record evidence of one phase of deformation earlier than pre-DF_1 (Naha et al., 1986; Naha and Mukhopadhyay, this volume). These are represented by isoclinal folds whose axial planes and related foliation trends are transected by the DF_1 isoclinal folds. However, the strong DF_1 deformation drags these early structures into parallelism with their axial plane trends within metres, obliterating evidence of this deformation on larger scales. Similar observations have been made by Hunter et al., (1985) in the Swaziland region of South Africa; they recognised in the gneissic rocks that evolved synkinematically with the deformation of supracrustal rocks, relicts of an extra deformation that preceded the deformation which affected the Barberton greenstone belt.

The gneissic complex that surrounds the Dharwar schist belts designated as Peninsular Gneiss has, therefore, components which preceded the Dharwar supracrustal sequence, as well as those that evolved during the deformation of the Dharwar supracrustal rock formations. Therefore, they have basement gneiss relicts as well as phases intrusive into Dharwar. The role of recycling through metamorphic, migmatitic and magmatic cycles are indeed factors that complicate the gneiss-schist relations in Archaean terranes (see Percival and Card, 1985).

Naha (1988) has documented the structural unity that pervades the South Indian Precambrian terrane, including the granulite province, and has adduced evidence for the formation of charnockites during DF_1 and DF_2 episodes. This implies that granulites and gneisses developed coevally at deep and shallow levels of the crust, respectively, and that they developed synkinematically with deformation of supracrustal rocks of the schist belts. The structural unity among the supracrustal rock formations, gneisses and granulites developed between 3300 Ma. and 2600 Ma. ago shows long-term stability of the stress regime in the Archaean lithosphere.

PALAEOBIOLOGICAL ACTIVITY

Although Pichamuthu (1945) recorded the finding of cyanobacterial filaments in cherts of the Dodguni area in the Chitradurga schist belt, it is only in recent years that more evidence of palaeobiological activity in the early Precambrian rock formations of Karnataka has come to light. Murthy and Reddy (1984), Baral (1986), Mallikarjuna et al., (1987) and Srinivasan et al., (1988) have recorded the occurrence of stromatolites in the carbonate rocks of the lower part of the Dharwar sequence. The stromatolites of the Dharwar craton are impressive from the point of view of

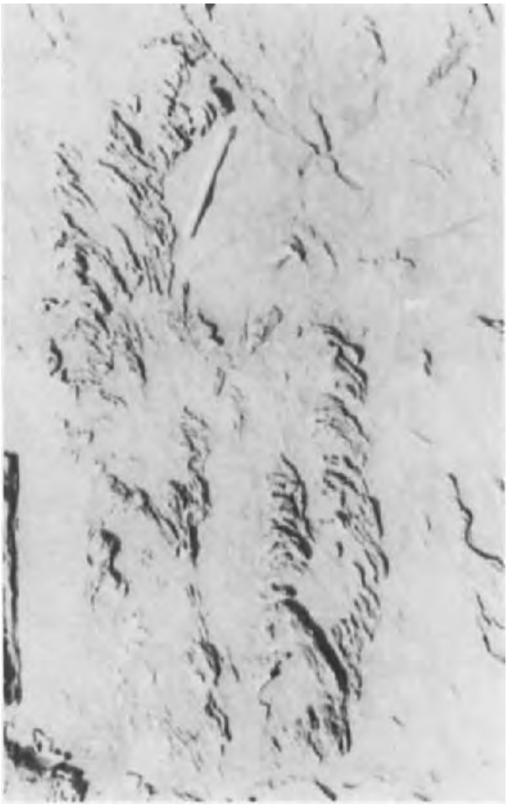

Figure 8. Actively and passively branched forms in Archaean (early Precambrian) stromatolites of the Chitradurga schist belt. Such forms are rare in pre-Riphean sequences.

morphological diverstiy, because such a diversity is rare in the pre-Riphean rocks. Srinivasan et al., (1988) record from the Chitradurga schist belt morphological forms which in outcroup resemble *Stratifera, Colonella, Kussiella, Gymnosolen* and *Tungussia* msp., (Fig.8) of Cloud and Semikhatov (1969).

Suresh (1982) provided evidence for syngenecity and biogenecity of the blue-green algal filaments reported earlier by Pichamuthu (1945). Naqvi et al., (1987) have recorded well-preserved permineralised cyanobacterial syngenetic filaments in the black cherts of Donimalai, Sandur schist belt. These observations suggest that cyanobacteria may have built the Archaean stromatolites of the Dharwar craton.

From C-isotopic evidence in the carbonate rocks of the Dharwar sequence, Kumar et al., (1983) suggested biological intervention in bringing about fractionation of carbon during the Dharwar sedimentation.

Carbon-isotopic data for some of the graphites associated with the banded iron-formations of the Dharwar Supergroup are given in Table 2. The $\delta^{13}C$ values varying from $-18^{o}/oo$ to $-34^{o}/oo$ PDB clearly suggest that the carbon in the graphite is biogenic (cf. Schidlowski, 1987).

Table 2.
$\delta^{12}C/_{13}C$ ratio of the organic carbon fraction and total organic carbon content of some graphites from the Dharwar Craton

Location	Description	Total Carbon content (%C)	Organic Carbon content (%C)	Carbon $\delta^{13}C^*$ ($^{o}/oo$)
Mavinahalli, Mysore Dt.	Metasediment ultramafic contact	1.27	0.73	-16.2
Chikbanavar Bangalore Dt.	Graphitic quartzite	0.55	0.46	-21.0
Ganacharpura Kolar Dt.	Graphitic schist	11.85	8.59	-35.4
Nagavand Dharwar Dt.	Graphitic phyllite	1.90	1.58	-21.8

* per mil vs. PDB

The magnitude of the biological activity during the Dharwar sedimentation must have been impressively large. This is indicated by extensive deposition of iron, manganese and limestone deposits in the Archaean Dharwar sedimentary basins.

CONCLUSION

No unique model of evolution is applicable to all the Archaean terranes of the world. The 2 Ga. time span of the Archaean must accommodate a great deal of diversity. The Archaean Dharwar craton has evidences for comparative stability of the earth's crust during the middle and late Archaean times. The structural unity among the various rock formations can be explained by long-term stability of stress regimes in the Archaean lithosphere, a condition difficult to reconcile with the high heat-flow conditions believed to have been operative during the Archaean. The morphological diversity of the stromatolites of the Dharwar craton indicates evolved ecological and biological conditions at least in late Archaean times. The Dharwar terrane is probably an unique middle to late Archaean terrrane with Proterozoic signatures. Indeed, the transition from Archaean to Proterozoic must have been gradual over a protracted period covered by the Zuluan wedge of Cloud (1976).

ACKNOWLEDGEMENTS

We thank Prof. Richard W.Ojakangas, University of Minnesota, Duluth, USA and Prof. K.Naha, IIT, Kharagpur for useful discussions on sedimentology and structural evolution, respectively. Dr. Jurgen Hahn, Max Planck Institut Fur Chemie, determined carbon isotope ratios for graphites and Dr.A.Y.Glikson, Bureau of Mineral Resources of Australia carried out electron- probe micro-analysis of chrome spinels. We are thankful to them. We wish to thank Prof. V.K.Gaur, Director, NGRI for encouragement and facilities.

REFERENCES

Baral, M.C., 1986. Archaean stromatolites from Dodguni belt, Karnataka craton, India. J. Geol. Soc. India, 28: 328-333.

Beckinsale, R.D., Drury, S.A. and Holt, R.W., 1980. 3360 m.y. old gneisses from the South Indian Craton. Nature, 283: 469-470.

Bauer, R.L., Huddleston, P.J. and Southwick, D.L., 1985. Correlation and contrasts in structural history and style between Archaean greenstone belt and adjacent gneiss belt, NE Minnesota. In: Tectonic evolution of greenstone belts, LPI, Technical Rep. No.86-10: 52-54.

Bickle, M.J., 1984. Variation in tectonic style with time; Alpine and Archaean systems. In: H.D. Holland and A.F. Trendall (Editors), Patterns of change in Earth evolution, Springer Verlag, Berlin, pp.357-370.

Chadwick, B., Ramakrishnan, M. and Viswanatha, M.N., 1985. A late Archaean intracratonic volcano-sedimentary basin, Karnataka, South India, Part I: Stratigraphy and basin development, J. Geol. Soc. India, 26: 769-801.

Cloud, P., 1976. Major features of crustal evolution, Geol. Soc. S. Africa, Annexure to volume 79: 1-33.

Cloud, P. and Semikhatov, M.A., 1969. Proterozoic stromatolite zonation, Am. J. Sci., 267: 1017-1061.

Condie, K.C., 1981. Archaean Greenstone belts, Elsevier, pp.1-434.

Condie, K.C., Allen, P. and Narayana, B.L., 1982. Geochemistry of the Archaean low-to high-grade transition zone, southern India. Contr. Min. Pet., 81: 157-167.

deWit, M.J. and Ashwal, L.D., 1985. Greenstone belt tectonics: some relevant outstanding questions. In: Tectonic Evolution of Greenstone belts, LPI, Technical Rep., 86-10: 11-12.

Dhoundial, D.P., Paul, D.K., Sarkar, A., Trivedi, J.R., Gopalan, K. and Potts, P.J., 1987. Geochronology of the Precambrian granitic rocks of Goa, SW India. Precamb. Res., 36: 287-302.

Drury, S.A., Holt, R.W., Reeves-Smith, G.J. and Weightman, R.T., 1984. Precambrian tectonics and crustal evolution in south India, J. Geol., 92: 3-20.

Glikson, A.Y., 1976. Stratigraphy and evolution of primary and secondary greenstones: significance of data from shields of the southern hemisphere. In: B.F. Windley (Editor), Early history of the Earth, John Wiley, pp.257-278.

Hansen, G.N., Krogstaad, E.J. and Rajamani, V., 1988. Tectonic setting of the Kolar schist belt, Karnataka, India. Proc. Workshop on Deep continental crust of South India, Geol. Soc. India, Bangalore: 40-42.

Hoffman, P., 1973. Evolution of an early Proterozoic continental margin: the Coronation geosyncline and associated aulacogens of the northwestern Canadian Shield : Phil. Trans. Roy. Soc. London, 273A: 547-581.

Huddleston, P.J., Schultz-Ela, D., Bauer, R.L. and Southwick, D.L., 1985. Transpression as the main deformation event in an Archaean greenstone belt, Northeastern Minnesota. In: Tectonic Evolution of Greenstone belts, LPI, Technical Rep., 86-10: 124-126.

Hunter, D.R., Wilson, A.H., Versfelt, J.A., Allen, A.R., Smith, R.G., Sleigh, D.W.W., Groenewald, P.P., Chutter, G.M. and Preston, V.A., 1985. A continuous record of tectonic evolution from 3.5 Ga to 2.6 Ga in Swaziland and Northern Natal. In: Tectonic Evolution of Greenstone belts, LPI, Technical Rep., 86-10: 127-131.

Jackson, E.D. and Thayer, T.P., 1972. Some criteria for distinguishing between stratiform, concentric and alpine-peridotite gabbro complexes, Proc. 24th Int. Geol. Congr., Sec.2: 289-296.

Janardhan, A.S., Newton, R.C. and Hansen, E.C., 1982. The transformation of amphibolite facies gneiss to charnockite in southern Karnataka and Northern Tamil Nadu, India, Contr. Min. Pet., 79: 130-149.

Knoll, A.H., 1984. The Archaean/Proterozoic transition : A sedimentary biological perspective. In: H.D. Holland and A.F. Trendall (Editors), Patterns of Change in Earth Evolution, Springer-Verlag, pp.221-242.

Kumar, B., Venkatasubramanian, V.S. and Rama Saxena., 1983. Carbon and oxygen isotopic composition of the carbonates from greenstone belts of Dharwar craton, India, In: S.M. Naqvi and J.J.W.Rogers (Editors), Precambrian of South India, Geol. Soc. India, Mem.4: pp.260-266.

Kroner, A., 1982. Archaean to Early Proterozoic tectonics and crustal evolution: A review, Revista Brasiliera De Geosciencias, 12: 15-31.

Lowe, D., 1980. Archaean sedimentation, Ann. Rev. Earth and Planet. Sci., 8: 145-167.

Lowe, D., 1982. Comparative sedimentalogy of the principal volcanic sequences of Archaean greenstone belts in South Africa, Western Australia and Canada, Precamb. Res., 17: 1-29.

Lowe, D., 1985. Proc. in Workshop on Early Crustal Genesis: The World's oldest rocks : LPI, Technical Rep., 86-10: 21-22.

Mallikarjuna, C., Devapriyan, G.V., Balachandran, V. and Harinadha Babu, 1987. Archaean stromatolites near Bhimasamudra, Karnataka, J. Geol. Soc. India, 13: 159-161.

Mukhopadhyay, D., 1986. Structural pattern in the Dharwar craton, Jour. Geol., 94: 167-186.

Murthy, P.S.N. and Reddy, K.R., 1984. 2900 m.y. old stromatolite from Sandur Greenstone belt of Karnataka craton, India. Jour. Geol. Soc. India, 25: 263-266.

Naha, K., 1988. Structural relations of charnockites of south India, Proc. Workshop on the Deep Continental Crust of south India, Geol. Soc. India: 99 (abst.)

Naha, K. and Mukhopadhyay, D., Structural styles in the Precambrian metamorphic terranes of Peninsular India: A synthesis (this volume).

Naha, K., Srinivasan, R. and Naqvi, S.M., 1986. Structural unity in the Precambrian Dharwar tectonic province, Peninsular India, Quart. J. Geol. Mining Met. Soc. India, 58: 219-243.

Naha, K., Srinivasan, R. and Jayaram, S., 1988. Structural evolution of the Peninsular gneiss - An early Precambrian migmatitic complex from south India. Geologische. Rund., (in press).

Naqvi, S.M., 1976. Physico-chemical conditions during the Archaean as indicated by Dharwar Geochemistry. In: B.F., Windley (Editor), Early History of the Earth, John Wiley and sons, London, pp.289-298.

Naqvi, S.M., 1981. The oldest supercrustals of the Dharwar craton, J. Geol. Soc. India, 22: 458-469.

Naqvi, S.M., 1985. Chitradurga schist belt - An Archaean suture (?), J. Geol. Soc. India, 26: 511-525.

Naqvi, S.M.,Divakara Rao, V., Rama Rao, P., Hussain, S.M., Narayana, B.L. and Jafri, S.M., 1978. The petrochemistry and geological implications of conglomerates from Archaean geosynclinal piles of southern India, Can. J. Earth Sci., 15: 1085-1100.

Naqvi, S.M., Venkatachala, B.S., Manoj Shukla, Kumar, B., Natarajan, R. and Mukund Sharma, 1987. Silicified Cyanobacteria from the cherts of Archaean Sandur schist belt. J. Geol. Soc. India, 29: 535-539.

Naqvi, S.M., Sawkar, R.H., Subba Rao, D.V., Govil, P.K. and Gnaneshwar Rao, T., 1988. Geology, Geochemistry and tectonic setting of greywackes from Karnataka Nucleus, India. Precamb. Res., 39: 193-216.

Ojakangas, R.W., Srinivasan, R. and Sawkar, R.H., 1988. Sedimentology of turbidite greywackes and conglomerates of the Chitradurga Group, Dharwar Craton, South India: Implications for Archaean crustal evolution (in preparation).

Percival, J.A. and Card, K.D., 1985. Greenstone belts: their boundaries, surrounding rock terrains and interrelationships. in: Tectonic evolution of Greenstone Belts, LPI, Technical Rep., 86-10: 170-173.

Pichamuthu, C.S., 1945. Algal structures in the cherts from Dodguni, Tumkur District, Ind. Sci. Congr. 32nd Session: 60.

Pichamuthu, C.S., 1951. Some observations on the structure and classification of Dharwars of Mysore State. Curr. Sci., 20: 117-119.

Pichamuthu, C.S. and Srinivasan, R., 1983. A billion year history of the Dharwar craton (3200 to 2100 m.y. ago), Mem. Geol. Soc. India. 4: 121-142.

Raase, P., Raith, M., Ackermand, D. and Lal, R.L., 1986. Progressive metamorphism of mafic rocks from greenschist to granulite facies in the Dharwar craton of south India, J. Geol. 94: 261-282.

Radhakrishna, B.P., 1976. The two greenstone groups in the Dharwar craton, Ind. Minerologist, 16: 12-15.

Radhakrishna, B.P., and Naqvi, S.M., 1986. Precambrian continental crust of India and its evolution, J. Geol., 94: 145-166.

Ramakrishnan, M., 1987. Tectonic evolution of the Proterozoic-type platform-fold belts of Archaean age in western Dharwar craton, Ind. Mineralogist, 27: 1-9.

Ramsay, J.G., 1963. Structural investigations in the Barberton Mountain Land, Eastern Transvaal, Trans. Geol. Soc. S. Africa, 66: 353-398.

Schidlowski, M., 1987. Application of stable carbon isotopes to early biochemical evolution on Earth, Ann. Rev. Earth. Planet. Sci., 15: 47-72.

Schopf, W., (Editor) 1983. Earth's earliest biosphere - its orign and evolution. Princeton Univ. Press, New Jersey, pp.1-543.

Shackleton, R.M., 1976. Shallow and deep level exposures of the Archaean crust in India and Africa. In: B.F. Windley (Editor), The Early History of the Earth, John Wiley and Sons, London, pp.317-322.

Srinivasan, R., 1985. Stratigraphical and geochemical characterization of the type sections of the Early Precambrian Rock Formations of Karnataka, Unpl. Ph.D. Thesis, Univesity of Mysore, India, pp.1-215.

Srinivasan, R. and Sreenivas, B.L., 1968. Sedimentation and tectonics in Dharwars (Archaeans), Mysore State, India, Ind. Mineralogist, 9 : 47-58.

Srinivasan, R. and Ojakangas, R.W., 1986. Sedimentology of quartz pebble conglomerates and quartzites of the Archaean Bababudan Group, Dharwar Craton, South India : Evidence for Early crustal stability J. Geol., 94: 199-214.

Srinivasan, R., Manoj Shukla, Naqvi, S.M., Yadav, V.K. Venkatachala, B.S., Uday Raj, B. and Subba Rao, D.V., 1988. Algal stromatolites from the Chitradurga schist belt, Dharwar craton, South India, Precamb. Res., (in press).

Suresh, R., 1982. Further evidence of biogenic nature of Dodguni microbiota, Dharwar craton, India, J. Geol. Soc. India, 23: 567-574.

Swami Nath, J. and Ramakrishnan, M., 1981. (Editors), Early Precambrian Supracrustals of southern Karnataka. Geol. Surv. India, Mem. 112, pp.1-350.

Tankard, A.J., Jackson, M.P.A., Erickson, K.A., Hobday, D.R., Hunter, D.R., Minter, W.E.L. and Ericksson, S.C., 1982. Crustal evolution of southern Africa 3.8 billion years of earth's history: Springer-Verlag, New York, Heidelberg, Berlin, pp.1-523.

Taylor, P., Moorbath, S., Chadwick, D., Ramakrishnan, M. and Viswanatha, M.N., 1984. Petrography, chemistry and isotope ages of Peninsular gneiss, Dharwar acid volcanic rocks, and the Chitradurga granite with special reference to the late Archaean evolution of the Karnataka craton, southern India, Precamb. Res., 23: 349-375.

Taylor, S.R. and McLennan, S.M., 1981. The composition and the evolution of the continental crust : Rare earth element evidence from seidmentary rocks, Phil. Trans. Roy. Soc. London, A301: 381-399.

Varentsov, I.M., 1964. Sedimentary manganese ores, Elsevier Publ. Co.,: 1-119.

Vasudev, V.N. and Srinivasan, R., 1979. Vanadium bearing titaniferous magnetite deposits of Karnataka, India, J. Geol. Soc. India, 20: 170-178.

Venktasubramanian. V.S. and Narayanaswamy, R., 1974. The age of some gneissic pebbles in Kaldurga conglomerates, Karnataka State, India. J.Geol. Soc. India, 15: 318-319.

Watson, J.V., 1983. Lewisian. In Craig (Editor), Geology of Scotland. Scottish Academic Press, Edinburgh, pp.23-73.

Windley, B.F., 1984a. The Archaean-Proterozoic boundary, Tectonophysics, 105: 43-54.

Windley, B.F., 1984b, The Evolving cotinents, John Wiley and Sons, London, pp.399.

GROWTH OF PRECAMBRIAN CONTINENTAL CRUST - A STUDY OF THE SINGHBHUM SEGMENT IN THE EASTERN INDIAN SHIELD

MIHIR K. BOSE

ABSTRACT

The trend of the Precambrian crustal evolution in a segment of the eastern Indian shield has been traced. The continental crust evolved though nucleation and growth of an Archaean sialic block (the Singhbhum Craton) which accreted a flanking Proterozoic basin to its north. The sialic block enlarged rather rapidly through repeated partial melting of the incipient crust. Formation of tonalite, an unique component of the craton, was very likely a two-stage melting process and this was followed by limited fractional crystallization to produce the early phases of granites. The development of the marginal basin with an apron of clastics and volcaniclastics together with strong compositional bimodality in volcanism is reminiscent of Archaean events (≈growth of greenstone belts). The mafic lavas constituting the bulk of the mid-basinal volcanic pile (the Dalma volcanics) has an analogy to basalts from back-arc basins. The sequence of volcanism was accompanied by some degree of mantle replenishment. Not only in volcanism, the Singhbhum Proterozoic basin reveals polarity also in sedimentation pattern and deformation plan in response to some regional unilateral tectonic process. The sediments in the proximal zone are characterised by mass-flow deposits accompanying basement unrest, whereas the distal zone shows flysch-type turbidites and increasing degree of mixing with volcanics. An overall suprasubduction zone situation is strongly indicated by the Proterozoic fossil marginal basin juxtaposed against a thickened crustal block in high-grade dress. A subduction analogue of successively grander scale is inferred to be the controlling mechanism in early continental crustal evolution in this segment of the Indian Shield.

INTRODUCTION

The present contribution attempts to highlight the trend of development of ancient crust in a segment of the eastern Indian

Shield. What can be established through this study is essentially a history of enlargement of an Archaean cratonic nucleus through accretion of a Proterozoic marginal basin coupled with an arc system now seen in vestiges. The present communication lays emphasis on the evolution of the Proterozoic marginal basin, often considered to have the same setting as that of the Archaean greenstone belt (Tarney and Windley,1981). Again, basinal history is considered to overshadow shelf sedimentation during the Archaean, the latter process is presumed to control the sedimentary process in the Proterozoic (Windley, 1984a). On the other hand, Eriksson and Donaldson (1986) pointed out that in terms of sedimentation pattern, designations like "Proterozoic style" should be discouraged as meaning shelf-controlled sedimentation, as also should reference to greenstone belts younger than 2.5 Ga as "Archaean type". The present contribution has important bearing on both these aspects of evolutionary style during early crustal growth.

GEOLOGICAL SETTING - THE SCENARIO

The investigated terrain is situated in the eastern part of the Indian Shield (Fig. 1) covering parts of the states of Bihar and

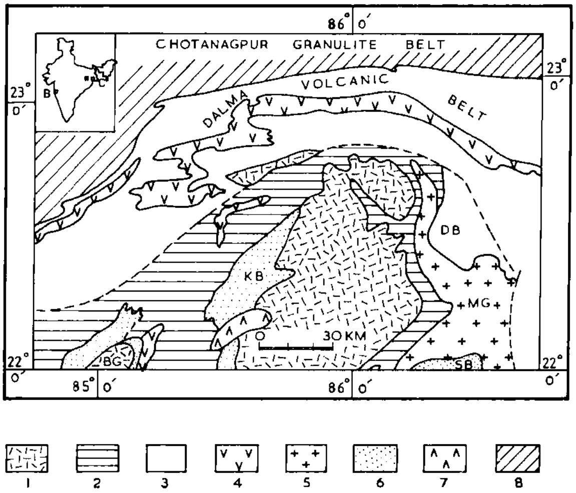

Figure.1 Generalized geological map of the study area. 1.Singhbhum Sialic block (basement), 2. Banded iron-formation enveloping the craton, 3. Singhbhum Proterozoic basin (volcaniclastic and clastic filling), 4. Dalma volcanic belt. 5. Mayurbhanj granite (MG) and Bonai granite (BG), 6. Younger basins (KB: Kolhan Basin, SB: Simlipal Basin, 7. Younger volcanics, 8. Chhotanagpur high-grade belt. DB:Dhanjori Basin. Inset is an index map showing location of study area (solid square), C: Calcutta, B: Bombay.

Orissa. An overview of the region brings out clearly three distinct morphotectonic-cum-lithotectonic zones from south to north (Dunn and Dey, 1942, Sarkar and Saha, 1977, Bose and Chakraborti, 1981, Banerji, 1984), viz., 1). The Singhbhum sialic platform with tonalitic and potassic granitoid components, all of Archaean age, ii) the (Proterozoic) Singhbhum Basin filled with volcaniclastics, platform wash and local mass-flow deposits with intrabasinal bimodal volcanics and iii) the Chhotanagpur plateau of high-grade metamorphic rocks, migmatites, para-gneisses and a characteristic calc-alkaline magmatic suite. The latter high-grade belt has many features in common with global granulite belts (Windley, 1984b). Available isotopic age data suggest a Proterozoic imprint on the Chhotanagpur high-grade terrane (Sarkar, 1980).

GROWTH OF THE SINGHBHUM SIALIC BLOCK

The basement platform of elongate plan (Fig. 1) is now represented by an extensive terrane of granite and gneissic complex with subordinate metabasic and minor metasedimentary rocks compositely described as the "Singbhum granite pluton" in the literature. In addition, a small patch of basement rocks comprising trondhjemite-granodiorite (designated as "Chakradharpur gneiss") is exposed to the northwest of the main block (Sengupta et al., 1983). Petrographic study on part of the Singhbhum pluton showed the existence of an older plagioclase-quartz assemblage (tonalitic) with relic tectonic fabric, on which was imprinted late potash feldspathization, viz., microclinization (Bose, 1960). Subsequent studies have revealed two temporal-cum-petrographic components within the sialic platform, viz., an older tonalite and a group of younger granodiorite-granite members. Earlier, the tonaltic gneiss, dated by the Sm-Nd method (3800 Ma) was considered as one of the oldest terrestrial rocks (Basu et al., 1981). Subsequently, Moorbath et al., (1986) did not confirm this old age and placed the rocks at an age level of 3378 Ma. The Singhbhum Granite, as previously reported, appears to be only slightly younger (Ca. 3300 Ma) (Saha et al., 1986; Moorbath et al., 1986). Thus, a trend of progressive potash enrichment in evolving magmas, as indicated by an earlier study (Bose, 1960), is corroborated. The origin of the tonalite unit again can be traced back to a basaltic source now represented by relict enclaves of ortho-amphibolites (Saha and Ray, 1984a) and as established for many other parts of the Indian Shield (Divakara Rao and Rama Rao, 1982). But a closer and critical look into trace-element distributions (Saha and Ray, 1984b) in this suite also seems necessary for an insight into the petrogenetic relations between the members. Apparently, the origin of tonalite is a two-stage melting process, viz. derivation of tholeiite (=Singhbhum ortho-amphibolite) from the mantle source and partial melting of basalt to produce tonalitic melt (Arth and Barker, 1976). The alternative model of fractional crystallization of basaltic magma is usually discarded simply in the absence of expected intermediate members in such cases (Sengupta et al., 1983; Condie, 1986).

Feeble LREE enrichment and accompanying high levels of alkali-earth metals in ortho-amphibolites of Singhbhum (Saha and Ray, 1984b) are apparently irreconcilable with their high Ni and Cr contents, for obvious reasons. On the other hand, the derived basaltic magma (from mantle source) was not picritic or komatiitic which presumably hints at the existence of an already thickened crust. The Ni and Cr enrichment in otherwise LIL-enriched basalt suggests a feeble boninitic impress on the melt, normally derived at an early stage of the subduction process. It may also be pointed out that the primary sinks (due to extraterrestial impact), which were supposed sites of magma generation, had unique tectonic settings. They were characterised by a bilateral subduction analogue process through which the upper enriched crustal zone melts to a greater extent.

The global advent of andesitic magmatism in the course of early crustal evolution is at about 4.0 to 3.5 Ga (Condie, 1980; 1986) and the Singhbhum tonalite event possibly falls within this range. The nucleation of the craton through tonalite magmatism under a falling thermal gradient resulted from partial melting of tholeiite basalt (according to the two-stage melting model). Melting models based on available geochemical data (Saha and Ray, 1984b) indicate that an extremely low degree ($\sim$ 3%) of melting of mantle source (Fig. 2a) was necessary to produce the relatively LREE-enriched ortho-amphibolite of Singhbhum. This may also imply that the basaltic magma had already attained a moderately evolved stage and there might have been limited fractionation following partial melting. The melting model further suggests that a partial melting of the order of 45% of the amphibolite source

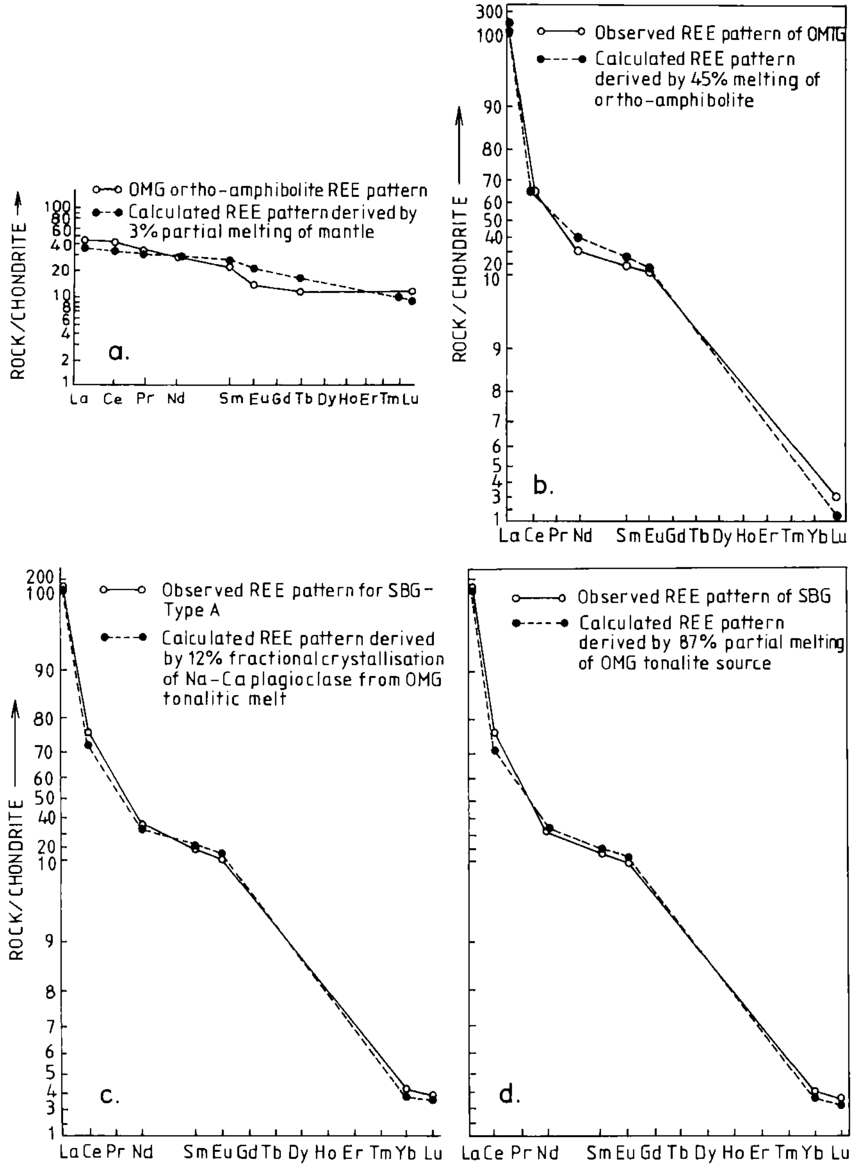

Figure 2. Chondrite-normalised REE distribution patterns in the Older Metamorphic magmatic suite compared with model melts. a) ortho-amphibolite (tholeiite) compared to model melting of spinel peridotite source; b) Tonalite, compared to model melting of tholeiite (ortho-amphibolite); c) Singhbhum Granite (type A) compared to fractional crystallization of tonalitic melt; d) Singhbhum Granite (type A) compared to melting product of OMG tonalite.

would produce the tonalitic melt of Singhbhum (Fig. 2b). It is also indicated that separation of the basaltic fraction would leave the mantle so depleted that the latter could not produce Singhbhum tonalite by direct partial melting. Singhbhum tonalite also does not bear any impress of a depleted source (except its positive epsilon Nd value, cf. Saha and Ray, 1984b). Like the Singhbhum tonalite, most of the Archaean tonalites involved in early crustal evolution have the apparently unresolvable impress of positive episilon Nd value (Saha and Ray, 1984b) on an otherwise fractionated character (Condie, 1986) which, in its turn, implies a short residence time. This has been explained through a very delicate balanced mixing of limited DMR and EMR in the course of a convective process which was relatively rapid (Condie, 1986).

A somewhat comparable mechanism of partial melting (with separation of Si-poor iron garnet) very likely continued to produce younger Singhbhum granites with high K/Na ratios. It is remarkable that REE abundances and their chondrite-normalised patterns are strikingly similar for Singhbhum tonalite and the early phase of Singhbhum Granite (Type A, Saha and Ray, 1984b), so much so that they are almost indistinguishable. Thus, the early granites could have formed by almost complete melting of the tonalite in thermal pools. Estimates on model melting show the degree of melting to be in the range 86 to 92 per cent (Fig. 3d). On the other hand, fractional crystallization of sodi-calcic plagioclase (in the order of 12 per cent) from tonalite melt can produce the same REE distribution pattern as in Singhbhum Granite (type A) (Fig. 2c). The still younger phases of Singhbhum granites might have been produced by partial melting of tonalite slabs involved in subduction analogue processes with a progressively lower degree of melting. For potash-rich pegmatoid granite, a possible sedimentay source rock can also be suggested (Sengupta et al., 1983), but field evidence in support of such regional sedimentation is as yet inconclusive.

The sialic crustal block serving as basement to the younger Proterozoic basin developed within a span of ca. 600 Ma. The spatial extension was possibly accompanied by growth in depth to add rigidity to the developing crustal plate (cf. Naqvi et al., 1974). The growth of the Singhbhum Craton started with the formation of sinks (caused by impact) or thermal pools, followed by repeated subduction analogue processes accompanied by partial melting of the incipient crust with progressively changing composition. The culmination of the process, with formation of potash rich granites at ca. 3100 Ma ago (Saha et al., 1986), was followed by more familiar rock.

DEVELOPMENT OF THE SINGHBHUM MARGINAL BASIN

Subsequent to the cratonization of the sialic block, the Singhbhum terrain witnessed, during the early Proterozoic, the emergence of a marginal basin girdling the northern fringe of the granitic platform. The Singhbhum Proterozoic basin demands the same status as many other fossil marginal basins of the world (Bose and Chakraborti, 1981; Windley, 1984b). Volcanism with a bimodal compositional character started from the very inception of the basin. The Dalma volcanic belt, developed along the spine of the linear marginal basin, runs for a distance of 180 km. (Dunn and Dey, 1942) and strikingly manifests the compositional bimodality, viz., ultrabasic volcanics at an early phase followed by the bulk of the basaltic eruption (1547 Ma). Such a compositional bimodality is reminiscent of analogous Archaean events in greenstone belts. Because of this striking similarity in geologic process across the time boundary, rather closer attention may be paid to the geochemistry of these volcanics. Further, as mentioned earlier, the sedimentation pattern in the basin, particularly to the immediate north of the Singhbhum platform, demands attention.

The mid-basinal Dalma volcanism is characterised by an early phase of Mg-rich products, their MgO contents being about 20 wt. per cent. On a normative basis, these volcanic rocks are picritic although, very rarely, they give indications of being boninitic. CaO/Al_2O_3 ratios of Dalma ultrabasic rocks range from 0.6 to 1.6 and in conventional chemographic schemes they appear to be akin to Geluk-type komatiites (Bose and Chakraborti, 1981). Al_2O_3/TiO_2 ratios in these rocks range from 16 to 19, which again is comparable to lower Proterozoic Cape Smith komatiites (A.D.Saunders, personal communication). Like most ultrabasic magmas, the Dalma picrites are also characterised by very low abundances of Na, K and Rb and most of the other incompatible elements such as Zr, Y, Ti and P along with Sr. Concentrations of these trace and minor elements in early Dalma lavas are much lower than in N-type mid-

TABLE I.

Trace-element ratios in Dalma lavas and other terrestrial magmas.

	1	2	3	4	5	6
Ti/Zr	89	100	110	110	110	70
TiO_2/P_2O_5	11.5	11.7	11	13	9-15	-
CaO/Al_2O_3	0.93	0.77	1	1	0.8	-
Zr/Y	2.6	2.6	2.5	2.6	2	3.2
Ti/V	12.2	18.1	14	19	22	16
Th/Ta	-	9.6	-	-	1.25	14
La/Ta	-	19	-	-	18	111
Zr/Hf	-	34.9	-	-	39	41

1. Dalma basalt, 2. Dalma ultrabasic rock, 3. STPK: Spinifex textured peridotitic komatiite (Nesbitt and Sun, 1980), 4. Cape Smith : Lower Proterozoic komatiite province (Nesbitt and Sun, 1980; Sun, 1980), 5. MORB : N-type midoceanic ridge basalt (compiled), 6. IAT :Island-arc tholeiite. Data source: Bose, Chakraborti and Saunders, in preparation. Representative (rather than average) values of least fractionated samples have been chosen.

oceanic-ridge basalts (Bose, Chakraborti and Saunders, in preparation). Ti/Zr ratios in these rocks often exceed 100, such values being comparable to modern-day MORB (Table 1). Consistent with this observation, the Dalma rocks show strong LREE depletion (Chakraborti and Bose, 1985, Bose, Chakraborti and Saunders, in preparation).

The Dalma basalts in bulk are low-potash, moderately evolved tholeiites with Mg values (100 x Mg/Mg + Fe) ranging from 41 to 64. Most of the analysed Dalma basalts are characterised by LREE depletion. Zr-Y relations and Ti/Zr ratios in Dalma basalts are comparable to N-type MORB (Table I). La/Ta ratios ranging from 14 to over 30 bring Dalma basalts close to modern N-type MORB (Table I). Local pillowed surfaces of the Dalma lavas attest to their subaqueous eruption.

In recent years there has developed a trend toward interpreting palaeo-tectonic settings of magmtism from "diagnostic" diagrams based on basalt geochemistry. Undue emphasis on some of the selected diagrams has given rise to confusion regarding tectonic interpretations of some volcanic provinces (Morrison, 1978; Thompson et al., 1980; Wood 1980). Although the applicability of some "diagnostic" diagrams has been questioned, most workers agree on the validity of such a chemographic approach in recognizing magma types. Further, increasing "available data" may lead to slight modifications of the diagrams, use of several diagrams in conjunction (Wood, 1980) and even reassessment of the "known" setting of the volcanics. The present contribution offers little scope to discussing the role of such "diagnostic" diagrams in evaluating the tectonic setting of Dalma lavas and such a chemographic presentation for them has not been incorporated in this study. It may, however, be mentioned that in most of the conventional discrimination diagrams based on incompatible elements and proportions, the Dalma basalts scatter over low-K tholeiites or ocean-floor basalt and some reveal their affinity to MORB. It is to be emphasized here that whatever may be the debate on the applicability of specific diagnostic *diagrams*, trace-element characteristics of different magma types are well established (Morrison, 1978) and from this view point particular significance should be attached to the depleted character of basalts in evidencing the signature of the mantle source, because it is hardly possible to derive depleted magma otherwise. Therefore, the overall depleted character of Dalma lavas, as described earlier may be considred diagnostic in recognizing their affinity with MORB (Table I) and this magma type is well known as being associated with distinct tectonic settings.

Dalma ultrabasic rocks have geochemical affinity with Archaean (spinifex textured) peridotitic komatiite (Table 1), which again documents that such magma genesis and related tectonics move across time planes from the Archaean into the Proterozoic. The geochemistry of Dalma basalts bears the signature of a parent depleted mantle source. The *MORB-like* trace-element character in Dalma basalt, viewed in conjunction with the geologic setting of the terrain, is indicative of rift tectonics developed along the *median zone* of the basin, as often manifested in ancient and present-day back-arc settings (Windley, 1984b). The signature of arc volcanism on the Dalma belt (Naha and Ghose, 1960) is almost illegible. On the other hand, Dalma lavas might have formed in a setting *analogous* to a back-arc basin. Back-arc basalts commonly exhibit compositions transitional between MORB and island arc basalts (Saunders and Tarney, 1979; Wood et al., 1979). Tarney, et al. (1976) have proposed a general model whereby greenstone belts originated in a back-arc setting and such a suggestion for the Dalma belt seems to be tenable. The occurrence of the bimodal basalt-ultrabasic couple in the Dalma belt suggests that the association and connected crustal history can continue into the Proterozoic too, though on a localized scale.

The inferred tectonic environment for the Dalma volcanism and thus for the Singhbhum Basin, finds support when the metamorphic and sedimentary history of the basin is viewed critically. A very important observation by Naha (1965) on the metamorphic evolution of the basin needs emphasis in this connection. According to Naha (1965, p.75), andalusite developed "*very early*" in the belt as a metamorphic mineral *independent* of the Barrovian zones and the mineral is spatially related to the site of volcanism. As suggested earlier (Bose and Chakraborti, 1981), as a precursor of Dalma volcanism and rifting, there was a regional rise of geoisotherms along the median zone of the basin which controlled the development of andalusite much earlier than regional metamorphism. The crustal swelling was followed by rifting and subsequent collapse which strongly controlled the sedimentary and tectonic history of the basin.

A very significant clue relating to the structure of the basin is furnished by a geophysical investigation over the region (Verma et al., 1984). The Singhbhum Basin to the north of the granitic platform is characterized by a significant positive gravity anomaly such as is normally observed over oceanic structures in general. For a similar situation in the western extension of the basin, these authors have inferred a basaltic floor for the cover sediments. It seems very likely that the positive gravity anomaly over the Singhbhum Basin is due to a simatic floor. Significantly, an earlier geophysical study on a section of the Dalma volcanic belt demonstrated its large depth extension (Bhattcharyya and Bhattacharyya, 1970). Taking into consideration the subsurface data, the absence of any floor for the Dalma lavas and profuse contemporaneous lavas interleaved with the sediments suggest a simatic oceanic floor for a larger part of the Singhbhum Basin with a possible mid-oceanic furrow along the median zone. Possibly, the lavas spreading over the basin ascended through attenuated crust via rifts and accompanying fracture zones. Thus the geochemistry of the lavas and the decipherable crustal history in the basin can be reconciled in terms of a back-arc situation.

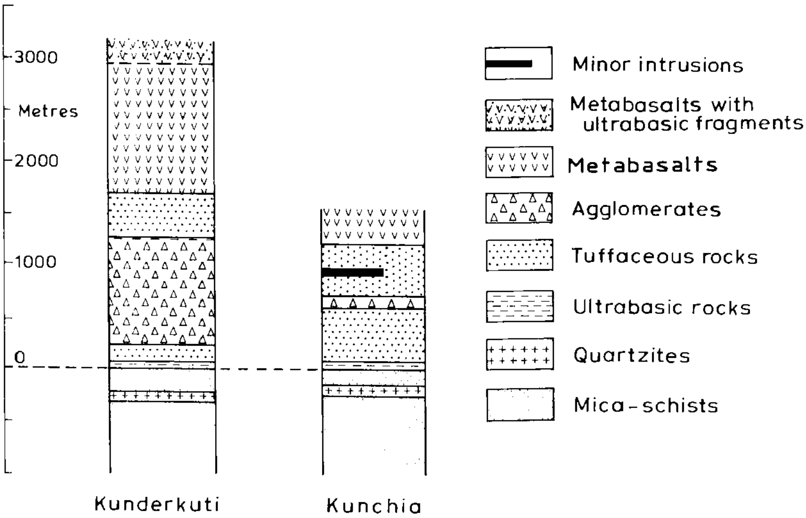

Figure 3. Profile showing stratigraphy of volcanics in the mid-basinal Dalma hill range

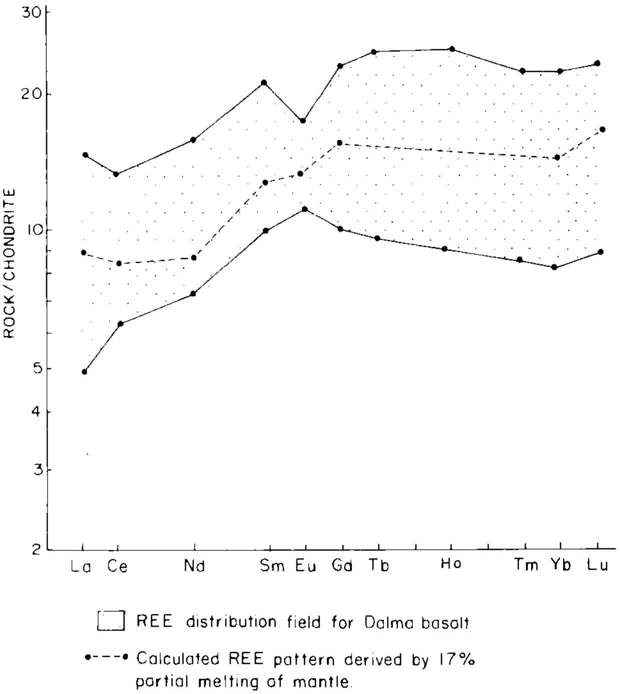

Figure 4. Chondrite-normalised REE distribution field for Dalma basalt along with REE pattern for a melt derived through 17% melting of mantle source.

Melting Model for Dalma Volcanism

A mantle-melting model based on the observed lava sequence has been tested. Field studies indicate that the basin filling was accompanied by contemporaneous thin mafic flows (Dunn and Dey, 1942; Bose, unpublished data), followed by picritic lavas (Bose and Chakraborti, 1981; Bose, 1982). This was followed by a period of cessation and deposition of locally reworked pyroclastics and finally by basaltic outpouring, manifesting the main Dalma volcanicity (Fig.4). The melting model based on this lava stratigraphy suggests that a spinel peridotite mantle, on limited (ca. 10%) melting, can generate the intial phase of minor mafic lavas, rendering a relatively depleted source which on 25 percent melting produced the Dalma picritic liquid with characteristic REE abundances. On separation of the picritic fraction, the source became too depleted to produce significant amounts of melt corresponding to the Dalma basalt. As mentioned earlier, during the cessation of magmatic activity some degree of mantle replenishment or mantle metasomatism took place in the sub-basinal zone. This might have been effected by limited mixing of EMR and DMR as conceived by Condie (1986). The partly replenished source suffered partial melting of about 17% to produce the bulk of Dalma basalt with its own geochemical characterisation (Fig. 4).

SEDIMENTATION PATTERN - A CASE OF POLARITY

The sedimentation pattern in the Singhbhum marginal basin, particularly along the northern fringe of the platform, is significant because of the imposed polarity, controlled by eroding basement on the one hand, and active volcanism along the mid--basinal zone (Fig.5). The mid-basinal ridge-rift system separated the whole marginal basin into two domains or sub-basins of which the southern basin was influenced by platform wash, mass gravity flow and melange, whereas the northern basinal domain was more restricted in nature, with relatively greater abundances of carbonate and carbonacous facies and volcanogenic clays (Bose, under preparation). The two sub-basins ultimately evolved as two discrete metamorphic belts during the closure of the basin. It may be mentioned that the depositional character of the Singhbhum Basin is consistent with the evolution of sedimentary rocks through the ages (Sutton and Windley, 1974) and the investigated sedimentary apron corresponds to an age level near 2200 Ma

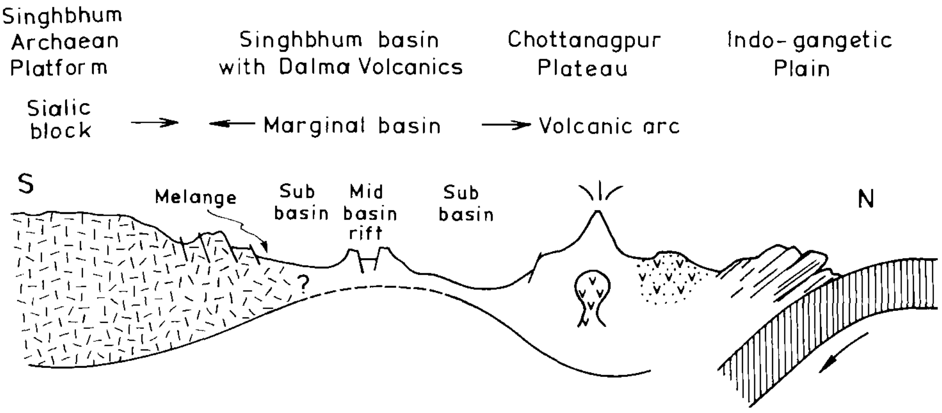

Schematic tectonic setting for Singhbhum fossil marginal basin.

Figure 5. Diagrammatic presentation of the tectonic setting of the Singhbhum Proterozoic basin.

(Bose and Chakraborti, 1981), which is in harmony with the available isotope age (2100 Ma) available for basinal rocks. The proximal zone immediately flanking the sialic platform to its north is characterized by dominance of mass-flow deposits, particularly pebble-oriented para-conglomerate (redeposited conglomerate), silici-clastic sediments and discontinuous bands of olistostromes (Bose, under preparation).

Several significant aspects of the conglomerate need to be mentioned here as they may serve as clues to the sedimentation pattern. In view of its pebble composition, the conglomerate may be designated as siliciclastic polymictic. The pebbles represent a highly mature assemblage and are compositionally unrelated to immediately underlying basement tonalite and the conglomerate may be said to have a non-erosive base. The conglomerate has a clast--oriented fabric and pebbles are usually floating in a phyllitic (muddy) matrix. Although, locally much flattened, the pebbles frequently reveal a primary character and are possibly protected from deformation by the matrix cushion. The preferred dimensional orientation of the pebbles is likely to be due to mass flowage and is to be reconciled in terms of the striking contrast between pebble composition and the matrix.

The conglomerate, with a local veneer of carbon shale and phyllite, is followed by siltstone. The least reconstituted rock is found to be quartzwacke with rounded to well - rounded

TABLE 2.

Chemical Compositions of mature and immature sediments from Proterozoic basin of Singhbhum, India.

	1	2	3	4	5	6
SiO_2	86.97	83.48	48.82	83.69	88.00	44.70
TiO_2	0.37	0.44	1.07	0.28	Tr	0.46
Al_2O_3	3.89	9.80	11.36	8.02	5.58	18.10
Fe_2O_3	4.49	0.40	25.35	2.50	0.38	1.79
FeO	-	-	-	-	0.98	10.72
Mgo	0.98	-	3.31	0.13	0.72	12.45
MnO	0.18	0.02	0.08	0.05	-	0.12
CaO	0.10	0.01	1.76	0.79	1.95	5.16
Na_2O	-	0.29	-	1.56	0.30	1.37
K_2O	0.46	2.70	1.93	1.15	0.30	0.08
P_2O_5	0.04	0.02	1.32	0.02	Tr	0.07
L.O.I.	1.64	1.45	4.61	1.07		
Total	99.12	98.61	99.61	99.26	98.21	95.02
SiO_2/Al_2O_3	22.36	8.52	4.30	10.43	15.77	2.47
$SiO_2/(Na_2O+K_2O)$	189.0	27.9	25.3	30.8	146.7	30.8

1. Siliciclastic rock (quartz-wacke) from basal part of Singhbhum cover sediment close to basement (Sp.No.160).
2. Siliceous Olistostrome from proximal zone of Singhbhum basin (Sp.No.191) contains carbon, not estimated.
3. Chlorite-quartz schist (with prophyroclasts of apatite and magnetite) approaching distal zone (Sp.No.GAR/1).
4. Arkosic-quartzite component of flysch type turbidite (rhythmite) in distal zone of the basin (Sp.No.GAR/1).
5. Average of 2 Archaean quartzites from Holenarasipur, (Naqvi 1978, Table 2).
6. Average of 5 chlorite schist from Holenarasipur (Naqvi, 1978, Table 2).

   Analysis of 1 to 4, carried out at AMSE laboratory, G.S.I., Bangalore. Total iron calculated as Fe_2O_3.

monocrystalline quartz grains set in a quartzose matrix. The wacke has K_2O/Na_2O <0.46 and Qz >65%. The compositional maturity of the rock is indicated by relatively high SiO_2/Al_2O_3 (Table 11). Moderately high roundness and good sorting of the framework may be suggestive of a recycled quartz-rich source or aeolian derivation of the grains which mixed with finer basin fillings (Bose, under preparation). Another significant feature of the proximal zone, and not hitherto reported, is the nonpersistent development of lithic wacke of intrabasinal origin. There is strong petrographic evidence that the rock fragments in this lithounit are largely derived from older parts of the sequence and such horizons are distinctly olistostromes. The clasts in the olistostrom are relatively angular (partly squashed) and poorly sorted. The flat and angular clasts, though matrix supported, are locally aligned in response to flow.

Far within the basin, the distal zone accommodated platform wash (with local uranium enrichment) and increasing amounts of chlorite which in its turn might indicate increasing non-terrigenous materials accompanying contemporaneous lava eruptions (Dunn and Dey, 1942; Bose and Chakraborti, 1981). Deeper within the basin, the latites are increasingly interlayered with arenaceous horizons. The intercalated arkosic sandstone shale sequence can be interpreted to be flysch type rhythmites (Table II). The rhythmites are regularly bedded and an individual sandstone bed continues for long distances without any sign of amalgamation. These sediments reaching the deeper part of the trough also flowed along the basinal axis in a restricted condition of fan development (Bose, under preparation).

The basin cover towards the southern contact with the platform (Fig. 5) is characterized by dismembered basement and ultramafic assemblages or tectonic slices (Bose and Chakraborti, 1981; Mukhopadhyay, 1984). This unstable platform edge triggering mass-flow deposits, therefore, defines a distinct melange which again manifests a polarity in the sedimentation pattern and deformation plan in the basin.

As mentioned at the outset, the Archaean basinal history has often been considered to be distinctive from the Proterozoic shelf guided sedimentation, the latter again characterized by quartz arenite. In contrast, the presently studied early Proterozoic belt has a basinal rather than a shelf-controlled history although the early sedimentary members are highly quartz rich (often supermature) as is often considered to be a Proterozoic imprint. Higher up in the sequence, the immature sediments are enriched in Ni and Co which may bring them closer to Archaean greywackes and this characteristic geochemistry again is controlled by a geological setting comparable to that in the Archaean, i.e., contemporaneous mafic volcanism and related volcanogenic sediments, although in a post-2.5 Ga terrane (Eriksson and Donaldson, 1986). Shelf sedimentation might have increased in abundance in comparison to basinal sediments across the Archaean - Proterozoic boundary, but at varying rates and degree of cratonization of the basement blocks (Eriksson and Danaldson, 1986).

CHOTANAGPUR HIGH-GRADE BELT

The Singhbhum Proterozoic basin has a tectonic boundary, a "boundary fault" against the northern high-grade metamorphic migmatite belt trending parallel to the basinal axis. The dominant component of this belt is a calc-alkaline gneiss interleaved with high-grade pelites and calc-magnesian metasediments. A significant feature, often considered as a signature of arc magmatism, is the abundant calc-alkaline magmatic emplacements in the belt. When in high-grade metamorphic dress, the dominant member of the suite, the hypersthene-bearing diorite, assumes the character of charnockites. The high-grade belt also accommodates massif-type anorthosite emplacements, thus bringing it to the status of well-known granulite belts such as are developed in many shield areas. Available data are strongly suggestive of a supra-subduction zone setting for this belt (Bose and Chakraborti, 1981). It is likely that bulk of the calc-alkaline sediments (now para-gneisses) along the belt is derived from erosion of felsic lavas. Recent gravity data from parts of the gneissic terrane (Mukhopadhyay, 1987) are suggestive of thickening of the crust by development of mafic slabs below this zone. This may be interpreted as underplating of parts of the mafic (oceanic) crust caused by collision tectonics. Thickened crust subjected to continued deformative forces lead to the development of graben formation perpendicular to the direction of tectonic transport. The belt also experienced late, minor alkaline and carbonatitic intrusions. It is therefore very likely that the Chotanagpur high-grade belt, like many other such Precambrian terranes (Windley, 1984b), developed through a process of plate destruction and is sited on a supra-subduction zone (Fig. 5). Further work to supplement the tectonic status of this high-grade belt is in progress.

CLUES TO DYNAMIC CAUSE - RESUME

The present study of the Singhbhum Precambrian terrane in the eastern Indian Shield offers an excellent opportunity to view closely the changing scenario of early crustal growth. At the same time, the area provides a case history to review the sweeping variation in the style of crustal tectonics through a span of Archaean to early Proterozoic. Windley (1984a) brought out elegantly the turning points in geologic processes during the

Archean-Proterozoic transition. The present study in a part of the Indian Shield evaluates some of the processes within a small spatial extent. The Archaean permobile crustal stage was dominated by repeated magmatism with changing chemistry of magmas, the major trail being increment in potassium at the expense of sodium (cf. Divakara Rao and Rama Rao, 1982), leading to the development of the Singhbhum sialic craton. The production of early tonalite was likely to be a two-stage process and the mechanism involved was analogous to subduction. In the melting process, the mantle was replenished repeatedly and also rapidly, affecting the growth rate of the nucleus.

The thickened Proterozoic crust accommadated a well-defined linear marginal basin (Singhbhum Basin, flanking the sialic craton) and gained rigidity adequate to respond to the processes of well-defined basinal growth accompanied by rifting and volcanism. These contributed to neocrustal growth both laterally and vertically. During the Proterozoic there was a distinct polarity in sedimentation, magmatism and tectonism, possibly in response to asymmetrical (unilateral) plate subduction. The present study distinctly identifies the Proterozoic crust to be closer to modern crust in terms of geologic processes. When looked at in detail, features like bimodal volcanism with an early phase of komatiitic chemistry and a later phase of depleted basalt, are reminiscent of Archaean episodes. It is also brought out through this study that the intimate volcano-sedimentary process in basin filling (simulating greenstone belts) is not confined to the Archean. It is evident that plate destruction (≈subduction) or its analogues were operative in a grander and well-defined style as the earth evolved from the Archaean to the Proterozoic.

ACKNOWLEDGEMENTS

I am thankful to Dr.A.D.Saunders, Department of Geology, University of Leicester, U.K., for his active co-operation in the study on Dalma volcanics and exciting discussions on the interpretative geochemistry of basalts. Valuable comments from Prof. D.E.Karig, Cornell University, Ithaca, N.Y., on the Singhbhum marginal basin are gratefully acknowledged. Sri. J.S.Ray, Department of Geology, Durgapur Government College, Durgapur, W.B., is thanked for his help in testing partial melting models.

Discussions with Dr.M.K.Chakraborti on the problems of Dalma volcanism have been very stimulating. I have benefitted from the encouragement received from Prof. A.K.Saha. The Director, AMSE Wing, Geological Survey of India, Banglore, is thanked for major-element analyses of a few samples.

REFERENCES

Arth, J.G. and Barker, F., 1976. Rare-earth partitioning between a hornblende and dacite liquid and implication for the genesis of trondhjemitic - tonalitic magmas. Geology, 4: 534-536.

Banerji, A.K., 1984. Crustal evolution and metallogeny of the Singhbhum region, eastern India. Indian. J. Earth Sci., CEISM Seminar, pp.171-182.

Basu, A.R., Ray, S.L., Saha, A.K. and Sarkar, S.N., 1981. Eastern Indian 3800 Ma old crust and early mantle differentiation. Science, 212: 1502-1506.

Bhattacharyya, D.S. and Bhattacharyya, T.K., 1970. Geological and geophysical investigations of a basaltic layer in Archaean terrain of eastern India. Bull. Geol. Soc. Amer., 81: 3073-7078.

Bose, M.K., 1960. On the gneissic granite of Champua, Keonjhar, Orissa. Proc. Nat. Inst. Sci. India, 26A: 143-151.

Bose, M.K. and Chakraborti, M.K., 1981. Fossil marginal basin from the Indian shield: a model for the evolution of Singhbhum Precambrian belt, Eastern India. Geol. Rundsch., 70: 504-518.

Bose, M.K., 1982. Precambrian picritic pillow lavas from Nominra, Keonthon, eastern India, Cur. Sci., 51: 14.

Chakraborti, M.K. and Bose, M.K., 1985. Evaluation of the tectonic setting of Precambrian Dalma volcanic belt, Eastern India, using trace element data. Precamb. Res., 28: 253-268.

Condie, K.C., 1980. Origin and early development of the earth's crust. Precamb. Res., 11: 183-197.

Condie, K.C., 1986. Origin and early growth rate of continents. Precamb. Res., 32: 261-278.

Divakara Rao, V. and Rama Rao, P., 1982. Granitic activity and crustal growth in the Indian shield. Precamb. Res., 16: 257-271.

Dunn, J.A. and Dey, A.K., 1942. Geology and petrology of eastern Singhbhum and surrounding areas. Mem. Geol. Surv. India, 69, 2: 281-356.

Eriksson, K.A. and Donaldson, J.A., 1986. Basinal and shelf sedimentation in relation to the Archaean Proterozoic Boundary. Precamb. Res., 33: 103-121.

Glikson, A.Y. and Lambert, I.B., 1976. Vertical zonation and petrogenesis of the early Precambrian crust in W. Australia. Tectonophysics. 30: 55-89.

Moorbath, S., Taylor, P.N. and Jones, N.W., 1986. Dating the oldest terrestrial rocks - fact and fiction. Chem. Geol, 57: 63-86.

Morrison, M.A., 1978. The use of 'immobile' trace elements to distinguish the palaeotectonic affinites of metabasalts: application to the Palaeocene basalts of Mull and Skye, northwest Scotland. Earth Planet. Sci. Letters, 39: 407-416.

Mukhopadhyay, D., 1984. The Singhbhum shear zone and its place in the evolution of the Precambrian mobile belt of north Singhbhum. Indian J. Earth Sci., CEISM Seminar, pp.205-212.

Mukhopadhyay, M., 1987. Gravity field and its significance to the origin of the Bengal anorthosite, J.Geol. Soc. India, 29: 489-499.

Naha, K., 1965. Metamorphism in relation to stratigraphy, structure and movement in E. Singhbhum, East India. Quart. J. Geol. Min. Met. Soc. India. 37: 41-88.

Naha, K. and Ghosh, S.K., 1960. Archaean Palaeogeography of eastern and northern Singhbhum, E. India. Geol. Mag., 97: 436-439.

Naqvi, S.M., 1978. Geochemistry of Archaean metasediments: evidence for prominent anorthosite - norite - troctolite (ANT) in the Archean basaltic primordial crust. In: B.F. Windley and S.M. Naqvi (Editors), Archaean Geochemistry. Elsevier, pp.343-360.

Naqvi, S.M., Divakara Rao, V. and Hari Narain, 1974. The protocontinental growth of the Indian shield and the antiquity of its rift valleys. Precamb. Res., 1: 345-398.

Nesbitt, R.W. and Sun, S. S., 1980. Geochemical features of some Archaean and post-Archaean high magnesian low alkali liquids. Phil. Trans. Roy. Soc. London, 297 A: 365-381.

Saha, A.K. and Ray, S.L., 1984a. The structural and geochemical evolution of the Singhbhum granite batholithic complex, India. Tectonophysics, 105: 163-176.

Saha, A.K., and Ray, S.L., 1984b. Early and middle Archaean crustal evolution of the Singhbhum-Orissa craton. Indian J. Earth Sci., CEISM Seminar, pp.1-18.

Saha, A.K., Ray, S.L. and Sarkar, S.N., 1986. Early history of the earth-evidence from the eastern Indian shield (Abstract). Group Discussion on Precambrian of the Eastern Indian shield, Dhanbad, pp.1-2.

Sarkar, S.N., 1980. Precambrian stratigraphy and geochronology of Peninsular India : a review. Indian J. Earth Sci., 7: 12-26.

Sarkar, S.N. and Saha, A.K., 1977. The present status of the Precambrian stratigraphy, tectonics and geochronology of Singhbhum-Keonjhar-Mayurbhanj region, East India. Indian J. Earth Sci., 4: 37-65.

Saunders, A.D. and Tarney, J., 1979. The geochemistry of basalt from a back-arc spreading centre in the east Scotia sea. Geochim. Cosmochim. Acta, 43: 555-572.

Sengupta, S., Bandopadhyay, P.K. and Van Den Hul, H.J., 1983. Geochemistry of the Chakradharpur granite-gneiss complex - A Precambrian trondhjemite body from west Singhbhum, eastern India. Precamb. Res., 23: 57-78.

Sun, S.S., 1980. Lead isotopic study of young volcanic rocks from mid-ocean ridges, ocean islands and island arcs. Phil. Trans. Roy. Soc. London, A 297: 409-446.

Sutton, J. and Windley, B.F., 1974. The Precambrian. Sci. Prog., 61: 401-420.

Tarney, J., Dalziel, I.W.D. and DeWit, M.J., 1976. Marginal basin Rocas-Verdes" complex from S.Chile: a model for Archaean greenstone belt formlation. In: B.F.Windley (Editor), The Early History of the Earth, Wiley, London, pp.131-146.

Tarney, J. and Windley, B.F., 1981. Marginal basins through geological time. Phil. Trans. R. Soc. London, Ser, A: 301: 217-232.

Thompson, R.N., Morrison, M.A., Mattey, D.P., Dickin, A.P. and Moorbath, S., 1980. An assessment of the Th-Hf-Ta diagram as a discriminant for tectono-magmatic classifications and detection of crustal contamination of magmas. Earth Planet. Sci. Letters, 50: 1-10.

Verma, R.K., Sarma, A.U.S. and Mukhopadhyay, M., 1984. Gravity field over Singhbhum, its relationship to geology and tectonic history. Tectonophysics, 106: 87-107.

Windley, B.F., 1984a. The Archaean-Proterozoic boundary. Tectonophysics, 105: 43-53.

Windley, B.F., 1984b. The Evolving Continents. 2nd Edn., John Wiley Sons.

Wood, D.A., 1980. The application of a Th-Hf-Ta diagram to problems of tectonomagmatic classification and to establishing the nature of crustal contamination of basaltic lavas of the British Tertiary volcanic Province. Earth Planet. Sci. Letters, 50: 11-30.

Wood, D.A., Joron, J.L. and Treuil, M., 1979. A reappraisal of the use of trace elements to classify and discriminate between magma series erupted in different tectonic settings. Earth Planet. Sci. Letters, 45: 326-336.

GEOCHEMISTRY OF AN EARLY PROTEROZOIC BASIC GRANULITE-GNEISS SUITE AND PETROGENETIC IMPLICATIONS, ARUNTA INLIER, CENTRAL AUSTRALIA

A.Y.GLIKSON AND J.FODEN

ABSTRACT

Granulite-gneiss terrains of the southwestern Arunta Inlier, central Australia, include basic granulites pervasively intruded by stringers, bands, lenses and stocks of gneiss. The basic granulites include LIL element-depleted types, continental tholeiitic compositions and Fe-rich garnetiferous granulites. All display light/heavy REE enrichment. The basic granulites include layered anorthosite-pyroxenite units, including both LIL element-depleted and LIL element-enriched meta-cumulates. Comparisons between depleted and enriched basic granulites suggest LIL element mobility in the increasing sequence: Sr<Ti<Y<P<Zr <K<Ce<Ba<Th. Major and trace elements modelling suggests that partial melting of LIL element-depleted Mt-Hay type basic granulite is only capable of producing K-high gneiss bands if alkali elements were added from an extraneous source. Partial melting of LIL element-normal to high Mt-Chapple type basic granulite is capable of producing Mt-Chapple type intermediate gneiss units if amphibole is accounted for as a residual phase. Petrogenetic modelling of the rare earth elements supports derivation of Mt Isa-type granitoid magmas by magmatic fractionation of basic source-derived acid melts. Partial melting of the basic granulites is consistent with P-T estimates based on garnet-pyroxene assemblages (680^{o}-770^{o}; 7.3-8.1 kb), locating these rocks between the dry and the wet gabbro solidi. No uniform depletion of LIL elements, including U and Th, is observed in the granulite/gneiss terrain, and some units are LIL element enriched. Comparisons of Ce/Y, Sm/Nd and Rb/Sr ratios in Archaean and early Proterozoic rocks suggest that the alkali and light REE enrichment may have been related to a secular increase in these values in the underlying lithosphere.

INTRODUCTION

Geochemical studies of high grade metamorphic suites allow insight into the nature of their protoliths, partial melting and magmatic fractionation processes, the origin of granitic magmas and chemical zonation of the continental crust. Marked depletion of Scourian granulites in K, Rb, Th, and U, was demonstrated by Sheraton (1970), Sheraton et al., (1973) and Weaver and Tarney (1981a). Lambert and Heier (1967 and 1968) showed that pyroxene granulites in central and Western Australia are significantly depleted in U and Th relative to associated lower grade rocks. However, depletion of large ion lithophile (LIL) elements in granulite facies terrains is not uniform (Tarney and Windley, 1977; Condie and Allen, 1984). Low LIL-element abundances have been variously attributed to original low-LIL compositions of the tonalite-trondhjemite protoliths (Glikson and Sheraton, 1972; Glikson, 1979; Sheraton and Black, 1983; Sheraton and Collerson, 1984), partial melting and/or loss of a fluid phase (Lambert and Heier, 1967; Sighinolfi and Gorgoni, 1978; Tarney, 1976; Tarney and Windley, 1977), and flushing by CO_2-rich volatiles (Newton et al., 1980; Hansen et al., 1984). In contrast to the alkali elements, the relative immobility of the rare earth (RE) and high field strength (HFS) (Ti, Zr, Nb, P, Y) elements during metamorphism (Condie et al., 1977; Humphries and Thomson, 1978; Beswick 1982, 1983) increases the primary petrogenetic significance of these elements, as discussed in this paper.

The importance of basic granulites and anorthosites in the lower continental crust has been emphasised by Fountain and Salisbury (1981), Arculus et al., (1985), Thompson (1985) and others from the study of high grade terrains, crustal xenoliths in alkaline lavas, and seismic reflection data. The high grade metamorphic terrain of the Arunta inlier, central Australia (Stewart et al., 1984; Shaw et al., 1984) allows the study of deep-seated palingenesis, related to the extensive igneous activity which occurred throughout the North Australian Precambrian shield 2.0-1.6 Ga. ago (Wyborn and Page, 1983; Etheridge et al., 1984). Basic granulites intruded by swarms of gneiss stringers and units of felsic-intermediate gneiss containing enclaves of basic granulite are exposed in large massifs in the southwestern part of the inlier (Fig. 1) (Glikson,

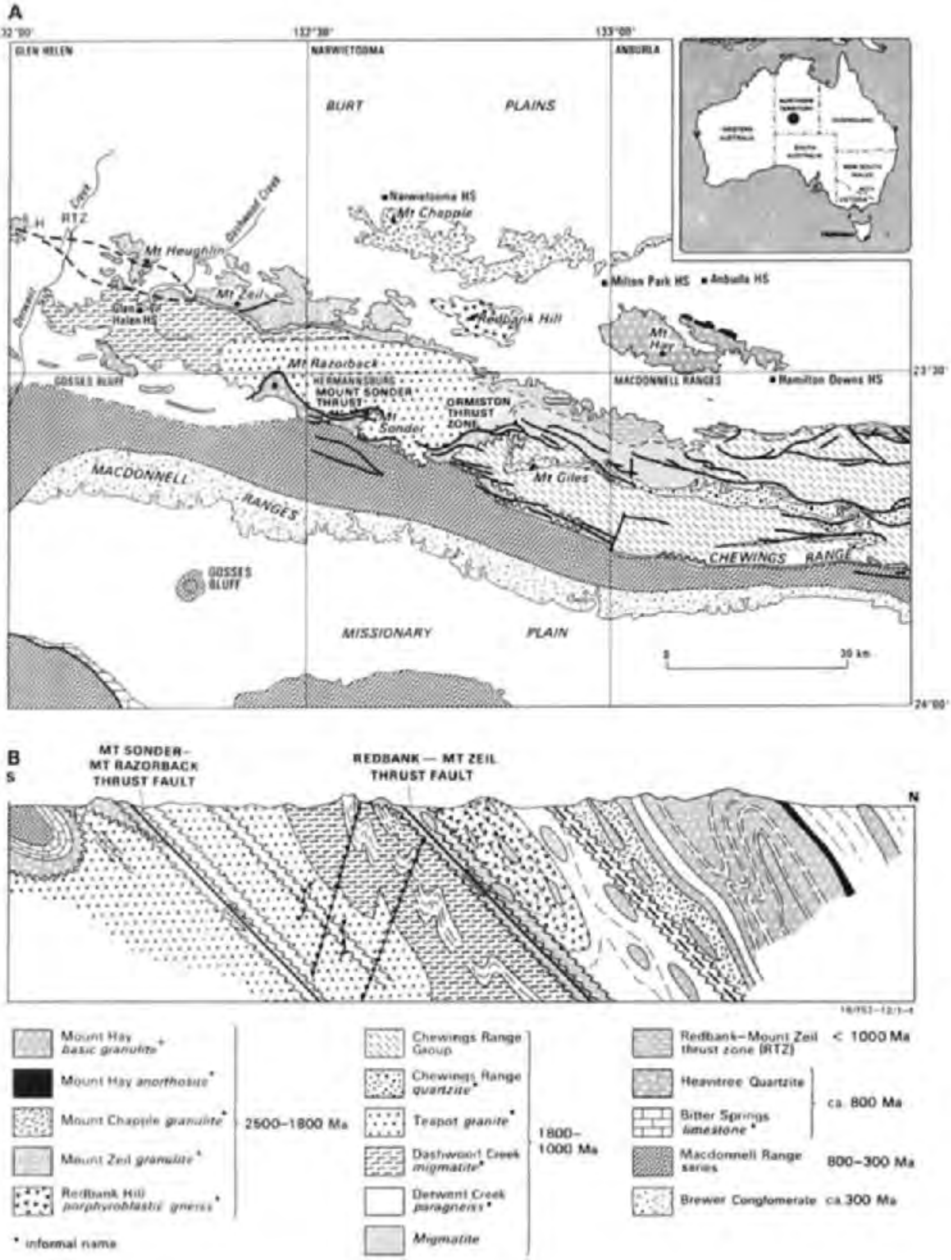

Figure 1. A geological sketch map and schematic cross section of part of Arunta Inlier, central Australia, showing the principal stratigraphic and structural units within the Hermannsburg 1:250,000 Sheet area.

A

B

C
Hermannsburg
granulites project
1974 (1)
A.Y Glikson
B.M.R., Canberra.

D
Hermannsburg
granulites project
1974 (1)
A.Y Glikson
B.M.R., Canberra.

1984, 1986, 1987). This paper is concerned with the geochemistry of these rocks, with reference to the nature and composition of the basic protoliths, the origin of the felsic-intermediate gneisses and their relationships with basic granulite.

GEOLOGY, PETROGRAPHY AND ISOTOPIC AGES

The southwestern part of the Arunta inlier consists of several latitudinal zones separated by major thrust faults, including the Mt Hay - Mt Chapple - Redbank Hill - Mt Zeil - Papunya granulite-gneiss zone (Fig. 1) located between the late Proterozoic-Palaeozoic Ngalia Basin to the north and the Redbank-Mt Zeil thrust fault to the south. The oldest recognized components in this zone are basic granulites of the Mt Hay massif and petrographically similar enclaves within felsic-intermediate amphibolite to granulite facies gneisses of the Mt Chapple, Redbank Hill and Mt Zeil massifs. The Mt Hay granulites yield Sm/Nd model ages of T^{Nd} =2.19 and 2.35 Ga. and T_{CHUR}=2.08 and 2.03 Ga. (Black and McCulloch, 1984). The same rocks yield Rb/Sr isochron ages of 1778 ± 20 Ma. (Ri = 0.7085) and 1728 ± 65 Ma. (Ri=0.706) which probably reflect metamorphic events (Black et al., 1983). The massifs include Qz-normative basic granulites, ferroan garnetiferous basic granulites, anorthosites interbanded with metapyroxenites, bimodal banded granulite-gneiss units, K-feldspar-orthopyroxene bearing granulites and supracrustal rocks including metapelites and calc-silicates. The felsic units occur as stringers and stromatic bands (Fig. 2a), porphyroblastic stringers (Fig. 2d), bands and lenses (Fig. 2c) of amphibolite to granulite facies gneiss. Agmatitic structures abound where concordant to subconcordant gneiss veins engulf basic relics (Fig.2b).

Figure 2. Relationships between basic granulites/amphibolites and gneiss/migmatite/charnockite units in the Mt Chapple, Redbank Hill and Mt Zeil massifs. A) Isoclinally-folded stromatically veined basic granulites-gneiss rock, showing mm to cm-scale plagioclase-dominated bands intruded concordantly along a weak gneissosity in the granulites. MT Chapple. B) Agmatitic structures in basic granulites, consisting of plagioclase- rich veins intruded subconcordantly in relation to the gneissosity of the granulites. Mt Chapple. C) Plagioclase-rich gneiss lenses and laminae in basic granulites, showing ortho-pyroxene-biotite-plagioclase-quartz gneiss intruding and or containing relics of two-pyroxene mafic granulite, Mt Chapple. D) Stromatic banded glomeroblastic/ porphyroblastic gneiss and basic granulite. Both plagioclase and K-feldspar porphyroblasts are present, in places outlining poorly defined rapakivi texture. Mt Chapple.

Felsic gneiss and charnockite terrains contain abundant xenoliths of basic granulite and migmatites contain abundant amphibolite xenoliths. Blastoporphyritic gneiss at Redbank Hill, 5 km north of the Redbank-Mt Zeil thrust zone (RTZ), has yielded a K-feldspar-whole-rock Rb-Sr isochron age of 893±97 Ma. (Ri=0.756) (Marjoribanks and Black, 1974), likely to reflect dislocation and retrogression along the RTZ.

The Mt Hay massif consists of isoclinally folded, massive to gneissose and lineated basic granulites (opx-cpx-plg±amph,biot, il,mt,qz) containing gneiss and charnockite bands (opx-plg± amph, biot,il,mt,qz) and layered anorthosite (opx-cpx-amph-plg)-metapyroxenite units. The gneiss bands consist of opx-plg assemblages and K-feld-plg-biot-qz (±gnt) assemblages paragneiss units comprising garnet-sillimanite gneiss, calc-granulite (cpx-plg±amph,scap,sph,gnt,ca,il,mt,qz) and rare quartzitic layers are intercalated with basic granulite lenses, along the northern flank of the Mt Hay massif. The Mt Chapple massif contains similar rock types although anorthosites have not yet been found. The estimated overall mafic/felsic rock ratio in this massif is less than 1/5. This terrain includes garnet-bearing basic granulites (gnt-opx-cpx-biot-amph-plg-qz) and is dominated by charnockites (opx-plg-qz±cpx,amph,biot,K-feld),including porphyroblastic gneiss with augen of sanidine. Paragneiss units are present, but their distinction from orthogneiss is difficult. In places, high grade gneiss and migmatite engulf enclaves of basic granulite and amphibolite (Fig. 2). Redbank Hill is characterized by very coarse grained deformed amphibolite-facies blastoporphyritic orthogneiss (gnt-amph-biot-plg-K-feld-qz) containing metre-scale and thicker basic granulite and hybridized granulite, the overall mafic/felsic ratio being estimated as about 1/20. An even lower mafic/felsic ratio pertains in the Mt Zeil massif, which consists predominantly of charnockite, garnet-biotite gneiss and biotite gneiss. The above terrains include garnet-sillimanite paragneiss layers. PT estimates on garnet-two pyroxene basic granulites from Mt Chapple suggest temperatures of 680-770°C and pressures of 7.3-8.1 kb (Glikson, 1984).

ANALYTICAL METHODS

Major element and minor element data, CIPW norms, selected ratios and petrographic definitions are given in Table 1.

TABLE 1 - CHEMICAL ANALYSIS, CIPW NORMS AND SELECTED RATIOS

	high-Mg basic granulites						tholeiitic basic granulites									garnet-bearing tholeiitic basic granulites			
	Mt Hay			Mt Chapple	Redbank Hill		Mt Hay					Mt Chapple				Mt Chapple			
	S43	S83	S86	S149	S239	S228	S73	S36	S80	S72	S82	S132	S133	S136	S197	S188	S201	S131	S203
SiO_2 % wt	49.54	49.46	50.56	52.37	49.05	50.40	49.98	50.43	50.03	51.04	48.15	53.21	52.29	55.81	52.12	50.42	53.63	53.57	52.81
TiO_2	0.44	0.41	0.47	0.59	0.90	0.68	1.13	1.11	0.92	1.04	1.01	0.82	0.91	1.01	1.15	0.92	1.32	1.64	1.57
Al_2O_3	16.66	16.65	15.85	7.40	10.85	15.00	15.61	15.23	14.55	14.33	15.05	15.21	15.10	14.81	14.06	15.40	13.56	16.04	13.89
Fe_2O_3	1.37	1.92	1.79	1.36	0.92	1.00	1.39	1.41	1.67	1.55	1.77	0.96	1.33	1.44	2.66	1.70	4.59	2.99	5.77
FeO	7.12	7.12	6.97	6.37	12.43	8.00	9.46	9.88	10.52	10.02	10.95	7.75	8.04	7.44	9.49	9.03	8.57	9.28	8.28
MnO	0.16	0.17	0.17	0.17	0.22	0.16	0.17	0.19	0.19	0.20	0.22	0.14	0.15	0.15	0.19	0.17	0.19	0.19	0.18
MgO	9.59	8.99	8.22	12.91	14.79	9.34	7.99	7.44	7.73	7.07	7.72	6.88	6.34	4.69	5.75	7.16	4.77	4.19	4.15
CaO	12.61	12.45	12.85	15.46	6.55	10.94	10.90	10.68	11.00	11.27	12.39	10.07	10.33	8.45	9.73	10.08	8.46	7.95	8.21
Na_2O	1.51	1.58	2.15	0.87	1.33	1.76	1.95	2.02	1.89	2.16	1.78	2.11	2.30	2.45	2.87	2.42	2.67	1.95	1.94
K_2O	0.08	0.09	0.15	0.83	0.43	0.79	0.54	0.69	0.47	0.77	0.15	1.30	1.23	1.82	1.11	0.83	1.39	1.11	1.55
P_2O_5	0.03	0.03	0.03	0.17	0.25	0.16	0.14	0.15	0.10	0.12	0.11	0.12	0.14	0.18	0.14	0.12	0.19	0.42	1.30
L.O.I.	1.01	1.13	0.94	0.11	1.35	1.41	0.92	0.96	0.99	0.79	1.00	0.93	0.86	0.79	0.93	0.99	0.71	0.72	0.72
Total	100.12	100.00	100.13	98.61	99.07	99.64	100.18	100.19	100.06	100.36	100.30	99.50	99.02	99.04	100.20	99.24	100.05	100.05	99.37
Mg^1*	70.6	68.1	66.8	78.1	70.0	68.8	61.0	58.3	57.4	56.5	56.3	62.6	59.0	43.0	50.4	58.7	44.1	42.3	39.2
CIPW norm % wt																			
Fo	1.25		0.77		5.45	1.19	0.48				3.07					0.83			
Fa	0.65		0.44		3.35	0.72	0.38				2.99					0.70			
En	15.90	16.37	11.59	14.21	27.72	24.99	14.45	13.84	14.11	11.59	8.86	12.38	10.73	8.29	9.07	12.20	7.53	9.54	7.19
Fs	7.47	7.91	5.97	4.24	15.48	16.14	10.42	11.31	12.03	10.14	7.83	8.73	8.27	7.67	8.45	9.35	6.19	10.84	5.46
Wo	10.08	9.92	12.79	26.17	3.63	9.58	8.80	9.07	10.15	11.74	11.82	8.89	9.82	7.10	10.58	8.72	8.33	2.08	5.99
En	6.42	6.72	7.94	18.43	2.20	5.84	4.91	4.83	5.32	6.09	6.11	5.00	5.35	3.60	5.35	4.76	4.43	0.97	3.28
Fs	3.01	3.03	4.09	5.50	1.23	3.20	3.54	3.95	4.54	5.33	5.40	3.52	4.12	3.33	4.98	3.65	3.64	1.10	2.49
Mt	2.00	2.82	2.62	2.00	1.37	1.48	2.03	2.06	2.44	2.26	2.58	1.41	1.96	2.13	3.89	2.51	6.70	4.36	8.48
Il	0.84	0.79	0.90	1.14	1.75	1.31	2.16	2.12	1.76	1.98	1.93	1.58	1.76	1.95	2.20	1.78	2.52	3.14	3.02
Ap	0.07	0.07	0.07	0.41	0.61	0.39	0.33	0.36	0.24	0.29	0.26	0.29	0.34	0.43	0.33	0.29	0.45	1.00	0.72
An	38.79	38.51	33.43	14.05	22.89	31.23	32.49	30.69	30.11	27.25	32.86	28.60	27.76	24.47	22.37	29.22	21.05	31.95	24.95
Ab	12.89	13.52	18.34	7.47	11.52	15.16	16.62	17.22	16.14	18.35	15.17	18.11	19.83	21.10	24.46	20.84	22.74	16.61	16.64
Or	0.48	0.54	0.89	4.98	2.60	4.75	3.21	4.11	2.80	4.57	0.89	7.79	7.40	10.95	6.61	4.99	8.27	6.60	9.28
Qz		0.09		1.23				0.23	0.16	0.22		3.55	2.51	8.85	1.53	7.97	11.63	12.32	
Ba ppm	30	38	43	381	239	242	130	191	129	165	261	226	261	381	249	290	371	328	447
Rb				48	12	40	8	20	9	13		69	47	92	28	29	37	42	49
Sr	277	280	300	119	216	144	104	114	94	96	144	100	105	139	131	113	140	278	109
Pb			2	5	10	9	6	6	5	7	3	9	10	12	8	8	9	8	11
Th	1	2		2	18	2	1	1	1			6	3	2	2	3	1	1	3
U					11	1		1				1			1	1			
zr	7	11	12	96	210	75	84	89	59	61	41	81	83	138	86	72	115	111	209
Nb				2	12	5	4	7	4	4	3	5	6	9	6	4	7	12	12
Y	5		6	22	22	19	30	51	27	30	21	25	29	42	35	23	37	34	46
La				24	74	17	14	24	14	12	7	20	20	27	23	16	23	29	36
Ce			3	47	121	31	28	55	25	24	15	35	38	54	40	28	49	61	67
Nd				26	47	14	13	31	13	13	13	17	20	29	22	15	25	36	35
Sc	31	29	33	48	36	26	32	36	35	36	46	27	29	29	32	29	31	35	31
V	165	134	141	173	184	146	194	221	198	211	264	164	174	161	234	179	229	201	271
Cr	220	254	219	1011	1254	354	363	158	239	213	17	230	210	87	24	105	13	62	18
Ni	93	106	49	272	318	173	132	68	90	51	41	89	75	39	33	101	16	23	33
Cu	38	34	15	173	44	22	64	63	65	62	99	50	48	36	41	62	44	29	91
Zn	45	48	46	52	139	78	86	88	98	87	96	70	76	86	97	85	102	125	114
Ga	15	15	16	9	13	15	17	18	17	18	18	16	16	17	18	17	18	22	18

* Mg^1 = 100 MgO/(MgO+o.85(0.9Fe_2O_3 +FeO)) Mol%

TABLE 1 CONTINUED

	high-Mg basic granulites						tholeiitic basic granulites									garnet-bearing tholeiitic basic granulites			
	Mt Hay		Mt Chapple	Redbank Hill			Mt Hay					Mt Chapple				Mt Chapple			
	S43	S83	S.86	S149	S239	S228	S73	S36	S80	S72	S82	S132	S133	S136	S197	S188	S201	S131	S203
TiO_2/P_2O_5	14.7	13.7	15.7	3.5	3.6	4.2	8.1	11.1	9.2	8.7	9.2	6.8	6.5	5.6	8.2	7.7	6.9	3.9	5.2
Ti/Zr	377	223	234	37	26	54	81	75	93	102	148	61	66	44	80	77	69	89	45
Ti/Y	528		470	160	245	214	226	130	204	208	288	197	188	144	197	220	214	289	205
Ti/Sc	85	85	85	74	150	156	211	184	158	173	131	182	188	209	215	190	255	281	304
Zr/Y	1.4		2.0	4.4	9.5	3.9	2.8	1.7	2.2	2.0	1.9	3.2	2.9	3.3	2.5	2.9	3.1	3.3	4.5
Zr/Nb				48.0	17.5	15.0	21	12.7	17.7	15.2	13.6	16.2	16.7	15.3	14.3	18.0	16.4	9.2	17.4
CaO/Al_2O_3	0.75	0.75	0.81	2.9	0.60	0.73	0.70	0.70	0.76	0.79	0.81	0.66	0.67	0.57	0.69	0.65	0.62	0.52	0.39
CaO/TiO_2	28.6	30.4	27.3	26.2	7.3	16.1	9.6	9.6	11.9	10.8	12.2	12.3	11.3	8.4	8.5	10.9	6.4	4.8	5.2
Al_2O_3/TiO_2	37.9	40.6	33.7	12.5	12.0	22.1	13.8	13.7	15.8	13.8	14.9	18.5	16.6	14.7	12.2	16.7	10.2	9.8	8.8
(Ce/Y)N				5.28	13.59	4.3	2.31	2.66	2.29	1.98	1.76	3.46	3.24	3.18	2.82	2.7	3.27	4.43	3.60
(Ce/Nb)N				1.31	1.87	1.61	1.57	1.29	1.4	1.34	0.84	1.50	1.38	1.36	1.32	1.36	1.42	1.23	0.82
(Nd/Y)N				4.01	7.25	2.50	1.47	2.06	1.63	1.47	2.10	2.31	2.34	2.34	2.13	2.03	2.29	3.59	2.58
K/Rb	665	748	1245	143	297	164	560	286	433	491	1245	156	217	164	329	237	312	219	262
K/Ba	22.1	19.7	28.9	18.1	14.9	27.1	34.5	30.0	30.2	38.7	20.4	47.7	39.1	39.6	37.0	23.7	31.1	28.1	28.8
K/Pb			622	1377	357	729	747	954	780	913	415	1199	1021	1259	1151	861	1282	1151	1169
Rb/Sr				0.40	0.05	0.28	0.08	0.17	0.09	0.13		0.69	0.45	0.66	0.21	0.26	0.26	0.15	0.44
Ca/Sr	325	317	306	928	217	542	749	669	836	838	614	719	703	434	530	637	431	204	538
Ba/Rb				7.9	19.9	6.1	16.2	9.5	14.3	12.6		3.3	5.5	4.1	8.9	10.0	10.0	7.8	9.1
Ba/Sr	0.11	0.13	0.14	3.20	1.10	1.68	1.25	1.67	1.37	1.72	0.42	2.26	2.48	2.74	1.90	2.56	2.65	1.18	4.10
Ni/Cr	0.42	0.41	0.22	0.27	0.25	0.49	0.36	0.43	0.37	0.23	2.4	0.38	0.36	0.45	1.37	0.96	1.23	0.37	1.83
Fe/V	393	513	473	470	559	1473	429	392	472	420	369	407	412	394	459	431	463	385	

	Calc-granulites		Anorthosites					intermediate-felsic gneiss							
								Mt Hay				Mt Chapple			Redbank Hill
								paragneiss							
	S53	S55	S28	S48	S65	S66	S45	S52	S57	S30	S71	S198	S196	S202	S130	S227
SiO_2 % wt	48.50	45.43	49.54	51.11	49.14	48.37	46.49	57.73	62.82	63.69	65.53	63.71	69.51	69.96	71.65	60.81
TiO_2	0.79	1.12	0.09	0.15	1.01	1.41	1.99	0.82	0.95	1.04	1.10	1.20	0.52	0.47	0.39	1.04
Al_2O_3	11.37	14.16	29.09	27.80	23.35	21.35	21.14	15.23	14.14	14.87	14.60	14.08	14.01	13.84	14.03	15.90
Fe_2O_3	0.65	2.33	0.31	0.26	2.07	2.37	4.52	4.10	4.64	1.27	1.37	3.00	1.51	0.96	1.32	2.42
FeO	7.60	7.58	1.44	1.49	5.46	7.42	7.36	6.97	6.04	7.08	4.03	5.07	2.86	2.61	1.34	6.06
MnO	0.13	0.18	0.05	0.04	0.10	0.13	0.13	0.13	0.16	0.11	0.08	0.08	0.05	0.04	0.01	0.13
MgO	7.43	7.76	2.30	2.18	2.66	3.43	5.40	5.49	2.38	3.68	2.16	1.97	1.31	1.17	0.60	2.24
CaO	22.09	17.88	14.62	13.50	11.41	10.86	9.61	7.49	6.15	4.44	3.43	5.24	3.70	3.10	3.61	5.68
Na_2O	0.54	1.16	2.12	2.88	2.96	2.82	2.57	0.57	1.58	0.72	1.64	2.15	2.34	2.33	2.02	2.46
K_2O	0.02	0.31	0.11	0.14	0.29	0.27	0.20	0.55	0.27	2.12	5.43	3.02	3.50	4.30	3.82	1.61
P_2O_5	0.09	0.12	0.03	0.03	0.28	0.35	0.04	0.12	0.22	0.09	0.08	0.24	0.13	0.11	0.08	0.35
L.O.I.	0.75	2.17	0.40	0.37	1.18	0.70	0.79	0.80	0.71	1.22	0.50	0.43	0.38	0.46	0.55	0.76
Total	99.96	100.20	100.07	99.95	99.91	99.48	100.24	99.82	100.06	100.23	99.95	100.19	100.02	99.25	99.42	99.46
Mg^1	65.6	62.7	73.7	72.6	43.2	42.9	49.8	51.9	32.8	48.4	46.2	34.7	39.4	41.4	33.2	36.3
DF index (Shaw, 1972								-5.6	-2.9	-4.8	-0.1	+0.02	+0.4	+0.8	+0.9	+0.13

TABLE 1 CONTINUED

	calc-granulites		anorthosites					intermediate - felsic gneiss								
								Mt Hay paragneiss					Mt Chapple			Redbank Hill
	S53	S55	S28	S48	S65	S66	S45	S52	S57	S30	S71	S198	S196	S202	S130	S227
CIPW Norm,% wt																
Fo		3.60					0.53									
Fa		2.08					0.28									
En			4.94	4.28			12.28	13.81	5.97	9.26	5.40	3.97	3.75	2.95	1.51	5.65
Fs			1.93	1.79			5.93	8.14	5.73	10.34	4.47	3.93	3.13	3.26	0.73	7.51
Wo	32.33	23.60	1.21	1.79	2.20	2.87	0.78					1.92				
En	18.65	14.57	0.08	1.17	1.08	1.35	0.49					0.95				
Fs	12.21	7.67	0.31	0.49	1.08	1.48	0.24					0.93				
Mt	0.95	3.45	0.45	0.38	3.04	3.48	6.59	6.0	6.77	1.86	2.00	4.36	2.20	1.41	1.94	3.56
Il	1.51	2.17	0.17	0.29	1.94	2.71	3.80	1.57	1.82	1.99	2.10	2.28	0.99	0.90	0.75	2.00
Ap	0.21	0.29	0.07	0.07	0.67	0.84	0.10	0.29	0.52	0.22	0.19	0.57	0.31	0.26	0.19	0.84
An	28.77	33.17	69.68	62.78	50.21	45.35	45.81	36.73	29.26	21.65	16.53	19.90	17.45	14.84	17.58	26.23
Ab	2.38	4.26	18.0	24.47	25.37	24.16	21.87	4.87	13.46	6.15	13.95	18.24	19.87	19.10	17.29	21.09
Or	0.12	1.87	0.65	0.83	1.74	1.16	1.19	3.28	1.61	12.65	32.26	17.89	20.76	25.72	22.83	9.64
C		HC1.20						0.37	0.60	3.57					0.20	0.63
Qz			1.73	1.63	1.31	0.76		24.79	34.12	32.20	22.98	25.00	31.40	31.37	36.97	22.74
Pl_2(An)	92	89	79	72	66	65	68	88	68	78	54	52	47	44	50	35
Ba ppm	8	92	23	26	83	80	45	148	371	492	1359	691§	728	770	1121	648
Rb		6			3	2		23	4	108	150	113	144	183	148	109
Sr	54	187	228	283	492	466	424	82	152	126	127	136	189	170	331	238
Pb	3				3	2		4		10	12	13	17	25	24	13
Th	4			1	1			1	8	21	2	3	2	9	1	21
U	7		1					2	1	1	1					2
Zr	40	57	3	2	25	29	5	47	360	174	179	153	141	134	163	255
Nb		2	3			2		3	8	13	6	7	7	7	3	35
Y	27	22	1		4	5	1	22	80	34	5	26	16	18	3	96
La	9	3			4	3		9	48	53	11	29	32	42	19	122
Ce	14	7			8	8		19	85	102	16	55	57	64	28	248
Nd	9	6			5			10	47	45	6	28	26	27	9	138
Sc	31	39	13	12	14	16	15	37	24	21	9	16	11	9	5	38
V	175	263	44	42	91	114	431	252	73	170	119	137	53	47	36	105
Cr	138	610	138	177	88	127	90	105	30	142	62	14	28	24	3	14
Ni	25	271	25	29	12	14	53	39	21	57	15	5	8	7		9
Cu	2	103	14	16	21	23	32	51	25	34	26	21	15	10	2	25
Zn	102	73	8	9	49	59	52	112	85	76	40	68	49	46	33	72
Ga	12	12	16	18	26	25	21	16	20	18	13	17	16	16	16	24

	S53	S55	S28	S48	S65	S66	S45
TiO_2/P_2O_5	8.8	9.3	3.0	5.0	3.6	4.0	49.7
Ti/Zr	118	118	180	449	242	291	2386
Ti/Y	175	305					
Ti/Sc	152	172	41	75	432	528	795
Zr/Y	1.48	2.59			6.25	5.80	5.0
Zr/Nb		28.5	3.0			14.5	
CaO/Al_2O_3	1.94	1.26	0.50	0.48	0.49	0.51	0.45
CaO/TiO_2	28.0	15.9	162	90	11.3	7.7	4.8
Al_2O_3/TiO_2	14.4	12.6	323	185	23.1	15.1	10.6
(Ce/Y)N	1.28	0.79			4.94	3.95	
(Ce/Nd)N	1.13	0.85				1.16	
(Nd/Y)N	1.13	0.92				3.40	

	S52	S57	S30	S71	S198	S196	S202	S130	S227
SI index	1.01	1.00	1.29	0.99	0.86	0.98	0.99	1.00	0.99
DI index	33	49	51	69	61	72	76	77	53
Solid index	32	16	25	15	13	13	10	7	15
Cryst index	47	34	30	20	25	20	17	19	31
K_2O/Na_2O	0.96	0.17	2.94	3.31	1.40	1.50	1.93	1.89	0.65
K/Rb	143	405	117	217	160	145	141	155	85
K/Ba	22	4.4	26	24	26	29	33	20	14
K/Pb	824		1270	2712	1392	1234	1031	954	715
Rb/Sr	0.28	0.26	0.85	1.18	0.83	0.76	1.07	0.44	0.45
Ba/Rb									
Ba/Sr	1.8	2.1	3.9	10.7	5.1	3.8	4.5	3.4	2.7

TABLE 1 CONTINUED

	Calc-granulites		Anorthosites				
	S53	S55	S28	S48	S65	S66	S45
K/Rb		310			580	809	
K/Ba	15	20	29	32	21	20	27
K/Pb	40				579	809	
Rb/Sr		0.03			0.006	0.004	
Ca/Sr	2923	683	450	341	165	166	162
Ba/Rb							
Ba/Sr	0.15	0.49	0.10	0.09	0.17	0.10	
Ni/Cr	0.18	0.44	0.18	0.16	0.13	0.11	0.59
V/Sc	5.6	6.7	3.4	3.5	6.5	7.1	28.7

	intermediate-felsic gneiss								
	Mt Hays				Mt Chapple				Redbank Hill
	S52	S57	S30	S71	S198	S196	S202	S130	S227
(Ce/Y)N	2.13	2.62	7.42	7.90	5.2	8.80	8.78	23.05	6.38
(Ce/Nd)N	1.38	1.32	1.65		1.43	1.60	1.73	2.26	1.31
(Nd/Y)N	1.54	1.99	4.49		3.66	5.52	5.09	10.19	4.88
Ni/Cr	0.37	0.70	0.40	0.24	0.35	0.28	0.29		0.64
V/Sc	6.8	3.0	8.1	13.2	8.5	4.8	5.2	7.2	2.8

Rock sample definitions for Table 1.

S43 - Am-Opx-Cpx-Plg high-Mg basic granulite (meta-pyroxenite).
Am-potassian Mg-hastingsite 9Ca:Mg:Fe = 32:33:35);
Opx-hypersthene (En:Fs = 63:38)
Cpx-salite (Wo:En:Fs = 47:40:12)
Plg-bytownite, An74
Ilm-100Ti/Ti+Fe = 45.1

S83 - Am-Opx-Cpx-Plg high-Mg basic granulite (meta-pyroxenite).
Am-potassian ferroan pargasite (Ca:Mg:Fe = 32:31:37).
Opx-hypersthene (En:Fs = 62:38).
Cpx-salite (Wo:En:Fs = 48:38:13)
Plg-bytownite, An73
Ilm-100Ti/Ti+Fe = 46.6

S86 - Opx-Cpx-Plg basic granulite

S149 - Bi-Opx-Cpx-Plg-Qz basic granulite

S239 - Biotite rich Opx-Am-Plg basic granulite

S228 - Bi-Am-Opx-Cpx-Plg high-Mg basic granulite.
Bi-Mg' = 62.7; TiO_2 =5.33%;

Am- potassian pargasitic hornblende (Ca:Mg:Fe = 32:35;32)
potassium edenite (Ca:Mg:Fe = 39:38:23)
Opx-hypersthene (Wo:En:Fs = 1:59:39)
Cpx-salite (Wo:En:Fs =47:39:12)
Ilm-100Ti/Ti+Fe = 47.8

S73 - Bi-Opx-Cpx-Plg basic granulite

S36 - Bi-Opx-Cpx-Plg basic granulite.
Bi-Mg" = 55.9; TiO_2 = 5.36%;

Opx-hypersthene (Wo:En:Fx = 1:53:45)
Cpx-salite (Wo:En;Fs - 46:35:18)
Plg-labradorite (An61)
Ilm-100Ti/Ti+Fe = 46.8

S80 - Am-Opx-Cpx-Plg basic granulite

S72 - Opx-Cpx-Plg basic granulite

S82 - Am-Opx-Cpx-Plg basic granulite

S132 - Opx-Cpx-Plg basic granulite

S133 - Opx-Cpx-Plg basic granulite

S136 - Am-Opx-Cpx-Plg basic granulite

S197 - Am-Opx-Cpx-Plg basic granulite

S188 - Gnt-Opx-Cpx-Bi-Am-Plg basic granulite.
Gnt-Ca:Mg:Fe = 20:20:59; MnO = 1.06%
Opx-hypersthene (Wo:En:Fs = 1:54:45)
Cpx-salite (Wo:En:Fs = 46:35:19)
Bi-Mg" = 53.9; TiO_2 = 4.78%;
Am-potassian magnesian hastingsite (Ca:Mg:Fe = 30:24:47).

S201 - Gnt-Opx-Cpx-Plg basic granulite

S131 - Gnt-bearing basic granulite band in felsic gneiss

S203 - Gnt-Opx-Cpx-Am-Plg-Qz basic granulite

S53 - Cpx-Sph-Plg basic calc-granulite
Cpx-salite (Wo:En:Fs = 49:31:19)

S55 - Scap-Am-Cpx-Plg basic calc-granulite
Scap-meionite, 100 Ca/Ca+Na = 78
Am-ferroan pargasite (Ca:Mg:Fe = 32:24:44)
Cpx-salite (Wo:En:Fs = 48:35:16)
Plg-anorthite An82

S28 - Opx-Am-Plg anorthosite
Opx-hypersthene (Wo:En;Fs = 1:60:38)
Am-Magnesian hornblende (Ca:Mg:Fe = 31:39:30)
Plg-bytownite, An73-78

S48 - Am-Opx-Cpx-Plg anorthosite
Am-titanian magnesian hornblende (Ca:Mg:Fe = 33:39:29)
Opx-Mg-hypersthene (En:Fs = 65:35)
Cpx-salite (Wo:En:Fs = 47:40:11)
Plg-labradorite, An57

S65 - Opx-Cpx-Plg anorthosite

S66 - Opx-Cpx-Plg anorthosite

S45 - Am-Opx-Cpx-Plg (+Ilm+Mt) anorthosite
Opx-hypersthene (En:Fs = 61.37)
Cpx-salite (Wo:En:Fs = 47:37:14)
Plg-labradorite, An65
Ilm-1--Ti/Ti+Fe = 46.3

S52 - Gnt-Opx-Am-Bi-Plg-Qz intermediate granulite
Gnt-Ca:Mg:Fe = 9:32:59
Opx-hypersthene (En:Fs = 62:36)
Am-tschermakitic hornblende (Ca:Mg:Fe = 31:36:34)
Bi-Mg'70.7; TiO_2 = 4.27%

Plg-bytownite, An86

S57 - Gnt-Bi-Kf-Plg-Qz gneiss
Gnt-Ca:Mg:Fe = 22:6:72
Bi-Mg' = 33; TiO_2 = 4.27%;
Plg-andesine, An34

S30 - Gnt-Bi-Plg-Qz gneiss
Gnt-Ca:Mg:Fe = 6:29:66
Bi-Mg' = 64; TiO_2 = 3.92%;
Plg-bytownite, An80

S57 - deformed Opx-Am-Plg-Kf (+ Ilm, Mt) intermediate granulite
Opx-hypersthene (Wo:En:Fs = 1:48:50)
Am-potassian ferroan pargasite (Ca:Mg:Fe = 31:22:47)
Plg-labradorite, An55-61

S198 - Gnt-Am-Opx-Kf-Plg-Qz felsic granulite

S196 - Gnt-Bi-Opx-Kf-Plg-Qz felsic granulite

S202 - Gnt-Bi-Am-Opx-Kf-Plg-Qz felsic granulite

S130 - Kf-Plg-Qz felsic gneiss

S227 - Gnt-Bi-Am-Plg-Qz gneiss
Gnt-Ca:Mg:Fe = 22:12:65
Bi-Mg'= 44; TiO_2 = 4.42%
An-Potassian ferroan pargasite (Ca:Mg:Fe = 30:19:51)
Plg-andesite, An42

Mineral compositions were analyzed by a TPD energy dispersive microprobe according to the method of Reed and Ware (1975). 35 rock samples were analyzed for major, trace, alkali and alkaline earth elements (Rb,Ba,Sr), large ion lithophile elements (U,Th, Pb), high field strength elements (Nb,Zr,Y), rare earth elements (La,Ce,Nd) and trace metals (V,Sc,Cr,Ni,Cu,Zn). The last four elements, as well as Na, were analysed by atomic absorption using a Varian-Techtron spectrometer (analyst: T.Slezak). All other elements were analyzed by X-ray fluorescence, using a Philips PW-1450 spectrometer (analyst: J.Pyke). Details of accuracy and precision are discussed in Sheraton and Labonne (1978). Seven samples were analyzed for Nd,Sm,Eu,Dy,Er and Yb by J. Foden, using isotope dilution mass spectrometry (Table 2).

LAYERED ANORTHOSITE-METAPYROXENITE UNITS

Major element characteristics of these rocks are plotted in Fig.3. Two types of anorthosite bodies are observed in the Mt Hay massif, each characterized by a different mode of occurrence and geochemistry:

(A) Type A - A contiguous unit of finely phase-laminated, hornblende-orthopyroxene-clinopyroxene labradorite to bytownite anorthosites exposed over a strike length of about 10km along the northern flanks of the Mt Hay massif (Fig. 1).

(B) Type B - centimeter to metre scale anorthositic bands intercalated with pyroxenite cumulates and basic granulites in parts of the Mt Hay massif and consisting of labradorite and a higher proportion of ferromagnesian minerals than type A.

Type A anorthosites (S28, S48) have less than 10% ferromagnesian phases, very high CaO and Al_2O_3, high Mg' values (~70) high Ni and Cr levels and very low LIL, HFS and RE element abundances (Table 1). Low Ga/Al, V/Sc and Ti/Sc, and high Ca/Sr pertain. The rocks are opx-normative, as reflected by low CaO/Al_2O_3 (~0.5), and have low normative Qz. Similar characteristics are shown by anorthositic gabbro from the Harts Range (Sivell and Foden, 1985).

Type B anorthosite and gabbroic anorthosite samples have up to 30% ferromagnesian phases, include opx-ol normative (S45) and Qz-normative (S65, S66) types, and have low Mg' values (39-46). These rocks have high levels of siderophile elements (Fe, Ti, Mn, V), chalcophile elements (Cu, Zn, Pb), alkali elements (K, Rb, Ba)

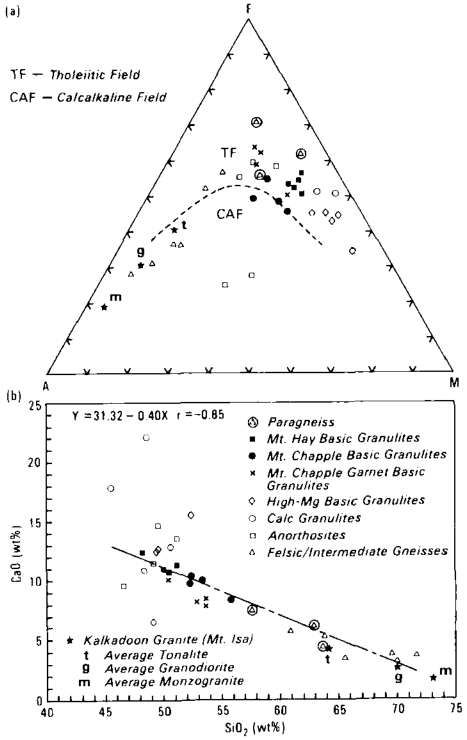

Figure 3. Major element characteristics of southwestern Arunta granulites and gneisses. A) FAM ($FeO+Fe_2O_3+MnO:Na_2O+K_2O:MgO$) ternary plot, showing the tholeiitic field (TF) and calc-alkali field (CAF). B) $CaO-SiO_2$ plots. Circled stars - average Mt Isa granitoid compositions (Wyborn and Page, 1983).

Pb and P relative to the type A anorthosites. The enrichment of HFS elements relative to chondrites is in the decreasing order P>Ti>Zr>Y. The rocks have high Ga/Al and (Ce/Y_N) (4-5) and low Ca/Sr. Sample S45 differs from the two other rocks by its high Fe, Ti, Mg and Ni, and lower LIL and HFS element levels.

High-Mg basic granulites (HMBG) representing probable metacumulates are interlayered with anorthosites at Mt Hay and are also interspersed with basic granulites in the Mt Chapple and Redbank Hill massifs. These rocks are geochemically characterized by high MgO (8-15%), high Mg' values (63-75) and are Ol-Or slightly Qz-normative (Table 1). However, LIL, HFS and RE element levels

Table 2.

Rare Earth Element analyses

Sample		S83 Mt Hay DHMG	S149 Mt Chapple EHMG	S80 Mt Hay TG	S82 Mt Hay TG	S57 Mt Hay Paragneiss	S196 Mt Chapple	S227 Redbank gneiss
ppm La								
" Ce	XRF		47	25	25	85	57	248
" Nd	IDMS	2.37	29.44	14.22	12.50	53.83	24.60	127.1
" Sm	"	0.77	6.64	3.64	3.26	12.25	4.39	27.7
" Ev	"	0.597	1.507	1.05	1.02	3.41	1.21	1.63
" Gd	"							
" Dy	"	0.89	4.30	4.19	3.51	14.36	2.66	19.58
" Er	"	0.52	2.32	2.72	2.81	10.14	1.49	10.22
" Yb	"	0.44	1.97	2.47	1.96	9.75	1.33	7.70
(Ce/Yb)	N		6.06	2.58	1.94	2.21	10.9	8.17
(Ce/Sm)	N		1.66	1.61	1.08	1.62	3.04	2.09
(Sm/Nd)	N	1.89	3.65	1.59	1.80	1.39	3.56	3.90
(Sm/Nd)	N	1.0007	0.70	0.79	0.81	0.706	0.55	0.67

vary considerably, allowing a two-fold division as follows:

(1)The Mt Hay HMBG are *LIL* and *HFS* element-depleted, of high Al_2O_3 and CaO abundances and very high Sr levels (280-300ppm).

(2)The Mt Hay and Mt Chapple HMBG are LIL and HFS element enriched.

The depleted HMBG have low K_2O (0.08-0.15%), Ba (30-43 ppm), P_2O_5 (0.03%), Zr (7-12 ppm), Y (5-6 ppm) and RE (Table 1). Rb, Pb, U, La, Ce and Nd are mostly below detection limits of BMR's XRF analysis and REE abundances are very low (Table 2). However, K, Sr, Ba and Th are not much lower than in the tholeiites and may have been re-enriched (Fig.4a). The $(Sm/Nd)_N$ ratio of S83 is chondritic whereas LRE/HRE are some what fractionated (Fig. 5). TiO_2, Cu and Zn are also low. Ca/Sr ratios are anomalously low (~310) relative to chondritic ratios (843; Sun, 1982). The very high K/Rb (~600) and very low Rb/Sr (~0.003), U and Th are consistent with the observed low values in some granulite terrains (Lambert and Heier, 1967; Sheraton, 1970; Tarney, 1976; Condie and Allen, 1984). The low Ba/Sr ratios (0.11-0.14), as compared to ratios above 0.5 in most basaltic rocks (Turekian and Wedepohl, 1961), are consistent with cumulates. Further evidence for a cumulate nature is furnished by marked departures from chondritic

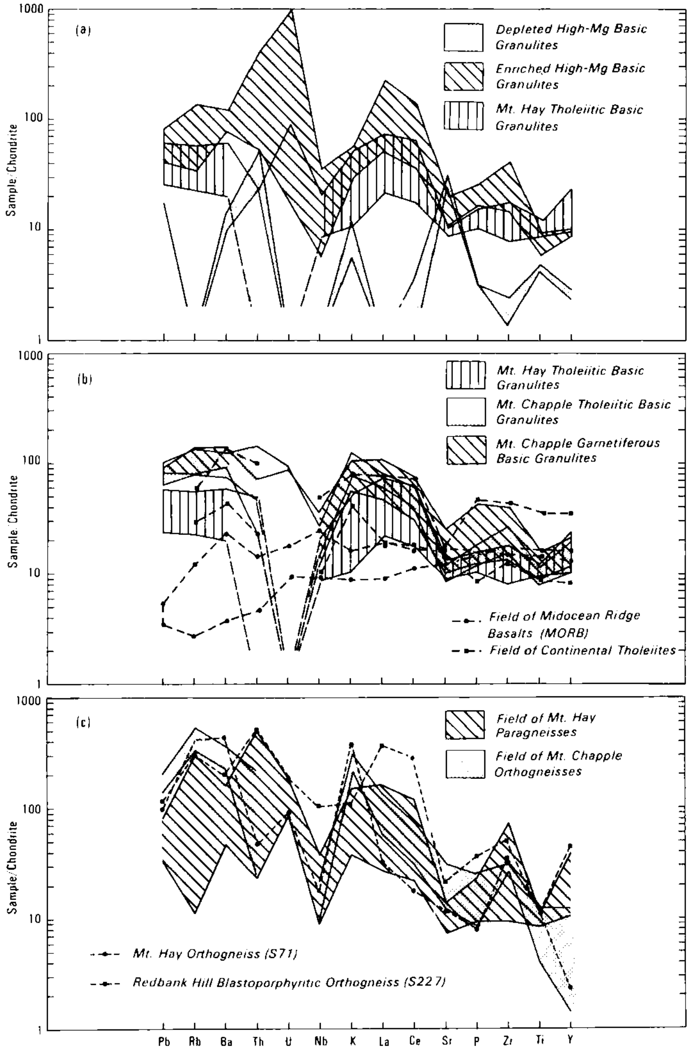

Figure 4. Chondrite-normalised incompatible element plots of south western Arunta Inlier granulite and gneiss compositions, compared to Mid-ocean ridge basalts(MORB) (after Sun et al., 1979) and continental tholeiite basalts (CB) (Scourie dolerites, Weaver and Tarney, 1981a). The element sequence corresponds to increase in incompatibility and secondary mobility from right to left.

a-Fields of LIL depleted high-Mg basic granulites and LIL-enriched high-Mg basic granulites, compared to Mt Hay depleted basic granulites.

b-Fields of Mt Hay depleted basic granulites, Mt Chapple tholeiitic basic granulites and Mt Chapple garnetiferous basic granulites, compared to MORB and CB.

c - Mt Hay - Mt Chapple - Redbank Hill gneisses compared to the high-Ca to low - Ca granite field of Turekian and Wedepohl (1961).

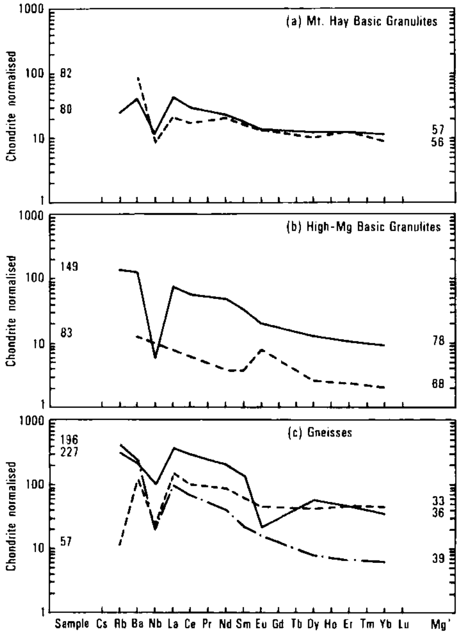

Figure 5. Chondrite-normalised rare earth elements, Rb, Ba and Nb patterns of LIL-depleted and enriched high Mg basic granulites (S83, S149), Mt Hay tholeiitic basic granulites (S80, S82), Mt Hay paragneiss (S57), Mt Chapple orthogneiss (S196), and Redbank Hill blastoporphyritic orthogneiss (S227). Analysis by isotope dilution mass spectrometry (J.Foden). Chondrite normalizing values after Sun (pers. comm.).

ratios of the HFS elements. Thus, Ti, Y, P and Zr display increased depletion, in this order, relative to chondritic primitive mantle (Fig. 4a), as reflected by high Ti/Zr (220-380), TiO_2/P_2O_5 (13-16) and Ti/Y (470-530). The measured $^{147}Sm/^{144}Nd$ of sample S43 of 0.20 (M.T. McCulloch, pers, comm., 1985) is close to the model chondritic ratio of 0.1967 (McCulloch and Wasserburg. 1978).

The LIL and HFS-enriched HMBG of Mt Chapple and Redbank Hill have similar or higher MgO and Mg' values, and similar or lower Al_2O_3 and CaO values, as compared to the depleted cumulates. On the other hand, LIL and HFS element abundances are similar to those of Mt Hay tholeiitic Qz-normative basic granulites. Thus, LIL elements (K_2O =0.4-0.8%; Rb = 12-48 ppm; Ba 240-380 ppm; Pb = 5-10 ppm), HFS elements (TiO_2 = 0.6-0.9%; P_2O_5 =0.16-0.25%; Zr =

75-210 ppm ; Y = 20 ppm; Ce = 30-120 ppm), U and Th may be even higher than in some Qz-normative basic granulites and continental basalts (Fig. 4a, b). The departure of the HFS elements from chondritic ratios is demonstrated by an increased depletion, relative to chondrites, in the order Zr, P, Nb, Y, Ti (Fig.4a). This is the opposite order to that shown by the depleted HMBG cumulates, a relationship with implications for the differential partitioning and mobility of the incompatible trace elements. Thus, the HFS enrichment/depletion factors, represented by the intervals between the enriched HMBG and depleted cumulates in Fig.4a. show that those elements which are very low in the cumulates (Y, Zr, Ce, Nb, U) are those which are high in the enriched HMBG. Conversely, elements relatively abundant in the cumulates (Ti, Sr) are those relatively low in the enriched HMBG. The average enrichment/depletion ratios for the various elements are, in increasing order: Sr (-10), Ti (3), Y (7), P (17), Zr (24), K (34), Ce (78), Ba (80), Th (194). La, Nb, Rb and U factors cannot be estimated since these elements are below detection limits in the depleted cumulates. The negative sign for Sr reflects its enrichment in plagioclase in the cumulates. This sequence is consistent with the relatively high Kd^{cpx}_{Y}, (0.5) Kd^{cpx}_{Sr} (0.12) and Kd^{cpx}_{Zr} (0.1) values as compared to K, Ba, Rb, Pb, Ce, La and Th, suggesting that the least mobile components are those which reside in clinopyroxene. That LIL and HFS element-enriched HMBG have, so far, been encountered only in the charnockite and gneiss-engulfed basic enclaves of Mt Chapple and Redbank Hill may, perhaps, be interpreted in terms of the introduction of these elements from the felsic magma with consequent growth of biotite and hornblende. Thus, the high-LIL HMBG may represent cumulates and/or depleted residues which were subsequently re-enriched in incompatible elements. An alternative interpretation is in terms of assimilation of sialic crust by the high temperature magnesian magmas, a possibility supported by high K, Ba and Rb of the rocks (Huppert and Sparks, 1985). The above mobility order varies somewhat from that observed by Weaver and Tarney (1981) in amphibolitized dykes, where the sequence is Rb>Ba>K>Sr>Th>La>Ce. It also varies from the diffusion sequence observed by Collerson et al., (1984) in a dyke in northern Labrador where K>Rb>Sr.

THOLEIITIC BASIC GRANULITES (TBG)

Tholeiitic basic granulites (TBG) constitute the bulk of the Mt Hay massif, are typically Qz-normative, and show a tholeiitic Fe-enrichment trend on the FAM diagram (Fig. 3) with Mg' values ranging from 57-35. The proportions of Opx and Cpx are about equal. The Mg' values, LIL and HFS element abundances and mineral assemblages allow a three-fold subdivision of the TBG.

(1) Mt Hay low-LIL element TBG
(2) Mt Chapple high-LIL element TBG
(3) Mt Chapple LIL, HFS and Fe-rich garnetiferous TBG.

Each of the above groups defines coherent patterns on the chondrite-normalized diagram (Fig.4b), which suggests that secondary geochemical redistribution was limited. The patterns feature Y, Zr, P, Ce, and La 'highs' and Ti, Sr, Nb, and Pb 'lows', broadly corresponding to continental tholeiites as represented by the field of the ca 2.4 Ga. old Scourie doleritic dykes (Weaver and Tarney, 1981). The fields of the tholeiitic basic granulites depart strongly from the field of mid-ocean ridge basalt (MORB) of Sun et al., (1979). The granulites have typically high Ba/Sr (1-4) and Rb/Sr (0.1-0.7) and low K/Rb (150-600). Among the HFS elements - TiO_2/P_2O_5 (5-9), Ti/Zr (40-90) and Ti/Y (140-290) are low as compared to chondritic values (Fig.4b). CaO/Al_2O_3, CaO/TiO_2 and Al_2O_3/TiO_2 are low (Table 1). Thus, the general decreasing enrichment order (relative to chondritic abundances) is Zr, P, Y, Sr, Ti, Al, Ca, Sc. The REE of Mt Hay basic granulites display weak fractionation (Table 2; Fig. 5). Sm/Nd data for S36 ($^{147}Sm/^{144}Nd = 0.1582$) (M.T. McCulloch, pers. comm., 1985) also indicate a $(Sm/Nd)_N$ value of 0.81 and for basic granulites from Mt Hay $(Sm/Nd)_N$ values of 0.78 and 0.50 (Black and McCulloch, 1984 REE of Mt Chapple basic granulites are even more fractionated (Figs.6,7). These samples have Rb/Sr ratios of 0.34 and 1.62, respectively, reflecting the wide range of this ratio in the analysed basic granulites (Table 1). These values, as well as the generally low K/Rb ratios, suggest little or no loss of Rb relative to K from the basic granulites. While the broad LIL and HFS chondrite-normalized profiles of basic granulites are similar (Fig. 4b), differences occur between the Mt Hay LIL element depleted TBG (Group 1), Mt Chapple TBG (Group 2) and Mt Chapple garnetiferous Fe-rich TBG (Group 3).

Group 1 - Mt Hay TBG have markedly low abundances of K, Rb, Ba, Pb, Th, U, Nb and REE. Mg' values are commonly higher, and normative Qz lower, than in group (2) and (3) rocks. HFS element ratios are closer to chondritic values than those of group (2) and (3). Thus, of all the rock types, the Mt Hay basic granulites may have preserved the most primitive geochemical characteristics. However, the possibility that some of these rocks have been depleted in LIL and HFS elements during high grade metamorphism should be kept in mind, e.g. S 82 - an Ol-normative (Mg' = 52.3) LIL element-depleted basic granulite (K/Rb = 1200). Light REE are depleted in this rock $(Ce/Nd)_N$ =0.88), although the $(Sm/Nd)_N$ value is less than unity. Sample S80 displays higher Ce and $(Ce/Yb)_N$ fractionation values. Whereas the HFS characteristics of group (1) granulites overlap the MORB field, larger radii elements show some affinities to the field of continental tholeiites.

Group 2 - The Mt Chapple TBG have higher SiO_2 (52.1-55.8%), and significantly higher LIL and HFS element abundances than group (1) samples. Thus, K_2O (1.1-1.8%), Ba (226-281 ppm), Rb (28-92 ppm) and Th (2-6 ppm) are high by several factors compared to the Mt Hay rocks. In contrast with Th, U is uniformly depleted in the granulites. However, differences with regard to HFS elements are more subtle, as REE, Zr and Nb overlap with, or exceed, the highest abundance levels of group (1) (Figs. 6,7), HFS element ratios depart more strongly from chondritic values, while Ba/Sr ratios (1.9-2.7) are high compared to the Mt Hay basic granulites (1.2-1.7). The sense of these departures from chondritic ratios is similar to that in the LIL and HFS element-enriched high-Mg basic granulites.

Group 3 - With the exception of an Ol-normative sample (S 188), the garnet-bearing basic granulites of Mt Chapple are high in SiO_2 (52.8-53.6%), total iron as FeO (12.6-13.5%), LIL and HFS elements, and have low Mg' values (35.4-40.1) and CaO(~8%). Whereas the fields of incompatible elements on chondrite normalized plots overlap, the garnet-bearing basic granulites tend to have higher Ti, Zr, P, Sr, Nb and REE than group 2 granulites (Fig. 4b). V and Zn have high values whereas Cr and Ni are low. While REE abundances are higher than in group 2, light/intermediate and intermediate/heavy REE ratios are similar (Fig. 6, 7). In most other respects the fields of groups 2 and 3 overlap. Thus, the garnet-bearing basic granulites can be regarded as somewhat more fractionated derivatives of the Mt Chapple tholeiitic suite.

Two samples (853, 855) of basic granulites from a supracrustal unit at Mt Hay are characterized by anomalously high CaO (22.09%, 17.88%) and thus clinopyroxene and calcic plagioclase (An92, An87)-rich norms, in agreement with probed feldspar compositions (An94, An82). These characteristics, and the sphene and scapolite rich mineral assemblages of these granulites may be alternatively interpreted in terms of de-carbonatization of originally carbonate-rich basic igneous rocks or metamorphosed calc-magnesian

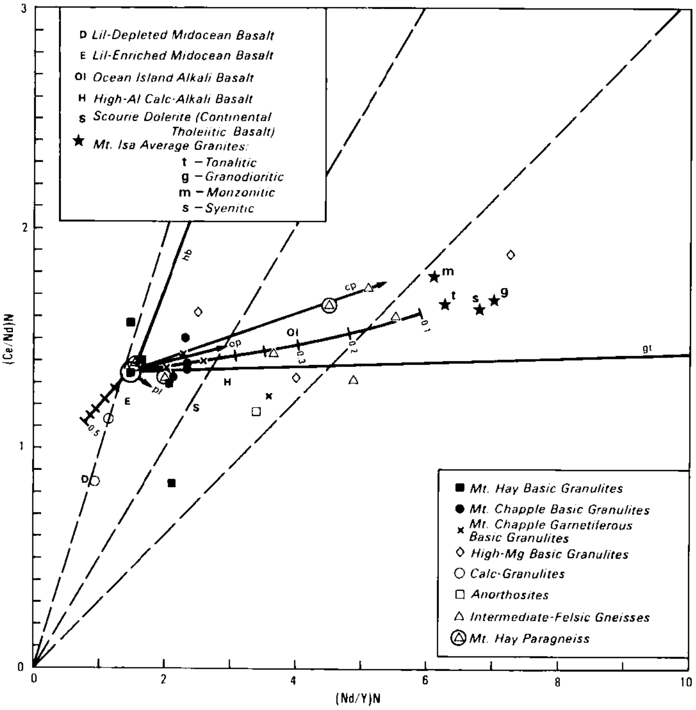

Figure 6. $(Ce/Nd)_N$ vs $(Nd/Y)_N$ plots of granulites and gneisses compared with mineral phase equilibrium fractionation trends, average modern basalts and average Mt Isa granites (Wyborn and Page, 1983). The model source composition is the average of 4 Mt Hay tholeiitic basalts. The arrow heads (pl-plagioclase; op-orthopyroxene; cp-clinopyroxene; gt-garnet; hb-hornblende) signify the composition of the partial melt where F=0.5. The numbered curves represent melt and residue compositions for the indicated F values and a residue of Cpx:Opx:Plg (0.23: 0.23: 0.54). Explanation in the text.

sediments. Comparisons between the calc-granulites and average sedimentary compositions suggest that the two samples are broadly consistent with derivation from a 4:1 shale/dolomite mixture with respect to their SiO_2, FeO_t, MgO and Na_2O abundances but are far too high in CaO (11.6% in the model sediment). Increase in the dolomite component would decrease the Al_2O_3 levels of the model sediment to well below calc-granulite abundances. K_2O levels in the granulites (0.02%, 0.31%) are well below those expected in clay-bearing sediments, although K was possibly depleted during metamorphism. On the other hand, concentrations of ferromagnesian and siderophile elements are not dissimilar to those of mid-ocean ridge basalts, i.e. FeO, MgO (7.43%, 7.73%), Mn, Ti, Cr, Ni and Sc abundances (Table 1). The near chondritic TiO_2/P_2O_5, Ti/Zr (118),

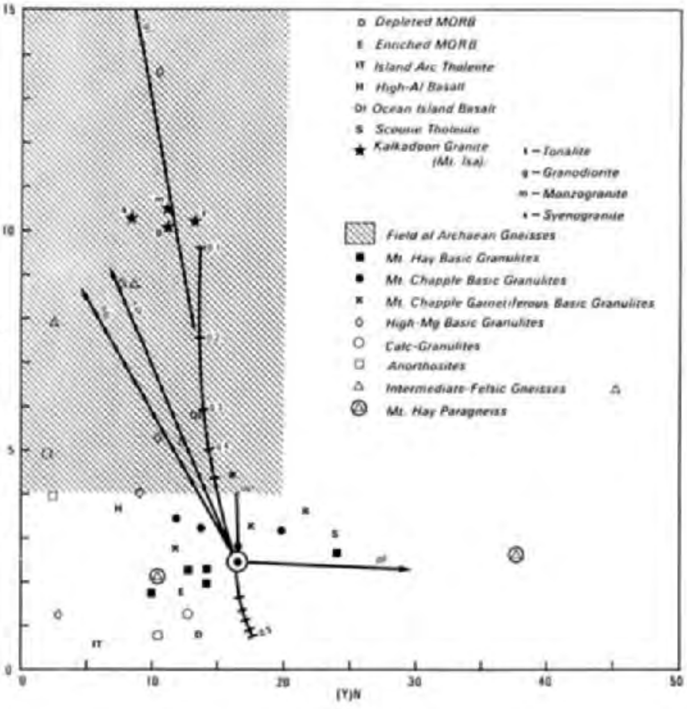

Figure 7. (Ce/Y)N vs (Y)N plots of granulites and gneisses compared with mineral phase equilibrium fractionation, average modern basalts and average Mt Isa granites (Wyborn and Page, 1983). Explanation in legend of Fig.6 and in the text.

Ti/Y and Zr/Y ratios support derivation from carbonated basic igneous rocks. A light/heavy REE ratio of less than unity (Ce/Y)N = 0.79) is observed in sample S55, which has Ol and Ne in the norm. These features, as well as the high CaO/Al_2O_3 (1.3-1.9), indicate strong departures from the composition of tholeiitic basic granulites, including marked depletion of Ce and Nd. These changes are likely to have been associated with the carbonatization of original basic igneous volcanic or hypabyssal parents followed by CO_2 loss during high grade metamorphism.

INTERMEDIATE TO FELSIC GNEISSES

Amphibolite to granulite facies gneiss units ranging from thin laminae to large intrusive stocks display a wide petrological and geochemical range from gneissose basic granulite to quartz monzonite gneiss. The type of band is commonly related to unit size, namely, thin mm- to cm-scale bands are commonly plagioclase -dominated orthopyroxene-bearing (± hornblende, biotite) types, whereas metre-scale lenses and larger bodies may consist of plagioclase, K-feldspar,biotite, garnet and quartz. These variations are reflected by increasing LIL and HFS element abundances. In addition to the orthogneisses, 3 samples of probable paragneiss from the northern flank of the Mt Hay massif were analyzed (Table 1). A metasedimentary origin is supported by the occurrence of sillimanite bearing bands alternating with quartzitic bands. The possible metasedimentary origin of these rocks is supported by their negative DF values (Table 1) according to Shaw's (1972) paragneiss-orthogneiss parameter: $DF = 10.44 - 0.21\ SiO_2 - 0.32\ Fe_2O_3$ (total) $- 0.98\ MgO + 0.55\ CaO + 1.46\ Na_2O + 0.54\ K_2O$. The intermediate to felsic gneiss and granulite analyzed in this study display a wide compositional range, i.e. SiO_2 (57-72%), Qz (23-37%), Or (1.6-32%) and Mg' values (48-29). Most gneisses plot on a calc-alkaline trend on the FAM diagram (Fig. 3a). Compositional ranges of gneisses from Mt Hay, Mt Chapple and Redbank Hill overlap (Fig. 4c). Sl indices (%mol $Al_2O_3/(CaO + Na_2O + K_2O$, Chappell and White, 1974) are mostly below 1.1, indicating an apparent igneous parenthood even for two of the paragneiss samples (S52, S57). Comparisons between the gneisses and average low-Ca and high-Ca granites (Turekian and Wedepohl, 1961) indicate the following.

(1) CaO levels are commensurate with, or higher than, those of

average high-Ca granite, as reflected by the high An content of plagioclase feldspars.

(2) Siderophile and chalcophile elements (Fe, Ti, V, Mn, Zn) and magnesian elements (Mg, Ni, Cr) show high abundances in the gneisses as compared to high-Ca granites.

(3) La, Ce, Nd, Nb and Th are generally significantly depleted in the gneisses as compared to average granites.

(4) With the exception of two samples of paragneiss (S 52, S 57), levels of K, Rb, Ba, Pb and Sr are within the range of low to high-Ca granites.

The high abundances of basic trace elements may result from incorporation by felsic magma of mafic restite derived from basic granulites. The high Rb levels suggest that little syn - metamorphic depletion of the type reported from some high grade terrains (Sheraton et al., 1973; Sheraton and Black, 1983; Condie and Allen, 1984) has taken place. The marked depletion of the gneisses in REE is accompanied by low (($Ce/Y)_N$ ratios relative to average granites and to Mt Isa Kalkadoon granites (Wyborn and Page, 1983) (Fig. 7). These values are low by almost an order of magnitude as compared to heavy REE-depleted tonalitic and trondhjemitic gneisses $(Ce/Y)_N$ = 5-100) (Tarney and Windley, 1977; Glikson, 1979). Of the 3 gneiss samples analyzed for REE, the Mt Hay paragneiss (S 57) shows low LRE/HRE fractionation ((Ce/Yb)N = 2.2), the Mt Chapple gneiss (S 196) has low total REE (Sm-4.39 ppm) and high $(Ce/Yb)_N$ (10.9), and the Redbank Hill blastoporphyritic gneiss has high Total REE (Sm=27.7 ppm), high $(Ce/Yb)_N$ and a marked negative Eu anomaly (Table 2; Fig. 5).

BASIC GRANULITE-GNEISS RELATIONS

Gravity studies indicate that the Mt Hay-Mt Chapple terrain and the Burt plain to the north (Fig. 1) are underlain by high-density crust, possibly dominated by basic rocks (Glikson, 1987). Thermobarometric studies of Mt. Hay and Mt. Chapple granulites and gneiss samples suggest equilibration T and P values which plot between the dry gabbro solidus and the H_2O-saturated gabbro solidus (Fig. 10) (Glikson, 1984). This suggests that, provided local hydration occurred, the rocks would undergo at least incipient partial melting. For this reason, although it is possible that the gneisses are derived from a sialic source, it is logical to test the origin of the intermediate to felsic gneisses in terms of partial melting of basic source materials. An anatectic derivation of the gneisses is consistent with the finely banded relations between the two components in the field and in thin section, displaying gradual to sharp interfingering of laminae and lenses of varying pyroxene/plagioclase ratios. However, no well substantiated ultramafic residues of partial melting have been observed. A partial melting model may be tested geochemically in two ways: (1) mass balance calculations which evaluate whether combinations of theoretical residue and observed intermediate-felsic gneiss compositions approximate observed source TBG chemistry, namely whether a closed or open geochemical source-residue-melt system may have applied;(2) model partial melting calculations, assuming a *basic granulite source*, using partitioning coefficients (Kd) from the literature and comparing calculated model partial melts compositions to the analyzed Mt Hay and Mt Chapple gneisses. It is emphasised that, since little evidence exists for in-situ partial melting, the models refer to possible anatexis of similar compositions at depth.

Combinations of residual and partial melt compositions for any particular element (e) can be obtained on the basis of:

$$FL_e + (1-F)R_e = S_e \qquad ......(1)$$

(F - fraction melting; S_e - abundance of element e in the source; R_e - abundance of element e in the residue; L_e - abundance of element e in the liquid).

Mg was chosen as the key element (e) from which the value of F is calculated, in view of the strong partitioning of this element between residue and liquid and its relative stability during high grade metamorphism. In the first model the average of four Mt Hay tholeiitic basic granulites was assumed as S_{Mg}. Problems are encountered in selecting a theoretical residue composition R_{Mg}. However, assuming that in any residue the level of incompatible elements is practically nil, this factor makes little difference. For L_{Mg} the MgO value of an orthogneiss band within basic granulites was assumed. For an R_{Mg} value of 9.6% the F value calculated according to equation (1) is 0.27. The combined compositions (R_e +L_e) vs S_e were then compared on a log-log plot for major and trace elements, allowing the following observations:

(1) The alkali (K, Rb, Ba) elements and Sr are strongly enriched in the model melt + residue system relative to the model source. Note that due to their relative mobility the alkali elements can not be used as a basis for petrogenetic modelling.

(2) Siderophile (Fe, Mn, V, Sc), chalcophile (Cu, Zn, Pb), RE (La, Ce, Nd) and high-field strength (Ti, Zr, Y, P, Nb) elements are markedly depleted in the model melt + residue system as compared to the model source.

These relations militate against closed-system derivation of the felsic magma by partial melting of LIL-depleted Mt Hay type basic granulites, indicating addition of alkalies from an external source. On the other hand, if a LIL-enriched basic source analogous to the Mt Chapple basic granulites is assumed, closed system partial melting relations are approached.

Comparisons between incompatible element abundances of the gneisses and model magma compositions derived by partial melting of basic granulite, may test possible genetic relations between these rocks. Applying equilibrium partial melting relation (Shaw, 1970; Arth, 1976):

$$C_L = C_o/(D+F(I-D) \qquad \ldots\ldots(2)$$

C_L - liquid composition; C_o - source rock composition;
D - bulk partition coefficient; F - fraction of melting.

The C_o values assumed in the model are (1) average Mt Hay basic granulites and (2) average Mt Chapple basic granulite. The bulk D partition coefficient was initially calculated by combining individual Kd mineral/melt partition values from the literature (Arth, 1976; Hanson, 1980; Pearce and Norry, 1979) with the normative proportions of Ol, Opx, Cpx and Plg in the model residue (depleted high-Mg granulite S 43). F values of 0.2 and 0.3 are assumed. Three models are considered:

1. Assuming a source composition of average Mt Hay basic granulite, a comparison with sample S 71; (an intrusive felsic gneiss band at Mt Hay) indicates that model values are too low in K, Rb, Ba and Sr by factors of 3-4, and too high in Ce, Nd, Y and Ti by factors of up to 6. Model and observed Zr and Nb values are similar (Fig. 8a).

2. Assuming a source composition of average Mt Chapple basic granulite, a comparison of partial melt compositions with the average Mt Chapple gneiss indicates a broad pattern agreement. K, Rb and Ba values of model partial melt and the average gneiss agree closely. Model values of Zr, Nb, Ce, Nd and Y are high by factors of up to 1.9 and Ti by a factor of 3.0.

3. The above discrepancies can be reduced further if the residue is assumed to contain amphibole, whose high Kd values for the REE, Y, Zr, Nb and Ti result in the closer approximation of model and gneiss compositions. Likewise, a lesser amount of residual plagioclase would improve the match of the Sr anomalies. Partial melting of Mt Chapple basic granulite leaving a residue of Cpx:

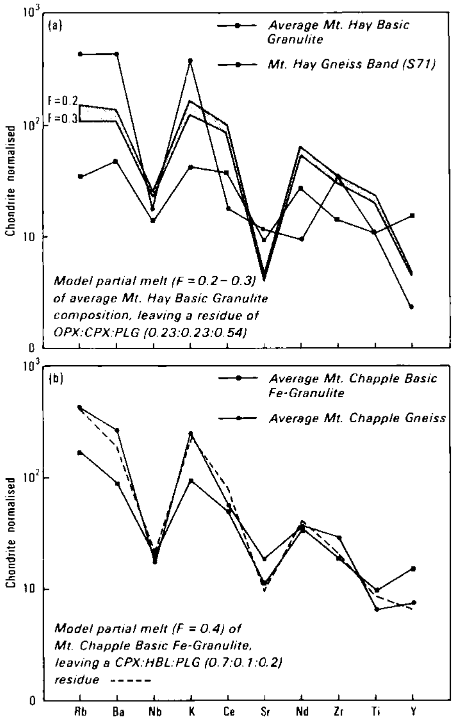

Figure 8. Partial melting models, assuming basic granulite source, model residual norms, Kd values from Arth (1976), Pearce and Norry (1979) and Hanson (1980),and varying F values, compared to analysed orthogneiss compositions. Chondrite normalizations valued after Sun (1982). See text for explanaltion. A)-Mt Hay granulite/gneiss; model specifications are given in the diagram. B)-Mt Chapple granulite/gneiss; model specifications are given in the diagram.

Hbl: Plg in the proportion 70:10:20 (F = 0.4) results in a magma composition which closely approximates the average Mt Chapple gneiss (Fig.8b). The only significant discrepancy is for Sr, possibly due to lower Kd^{Plg}_{Sr} values.

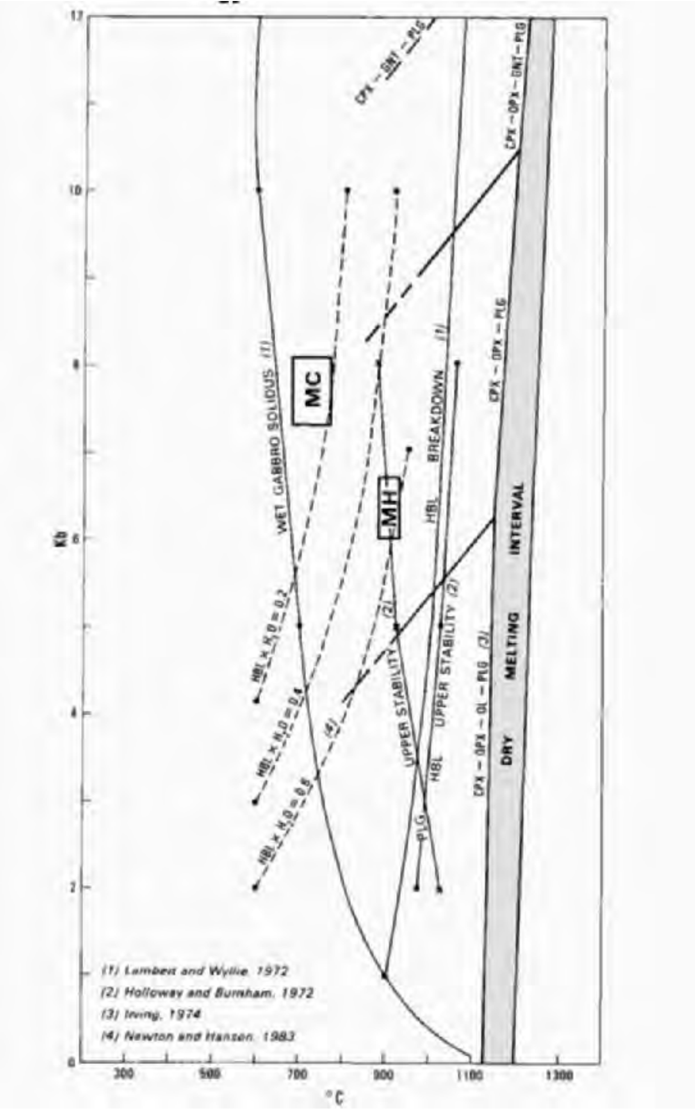

Figure 9. Pressure-temperature relations of components relevant to metamorphic phase transformation and partial melting of basic igneous rocks, showing P-T parameters estimated for the Mt Hay and Mt Chapple granulite/gneiss suites from garnet-two pyroxene assemblages (Glikson, 1984). Experimental stability fields of Cpx-Opx-Ol-Plg, Cpx-Opx-Plg, Cpx-Opx-Gnt-Plg, and Cpx-Gnt-Plg are from Irving (1974). Phase boundaries are after Lambert and Wyllie (1972) and Helz (1976). Model Proterozoic geothermal gradients are after Lambert (1983).

These comparisons indicate, in agreement with mass balance considerations, that if the felsic magmas were derived by partial melting of Mt Hay-type basic granulite, significant amounts of alkali elements (K, Rb, Ba) have been added. However, the Mt Chapple felsic gneisses are broadly consistent with derivation by partial melting of the alkali and HFS element-enriched Mt Chapple basic granulites, particularly if amphibole is present in the residue. The role of amphibole as a minor (~10%) residual phase during partial melting processes (Helz, 1976) has been pointed out by Sivell and Foden (1985) in connection with Harts Range amphibolites. The amount of residual amphibole is limited by the moderate Ce/Yb ratios of the gneisses (11), since any significant fractionation of this phase and/or garnet would elevate this value (Hanson, 1980). The petrogenetic relations portrayed on a PT phase diagram (Fig. 9) suggest melting at temperature and pressure commensurate with those estimated from garnet-pyroxene assemblages as Ca. 680-770^{o}C and 7.3-8.1 kb (Glikson, 1984) under high partial pH_2O pressures, underlying the role of amphibole. The close to unity $(Sm/Yb)_N$ ratios militate against equilibration with garnet, thus supporting partial melting under pressures below 9 kb (Fig. 9) (Lambert and Wyllie, 1972).

Comparisons between the basic/granulite and gneiss compositions and experimental partial melts studied by Holloway and Burnham (1972) and Helz (1976) are relevant to their relations. The Mt Hay gneiss (S 71) is too K-rich and not siliceous enough to represent partial melt of Mt Hay granulite. The high FeO and MgO abundances of Mt Chapple gneisses exceed those obtained by high degree melting of Picture Gorge tholeiite (at 1000^{o}C:FeO_t = 4.22%; MgO = 1.03%, Helz, 1976). The CaO/Na_2O of the gneisses, which are low by about a factor of 2 compared to the basic granulites, are still higher than average granites - supporting the role of mafic source or contaminant. The moderate to low Al_2O_3 abundances of the gneisses, as compared to island arc compositions, are consistent with a retention of amphibole in the residue. Plots of amphibole breakdown curves as a function of XH_2O (mol. fraction) after Newton and Hansen (1983) indicate that this parameter was at least 0.2 for Mt Chapple granulites and 0.6 for Mt Hay granulites (Fig. 10).

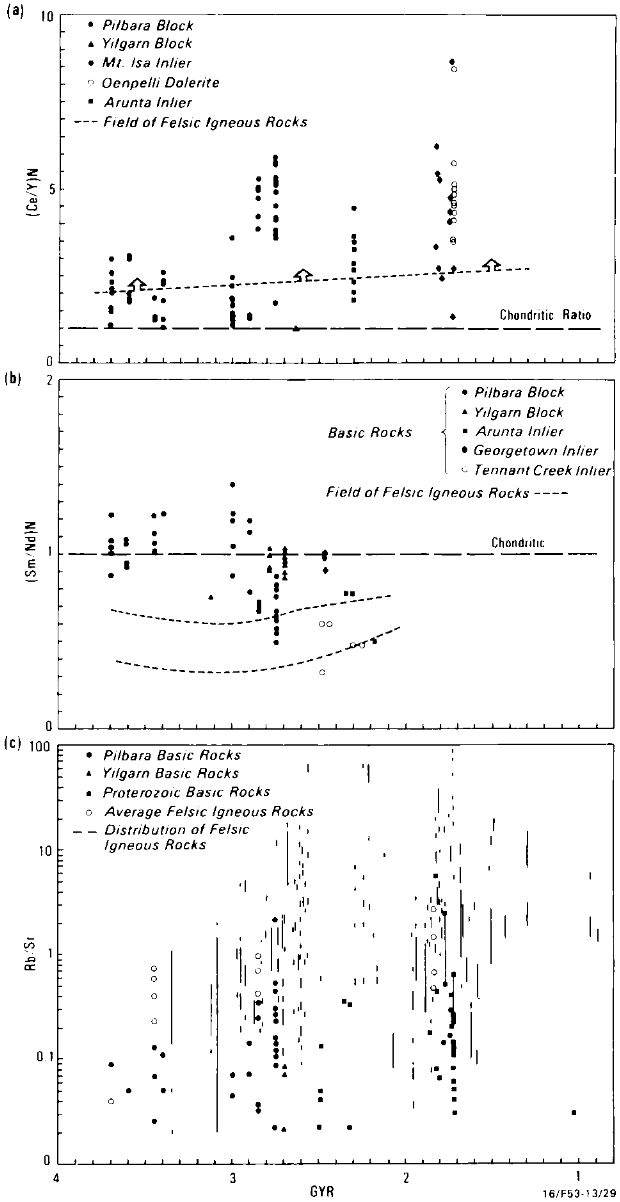

Figure 10. Secular evolution of selected trace element ratios in Precambrian basic and felsic igneous rocks.

A-(Ce/Y)N ratios. Principal data sources: Glikson and Hickman, (1981); Glikson et al., (1985); Sun and Nesbitt, (1978); Wyborn and Page, (1983); Stuart Smith and Ferguson, (1978); this study.

B-(Sm/Nd)N ratios. Principal data sources: Glikson et al., (1985); Sun and Nesbitt, (1978); Black and McCulloch, (1984).

C-Rb/Sr ratios. Principal data sources: Glikson and Hickman, (1981); Hallberg and Glikson, (1979); Glikson, (1980); Wyborn and Page, (1983); Bultitude and Wyborn, (1982).

REE FRACTIONATION

All samples were analyzed for Ce, Nd and Y (Table 1) by XRF and seven samples were analyzed for Nd, Sm, Eu, Dy, Er and Yb by IDMS (Fig.5). The samples analyzed by IDMS include a LIL element-depleted metapyroxenitc cumulate (S 83), a LIL element-enriched high-Mg basic granulite (S 149), two Mt Hay tholeiitic basic granulites (S 80, S 82), a paragneiss from Mt Hay (S 57) and orthogneiss samples from Mt Chapple (S 196) and Redbank Hill (S 227).

With the exception of the depleted cumulate, which has $(Sm/Nd)_N$ about 1 and a strong positive Eu anomaly, corresponding to its marked Sr enrichment (Fig. 4a), all samples show marked increase in light/medium REE ratios relative to chondrites. Possible genetic relationships between the basic granulites and the gneisses are compared in Figs. 6 and 7 where equilibrium fractionation trends for Cpx, Opx, Hbl, Gnt and Plg are plotted.

Assuming an average Mt Hay basic granulite as a source composition, the Ce-Nd-Y relations in the gneisses can be interpreted in terms of separation of various combinations of Cpx, Opx and, in some samples Gnt (Figs. 6 and 7). A fractionation trend produced by separation of an Cpx-Opx-Plg residue in the proportion 23:23:54, respectively, plots close to most gneiss points on the $(Ce/Nd)_N$ vs $(Nd/Y)_N$ diagram. An extension of this trend intersects the average granite, tonalite, granodiorite and monzonite composition of Mt Isa plutons (Wyborn and Page, 1983). However, due to the low percentage of melting required (<10%), no direct derivation is possible and a two-stage melting process may be envisaged instead. The lack of negative Eu anomalies in the gneisses, except for the Redbank Hill blastoporphyritic gneiss, constrains plagioclase fractionation.

The REE model patterns indicate that, to obtain a model partial melt composition similar to the strongly light REE enriched Mt Chapple gneiss (S196) separation of clinopyroxene and hornblende is required (Fig. 7). To obtain a model partial melt composition similar to the light/medium REE-fractionated, medium/heavy REE-flat, and Eu-depleted profile of the Redbank blastoporphyritic gneiss (S227), significant plagioclase must remain in the residue. Further REE modelling of the granulite-gneiss suite is in progress (Foden and Glikson, in prep.).

DISCUSSION

The difficulties in deriving some alkali element rich orthogneiss compositions by partial melting of basic granulites within a closed chemical system suggest that, in addition to, or instead of, LIL element depletion processes operating during metamorphism (Condie and Allen, 1984), the granulite-gneiss complex has experienced in places introduction of mobile incompatible elements (K, Rb, Ba). Three alternative sources may be invoked for these components:

(1) The alkali elements were enriched by progressive fractional crystallization of partial melts of the basic granulites. This may be supported by the generally positive correlation between the size of gneiss units and the fractionation of the rocks.
(2) Alkali element-bearing liquids or fluids may have been derived by partial melting of, or contamination by, sialic materials from below the basic granulites.
(3) Alkali-bearing fluids may have been derived from the underlying mantle.

A distinction between these possibilities must rely on isotopic criteria. Since the initial Sr^{87}/Sr^{86} ratios of Rb-Sr isochron ages of Mt Hay granulites (0.7085, 0.706; Black et al., 1983) are perhaps not high enough to suggest occurrence of Archaean sialic crust beneath the basic granulites, anatexis of relatively young granitic material could account for the alkali addition. Alternatively, the enrichment of alkalies and LREE in the basic granulites is related to upper mantle enrichment. While the initial Nd^{143}/Nd^{144} of Strangways granulites (2015±120 m.y.; E_{Nd} = +1.4) (Windrim and McCulloch, 1983) suggests a long term LREE-depleted mantle source, the almost invariably high LREE/HREE values of .cwl0 the basic granulites, also observed by Sivell and Foden (1985) in amphibolites of the Harts Range, suggests short term upper mantle enrichment and/or synmagmatic enrichment in light REE.

While no clear discrimination between the two latter models seems possible, the general elevation of Ce/Y and Rb/Sr and the decline of Sm/Nd ratios from the Archaean to the early Proterozoic (Fig. 10) may suggest an upper mantle fractionation trend. A secular lithospheric enrichment in LIL and HFS elements would go a long way to explain the geochemical differences between

Archaean and early Proterozoic gneiss-granulite suites. A general increase in the range of Ce/Y ratios is shown by volcanics of the Pilbara Block and persists into the early Proterozoic in the Mt Isa and Pine Creek rocks (Fig. 10a). The increase in light/heavy REE fractionation is also reflected by a secular decline in the Sm/Nd ratios (Fig. 10b). An overall increase in Rb/Sr ratios from early Archaean to the middle Proterozoic (Fig. 10c) underlies the secular rise in initial Sr^{87}/Sr^{86} ratios (Glikson, 1980). In veiw of the short lived crustal prehistory of early Proterozoic sial, as shown by Sm-Nd isotopes (Black et al., 1983; Black and McCulloch, 1984; Windrim and McCulloch, 1984), it seems probable that early Proterozoic sequences formed above young sialic and/or simatic crustal environments rather than above Archaean basement.

To summarize

(1) Basic granulites of the southwestern Arunta Inlier consist of high LREE/HREE, Qz-normative, continental-type LIL element-depleted to enriched tholeiitic basic granulites, probably metagabbros, together with layered anorthosite-pyroxenite complexes, forming a part of a supracrustal pile.

(2) It is likely that the basic granulites have been subjected to some partial melting, producing stringers, bands, stocks and lenses of tonalitic to adamellitic orthogneiss. However, only limited evidence for anatexis is seen at the crustal levels and it is inferred that more extensive melting of similar rocks occurred at depth. Models which assume a LIL element-rich Fe tholeiitic granulite source are consistent with an almost chemically closed partial melting system involving minor residual amphibole. Models which assume a LIL element depleted basic granulite source suggest that alkali elements (K, Rb, Ba) have been added to the felsic-inter mediate melts from an extraneous source, i.e. either underlying sial or the mantle.

(3) Large massifs of gneiss and charnockitic gneiss (Mt Chapple, Mt Zeil) engulf relic enclaves of basic granulites and high-Mg basic granulite with high LIL and HFS (Ti, Zr, Nb, P, Y) elements, possibly introduced from the magmas.

(4) Comparisons between elements depletion orders in cumulate metapyroxenites and enrichment orders in high-Mg basic granulites indicate decreasing mobility in the sequence: Th, Ba, Ce, K, Zr, P, Y, Ti, Sr.

(5) The light REE and alkali elements enrichment of the basic granulites and gneiss, respectively, may have been related to secular enrichment of upper mantle source regions in these elements, as reflected by comparisons between early Archaean, late Archaean and early Proterozoic igneous suites.

ACKNOWLEDGEMENTS

We thank Dr. J.W. Sheraton and Dr. S. Sun for their comments and criticism. This paper is published with the permission of the Director, Bureau of Mineral Resources, Geology and Geophysics.

REFERENCES

Arculus, R.J., Ferguson, J., Chappell, B.W., Smith, D., McCulloch, M.T., Jackson, I., Hensel, H.D., Taylor, S.R., Knutson, I. and Gust, D.A., 1985. Eclogites and granulites in the lower continental crust: examples from eastern Australia and SW U.S.A., Chem. Geol. 50: 1-3.

Arth, J.G., 1976. Behaviour of trace elements during magmatic processes: a summary of theoretical models and their application. U.S. Geol. Survey J. Research. 4: 41-47.

Beswick, A.E., 1982. Some geochemical aspects of alteration and genetic relations in komatiitic suites. In: N.T. Arndt and E.G. Nisbet (Editors), Komatiites. Allen, London, pp.283-308.

Beswick, A.E., 1983. Primary fractionation and secondary alteration within an Archaean ultramafic lava flow. Contr. Min. Pet. 82: 221-231.

Black, L.P., Shaw, R.D. and Stewart, A.J., 1983. Rb-Sr Geochronology of Proterozoic events in the Arunta inlier, central Australia. Bur. Miner. Resour. J. Aust. Geol. Geophys. 8: 129-137.

Black, L.P. and McCulloch, M.T., 1984. Sm-Nd ages of the Arunta, Tennant Creek, and Georgetown inliers of northern Australia. Aust. J. Earth Sci., 31: 49-60.

Bultitude, R.J. and Wyborn, L.A.I., 1982. Distribution and geochemistry of volcanic rocks in the Duchess-Urandanji region, Queensland. Bur. Miner. Resour. J. Aust. Geol. Geophys. 7: 99-112.

Chappell, B.W. and White, A.J.R., 1974. Two contrasting granite types. Pacif. Geol. 8: 173-174.

Collerson, K.C., McCulloch, M.T. and Bridgwater, D., 1984. Nd and Sr isotopic crustal contamination patterns in an Archaean meta-basic dyke from northern Labrador. Geochim. Cosmochim. Acta 48: 71-83.

Condie, K.C., Viljoen, M.J. and Kable, E.J.D., 1977. Effects of alteration on element distributions in Archaean tholeiites from the Barberton greenstone belt, South Africa. Contr. Min. Pet. 64: 75-89.

Condie, K.C. and Allen, P., 1984. Origin of Archaean charnockites from southern India. In: A. Kroner, G.N., Hanson, A.M. Goodwin (Editors), Archaean Geochemistry. Springer Verlag, Berlin, pp. 182-203.

Etheridge, M.E., Wyborn, L.A.I., Rutland, R.W.R., Page, R.W., Blake, D.H. and Drummond, B.J., 1984. The BMR model - a discussion paper. Aust. Bur. Miner. Resour. Record, 84-31.

Fountain, D.M. and Salisbury, M.H., 1981. Exposed cross-sections through the continental crust: implications for crustal structure, petrology and evolution. Earth Planet. Sci. Lett. 56: 263-277.

Glikson, A.Y., 1979. Early Precambrian tonalite - trondhjemite sialic nuclei. Earth Sci. Rev. 15: 1-73.

Glikson, A.Y., 1980. Precambrian sial-sima relations: evidence for earth expansion? Tectonophysics, 63: 193-234.

Glikson, A.Y., 1984. Granulite-gneiss terrains of the southwestern Arunta Block, central Australia: Glen Helen, Narwietooma and Anburla 1:100 000 Sheet areas. Bur. Miner. Resour. Rec. 84-22.

Glikson, A.Y., 1986. An upthrusted early Proterozoic mafic granulite-anorthosite suite and anatectic gneisses, southwest Arunta Block, central Australia: evidence on the nature of the lower crust. Trans. Geol. Soc. S. Africa 89: 263-283.

Glikson, A.Y., 1987. Regional structure and evolution of the Redbank-Mount Zeil thrust zone: a major lineament in the Arunta Inlier, Central Australia. BMR J. Aust. Geol. Geophys. 10: 89-107.

Glikson, A.Y. and Sheraton, J.W., 1972. Early Precambrian trondhjemitic suites in Western Australia and northwestern Scotland, and the geochemical evolution of shields. Earth Planet. Sci. Lett. 17: 227-242.

Glikson, A.Y. and Hickman, A.H., 1981. Geochemistry of Archaean volcanic successions, eastern Pilabra Block, Western Australia Aust. Bur. Miner. Resour. Geol. Geophys. Record, 1981-36.

Glikson, A.Y., Pride, C., Jahn, B., Davy, R. and Hickman, A.H., 1985. RE and HFS (Ti, Zr, Nb, P, Y) element evolution of Archaean mafic-ultramafic volcanic suites. Pilbara Block, Western Australia. Aust. Bur. Miner. Resour. Geol. Geophys. Record, 1985.

Hallberg, J.A. and Glikson, A.Y., 1979. Archaean granite-greenstone terrains of western Australia. In: D.R. Hunter (Editor), Precambrian Shields of the Southern Hemisphere: Elsevier, Amsterdam.

Hansen, E.C., Newton, R.C. and Janardhan, A.S., 1984. Pressures, temperatures and metamorphic fluids across an unbroken amphibolite facies to granulite facies transition in Southern Karnataka, India. In: A. Kroner, G.N. Hanson, A.M. Goodwin (Editors), Archaean Geochemistry. Springer Verlag, Berlin, pp.161-181.

Hanson, G.N., 1980. Rare earth elements in Petrogenetic studies of igneous systems. Ann. Rev. Earth Planet. Sci. 8: 371-406.

Helz, R.T., 1976. Phase relations of basalts and their melting ranges at PH_2O = 5 kb. Part II: melt compositions. J. Petrol. 17: 139-193.

Holloway, J.R. and Burnham, W.C., 1972. Melting relations of basalt with equilibrium water pressure less than total pressure. J. Petrol. 13: 1-29.

Humphries, H.E., and Thomson, G., 1978. Trace element mobility during hydrothermal alteration of oceanic basalts. Geochim Cosmochim Acta, 42: 127-136.

Huppert, H.E. and Sparks, S.J., 1985. Cooling and contamination of mafic and ultramafic magmas during ascent through continental crust. Earth Planet. Sci. Lett. 74: 371-386.

Irving, A.J., 1974. Geochemical and high pressure experimental studies of garnet pyroxenite and pyroxene granulite xenoliths from the Delegate basaltic pipes. Australia. J. Petrol. 15: 1-40.

Lambert, I.B. and Heier, K.S., 1967. The vertical distribution of uranium, thorium and potassium in the Continental Crust. Geochim. Cosmochim. Acta. 31: 377-390.

Lambert, I.B. and Heier, K.S., 1968. Geochemical investigations of deep seated rocks in the Australian shield. Lithos 1: 30-53.

Lambert, I.B. and Wyllie, P.J., 1972. Melting of gabbro (quartz eclogite) with excess water to 35 kb, with geological implications. J. Geol. 80: 693-708

Lambert, R. St. J., 1983. Metamorphism and thermal gradients in the Proterozoic continental crust. Geol. Soc. Am. Memoir. 161: 155-166.

Marjoribanks, R.W. and Black, L.P., 1974. The Geology and geochronology of the Arunta complex north of Ormiston Gorge, central Australia. J. Geol. Soc. Aust. 21: 291-299.

McCulloch, M.T. and Wasserburg, G.J., 1978. Sm-Nd and Rb-Sr chronology of continental crust formation. Science 200: 1003-1011.

Newton, R.C., Smith, J.V. and Windley, B.F., 1980. Carbonic metamorphism, granulites and crustal growth. Nature, 288: 45-50.

Newton, R.C. and Hansen, E.C., 1983. The origin of Proterozoic and late Archaean charnockites: evidence from field relations and experimental petrology. Geol. Soc. Am. Memoir, 161: 167-178.

Pearce, J.A. and Norry, M.J., 1979. Petrogenetic implications of Ti, Zr, Y and Nb variations in volcanic rocks. Contr. Min. Pet. 69: 33-47.

Reed, S.J.B. and Ware, N.G., 1975. Quantitative electron probe analysis of silicates using energy dispersive X-ray spectrometry. J. Petrol. 16: 499-519

Shaw, D.M., 1970. Trace elements fractionation during anatexis. Geochim. Cosmochim. Acta 34: 237-243.

Shaw, D.M., 1972. The origin of the Apsley gneiss, Ontario. Can. J. Earth Sci., 9: 18-35.

Shaw, R.D., Stewart, A.J. and Black, L.P. 1984. The Arunta Inlier: a complex ensialic mobile belt in central Australia. Part 2: tectonic history. Aust. J. Earth Sci. 31: 457-484.

Sheraton, J.W., 1970. The origin of the Lewisian gneisses of Northwest Scotland, with particular reference to the Drumbeg Area, Sutherland. Earth Planet. Sci. Lett. 8: 301-310.

Sheraton, J.W., Skinner, A.C., and Tarney, J., 1973. The geochemistry of the Scourian gneisses of the Assynt District. In: R.G. Park and J. Tarney (Editors), The early Precambrian of Scotland and Related Rocks of Greenland. University of Keele, pp.

Sheraton, J.W. and Labonne, B., 1978. Petrology and geochemistry of acid igneous rocks of northeast Queensland. Aust. Bur. Miner. Resourc. Bull. 169.

Sheraton, J.W. and Black. L.P., 1983. Geochemistry of Precambrian gneisses: relevance for the evolution of the east antarctic shield. Lithos, 16: 274-296.

Sheraton, J.W. and Collerson, K.D., 1984. Geochemical evolution of Archaean granulite facies gneisses in the Vestfold Block: Comparisons with other Archaean complexes in the east Antarctic shield. Contr. Min. Pet. 87: 51-64.

Sighinolfi, G.P. and Gorgoni, C., 1978. Chemical evolution of high grade metamorphic rocks - anatexis and removal of material from granulite terrains. Chem. Geol. 22: 157-176.

Sivell, W.J. and Foden, J.D., 1985. Banded amphibolites of the Harts Range meta-igneous complex, central Australia: an early Proterozoic basalt-tonalite suite. Precamb. Res. 28: 223-252.

Stewart, A.J., Shaw, R.D. and Black, L.P., 1984. The Arunta Inlier: a complex ensialic mobile belt in central Australia: Part I: stratigraphy, correlations and origin. Aust. J. Earth. Sci. 31: 445-455.

Stuart-Smith, P.G., and Ferguson, J. 1978. The Oenpelli dolerite - a Precambrian continental tholeiite suite from the Northern Territory, Australia. Bur. Miner. Resourc. J. Aust. Geol. Geophys. 3: 125-133.

Sun, S., 1982. Chemical composition and origin of the Earth's primitive mantle. Geochim. Cosmochim. Acta, 46: 179-192.

Sun, S. and Nesbitt, R.W., 1978. Petrogenesis of Archaean ultrabasic and basic volcanics: evidence from rare earth elements. Contr. Min. Pet., 65: 301-325.

Sun, S., Nesbitt, R.W. and Sharaskin, A.Y. 1979. Chemical characteristics of Mid-Ocean ridge basalts. Earth Planet. Sci. Lett., 44: 119-138.

Tarney, J., 1976. Geochemistry of Archaean high-grade gneisses, with implications to the origin and evolution of the Precambrian crust. In: B.F. Windley (Editor), Early History of the Earth. Wiley & Sons: London, pp.405-418.

Tarney, J. and Windley, B.F., 1977. Chemistry, thermal gradients and evolution of the lower continental crust. J. Geol. Soc. London 134: 153-172.

Thompson, A.B., 1985. Melting of the continental crust (abst.) Terra Cognita, 5: 228.

Turekian, K.K. and Wedepohl, K.H., 1961. Distribution of the elements in some units of the Earth's crust. Geol. Soc. Am. Bull. 72: 175.

Weaver, B.L. and Tarney, J., 1981a. The Scourie dyke suite: Petrogenesis and geochemical nature of the Proterozoic sub continental mantle. Contr. Min. Pet. 78: 175-188.

Weaver, B.L. and Tarney, J., 1981b. Chemical changes during dyke metamorphism in high grade basement terrains. Nature 289: 47-49.

Windrim, D.P. and McCulloch, M.T., 1983. Nd and Sm chronology of Strangways Range granulites: implications for crustal growth and reworking in the Proterozoic of central Australia. Geol. Soc. Aust. 6th Aust. Geol. Conv. Abstr. 9: 192-193.

Wyborn, L.A.I and Page, R.W., 1983. The Proterozoic Kalkadoon and Ewen batholiths. Mt. Isa inlier, Queensland: Source, chemistry, age and metamorphism. Bur. Miner. Resour. J. Aust. Geol. and Geophys. 8: 53-69.

EVOLUTION OF THE PRECAMBRIAN CRUST OF THE ARAVALLI MOUNTAIN RANGE

A.B.ROY

ABSTRACT

The Precambrian crust of the Aravalli Mountain Range comprises a number of Proterozoic fold belts underlain and delimited by schist-gneiss-granitic rocks of Archaean age. The basement, which was partly remobilized during the Proterozoic orogenesis, includes a heterogeneous assemblage of biotite gneiss, amphibolite, aluminous paragneiss, quartzite and marble formed during the time span 3.5-2.5 Ga. The three major Proterozoic cover units: the Aravalli Supergroup (~2.5-1.90 Ga), the Delhi Supergroup (~1.9-1.45 Ga), and the Champaner Group (closing at ~0.9 Ga), evolved as ensialic fold belts through development of a series of rift-basins, grabens with intervening horsts. The basin-fills included sediments and volcanics laid down in several successive stages punctuated by great hiatuses. Sedimentation and volcanicity in these basins recorded several secular changes in terms of basin formation, lithologic characters, biological evolution, magmatism and metallogeny. The Proterozoic, which started with the formation of linear fold belts, culminated in abortive rifting and associated anorogenic multimodal magmatism in the axial zone of the mountain range and west of it.

INTRODUCTION

The Aravalli Mountain Range which fringes the northwestern margin of the Peninsular Indian Shield, is thought to be one of the most ancient mountain ranges in the world. Running for more than 700 km between the sandy waste land of the Thar in the west and the Malwa Plataeu in the east, this ancient orographic belt resembles a distorted hour-glass-like feature on the satellite imagery. The general trend of the mountain range is northeast-southwest . It swings gradually to east-southeast in the southern part. The average elevation of the Aravalli Mountains is 700 metres. The highest elevation is 1722 metres at Mt. Abu.

Significant information is now available on the gravity field over the Aravalli Mountains. Published Bouguer, free-air and isostatic maps show, a regional gravity 'high' of considerable magnitude all along the length of the mountains, flanked by linear belts of negative gravity values on the southwestern and northeastern sides of the mountain range. The gravity 'high' suggests that the underlying crust has higher than normal density, and the gravity lows are the regions where root formations have taken place (Verma and Subrahmanyam, 1984).

TABLE I.
Stratigraphic succession of the Precambrian rocks of the Aravalli Mountains.

		Age in Ga.
	Vindhyan Supergroup	
	Malani rhyolite suite	0.75
	Erinpura granite and Godra granite	0.75-0.90
	Champaner Group (Sirohi Group ?)	
	Post-Delhi granites	1.45
Delhi Supergroup	Ajabgarh Group	
	Alwar Group	
	Ryanhalla Group [1]	
	Post-Aravalli granites (Darwal and Amet granites)	1.9
Aravalli Supergroup	Upper Aravalli Group	
	Middle Aravalli Group	
	Lower Aravalli Group	
Mewar Gneiss & Granite	Berach granite	(~2.6)
	Untala and Gingla granite	3.0
	Pelitic gneiss, quartzite, marble, calc-silicates	
	Tonalitic biotite gneiss, amphibolite	3.5

[1] sensu Roy (1988), Raialo 'series' sensu Heron (1917)

The geological foundation of this great mountain range comprises a number of metasedimentary and metavolcanic units deposited successively over an Archaean basement. The Aravalli Supergroup is the oldest Proterozoic cover unit. The Delhi

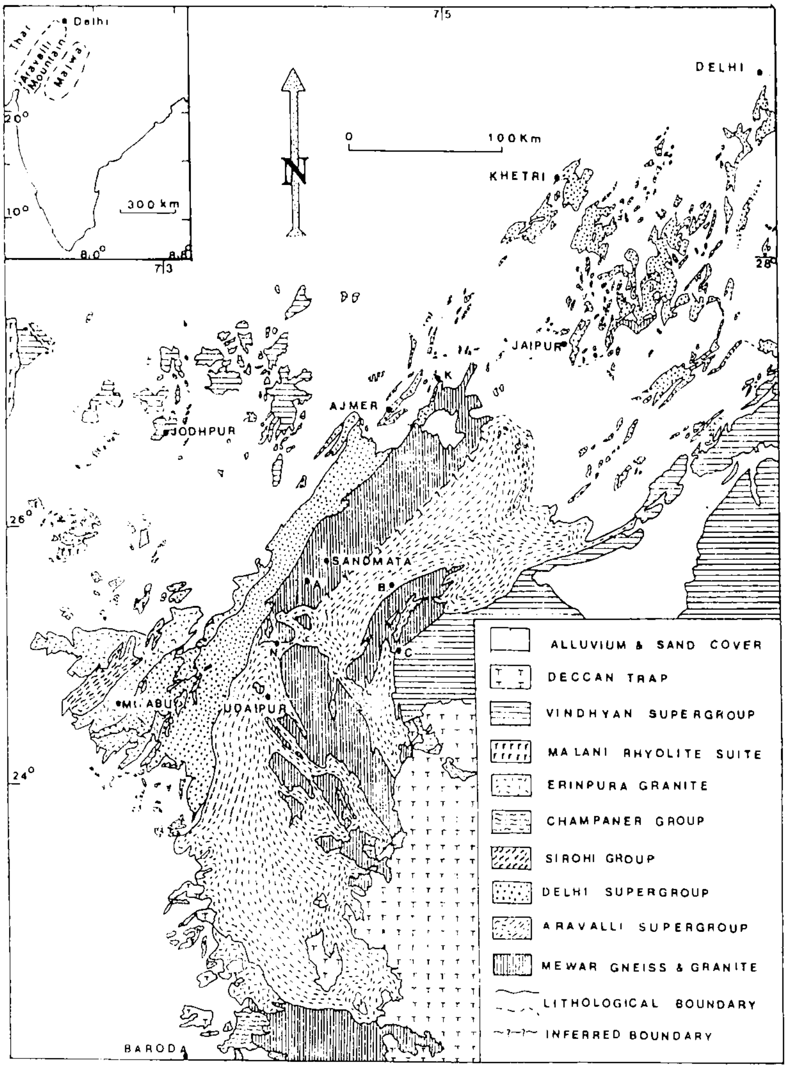

Figure 1. Generalized geological map of the Aravalli Mountain Range and its vicinity (modified after the map published by the Geological Survey of India, 1969). A = Amet; B = Bhilwara; C = Chittaurgarh; K = Kishangarh; N = Nathdwara.

Inset: Map of the Indian Peninsula showing the location of the Aravalli Mountain Range in between the Thar desert and the Malwa Plateau.

Supergroup and the Champaner Group are the two successive younger units (Table 1). There are several intrusions of granitic, mafic, ultramafic and alkaline rocks into the cover as well as the basement rocks. Rhyolite flows, ignimbrites and tuffs (late Proterozoic Malani suite of igneous rocks) occur in isolated hills and ridges west of the Aravalli Mountain Range.

The Proterozoic rocks occur along well-defined fold belts delimited by blocks of Archaean rocks. The distribution of the Archaean basement rocks and the Proterozoic fold belts exposing the Aravalli and Delhi Supergroups and the Champaner Group is shown in Fig. 1.

BASEMENT ROCKS: AGE AND LITHOLOGICAL CHARACTER

The records of the continental rocks in the Aravalli Mountain Range (in Rajasthan and northern Gujarat) extend back to about 3.5 billion years. Information regarding this antiquity of the basement rocks of the region comes from two different sources. First is an indirect evidence of a Pb-isochron age of 3.5 Ga from detrital zircons in the overlying Aravalli (Supergroup) phyllite (Vinogradov et al., 1964). The actual confirmation of such an old age is provided by the recent Sm/Nd isotopic study of amphibolite and biotite gneiss from the area east of Udaipur. The study suggests that the two rocks are cogenetic and have evolved from a protolith of mantle origin at 3.5 Ga (Macdougall et al., 1983). The different gneisses and amphibolite which form the bulk of the pre-Proterozoic basement were syn- or late-kinematically intruded by granitic rocks at around ca. 3.0 Ga (Choudhary et al., 1984). A part of the pre-Proterozoic basement was either formed or reconstituted at around 2.6 Ga, as indicated by the U-Pb discordia age of zircons from the Berach granite (Sivaraman and Odom, 1982).

The basement rocks (described subsequently as the Mewar Gneiss to differentiate them from those components of the Banded Gneissic Complex of Heron (1953) which could be migmatized Proterozoic rocks) comprise heterogenous assemblages of biotite (or hornblende) gneiss, granitic rocks, amphibolite, aluminous paragneiss, quartzite, marble, calc-silicate rocks, and pegmatites. The gneisses of different lithology and the granitic rocks are by far the most common rock types of the Mewar gneiss. The biotite (locally hornblende) gneisses are dominantly tonalitic in composition (Table II); a few samples, however, plot in the

TABLE 2.

Selected chemical analyses of Archaean biotite gneiss (1-8) and intrusive granites (9-16) of the Aravalli Mountain Range.

Sample No.	1	2	3	4	5	6	7	8	9	10	11	12	13	14	15	16
SiO_2	66.04	72.04	71.96	72.21	60.68	73.21	74.15	70.73	71.52	71.03	72.59	73.57	71.78	65.90	72.74	66.82
TiO_2	0.84	0.50	Tr	Tr	0.62	0.72	0.56	0.38	0.24	0.23	0.23	0.13	Tr	0.15	0.08	0.15
Al_2O_3	16.57	14.12	13.35	14.43	14.10	12.60	12.10	15.61	12.80	13.39	13.72	13.89	13.75	16.63	12.28	14.33
Fe_2O_3	1.94	4.91^T	4.75^T	5.12^T	3.12	1.96	4.29^T	2.79^T	2.68	2.02^T	2.24^T	1.78^T	0.78	1.00	0.85^T	0.93^T
FeO	4.12	-	-	-	5.45	4.33	-	-	-	-	-	-	5.60	4.11	-	-
MnO	0.11	-	-	-	Tr	Tr	-	-	0.05	0.04	0.04	0.03	0.05	-	-	-
MgO	1.32	0.15	0.20	0.39	3.19	1.05	1.05	1.22	0.45	0.25	0.01	0.07	0.22	1.70	0.31	0.76
CaO	4.39	1.34	1.96	1.47	5.09	1.14	2.03	1.61	0.85	1.02	1.17	1.63	0.90	1.40	1.15	1.60
Na_2O	3.21	4.63	3.50	4.32	2.60	2.62	3.63	5.29	3.01	3.60	2.46	2.64	2.65	2.70	7.04	8.47
K_2O	2.57	1.48	1.45	1.30	3.49	2.20	1.09	1.77	5.07	4.99	5.49	3.95	3.33	4.38	2.80	5.27
P_2O_5	0.19	-	-	-	-	-	0.15	0.80	0.05	0.04	0.05	0.04	0.07	0.10	0.06	0.06
Total	101.30	99.17	99.17	99.24	98.34	99.83	99.05	100.2	96.72	86.61	99.00	98.73	99.13	98.47	97.31	98.39

Data source : 1. K.C. Gyani (1979) Ph.D. thesis - Univ. Rajasthan (published)
2-4. S.S.Shekhawat (1982). Ph.D. thesis. Univ. Rajasthan (unpublished)
5,6,13,14 - Heron (1953)
4, 8 - J.D. Macdougall (unpublished work)
9 - 12 - A.K. Choudhary (1984). Ph.D. thesis. Gujarat Univ. (unpublished)
15, 16 - Roy *et al.* (1985)

adamellite-granodiorite field in the Na_2O-K_2O diagram (Fig. 2). The Sm/Nd isotopic studies indicate that these rocks (biotite gneiss and cogenetic amphibolite) were derived from a LREE depleted mantle source (E_{juv} (T)=3.5, see Macdougall et al., 1983).

TABLE III.

Chronology of Precambrian crust-building events in the Aravalli Mountain Range

Age in Ga.	Event
0.75 -0.90	Folding of Champaner Group (and possibly Sirohi Group). Development of ductile shear zones in the Delhi fold belt. Low grade metamorphism;high-temp. thermal metamorphism (M4) at intrusive contacts. Intrusion of diapiric granite-granodiorite, mafic-ultramafic (anorogenic)bodies. Acid effusives in in the west of the mountain range.
1.45	Two (or three) phases of folding. Lowest green schist to amphibolite facies metamorphism (M3). Intrusion of synkinematic granite, and remobilization of basement granites.
1.9	Formation of Delhi basins as grabens. Intrusion of granites synkinematically with isoclinal folding of the Aravalli Supergroup under greenschist to amphibolite facies metamorphism (M2). Extensive basement remobilization and diapiric intrusion, granulitic rocks with the basement blocks.
~2.5	Formation of Aravalli grabens on peneplained Mewar gneiss and granite, and deposition of terrigenous sediments and minor volcanics.
2.6(?)	Emplacement of granites (Berach granite, for example).
3.0	Intrusion of Untala, Gingla and other similar granites synkimatically or late synkinematically with one or two phases of folding of para and ortho-gneisses, amphibolite facies metamorphism (M1).
3.5*	Deposition of metasediments in shallow linear basins, intrusion of basic (minor ultramafic) and tonalitic gneisses.
Pre - 3.5	History is unknown

Note: Geochronological data compiled from Choudhary et al., (1984), Gopalan et al., (1979) and Macdougall et al., (1983). Use of new values of decay constant (1.42×10^{-11} Yr^{-1}) for ^{87}Rb would reduce Rb/Sr ages by about 2% (Choudhary, 1984).

* Sm/Nd isotopic data.

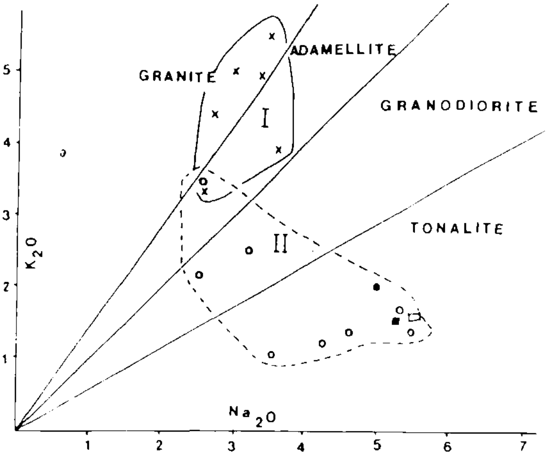

Figure 2. Na_2O - K_2O plot of grey biotite gneisses (open circle) and intrusive Archaean granites (cross). Averages of leuco biotite-quartz tonalite gneiss of Barberton (closed circle) (Viljoen and Viljoen, 1969), Older Metamorphic Group (OMG) tonalite gneiss Singhbhum Craton, Eastern India, (solid square) (Saha and Ray,1984), and the oldest tonalite-trondhjemite gneisses of the Dharwar 'Protocontinent' (open rectangle) (Bhaskar Rao et al., 1983) are plotted for comparison).

The amphibolite gneiss constitutes a major constituent of the Mewar Gneiss. These basic rocks showing low Zr, Nb, and Rb, and moderate Cr, Ni, V, and Sr, have a tholeiitic parentage with probable oceanic affinity (Kataria et al., 1988). Some amphibolites occurring east of Ajmer are reportedly metamorphosed komatiite in composition (Gyani and Pandya, 1986). There are some minor bodies of ultramafic rocks, which are troctolitic in composition (P.K.Kataria, personal communication). Patches of small bodies of altered ultramafic rocks occur in some parts of the Mewar Gneiss. These are manifestations of Proterozoic intrusions.

High-alumina para-gneisses occur as comformable bodies with other lithologic units of the Mewar Gneiss. These rocks, which show a considerable areal distribution, gradually pass on to migmatites of various types. Quartzite (containing fuchsite mica) and marble (poor in MgO content) occur as isolated linear bodies within the Mewar gneiss. The quartzite and marble, unlike their Proterozoic counterparts, do not occur in close association. There are a few minor occurrences of calc-silicate rocks and para-amphibolite in the Mewar Gneiss.

Intrusion of normal potassic granite and adamellite (Table II; Fig. 2) into the early formed ortho-and para-gneissic rocks took place at ca. 3.00 Ga and also probably at 2.6 Ga (Choudhary et al., 1984). Sr isotopic initial ratios of these granites are in the range of 0.7033 ± 208 to 0.7043 ± 33 (Choudhary, 1984). The low values possibly suggest a mantle origin for the granites.

There is hardly any information available on the stratigraphic relationship of the different ortho- and paragneisses constituting the Mewar Gneiss. The mode of emplacement of the mafic rocks now metamorphosed to amphibolite is also difficult to determine. However, when seen in association with quartzite, a very intimate interleaving is noticeable. Possibly, the mafic bodies represent flows (and tuff ?) accumulated in a shallow-water environment. The parentage of biotite schist and gneiss makes interesting study. These rocks, which on the one hand are intimately associated with amphibolite, appear inseparable at places, from the true pelitic rocks. The rare presence of thin folia and bands of amphibolite in biotite schist, coupled with petrographic evidence of alteration of hornblende to biotite, might suggest formation of at least a part of the biotite gneiss and schist by potash metasomatism of amphibolite during migmatization. Mention has already been made of the bodies of biotite gneiss which show mantle characteristics as indicated by the Sm/Nd isotopic data.

The quartzite and marble which occur as linear bodies in the Mewar Gneiss are evidently the youngest metasedimentary units deposited in narrow troughs. There is, however, no clear evidence of unconformity between these and other gneissic rocks, nor is there any record of a conglomerate horizon in the basement rocks.

Metamorphic assemblages in the para-and/or orthogneisses, which are unaffected by the proterozoic events, show amphibolite facies metamorphism (M 1). Superimposition of a later phase of Proterozoic metamorphism (M 2) on the earlier one produced polymetamorphic assemblages over a large region in central Rajasthan. M 2 metamorphism caused widespread anatexis in the region and locally produced several anhydrous assemblages of amphibolite-granulite transition facies (Sharma and Narayan, 1975; Sharma, 1988). Patches of very high pressure granulites, presumably emplaced from deeper crustal levels, have been reported from this belt.

Although the basement rocks have been considerably remobilized over a large region (Naha and Roy, 1983), some evidence of Archaean folding and deformation is preserved in areas which remained as a zone of very low strain during the Proterozoic deformation. The earliest folds are isoclinal and are coaxially refolded by open, upright folds. Locally, a third phase of folding with subhorizontal axial plane can be observed. In spite of polyphase folding, the gneissic foliation remains the most dominant planar fabric in all the rock types. Bedding is identifiable at places in the metasedimentary rocks. Nowhere could any angular relationship be observed to prove that the foliation or (schistosity) is axial planar to any such folds.

The earliest deformation noted in the Mewar gneiss is pre-3.00 Ga in age (Fig.3). Very little information is available about the most primitive crust-building events, although preliminary Sm/Nd

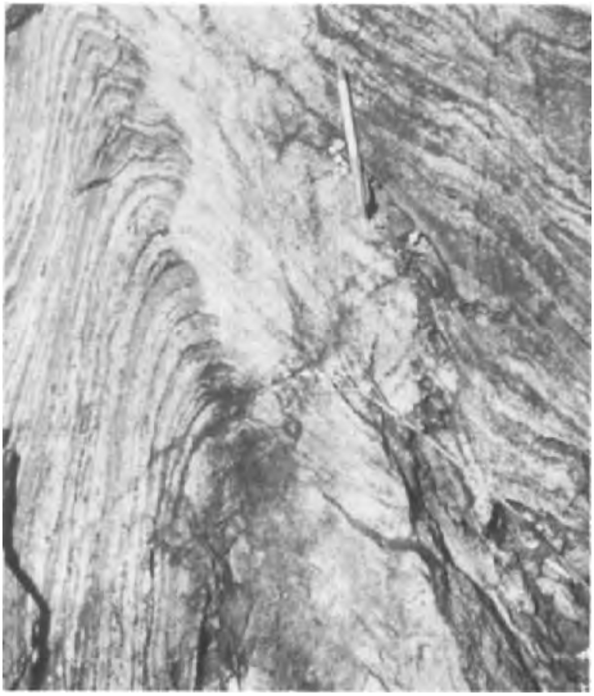

Figure 3. Mobilization of granitic material (3.0 Ga Untala phase) along a thin zone subparallel to the axial plane of a fold in the biotite gneiss (Mewar Gneiss).

data suggest the presence of 3.5 Ga old crustal remnants in Rajasthan. The presence of highly fractionated metasediments (quartz arenite, calcite marble and high-aluminous pelites) and normal granites in pre-3.5 Ga rocks indicates the evolved nature of the Archaean crust in Rajasthan.

EVOLUTION OF THE ARAVALLI FOLD BELTS (~2.5 - 1.90 Ga)

With the onset of the Proterozoic, a number of elongate, fault-bounded grabens were developed on the denuded Archaean crust (Fig.4) which had attained a thickness in the range of 20-25 km. These grabens, which were either detached or partially linked, became receptacles of a thick terrigenous debris, chemogenic sediments and volcanic rocks. The total sedimentary-volcanic package (the Aravalli Supergroup) comprises three Groups separated by an unconformity (Table 1). A continuous change in depositional environment, reflecting the interplay of tectonism, erosion and sedimentation, is recorded in lithological attributes of the successively deposited rocks. The chemistry of the volcanic rocks (high-alumina tholeiitic basalts), and the presence of coarse fanglomerates along basin margins, proximal greywacke towards centres of shallow-water depositories, rapid lithofacies changes across the belts and the presence of ultramafic rocks within the basins, are characteristics of pull-apart basins. Vertical movements changing relief between the basins and the

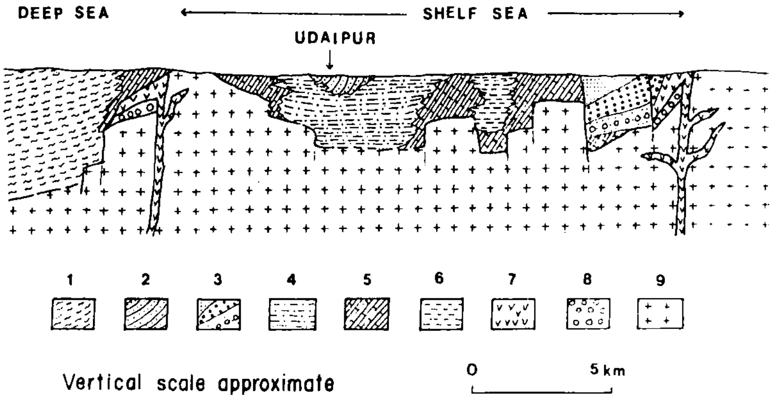

Figure 4. Restored east-west stratigraphic section of the Aravalli basin through Udaipur, showing relationships between lithological facies, environment and time.

uplifted basement blocks seem to be the primary factor controlling the sedimentation pattern during the Aravalli depositional history. The general upward increase in the amount of granite-derived sediments suggests progressive uplift and denudation of the sialic crust (Roy and Paliwal, 1981).

There are two distinctly different 'facies sequences' in the rocks of the Aravalli Supergroup, indicating deep-sea and near-shore shelf environments of deposition (Roy and Paliwal, 1981). This bimodal character of sediments may appear comparable to that of the sediments deposited in an eugeosynclinal and miogeosynclinal couplet, as in the Alpine orogenic belts. Such 'eu- and miogeosynclinal' characters are seemingly unknown in the pre-Proterozoic rocks (cf. Salop and Scheinmann, 1969).

Ultramafic rocks now represented by serpentinites were intruded during the terminal phase of the Aravalli sedimentation. Most of these rocks occur along the boundary of deep-water and shelf-seas in the southern part of the Aravalli belt; only a few are confined to the deep-sea region. Field associations and chemical characteristics of the serpentinites suggest that these could represent 'cumulate phases' emplaced at the time of deepening of basins.

Many of the synsedimentary basin-margin faults were listric in nature. Movement along these faults, either during or subsequent to the deposition of beds, rotated some of the formations sinistrally (viewing north) to steeply dipping positions before the initiation of folding.

The deformation of the Aravalli rocks was due to a combination of pure shear and simple shear movements (cf. Naha and Halyburton, 1977). A series of isoclinal reclined or inclined folds with dominant easterly or westerly plunge were the earliest structures to form. Schistosity axial planar to these folds is marked by down-dip or steeply plunging mineral lineations, mullions and stretched pebbles developed along with folding (Fig. 5). The strain pattern over the Aravlli basins is extremely heterogeneous in nature. Thus, there are certain high-strain zones, mainly along the steep-sided walls of the depositional grabens, producing wide zones of mylonites and phyllonites. By contrast, there are cover (Aravalli) rocks overlying blocks of basement which virtually escaped this deformation.

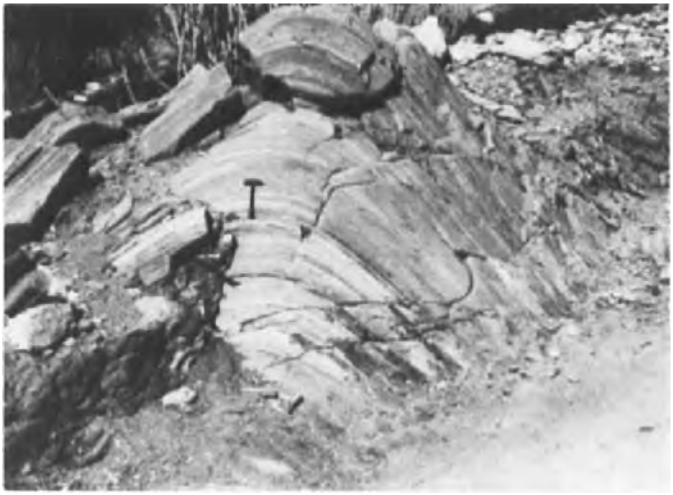

Figure 5. Strongly lineated Aravalli (Supergroup) quartzite showing folding formed during the Delhi phase of deformation.

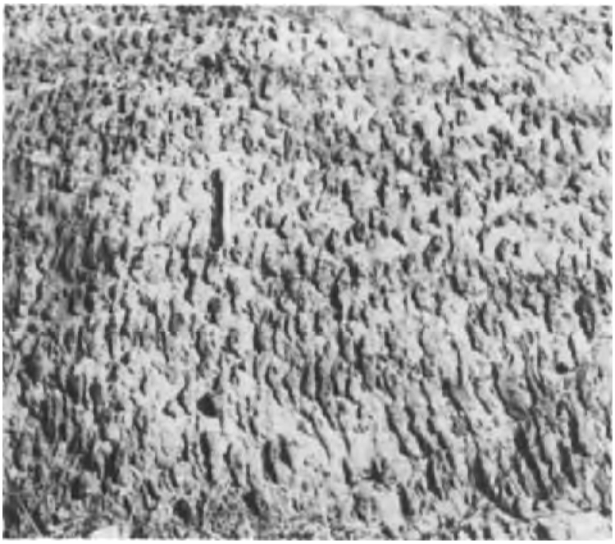

Figure 6. Stromatolitic phosphorite in dolomite of the Aravallli Supergroup.

Metamorphism synkinematic with this deformation is generally of low to extremely low grade in the shelf-facies zone of the

Aravalli Supergroup, around Udaipur as well as in the easternmost basins to the northeast and southeast of Chittaurgarh (i.e., the Hindoli and Badesar-Kharmalia belts, respectively). High-grade metamorphic rocks occur in patches in the Udaipur-Jharol basins and over a wide region in the Nathdwara-Bhilwara regions. The granulite-facies metamorphism of the basement rocks of the Sandmata region (Sharma, 1988) can be tied up with the thermal rise during the Aravalli orogeny.

The culmination of the Aravalli orogeny is marked by emplacement of synkinematic or late-synkinematic granites at ca. 2000 Ma (Choudhary et al., 1984). The Darwal granite, emplaced in the Aravalli rocks is an example of this type of granite activity. Contemporary granitic rocks occur around Amet and other places where they intrude the basement gneisses. Initial ratios of Sr isotopes range between 0.7053 and 0.7093 (Choudhary, 1984). The values possibly suggest a mixed source for the post-Aravalli granites.

The nepheline syenite of Kishangarh is, in all probability, an early-Proterozoic intrusion in rocks which could be correlated with the Aravalli Supergroup.

A strong contrast in the pattern of crustal growth is clearly reflected not only in the lithology but also in the nature of mineralization during the Archaean and Proterozoic. The Archaean basement is virtually devoid of mineral deposits, except along zones of basement-cover interactions. The first sign of mineralization is recorded in the basal Aravalli volcanics in the form of copper ores (and locally of baryte). The association of copper minerals with the volcanic rocks suggests a volcanogenic process of mineralization. The most important mineral deposits which make the Aravalli Supergroup unique, are the stromatolitic phosphorites (Fig. 6). Prolific but extremely restricted occurrences of stromatolitic phosphorites are known in the Lower Aravalli Group of the Udaipur region (Roy and Paliwal, 1981; Choudhuri and Roy, 1986). The sudden growth of stromatolitic structures in the lower-carbonate sequence of the Aravalli Supergroup marks a biologic explosion unknown in the Archaean rocks (cf. Goodwin, 1981). The other secular changes which can be noticed in the stratigraphic record are the abundance of dolomite (probably reflecting the high CO_2 content of the Proterozoic atmosphere), and the first appearance of lateritic horizons in the Proterozoic rocks. Extension laterite cappings on the Aravalli dolomites clearly imply increased oxidizing conditions resulting from enhanced photosynthetic production of O_2 (cf. Windley, 1973; Goodwin, 1981).

Associated with the stromatolitic phosphorite, but not occurring together, are the deposits of uranium and copper. In the Middle Aravalli Group of the shelf facies, which comprises a thick pile of terrigenous clasts, there is an important carbonate (or rarely shale) hosted lead-zinc silver horizon. All these mineral deposits appear for the first time in the Precambrian history of the rocks of the region.

EVOLUTION OF THE DELHI FOLD BELT (~1.9 - 1.45 Ga)

The Delhi basins opened up as a system of linear grabens (or half grabens) with intervening horsts, closely following the culmination of the Aravalli crust-building events. Initially, the basins formed in the northeastern part of Rajasthan. Later on basins extended all along the axial zone of the Aravalli Mountain Range. Volcano-sedimentary rocks about 10 km thick were laid down in these basins in three successive sequences: the Raialo (Sensu Heron, 1917, renamed as the Rayanhalla Group), Alwar and Ajabgarh groups (Singh, 1982a).

Sedimentation in the Delhi grabens registers a significant change in the proportion of volcanic to terrigenous clastic sediments compared to that in the earlier Aravalli basins. Thus, unlike the Aravalli basins in which volcanic rocks formed only during the initial phases of basin formation, the Delhi basins included a significant proportion of volcanic flows and tuff-materials. A shallow-water (fluvial and marginal marine) depositional environment has been envisaged for the sedimentary sequences of the Delhi Supergroup (Deb, 1980; Singh, 1982a). The deposits show a dominance of immature clastics derived from rapidly uplifted granitic source terranes in the basal parts (Singh, 1982b). In strong contrast to the pattern of sedimentation observed in the Aravalli Basin of the Udaipur-Jharol area, there is no apparent differentiation of shallow and deep-water sediments in any of the Delhi basins. Further, the black-shale facies, developed so extensively in the Aravalli Supergroup, is either absent or insignificantly developed in the Delhi rocks.

Other significant secular changes reflected in the lithological characters of the Delhi rocks in contrast to the Aravalli rocks are: (i) the virtual absence of stromatolitic phosphorite, and (ii) dominance of calcitic marbles (limestones) over the dolomitic in the Delhi sequences.

Basinwise, the Delhi grabens are more linear in pattern, having well-defined clean-cut boundaries. Episodic synsedimentary dislocation along the basin margin faults seems to be the primary factor controlling the sedimentary facies. Features providing evidence for a rift-framework of sedimentation (Fig.7) (Singh, 1984) are: (i) thick accumulations of shallow-water deposits, (ii) a preponderance of coarse clastics (fanglomerates and fan delta deposits), (iii) an abrupt change in thickness, (iv) rapid changes in lithology across the basin axis, (v) a strong overlapping relationship, and (vi) the presence of synsedimentary volcanics including coarse pyroclastics.

The volcanics in the Delhi sequences show a bimodal rhyolite - basalt association. In the Rayanhalla Group (oldest Group of the Delhi Supergroup), the volcanics comprise lava flows, agglomerates, volcanic breccias and tuffs interbedded with quartzite and conglomerate. These volcanics chemically resemble high-K_2O continental tholeiites (Singh, 1985). In additon to basaltic flows, there are also flows of andesite, trachyte, rhyolite and even ultramafic rocks (Singh, 1982a). Ultramafic rocks have been reported from the basal part of individual flows. Volcanic rocks occur extensively in both the Alwar and Ajabgarh groups all along the axial zone of the Aravalli Mountain. The basic volcanics are tholeiitic in composition, showing continental (or partly oceanic, Bhattacharyya and Mukherjee, 1984) affinity. Felsic volcanics and volcanoclastic sediments occur as bands in the basic volcanics occurring southwest of Ajmer (J.Bhattacharjee, personal communication).

The terrigenous sediment - volcanic association of the Delhi basins matches well with the 'Assembly II' of Condie (1982), implying their deposition in intracratonic rift basins or aulacogens. The entire sequence, except for some basin-margin formations (Singh, 1982a), was affected by three phases of folding (Naha et al., 1984; Roy and Das, 1985). The earliest deformation produced isoclinal (or tight) folds with a penetrative axial

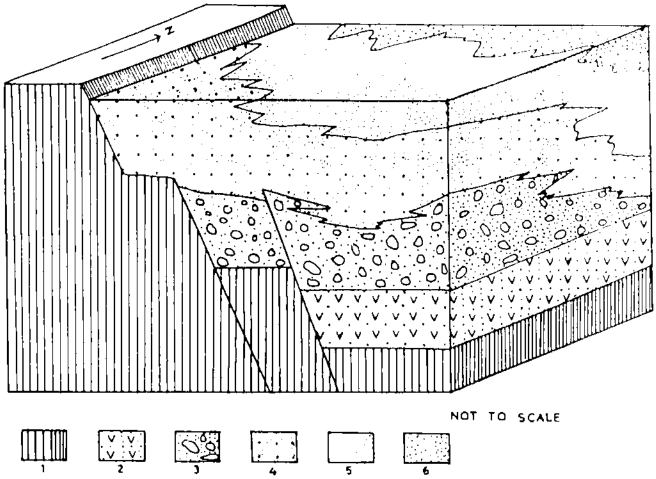

Figure 7. Schematic representation of the basin filling in the Lalgarh (Delhi) graben (Data from Singh, 1984). 1. Pre-Delhi basement; 2. Basal Alwar volcanics, 3. Boulder conglomerate, 4. Red boulder conglomerate with sandstone-siltstone interbeds, 5. Sandstone-conglomerate interbeds showing profuse cross-bedding, 6. arkosic sandstone.

planar schistosity. These early formed folds were coaxially refolded to open to tight upright folds. This deformation marks the major crustal shortening phase affecting not only the Delhi rocks, but also other pre-Delhi rocks except those which remained as zones of low strain. The third-generation structures are cross-folds, showing open or very gentle profiles. The metamorphic climax of the Delhi Supergroup rocks (M3) was during the first and second phases of folding (Bhattacharyya, 1980; Lal and Ackermand, 1981; Roy and Das, 1985). A number of granitic bodies intruded the Delhi rocks concomitantly with the peak of metamorphism and the first two phases of folding (Roy and Das, 1985) (Fig. 8). Rb/Sr dating of these granites reveal that the peak of the tectono-thermal event of the Delhi orogeny was reached at ca. 1.45 Ga (Choudhary et al., 1984). These granites have rather low Sr initial ratios (e.g., 0.7075 ± 40 for Seoli granite, Choudhary, 1984). Choudhary (1984) and Choudhary et al., (1984) have also studied other granites in the Delhi fold belt and reported disturbed isochron patterns having quite high computed intial Sr ratios (0.7289 ± 120 for Dadikar granite and 0.7197±29 for

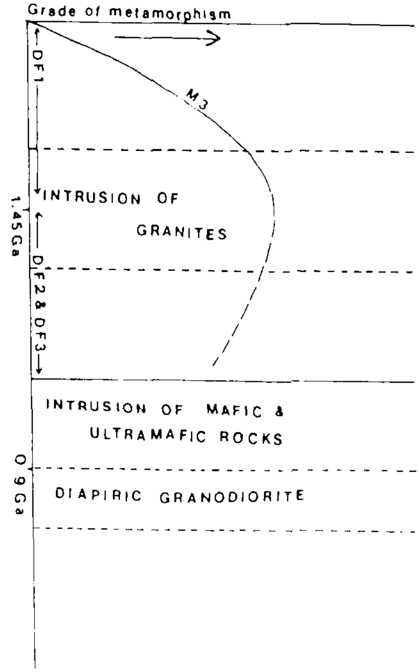

Figure 8. A diagrammatic correlation between folding (DF1, DF2 and DF3), metamorphism (M3 and M4) and intrusions of granite, gabbro, diorite-ultramafic-mafic rocks in the Delhi fold belt.

Ajmer granite). These could be pre-Delhi granites partly reconstituted during the Delhi orogeny (Roy, 1988).

The Delhi granites show high K_2O values and the majority fall in the granite field in the Na_2O-K_2O diagram (Fig. 9). There is an apparent increase in the Na_2O/K_2O ratio from north to south.

LATE PROTEROZOIC TECTONO-MAGMATIC EVENT ($\sim$1.0 - 0.75 Ga)

The opening of Champaner Basin in the southern fringe and possibly the Sirohi Basin along the southwestern flanks of the Aravalli Mountains marks the culminating phases in the cratonization process of the Precambrian crust in this part of the Peninsular Indian Shield. Both the depositories are characterized by shallow-water sediments. Volcanic rocks occur in significant proportion in the Sirohi Group. The sediments comprising the Champaner Group include a thick sequence of conglomerate quartzite, greywacke, dolomitic limestone and manganese-and

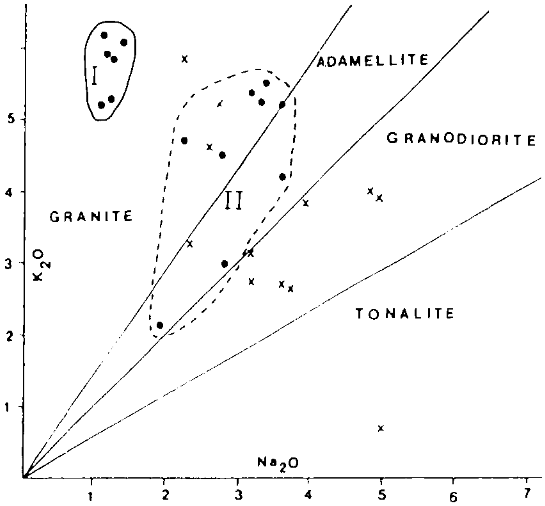

Figure 9. Na_2O-K_2O plot of granites intrusive into the Delhi Supergroup rocks. Solid circle - 1.45 Ga granites; Cross - 0.9 - 0.85 granites. I. Field of Khetri granites. II. Field of Alwar - Jaipur granites.

phosphorite-bearing beds. The entire sequence was folded into a series of open antiforms and synforms with WNW-ESE axial trends. Godhra granite which intruded the Champaner yielded a 0.9 Ga Rb/Sr isochron age (Gopalan et al., 1979). Very little information is as yet available on the deformation pattern of the Sirohi Group rocks. Folds of more than one generation have, however, been reported in the group.

The time span between 0.85 - 0.75 Ga is a period of extensive granitic activity over a wide area in the southwestern and western flanks of the Aravalli Mountain Range. In its axial zone, a series of diapiric granites, and locally alkali syenite (Deb, 1980), intruded the folded and regionally metamorphosed rocks of Delhi Supergroup along with ultramafic rocks (altered to serpentinites), gabbro and diorite. Field evidence suggests that the mafic ultramafic intrusives were emplaced earlier than the acid intrusives. A number of ductile shear zones developed at this stage in the Delhi fold belt, affecting even the mafic intrusive rocks. Granitic rocks (dominantly granodioritic in composition) showing a synkinematic fabric intruded the diorite at several places. A rather high Sr initial ratio of these granites (0.7148 - 0.7226, Choudhary, 1984) suggests their evolution from reworked materials. The magmatic activity in this part of the Aravalli Mountains caused extensive thermal metamorphism (M4) of the pre-exsting rocks.

The tectono-magmatic activity described above is a part of the anorogenic magmatism resulting from aborted rifting. Extensive acid-magmatic eruptions over a wide area west of the Aravalli Mountains is also related to this tectono-thermal event.

Deposition of the late Proterozoic-Cambrian flat-lying platform sediments (the Vindhyans) on either side of the Aravalli Mountains indicates that the Precambrian crust had been cratonized by that time. A summary of the chronology of the Precambrian crust-building events is given in Table III.

ACKNOWLEDGEMENTS

I had many fruitful discussions with my colleagues on several topics covered in this paper. Thanks are due to Dr.Dilip Nagori for his assistance in preparation of the manuscript.

REFERENCES

Bhaskar Rao, Y.J., Beck, W., Rama Murthy, Y., Nirmal Charan, S., and Naqvi, S.M., 1983. Geology, geochemistry and age of metamorphism of Archaean grey gneisses around Channarayapatna, Hassan district, Karnataka, South India. In: S.M.Naqvi and J.J.W.Rogers, (Editors), Precambrian of South India. Geol. Soc. India, Mem., 4, pp.309-328.

Bhattacharyya, P.K., 1980. Metamorphic reaction in static and dynamic environments, a petrographic illustration from the metapelites in the Khetri Copper Belt, Rajasthan, India. N. Jb. Miner. Abh., 139: 191-204.

Bhattacharyya, P.K. and Mukherjee, A.D., 1984. Petrochemistry of metamorphosed pillows and the geochemical status of the amphibolites (Proterozoic) from the Sirohi district, Rajasthan, India. Geol. Mag., 121: 465-473.

Choudhary, A.K., 1984. Precambrian Geochronology of Rajasthan, Western India. Ph.D. - Thesis, Gujarat University, Ahmedabad (unpublished).

Choudhary, A.K., Gopalan, K. and Sastry, C.A., 1984. Present status of the geochronology of the Precambrian rocks of Rajasthan. Tectonophysics, 105: 131-140.

Choudhuri, B. and Roy, A.B., 1986. Proterozoic - Cambrian Phosphorite deposits: Jhamarkotra, Rajasthan, India. In: P.J. Cook and J.H. Shergold (Editors), Proterozoic-Cambrian Phosphorites, v.1, Cambridge University Press, pp.202-219.

Deb., M., 1980. Genesis and metamorphism of two stratiform massive sulphide deposits at Ambaji and Deri in the Precambrian of Western India. Econ. Geol., 75: 577-591.

Goodwin, A.M., 1981. Precambrian Perspectives. Science, 213 (4503): 55-61.

Gopalan, K., Trivedi, J.R., Merh, S.S., Patel, P.P., Patel, S.G., 1979. Rb-Sr age of Godra and related granites, Gujarat (India). Proc. Indian Acad. Sci. (Earth Planet. Sci.), 88A: 7-17.

Gyani, K.C. and Pandya, M.K., 1986. Geology and Geochemistry of the Archaean granulite-gneiss belt of Rajasthan. Proc. Seminar on Evolution of the Precambrian Crust in the Aravalli Mountain Belt, University of Rajasthan, Udaipur (abst.), pp.62-64.

Heron, A.M., 1917. Geology of northeastern Rajputana and adjacent districts. Geol. Surv. India, Mem., 45: 128.

Heron, A.M., 1953. Geology of central Rajputana. Geol. Surv. India, Mem., 79: 389.

Kataria, P., Chaudhari, M.W. and Althaus, E., 1988. Petrochemistry of amphibolites from the Banded Gneissic Complex of Amet, Rajasthan, northwestern India, N.Jb. Miner. Abh. (in press).

Lal, R.K. and Ackermand, D., 1981. Phase petrology and polyphase andalusite-sillimanite type regional metamorphism in pelitic schists of the area around Akhwali, Khetri Copper Belt, Rajasthan, India. N. Jb. Miner. Abh., 141: 161-185.

Macdougall, J.D., Gopalan, K., Lugmair, G.W. and Roy, A.B., 1983. The Banded Gneissic Complex of Rajasthan, India, Early crust from depleted mantle at 3.5 AE. Trans. Am. Geophys. Union, 64(18), 351pp.

Naha, K. and Halyburton, R.V., 1977. Structural pattern and strain history of a superposed fold system in the Precambrian of central Rajasthan, India. II, Strain history. Precamb. Res., 4: 85-111

Naha, K. and Roy, A.B., 1983. The problem of the Precambrian basement in Rajasthan, western India. Precamb. Res., 19: 217-223.

Naha, K., Mukhopadhyay, D.K., Mohanty, R., Mitra, S.K., and Biswal, T.K., 1984. Significance of contrast in the early stages of the structural history of the Delhi and the pre-Delhi rock groups in the Proterozoic of Rajasthan, western India. Tectonophysics, 105: 195-206.

Roy, A.B., 1988. Stratigraphic and tectonic framework of the Aravalli Mountain Range. In: A.B.Roy (Editor), Precambrian of the Aravalli Mountains. Geol. Soc. India, Mem., 7, pp.3-31.

Roy, A.B. and Das. A.R., 1985. A study of time relations between movements, metamorphism and granite emplacement in the middle-Proterozoic Delhi Supergroup of Rajasthan. J.Geol. Soc. India, 26: 726-733.

Roy, A.B. and Paliwal, B.S., 1981. Evolution of Lower Proterozoic epicontinental deposits: Stromatolite bearing Aravalli rocks of Udaipur, Rajasthan, India. Precamb. Res., 14: 49-74.

Saha, A.K., and Ray, S.L., 1984. The structural and geochemical evolution of the Singhbhum granite batholithic complex, India. Tectonophysics, 105: 163-176.

Salop, L.I. and Scheinmann, Yu. M., 1969. Tectonic history and structures of platforms and shields. Tectonophysics, 7: 565-597.

Sharma, R.S. and Narayan, V., 1975. Petrology of the polymetamorphic schist from an Archaean complex terrain, southwest of Beawer, Rajasthan, India. N. Jb. Miner. Abh., 124: 190-222.

Sharma, R.S., 1988. Patterns of metamorphism in the Precambrian rocks of the Aravalli Mountain Belt. In: A.B.Roy (Editor), Precambrian of the Aravalli Mountains. Geol. Soc. India, Mem. 7, pp.33-75.

Singh, S.P., 1982a. Palaegeography and sedimentation history of the Delhi Supergroup - a study from the Bayana sub basin, northeastern Rajasthan, Ph.D. - thesis. University of Rajasthan, Jaipur (unpublished).

Singh, S.P., 1982b. Stratigraphy of the Delhi Supergroup in the Bayana sub-basin, northeastern Rajasthan. Rec. Geol. Surv. India. 112(7): 46-62.

Singh, S.P., 1984. Evolution of the Proterozoic Alwar sub-basin, northeastern Rajasthan. Indian J. Earth Sci., CEISM Seminar Volume, pp.113-124.

Singh, S.P., 1985. Geochemistry of Jahaj-Govindpura volcanics, Bayana sub-basin, Northeastern Rajasthan. J. Geol. Soc. India., 24: 208-215.

Sivaraman, T.V. and Odom, A.L. 1982. Zircon geochronology of Berach Granite of Chittaurgarh, Rajasthan. J. Geol. Soc. India, 23: 575-577.

Verma, R.K., Mitra, S. and Mukhopadhyay, M., 1986. An analysis of gravity field over Aravallis and the surrounding region. Geophys. Res. Bull., 24(1).

Verma, R.K. and Subrahmanyam, C., 1984. Gravity anomalies and the Indian lithosphere: review and analysis of existing gravity data. Tectonopysics, 105: 141-162.

Viljoen, M.J. and Vilijoen, R.P., 1969. The geochemical evolution of the granitic rocks of Barberton region. Geol. Soc. S. Afr. Spec. Publ. 2: 189-219.

Vinogradov, A., Tugarinov, A., Zhykov, C., Stapnikova, N., Bibikova, E. and Khorre, K., 1964. Geochronology of Indian Precambrian. Proc. Int. Geol. Cong. New Delhi - 2, Pt. X-Archaean and Precambrian Geology: 552-567.

METAMORPHIC EVOLUTION OF ROCKS FROM THE RAJASTHAN CRATON, NW INDIAN SHIELD

Ram S. Sharma

ABSTRACT

This paper describes the metamorphic characteristics of rocks of the Banded Gneissic Complex (3500 to 2600 Ma) and of the supracrustals of the Aravalli (ca. 2000 Ma) and Delhi (1650 to 950 Ma) Supergroups, constituting the Rajasthan Craton and Aravalli mobile belt in the NW Indian Shield. Two regional recrystallization events, separated in space and time, are recorded in the complex, whereas only one regional metamorphism (excluding thermal imprints) is documented in the Proterozoic supracrustals. Sand Mata granulites, a possible component of the Basement Complex and having a shear contact with it, reveal a tectonic path which contrasts with the 'normal' P-T path of most metamorphic terrains and collision zones.

In view of the fact that gneissic rocks as old as 3.5 Ga. constitute the Banded Gneissic Complex (BGC) and from the consideration that the Aravalli sequence of the Precambrian gneissic rocks in the NW Indian Shield is ensialic, the present author proposes a model of ensialic orogenesis, instead of the plate tectonic model, for the evolution of the Aravalli fold belt. In this model, the development of large basins (characteristic of the Aravalli-Delhi sediments) is visualized as having formed as a result of ductile extension of hot sialic material, rather than by brittle rupture. Ductile spreading followed by contraction of crust, rather than subduction or plate collision, is considered the dominant process in the evolution of this Proterozoic belt. This large-scale ensialic orogenesis in the NW Indian Shield involved the re-working of the granite gneiss complex, whereby deformed cover rocks are now seen to rest on a mobilized basement. However, there are areas, for example the Berach and Sarara, where deformed cover rocks lie on unmobilized or less mobilized basement.

INTRODUCTION

The Rajasthan Craton, a part of the Indian Shield, is formed of the Archaean Complex and Proterozoic supracrustals which have undergone superposed deformation, metamorphism and granitic emplacements throughout the late Precambrian, culminating in the crustal thickening that built the Aravalli Mountains. This orogen is the major mountain range of Peninsular India, striking at right angles to the Himalaya in which the NW Shield elements can be traced. South of 25^o latitude in central Rajasthan (Fig. 1), the Aravalli orographic trend veers from NE-SW to N-S and then NNW-SSE and finally WNW-ESE near the NE-trending Son-Narmada lineament. The fold belt is bounded on the east by the Great Boundary Fault, east of which lies the Bundelkhand Massif and the younger cover rocks. The purpose of this paper is to provide information on the nature of metamorphism in the basement and cover rocks and to propose an evolutionary history of the Precambrian crust of the NW Indian Shield.

The distribution and geologic relations of the rocks occurring in Rajasthan have been comprehensively documented by Heron and co-workers (see Heron, 1953) and their maps (see Fig. 1) provide a foundation upon which subsequent work has been based. Almost all geologists working in Rajasthan are unanimous in accepting three metamorphosed stratigraphic units which in ascending order are:

1 Banded Gneissic Complex (3500 to 2600 Ma): recently modified and renamed as the Bhilwara Supergroup by the officers of the Geological Survey of India (Gupta et al., 1980).

2. Aravalli Supergroup (ca. 2000 Ma)

3. Delhi Supergroup (1650 to 950±50 Ma)

Detailed structural studies (see Naha, 1983; Roy, 1985), geochronological results (Gopalan and Choudhary, 1984) and petrological investigations (Sharma, 1977; 1983a,b,c; 1988) of rocks from the Banded Gneissic Complex (BGC) and the supracrustals of the Aravalli and Delhi supergroups have raised many problems with regard to (i) the nature of the BGC and its recognition as a basement in Rajasthan (ii) the grade of metamorphism in the Aravalli rocks which is largely lower than in the underlying BGC and the overlying Delhis in central Rajasthan; (iii) the reported

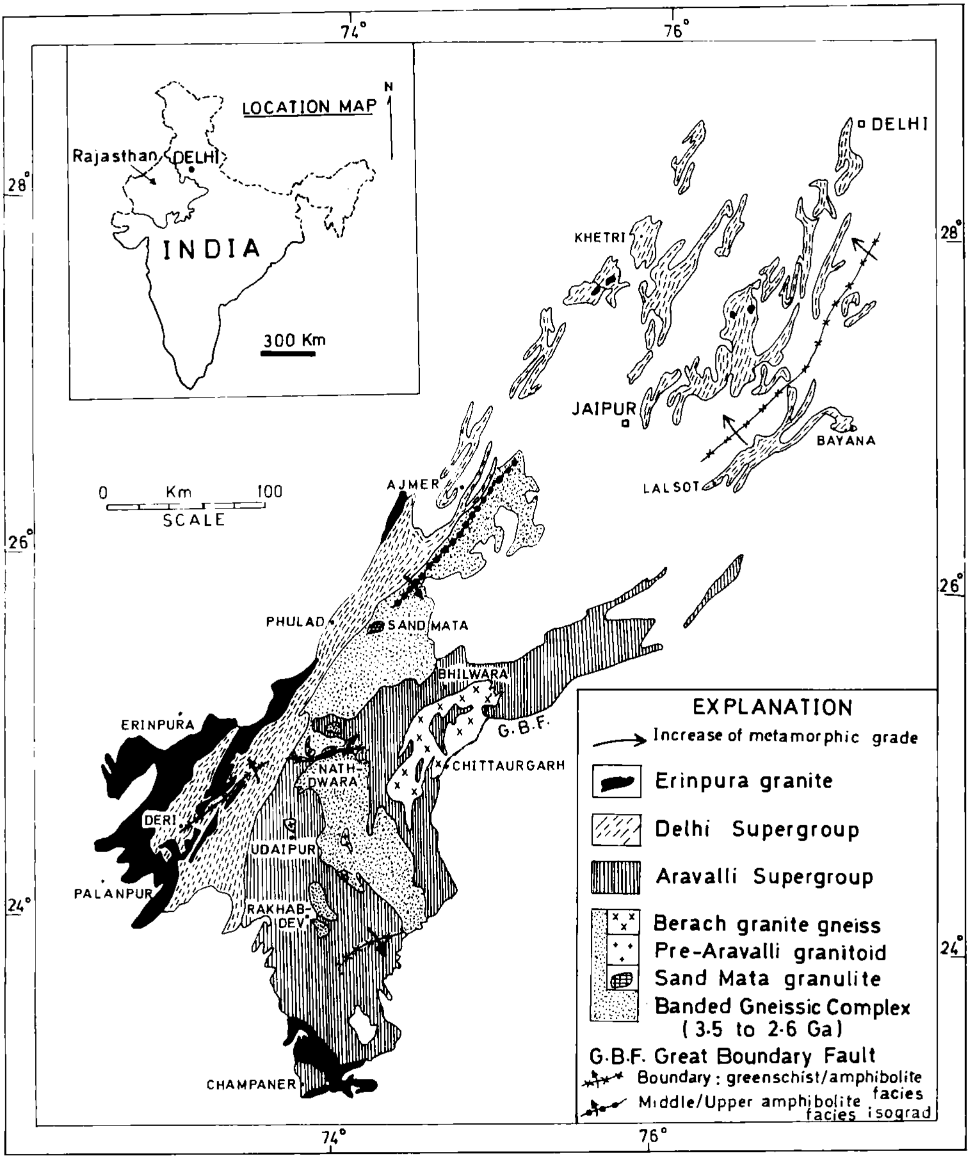

Figure 1. Map showing the distribution of the Precambrian crystalline rocks from the Rajasthan Craton, NW Indian Shield (simplified after published maps of the Geological Survey of India). The delineated isograds and facies boundaries are after Sharma (in press).

difference in isotopic ages of the granitic intrusives in the Delhi Supergroup from the northern and southern parts of the Aravalli belt; and (iv) the orogenic events and evolutionary models for the Aravalli mobile belt.

BANDED GNEISSIC COMPLEX, ITS ROCKS AND METAMORPHISM

The term, Banded Gneissic Complex, was coined by Heron in 1917 (see Heron, 1953) for a Pre-Aravalli stratigraphic unit in which metasediments and igneous (-like) materials of different compositions and ages were recrystallised together under plutonic conditions and in which original rock units are only seen in the form of xenoliths, streaks and patches. The term is preferred here rather than the newly coined Bhilwara Supergroup for the reasons stated by Sharma (see Sharma, 1988). Four rock types are generally distinguishable in the BGC: (a) schist, (b) gneiss, (c) amphibolite and ultramafic rocks, and (d) late intrusives. These four rock types encompass a large variety of lithologies.

The pelitic schists are characterized by garnet, staurolite, kyanite, sillimanite and biotite in different combinations. They are dark coloured and generally devoid of or impoverished in white mica. The schists are often interlayered with or veined by quartzo-feldspathic material and form different migmatitic rocks. Often, the schist and gneiss alternate and produce the characteristic banded gneiss of the BGC. Occasionally, the schists are found as schlieren within the gneisses and show a variety of polymineralic assemblages (Sharma and Althaus, 1977; Sharma and MacRae, 1981; Sharma et al., 1985):

(i) gedrite-cordierite-biotite-kyanite-sillimanite-quartz-plagioclase;
(ii) garnet-cordierite-gedrite-biotite-kyanite-sillimanite-quartz
(iii) garnet-gedrite-staurolite-spinel-cordierite-kyanite-sillimanite;
(iv) garnet-biotite-sillimanite-kyanite-quartz-plagioclase- K-feldspar;
(v) sapphirine-cordierite-spinel-kyanite-sillimanite-tourmaline-garnet;
(vi) kornerupine-tourmaline-staurolite-biotite-kyanite-sillimanite-cordierite-garnet;
(vii) kornerupine-tourmaline-gedrite-biotite-kyanite-sillimanite-(-quartz);
(viii) hypersthene-bioite-plagioclse-K-feldspar-quartz-garnet;
(ix) hypersthene-sillimanite-kyanite-gedrite-plagioclase-bioite.

These assemblages evidently are the outcome of polymetamorphism and partial melting of the meta-pelitic component of the BGC (Sharma, 1983a). From metamorphic investigations of the rocks, the present author showed that the BGC had crystallized in upper amphibolite facies conditions (Sharma, 1988). The schistose components are found to record mineral assemblages of two regional metamorphic events. Relics of kyanite within a late

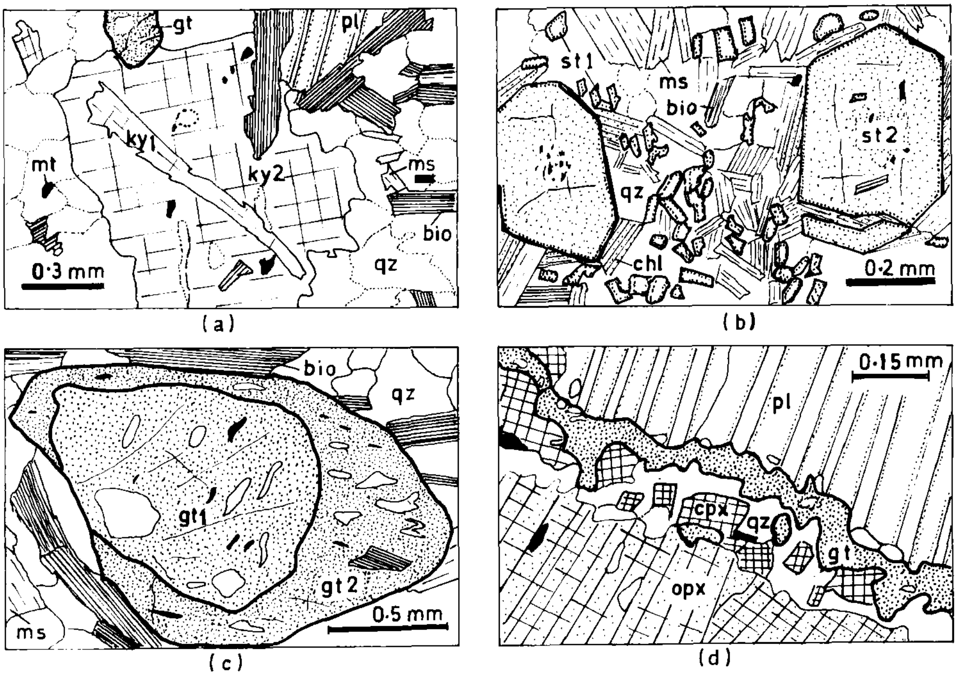

(a) (b) (c) (d)

Figure 2. Mineral textures showing two regional metamorphic events in rocks of the Banded Gneissic Complex. (a) inclusion of an earlier 'resorbed' kyanite (ky 1) within a later recrystallized kyanite (ky 2). (b) Two generations of staurolite. (c) Overgrowth of garnet (gt 2) on an earlier Pre-Aravalli garnet (gt 1) in schist of BGC. The internal schistosity (si) of the outer garnet truncates against the rim of the inner garnet, suggesting a hiatus in growth of the two garnets, which is called a tectono-metamorphic unconformity on a small scale (Sharma, 1983b). (d) Corona of garnet-clinopyroxene-quartz at the interface of hypersthene and plagioclase in basic granulite from Sand Mata.

Mineral abbreviations : bio = biotite, chl = chlorite, cpx = clinopyroxene, gt = garnet, ky = kyanite, ms = muscovite, mt = magnetite, opx = orthopyroxene, pl = plagioclase, st = staurolite, qz = quartz.

crystallized kyanite (Fig. 2a) and two generations of staurolite (Fig. 2b) point to an earlier metamorphism of amphibolite facies, at least up to the staurolite-kyanite zone of regional metamorphism. During the second metamorphism, assemblages containing gedrite, cordierite, kornerupine and hypersthene were formed by complex mineral reactions associated with partial melting of metapelites in deeper levels. A most convincing evidence of two distinct regional metamorphisms of the BGC schist is documented in garnet, wherein the pre-Aravalli schistosity is preserved in the core of an early formed garnet which was later overgrown by another garnet during the Aravalli metamorphic event (Fig. 2c). In this overgrowth texture, the contact between the two garnets is not only sharply demarcated by the difference in their colour, refractive index and type of inclusions, but also the orientation of internal schsitosity (si) in the inner garnet is truncated against the boundary of the outer garnet (Sharma, 1983b). Late muscovite blasts containing relics of Al-silicate are also found in these high-grade schists/paragneisses. All these features make the mapping of isograds difficult, although a first attempt was made by Sharma and Narayan (1975) and Sharma (1977) in the BGC terrain of north-central Rajasthan (see Fig. 1).

Gneisses are the dominating rocks of the BGC. Some varieties are clearly paragneisses, particularly those associated with schists, and contain dark schlieren within them. Others, for example the Berach granite gneiss, appear to be deformed magmatic protoliths. The chemical nature of these orthogneisses, however, remains to be studied, but some Rb/Sr age data have been determined on them. The whole-rock Rb-Sr age of the Berach granite gneiss is found to be about 2600 Ma. (Crawford, 1970; Sivaraman and Odom, 1982). Others, such as the porphyroblastic Anjana gneiss from Udaipur district, have not yet been dated but could be equivalent in age to the Berach granite gneiss, or could be even older, like the Untala and Gingla granites (2950 Ma; Choudhary et al., 1981).

Amphibolite from the BGC is subordinate in aerial extent to schists, gneiss and migmatites. Their parent composition in all cases is not proven due to the possible chemical changes that may have occurred during the two regional recrystallization events. However, the amphibolites near Udaipur are evidently of igneous origin. They gave the same age (3.5 Ga) by the Sm/Nd method as the nearby tonalitic gneiss, implying that these rock components represent early crust from the depleted mantle (Macdougall et al., 1983). At some places the amphbolites are associated with minor calc-silicate bands which contain diopside, grossularite, forsterite, scapolite, wollastonite, plagioclase and calcite in various combinations. Ultrabasic rocks are scarce and are found as intrusive bodies, e.g., at Tikhi mines to the south of Devgarh-Madaria in Udaipur district. These rocks are almost serpentinized and are similar in composition to the ultramafic bodies occurring in the supracrustals of the Aravalli and Delhi Supergroup. At places they are emerald bearing and are traversed by pegmatitic dykes.

The BGC also contains several granitoid rocks from which it is conceivable that during regional metamorphism large-scale crustal melting occurred which generated granitoid plutonism in different structural levels. At many places the BGC is intruded by basic rocks, mainly dolerite and sometimes norite.

Recent studies by the author (Sharma, 1983c) have shown that the BGC also contains segments of deep crust, as at Sand Mata. Here the rocks are composed of:

(i) garnet-pyroxene granulite with garnet-diopside-hydersthene-plagioclase-quartz;

(ii) pelitic granulite with kyanite-sillimanite-biotite-garnet-quartz-plagioclase with or without hypersthene and cordierite;

(iii) mafic norite dyke with blastophitic texture.

The age of the norite dyke is unknown. It certainly intruded during the waning stages of granulite-facies metamorphism (Sharma et al., 1987). The garnet-bearing basic granulite, on the other hand, is characterised by coronitic texture in which a garnet-clinopyroxene-quartz corona has developed at the interface of hypersthene and plagioclase (Fig. 2d), suggesting the reaction (Green and Ringwood, 1967; Hansen, 1981):

Hypersthene + plagioclase = garnet + diopside + quartz,

which is divariant in the ACFM system. That the corona texture has not formed during cooling is revealed by the P-T estimates and by the development of garnet in the norite dyke showing igneous texture. The intrusion presumably provided additional heat and caused an almost complete re-equilibration of the assemblages in the granulites.

The above-stated texture in the high-pressure granulites also reveals a two-stage recrystallization history (polymetamorphism) similar to the schist component of the BGC. In the first metamorphic event (M1), the hypersthene-plagioclase pair remained stable but during the second metamorphism (M2), operating under higher load pressure, the mineral pair became incompatible to produce the garnet-clinopyroxene-quartz corona.

Calculations of metamorphic conditions in the granulite assemblages gave temperature concentrations at 850^{o}C and 650^{o}C and pressure values at 8-10 kb and 5 kb according to different geothermobarometric models. Interestingly, the P estimate in the pelitic granulite was found to be higher for the garnet rim than for the garnet core involving garnet-cordierite-Al-silicate-quartz and garnet-plagioclase-Al-silicate-quartz equilibria. This implies that there was loading during cooling of the Sand Mata granulites. Furthermore, the concentration of pressure values at 8-10 kb and at 5 kb, without intermediate values, is interpreted to suggest that the granulites were suddenly transported from deeper levels of the crust and emplaced at shallower depths of ca.15 kilometers (corresponding to 5 kb). A strong evidence in support of this geological event is cited by the presence of the shear zone which surrounds the Sand Mata granulites against their contact with the BGC, as stated earlier.

The P-T estimates, textural criteria, and the chronology of crystallization of aluminium silicates (in the order Ky Sill Ky) in the pelitic granulites, have been used to derive a tectonic path which has an anticlockwise sense in P-T space, and can be summarised as follows:

1) T increase up to 850^{o}C and partial melting at depths of 30-35 km (8-11 kb).
2) Loading during cooling of the granulites in the T range of 750^{o} - 650^{o}C, which is consistent with the higher pressure value for garnet rim than for the garnet core composition.

3) Nearly isothermal decompression and emplacement of the granulite (along a ductile shear zone) at about 5 kb and 650°C, followed by erosion.

The deduced tectonic path for the Sand Mata granulites places considerable constraints on the crustal evolution in the NW Indian Shield, as discussed in a later section.

ARAVALLI SUPERGROUP AND ITS METAMORPHIC CHARACTERISTICS

The supracrustals of the Aravalli Supergroup mainly include the rocks of the Aravalli System and Raialo Series of Heron (1953) and are composed of pelitic and calcareous metasediments with minor basic flows. They predominantly occur in central and southern Rajasthan. However, the metasediments of middle amphibolite facies extending with a NE trend through Bhilwara, as also the greenschist facies rocks outcropping in the Berach-Chittaurgarh region, have been recently grouped, rather arbitrarily, in the pre-Aravalli Bhilwara Supergroup by the Geological Survey of India (Gupta et al., 1980). These metasediments are, however, found to have imprints of only one regional metamorphism in contrast to the polymetamorphism recorded by the schist component of the BGC. Moreover, there is a recognizable metamorphic discordance between these medium to low-grade metamorphics and the underlying coarsely crystalline, high-grade schists and gneisses of the BGC. From these criteria, it is difficult to visualise the mechanism of metasomatism/granitization to produce high-grade schists and migmatites from the overlying lower-grade metamorphics, even if the two rock units exhibit structural accordance in some areas. Furthermore, these migmatitic rocks do not show spatial relations to granitoid bodies that could have served either as a source of granitic material to inject into the metamorphic rocks or as a source of metasomatizing fluids.

The Aravalli metasediments from the type area to the south of Nathdwara in Udaipur district contain assemblages of greenschist facies, despite the different depositional environments, with (carbonate-bearing) shelf facies or miogeosynclinal deposits in the east and deep-sea deposits in the west (see Roy and Paliwal, 1981). The mineral assemblages in the Aravalli rocks facilitate delineation of an isograd along the Banas River Valley in the area north of Udaipur (see Fig. 1). The trend of this isograd is across the regional strike of the Aravalli Range, suggesting that recrystallization outlasted deformation in the Aravalli rocks. These rocks appear to be free from thermal effects, and the granitic outcrops such as the Untala, Ahar River, etc. within the Aravalli terrain represent sialic basement for these supracrustals.

There are some ultrabasic intrusives in the Aravalli rocks, for instance at Rakhab Dev, Gogunda, etc. They are largely altered and contain a talc-chlorite-serpentine ± tremolite assemblage with some relict igneous mineralogy. Pillow structure is not convincingly reported in these ultramafics.

DELHI SUPERGORUP, ITS METAMORPHISM AND GRANITIC INTRUSIONS

The rocks of Delhi Supergroup are the major components making up the Aravalli Mountains. They are composed of meta-arenites and meta-volcanics in the lower part (Alwar Series of Heron), whereas the upper part (Ajabgarh Series) consists of metamorphosed argillaceous to marly sediments with volcanics. Some authors also include in this Supergroup the meta-carbonate and meta-volcanic sequence named by Heron the Raialo Series as an intermediate formation between the Aravalli and Delhi 'Systems'.

The Delhi rocks are found to have recrystallized first under regional metamorphism associated with the Delhi orogeny, leading to an extensive development of amphibolite-facies assemblages, except in the Lalsot-Bayana tract in the NE and in the terrain extending from Deri-Ambaji near the State boundary of Rajasthan and Gujarat to the contact of Delhi-Aravalli further southeastwards, where greenschist facies assemblages are reported (Singh, 1982; Deb, 1980). In some areas, such as in the NE and SW sectors of the fold belt, andalusite overprints the regional schistosity and the texture becomes hornfelsic, obviously related to the intrusions of late-to post-kinematic Erinpura granites.

Recent geochronological work (Gopalan and Choudhary, 1984; Choudhary et al., 1984) indicates that the granites within the Delhi rocks are of two distinct ages. The granites which occur in the fold belt to the north of Ajmer give isochron ages between 1700 and 1480 Ma; those which occur along the axial zones of the Aravalli Mountain to the south of Ajmer yield younger ages of 850 and 750 million years.

The radiometric age determinations, analogous to geothermometry and geobarometry, give us only numbers whose geological significance is a matter of interpretation. The stated difference in age of the granite from the northern and southern Delhi fold belt could be a reflection of the possible difference in the "residence" time of the granitoid rocks in the crustal depths before they were emplaced in the Delhi supracrustals. It is for this reason that one cannot be sure of the tectonic significance of an isotopic age in a terrain. A rock that is now at the surface could have remained at middle crustal depths for hundreds of million years, after it dropped below its closure temperature, and been brought to the surface by a tectonic event distinct from that which the isotopic age records. The different granitic plutons in the Delhi supracrustals may be the consequence of this possible geological behaviour. Alternatively, it can also be argued that the observed difference in age of the granitic plutons (1700-1480 Ma and 850-750 Ma) in the Delhi fold belt is due to different parent source pristine granitic rock or metasediments that underwent partial melting. The younger mineral ages in the older granitoids are obviously due to a late tectonic or thermal (reheating) event, as has been documented by 700 Ma biotite from 1480 Ma Khetri granites (Gopalan et al., 1979).

The important inference that can be drawn from these granitic intrusives can be stated as follows: Melting occurred at two distinct levels within the crust; one towards the base of the Delhi metasedimentary sequence and the other in the lower crust from where the magmas subsequently invaded higher structural levels. This conclusion can be further substantiated when geochemical and more detailed geochronological works are carried out on the granitoid rocks and associated metasediments.

Akin to the Rakhab Dev ultramafics, as stated earlier we encounter these rocks in the Delhi fold belt also. More often these are sepentinites and are located near lineaments (shear zone or fault plane) running close to the BGC-Delhi boundary, e.g., at Phulad. However, these are serpentinites and not spinel peridotites or lherzolites and are devoid of any layered rock group to suggest mantle material or magmatic differentiate of upper mantle.

EVOLUTIONARY HISTORY OF THE PRECAMBRIAN ROCKS IN THE ARAVALLI BELT

The evolutionary history of the rocks from the Aravalli belt has been recently attempted in view of the developments in the stratigraphy, structure, metamorphism and radiometric dating of the Precambrian rocks from Rajasthan (see Sharma and Roy, 1986). The BGC comprises high-grade quartzo-feldspathic gneisses with striped amphibolites and pelitic schists and rare quartzites. The 3500 Ma. old amphibolites and grey tonalite gneiss from near Udaipur city represent early crust derived from depleted mantle (Macdougall et al., 1983). On this evolving crust, a thin veneer of sediments is conceived to have accumulated, and later been involved in regional metamorphism (Pre-Aravalli) and igneous intrusions (2950 to 2600 Ma) to form the Banded Gneissic Complex. Stabilization of the crust presumably occurred in the early Proterozoic with the development of the Aravalli basins. Along the margins of the basins, basic lavas poured out, as evidenced by the volcanic flows at the base of the Aravalli sequence. These rocks were subsequently involved in the Aravalli cycle (ca. 2000 Ma) during which they have been folded on the E-W fold axes. After a hiatus, sedimentation of the Delhi Supergroup commenced with terrigenous clastics. The upper part of the sequence is dominantly argillaceous and is accompanied by coeval shallow--marine volcanism in different sectors. In the Delhi orogeny these supracrustals were recrystallized and intruded extensively by the Erinpura granite (950 Ma).

ARAVALLI OROGENY AND PLATE TECTONIC MODEL

Sychanthavong and Desai (1977), apparently believing that thc Aravalli Mountains are exclusively made up of Delhi "system" rocks, assumed a BGC-Aravalli Protocontinent in the east and a hypothetical Precambrian oceanic plate with a mid-oceanic ridge in the west; the intervening trough (geosyncline) being the site of Delhi sedimentation. These authors further believed that the oceanic plate (and the ridge) moved eastward and squeezed the Delhi sediments against the protocontinental foreland in the east; this culminated in the Delhi orogeny and generated the Aravalli fold belt.

Sinha-Roy (1984), however, considered crustal under thrusting from the east, due to westward movement of the

Aravalli-BGC-Berach block, which resulted in deformation of the Delhi sedimentary basin. He also visualised the plate-tectonic mechanism for the Aravalli Supergroup. According to him, the BGC-Bundelkhand (Berach) Craton (abbreviated BBC) rifted to form N-S linear troughs for the Aravalli sedimentation and igneous eruptions. Sinha-Roy conceived eastward underthrusting of an oceanic crust (at the axial part of the Aravalli rift) against the BBC block, whereby the Aravalli trough was closed, deformed and metamorphosed along with reactivation of the basement and granitic emplacement.

The absence of any definite unconformity between the Delhi and Aravalli supergroups and the stated metamorphic characteristics in these supracrustals, do not favour an Aravalli orogeny as an additional event between the Delhi and pre-Aravalli orogenies. The basic objection to the Aravalli orogeny is that the Aravalli rocks, sandwiched between the Delhis and the underlying BGC (as the youngest and oldest rock units, respectively), show lower grade regional metamorphism. Unless the two supracrutals, namely the Delhis and Aravallis, were involved together in the same orogeny, it is difficult to explain why the Delhis, as a younger formation, are higher grade than the older Aravallis. The radiometric age data on the Aravalli rocks are inconclusive in this regard, since the samples of the Aravalli lavas (metamorphosed) are poorly enriched in radiogenic Sr and the ages on the Aravalli rocks show a large scatter, indicating isotopic exchange or different cooling rates following a single regional metamorphism. Hence, the older age obtained for the Aravalli rocks does not mean a major regional recrystallization event, i.e., orogeny.

From the available metamorphic and other geologic evidence in the Precambrian rocks of the Aravalli fold belt, the plate--tectonic model is not tenable for the evolution of the Aravalli belt. The main criteria against this model are : (i)The Delhi-Aravalli contact at many places in Rajasthan is without a structural hiatus and metamorphic discordance (Chattopadhyay and Mukhopadhyay, 1985; Sharma, 1988). On either side of the Delhi-Aravalli contact in southern Rajasthan, the rocks are isogradic in that the Delhi rocks in the Deri-Ambaji and underlying Aravallis on the eastern side of the contact line contain metamorphic assemblages of greenschist facies. This contact line at the interface of the two formations cannot be conceived as a plate junction or subduction zone; (ii) The linear fractures, particularly the Idar-Devgarh-Ajmer fault, also cannot represent a palaeosuture or plate boundary (Sen, 1981), since the lineament occurring at the contact of the two rock formations shows a wide zone of cataclasis of the affected rocks, including the late-kinematic granitic intrusion. The fracture is therefore a shallow-level deformation feature, and not a ductile shear zone, and post-dates both regional and thermal events in the rocks; (iii) The Aravalli rocks from southern Rajasthan are low grade over a vast terrain and their metamorphic grade increases north- ward along the Aravalli strike in the Udaipur-Rajnagar area. This feature plus the possible extension of this isograd across the Delhi-Aravalli boundary in central Rajasthan, do not accord with the suggested plate-tectonic model for the Aravalli fold belt which is constituted of both Aravalli and Delhi supergroups; (iv) The tectonic path for the Sand Mata granulites is found to be the reverse as compared to that characterizing collision-tectonic regions.

ENSIALIC OROGENESIS MODEL FOR EVOLUTION OF THE ARAVALLI BELT

The present author (Sharma 1988), therefore, suggested an alternative model which satisfactorily accounts for the observed metamorphic characteristics in the basement complex and the supracrustals from Rajasthan. The model, is briefly described below.

The available geologic evidence indicates that the Aravalli orogen 'rests' on the Precambrian gneissic rocks (analogous to other continental terrains), many of which have older ages of from 3.5 to 2.6 Ga. (Crawford, 1970; Sivaraman and Odom, 1982; MacDougall et al., 1983). From this fact and from the metamorphic criteria recorded in the rocks from Rajasthan, the present author conceives a large-scale ensialic orogenesis for the evolution of the Aravalli mobile belt. In this model it is suggested that the Aravalli and Delhi successions are ensialic, and that the continental basement was stretched and thinned as a result of ductile extension of hot sialic material. The basins formed in this way were floored with thin crust and accompanied by sedimentation and eruption of basic/ultrabasic material. It should be stated here that the development of the different basins was not essentially contemporaneous. Variations of facies and

Table 1.
Evolutionary history of Rajasthan Craton, NW Indian Shield.

Intrusion of Erinpura granite (MAINLY IN DELHI FOLD BELT)	0·95 GA
Deformation & metamorphism of supracrustals and evolution of Aravalli mobile belt; Remobilization & recrystallization of B.G.C. and Uplift of lower crust (e.g. at Sand Mata)	Age(?)
Deposition of supracrustals of Aravalli Supergroup & Delhi Supergroup on peneplained B.G.C.	2-1·6 GA
UNCONFORMITY	
Emplacement of Berach granite (LAST EVENT OF FORMATION & STABILIZATION OF CRATON)	2·6 GA
Intrusion of older Granites (UNTALA, GINGLA etc.)	2·9 GA
Intense ductile deformation & metamorphism; Partial melting at deep crustal levels; Underplating of crust by magma addition; (FIRST EVENT OF DEVELOPMENT OF B.G.C.)	3 GA (?)
Deposition of thin veneer of sediments (incl. Al- & Cr-rich layers)	Age (?)
Formation of Early Crust, mainly Tonalitic with minor mafic & ultramafics	3·5 GA

thickness in the supracrustal sequences indicate that tectonic instability increased southwards in the Aravalli basins. Perhaps the older rocks were deposited in a shelf environment to deepwater conditions and the younger sequences in a series of fault-bounded basins (cf. Roy and Paliwal, 1981; Singh, 1982). In the final stage there occurred contraction of crust (presumably related to convection currents in the Aravalli lithosphere), rather than subduction or plate collision, resulting in deformation, metamorphism and partial melting of rocks at deeper levels. Repeated deformation of crust and its thickening built the Aravalli Mountains, the rocks of which were intruded by anatectic melts at different structural levels. The buoyant force of the anatectic melt may have also contributed in the elevation of the rock-pile of the Aravalli lithosphere.

From the patterns of isograds (Sharma, 1988), it is suggested that the Delhi and Aravalli supracrustals were subjected to gentle thermal gradients developed during the Aravalli (=Delhi) orogeny. The low-grade metamorphism of the Aravallis as compared to the overlying Delhis could be a progressive effect of the same regional metamorphism during the Delhi orogeny and also a possible reflection of the absence of heat producers in the Aravallis.

The author believes that large-scale ensialic orogenesis in the western Indian Shield involved the re-working of the granite-gneiss complex, presumably at varying depths, whereby deformed cover rocks are now seen resting on a mobilized basement with equivalent ductility at most places in Rajasthan. However, there are areas, e.g. Sarara, where deformed cover rocks lie on an unmobilized or less mobilized basement.

The evolutionary history of the rocks from Rajasthan Craton is summarized in Table 1.

ACKNOWLEDGEMENTS

Sincere thanks are due to colleagues and friends, particularly R.K.Lal and A.B.Roy, for encouragement and to the present and past students for their enquiries on several problems of Rajasthan geology.

REFERENCES

Chattopadhyay, A.K. and Mukhopadhyay, D., 1985. Delhi-pre-Delhi relation along the eastern flank of the Delhi synclinorium near Hira-Ka-Baria, southeast of Beawar, central Rajasthan. Indian J. Earth Sci., 12: 145-149.

Choudhary, A.K., Gopalan, K. and Sastry, C.A., 1984. Present status of the geochronology of the Precambrian rocks of Rajasthan. Tectonophysics, 105: 131-140.

Choudhary, A.K., Gopalan, K., Bose, U., Gupta, S.N., Ravindra, R. and Sastry, C.A., 1981. Rb-Sr chronology of granites from the Delhi Formations, Rajasthan. Proc. Symp. "Three Decades of Developments in Petrology, Mineralogy and Geochemistry in India", Jaipur (abst.), pp.52.

Crawford, A.R., 1970. The Precambrian geochronology of Rajasthan and Bundelkhand, northern India. Can. J. Earth Sci., 7: 91-110.

Deb, M., 1980. Genesis and metamorphism of two stratiform massive sulphide deposits at Ambaji and Deri in the Precambrians of Western India. Econ. Geol., 75: 572-591.

Gopalan, K. and Choudhary, A.K., 1984. The crustal record in Rajasthan. Proc. Indian Acad. Sci. (Earth Planet. Sci.), 93: 337-342.

Gopalan, K., Trivedi, J.R., Balasubrahmanyan, M.N., Ray, S.K. and Sastry, C.A., 1979. Rb-Sr chronology of the Khetri Copper Belt, Rajasthan. J. Geol. Soc. India, 20: 450-456.

Green, D.H. and Ringwood, A.E., 1967. An experimental investigation of the gabbro to eclogite transformation and its petrological implications. Geochim. Cosmochim. Acta, 31: 767-833.

Gupta, S.N., Arora, Y.K., Mathur, R.K., Iqbaluddin, Prasad, B., Sahai, T.N. and Sharma, S.B., 1980. Lithostratigraphic map of Aravalli region, southern Rajasthan and northern Gujarat. Geological Survey of India, Calcutta.

Hansen, B., 1981. The transition from pyroxene granulite facies to garnet-clinopyroxene facies: Experiments in the system $CaO-MgO-Al_2O_3-SiO_2$. Contr. Min. Pet., 86: 234-242.

Heron, A.M., 1953. The geology of Central Rajputana. Mem. Geol. Surv. India, 79, pp.1-389.

MacDougall, J.D., Gopalan, K., Lugmair, G.W. and Roy, A.B., 1983. The Banded Gneiss Complex of Rajasthan, India: Early crust from depleted mantle at 3.5 A.E. Trans. Amer. Geophys. Union. 64 (18): 351.

Naha, K., 1983. Structural and stratigraphic relation of the pre-Delhi rocks of south-central Rajasthan : a summary, In: S.Sinha-Roy (Editor), Recent Researches in Geology, v.10 Structure and Tectonics of the Precambrians rocks. Hindustan Publ. Corpn., Delhi.

Roy, A.B., 1985. Tectonic and stratigraphic framework of the early Precambrian rocks of Rajasthan and northern Gujarat. Bull. Geol. Min. Met. Soc. India, 53: 100-114.

Roy, A.B. and Paliwal, B.S., 1981. Evolution of lower Proterozoic epicontinental deposits: stromatolite bearing Aravalli rocks of Udaipur, Rajasthan, India. Precamb. Res., 14: 49-74.

Sen, S., 1981. Proterozoic palaeotectonics in the evolution of crust and location of metalliferous deposits, Rajasthan. Q. J. Geol. Min. Metal. Soc. India, 53: 63-75.

Sharma, R.S., 1977. Deformational and crystallization history of the Precambrian rocks in north-central Aravalli Mountains. Rajasthan, India. Precamb. Res., 4: 133-162.

Sharma, R.S., 1988a. On the polymineralic paragneisses from Karera, district Bhilwara, Rajasthan, III-Metamorphic conditions and Petrogenesis. Indian J. Earth Sci., 10: 152-169.

Sharma, R.S., 1983b. Basement-cover rocks relations in north central Aravalli Range: a tectonic and metamorphic synthesis. In: S. Sinha-Roy (Editor), Recent Researches in Geology, v.10 Structure and Tectonics of the Precambrian rocks. Hindustan Publ. Corpn., Delhi, pp.52-71.

Sharma, R.S., 1983c. Pressure, temperature and time indicators in granulites from Rajasthan, NW India. Geophys. J.R. Astr. Soc., 73: 291.

Sharma, R.S., 1988. Patterns of metamorphism in the Precambrian rocks of the Aravalli Mountain belt. In: A.B. Roy (Editor), Precambrian of the Aravalli Mountain, Rajasthan, India, Mem. Geol. Soc. India, 7: pp.33-75.

Sharma, R.S. and Narayan, V., 1975. Petrology of polymetamorphic schists from an Archaean complex terrain, southeast Beawar, Rajasthan, India. Neues Jb. Mineral. Abh., 124: 190-222.

Sharma, R.S. and Althaus, E., 1977. Stability relations of sapphirine in the Banded Gneissic Complex of Bhilwara district, Rajasthan, India. Fortschr. Mineral., 55: 128-130.

Sharma, R.S. and MacRae, N.D., 1981. Paragenetic relation in gedrite-cordierite-staurolite-biotite-sillimanite-kyanite gneisses at Ajitpura, Rajasthan, India. Contr. Min. Pet., 78: 46-60.

Sharma, R.S. and Roy, A.B. 1986. Evolution of Precambrian lithosphere. The Indian Lithosphere, Publ. Indian National Sci. Acad., New Delhi, pp.1-14.

Sharma, R.S., Althaus, E. and Wilson, R.N., 1985. Kornerupine in aluminous enclaves of the Archaean complex from Rajasthan, NW India : Paragenesis and stability. Terra Cognita, 5: 328.

Sharma, R.S., Sills, J.D. and Joshi, M., 1987. Mineralogy and metamorphic history of norite dykes within granulite facies gneisses from Sand Mata, Rajasthan, NW India. Min. Mag., 51: 207-215.

Singh, S.P., 1982. Stratigraphy of the Delhi Supergroup in Bayana Sub-basin, northeastern Rajasthan. Rec. Geol. Surv. India, 112(7): 46-62.

Sinha-Roy, S., 1985. Precambrian crustal interaction in Rajasthan, NW India. Indian J. Earth Sci., (CEISM Volume), pp.84-91.

Sivaraman, T.V. and Odom, A.L., 1982. Zircon geochronology of Berach granite of Chittorgarh, Rajasthan. J. Geol. Soc. India, 23: 575-577.

Sychanthavong, S.P. and Desai, S.D., 1977. Proto-plate tectonics controlling the Precambrian deformations and metallogenetic epoch of north-western Peninsular India. Mineral Sci. Engg., 9: 218-236.

THE TECTONIC SETTING OF MINERALISATION IN THE PROTEROZOIC ARAVALLI DELHI OROGENIC BELT, NW INDIA

T.J.SUGDEN, M.DEB AND B.F.WINDLEY

ABSTRACT

The Proterozoic Aravalli-Delhi orogenic belt in NW India shows remarkable similarity to Mesozoic-Cenozoic Himalayan-type orogenic belts in terms of component parts and appears to have passed through a near-orderly Wilson cycle of events. Its evolution involved: rifting of a rigid Archaean continent represented by the Banded Gneissic Complex at ~2.2 Ga with the concomitant formation of the Bhilwara aulacogen in the eastern part and eventual rupturing and separation of the continent along a line parallel to the Rakhabdev lineament to the west; simultaneous development of a passive continental margin with the shelf rise sediments of the Aravalli-Jharol belts depositing on the attenuated crust on the eastern flank of the separated continent; subsequent destruction of the margin by accretion of the Delhi island arc from the west at Ca 1.5 Ga. The collisional event involved early thrusting with partial obduction of the oceanic crust along the Rakhabdev lineament, flattening and eventual wrenching parallel to the collision zone. The basement served as a rigid indentor which controlled the overall wedge shaped geometry of the orogen.

Exhalative sedimentary base metal sulfide ores formed extensively along several, long, linear zones in the Bhilwara aulacogen or produced local concentration in the rifted Aravalli continental margin, where rich stromatolitic phosphorites also formed. In the southern part of the arc complex base metal sulfides were generated near the subduction zone on the western fringe or in zones of back-arc extension to the south-east. Continued subduction produced W-Sn mineralisation in S-type felsic plutons. The tectonic setting of Cu sulfide mineralization in the northern part of the Delhis remains unclear.

INTRODUCTION

A variety of geological, geochemical and geophysical constraints suggest that by 2.5 Ga the growth of the continental crust had reached to within 50 - 90% of its present mass, and therefore it was able to respond to deposition, deformation, intrusion and metamorphism in a mode almost comparable with that of today, and thus from this time it was possible for modern-style plate tectonics to operate (Dewey and Windley, 1981; Windley, 1983; Taylor and McLennan, 1985; Patchett and Arndt, 1986). In consequence several early to mid-Proterozoic orogenic belts have geological features and relationships which are broadly similar to those in Mesozoic-Cenozoic belts (Windley, 1984).

The well-exposed Aravalli-Delhi orogenic belt in NW India is 30-200 km wide and it extends for some 700 km in a NE-SW direction from Delhi through Rajasthan to Gujarat state (Fig. 1). Post-Neogene tectonism (Sen and Sen, 1982), related to flexuring of the Indian crust, has uplifted the Aravalli-Delhi orogenic belt to form a horst block.

The orogen is roughly bisected along its trend by a major lineament passing through Rakhabdev in the south, Gogunda in the central part and Kishangarh in the north. To the east the Archaean crust, represented by the Banded Gneissic Complex (BGC) and the Bundelkhand massif (further to the east) is overlain by the mid-Proterozoic Aravalli and Bhilwara supracrustal belts or the upper Proterozoic sediments of the Vindhyan Supergroup. To the west of the lineament lie the Jharol and Delhi belts comprising metasedimentary and metavolcanic rocks intruded extensively by granitic suites. This 'Rakhabdev lineament' appears to be an important tectonic divide, separating belts with highly contrasting depositional histories.

The Aravalli-Delhi orogen contains many important base metal sulfide deposits (Deb, 1982; Pawar and Patwardhan, 1984) and accounts for the biggest reserves of Pb-Zn and a substantial part of the Cu production in India. In addition, the region has noteworthy occurrences of tungsten-tin and uranium, minor manganese and vast resources of sedimentary phosphorites (Banerjee, 1971).

Modern studies in Rajasthan owe much to the classic work of Heron (1953). Earlier attempts to analyse the belt from a plate tectonic standpoint are by Sychanthavong and Desai (1977), Sen (1981) and Sinha Roy (1984). In this paper we aim to present a complete geological tectonic profile across the southern part of the belt, to interpret this profile in terms of the most likely plate tectonic model, and in particular to relate the mineralisation to this geodynamic framework.

TECTONIC FRAMEWORK

The Aravalli-Delhi orogenic belt consists of several sub-parallel units which we describe separately from east to west (Fig. 1).

Terrain east of the Rakhabdev Lineament

Archaean Basement. The Banded Gneissic Complex (BGC) consists of amphibolite and granulite facies gneisses (with complex minor folds), migmatites, amphibolite bodies and metasedimentary enclaves. Although Crookshank (1948) and Naha and Halyburton (1974) suggested that much of the BGC formed by migmatisation of Aravalli sediments, we are in agreement with Heron (1953) that the BGC constitutes an Archaean basement to the Aravalli Group because Pb isochron data on Aravalli schists with a lot of detrital zircon by Vinogradov et al (1964), and Sm-Nd isochron data by MacDougall et al., (1983) show that the BGC contains material as old as 3500 Ma and because locally the Aravalli Group lies with clear unconformity on the BGC (Roy and Paliwal, 1981). The BGC has two tectonic blocks (Sen, 1970). In the north, a high grade block showing metamorphism from upper amphibolite, amphibolite - granulite transition to granulite facies (Sharma, 1986) is bounded on the west by a shear zone (suture ?) against the Delhi Supergroup and to the east by a major lineament with mylonites and pseudo-tachylites against the Bhilwara belt. In the south there are amphibolite facies gneisses with migmatites, schists, meta-sedimentary inclusions, and plutons of synorogenic granite with Rb-Sr isochron ages of 3,000 Ma (Choudhary et al., 1984). The emplacement of the potassic Berach granite around 2600 Ma (Crawford, 1970) marked the process of cratonization of the basement and the initiation of its rifting.

The Bhilwara Belt. This metasedimentary belt was considered contemporaneous with the Aravallis by Gupta (1934) and Heron (1953). However, later workers (Raja Rao et al., 1971; Raja Rao, 1976) suggested that it is older than the type-Aravallis around Udaipur and redesignated them as the 'Bhilwara Group'. In a recent re-examination of the structural-stratigraphic status of these so-called 'Pre-Aravalli'rocks around Bhinder, Roy et al., (1981) provided convincing field evidence against the above suggestions

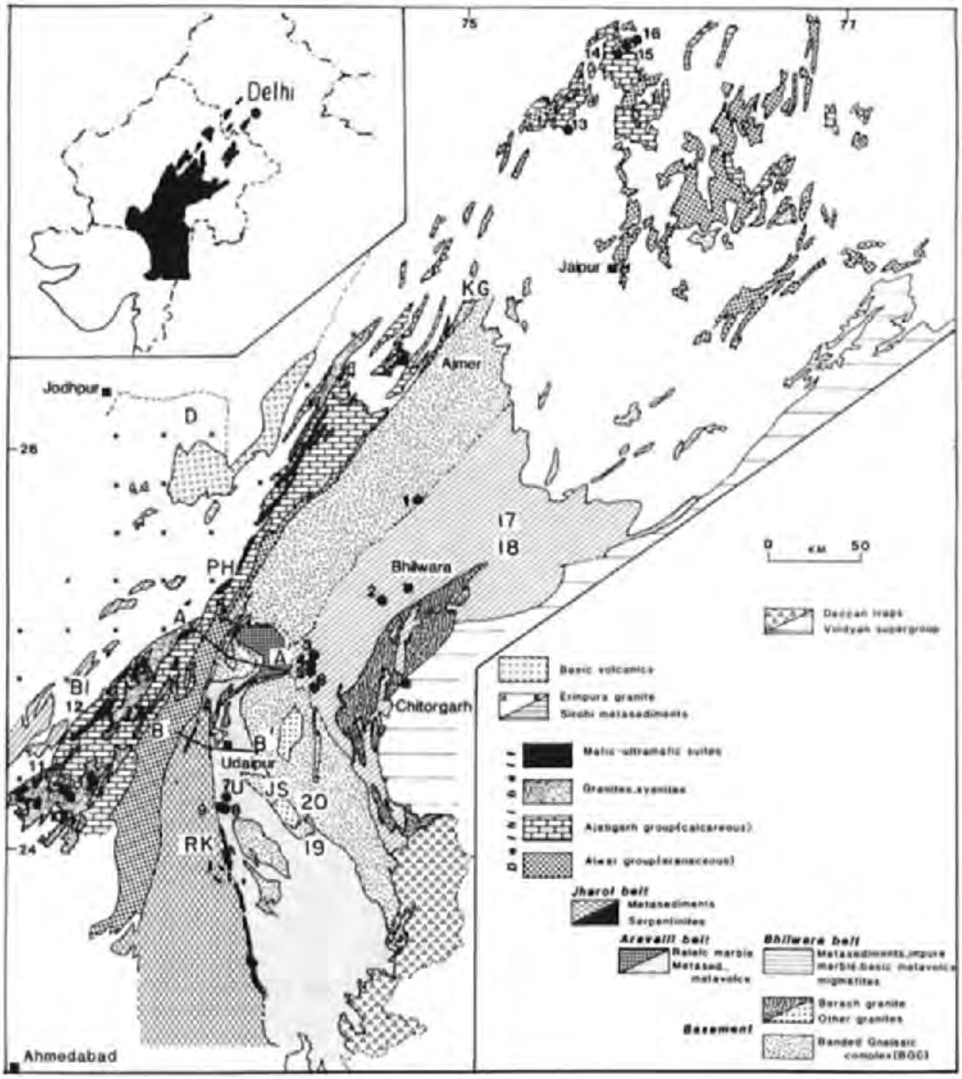

Figure 1. Geological map of the Aravalli-Delhi orogenic belt (modified after Heron, 1953 and Gupta et al., 1980). Inset shows the location of the orogen (black). Sulfide deposits/prospects: (1) Rampura-Agucha (2) Tiranga, (3)Sindeswar Kalan, (4) Rajpura, (5) Dariba, (6) Wari, (7) Mochia-Balaria, (8) Zawar Mala, (9) Baroi Magra, (10) Ambaji, (11) Deri, (12) Basantgarh, (13) Saladipura, (14) Chandmari, (15) Kolihan, (16) Madan Kudan, (17) Sawar, (18) Jahazpur, (19) Anjeni, (20) Phalet. Tungsten deposits/ prospects: D=Degana; Bl=Balda; Phosphorite: JS=Jhamarkotra-Sameta; Uranium : U=Umra; RK=Rakhabdev; PH=Phulad; KG=Kishangarh.

and showed that the Aravalli-Pre-Aravalli boundary is clearly a time-transgressive plane.

To the east the Bhilwara belt is juxtaposed against the Vindhyan Supergroup along the Great Boundary Fault and there it comprises low-grade (greenschist facies) metapelites, metagreywackes and metabasics in a turbidite sequence. These rocks are overlain in the north-central part of the belt by a dominantly metamorphosed dolomite-orthoquartzite sequence with a folded unconformity between the two (Sinha Roy, 1984). In the Sawar area, sillimanite-bearing pelitic schists and diopside marble, enclosed within a patch of BGC, host Cu and Pb-Zn mineralization (Ray, 1986). In the Pur-Banera mineralised zone, metavolcanics occupy substantial areas and the repetitive sequence of argillaceous, arenaceous and calcareous metasediments of the amphibolite facies is characterised by a marker bed of metamorphosed banded iron formation and by folded conglomerates (Basu, 1971). Further south amphibolitic basic sills, dolomitic marbles, kyanite/staurolite-bearing graphitic mica schists and bedded cherts characterise the Rajpura-Dariba mineralised belt (Deb and Bhattacharya, 1980). In the west, along the eastern margin of the BGC amphibolite-granulite transition facies schists (Deb and Sehgal, in prep.) and gneisses host the massive Zn sulfide ore body at Rampura-Agucha.

The Aravalli Belt. The Aravalli Group occupies a 200 km long belt which varies in width from 70 km in the south to <10 km in the north. The stratigraphy is well known (Roy and Paliwal, 1981). A dominantly argillaceous sequence lies unconformably on the BGC. The base of the sequence is commonly marked by an aluminous pyrophyllite-muscovite-sericite horizon which is probably derived from a palaeosol developed on the peneplained basement. The main basal formation consists of fine grained fuchsite-bearing quartzites, occasionally associated with calc-schists, barite and thin amphibolite bands with manganese-iron-copper mineralisation. There follows a 500 m - 3 km thick unit of greenschists and amphibolites showing komatiitic affinity (Ahmed and Rajamani, 1986) or derived from tholeiitic to andesitic volcanics (Deb et al., in prep.).

The overlying unit is mainly carbonate, dominated by ferruginous and manganiferous dolomites. The occurrence of phosphorite bearing stromatolites here indicates a warm shelf environment (Banerjee, 1971). Dolomites with or without stromatolites are often associated with basement inliers suggesting that these formed stable horsts. Carbonaceous phyllites with uranium minerals are associated with the carbonates and probably formed in deeper anoxic basins adjacent to the horst block.

Carbonate gave way to clastic deposition. A conglomerate-arkose-quartzite sequence, which in places overlies the original basement-cover contact, reflects rapid uplift of the marginal parts of the basin. Clasts in the conglomerate are often very large and poorly sorted. The clasts are composed dominantly of quartzite with rare dolomite and phyllite. The composition varies considerably along strike, indicating a complex of fans and fan deltas. A thick rhythmic sequence of greywackes and phyllites developed through turbidite currents in the deeper subsiding parts of the basin. Finally oolitic Raialo limestones were deposited in the distal parts of the shelf and the overlying phyllites marked the end of sedimentation on the Aravalli margin.

To the north the Aravallis thin out substantially, occurring intermittently along the fault zone/lineament separating the Delhi metasediments from the BGC. At Kishangarh, near Ajmer, Aravalli metasediments and metabasites hosting Cu mineralisation (Chattopadhyay and Misra, 1986) are associated with nepheline syenites on the lineament. The Rakhabdev lineament forms the western edge of the Aravalli belt. In the Rakhabdev area, the lineament passes through a melange of phyllites (flysch ?), dolomites, sheared amphibolites, ferruginous cherts and chromite-bearing serpentinites, representing in all likelihood, a dismembered ophiolite.

Terrain west of the Rakhabdev lineament

The Jharol Belt. This belt is parallel to and directly west of the Aravalli belt. It comprises a monotonous series of phyllites and lutites with occasional thin beds of quartzite and limestone. An oval-shaped anticlinal structure in the Bagdunda area (Sharma et al., 1986) reveals a gneissic basement. Throughout the belt there are slices of ultrabasic rocks which are highly tectonised with sheared contacts suggesting a tectonic mode of emplacement. Highly sheared and folded quartz veins are ubiquitous throughout the belt. Like the Aravallis, the Jharol belt thins northwards and is ultimately preserved only as a smear along the

Rakhabdev lineament.

The Delhi Belt. This is a major NE-SW trending linear belt, which narrows to 10 km width in its central part. The belt is petrologically and structurally different from the Aravalli and Bhilwara belts. Heron (1953) recognised two major stratigraphic units. To the east, a lower dominantly arenaceous Alwar unit consists of quartzites, biotite gneisses, amphibolites and calc-schists. This is overlain by the dominantly calcareous Ajabgarh unit of calc-schists, calc-gneisses and amphibolites. These two units are intruded by a variety of pegmatites, granites and granodiorites of several ages along the axis of the Delhi belt. No definite Archaean crust is known in the Delhi belt. In the southernmost part there are hypersthene bearing gabbroic rocks with patches of peridotite, troctolite and leuco gabbro. Field relationships suggest that by and large, these plutonic rocks are later than the Ajabgarh metasediments (Deb and Sharma, in prep.).

The western boundary of the Delhi belt is a major fault zone along which there are cherts, epidiorites, hornblende schists, gabbros, pyroxene granulites, chromite-bearing serpentinites, serpentinite melange (talc-chlorite-kyanite) with rare fragments of high pressure grospydite (garnet-pyroxene rocks with a density of 3.65-Sychanthavong and Mehr, 1984), and amphibolites which represent metavolcanics with well preserved relict pillows in low strain zones. These metavolcanics are low-K tholeiites comparable with modern oceanic tholeiites occurring close to trenches in island arcs (Bhattacharyya and Mukherjee, 1984). All these rocks are collectively termed the Phulad ophiolite suite (1:1,000,000 map of Rajasthan, Gupta et al., 1980).

The Vindhyan. The Vindhyan Supergroup occupies a series of vast intracratonic basins in northern India. It reaches a maximum thickness of 4 km and consists largely of conglomerates, sandstones and shales and was deposited under shallow water continental to marine conditions in a mosaic of tidal flat, lagoonal and beach environments (Valdiya et al., 1982). Its age range has long been difficult to define because of lack of megafossils, but an age of 1400 Ma is commonly accepted for the beginning of sedimentation (Crawford and Compston, 1970). Although the type area lies to the south east of the Aravalli belt,

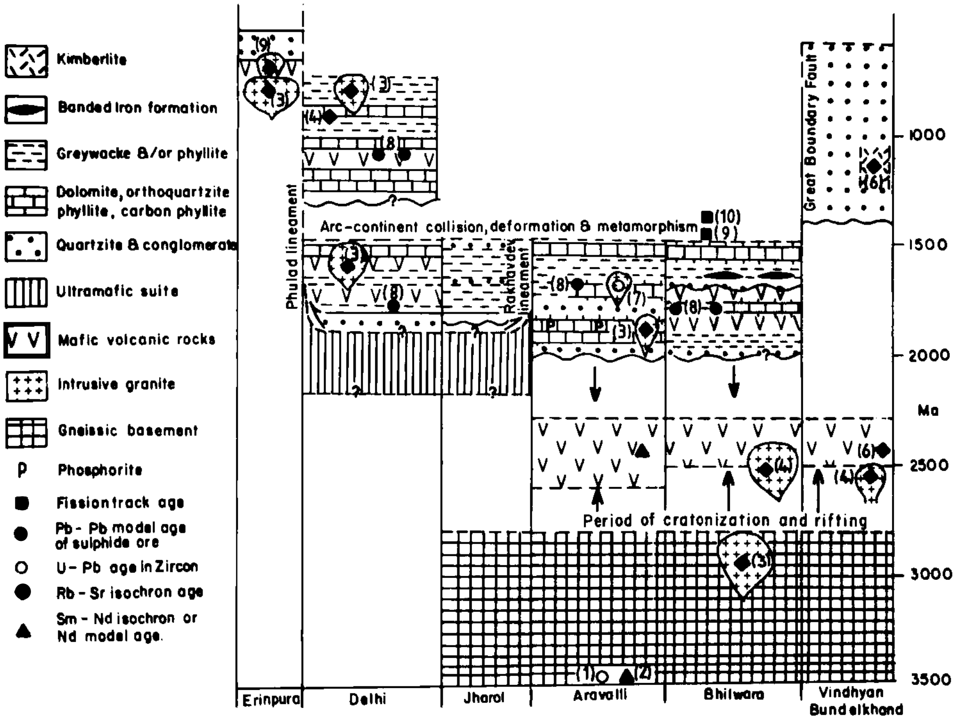

Figure 2. Time-space framework for the evolution of the Aravalli - Delhi orogenic belt, Geochronologic data from (1): Vinogradov et al., (1964); (2) MacDougall et al., (1983); (3)Choudhary et al., (1984); (4): Crawford, (1975); (5): MacDougall et al., (1984); (6): Crawford and Compston, (1970); (7) : Sivaraman, (1982); (8): Deb et al., (in press); (9): Crawford, (1975).

comparable sediments lie to the west of the Delhi belt. They are all post-tectonic with respect to the Aravalli-Delhi orogeny. A time-space relationship between the different constituent belts of the Aravalli-Delhi orogen, based on available geochronological data is shown in Fig.2.

STRUCTURAL PROFILE

Detailed structural analyses of rocks in Udaipur district of southern Rajasthan have been carried out by Sugden (1987). Two structural sections from this study, depicting the entire width of

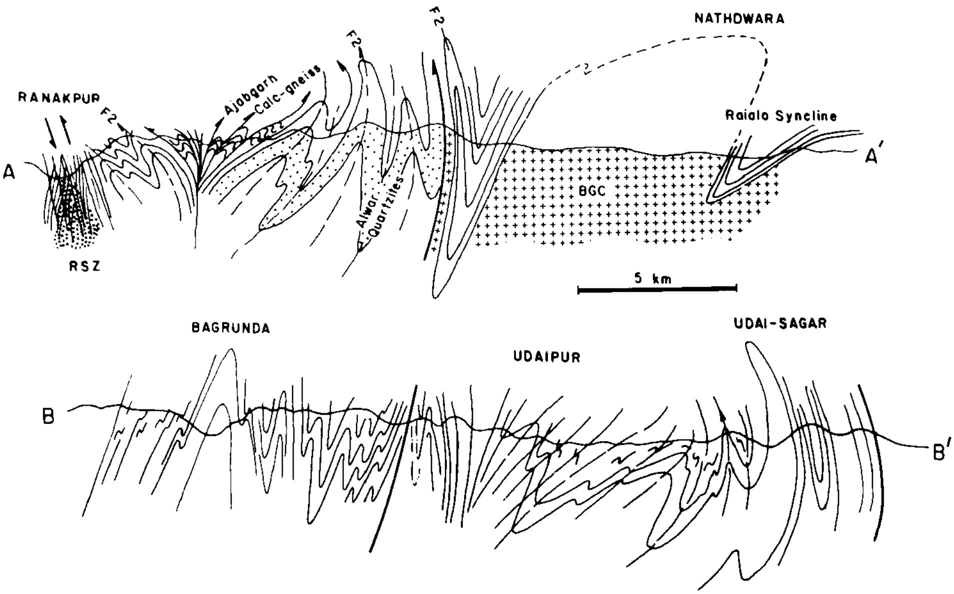

Figure 3. Structural profiles across the Aravalli-Delhi orogenic belt. See. Fig.1 for location of the profiles.

the orogen, are shown in Fig. 3. A resume of conclusions drawn from the analyses is presented below.

The structure of the Aravalli belt has been described by Naha and his associates (1968, 1974, 1977, 1984) and Roy and his co-workers (1971, 1974), and that of Bhilwara belt by Roy et al., (1981). Both these belts, along with the Jharol belts, record a similar tectonic history, intense E-W stretching bringing early (F_1) folds in parallelism. This episode is associated with intense mylonitisation at basement-cover contacts (Roy et al., 1985) indicating that the Aravalli belt has been thrust bodily over the craton. A great deal of other evidences (cf. Sugden, op. cit.) also support the allochthonous nature of the Aravalli rocks relative to the basement complex, which has not been identified by earlier workers. Shear criteria and strain data are consistent with a model involving thrusting combined with wrenching and a (gravity induced ?) longitudinal stretch in the direction of flow. The bulk shear strain increases towards the base of the system. The high strain pyrophyllite - muscovite horizon between the basement and the Aravalli may have acted as a glide horizon (decollement). D_1 strain estimated at 80 localities in deformed conglomerates show that atleast 10 km of strain was accommodated by grain boundary sliding and crystal plasticity but an unknown displacment took place at the basal decollement.

The subhorizontal fabric and E-W stretching lineation, generated during D_1, were buckled and rotated to a subvertical position during D_2. The bulk kinematic axes during D_2 remained roughly parallel to the D1 axes, indicating that the two phases record an essentially coaxial stress history, progressing from dominantly simple shear to dominantly pure shear. F_2 folds are upright and trend consistently N-S. The complex fold superimposition pattern (e.g. the 'hook syncline') have been subjected to detailed analyses (Naha et al., 1966). The intensity of flattening of F_2 folds is negligible in the southern (wide) part of the terrain but increases considerably northwards, maximum flattening occurring in the narrowest part of the belt. There is a clear correlation between cleavage orientation, fold flattening and the overall thinning of the Aravalli-Jharol belts northwards. The present wedge-like geometry of these belts is primarily an effect of D_2 flattening. In the Aravalli belt, the principal D_2 compression direction swings round the basement indicating that the basement behaved as a rigid indentor.

The third movement phase (D_3) was dominated by subhorizontal shear parallel to the trend of the orogen. The basement was backthrust as a 'flake' over the subvertical fabric of the Aravalli rocks, resulting in the development of a series of shallow, south-easterly dipping shears and NE trending recumbent folds. This phase is important in terms of collisional tectonics because it represents the time when colliding lithospheric plates had effectively 'locked' and further convergence was accommodated by wrenching parallel to the plate boundaries.

The Delhi belt is a flower structure (cf. Ramsay and Huber, 1987) and a zone of dextral transpression. The earliest folds in the Delhi belt are generally isoclinal and recumbent with NNE-trending axes, described by Naha et al., (1984) as 'gravity induced' structures. The F_1 folds, contemporaneous with thrusting in the Aravalli belt, are coaxially refolded by progressively steeper F_2 folds with upright axial planes. These later folds are considerably flattened especially in the central, narrow part of the belt and appear to be of the same age as F_2 folds in the eastern terrain. Vertical extrusion of high grade calc-gneisses was accommodated by displacement by discrete upward-splaying shear zones during a third deformation phase which provided several major discontinuities e.g. the Ranakpur shear zone, on the western edge of the Delhi belt.

Structures can be fairly confidently correlated across the two terrains and strains can be partitioned throughout the evolution of the belt. Accepting that F_2 folds are of the same age in both terrains, the major difference is the orientation of F_1 folds. The early east-west trending folds of the Aravalli and Bhilwara belts have led some workers to suggest an early "Aravalli" orogeny (Naha et al., op. cit.). However, as already mentioned, these can be adequately explained by a simple shear mechanism.

The Vindhyan system is generally flat lying and undisturbed, although considerably folded and faulted at its margins, such as along the Great Boundary Fault (Valdiya et al., 1982).

MINERALISATION

The locations of the major mineral deposits and occurrences in the Aravalli-Delhi orogenic belt are shown in Fig.1. Their geologic setting and salient features are summarised by Deb (this volume, Table 1).

The BGC to-date, is known to contain very little mineralisation. Exceptions are minor copper prospects in quartzose rocks at Anjeni and Phalet (Raghunandan et al., 1981), which occur near the margin of the BGC and are also not stratigraphically aligned. The massive sulfide ore body at Rampura-Agucha, considered so far (Gandhi et al., 1984) to be located within the BGC, has been shown recently (Deb et al., in press) to be hosted by high-grade Bhilwara metasediments on the basis of extensive Pb isotope data.

The Bhilwara belt hosts several linear zones of base metal sulfide mineralisation e.g. (from east to west): Jahazpur Cu belt, Sawar and Pur Banera Cu and Pb-Zn belts, Bethumni-Bamnia-Rajpura-Dariba-Wari polymetallic belt and Rampura-Agucha Zn (Pb) ore body. The largest Pb-Zn sulfide concentration in India occurs in the Zawar ore district, in the southern part of the Aravalli belt, close to the basement. A large concentration of sedimentary phosphorite with >25% P_2O_5 also occurs in the Aravalli margin at Jhamarkotra - Sameta and Matoon. The Jharol belt appears to be completely devoid of any mineralisation. The Delhi belt, however, contains a northern and a southern metallogenic province. In the north, the third largest Cu reserve in India is located along the Khetri Copper belt. In the southernmost part, polymetallic sulfides in the Ambaji-Deri zone and Cu(Zn) sulfide in the Basantgarh-Golia Pipela belt occur in sedimentary intercalations within mafic metavolcanics.

In addition to the base metals, occurrences of tungsten with minor tin or tin with minor tungsten are found associated with pegmatites or granitic intrusives in widely separated regions along the Delhi belt. Tungsten mineralisation at Balda near Sirohi, in the Sirohi district of Rajasthan, occur along greisenized and pneumatolytic shear zones in syn- to post-orogenic potassic granite intrusives, correlated with the Erinpura phase of acidic magmatism (Banerjee et al., 1983). The occurrence of scheelite-molybdenite has also been noted in the Phalwadi-Positara area in the same district (Mukhopadhyay, 1981). The best known wolframite mineralisation as fracture fillings occurs in Rewat hill at Degana in Nagaur district of western Rajasthan, in a quartz monzonite stock intruding Aravalli phyllites (Dekate, 1967). These acidic intrusives are now believed to be 'Jalor type' high level granitic plutons related to the 700-500 Ma old Malani igneous suite, intruding into Delhi Supergroup metasediments (Murthy, 1983). Stocks and bosses of porphyritic, potassic granites and rhyolites belonging to the same suite and intruding andalusite-bearing metasediments of the Delhi Supergroup contain tin-tungsten mineralisation in and around Tosham, about 150 kms WNW of Delhi in the Bhiwani district of Haryana (Chowdhary et al., 1984).

PLATE TECTONIC INTERPRETATION

Based on the foregoing discussion of the geology and mineralisation in the constituent terranes, delineation of the discontinuities and strain and kinematic history of the region, a plate tectonic model involving rifting of a rigid Archaean continent, development of a passive continental margin and its subsequent destruction by arc accretion provides a simple and acceptable paradigm in which to view the evolution of the

Aravalli-Delhi orogen. We give here reasons for our choice of specific plate tectonic environments for certain rock groups. Such choice inevitably determines the polarity of subduction, and this in turn controls the type of deformation patterns across the belt. Also we emphasize that there is commonly no unique solution for such an interpretation, and therefore we must be prepared to consider alternatives for the most viable plate tectonic scenario. Mineralisation is also considered in terms of paleotectonic setting and related to the plate tectonic environment (cf. Table 1).

We interpret the Bhilwara belt as an aulacogen. It is a linear belt within the Archaean Basement Gneissic Complex and it projects

Table 1.
Paleotectonic setting of mineral deposits/prospects, in the Aravalli-Delhi orogenic belt, NW India.

Basement	Intraplate (ensialic) setting incipient divergent boundary	Convergent plate boundary setting
Minor	a) In Bhilwara aulacogen:	a) Subduction-related deposits:

Cu sulfides at Anjeni & Phalet	i) Sawar Cu & Pb-Zn belt;
	ii) Jahazpur Cu belt;
	iii) Pur-Banera Pb-Zn-Cu belt;
	iv) Bethumni-Bamnia-Rajpura-Dariba-Wari Zn-Pb-Cu belt; with subsidiary Cd,Sb,As, Ag,Au and Hg;
	v) Rampura-Agucha Zn(Pb) ore body.
		i) Basantgarh-Golia Pipela Zn-Cu deposits associated with mafic volcanics;
		ii) Balda W;
		iii) Phalwadi-Positara scheelite-molybdenite in potassic granites;
		iv) Degana W in Jalor-type high level granite;
		v) Tosham Sn-W-Cu in Malani igneous suite.

	b) In rifted Aravalli continental margin: i) Stromatolitic phosphorites at Jhamarkotra-Sameta and Matoon. ii) Low grade U-Oxide and Cu sulfide in carbon phyllite at Umra-Udaisagar. iii) Pb-Zn deposits in Zawar area: Mochia Magra, Balaria, Zawar Mala, Baroi Magra.	b) Back-arc related deposits: i) Ambaji-Deri Zn-Pb-Cu; ii) Khetri Cu belt (?) iii) Saladipura Pyrite (?)

westwards towards the contemporaneous Aravalli continental margin. The association of dolomites, quartzites, ferruginous and carbonaceous cherts, graphitic shales, early basic volcanic flows, with characteristic geochemical signatures (Deb, 1987) along with long, linear zones of base metal mineralisation are entirely consistent with formation in an aulacogen. Strata bound Cu-Pb-Zn mineralisation in carbonate rocks such as along the Rajpura-Dariba and Sawar belts or in carbonaceous shales, such as in the Pur-Banera belt and at Rampura - Agucha, is typical of rifts ranging from the mid-Proterozoic McArthur river area of Australia to those associated with the break up of Pangea in the Benue trough in Nigeria and in the margins of the Red Sea (Sawkins, 1982).

The Aravalli belt formed on a passive continental margin (MacDougall et al., 1984). As in a modern passive margin setting, thinning of the continental crust eastward may be imagined to have been accommodated by a combination of ductile extension and motion along a series of normal listric faults which controlled the sedimentation rate. In the proximal part of the shelf, the early volcanics (high K-tholeiitic andesites) and clastics belong to the rifting stage, as also do the nepheline syenites at Kishangarh. With continued crustal attenuation a stable carbonate platform with stromatolites and phosphorites developed above the rift facies rocks, probably prior to complete separation. In a thick sequence of such clastics and non-clastics, the stratabound Pb-Zn ores of the Zawar area were generated in subsiding second order basins, probably formed as fault controlled embayments in the Aravalli continental margin. An exhalative-sedimentary origin for these ores is compatible with their formation in a rifted continental margin.

Ultimately the BGC continent ruptured along a line parallel to the Rakhabdev lineament. Necks between separated and thinned continental crust were sites for asthenospheric upwelling and subsequent ocean crust formation. The chromite-bearing serpentinites along the Rakhabdev lineament, delineating the shelf-rise boundary represent this ocean floor material, interthrust during partial obduction against the continental rise sediments. A thick apron of phyllites and lutites (distal turbidites) were deposited on the continental rise, now represented by the Jharol belt and probably buried the spreading centre and basement relicts which rarely bulged out, as at Bagrunda, during accretion. The Debari clastic formation which covers the phosphorite-bearing carbonates at Jhamarkotra developed in response to flexuring of the continental margin, whether this is due to load-induced subsidence or due to downwarping associated with early collision is uncertain.

Though extreme tectonic thinning, wrench-faulting and amphibolite-granulite grade metamorphism have transposed most of its original characteristics, a variety of data indicate that the Delhi belt evolved as an island arc. We recognise a calc-alkaline gabbro-granodiorite-granite suite with stable hornblende, but there is more than one generation of granitic material. Early intrusives are deformed into gneisses, whereas late ones are undeformed; this is similar to the history of the Cretaceous-Tertiary Kohistan arc-batholith in the Himalayas of North Pakistan (Coward et al., 1987). Radiometric studies (Choudhary et al., 1984) indicate that felsic magmas were being intruded into the arc complex by atleast 1.7 Ga. The recrystallised norites, troctolites and layered peridotite-anorthosite sequences (Desai et al., 1978) are very similar to the Chilas complex of orthopyroxene-bearing cumulates which formed in the deep levels of the Kohistan island arc (Jan et al., 1984; Coward et al., 1987) and of equivalents in the root of the Jurassic Border Range island arc of Alaska (Burns, 1985). However, the exact time of emplacement of these plutonic bodies needs to be worked out accurately. The sequence of chromite-bearing serpentinites, diorites, xenolithic tonalites and granites in the Ranakpur shear zone resembles a typical plutonic island arc suite.

The Phulad ophiolite belt (laterally equivalent to the Ranakpur shear zone) defines a suture on the western side of the arc. We agree with the 1980, 1:1,000,000 map of Rajasthan by the Geological Survey of India (Gupta et al., 1980) which interprets the Phulad rocks as "metamorphosed thrusted wedges of oceanic crust". However we reinterpret the "deep-seated fracture zone marking the boundary of the continental shelf and geosynclinal trough" as a suture between the Delhi arc and a shallow water foreland to the west. Serpentinite melanges with relicts of grospydite, and talc-chlorite-kyanite rocks indicate high pressure metamorphism to be expected in a subduction zone (Sychanthavong and Mehr, 1984). Further south, amphibolites with relict pillows in the Sirohi area, geochemically resemble low K-tholeiites occurring nearest to trenches in modern island arcs (Bhattacharya and Mukherjee, 1984).

The major lithologies in the Delhi belt are calc gneissses, orthoquartzites and minor amphibolites. These were probably deposited in a back-arc or fore-arc basin (depending on the inferred direction of subduction). The general lack of rocks of volcanic origin would indicate that the basin was a considerable distance from the arc.

The base metal mineralisations in the southern half of the Delhi belt also have certain similarities with those formed in island arc environments. The Basantgarh-Ajari-Pipela-Golia section in Sirohi district of southern Rajasthan hosts conformable, lenticular pyritic Cu-Zn sulfide ore bodies in sedimentary intercalations in tholeiitic metabasites of island arc affinity, mentioned above. The narrow time-stratigraphic interval of the ore zones and alignment of the ore bodies in small, linear fault-controlled basins appears to suggest that they were generated over steeply dipping subduction zones. The rich polymetallic sulfide lenses in the Ambaji-Deri zone across the Rajasthan-Gujarat border constitute another important base metal concentration in the region, further to the south-east. The stratiform ore bodies are hosted by magnesian sediments overlying massive to schistose metavolcanic amphibolites. Geochemically these amphibolites suggest an ocean floor setting of emplacement while showing an overall island are affinity (Deb et al., in prep.). Such signatures, together with the presence of an alkali syenite pluton at Deri support the back-arc regime for this ore zone within the Ajabgarh Group. The subduction zone along the western fringe of Delhis presumably became shallower and deeper-penetrating with time to produce the tungsten-tin deposits in S-type magmas (cf. Sawkins, 1984). In this context it is worth noting that the Ambaji-Deri ores formed around 1100 Ma (Deb et al. in press) while the tungsten-tin occurrences associated with the Erinpura, Jalor or Malani igneous phases are between 850 and 735 Ma respectively (Crawford, 1975; Gopalan., 1986).

Recent Pb isotopic studies by Deb et al., (in press) have also brought to light certain interesting aspects of the Delhi arc and its mineralisations: the 207/204 Pb ratios of the otherwise homogeneous Ambaji-Deri lead point to the involvement of a substantial part of continental crustal material in the ore-forming environment as is typical in mature arcs. Further, the Saladipura deposit in the northern part of the Delhi belt is isotopically distinct from Ambaji-Deri and is of mid-Proterozoic (1800 Ma) age. There are two possible implications to this observation: a) the Delhi belt evolved episodically over a much longer time span (700 Ma or more), compared to any Phanerozoic/ Cenozoic arc and was characterised by volanogenic sulfides in the early as well as later arc sequences; b) since Saladipura model age is Aravalli equivalent the stratigraphic assignments in the northern part of the Delhi belt should be re-examined keeping in mind the possibility of suspect terrains, formed by arc-continent collision.

The Vindhayan sediments were laid down in successor basins immediately following the Aravalli-Delhi orogeny. They are shallow-water molasse deposits derived by erosion of the uplifted orogenic belt.

The above section demonstrates that all the component parts of the orogenic belt are remarkably similar to equivalents in a Mesozoic-Cenozoic Himalayan-type orogenic belt. All the rock groups are in their expected order, and to such an extent that it is possible to predict correctly their occurrence. Therefore, it is very likely that the orogenic belt went through an orderly Wilson cycle of events in a manner little different from a late Phanerozoic orogenic belt. The times of formation of the early rifts, the Bhilwara aulacogen and the Aravalli continental margin (Fig.4a) are difficult to define with any degree of precision. The alkaline Berach granite which underlies the Bhilwara rift succession has a Rb/Sr model age of 2600 ± 150 Ma (Crawford, 1970); this is the earliest evidence of any rift-related activity. Nd model ages for several metavolcanics for the basal part of the Aravalli succession are in the range 2600-2300 Ma (MacDougall et al., 1984), but Choudhary et al. (1984), place a lower limit of 2000 Ma on the age of the early Aravalli sediments. The nepheline syenites at Kishangarh no doubt formed earlier than their K/Ar age of 1490 Ma (Chaudhuri and Mukherjee, 1978) and were probably intruded into an early rift. We envisage that, although intra-cratonic rifting may have begun as early as 2500 Ma, the

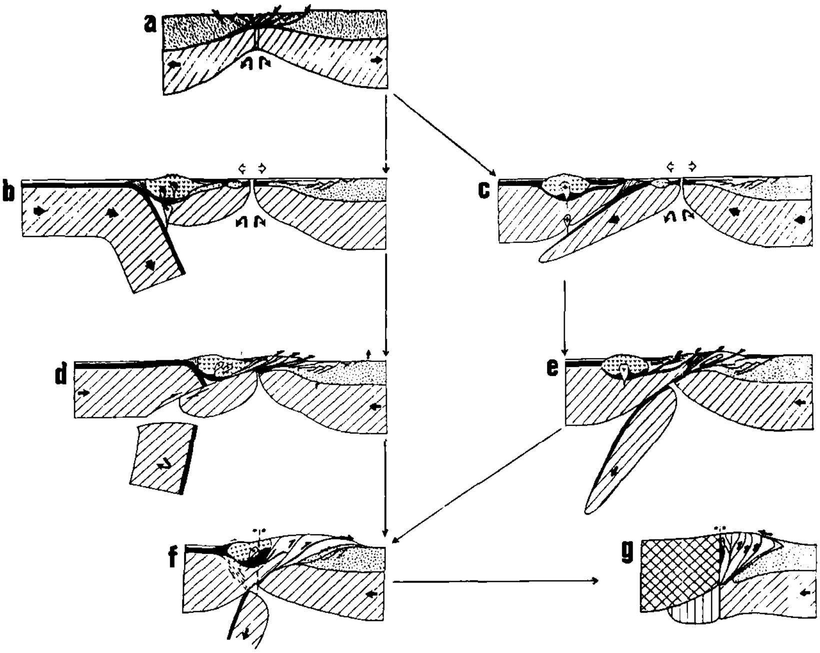

Figure 4. Suggested models of evolution of the Aravalli-Delhi orogenic belt. See text for details.

eastern side of the rifts did not develop into a passive continental margin for several hundred million years, i.e., till complete separation occurred sometime between 2.2 and 1.8 Ga.

Figure 4b and c illustrate two possible alternatives for a plate tectonic scenario for the development of the Delhi island arc and the possible environments of the Jharol belt, which are dependent on the speculations on the polarity of subduction. We wish to emphasise the fact that it is hardly more easy to understand such questions in a Mesozoic-Cenozoic orogenic belt such as the NW Himalayas, as the speculative models of Reynolds et al., (1983) illustrate, for the possible evolution of the Kohistan arc and Karakorum batholiths of N. Pakistan. Indeed there is little unequivocal field evidence to indicate which of the two sutures bordering the island arc formed first. The same problems apply to Proterozoic orogenic belts. (1) If the Jharol belt is interpreted as a telescoped sequence of deep pelagic continental rise sediments, then eastward subduction took place below the western side of the arc, and the Alwar and Ajabgarh sediments formed in the back-arc basin possibly underlain by attenuated remnants of continental crust. The contact between the Alwar Group and the Jharol belt in the southern part of the orogen is conformable and not (obviously) a thrust contact, indicating that the back-arc sediments were deposited directly over distal shelf-rise sediments. The occurrence of high pressure grospydite in the Phulad belt suggests that this was the site of the main subduction zone of an oceanic plate rather than of a back arc basin. (2) The belt may be an accretionary prism formed tectonically above a subduction zone which dipped westward below the Delhi magmatic arc, and accordingly the Alwar and Ajabgarh sediments were deposited in the fore arc and the Phulad ophiolite suite is the remnant of the back arc. This model cannot explain continental crust contamination as easily as the other model. It also requires the arc to be mid-oceanic.

Formation of the Delhi rocks is better constrained particularly in the region north of Ajmer. Crawford (1970) produced a single model Rb/Sr age of 1650 Ma for a granite in the Delhi belt, and Choudhary et al., (1984) have measured Rb-Sr whole rock isochrons in the range 1700-1500 Ma for a number of granites intrusive into the Delhi rocks and some of these granites are believed to be synkinematic with the first Delhi deformation (Goswami and Gangopadhyay, 1971).

Most metamorphic ages in both the Aravalli and Delhi belts cluster around 1500 Ma; we interpret this as the time of terminal collision. The early stretching lineations in the Aravalli and Bhilwara belts suggest oblique convergence of the arc and continental margin. This was a time when the Aravalli and Jharol sediments were thrust eastward over the BGC craton, with restacking accommodated by reactivation of old listric normal faults. During arc-continent collision, continental lithosphere is thrust under the arc complex in both models (Fig.4d & e). Thinning of the Aravalli continental margin leads to subsidence and subsequent influx of (Debari clastics) from the east. In both models (Fig. 4d and e) a thrust stack of back-arc (or fore-arc) and shelf-rise sediments are transported eastwards over the continental margin. The Rakhabdev lineament evolved into a major shallow west-dipping thrust. With continued convergence (Fig. 4f), the early thrusts steepen and wrenching parallel to the belt is initiated.

Ultimately, the early thrusts are rotated to a vertical attitude (Fig.4g) and material is extruded laterally and vertically. At this stage, dextral strike-slip motion parallel to the belt is great and 'flakes' of continental crust are back-thrust over the Aravalli thrusts. In the northern narrow part of the belt, shortening was so great that slices of lower crust (represented by upper amphibolite to granulite facies BGC block) were back-thrust over the Bhilwara aulacogen (not shown in Fig.4). The final configuration of the constituent belts was controlled by possible indentation of the eastern basement block into the accreted orogen.

There are interesting problems associated with the rocks to the west of the Delhi belt. Choudhary et al., (1984) have Rb/Sr whole rock isochron data which indicate that the Erinpura granites have ages of 800 ± 50 Ma which is close to the 735 Ma Rb/Sr model age for the alkaline Malani granites and associated acid volcanics further west (Crawford., 1975). These Malani alkaline rocks are associated with cauldron subsidence and ring structures (Kochhar, 1984). We suggest that these Erinpura and Malani rocks are an expression of a Pan-African belt on the western side of the Delhi belt. However, little is as yet known about this westernmost belt. There is a possibility that during the 1500 Ma event an arc or continental block collided and was accreted to the western side of the Delhi belt. If this were so, the Malani alkaline rocks could have formed either in a late Proterozoic intra-continental rift or in a post-collisional rift which would be related to a Pan-African orogenic belt which was situated to the west of India (Saudi Arabia, E. Africa ?). Alternatively oceanic crust may have lain to the west of the Delhi belt after the 1500 Ma event until a Pan-African block was accreted to it from the west and the Malani rocks would then be situated within a sequence of folded and metamorphosed rocks of Pan-African age. To solve such problems we recommend geological studies and isotopic dating of the 'orogenic belt' rocks in which the Malani rocks are situated. Such data are currently not available. The above suggestions may provide useful models to test with the new data.

ACKNOWLEDGEMENTS

Mihir Deb thanks the Alexander von Humboldt Stiftung, Bonn, for the grant of an 'Europastipendium' at the University of Leicester, U.K., where this collaborative study was undertaken. Sugden acknowledges an NERC studentship.

REFERENCES

Ahmed, T. and Rajamani, V., 1986. Petrogenesis of Aravalli Komatiitic rocks near Nathdwara, Rajasthan. Seminar on Evolution of the Precambrian crust in the Aravalli mountain belt. Udaipur (abst.), 310pp.

Banerjee, G.M., Mukhopadhyay, A.K. and Singhal, R.K., 1983. Tungsten mineralisation of Sirohi, district Sirohi, Rajasthan. Proc. Workshop on Mawam, 1979. Geol. Surv. India. Sp. Publ. 13: 'Mineralisation associated with acid magmatism', pp.130-133.

Banerjee, D.M., 1971. Precambrian stromatolitic phosphorites from Udaipur, Rajasthan, India. Bull. Geol. Soc. Am. 82: 2319-2330.

Basu, K.K., 1971. Base metal mineralisation along the Pur-Banera belt, Bhilwara district, Rajasthan. Misc. Publ. Geol. Surv. India. 16: 153-159.

Bhattacharya, P.K. and Mukherjee, A.D., 1984. Petrochemistry of metamorphosed pillows and the geochemical status of the amphibolites (Proterozoic) from the Sirohi district, Rajasthan, India. Geol. Mag., 121: 465-473.

Burns, L.E., 1985. The Border Ranges ultramafic and mafic complex, south-central Alaska: Cumulate fractionates of island arc volcanics. Can. J. Earth Sci., 22: 1020-1038.

Chattopadhyay, A.K. and Misra, A.K., 1986. Metallogeny in Aravallis with special reference to Kishangarh and Ghugra areas, Ajmer district, Rajasthan. Seminar on Evolution of the Precambrian crust in the Aravalli mountain belt. Udaipur. (abst.), pp.53-54.

Chaudhari, A.K. and Mukherjee, D., 1978. Superposed folding in nepheline syenites and associated metamorphites around Kishangarh, Rajasthan, India. J. Geol. Soc. India, 19: 46-52.

Choudhari, A.K., Gopalan, K. and Sastry, C.A., 1984. Present status of the geochronology of the Precambrian rocks of Rajasthan. Tectonophysics, 105: 131-140.

Chowdhary, S.V., Wakhaloo, R.K. and Prasad, S., 1984. Geology and tin mineralisation in Precambrian rocks, Tosham, Haryana, India. Seminaron Geology of Tin Deposits. Nanning, China. (abst.), 35pp.

Coward, M.P., Butler, R.W.H., Asif Khan, M. and Knipe, R.J., 1987. The tectonic history of Kohistan and its implications for Himalayan structures. J. Geol. Soc. Lond., 144: 369-377.

Crawford, A.R., 1970. The Precambrian geochronology of Rajasthan and Bundelkhand, northern India. Can. J. Earth Sci. 7: 91-110.

Crawford, A.R. and Compston, W., 1970. The age of the Vindhyan system of Peninsular India. Q.J. Geol. Soc. London, 125: 351-372.

Crawford, A.R., 1975. Rb-Sr age determinations for the Mount Abu granite and related rocks of Gujarat. J. Geol. Soc. India, 16: 20-28.

Crookshank, H., 1948. Minerals of the Rajputana pegmatites. Trans. Min. Geol. Met. Inst. India, 42: 105-189.

Deb, M. and Bhattacharya, A.K., 1980. Geological setting and conditions of metamorphism of Rajpura-Dariba polymetallic ore deposit, Rajasthan, India. Vth IAGOD Symp., Utah, 1978. Schweiz. Verlag., Stuttgart, pp.689-697.

Deb, M., 1982. Crustal evolution and Precambrian metallogenesis in western India. Rev. Brasilier de Geol., 12: 94-104.

Deb, M., 1987. Lithogeochemistry around Rampura-Agucha massive sulfide orebody, Proterozoic Aravalli-Delhi orogenic belt, NW India-implications on the evolution of the Archaean crust of western India. IGCP Conf.: Proterozoic geochemistry. Lund, Sweden, (abst.), pp.28-29.

Deb, M., Thorpe, R.S., Cumming, G.L. and Wagner, P.A., 1989. Age, source and stratigraphic implication of lead isotope data for conformable sediment-hosted base metal deposits in the Proterozoic Aravalli-Delhi orogenic belt, Northwestern India. Precamb. Res., (in press).

Deb, M., Sugden, T. and Windley, B.F. Geochemistry of meta-volcanic amphibolites in relation to tectonic environment and mineralisation in the Proterozoic Aravalli-Delhi orogenic belt NW India., (in prep.).

Dekate, Y.G., 1967. Tungsten occurrences in India and their genesis Econ. Geol., 62: 556-561.

Desai, S.J., Patel, M.P. and Merh, S.S., 1978. Polymetamorphites of Balaram-Abu road area, N. Gujarat and SW Rajasthan. J. Geol. Soc. India, 19: 383-394.

Dewey, J. and Windley, B.F., 1981. Origin and differentiation of the continental crust. Phil. Trans. R. Soc. London, A301: 189-206.

Gandhi, S.M., Paliwal, H.V., Bhatnagar, S.N., 1984. Geology and ore reserve estimates of Rampura-Agucha zinc-lead deposit, Bhilwara district, Rajasthan. J. Geol. Soc. India, 25: 689-705.

Gopalan, K., 1986. Geochronology of the Precambrian rocks of Rajasthan: problems and prospects. Seminar on Evolution of the Precambrian crust in the Aravalli mountain belt. Udaipur. (abst.), pp.64-65.

Goswami, P.C. and Gangopadhyay, P.K., 1971. Petrology and structure of Bairat granite in the districts of Alwar and Jaipur, Rajasthan. Q.J. Geol. Min. Met. Soc. India, 43: 141-147.

Gupta, B.C., 1934. The geology of central Mewar, Mem. Geol. Surv. India, 65: 107-169.

Gupta, S.N., Arora, Y.K., Mathur, R.K., Iqbaluddin, Prasad, B., Sahai, T.N. and Sharma, S.B., 1980. Lithostratigraphic map of Aravalli region. Geol. Surv. India, Calcutta.

Heron, A.M., 1953. The geology of central Rajputana. Mem. Geol. Surv. India, 79: 389pp.

Jan, M.Q., Khattak, M.U.K., Parvez, M.K. and Windley, B.F., 1984. The Chilas stratiform complex: field and mineralogical aspects. Geol. Bull. Univ. Peshawar, 17: 153-169.

Kochhar, N., 1984. Malani igneous suite: Hot-spot magmatism and cratonization of the northern part of the Indian Shield. J. Geol. Soc. India, 25: 155-161.

MacDougall, J.D., Gopalan, K., Lugmair, G.W., and Roy, A.B., 1983. The Banded Gneissic Complex of Rajasthan, India: early crust from depleted mantle at 3.5 AE ? EOS transactions. Am. Geoph. Union., 64, (1-26): 351.

MacDougall, J.D., Willis, R., Lugmair, G.W. and Roy, A.B. and Gopalan, K., 1984. The Aravalli sequence of Rajasthan, India: A Precambrian continental margin. Workshop on the Early Earth: the Interval from Accretion to the older Archaean. Lunar Planet. Inst. Houston, Texas: 55-56.

Mukhopadhyay, A.K., 1981. A new occurrence of scheelite, molybdenite, powellite and gadolinite in Phalwadi-Positara area, district Sirohi, Rajasthan. J. Geol. Soc. India, 22: 147-148.

Murthy, M.V.N., 1983. Some aspects of mineralisation associated with acid magmatism in Rajasthan. Proc. Workshop on MAWAM, 1979. Geol. Surv. India Sp. Publ. 13: 'Mineralisation associated with acid magmatism': 15-24.

Naha, K., Chaudhuri, A.K. and Bhattacharyya, A.C., 1966. Superposed folding in the older Precambrian rocks around Sangat, central Rajasthan, India. Neues Jharb. Geol. Palaeontol., ABH, 126: 205-231.

Naha, K. and Chaudhuri, A.K., 1968. Large scale fold interference in a metamorphic-migmatitic complex. Tectonophysics, 6: 127-142.

Naha, K. and Halyburton, R.V., 1974. Early Precambrian stratigraphy of central and southern Rajasthan, India. Precamb. Res., 1: 55-73.

Naha, K. and Halyburton, R.V., 1977. Structural pattern and strain history of a superposed fold system in the Pre-Cambrians of Central Rajasthan. India. I and II. Precamb. Res, 4: 39-111.

Naha, K., Mukhopadhyay, D.K., Mohanty, R., Mitra, S.K. and Biswal, T.K., 1984. Significance of contrast in the early stages of the structural history of the Delhi and the Pre-Delhi rock groups in the Proterozoic of Rajasthan, Western India. Tectonophysics, 105: 193-206.

Patchett, P.J. and Arndt, N.T., 1986. Nd isotopes and tectonics of 1.9-1.7 Ga crustal genesis. Earth Planet. Sci. Lett., 78: 329-338.

Pawar, K.B. and Patwardhan, A.M., 1984. Tectonic evolution and basemetal mineralisation in the Aravalli-Delhi belt, India. Precamb. Res., 25: 309-323.

Raghunandan, K.R., Dhruba Rao, B.K. and Singhal, M.L., 1981. Exploration for copper, lead and zinc ores in India. Bull. Geol. Surv. India, Ser. A 47: 222.

Raja Rao, C.S., 1976. Precambrian sequences of Rajasthan. Misc. Publ. Geol. Surv. India, 23: 497-516.

Raja Rao, C.S., Poddar, B.C., Basu, K.K. and Dutta, A.K., 1971. Precambrian stratigraphy of Rajasthan - a review. Rec. Geol. Surv. India, 101: 60-79.

Ramsay, J.G. and Huber, M.I., 1987. The techniques of modern structural geology, V.2. Folds and fractures. Academic Press: 700pp.

Ray, S.K., 1986. Structural control of copper mineralisation in the Sawar group of rocks, Ajmer district, Rajasthan. Seminar: Evolution of the Precambrian crust in the Aravalli mountain belt. Udaipur, (abst.), 46pp.

Reynolds, P.H., Brookfield. M.E. and McNutt, R.H., 1983. The age and nature of Mesozoic-Tertiary magmatism across the Indus suture zone in Kashmir and Ladakh (NW India and Pakistan). Geol. Rund., 72: 981-1004.

Roy, A.B., Paliwal, B.S. and Goel, O.P., 1971. Superposed folding in the Aravalli rocks of the type area around Udaipur, Rajasthan. J. Geol. Soc. India, 12: 342-348.

Roy, A.B. and Jain, A.K., 1974. Polyphase deformation in the Pb-Zn bearing Precambrian rocks of Zawarmala, district Udaipur, southern Rajasthan. Q.J. Geol. Min. Met. Soc. India., 46: 81-86.

Roy, A.B. and Paliwal, B.S., 1981. Evolution of lower Proterozoic epicontinental deposits: stromatolite-bearing Aravalli rocks of Udaipur, Rajasthan, India. Precamb. Res., 14: 49-74.

Roy, A.B., Somani, M.K. and Sharma, N.K., 1981. Aravalli-pre-Aravalli relationship: a study from the Bhinder region, southern Rajasthan. Indian J. Earth. Sci., 8: 119-130.

Roy, A.B., Golani, P.R. and Bejarniya, B.R., 1985. The Ahar River granite, its stratigraphic and structural relations with the early Proterozoic rocks of south-eastern Rajasthan. J. Geol. Soc. India. 26: 315-325.

Sawkins, F.J., 1982. Metallogenesis in relation to rifting. In: Palmeson, G. (Editor), Continental and Oceanic rifts. Geodynamics ser. 8, Am. Geophys. Union, pp.259-269.

Sawkins, F.J., 1984. Metal deposits in relation to plate tectonics. Springer-Verlag, Berlin, 325pp.

Sen, D. and Sen, S., 1982. Post-Neogene tectonism along Aravalli range, Rajasthan: Tectonophysics, 93: 75-98.

Sen, S., 1970. Some problems of Precambrian geology of the central and southern Aravalli range. J. Geol. Soc. India, 11: 217-231.

Sen, S., 1981. Proterozoic palaeotectonics in the evolution of crust and location of metalliferous deposits, Rajasthan. Q. J. Geol. Min. Met. Soc. India, 53: 162-185.

Sharma, B.L., Chauhan, N.K. and Bhu, H., 1986. Strain history of the Pre-Cambrian rocks of Bagdunda area, Distt, Udaipur, Rajasthan. Seminar on Evolution of the Precambrian crust in the Aravalli mountain belt, Udaipur, (abst.), 35pp.

Sharma, R.S., 1986. Patterns of metamorphism in the Precambrian rocks of the Aravalli mountain belt. Seminar on Evolution of the Precambrian crust in the Aravalli mountain belt, Udaipur, (abst.), pp.13-14.

Sinha-Roy, S., 1984. Precambrian folded unconformity in Rajasthan. Curr. Sci., 53(22): 1205-1207.

Sinha-Roy, S., 1984. Precambrian crustal interaction in Rajasthan, NW India. Indian J. Earth Sci., CEISM Seminar volume: 84-91.

Sivaraman, T.V., 1982. Zircon geochronology of granites from the Precambrian of Rajasthan, India. G.S.A. Abstr., 14(7): 618.

Sugden, T.J., 1987. Evolution of the southern part of the Aravalli-Delhi orogen, western India. (Unpubl. Ph.D. thesis), Univ. of Leicester, U.K., 241pp.

Sychanthavong, S.P.H. and Desai, S.D., 1977. Proto-plate tecotonics controlling the Precambrian deformation and metallogenetic epochs of north-western peninsular India. Minerals. Sci. Engng., 9: 218-236.

Sychanthavong, S.P.H. and Mehr. S.S., 1984. Proto-plate tectonics-the energetic model for the structural, metamorphic and igneous evolution of the Precambrian rocks, NW peninsular India. Sp. Publ. Geol. Surv. India, 12: 419-458.

Taylor, S.R. and McLennan, S.M., 1985. The continental crust: its composition and evolution. Blackwell, Oxford, 312pp.

Valdiya, K.S., Bhatia, S.B. and Gaur, V,K. (Editors), 1982. Geology of Vindhyachal, Hindustan Publ. Co. Delhi, 231pp.

Vinogradov, A., Tugarinov, A., Zhykov, C., Stapnikova, N., Bibikova, E. and Khorre, K., 1964. Geochronology of the Indian Precambrian. 22nd Int. Geol. Congr. Delhi Pt. X, Archaean and Precambrian geology, pp.553-567.

Windley, B.F., 1983. A tectonic review of the Proterozoic. Geol. Soc. Am. Mem., 161: 1-10.

Windley, B.F., 1984. The Evolving Continents, 2nd edition, Wiley, Chichester, 399pp.

ON THE GEOLOGY OF THE EASTERN GHATS OF ORISSA AND ANDHRA PRADESH, INDIA

P.K.BANERJI

ABSTRACT

The Eastern Ghats granulite - gneiss tract of Orissa and Andhra Pradesh, dominantly composed of the khondalite group with moderately extensive charnockites, granites, migmatites and local pegmatites, besides a few anorthosites-alkaline syenite complexes, covers approximately 52000 Sq. km. Serious problems have been faced in systematic lithofacies mapping owing to lack of marker bands, absence of unconformities, the thick weathered crust and limited accessibility. As a result, first-generation systematic mapping of this tract has not been very successful in spatial and temporal discrimination/classification of the granites and migmatites in relation to the associated granulites.

This horst-shaped tract carries a clear impress of three cycles of acid igneous plutonism, deformation and prograde/retrograde metamorphism and more than two phases of basic igneous magmatism. There is extensive reactivation along its margins by rifting, local emplacement of mafic/ultramafic complexes and then collision with the Gorumahisani and equivalent Iron Ore Group sequences lying to its north and west. Deep inside the Eastern Ghats, the orogenic cycles were not interleaved with sedimentation; and there is a recognisable contrast in their metamorphic P.T from the granulite-gneiss terrane of South Andhra Pradesh and Tamil Nadu beyond the Proterozoic to Recent Godavari - Krishna aulacogen, where charnockites become dominant at the expense of khondalites: high P.T granulite-facies assemblages become more extensive and abundant: and even the metamorphic impress of the border (reactivated) zone assumes a higher grade.

One suspects one or more fundamental mid-Proterozoic event(s) of differential uplift between the North and the South Eastern Ghats, possibly coinciding with Pakhal sedimentation, deformation and igneous (granitic and alkaline) intrusions.

INTRODUCTION

First-generation surface geological mapping of a major part of the Eastern Ghats on a 1:63,360 scale has been carried out by the Geological Survey of India during the period 1945 - 1985. Coincidentally, this period witnessed a dramatic change in the analysis and understanding of granites, migmatites and granulites following new researches in the advanced countries on mineral equilibria, structural analysis and geothermometric and barometric indicators in co-existing mineral phases. But the universal phenomenon of a variable lag effect between new research finds in the laboratories and orthodox mapping techniques adopted by the geologists could not be overcome in the Eastern Ghats during the first-generation mapping programme. Industrial developments during the last 40 years have made the Eastern Ghats terrain relatively more accessible.

The present paper highlights some of the practical problems of systematic mapping of the Eastern Ghats, briefly reviews the existing information and makes a case for taking up second-generation mapping of selected sectors of this area along modern lines.

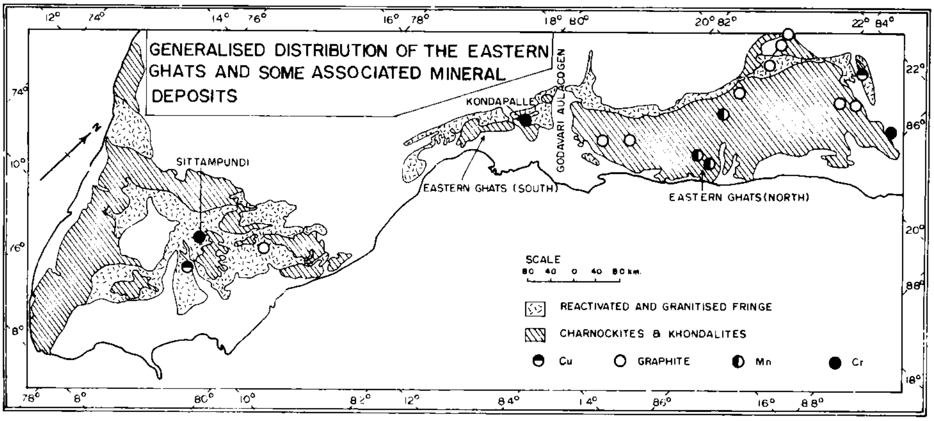

Figure 1. Generalized geological map of the Eastern Ghats and some associated mineral deposits.

The Eastern Ghats have an overall NE-SW trend from the southern bank of the Brahmani river in Orissa to the Nilgiri Mountains of Tamil Nadu, with a pronounced break between the Godavari and Krishna rivers of Andhra Pradesh (Fig.1). The area to the north of the Godavari river comprises the Eastern Ghats (North) and is the central theme of this paper. The area south of the Krishna river from Vijaywada onwards forms a distinctly different geomorphic, geologic ensemble and is hereafter referred to as the Eastern Ghats (South).

The geology of the Eastern Ghats (North) was established in broad outline by the traverses by V.Ball, T.L. Walker, C.S. Middlemiss, H. Crookshank, M.S. Krishnan, P.K. Ghosh (in adjoining Bastar dt. of M.P.) and others. (Pascoe, 1950).

During the last four decades, systematic geological mapping of almost the whole Eastern Ghats (North) terrain on a scale of 1:63,360 has been undertaken by Geological Survey of India. Ground observations on lithology and structure have been supplemented sporadically with modern aids like aerial photos, satellite imageries, isotope geochronology, etc. Some interesting data have been collected, but this high grade terrain remains comparatively ill understood.

STRATIGRAPHY

On the basis of systematic geological mapping and some isotope geochronologic data, the stratigraphic arrangement of the rocks is generally believed to be as follows:

U.Proterozoic (900 - 550 m.y)	Porphyritic gneiss, granite, pegmatite and quartz-vein, dolerites.
M. Proterozoic (1600 - 900 m.y)	Anorthosite, quartz mangerite, granite, nepheline syenite, gabbro and norite.
Archaean to L. Proterozoic	Migmatites, biotite granite gneiss, pegmatite and quartz vein.
	Charnockite (acid to basic) suite; Khondalite group (metamorphosed arenaceous, argillaceous and carbonate sediments and some intercalated volcanics).

Detailed lithofacies mapping of the khondalites has nowhere been possible during the programme of mapping on the scale of 1:63,360. Outcrops are few except on hill crests and road cuttings. Similarly, the contact between the charnockites and khondalites is obscure; nowhere is any acid or intermediate charnockite seen to be cutting through the metasediments of the khondalite group. The original discordance, if any, has possibly been transposed by repeated folding. The alternative possibilty that the charnockites were the basement over which the Khondalite group sediments accumulated, is rather thin. Quartzites are the dominant facies of the khondalite group in many areas of the Eastern Ghats (North); but these do not carry any rutile,a characteristic accessory mineral of the charnockites; nor do the khondalites include any basal or intraformational conglomerate with pebbles or boulders of charnockite. The bulk chemistry of khondalite s.s. (quartz + garnet + sillimanite + graphite) is unlike any modern magmatic rocks. In fact, Walker (1902) had commented upon its possible sedimentary analogue, a well-leached clay, mixed with a little quartz. The association with calc-silicate granulites and manganiferous quartzites is also suggestive of a sedimentary parentage.

The charnockite suite ranges from alaskite/leucogranodiorite through hypersthene granite, enderbite (with antiperthitic plagioclase and mesoperthitic microperthite), quartz syenite and diorite to hypersthene granulite, the basic member occurring frequently as xenolithic enclaves in acid charnockite. The basic charnockites also occur as small bodies within khondalites; but the abundance of the basic enclaves is extremely erratic. It may be more than a coincidence that the acid charnockites in both the northern and southern Eastern Ghats appear to have whole-rock Rb-Sr dates of around 2695 Ma. (Perraju et al., 1979) to 2600 Ma. (Vinogradov et al., 1864) and compare well with the Rb/Sr isochrons of 2580 ± 80 Ma. for the Madras city and Nilgiri Hills charnockites (Crawford., 1969). Recent determinations of whole rock Rb-Sr isochrons and lower intercept data of U-Pb in zircon from the charnockite of Kabbaldurga, Karnataka (Raith et al., 1988) are also in conformity with an estimate of about 2500 Ma. as a major phase of charnockitization of diverse types of hypozonal plutonic assemblages near the Archaean-Proterozoic boundary.

The intrusive/infiltrative nature of the granites and migmatites towards both charnockites and khondalites is well displayed in various outcrops and road cuttings in Sambalpur, Dhenkanal, Ganjam and other districts. All stages of conversion of khondalite s.s. (Banerji, 1982b) into migmatites are exposed lending credence to the concept of anatectic derivation of some of these migmatites from pelitic assemblages (Bose and Sanyal, 1987). Anastomosing veins of leucogranite in acid charnockites (quartz + K-feldspar + plagioclase + orthopyroxene) are also frequently noted.

But the crucial issue, which has so far baffled the geologist mapping hundreds of square kilometers every year (mostly on the basis of observations of outcrops and hand specimens), is the problem of stratigraphic ordering of the different granites and migmatites. Unlike the surrounding greenstone terranes there are no easily recognisable (and mappable) cycles of sedimentary and/or volcanic sequences starting with unconformities marking the onset of the different stratigraphic sequences. For example, around the Chilka Lake of Orissa, there are khondalites and a garnetiferous granite gneiss, which is intruded by anorthosite (Rb/Sr isochron age 1404 ± 89 Ma.). Besides there is a garnetiferous quartz mangerite bearing subangular inclusions of anorthosites (Sarkar et al., 1981). One has to be very careful to decipher the subtleties contained within such "similar looking" rocks. To cite another example, south of Phulbani town at the heart of the E. Ghats province, the charnockites are retrograded to garnetiferous, amphibole- and biotite-bearing rocks by tectono-metamorphic differentiation (Kamenev, 1982) and later metasomatism. They show faintly pleochroic orthopyroxene with rims either of dactylitic aggregates of garnet or of uralite, red-brown biotite and chlorite. These rocks were intruded by a porphyritic granite gneiss (quartz + microperthite + garnet + brown biotite + zircon). Careful Pb-Pb dating of zircon, apparently infiltrated into these charnockites, yielded a good isochron of about 800 Ma. (D.K.Paul, Pers. Comm.). Without the benefit of such isotope geochronologic signposts, the granites associated with these charnockites could hardly be suspected to be upper Proterozoic. In fact, I had sampled these rocks with the hope of getting some Early Proterozoic to Archaean dates.

Such upper Proterozoic granites have also been reported by Perraju et al., (1979) from the Srikakulam area of Andhra Pradesh on the basis of Rb-Sr dating.

Such repeated granite emplacements, many of which cannot be stratigraphically classified in space (at the present level of availability and speed of dependable isotope geochronologic data in India) have also been a source of considerable uncertainty in tectonic and metallogenic modelling. A regional-scale understanding of the controls and geometry of magmatism in space and time is lacking. Hundreds of careful geochronologic measurements will be needed before the granitic suites of this area can be correlated and arranged sequentially over the whole region.

STRUCTURAL FEATURES

The geologist engaged in systematic mapping is equally handicapped in delineating regional fold forms. There are no marker bands within the khondalite group except for calc silicates and manganiferous zones which occur only at a few localities as small strips. The charnockites are massive looking. On top of it, there is a thick lateritic cover at many places. Consequently, structural analysis is on either mesoscopic and microscopic scale or on the scale of satellite imagery (1:250,000). Lineaments identified in black and white Landsat imageries of Band 5 and 7 are quite abundant in this tract. These are generally oriented in NE-SW, NW-SE and E-W directions. Many of these are possibly expressions of regional-scale fold trends, which appear on mesoscopic scale as tightly appressed, isoclinal and coaxially refolded systems in rocks of the khondalite group and in the migmatites. The dominant foliation is axial planar to these isoclinal folds and is also parallel/subparallel to the axial planes of intrafolial folds, which are generally believed to be F_1, e.g., near Angul (Halden et al., 1982). Other open fold forms are also noticed around plutonic emplacements, e.g., of anorthosites and porphyritic granites around Chilka Lake, Mandibisi (Koraput), Kottauru (Visakhapatnam), etc. Elsewhere, these open fold forms are subdued and do not show up in Landsat imageries, although in the field, they appear to be quite pervasive.

The porphyritic granites are intermittently characterised on mesoscopic scale by swirls of feldspar porphyroblasts sub-horizontally oriented, indicating viscous, lateral flowage of the rock mass during semisolid emplacement. It would be naive to expect that all these porphyritic granitoids with such flowage features are of the same age (U. Proterozoic). But no further stratigraphic refinement is possible with the available data.

Besides the fold-parallel lineaments, there are other lineaments, which appear to cut across the regional folds, e.g., along the Tel, the Vansadhara, etc. These appear to define major fracture/fault zones (Prudhivi Raju and Vaidyanadhan, 1981). Discrete mylonite zones, parallel to such features, have been mapped locally (e.g., P.Perraju in Puri district, Orissa).

The northern, western and southern margins of the Eastern Ghats (North) are intruded by granophyres, K-granites, alkaline syenites, gabbros and anorthosites, ultramafic rocks, etc., and carry distinct and overlapping dislocation zones. The "so-called" Mahanadi trend is a part of this domain, wrapped around by the greenstone-granite provinces of the Gorumahisani and Bengpal groups. The western margin was described by Crookshank (1938), who noted albitization and crushing. Road cuttings to the power house of the upper Kolab dam, near Jeypore, expose this crush zone clearly.

The northern margin of the Eastern Ghats (North) is characterised by impersistent blastomylonites and crush zones. There is a motley crowd of specialised facies in this area: K-granites and pegmatites with beryl (Sambalpur), chromiferous ultramafic masses (Dhenkanal district), impersistent sulphide ores (Adas), magnetite-bearing granophyre (Sukinda), etc. This sector has recently been described by Banerji et al., (1987). Early Proterozoic rifting followed by collision appears to have dominated the growth of this remobilized sector, prompting this author to compare a part of its evolution with the northern Red Sea rift (Banerji and Chatterjee, 1988).

The southern margin is defined by the Godavari graben which has been a depocenter for upper Proterozoic, Gondwana and Meso-Cenozoic sediments beginning with the Pakhal Basin (Rao, 1987). Repeated reactivation on diversely oriented surfaces, locally orthogonal to the graben margins, has been recorded (Sastri, 1980; Rao, 1987).

Recent offshore wells of Oil India, off the Mahanadi delta, show that rocks of this province continue below the continental shelf sediments of the Bay of Bengal. Late Mesozoic to Cenozoic reactivation is attested to by a network of faults and thick sequences of volcanic rocks (Baishya et al., 1986).

In totality, therefore, the Eastern Ghats (North) province appears to be a prominent horst, bounded on all sides by a large number of faults. Ductile to brittle state dislocations along these faults of various ages were superposed on polycyclic ductile state folding movements, accompanying magmatic and metamorphic-metasomatic processes.

METAMORPHISM

The khondalites and migmatites bear high-grade index minerals like sillimanite, kyanite and cordierite and reflect, by their different textural characters, cycles of high PT (Banerji, 1982b; Dash, 1982). Inclusions of spinel, sapphirine and sillimanite in garnet, and sillimanite and sapphirine rims around spinel are locally observed. Other index associations viz., hypersthene + sillimanite, cordierite + garnet + sillimanite + biotite + quartz + ilmenite ± spinel ± plagioclase ± corundum ± anothophyllite ± hypersthene, sapphirine + sillimanite + sapphirine + spinel + sillimanite, kornerupine + spinel, wollastonite + calcite, etc. reflect high temperature and high-to medium-pressure environments. In the charnockitic suite, partial alteration of the pyroxenes to hornblende and/or to biotite, the presence of dactylitic rims of garnet around pyroxenes, and symplectitic intergrowth of felspars suggest retrogression to hornblende granulite/almandine amphibolite facies. This retrogression was of varying intensity from place to place.

Consequent upon such repeated metamorphism and deformation, it has not been possible to prepare an accurate metamorphic facies map of this terrain either. In south-west Orissa and north Andhra Pradesh, comprising the districts of Koraput, Visakhapatnam Srikakulam and Prakasam, the higher grade assemblages are more abundant and the retrograded variants occupy less area than in the northern parts viz., the districts of Ganjam, the Kalahandi, Bolangir, Sambalpur, Dhenkanal, Puri and Cuttack. It may be more than a concidence that the latter are more closely traversed by a network of fracture lineaments and rectangular drainage courses.

ALKALINE AND MAFIC-ULTRAMAFIC MAGMATISM ALONG THE MARGINS

The present boundary of the Eastern Ghats (North) provides a classic example of recurrent deep-seated tectonism and related igneous activity. A number of alkaline and mafic to ultramafic igneous masses have been identified along the northern and the western reactivated margins with characteristic ore deposits of Cr, Ni, Cu, Zr, apatite, REE, etc. But these intrusive masses along the margins of the Eastern Ghats (North) province viz., the ultramafic masses around Asurbandh and Moulabhanj Parbat, the Bolangir and Kalahandi anorthosites, Koraput syenite, Borra syenite-carbonatite (?), Cheruvakonda olivine gabbro-norite, Kunavaram syenite, etc., did not suffer any high granulite-grade metamorphic alteration or any strong regional scale folding movement after their emplacement within the charnockite tract, although in selected sectors (e.g., near Moulabhanj Parbat, Orissa), they were intruded by granophyric rocks.

This habitat is in sharp contrast to similar emplacements within the Eastern Ghats (South) tract, south of the Krishna river. Recent studies by this author (Banerji, in press) suggest that the Kondapalle chromiferous orthopyroxenite, norite and anorthosite in the Eastern Ghats (South) province suffered strong folding movements. In the Rama quarry of Kondapalle (sunk by the Ferro- Alloys Corporation), chromitite-silicate interbands show both tightly appressed, reclined folds as well as open and upright folds. Further south in the Sittampundi field also, the chromiferous pyroxenites and norites (retrograded) have suffered intense folding and brecciation and occur as isolated rafts with a style of folding and shearing different from the tightly folded and boudinaged host anorthosite, emplaced within garnet-hypersthene granulite and garnet-corundum diorite gneiss. Partial retrogression of all these rocks is witnessed by the sporadic formation of large prismatic crystals of zoisite-epidote within Sittampundi anorthosite, e.g., near Nallkavundan-Palliyan ($11^{o}19$'N: $78^{o}02$'E: 58), development of hornblende with release of opaque granules from garnet in the garnet-hypersthene granulite, development of amphiboles, chlorite and magnetite in the chromitite suite, etc. The geological habitat of the Sittampundi mass appears to be similar to the Oddanchatram anorthosite (Wiebe and Janardhan, 1988) of the Tamilnadu and the Kurihundi anorthosites of Karnataka (Ramakrishnan et al., 1978) although this author is in complete agreement with Ashwal (1988) that the similarity among these anorthosites does not imply "a distinct anorthosite event". A comparative geological and geochemical re-study of these anorthosite masses of South India associated with granulites, granitic gneisses and greenstones might be useful in unravelling their similarities and contrasts with East Indian (Chilka, Bankura, Kalahandi, Bolangir, Nausahi, Kumardubi, etc.) anorthosites and related rocks.

CONTRASTS BETWEEN EASTERN GHATS (NORTH) AND EASTERN GHATS (SOUTH)

The contrast in the time and level of emplacement of chromite-rich mafic-ultramafic bodies vis-a-vis folding movements between the Eastern Ghats (North) and the Eastern Ghats (South) provinces is also reflected in the overall rock assemblages.

From Vijaywada south and southwestward up to the Nilgiri hills, the khondalite-charnockite association of the Eastern Ghats (South) possibly reflects a more complex and initially higher metamorphic PT than the rocks of the Eastern Ghats (North). Dhanaraju's (1977) estimate of 600^o - 700^oC and a P_{load} of 6-7 Kb for the temperature of crystallisation of orthopyroxene in rocks of the Chipurupalle-Razam area, together with the recent work of Murthy and Nirmal Charan (1988) on the cordierite gneisses near Guntur, suggest a general range of 600^o - 750^o and P_{load} of 6 - 7 Kb for metamorphism of the rocks of the Eastern Ghats (north). However, estimates of 720^o - 840^oC and a P_{load} of 9 - 10 Kb for the Madras granulites by Weaver et al., (1978) and of 700^o - 920^oC and a P_{load} of 8.8 - 11.3 Kb for the Oddanchatram anorthosites and charnockites (Wiebe and Janardhan, 1988) suggest a higher P,T environment preserved in some assemblages, although the later cycle of charnockite formation around Kabbaldurga at 750^oC and P_{load} of 5.5 Kb is generally believed to be a shallower event (Raith et al., 1988), possibly related to localised higher geothermal gradients.

The relatively lower and simpler P-T history of the northern sector is also borne out by the three following observations:

1. The transitional nature of the contact between the Eastern Ghats gneisses and the Bonai granite off Riamal, Sambalpur district, (Banerji et al., 1987); not far from the contact with

the Eastern Ghats the Bonai granite bears enclaves of khondalites, the latter infiltrated by K-granite and granophyre at the margin.

2. The absence of any field evidence in the E. Ghats (North) suggesting development of charnockites from granites, unlike such evidence in the southern sector, e.g., from the Kabbal and Krishnagiri areas (Pichamuthu, 1961; Ramiengar et al., 1978; Janardhan et al., 1982). This contrast suggests that the metamorphic cycles following various episodes of granite emplacement in the Eastern Ghats (North) did not again reach appropriate P,T,X for their conversion into charnockites.
3. The khondalite group of rocks is much less abundant in the Eastern Ghats (South), where high grade charnockites and gneisses dominate.

The Krishna-Godavari graben, lying in between the northern and the southern provinces, bears clastic sediments from (U. Proterozoic onwards). Repeated reactivation of this graben appears to have begun in late Proterozoic times and the metamorphic event within the Pakhal sequence of this graben could conceivably be near-isochronous with the young pegmatites across the Eastern Ghats.

MINERAL DEPOSITS IN THE EASTERN GHATS

Compared to the B.I.F. provinces to its north and west, this terrain is comparatively poor in known mineral resources. This may partly be due to incomplete investigation. Dense vegetation and abundant colluvium on the hill slopes and fairly thick alluvial or laterite cover in the plains and plateaus render a visual search for mineral deposits in the course of systematic mapping an accidental event; certain significant indications of a higher mineral potential are obtained now and then, e.g.: (1) the discovery of a large graphite deposit at Tumudibandh, Kalahandi district, Orissa by boulder trains in a first-order nullah in a densely forested, almost inaccessible part of the Eastern Ghats (North) during the late forties/early fifties and (2) the discovery of a small copper sulphide deposit at Adas, Sambalpur district, Orissa, in the early eighties (Banerji et al., 1988) prompted by an accidental misinterpretation of a laterite saprolite as gossan in the seventies. Perceptive, concept-oriented geophysical and geochemical surveys in this tract would probably lead to new mineral discoveries. An airborne survey has been undertaken over a part of this area. It is hoped that ground follow-up geophysical and geochemical search will prove rewarding.

Economically important mineral occurrences so far known include high- to medium-grade graphite (both flaky and massive varieties), low- to medium-grade and generally high-phosphorus (due to apatite) manganese ore (mainly pyrolusite and psilomelane), local enrichments of apatite-magnetite and sporadic occurrences of semi-precious emerald, beryl,zircon and garnet. There are also reports of sapphire.

The graphite deposits occur as bedded to massive deposits i grey quartzites of the khondalite group, e.g., in Tumudibandh in Orissa (which is the largest single deposit in the State); as concentrated palaeosomes from graphite-rich schists of the Khondalite group in migmatite terranes, e.g., in Bolangir and Sambalpur districts; and as clots of pure, coarsely flaky graphite in pegmatites. The graphite reserves are huge, although large single deposits are exceptions. At a few places, graphite deposits are associated with sulphides, e.g., at Adas, Sambalpur dt. In relatively flat terrains with extensive soil/laterite/alluvium cover, ground geophysical exploration has proved useful in Bolangir district and elsewhere.

The small (1-2 million tonnes) manganese-ore deposits of Visakhapatnam, Srikakulam, Vizianagaram and Koraput districts have been explored and studied in detail by GSI officers. According to Krishna Rao et al., (1982), manganese silicate, oxide and carbonate minerals form the protores in the A.P. sector and form a part of the khondalite group. The deposits occur within banded quartzites and at the contact of calc-granulite and quartzite. In the Koraput Dt, the ore bodies are associated with ferruginous and cherty quartzites. On supergene alteration these have given rise to economic ore bodies.

The precious and semiprecious stones (aquamarine, yellow beryl, amethyst, sapphire, etc) are mostly associated with aegirine-augite/nepheline syenites and zoned pegmatites along the western and northwestern reactivated border of the Eastern Ghats. Fresh and locally large garnet crystals are common in some granites. The fluor-apatite and magnetite-bearing veins in Kasipatnam, southeast of the Borra pyroxenite-syenite-carbonatite(?) occurence in Andhra

Pradesh, appear to lie in extension of the reactivated fringe. The currently disputed (Rao and Narendra, 1986) Borra carbonatite (?) carries bastnaesite - a REE-rich mineral - in small quantities (Ramam and Viswanathan, 1977). The deposit is high grade (P_2O_5 : ~39%) but erratic.

Besides these, local (e.g., near Palasama in Sambalpur district) low-grade (40-70%) sillimanite deposits have been located by GSI within sillimanite-quartz schists, with or without garnet and magnetite. The northern reactivated fringe of the Eastern Ghats also bears small auriferous pyrite - chalcopyrite ore bodies in garnetiferous amphibolites at Adas, Sambalpur district (Banerji et al., 1988), and pods of high-to medium-grade chromite associated with serpentinites, e.g., at Asurbandh and Maulabhanj Parbat (Banerji, 1972).

The most important mineral deposit in this tract is, however, an exogenetic blanket of red and brown bauxite, popularly known as the East Coast Bauxite deposits. This is associated with the highest planation surface, which shows up as large to small mesa-type plateaus in the western and southern part of the granulite tract. The deposits are essentially made up of gibbsite, haematite and geothite and are characterised by very low silica and titanium (Rao and Ramam, 1979).

CONCLUSION

The Eastern Ghats rock assemblages, north of the Krishna-Godvari graben, record a complex sequence of metamorphism, magmatism and deformation. Isotope geochronologic measurements on these rocks span almost the whole of the Proterozoic and possibly a part of the Archaean era. The available data are, however, inadequate and some are equivocal. But the absence of sedimentary and/or volcanic sequences, alternating with the various cycles of granite emplacement, is an observable fact in the field and so is the suspected contrast in metamorphic history between the blocks, north and south of the Krishna-Godavari graben. It appears that the khondalite group represents an Archaean clastic (and minor chemogenic) sedimentary pile, which was dragged down to depths of approx. 20-30 km from the surface by intense compressive stress reaching below or near the Conrad discontinuity. Subsequently, uplift of these rocks to surface levels did not upwarp the corresponding M discontinuity, as is revealed by extensive negative

Bouguer gravity anomalies below the Eastern Ghats. This feature is comparable to the gravity anomaly pattern in the granulites from Enderby Land, Antartica (Wellman and Tingey, 1977). One explanation for this feature (Banerji, 1982a) could be underpinning by lateral flow of acidic material accompanying uplift of this early Proterozoic lower crust, although what forces caused such underpinning, possibly in stages, and what relation, if any, this mass flowage had with the development of the surrounding greenstone provinces and subsequent development of sedimentary basins (Cuddapah-style) are still in the domain of speculation. Alternatively, one has to agree with the interpretation of Wiebe and Janardhan (1988) and Leelanandam et al., (1988) that these granulites represent the lower parts of a Himalaya-type collision zone, which attained an estimated crustal thickness of about 75 Km during the early- to mid-Proterozoic era.

In order to choose between these alternatives, it is necessary to map these rocks in detail with proper isotope geochronologic, petrologic and geochemical back up. This will provide us with a dynamic view of the evolution of the deeper crust and should prove to be of interest for the International Lithosphere Project. In an era when the superdeep borehole at Kola Peninsula has already intersected granulites at depths close to the Conrad discontinuity, the Eastern Ghats at our doorstep could provide an equally interesting 3D X T view, if a proper work programme could be executed. Needless to mention that such a programme, forming second-generation mapping along selected transects on a scale of 1:10,000 (10 Km- wide approx.) needs to have large-scale inputs from isotope geochronology and geochemistry, not to mention refraction seismic profiling, which together with airborne magnetic and regional gravity data will provide adequate constraints in modelling the evolution of the Eastern Ghats.

ACKNOWLEDGEMENTS

The paper is published with the approval of the Director General, Geological Survey of India. I am also obliged to Shri. S.K. Bandopadhyay of Wing Hqrs., for repeated typing of the manuscript.

REFERENCES

Ashwal, L.D., 1988. Anorthosites: classification, mythology, trivia and a simple unified theory. J. Geol. Soc. Ind., 31(1):6-7.

Baishya, N.C., Srivastava, S.K. and Singh, S.N., 1986. Indentification of lower Cretaceous sediment below thick volcanics sequence in Mahanadi Offshore Basin from Vertical Seismic Profiling: A case history. J. Assoc. Expl. Geophs., 7(4): 195-203.

Banerji, P.K., 1972. Geology and Geochemistry of the Sukinda ultramafic field, Cuttack Dt, Orissa. Mem. Geol. Surv. Ind., 103: 1-171.

Banerji, P.K., 1982a. A morphotectonic classification of laterite and ironstone covered basements in Gondwanaland, a case study from Orissa, India. Proc. 2nd Int. Sem. IGCP 129 (Lateritisation Processes), Sao Paolo, Brazil, pp.360-371.

Banerji, P.K., 1982b. The Khondalites of Orissa, India - a case history of confusing terminology. J. Geol. Soc. Ind., 23: 15-159.

Banerji, P.K., In press: On some traits of the chromite occurrences at Kondapalli and Lingampeta (A.P) and Sittampundi, Tamil Nadu. Ind. Minerals.

Banerji, P.K. and Chatterjee, Saswati, 1988. Tectonic models for Proterozoic metallogeny in parts of folded and metamorphosed rock assemblages of East and South India. Proc. International Conference of IGCP Project 247 (abst.), Jadavpur, India.

Banerji, P.K. Mahakud, S.P., Bhattacharya, A.K. Mohanty, A.K., 1987. On the northern margin of the Eastern Ghats in Orissa. Rec. Geol. Surv. Ind., 118(2): 1-8.

Banerji, P.K., Mohanty, A.K. and Mahakud, S.P., 1988. Secondary geochemical dispersion in the lateritic tracts over two copper sulphide deposits in Orissa, India. J. Geol. Soc. Ind., 31: 404-416.

Bose, S.K. and Sanyal, T., 1987. Migmatites from Kondapalli Hills, Krishna district, Andhra Pradesh. Ind., J. Geol., 59(4): 253-264.

Crawford, A.R., 1969. Reconnaissance Rb-Sr dating of the Precambrian rocks of Southern Peninsular India. J. Geol. Soc. Ind., 10: 117-166.

Crookshank, H., 1938. The western margin of the Eastern Ghats in Southern Jeypore. Rec. Geol. Surv. Ind., 73(3): 398-434.

Dash, B., 1982. Textural and chemical features of sillimanite in Khondalite. Proc. Workshop on Eastern Ghats, Waltair. (Unpublished).

Dhanaraju, R., 1977. P-T conditions of granulite-upper amphibolite facies metamorphism in the Precambrian granitic rocks of Chipurupalle - Razam area of the Eastern Ghats. J. Geol. Soc. Ind., 18: 281-287.

Halden, N.H., Bowes, D.R. and Dash, B., 1982. Structural evolution of migmatites in granulite facies terrain: Precambrian Crystalline Complex of Angul, Orissa, India. Trans Roy. Soc. Edin., Earth Sci., 73: 109-118.

Janardhan, A.S., Newton, R.C., and Hansen, E.C., 1982. The transformation of amphibolite facies gneiss to Charnockite in southern Karnataka and northern Tamil Nadu, India. Contr. Min. Pet. 79: 130-149.

Kamenev, E.N., 1982. Antartica's oldest metamorphic rocks in the Fyfe Hills, Enderby Land In: C.Craddock (Editor), Antarctic Geoscience. Univ. of Wisconsin, IUGS Ser B(4): 505-510.

Krishna Rao, S.V.G., Sarma, K.S. and Bhattacharya, S., 1982. Manganese ore deposits in parts of Eastern Ghats of Andhra Pradesh. Proc. Workshop on Eastern Ghats, Waltair (Unpublished).

Leelandandam, C., Ratnakar, J. and Narasimha Reddy, M., 1988. Anorthosites and alkaline rocks from the deep crust of Peninsular India. J. Geol. Soc. Ind., 31: 66-68.

Murthy, D.S.N. and Nirmal Charan, S., 1988. Metamorphism of cordierite gneiss from Eastern Ghat granulite terrain, Andhra Pradesh, S. India. J. Geol. Soc. Ind., 31(1): 97-98.

Pascoe, E.H., 1950. A manual of the geology of India and Burma. 1: 485pp.

Perraju, P., Kovach, A and Svingor, E., 1979. Rubidium strontium ages of some rocks from parts of the Eastern Ghats in Orissa and Andra Pradesh, India. J. Geol. Soc. Ind., 20: 290-296.

Pichamuthu, C.S., 1961. Transformation of Peninsular gneiss into charnockite in Mysore State, India. J. Geol. Soc. Ind., 2: 46-49.

Prudhvi Raju, K.N. and Vaidyanadhan, R., 1981. Fracture pattern study from Landsat imagery and aerial photos of a part of the Eastern Ghats in Indian Peninsula. J. Geol. Soc. Ind., 22: 17-21.

Raith, M., Stahle, and Hoernes, S., 1988. Kabbaldurga-type charnockitisation: A local phenomenon in the granulite to amphibolite grade transition zone. J. Geol. Soc. Ind., 31(1): 116-117.

Ramakrishnan, M., Viswanatha, M.N., Chayapathi, N. and Narayanan Kutty, T.R., 1978. Geology and geochemistry of anorthosites of Karnataka craton and their tectonic significance. J. Geol. Soc. Ind., 19: 115-134.

Ramam, P.K. and Viswanthan, T.V., 1977. Carbonatite Complex near Borra, Visakhapatnam district, Andhra Pradesh. J. Geol. Soc. Ind., 18: 605-610.

Ramienger, A.S., Ramakrishnan, M. and Viswanatha, M.N., 1978. Charnockite - gneiss complex relationship in Southern Karnataka. J. Geol. Soc. Ind., 19: 411-419.

Rao, A.T. and Narendra, K., 1986. Granite tectonics and apatite - phlogopite mineralisation around Borra in the Eastern Ghats mobile belt. Proc. Sem. Crustal Dynamics, Ind. Geophysical Union, Hyderabad.

Rao, M.G., and Ramam, P.K., 1979. The East Coast Bauxite deposit of India. Bull. Geol. Surv. Ind., Ser A, 46: 24.

Sarkar, A., Bhanumathi, L. and Balasubrahmanyan, M.N., 1984. Petrology, geochemistry and geochronology of the Chilka Lake igneous complex, Orissa State, India. Lithos., 14: 93-111.

Sastri, V.V., 1980. Stratigraphy and sediments of some coastal basins of India - An overview. Bull. ONGC 17(1): 269-276.

Sreenivasa Rao, T., 1987. The Pakhal Basin - A perspective Mem. Geol. Soc. Ind., 6, 161-187.

Vinogradov, A., Tugarinov, A., Zhykov, C., Stapnikova, N., Bibikova, E. and Khorre, K., 1964. Geochronlogy of the Indian Precambrian. Report 22nd Int. Geol. Cong., Pt. 10, pp.553-567.

Walker, T.L., 1902. Geology of Kalahandi State, Central Provinces. Mem. Geol. Surv. Ind., 33(3).

Weaver, B.L., Tarney, J., Windley, B.I., Sugavanam, B.P. and Venkata Rao, V., 1978. Madras granulites: geochemistry and P-T conditions of crystallisation. In: B.F. Windley and S.M. Naqvi (Editors), Archaean Geochemistry. Elsevier, Amsterdam, pp.177-204.

Wellman, P. and Tingey, R.J., 1977. A gravity survey of Enderby and Kemp Lands. 3rd symposium on Antartic Geology and Geophysics, Madison, USA.

Wiebe, R.A. and Janardhan, A.S., 1988. Metamorphism of the Oddanchatram anorthosite, Tamil Nadu, South India. J. Geol. Soc. Ind., 31(1): 163-165.

This Page Intentionally Left Blank

THE ANORTHOSITE COMPLEXES AND PROTEROZOIC MOBILE BELT OF PENINSULAR INDIA: A REVIEW

C.LEELANANDAM

ABSTRACT

The Precambrian anorthosite bodies of eastern and southern Peninsular India can be grouped into seven types: (1) metamorphosed layered complexes (MLC); (2) igneous layered complexes (ILC); (3) metamorphosed massif labradorite type (MML); (4) metamorphosed massif andesine type (MMA); (5) gabbro-anorthosite basic plutons (GAP); (6) anatectic type (ATT); and (7) mixed type. The type and areal extent of all the known occurrences, numbering more than fifty, are depicted on the maps showing various tectonic elements, and certain aspects of the most abundant massif-type anorthosites of Proterozoic age are discussed. The anorthosite massifs occur in the Eastern Ghat granulite (mobile) belt, and some of them yield final equilibration temperatures of 600-750°C and pressures of 5-7 kbar. The granulite facies terrain of south India represents the mid- to lower-levels of greatly thickened crust, and the regional variation in P(6.5-9.5 kbar) is attributed to the differntial uplift of smaller blocks. Problems pertaining to the over-all development of the Proterozoic mobile belts are evaluated with particular emphasis on the collision tectonics and granulite (including carbonic) metamorphism.

INTRODUCTION

The anorthosites are cumulates of plagioclase feldspar from mantle-derived basaltic magmas (Ashwal, 1988). The anorthosite occurrences of eastern and southern Peninsular India are classified into seven groups: (1) metamorphosed layered complexes (MLC); (2) igneous layered complexes (ILC); (3) metamorphosed massif labradorite type (MML); (4) metamorphosed massif andesine type (MMA); (5) gabbro-anorthosite basic plutons (GAP); (6) anatectic type (ATT); and (7) mixed type (MT). They are shown on various tectonic maps (Figs. 1-6); the affirmed or inferred 'type' of each occurrence and its areal extent (Fig.7) are depicted in Figs. 2-6; the occurrences are numbered and keyed in Table 1.

The Archaean high-calcic anorthosites (Leelanandam, 1987a) are prominently represented by the well-known Sittampundi complex (~60 km^2) in Tamil Nadu (Fig.3) and the recently described Chimalpahad complex (200 km^2), in Andhra Pradesh (Fig. 5) (Leelanandam and Narsimha Reddy, 1983, 1985). The initial megacrystic textures, characteristic of the Archaean type, are not exhibited by these two complexes (see Phinney et al., 1988). The Chimalpahad complex exhibits spectacular layering and the primary Chimalpahad magma approximates the composition of a moderately aluminous tholeiitic basalt. The general consensus among petrologists is that the early Archaean anorthositic complexes exhibit typical calc-alkaline trends (with no iron enrichment at all); however, this is open to debate (see Leelanandam and Narsimha Reddy, 1985). The differentiation trends are not always strictly calc-alkaline and a rather broad zone of compositions (probably due to cumulates with various proportions of phases)crosses from the field of calc-alkaline rocks into the field of tholeiitic rocks, and there is some enrichment of iron (small and variable) in the different trends. In the southern part of the western Dharwar craton (WDC in Fig. 1), some high-calcic metamorphosed (layered or cumulus or volcanic flows of) anorthosites occur as components in the ultramafic units of the schist belts and also in the high-grade rocks of the transition zone from amphibolite to granulite facies; these are to be distinguished separately from the major Archaean anorthosite complexes such as Sittampundi and Chimalpahad. As this paper is essentially aimed at a review of the Proterozoic anorthosite massifs and the Proterozoic mobile belt, the Archaean anorthosites are not further referred to.

Theories on the origin of Proterozoic anorthosites are generally clouded due to the unfounded notion that there is some genetic relationship among the composition of the constituent plagioclase, layered structures and metamorphic textural features. The fact that the metamorphosed massif anorthosites display layered structures, have high An values for the plagioclase, and exhibit primary igneous characteristics (mineralogical and textural), even after they were metamorphosed under granulite facies conditions, leads us to re-examine the existing views. Furthermore, the realisation that metamorphism is not the causative factor for the anorthosite genesis, that the late residual liquids may be mafic rather than acidic, and that the

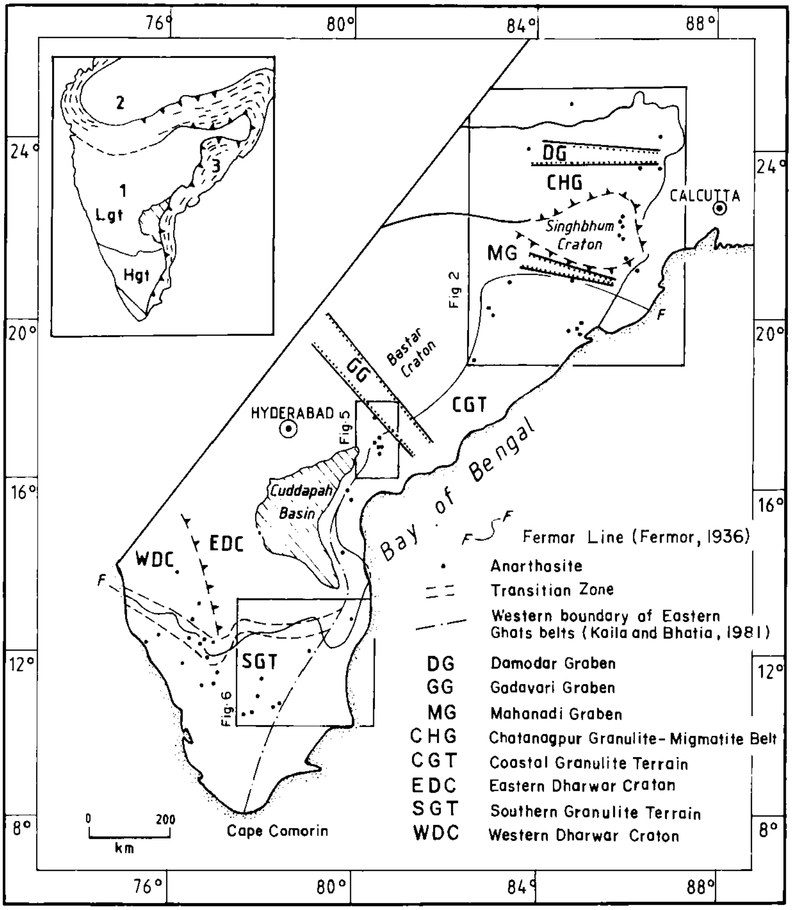

Figure 1. Map showing the Precambrian anorthosite occurrences in a part of Peninsular India. The inset map (after Radhakrishna and Naqvi, 1986) shows (1) Dharwar-Singhbhum Protocontinent with low grade terrain (Lgt) separated from high grade terrain (Hgt) with a transition zone; (2) Bundelkhand Protocontinent; and, (3) Middle Proterozoic Mobile belts. See also Figs.2-6.

associated acidic rocks of the anorthosites are at the most coeval (but not comagmatic and not cogenetic) compels us to view the massifs in an altogether different perspective (Leelanandam, 1987b; Leelanandam and Narsimha Reddy, 1988).

The relations between the emplacement of anorthosites, Proterozoic tectonics and granulite facies metamorphism are, in a way, interwoven and an understanding of these relations is essential to an understanding of the evolutionary history of the Proterozoic

TABLE 1

Anorthosite occurrences (plotted in Figs. 1-6). The numbers correspond to those (Fig.7) marked on Figs.2-6. For brief descriptions of the anorthosite occurrences, see Leelandandam and Narsimha Reddy (1988). For an alphabetical list of anorthosite occurrences, see Table 2.

1. Bela
2. Dumka
3. Biwabathan
4. Bankura
5. North Manbhum
6. Dublabera
7. Sundhal
8. Hatichhar
9. Bhelupani
10.Khejuri
11.Nausahi
12.Bhadrak
13.Angul
14.Banpur-Balugaon
15.Kallikota
16.Rambha
17.Kodala
18.Bolangir
19.Turkel
20.Bhawanipatna
21.Koraput
22.Chimalpahad
23.Erukopadu (Tiruvur)
24.Dendukur
25.Pangidi Chervu
26.Gangineni
27.Kondapalli
28. Pasupugallu
29. Chimakurti
30. Nadimidoddi
31. Inukurti (Nellore)
32. Chinglepet
33. Mamandur
34. Sittampundi
35. Chinnadharapuram
36. Manappparai
37. Kadavur
38. Oddanchatram
39. Palni
40. Attapadi
41. Togamalai
42. Kotagiri
43. Kabbani
44. Gundlupet
45. Konkanahundi
46. Hullahalli
47. Sinduvalli
48. Hunsur
49. Perinthatta
50. Kottanjariparambu
51. Holanarasipur
52. Nuggihalli
53. Masanikere

TABLE 2

Anorthosite occurrences (plotted in Figs. 2-6) arranged in alphabetical order.

The numbers correspond to those marked on Figs.2-6; see also Fig.7.

Angul (13)
Attapadi (40)
Bankura (4)
Banpur-Balugaon (14)
Bela (1)
Bhadrak (12)
Bhawanipatna (20)
Bhelupani (9)
Biwabathan (3)
Bolangir (18)
Chimakurti (29)
Chimalpahad (22)
Chinglepet (32)
Chinnadharapuram (35)
Dublabera (6)
Dumka (2)
Dendukur (24)
Erukopadu (Tiruvur) (23)
Gangineni (26)
Gundlupet (44)
Hatichhar (8)
Holenarasipur (51)
Hullahalli (46)
Hunsur (48)
Inukurti (Nellore) (31)
Kabbani (43)
Kadavur (37)
Kallikota (15)
Khejuri (10)
Kodala (17)
Kondapalli (27)
Konkanahundi (45)
Koraput (21)
Kotagiri (42)
Kottanjariparambu (50)
Mamandur (33)
Manapparai (36)
North Manbhum (5)
Masanikere (53)
Nadimidoddi (30)
Nausahi (11)
Nuggihalli (52)
Oddanchatram (38)
Palni (39)
Pangidi Chervu (25)
Pasupugallu (28)
Perinthatta (49)
Rambha (16)
Sinduvalli (47)
Sittampundi (34)
Sundhal (7)
Togamalai (41)
Turkel (19)

mobile belt of Peninsular India. The earlier overviews on the Archaean and Proterozoic anorthosite complexes by Leelanandam (1987a, 1987b) and by Leelanandam and Narsimha Reddy (1988) form the backdrop for the present contribution, in which the emphasis on the descriptions of the massifs is mineralogical and of the mobile belt petrological. For a comprehensive list of references on the Indian occurrences, see Leelanandam and Narsimha Reddy (1988).

PROTEROZOIC ANORTHOSITE MASSIFS

A general survey

There are about fifty individual Proterozoic anorthosite occurrences of various dimensions in Peninsular India, and they occur largely within the Proterozoic mobile belts in southern and eastern India (Fig. 1). The state of Orissa hosts many major and minor anorthosite bodies: Bolangir (~450 km^2); Banpur-Balugaon (250 km^2), Rambha (12 km^2) and Kallikota (7 km^2) of the Chilka Lake igneous complex; Turkel (7 km^2); Angul; Nausahi; Bhadrak; Koraput and Bhawanipatna (Fig. 2). Bankura (~250 km^2) in Bengal, Perinthatta (65 km^2) in Kerala, and Oddanchatram (~35 km^2) and Kadavur (35 km^2) in Tamil Nadu are some of the other major massifs which, together with those in Orissa, have been well described.The metamorphosed anorthosite massifs should be clearly distinguished from the unmetamorphosed gabbro (-anorthosite) plutons (6-10 in Fig.2 and 28 and 29 in Fig.3). Some of the massifs which are geographically close display disparate mafic mineralogies and textures, while others which are spatially far separated exhibit remarkable similarities.

The massifs, within themselves, do not exhibit uniform metamorphic effects. In general, the central parts of the massifs are massive, coarse-grained and anorthositic with practically no effects of recrystallization and mineralogical reconstitution, while the marginal parts are foliated, medium-grained and gabbroic with effects of metamorphism, metasomatism and tectonism. Many massifs which are construed as exhibiting primary mineralogies and structural patterns are not totally devoid of the presence of metamorphic (and also metasomatic) minerals, and are not completely free from tectonic effects; effects of late potash enrichment, migmatizastion and hybridization, though in general on

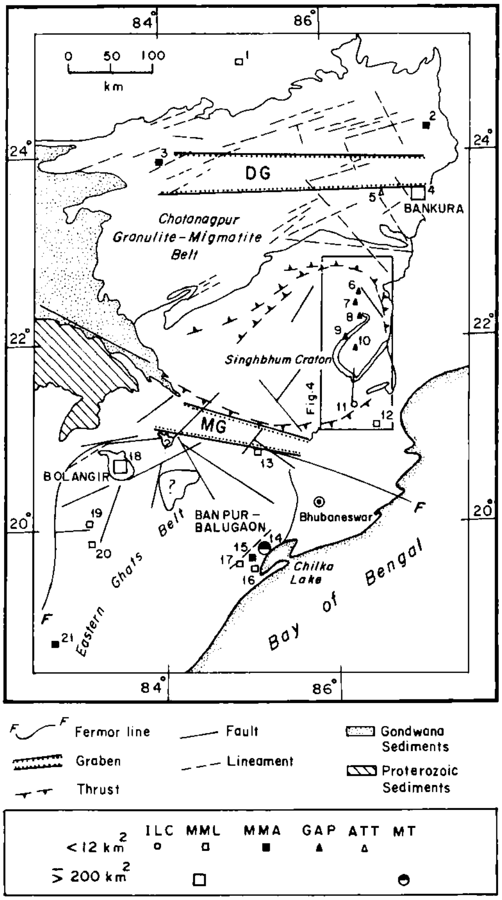

Figure 2. Generalised tectonic map of a part of eastern India (after Banerji, 1975; Sarkar, 1982; Bhan and Hegde, 1985) showing the anorthosite occurrences (nos.1-21). The type and areal extent of individual anorthosite occurrences are indicated and the numbers are keyed in Table 1. The shape of the largest anorthosite body at Bolangir is shown. Other enclosed areas (with question marks) are "suspected" gabbro-anorthosite intrusives (after Bhan and Hedge, 1985). (See also Figs. 1,4 and 7).

a minor scale, seem to be a rule rather than exception, especially in the marginal zones of the massifs.

Efforts to make gross general characterizations of massifs in different tectonic provinces or in different parts of the same province have not met with success. Similarly, attempts to unravel relationships (if any) between the deformational and mineralogical characters of the individual massifs and their specific tectonic

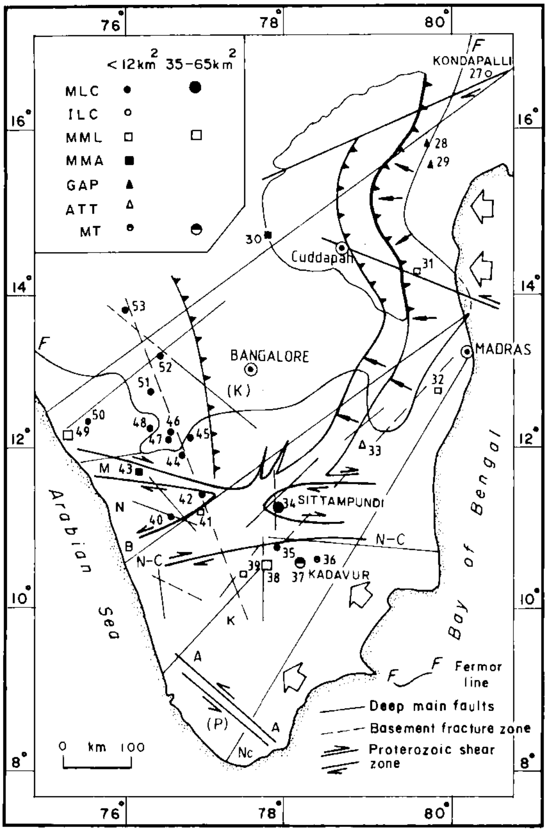

Figure 3. Generalised tectonic map of south India (after Harris et al., 1982; Drury et al., 1984; Venkatakrishnan and Dotiwalla, 1987 showing the anorthosite occurrences (nos.27-53). The type and areal extent of individual anorthosite occurrences are indicated and the numbers are keyed in Table 1. See also Figs. 1,6 and 7. (K) = Kabbal; (P) = Ponmudi; Shear zones: A-Achankovil; B-Bhavani; M-Moyar; N-C-Noyil-Cauvery; Massifs: K-Kodaikanal; N-Nilgiri; Nc-Nagercoil.

environments (see Figs. 2-6) are not particularly encouraging. Whether the massifs are pre-, syn-, or post-orogenic is difficult to decide in a majority of cases from the available literature (Leelanandam and Narsimha Reddy, 1988). Many complexes show features intermediate between metamorphosed anorthosite massifs and unmetamorphosed mafic (layered) intrusions, and it is not easy to classify them with certainty; the Banpur-Balugaon,

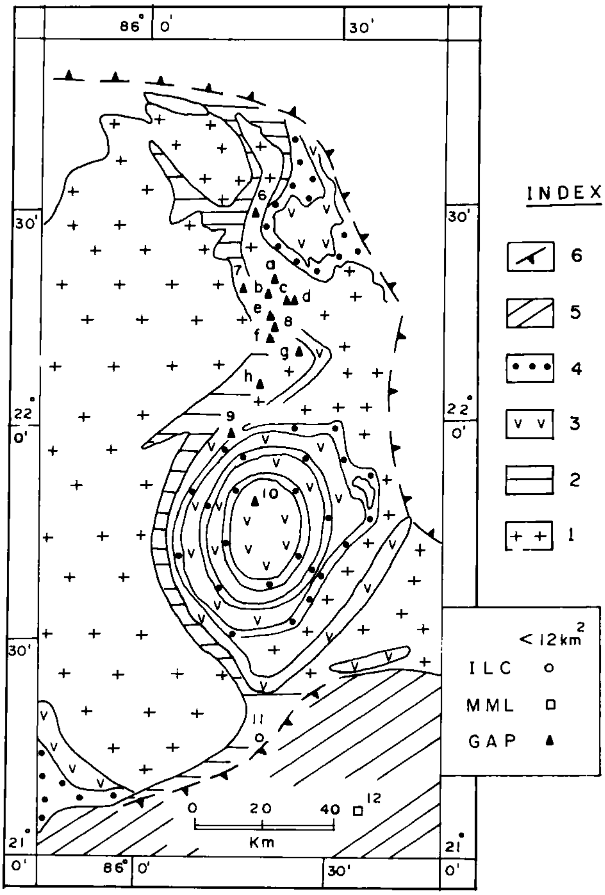

Figure 4. Geological map of a part of the Singhbhum craton, eastern India (after Banerji, 1975; Saha et al., 1977) showing anorthosite occurrences (nos 6-12; a-h). The numbers (6-12) are keyed in Table 1 and also shown in Figs. 1,2 and 7. The additional occurrences of anorthosites. a-Chattrmandal; b-Kumhardubi; c-Bara Bantha; d-Betjharan; e-Luhasila; f-Amdabera; g-Bisoi; and h-Asana are not shown in Figs. 1,2and 7 and are not keyed in Table 1. 1. Granitic rocks; 2. Iron ore series; 3. Basic volcanics; 4. Quartzites; 5. Cenozoic cover, and 6. Thrust.

Kadavur and Manapparai occurrences are classified as mixed type. The well known unmetamorphosed gabbro (-anorthosite) plutons of Mayurbhanj district (Orissa) (Fig.4) and the recently reported Chimakurti and Pesupugallu plutons (Prasad Rao et al., 1988) of Prakasam district (Andhra Pradesh) are a class by themselves and they should not be grouped with the metamorphosed anorthosite massifs.

For those anorthosite massifs (especially the central parts) that are inferred to be unmetamorphosed and also contain xenoliths of granulite one is led to infer (rather erroneously ?) that anorthosite emplacement apparently took place subsequent to a granulite metamorphism. The general consensus is that anorthosite emplacement can occur at any depth in the crust, and that the association of anorthosites and granulite metamorphic conditions is *purely* fortuitous. Valley (1985) shows that only the emplacement of the Adirondack Marcy massif was *prior* to granulite facies metamorphism. His results do not indicate that anorthosite emplacement *in general* is prior to metamorphism.

The early crystallization of plagioclase, relative to ferromagnesian minerals, is a common feature in the anorthosite massifs. Accordingly, plagioclase is more calcic in anorthosites than in the associated gabbros. Hence mafic rocks (with less calcic plagioclase) form members late in the fractionation sequence and they contain autolithic inclusions of early formed anorthosite. Though the An contents of the plagioclase are in conformity with the magnesian contents of the coexisting ferromagnesian mineral (Chilka Lake), exceptions are not unknown (Bolangir). The plagioclase in anorthosites of the Bolangir and Oddanchatram massifs is, contrary to the general expectations, less calcic than that in the gabbros (norites). There is no discernible variation in the plagioclase compositions in different units of major gabbro plutons (associated with minor anorthosites) of Mayurbhanj (Orissa) and Prakasam (Andhra Pradesh) districts. Primary plagioclase in many massifs is more calcic than the secondary (metamorphic) plagioclase, though in the Oddanchatram massif the secondary plagioclase is extraordinarily calcic.

The major mafic mineralogy is essentially the same (Hb>>Cpx>Opx) in the Bankura and Oddanchatram massifs; it is different (Opx>>Cpx) in the Banpur-Balugaon, Bolangir, Turkel and Kadavur (Unit II) massifs. While the hornblende at Oddanchatram (Fig.6) is recognised as primary (? obtained from feldspathic parental magma with higher f(H_2O)), that at Kadavur (Units I and III) is identified as secondary derived from primary pyroxenes.

The occurrence of olivine in gabbros associated with the massif anorthosites (as at Bankura and Turkel) suggests lower pressures (shallower/higher levels) for their emplacement. Similarly, the occurrence of olivine in gabbro plutons of Mayurbhanj (Orissa) and Prakasam (Andhra Pradesh) districts suggests shallower levels of emplacement. The occurrence of wollastonite in the calc-silicate band metamorphosed by the anorthosite in pyroxene-hornfels facies at Rambha points to the high temperature (low pressure and shallow level) of emplacement.

The formation of garnet coronas is consistent with polymetamorphism, the prograde garnet growth being due to increasing P and T of granulite metamorphism. However, some workers have attributed coronas to isobaric cooling with retrograde garnet growth due to decreasing T at constant P after igneous intrusion.

In the study of individual anorthosite massifs (see next section), a clear distinction has to be made between the magmatic, metamorphic and alteration products.

SELECTED EXAMPLES

The Chilka Lake igneous complex (Nos. 14,15 and 16 in Fig.2).

This is a "syntectonic composite complex", emplaced 1400 Ma ago, and cut by a suite of "atectonic" noritic dykes ~850 Ma ago. It exhibits primary compositional layering and is characterized by the adcumulus growth of plagioclase, total absence of hornblende and presence of orthopyroxene (some with (100) lamellae of clinopyroxene). Garnet (as a metamorphic reaction product between plagioclase and orthopyroxene), together with quartz and K-feldspar, occurs along marginal zones. Large xenoliths of pyroxene granulite and gneisses occur in the Balugaon dome (Sarkar et al., 1981). Perraju (1973) earlier reported that the Banpur-Balugaon anorthosites are absolutely free from deformational effects, and are either late-tectonic or post-tectonic; he, however, also noted the protoclastic granulation in these rocks. Sarkar et al. (1981) suggest that the massif exhibits gradation from "orogenic-plutonic" type to "gravity-stratified" class, with significant metasomatic exchange between the anorthositic rocks and the host rocks. The massif is associated, like the Unit II of Kadavur, with rapakivi granites. The occurrence of wollastonite-bearing calc-silicate skarn rock as a xenolith in the Rambha unit of the complex bears testimony to the contact metamorphism by the emplacement of anorthosite at high temperature.

Bankura (No. 4 in Fig. 2)

The absence of chilled margins and of contact aureoles in the enveloping and enclosed granulites of the Bankura massif suggests that the anorthosite emplacement took place in a hot environment prior to cooling (Bhattacharyya and Mukherjee, 1987); simultaneous deformation of both the intrusive and country rocks as a part of the intrusive event suggests that the massif is syntectonic. During the subsolidus equilibration under granulite facies conditions, it interacted with a granitic fluid probably derived from the partial melting of granites or their precursors (Sen and Bhattacharya, 1986). Though Manna and Sen (1974) argue that garnet appeared during subsolidus cooling of the Bankura complex, Bhattacharyya and Mukherjee (1987) demonstrated that it is a late prograde metamorphic overprint. In recent years, many investigators elsewhere have established that the coronal garnet is a prograde metamorphic product rather than due to an isobaric retrogression. What is more important is that the final equilibration conditions are supposed to be similar for both anorthositic and different granulitic assemblages of Bankura.

Bolangir (No. 18 in Fig. 2)

The Bolangir anorthosite massif, the largest in India, was forcibly intruded into the granulitic cover and contains inclusions of garnet-pyroxene-granulites (Tak et al., 1966) and is devoid of penetrative post-intrusion tectonic overprint. The un common Bolangir fractionation trend from anorthositic norite to noritic anorthosite to anorthosite, though supplemented by the median plagioclase compositions of An_{75}, An_{70} and An_{52} respectively, is not substantiated by the compositional trend of orthopyroxenes. Curiously, orthopyroxene is more magnesian (plagioclase is less calcic) in anorthosites than in anorthositic norites (Mukherjee et al., 1986). Wollastonite is not reported in the calc granulites bordering the Bolangir body (Mukherjee et al., 1986), though its occurrence is known in the calc-silicate rocks from the Bolangir-Patna district (Tak, 1973).

In order to explain the present anorthosite and granulite mineralogies of Bolangir, Mukherjee et al., (1986) prefer "a single episode of prolonged and very slow cooling and annealing" of the pluton after its intrusion, rather than the "over-print of a post-intrusion high grade metamorphism". They assume that the

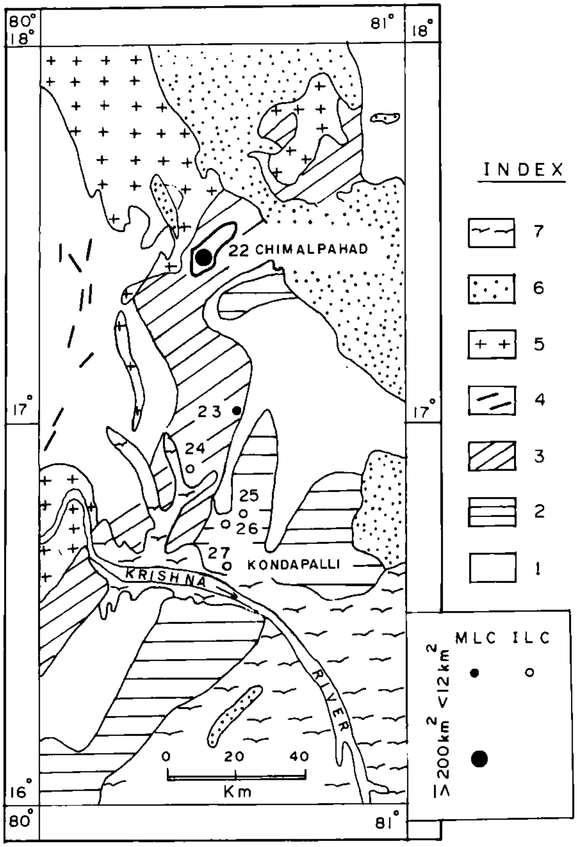

Figure 5. A part of geological map of Andhra Pradesh showing the anorthosite occurrences (nos. 22-27). The shape of Chimalpahad anorthosite complex (22) is given. The type and areal extent of individual anorthosite occurrences are indicated, and the numbers are keyed in Table 1 and are also shown in Figs. 1 and 7. 1. Unclassified crystalline rock; 2. Charnockite-Khondalite; 3. Schist belt; 4. Basic intrusive; 5. Proterozoic; 6. Gondwana and 7. Alluvium.

Proterozoic crust (>15-25 km) at around 1300 Ma was not substantially thicker than the present average continental crust and indeed might have been considerably thinner.

Oddanchatram (No. 39 in Figs. 3 and 6)

The dome-shaped unmetamorphosed labradorite-type pluton characteristiccally contains central coarse-grained anorthosite facies and marginal fine-grained gabbroic facies; it is only the border

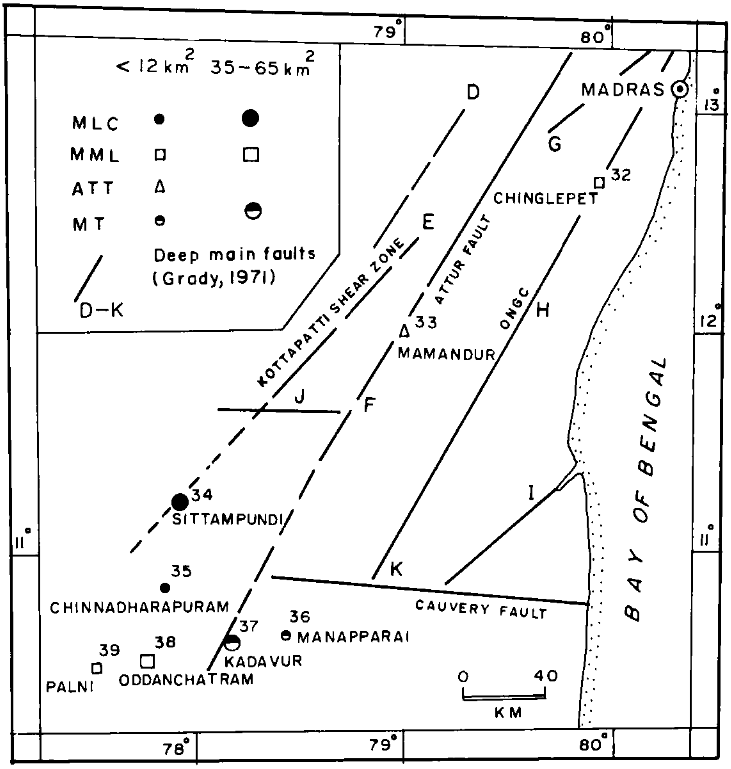

Figure 6. Map of a part of Tamil Nadu showing the anorthosite occurrences (nos32-39) and deep main faults D-K (after Grady, 1971). The type and areal extent of individual anorthosite occurrences are indicated and the numbers are keyed in Table 1 and are also shown in Figs. 1, 3 and 7.

zones of the massif that bear an overprint of metamorphism; the pluton exhibits protoclastic granulation and flow differentiation (Narasimha Rao, 1977). The occurrence of cordierite-bearing metasediments as enclosing rocks to the pluton and of skarn xenoliths (of pyroxene-hornfels facies) within the pluton is noteworthy. The presence of discrete euhedral crystals of primary hornblende in the anorthosites is suggestive of (but not necessarily) the initial high water pressure in the magma during the early stages of crystallizatin (Narsimha Rao, 1977); the Cl content of hornblende is not known.

Though the Oddanchatram massif was considered as unmetamorphosed, retaining its primary igneous texture, primary orthopyroxene and primary hornblende (Janardhan and Wiebe., 1985), the presence of garnet, biotite, quartz, K-feldspar and secondary high-calcic plagioclase (An_{94}) makes this conclusion tenuous. Symplectites of orthopyroxene and plagioclase (An_{94}) were derived as the break-down products of garnet at pressures <5 kbar. The problems inherent in identifying the primary hornblende from secondary hornblende in metamorphic rocks are only too well known. In fact, Wiebe and Janardhan (1988) subsequently realised that the massif has been affected by later metamorphism and deformation. Metamorphic equilibration temperatures (920^{o}-700^{o}C) and pressures (11.3 kbar at 920^{o}C and 7.3-5.6 kbar at 775^{o}C) in the anorthositic rocks are variable, the lower values corresponding to the formation of symplectites.

Krishna and Khammam districts (Andhra Pradesh) (Nos.22-27 in Fig.5)

The Kondapalli complex is tentatively classified as the Bushveld type (with apparent magmatic textures; cf. Leelanandam, 1967, 1972), and the chromite-bearing ultramafics (some containing a highly calcic plagioclase, An $_{>99.5}$) constitute a part of the complex, having no genetic relationship with the enclosing granulites (charnockites). The Gangineni and Pangudi occurrences (Nanda and Natarajan, 1980) are similar to that of Kondapalli, and all of them show spectacular layered characters. The Dendukur occurrence, though similar to Kondapalli, is situated in the schistose country rock (like the metamorphosed Chimalpahad complex which contains both chromite-bearing and magnetite-bearing units). The Erukapodu (Tiruvur) occurrence with the magnetite-bearing unit, though small, is similar to the huge Chimalpahad complex.

The Erukapodu and Dendukur occurrences (Nos. 23 and 24 in Fig. 5) are reported here for the first time.

Inukurti (Nellore) (No. 31 in Fig. 3)

The nearly circular, plug-shaped Inukurti (Nellore) anorthosite body (~2 km^2), though extremely small, is an epitome of the Adirondack variety, and yet it is unique in the sense that it occurs in a typical schist belt (known as the Nellore Mica-Pegmatite Belt) which lies in the "non-charnockitic region" (Fermor, 1936) of the Eastern Ghats Belt (see Figs. 1 and 3). The increase in the mafic mineral content and decrease in grain size from the central anorthosite (An_{50-60}) to peripheral anorthositic gabbro (with less calcic plagioclase ?) is attributed to flow

Area / Type		$< 12\ \mathrm{km}^2$	$35-65\ \mathrm{km}^2$	$\geqslant 200\ \mathrm{km}^2$
MLC	Metamorphosed layered complex	● 23, 35, 40, 42, 44, 45, 46 47, 48, 50, 51, 52, 53	● 34	● 22
ILC	Igneous layered complex	○ 11, 24, 25, 26, 27		
MML	Metamorphosed massif labradorite type	□ 1, 12, 13, 16, 17, 19, 20, 31, 32, 39, 41	□ 38, 49	□ 4, 18
MMA	Metamorphosed massif andesine type	■ 2, 3, 15, 21, 30, 43		
GAP	Gabbro - anorthosite basic pluton	▲ 6, 7, 8, 9, 10, 28, 29		
ATT	Anatectic type	△ 5, 33		
MT	Mixed type	◓ 36	◓ 37	◓ 14

Figure 7. The type and areal extent of individual anorthosite occurrences are shown in a tabular form. The numbers correspond to those plotted in Figs. 2-6. See also Table 1.

differentiation (Kanungo et al., 1986). Foliation in the anorthosites (defined by the parallel arrangement of the major mafic minerals hornblende and garnet) is well developed at the contacts with host rocks and gradually becomes less distinct away from the contacts, and finally disappears towards the central portion of the body; some marginal portions even exhibit shearing. The body contains the intensely folded xenoliths of some of the host rocks (amphibolite, hornblende schist, quartzite, quartz-mica schist, and staurolite-kyanite schist). The accessory minerals in the rocks are epidote, zoisite, clinozoisite, chlorite, quartz, biotite, apatite and sphene. It is inferred that the body was subjected to almandine - amphibolite facies metamorphism, subsequent to its emplacement. The work of Bhushan et al. (1988) suggests that the Inukurti anorthositic rocks (An_{40-50}) are essentially cumulates and were formed at about 625°C and >5 kbar, the mafic and ultramafic xenoliths (or? late intrusives) contain a sodic plagioclase (An_{26-35}), and the marginal meta-diorite (An_{35-40}) may be parental (and the adjoining amphibolites are chemically unrelated) to the anorthositic rocks.

Chimakurti - Pasupugallu (Nos. 29 and 28 in Fig. 3)

The anorthosites (with olivine, clinopyroxene and orthopyroxene) of the oval-shaped concentrically zoned Chimakurti pluton occur as arcuate bodies (An_{55-70}) in between the central coarse-grained (olivine-) clinopyroxenite unit (An_{50}) and the broad outer zone of gabbro-norite (± olivine) unit (An_{70}) which is slightly deformed at the peripheral portions (An_{58-45}). While the (late ?) ultrabasic dykes of dunite, wehrlite and pyroxenite are restricted to the central unit, (late ?) basic dykes of gabbronorite and dolerite occur in the remaining portions of the pluton (Prasad Rao et al., 1988). In the nearby Pasupugallu pluton, anorthosites (An_{64}) and leuco-gabbros (An_{60-66}) occur as minor patches in gabbros (An_{56-60}); ultramafic unit (An_{40}) is scarce and a hornblende-bearing anorthosite dyke (An_{56}) is present (unpublished work of C.Leelanandam and Y.Jyothender Reddy). Lack of data on the composition of the constituent minerals in various rock units prevents us from establishing the differentiation sequence for the plutons. The plutons exhibit cumulus (and layered ?) characters and are totally devoid of metamorphic effects. While the Chimakurti pluton is associated with ferrosyenite as the late differentiate, the Pasupugallu pluton is cut by nepheline syenite (and dolerite) dykes. Both the plutons are associated with (and probably intrusive into) cordierite-bearing gneisses.

Perinthatta (No.49 in Fig.3) (and other plutons of Kerala)

The syntectonic non-migmatized zoned Perinthatta pluton, the largest anorthosite massif in South India, contains anorthosite, gabbroic anorthosite and gabbro in that order from the central to peripheral portions, and the plagioclase shows intense effects of shearing (Vidyadharan et al., 1977). The gabbros of Ezhimala are associated with (rapakivi) granite and granophyre. These and other gabbro (-anorthosite) bodies -- Kadannapalli, Karauq, Kartikulam, Adakkathodu and Vatekolli situated along the Bavali lineament in Kerala (Nair and Vidyadharan, 1982) -- are in general non-layered, highly deformed and metamorphosed with destruction of primary igneous structures. Effects of retrogressive metamorphism, migmatisation and metasomatism are recorded, with the presence of minerals such as sericite, zeolite, amphibole, biotite, chlorite, garnet, quartz, K-feldspar perthite, myrmekite, epidote and calcite. Though the Perinthatta massif was metamorphosed isochemically under granulite-facies conditions, the primary igneous features are retained (Raghavan Nambiar et al., 1982); however, Ravindra Kumar and Chacko (1986) maintain that the primary igneous structures are absent.

Mayurbhanj district (Orissa) (Nos.6-10 and a-h in Fig.4)

More than a dozen minor anorthosite occurrences are associated with the gabbroic bodies of the Mayurbhanj district of Orissa. These are situated in the typical cratonic setting and are absolutely free from tectonic and metamorphic effects. Though the gabbros (± olivine/quartz) are well studied, very little is known about the anorthosites: they are locally associated with pyroxene granite, riebeckite granite and granophyre; they contain the following secondary minerals: K-feldspar, quartz, biotite, chlorite, actinolite, hornblende, epidote, sphene, micropegmatite, myrmekite and saussurite. The Kerala gabbro - anorthosite bodies (along the Bavali lineament), as well as the recently reported ones from the Prakasam district of Andhra Pradesh (Prasad Rao et al., 1988), are grossly comparable to the Mayurbhanj occurrences. It appears that a considerable number of gabbroic bodies of various dimensions, both in the mobile belt and cratonic regions of Peninsular India (including Rajasthan), are not brought to light in the proper perspective, and the chances of anorthosite occurring as a major or minor component in these bodies cannot be ruled out.

THE MOBILE (GRANULITE) BELT

Tectonic aspects

Anorthosite intrusion may have been at various crustal levels through the Eastern Ghat province. The majority of the massif anorthosites occur within or adjacent to the Eastern Ghats province (Fig. 1). There is no conspicuous clustering of the anorthosite bodies in the Proterozoic shear belts in South India (Fig. 3). The relative age relationships between the periods of emplacement of the anorthosite complexes and the formation of the Proterozoic shear zones are far from clear.

The Eastern Ghat mobile belt (Figs. 1-3) is considered as a fault-bounded, ensialic and linear rift zone (Katz, 1978), and represents an isostatically uplifted boundary portion of the Dharwarian nucleus (Grady., 1971). The charnockitic (gneiss-granulite) region of Peninsular India (CGT and SGT of Fig. 1) is uplifted as a whole relative to the non-charnockitic (granite-greenstone) region, and Fermor's line (Fermor, 1936) forms an abrupt discontinuity between contrasting geologic terrains (Fig.1). The metamorphic discontinuity across the boundary between the Eastern Ghats and the adjoining cratons suggests thrusting of the deeper level eastern terrain over the shallower level western terrain. The boundary (possibly comparable to the Grenville Front) is marked by the presence of an east dipping thrust zone separating the younger (slightly denser and significantly thicker) crustal blocks of the Eastern Ghat province from the older blocks of the craton (see the inset map of Fig. 1). "The charnockites with their granitic basement are upthrusted against the Dharwars during the post-Dharwar period" (Kaila and Tewari, 1985). The eastern margin of the Cuddapah basin (see Fig.3) is a site of crustal shorterning during the E-W compression, and the higher heat flow along this margin may indicate recurrent igneous intrusive activity along the faulted boundary which probably was originally a collisional front (Narain and Subrahmanyam, 1986), though Drury et al., (1984) suggest that the thrust zone does not represent a plate collision zone.

Gravity data from the Indian shield indicates that the boundary between the Eastern Ghats and the adjoining craton extends from the Mahanadi lineament in the north all the way down to Cape Comorin in the south (Fig. 1). The gravity anomaly pattern, a steep eastward positive gradient along the entire Eastern Ghat belt is interpreted to result from the presence of a subsurface ridge-like feature of high density material at shallow depth, and the (gabbroic) anorthosites, according to Kaila and Bhatia (1981), are perhaps the surface manifestations of this feature. As the gravity gradient along the western edge of the Eastern Ghat province is identical to that along the Grenville front of the Canadian shield, the boundary is interpreted to indicate a Proterozoic "cryptic suture"(?) resulting from collision tectonics (Subrahmanyam, 1978). It is of interest to note that the anorthosites in the eastern part of the Grenville province and the anorthosites of the Adirondacks and Nain complexes are associated with strong negative gravity anomalies. Large negative Bouguer gravity anomalies associated with many massifs attest to: (1) the low average density of anorthosite complexes relative to their surrounding country rocks; and (2) the absence of large quantities of associated ultramafic rocks. With the presently available gravity data, it will be extremely difficult to correlate the known anorthosite complxes, barring Bankura, with the gravity anomalies.

Early orogenic, large-scale thrusting and nappe stacking occurred in south India (Drury et al., 1984; Newton, 1985), wherein some areas show increase of pressure towards higher grade, compatible with the depth zone concept (i.e., no isobaric increase of grade). The generalization that deeper crustal levels are exposed to the south does not extend south of the Noil-Cauvery Proterozoic shear zone (Fig.3). Immediately south of the low to high grade transition zone, profound late-Archaean crustal shorterning and thickening is affected (prior to granulite facies metamorphism) by the downward-steepening crustal underthrusting due to the northward underthrusting of the southern block (SGT in Fig. 1) in the continent-continent collision model; thus the southern granulite terrain (SGT) was underthrusted northwards under the Dharwar craton (WDC and EDC of Fig. 1), while the coastal granulite terrain (CGT) was upthrusted westwards over the Dharwar and Bastar cratons (see Drury et al., 1984).

Petrological aspects

The high temperatures (700-900^{o}C) and high pressures (8±2 kbar) in a thick continental crust yielded charnockites, and the Proterozoic Adirondack and Grenville charnockite bodies are the result of a high-pressure metamorphic overprint on plutonic rocks that may have been originally emplaced at relatively shallow levels (Newton and Hansen, 1983). The most recent studies on the granulites from Madras (Tamil Nadu), Kabbal (Karnataka) and Ponmudi (Kerala) suggest high T (650-850^{o}C) and P (5-7.5 kbar) for the equilibration of metamorphic assemblages (Bhattacharya and Sen, 1986; Chacko et al., 1987; Hansen et al., 1987; Santosh., 1987). All these data indicate that the presently exposed granulite terrains (all along the mobile belt) must have been formed at depths of more than 20 km. The present Moho discontinuity lies 35-40 km beneath the current level of erosion (Kaila et al., 1987) implying an anomalously thickened (>60 km) continental crust during the metamorphism.

Though the intrusive temperatures (980 ± 20°C for Oddanchatram), final equilibrium P-T conditions (4.7-7 kbar and 620-740°C for Bolangir; 6 ± 1.0 kbar and 680 ± 35°C for Bankura) of the prograde phases (6.25 ± 0.5 kbar and 650°C for Bankura), retrogressive pressure (~5.3 kbar for Oddanchatram), and also high-pressure and retrogressive events (12 kbar and 800°C; 7-8 kbar and 675 ± 25°C for Sittampundi) for some anorthosite complexes are known (see Leelanandam and Narsimha Reddy., 1988), data pertaining to the P-T-time paths are virtually non-existent.

Gopalakrishna et al., (1986) suggest that the granulite facies terrains commonly exposed at the surface in shield areas represent the mid-levels of greatly thickened crust (rather than the deepest crustal levels) and that the deepest crustal levels have rarely or never become subsequently uplifted to the surface.

The high P (9.9 ± 1 kbar) values of the "less retrogressed" (?) samples from the northern slopes of the Nilgiri massif (Moyar shear zone; Fig.3), in contrast to the low P (6.6 ± 0.6 kbar) values for the "more retrogressed" (?) samples from the central portions (highland terrane) of the Nilgiri massif (south of the Moyar shear zone and north of the Bhavani shear zone), for similar T (720 ± 80°C) values (Raase et al., 1986), are rather intriguing; further,the P values tend to decrease farther south in the Kodaikanal (5.3 ± 0.5 kbar ; 750 ± 50°C) and Nagercoil (5.0 ± 1 kbar; 700 ± 20°C) massifs (Fig.3) of the southern granulite terrain (Harris et al., 1982). Petrologists actually know less about the pressure and temperature conditions of granulite metamorphism than is generally accepted (Frost and Chacko, 1989).

Many granulite terrains record the effects of either rapid and virtually isothermal decompression (crustal uplift) or slow and nearly isobaric cooling (thermal relaxation) at depth with little uplift. The regional variation of the pressure data in the granulite facies terrain of south India (6.5 - 9.5 kbar; 730 - 800°C) is attributed to the differential uplift of smaller blocks (Raith et al., 1983).

Carbonic metamorphism

Though the CO_2-streaming hypothesis (carbonic metamorphism) for the generation of granulite (especially in the transition zones of south India) is increasingly favoured by many researchers in recent years, vapour-absent metamorphism (or metamorphism of already dry rocks as in the Adirondacks) is not ruled out to explain the genesis of huge massifs. The mechanism of internal fluid buffering (instead of CO_2 influx from external sources) and participation of an anatectic melt (generated by dehydration melting) can explain the genesis of Madras granulite (Bhattacharya and Sen, 1986). The ultimate cause for the unusual impoverishment of structurally combined water (H_2O^+), coupled with the exceptional enrichment of F and Cl, in the hornblendes and biotites of the Kondapalli granulites (Leelanandam, 1970) is yet to be explored. The efficacy of carbonic metamorphism for the genesis of huge charnockitic massifs in Andhra Pradesh and Orissa of the Eastern Ghat Province is not tested, and this field of research is wide open for future investigators.

Prograde charnockitization of (or retrograde de-charnockitization to) lower grade rocks is probably aided by high P_{CO2} (or high P_{H2O}) conditions, and the prograde relationships that exist in the amphibolite-granulite transition zone are reversed in the Proterozoic shear zones (Allen et al., 1985).

The charnockite (orthopyroxene)-producing reactions involve either the breakdown of calcic amphibole (in the graphite-free environment), as at Kabbal, or the reaction between biotite and quartz (in the presence of graphite), as at Ponmudi. Though the P-T conditions of the carbonic granulite-facies metamorphism of both the Kabbal-type and Ponmudi-type localities (separated by 500 km; Fig.3), were generally the same (5-6 kbar; 700-800°C), the Ponmudi-type metamorphism represents a higher grade or more probably lower H_2O activity (Hansen et al., 1987). Srikantappa et al., (1985) suggest that the charnockitization was induced in the Ponmudi area by an isothermal decrease of fluid pressure relative to lithostatic pressure, but was not due to carbonic metamorphism. This was refuted by Ravindra Kumar and Chacko (1986) who believe that carbonic metamorphism was not restricted to the amphibolite-granulite transition zone, but was important to the evolution of the entire southern Indian granulite terrain. Santosh and Yoshida (1986) recorded the evidences of both breaking and making of charnockites in the same localities in south Kerala. The khondalite belt of Kerala, possibly formed at nearly uniform depths of 15-21 km (4.5-6.5 kbar; 650-850°C), could be due to an "A-subduction" model, in which a continental shelf sequence was entrained at the flat interface of colliding continents in near-horizontal subduction (Chacko et al., 1987).

EPILOGUE

Most speculations interpret the granulite terrains as the result of continental rifting and collision processes (Newton, 1985). In the Proterozoic Grenville province of Canada, granulite metamorphism occurred a few hundred million years after accretion. If the original anorthosite emplacement took place at relatively shallow levels and was a separate (earlier) tectonic event from the (later) regional metamorphism as in the Adirondacks, then models of anorthosite genesis during crustal rifting and spreading followed by regional metamorphism during continent-continent collision can be supported.

The temporal relationship between the anorthosite intrusion, crustal accretion and granulite metamorphism are far from clear for almost all the massifs in the Proterozoic mobile belt of Peninsular India. The amount, rate and (specifically) timing of the uplift (cooling), and also particularly the subsequent amount and rate of erosion of the terrains are of crucial significance in tracing their evolutionary histories. It is hoped that the present paper will initially help in clearly understanding these problems and eventually aid in solving at least some, if not all, of them.

ACKNOWLEDGEMENTS

The writer is indebted to Drs. L.D.Ashwal, B.R.Frost, J.Morrison and W.C.Phinney for their critical reviews of the manuscript. He thanks Dr.M. Narsimha Reddy for the help he has provided in preparing the figures and in checking the references.

REFERENCES

Allen, P., Condie., K.C. and Narayana, B.L., 1985. The geochemistry of prograde and retrograde charnockite-gneiss reactions in southern India. Geochim. Cosmochim. Acta, 49: 323-336.

Ashwal, L.D., 1988. Anorthosites: classification, mythology, trivia, and a simple unified theory. J. Geol. Soc. India, 31: 6-8.

Banerji, A.K., 1975. On the evolution of the Singhbhum nucleus, eastern India. Quart. J. Geol. Min. Met. Soc. India, 47: 51-60.

Bhan, S.K. and Hegde, V.S., 1985. Targeting areas for mineral exploration: a case study from Orissa, India. Int. J. Remote Sensing, 6: 473-479.

Bhattacharya, A and Sen., S.K., 1986. Granulite metamorphism, fluid buffering, and dehydration melting in the Madras charnockites and metapelites. J. Petrol., 27: 1119-1141.

Bhattacharyya, P.K. and Mukherjee, S., 1987. Granulites in and around the Bengal anorthosite, eastern India: genesis of coronal garnet, and evolution of the granulite-anorthosite complex. Geol. Mag., 124: 21-32.

Bhushan, K.S., Bhaskar, B., Parthasarathy, R. and Nambiar, C.G., 1988. Geochemistry and genesis of the meta-anorthositic rocks near Inukurti, Nellore district, Andhra Pradesh, South India. Neues. Jb. Miner. Abh., 159: 153-164.

Chacko, T., Ravindra Kumar, G.R. and Newton, R.C., 1987. Metamorphic P-T conditions of the Kerala (South India) khondalite belt, a granulite facies supracrustal terrain. J. Geol., 95: 343-358.

Drury, S.A., Harris, N.B.W., Holt, R.W., Smith, G.J.R. and Wightman, R.T., 1984. Precambrian tectonics and crustal evolution in South India. J. Geol., 92: 3-20.

Fermor, L.L., 1936. An attempt at correlation of the ancient schistose rocks of Peninsular India. Mem. Geol. Surv. India, 70: 1-324.

Frost, B.R. and Chacko, T., 1989. The granulite uncertainty principle: limitations to thermobarometry in granulite. Geology, 17: (in press).

Gopalakrishna, D., Hansen, E.C., Janardhan, A.S. and Newton, R.C., 1986. The southern high-grade margin of the Dharwar craton. J. Geol., 94: 247-260.

Grady, J.C., 1971. Deep main faults in south India. J. Geol. Soc. India, 12: 56-62.

Hansen, E.C., Janardhan, A.S., Newton, R.C., Prame, W.K.B.N. and Ravindra Kumar, G.R., 1987. Arrested charnockite formation in southern India and Sri Lanka. Contr. Min. Pet., 225-244.

Harris, N.B.W., Holt, R.W. and Drury., S.A., 1982. Geobarometry, geothermometry, and late Archaean geotherms from the granulite facies terrain of South India. J. Geol., 90: 509-527.

Janardhan, A.S. and Wiebe, R.A., 1985. Petrology and geochemistry of the Oddanchatram anorthosite and associated basic granulites, Tamil Nadu, South India. J. Geol. Soc. India., 26: 163-176.

Kaila, K.L. and Bhatia, S.C., 1981. Gravity study along the Kavali-Udipi deep seismic sounding profile in the Indian Peninsular shield: some inferences about the origin of anorthosites and the Eastern Ghats orogeny. Tectonophysics, 79: 129-143.

Kaila, K.L. and Tewari, H.C., 1985. Structural trends in the Cuddapah basin from deep seismic soundings (DSS) and their tectonic implications. Tectonophysics, 115: 69-86.

Kaila, K.L., Tewari, H.C., Roy Chowdhury, K., Rao, V.K., Sridhar, A.R. and Mall, D.M., 1987. Crustal structure of the northern part of the Proterozoic Cuddapah basin of India from deep seismic soundings and gravity data. In: S. Asano and W.D. Mooney (Editors), Seismic Studies of the Continental Lithosphere. Tectonophysics, 140, pp.1-12.

Kanungo, D.N., Chetty, T.R.K. and Mallikarjuna Rao, J., 1986. Anorthosites and associated rocks of Nellore - Gudur, South India. J. Geol. Soc. India, 27: 428-439.

Katz, M.B., 1978. Tectonic evolution of the Archaean granulite facies belt of Sri Lanka - South India. J. Geol. Soc. India, 19: 185-205.

Leelanandam, C., 1967. Occurrence of anorthosites from the charnockitic area of Kondapalli, Andhra Pradesh. Bull. Geol. Soc. India, 4: 5-7.

Leelanandam, C., 1970. Chemical mineralogy of hornblendes and biotites from the charnockitic rocks of Kondapalli, India, J. Petrol., 11: 475-505.

Leelanandam, C., 1972. An anorthositic layered complex near Kondapalli, Andhra Pradesh. Quart. J. Geol. Min. Met. Soc. India, 44: 105-107.

Leelanandam, C., 1987a. Archaean anorthosite complexes: an overview. In: A.K. Saha (Editor), Geological Evolution of the Peninsular India-Petrological and Structural Aspects. Hindustan Publ. Corp., Delhi, pp.108-116.

Leelanandam, C., 1987b. Proterozoic anorthosite massifs: an overview. Ind. J. Geology, 59: 179-194.

Leelanandam, C. and Narsimha Reddy, M., 1988. Precambrian anorthosites from Peninsular India: Problems and perspectives. Ind. J. Geol., 60: 111-136.

Leelanandam, C. and Narsimha Reddy, M., 1983. Plagioclase feldspars and hornblendes from the Chimalpahad complex, Andhra Pradesh, India. Neues Jb. Miner. Abh., 148: 200-222.

Leelanandam, C. and Narsimha Reddy, M., 1985. Petrology of the Chimalpahad anorthosite complex, Andhra Pradesh, India. Neues Jb. Miner. Abh., 153: 91-119.

Manna, S.S. and Sen, S.K., 1974. Origin of garnet in basic granulites around Saltora, West Bengal, India. Contr. Min. Pet., 44: 195-218.

Mukherjee, A., Bhattacharya, A. and Chakraborty, S.C., 1986. Convergent phase equilibria at the massif anorthosite-granulite interface near Bolangir, Orissa, India and thermal evolution of a part of the Indian shield. Precamb. Res., 34: 69-104.

Nair, M.M. and Vidyadharan, K.T., 1982. Rapakivi granite of Ezhimala complex and its significance. J. Geol. Soc. India, 23: 46-51.

Nanda, J.K. and Natarajan, V., 1980. Anorthosites and related rocks of the Kondapalli hills, Andhra Pradesh, Rec. Geol. Surv. India, 113: 57-67.

Narain, H. and Subrahmanyam, C., 1986. Precambrian tectonics of the South Indian shield inferred from geophysical data. J. Geol., 94: 187-198.

Narasimha Rao, P., 1977. Petrology and geochemistry of the anorthositic suite of Oddanchatram, Madurai district, Tamilnadu, India (abst.). Symposium on Archaean Geochemistry: the origin and evolution of the Archaean continental crust. Hyderabad, pp.92-94.

Newton, R.C., 1985. Temperature, Pressure and metamorphic fluid regimes in the amphibolite facies to granulite facies transition zones. In: A.C. Tobi and J.L.R. Touret (Editors), The Deep Proterozoic Crust in the North Atlantic Provinces. Reidel, Amsterdam, pp.75-104.

Newton, R.C. and Hansen, E.C., 1983. The origin of Proterozoic and late Archaean charnockites: evidence from field relations and experimental petrology. Mem. Geol. Soc. Amer., 161: 167-178.

Perraju, P., 1973. Anorthosites of Puri district, Orissa. Rec. Geol. Surv. India, 105: 101-116.

Phinney, W.C., Morrison, D.A. and Maczuga, D.E., 1988. Anorthosites and related megacrystic units in the evolution of Archaean crust. J. Petrol., 29: 1283-1323.

Prasad Rao, A.D., Rao, K.N. and Murty, Y.G.K., 1988. Gabbro - anorthosite - pyroxenite complexes and alkaline rocks of Chimakurti - Elchuru area, Prakasam district, Andhra Pradesh. Recs. Geol. Surv. India, 116: 1-20.

Raase, P., Raith, M., Ackermand, D. and Lal, R.K., 1986. Progressive metamorphism of mafic rocks from greenschist to granulite facies in the Dharwar craton of South India. J. Geol., 94: 261-282.

Radhakrishna, B.P. and Naqvi, S.M., 1986. Precambrian continental crust of India and its evolution. J. Geol. 94: 145-166.

Raghavan Nambiar, A., Vidyadharan, K.T. and Sukumaran, P.V., 1982. Petrology of anorthosites of Kerala, Recs. Geol. Surv. India, 114: 60-70.

Ravindra Kumar, G.R. and Chacko, T., 1986. Mechanisms of charnockite formation and breakdown in southern Kerala: implications for the origin of the southern Indian granulite terrains. J. Geol. Soc. India, 28: 277-288.

Saha, A.K., Bose, R., Ghosh, S.N. and Roy, A., 1977. Petrology and emplacement of the Mayurbhanj granite batholith, eastern India. Bull. Geol. Min. Met. Soc. India, 49: 1-34.

Santosh, M., 1987. Cordierite gneisses of southern Kerala, India: petrology, fluid inclusions and implications for crustal uplift history. Contr. Min. Pet., 96: 343-356.

Santosh, M. and Yoshida, M., 1986. Chanockite in the breaking: evidence from the Trivandrum region, South Kerala. J. Geol. Soc. India, 28: 306-310.

Sarkar, A., Bhanumathi, L. and Balasubrahmanyan, M.N., 1981. Petrology, geochemistry and geochronology of the Chilka Lake igneous complex, Orissa state, India. Lithos, 14: 93-111.

Sarkar, A.N., 1982. Precambrian tectonic evolution of eastern India: a model of converging microplates. Tectonophysics, 86: 363-397.

Sen, S.K. and Bhattacharya, A., 1986. Fluid induced metamorphic changes in the Bengal anorthosite around Saltora, West Bengal. Ind. J. Earth Sci., 13: 45-68.

Srikantappa, C., Raith, M. and Ackermand, D., 1985. High-grade regional metamorphism of ultramafic and mafic rocks from the Archaean Sargur terrane, Karnataka, South India. Precamb. Res., 30: 189-219.

Subrahmanyam, C., 1978. On the relation of gravity anomalies to geotectonics of the Precambrian terrains of the South Indian shield. J. Geol. Soc. India, 19: 251-263.

Tak, M.W., 1973. Calc-silicate rocks of Bolangir-Patna district, Orissa. Rec. Geol. Surv. India, 105: 117-120.

Tak, M.W., Mitra, D. and Chatterjee, P.K., 1966. A note on the occurrence of anorthosite in the Bolangir - Patna district, Orissa. Ind. Minerals, 20: 339-342.

Valley, J.W., 1985. Polymetamorphism in the Adirondacks: wollastonite at contacts of shallowly intruded anorthosite. In: A.C. Tobi and J.L.R. Touret (Editors), The Deep Proterozoic Crust in the North Atlantic Provinces. Reidel, Amsterdam, pp.217-236.

Venkatakrishnan, R. and Dotiwalla, F.E., 1987. The Cuddapah Salient: a tectonic model for the Cuddapah Basin, India, based on Landsat image interpretation, Tectonopysics, 136: 237-253.

Vidyadharan, K.T., Sukamaran, P.V. and Nair, M.M., 1977. A note on the occurrence of anorthosite near Perinthatta, Taliparamba taluk, Cannanore district, Kerala. J. Geol. Soc. India, 18: 519-520.

Wiebe, R.A. and Janardhan, A.S., 1988. Metamorphism of the Oddanchatram anorthosite, Tamil Nadu, South India. J. Geol. Soc. India, 31: 163-165.

This Page Intentionally Left Blank

EARLY PROTEROZOIC TECTOFACIES IN EASTERN AND NORTHERN FINLAND

KAUKO LAAJOKI

ABSTRACT

The late Archaean basement of the Fennoscandian (Baltic) Shield is covered by early Proterozoic (c. 2500-1900 Ma) peri/epicontinental Karelia and flyschoidic Kaleva rocks in eastern and northern Finland.

The Karelia supracrustal rocks form three tectofacies: the oldest, the Sumi-Sariola, consists of immature conglomerates, arenites and subaerial basic metalavas of the incipient rifting stage of the Archaean craton. The 2440 Ma old layered basic intrusions are also included in this stage. The Kainuu-Lapponi tectofacies, separated by a period of deep chemical weathering from the former, represent either a narrow sea or inland basin system with its shallower-water parts characterized by quartz-pebble conglomerates and mature arenites while the deeper-water assemblages include turbiditic arenites overlain by hummocky, cross-stratified micaceous arenites, cross-bedded quartzites and shallow-water muddy metasediments with metalavas, the latter being especially abundant in Lapland. The Jatuli, the youngest Karelia tectofacies, is dominated by mature quartzites with minor dolomites and mica shists. It consists of at least two major transgressive cycles and represents fluvial and shelf-type sediments of an open-sea stage.

The Kaleva rocks are divided into the Lower-Kaleva, the Middle Kaleva, and the Upper Kaleva tectofacies, of which the first consists of the c. 1960 Ma old Jormua Ophiolite Complex and associated sediments and the Outokumpu allochthon of ophiolitic serpentinites and associated pelitic metasediments and Cu-ores. The Middle Kaleva consists of turbiditic arenites and metapelites with minor black schist and banded iron formations. The upper Kaleva has a very restricted distribution comprising a few erosional relics of molassic quartzites and conglomerates in northern Finland. The tectonosedimentary evolution of the Kaleva tectofacies is debated. The models proposed include Svecofennidic

back-arc flysch, Kolalappidic foredeep sediments or a Kalevian passive margin sequence.

As a whole the Karelia and Kaleva tectofacies form a supracrustal sequence very similar to the Wopmay Orogen which is interpreted as a complete early Proterozoic Wilson Cycle (Hoffman 1980).

INTRODUCTION

On most continents the early Proterozoic supracrustal rocks which are preserved are epi/pericontinental or platformal rocks covering the Archaean basement and they generally fall into Condie's (1982) quartzite-carbonate-shale succession (assemblage 1). Well-studied exmples from the Canadian Shield include the Coronation Supergroup (Hoffman, 1980), the Huronian Supergroup Young (1973), the Circum-Ungava belt (e.g. Dimroth, 1970; Ricketts and Donaldson, 1981; Wardle and Bailey, 1981) and the Lake Superior area (e.g. Sims et al., 1981; Morey, 1983) all of which bear specific lithostratigraphic and chronostratigraphic similarities with the Karelian formations of the Fennoscandian (Baltic) Shield. Plate-tectonic models including rifting, continental break-up, and development of an Atlantic-type continental margin have been used to interpret the evolution of the North American successions (e.g. Hoffman, 1980; Larue, 1983; Stauffer, 1984).

The sedimentology and stratigraphy of the early Proterozoic Karelian formations in the Soviet Karelia have been studied intensively and they have been interpreted by Sokolov and Heiskanen (1985) in terms of molasse troughs (Sumi-Sariola), protoplatform (Jatuli) and aulacogens (Ludicovian) and flysch troughs (Livvian).

In Finland, plate tectonics has generally become paramount in the interpretation of the evolution of the Svecofennian Belt, whose supracrustal rocks from a counterpart of Condie's (1982) assemblage III (e.g. Hietanen, 1975; Piirainen, 1975; Park et al., 1984; Gaal and Gorbatschev, 1987). The tectonic settings of the Karelian formations have, however, received relatively little attention. This is partly due to the fact that the Karelian formations do not form large continuous deposits but are encountered as smaller schist areas separated by tectonic and metamorphic zones

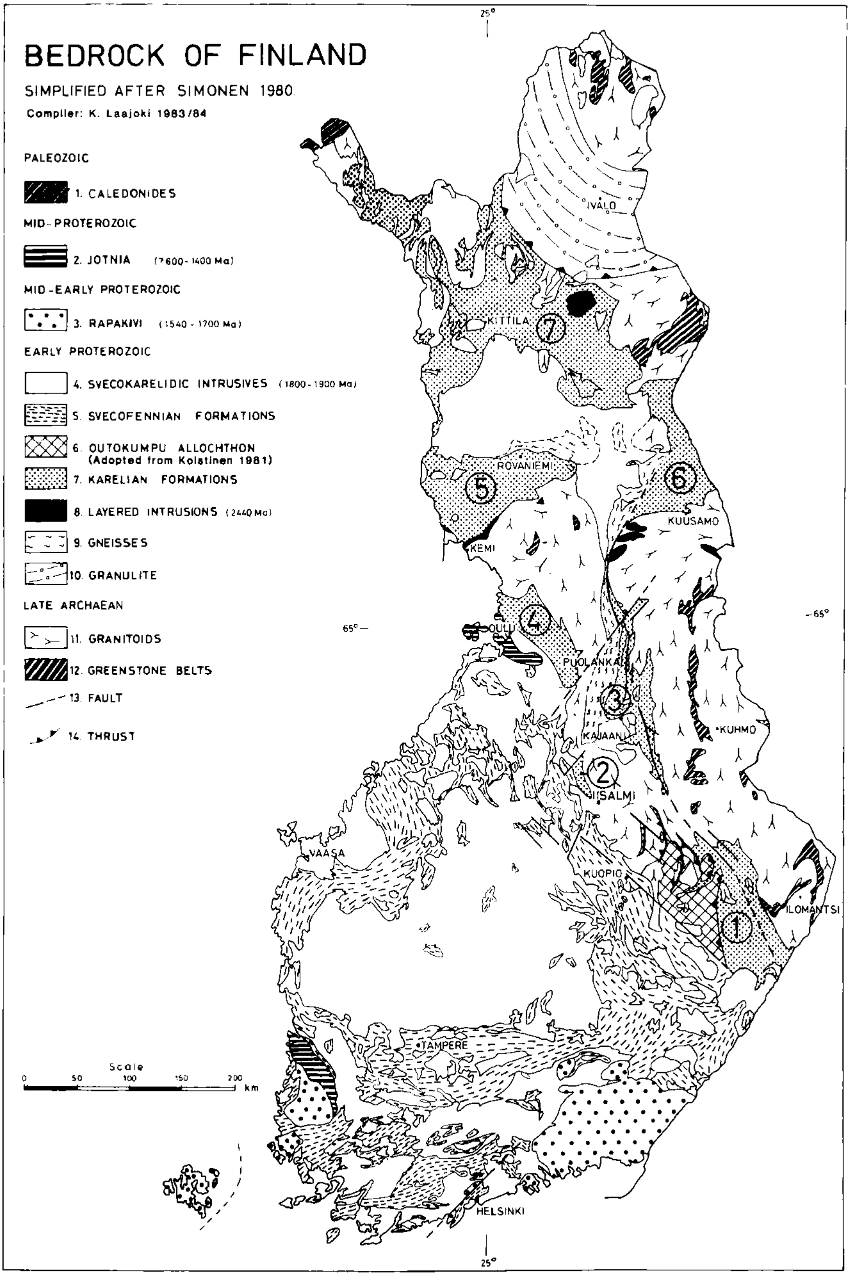

Figure 1. Simplified geological map of Finland showing the distribution of the major Karelian schist areas: 1. North Karelia, 2. Salahmi, 3. Kainuu, 4. Northern Pohjanmaa, 5. Perapohja, 6. Kuusamo, 7. Central Lapland schist belts. Letters LR and BB show, repectively, the approximate locations of the Raahe-Ladoga zone and the Baltic-Bothnia megashear.

(Fig.1). On the basis of palaeosedimentological, stratigraphical and structural studies in northern Finland, the author has treated the general evolution of the Karelian formations in terms of a Wilson cycle (Laajoki, 1986a). However, recently a lot of new information concerning these subjects has become available (e.g. Kontinen, 1987; Ward, 1987; Laajoki and Paakkola, 1988) which helps to establish more detailed models.

This paper concentrates on the supracrustal cover rocks of the late Archaean granitoid-greenstone basement of eastern and northern Finland and interprets their evolution in terms of tectofacies. A *tectofacies* is defined as including all the sedimentary, volcanic and hypabyssal intrusive rocks deposited, extruded or intruded into a tectonosedimentary system.

GENERAL FEATURES OF THE PRECAMBRIAN BEDROCK OF FINLAND

The bedrock of Finland consists almost entirely of Precambrian rocks which form three major units (Fig. 1) : 1) the late Archaean granitoid basement with minor greenstone-belt relics of eastern and northern Finland, 2) the early Proterozoic metasedimentary and associated metavolcanic rocks deposited nonconformably on the late Archaean cratonized basement and collectively known in Finland as the Karelian formations, 3) the Svecofennian formations and associated plutonic rocks (c. 1900-1800 Ma) of central and southern Finland, which represent an island-arc association, are obviously exotic in relation to the Karelian areas. The fourth unit is the Granulite Arc in Lapland which represents either reworked Archaean basement or granulitized Proterozoic formations or both. For general reviews of the bedrock of Finland see Simonen (1980), Laajoki (1986a) and Gaal and Gorbatschev (1987).

The Karelian formations consist of schist areas separated by tectonic and metamorphic zones. The major schist areas are encountered in North Karelia, Kainuu, Northern Pohjanmaa, Kemi, Kuusamo and in Central Lapland (Fig. 1). Furthermore, Karelian schists occur in North Savo where they change into highly metamorphic and plutonic rocks of the Karelia - Svecofennia boundary called the Raahe-Ladoga zone (Laajoki, 1986a). The degree of metamorphism of the schist belts varies from greenschist facies to upper amphibolite facies and many of the belts underwent repeated deformation.

Lithologically the Karelian formations can be divided into two major successions: the lower arenite-dominated sequences and the overlying turbidite-dominated sequences, which represent two tectofacies associations called, respectively, the Karelia and the Kaleva tectofacies.

KARELIA TECTOFACIES

The Karelia rocks are classified into three tectofacies:the Sumi-Sariola, the Kainuu-Lapponi and the Jatuli (Fig. 2).

The Sumi-Sariola, the oldest one, comprises conglomerates and arkosites, originally immature fluvial and alluvial gravels and sands, and associated subaerial basic or intermediate lavas now mostly amygdaloid rocks (e.g. Pekkarinen, 1979; Marmo et al., 1988; Strand, 1988). Marmo and Ojakangas (1984) have described glacial rocks from this tectofacies from North Karelia. The Sumi-Sariola rocks were deposited in narrow fault-controlled basins in eastern and northern Finland (Fig. 3). The 2440 Ma old basic intrusions (Alapieti, 1982) are included in this tectofacies (cf. Park et al., 1984).

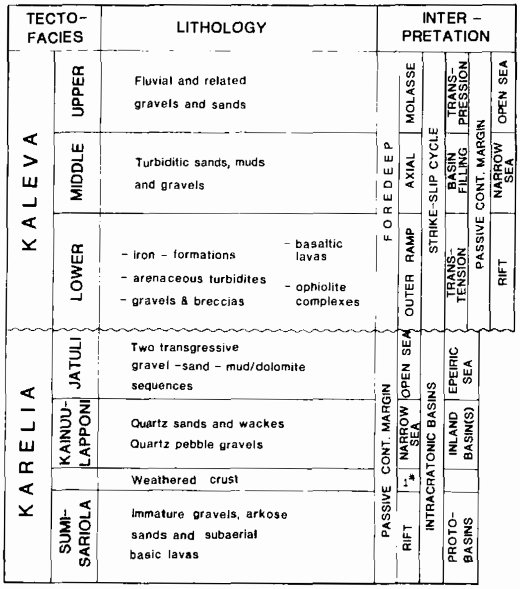

Figure 2. Karelia and Kaleva tectofacies in Finland, their primary (now metamorphosed) lithological contents and possible interpretations (see discussion in the text).

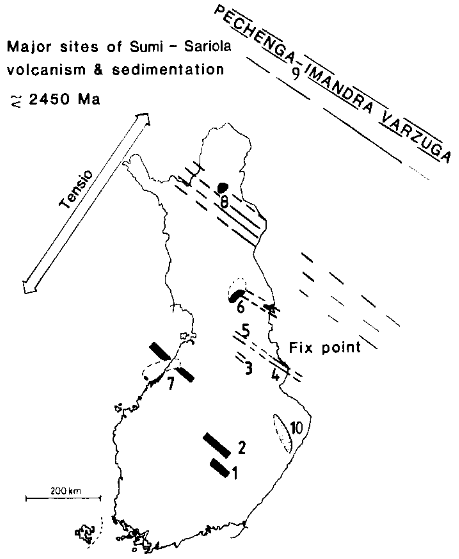

Figure 3. Arbitrary reconstruction of the distribution of the Sumi-Sariola rifts (Nos. 1-9) (About 2400 Ma ago) supposing that the Kemi occurrence (No.7) was moved about 200 km from the southwest to its present location. Black colour shows the basic layered intrusions of northern Finland. (6. Koillismaa, see Alapieti 1982, 7. Kemi, 8. Koitelainen). No.10 indicates the Sariola of North Karelia. The fix point (rift No. 4) is a reference point relatively unaffected by the Svecokarelidic orogenic movements. The major Svecokarelidic crustal shortening was caused by NE-SW compression causing thrusting to the northeast along the North Karelia-Kianuu thrust belt (indented). Later movements followed the wrench faults of Auho and Kalhama.

In eastern Finland, the Kainuu-Lapponi tectofacies is mostly built up of more mature quartzites and sericite quartzites, originally quartz sands and wackes underlain by a chemical palaeosol (Fig. 4) (Marmo et al., 1988; Strand, 1988). The western part of the Kainuu Schist Belt and the Central Lapland Schist Belt (belts 3 and 7, respectively in Fig. 1), however, include progradational turbidite - shallow-water sand and mud sequences (Laajoki, 1986b) and it may be that the khondalite suite of the Granulite Belt (the area around Ivalo in Fig. 1) originated from the turbidites of this cycle (cf. Barbey et al., 1984). Laajoki and Korkiakoski (in print) have described a turbidite-tempestite transition from this tectofacies. In Lapland, the tectofacies may include abundant volcanic rocks at the top of the succession, mostly basaltic metalavas and komatiitic pyroclastics

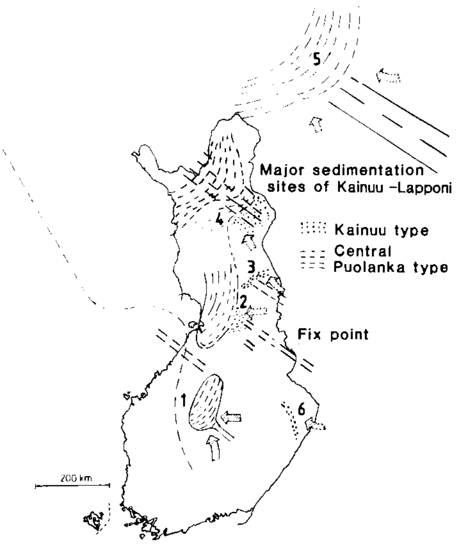

Figure 4. Arbitrary original distribution of the Kainuu-Lapponi tectofacies supposing that the Sumi-Sariola rifts (Fig. 3) controlled the sedimentation of the fluvial Kainuu-type sands (stippled areas) and the deeper-water Central Puolanka-type turbiditic sequences (ruled) and associated volcanic rocks. 1. Otanmaki deep-water palaeofan, 2. Central Puolanka deep-water (see Laajoki 1986b, Laajoki and Korkiakoski in print), 3. Paljakkavaara quartzite, 4. Central Lapland, 5. Possible "granulite arc" deep-water palaeofan. 6. Kainuu-type quartzites in North Karelia.

rocks. Since the stratigraphy of Lapland is still under debate, however, part of them may belong either to older or younger cycles.

In Kainuu and Northern Finland, the Jatuli tectofacies, separated by the so-called Nenakangas unconformity (Fig. 5) from the Kainuu-Lapponi tectofacies (Laajoki, 1988a) consists of at least two transgressive shelf-type quartzite-dolomite-pelite sequences with minor volcanic rocks (Perttunen, 1985; Kangas, 1985). In North Karelia the equivalent rocks are mostly fluvial sands (Marmo et al., 1988), which indicates that the Jatuli Sea transgressed from northwest to southeast (Fig. 6). The Kainuu-Karelia seaway in Fig. 6 represents the basin where the Jatuli of North Karelia and Kainuu was deposited and which was later closed to form the Kainuu and North Karelia schist belts of Fig. 1. In Lapland, this tectofacies is encountered only as solitary quartzite hills (Nikula, 1988; Rasanen and Makela, 1988).

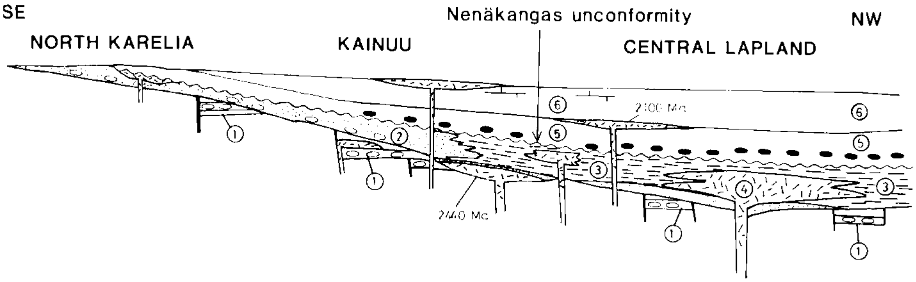

Figure 5. A schematic reconstructed cross-section of the Karelia tectofacies from North Karelia via the Kainuu Schist Belt to Central Lapland (see Fig. 1). 1 Sumi-Sariola, 2. and 3. Proximal and distal metasediments of the Kainuu-Lapponi tectofacies, 4. Lapponi metavolcanics, 5 and 6. First and second transgressions of the Jatuli tectofacies. The solid circles indicate the conglomerate at the base of the Jatuli. Also shown are the 2440 Ma old layered intrusions of Koillismaa and the Jatulian metalavas. Notice that the Kainuu-Lapponi tectofacies may consist of several individual basins or sub-basins. Adapted from Laajoki (1988a).

The Karelia tectofacies represents a transition from continental fluvial sedimentation and volcanism to shelf-type sedimentation. This evolution is interpreted in terms of a passive continental margin in such a way that the Sumi-Sariola, the Kainuu-Lapponi and the Jatuli represent, respectively, the rifting, the narrow sea and the open sea stages (Fig. 2) (cf. Laajoki, 1986a). The unconformity below the Kainuu-Lapponi is interpreted to mark the onset of drifting and is called after Falvey (cited by Balley, 1981) the "breakup unconformity". In comparison with more recent passive continental margins the relatively large volume of volcanic rocks is exceptional; especially in the case of the Lapponian rocks in Lapland, but volcanic rocks are also encountered in the Jatuli. This reflects the same kind of deviation that the early Proterozoic foredeeps of North America have when compared with younger foredeeps (Hoffman, in print). Park et al., (1984) interpret this "continental" basic igneous activity as being related to a phase of tensional activity in the craton which included stretching of the continental margin.

As an alternative to the passive continental margin development the Karelia tectofacies could represent intracratonic basins deposited successively upon each other as in the case of the

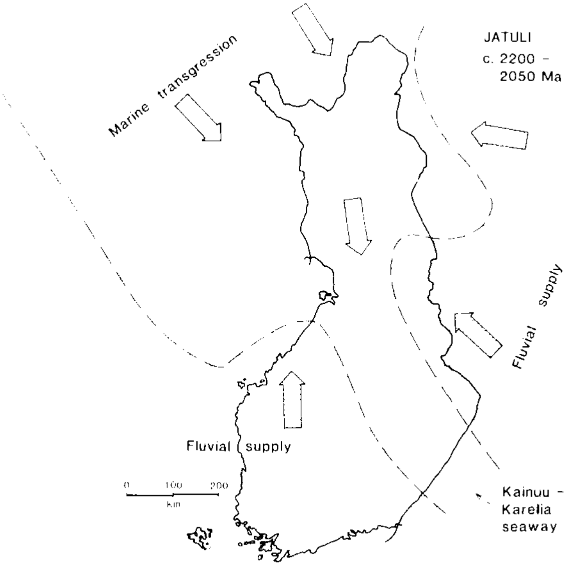

Figure 6. A Schematic reconstruction of the depositional environments of the Jatuli tectofacies (c. 2200-2050 Ma ago).

Precambrian Witwatersrand and Transvaal basins of South Africa (Tankard et al., 1982). In this case the Sumi-Sariola, the Kainuu-Lapponi and the Jatuli could represent, for instance, protobasin, inland basin and epeiric sea stages, respectively (Fig. 2). The abundant basaltic rocks indicate that the craton was repeatedly fractured by faults probing down to the mantle. Gaal and Gorbatschev (1987) support this interpretation and consider that the majority of the Karelian rocks were formed by intracratonic, anorogenic processes, including intracratonic volcanism (cf. Sokolov and Heiskanen, 1985).

KALEVA TECTOFACIES

The Kaleva can also be divided into three tectofacies, which are called the Lower Kaleva, the Middle Kaleva and the Upper Kaleva. The unconformity between the Kaleva and the Karelia is established by the basal sedimentary breccias and conglomerates (Vayrynen, 1933; Gehor and Havola, 1988; Karki, 1988) of the Lower Kaleva overlain by turbiditic meta-arenites and metapelites, phosphogenic banded iron-formations and black schists (Laajoki and Saikkonen, 1977; Kontinen, 1986). In the area of Outokumpu in North Karelia (Koistinen, 1981) and at Jormua in Kainuu (Kontinen,

1987) ophiolite complexes about 1970 Ma old occur which are included in the Lower Kaleva. The Middle Kaleva consists mainly of basinal micaceous turbidites encountered in North Karelia, Savo, Kainuu, Northern Pohjanmaa, and Kemi, but not in Lapland. Its relation with the Lower Kaleva turbidite sequence has not yet been established (cf. Ward, 1987). The upper Kaleva rocks are seen only as two minor fluvial quartzite occurrences in Kainuu (Gehor and Havola,1988; Laajoki, 1988b).

As a whole the Kaleva is a flyschoidic or geosynclinal unit and it has traditionally been stated that the Kaleva and the Jatuli represent, respectively, the eugeosynclinal and miogeosynclinal facies of the Svecokarelidic orogeny. Recent studies have revealed, however, that the Kaleva - Karelia relation is complicated and there are many ways in which it may be explained.

One possibility is that the Kaleva is a back-arc flysch of the Svecofennides (Park et al., 1984), but this interpretation seems not to be valid because the Kaleva has received its material mainly from the Karelia or from basement sources. This model is close to the marginal basin settings supported for example by Gaal (1986).

A second possibility is that the Kaleva represents a foredeep sequence, in which case the Lower, the Middle and the Upper Kaleva could be interpreted as the outer ramp, the axial, and the molasse sediments, respectively (Fig.2, Laajoki and Gehor, in print). In this model the presence of basaltic lavas, e.g. in Northern Pohjanmaa, could be explained in terms of products of foredeep magmatism (cf. Hoffman, in print). To explain the Kaleva ophiolite complexes, however, demands that there was also some extension of the crust of the continent margin that was overridden by the fold-and-thrust belt. A possible connection between the Kaleva foredeep and the Kolalappidic (for definition see Laajoki, 1986a), or the Svecofennidic orogenies is problematical. Since the Middle Kaleva turbidites occupy a northwest-trending zone from North Karelia to Perapohja (schist belt 1-5 in Fig.1), the axial zone was probably located close to the Svecofennian area and so the Kaleva could be a foredeep of the Svecofennides, receiving its detritus mainly from the foreland in the northeast. Another alternative is that the Kaleva foredeep developed in front of the Granulite Belt thrust upon the Central Lapland Schist Belt from the northeast and that this Kolalappidic foredeep was later involved in the Svecokarelidic orogeny migrating from the southwest. This model resembles Barbey et al.'s (1984) idea that the Kaleva rocks were the molasse of the Kolalappidic fold belt and that the Kolalappidic and the Svecofennidic orogenies are closely related.

The third alternative is to interpret the Kaleva as a strike-slip (or pull-apart) basin cycle, in which case the Lower, the Middle and the Upper Kaleva could have been deposited, during the transtensional, the basin filling, and the transpressional phases respectively (cf. Reading, 1980). This model would explain the Kaleva ophiolite complexes as ensialic ophiolites developed during the transtensional stage (cf. the ophiolites of the innermost Hellenides; Bebien et al., 1986) and it has been applied by Ward (1987) to the Kaleva rocks of the Hoytiainen province in North Karelia.

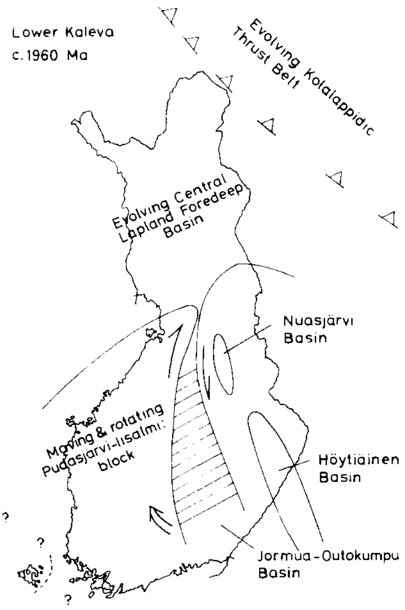
Lower Kaleva
c.1960 Ma
Evolving Kolalappidic Thrust Belt
Evolving Central Lapland Foredeep Basin
Nuasjärvi Basin
Moving & rotating Pudasjärvi-Iisalmi block
Höytiäinen Basin
Jormua-Outokumpu Basin
?
?
?

Figure 7. A schematic reconstruction of the Lower Kaleva (c. 1960 Ma ago) showing the formation of the Jormua-Outokumpu Basin with its ensialic (?) ophiolites due to the breakup and rotation of the Pudasjarvi-Iisalmi Archaean block. The Nuasjarvi and Hoytiainen basins probably began to evolve during this stage (see Ward, 1987) and the Kolalappidic orogen began in the north. The relative block movements are indicated by arrows.

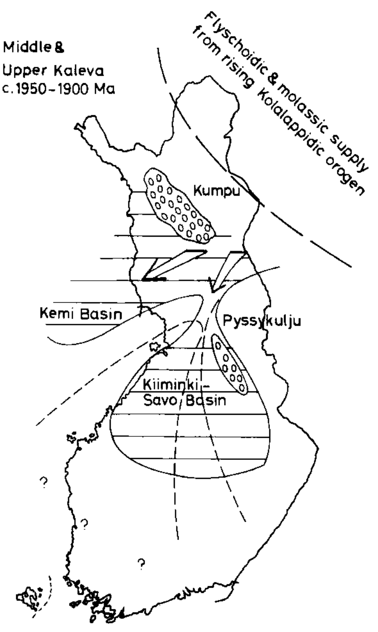

Figure 8. A schematic reconstruction of the Middle (horizontal ruling) and Upper Kaleva (circles) tectofacies (c. 1950-1900 Ma ago) in the case that they represent, respectively, flyschoidic and molassic foredeep sediments of the Kolalappidic orogeny. Arrows indicate supposed sediment transportation directions.

The last possibility is that the Kaleva was a passive continental margin sequence developed during the breakup of the Archaean craton (Gaal and Gorbatschev, 1987). This interpretation relies on the Jormua and Outokumpu ophiolites representing Proterozoic ocean floor as interpreted by Koistinen (1981) and Kontinen (1987). The latter author interprets the Jormua complex as divergent-margin ophiolites. In this case, the Lower, the Middle and the Upper Kaleva would form counterparts of the rifting, the narrow sea and the open sea stages, respectively. Evidence for open sea deposits is, however, scanty and one has to suppose that they have been eroded away. The Middle Kaleva of the Salahmi, Northern Pohjanmaa and Perapohja schist belts (Fig. 1) is also difficult to explain with this model. Furthermore, as stated by Hoffman (in print) the Precambrian foredeeps and rifted continental margin sequences are easily confused with each other.

With respect to the Kaleva, the ophiolite complexes serve as evidence of some degree of extension and consequently the Kaleva development may be explained most logically by the strike-slip basins or by a combined foredeep-strike-slip basin model (Figs. 7 and 8). Furthermore, the Kaleva may, as pointed out by Ward (1987), be composed of separate basins whose origins differ and so the scheme depicted above may be too simple.

THE RELATIONSHIP BETWEEN THE KARELIA AND KALEVA TECTOFACIES

As to the relationship between the Karelia and Kaleva tectofacies, there are two major choices. Firstly, as favoured in this paper, they represent a single passive margin-foredeep or related couplet. Secondly, as stated by Gaal and Gorbatschev (1987), the Karelia should be considered as "anorogenic" and the Kaleva as a passive margin "prelude" to the "orogenic" development of the Svecofennian rocks (cf. Kontinen.,1987). At this stage this dilemma cannot be solved and in fact this problem calls for a regional tectonosedimentary synthesis covering the whole Fennoscandian Shield; e.g. the relationship between the Central Lapland plutonometamorphic complex (the area bordered by the schist belts 5, 6 and 7 in Fig. 1) and the areal distribution of the reactivated basement area of northern Sweden (cf. Ohlander et al., 1987) should be known and the significance of the major fault zones of the Fennoscandian Shield should be better understood than at present. For instance, the so-called Raahe-Ladoga zone seems to be a rather young feature, at least post-Kaleva and the Baltic-Bothnia megashear has just recently been discussed by Berthelsen and Marker (1986).

The many major tectonic contacts and the polyphase deformation of the Karelian schist area call for careful structural and tectonic studies. Only after these studies connected with basin analyses have been concluded will it be possible to choose the most probable of the models discussed in this paper. It should be kept in mind, as stressed by the author (Laajoki, 1986a) and Welin (1987), that the entire Fennoscandian Shield is of very limited size when compared with modern plates.

ACKNOWLEDGEMENTS

This paper is based on a lecture delivered to the 4th European Union of Geosciences (EUG) Biannale, Strasbourg, 13-16 April 1987. A travel grant from the Academy of Finland and the comments of Dr.G.Gaal and an anonymous referee are acknowledged.

REFERENCES

Alapieti, T., 1982. The Koillismaa layered igneous complex, Finland its structure, mineralogy and geochemistry, with emphasis on the distribution of chromium. Geol. Surv. Finland, Bull., 319: 116.

Balley, A.W., 1981. Atlantic-type margins. In: Geology of Passive Margins. Education Course Note Series 19, Am. Assoc. Petroleum Geol., 1-1 - 1-45pp.

Barbey, P., Convert, J., Moreau, B., Capdevila, R. and Hameurt, J., 1984. Petrogenesis and evolution of an early Proterozoic collisional orogenic belt. The granulite belt of Lapland and the Belomorides (Fennoscandia). Bull. Geol. Soc. Finland, 56: 161-188.

Bebien, J., Dubois, R. and Gauthier, A., 1986. Example of ensialic ophiolites emplaced in a wrench zone: Innermost Hellenic ophiolite belt (Greek Macedonia). Geology, 14: 1016-1019.

Berthelsen, A. and Marker, M., 1986. 1.9-1.8 Ga old strike-slip megashears in the Baltic Shield, and their Plate tectonic implications. Tectonophysics, 128: 163-181.

Condie, K.C., 1982. Early and middle Proterozoic supracrustal successions and their tectonic settings. Am. J. Sci., 282: 341-357.

Dimroth, E., 1970. Evolution of the Labrador Geosyncline. Geol. Soc. Am. Bull., 81: 2717-2742.

Gaal, G., 1986. 2200 million years of crustal evolution: The Baltic Shield. Bull. Geol. Soc. Finland, 58: 149-168.

Gaal, G. and Gorbatschev, R., 1987. An outline of the Precambrian evolution of the Baltic Shield, Precamb. Res., 35: 15-52.

Gehor, S. and Havola, M., 1988. The depositional environment of the early Proterozoic Tuomivaara iron-formation and associated metasediments, eastern Finland. Geol. Surv. Finland. Spec. Pap., 5.

Hietanen, A., 1975. Generation of potassium-poor magmas in the northern Sierra Nevada and the Svecofennian of Finland. Jour. Res. U.S. Geol. Surv., 316: 631-645.

Hoffman, P.F., 1980. Wopmay Orogen: A Wilson Cycle of early Proterozoic age in the northwest of the Canadian Shield. Geol. Assoc. Canada. Spec. Pap., 20: 523-549.

Hoffman, P.F., (in print). Early Proterozoic foredeeps, foredeep magmatism, and Superior-type iron-formations of the Canadian Shield. In: A. Kroner (Editor), Proterozoic Lithospheric Evolution. American Geophysical Union, Geodynamics Series.

Kangas, R., 1985. Alaproterotsooisen Ita-Puolangan ryhman lansiosan litostratigrafia, paleosedimentaatio ja rakenne, Puolanka. Res Terrae, Ser. B, No. 8. 111pp.

Karki, A., 1988. Stratigraphy of the Kainuu Schist Belt and the palaeosedimentology of its Kalevian metasediments at Melalahti, northern Finland, Geol. Surv. Finland, Spec. Pap., 5.

Koistinen, T., 1981. Structural evolution of an early Proterozoic stratabound Cu-Co-Zn deposit, Outokumpu, Finland. Transact. Royal Soc. Edinburgh Earth Sciences, 72: 115-158.

Kontinen, A., 1986. Early Proterozoic stratigraphy and sedimentation in the Hyrynsalmi area, eastern Finland. In: V.A. Sokolov and K.I. Heiskanen (Editors), Early Proterozoic of the Baltic Shield. Proceedings of the Finnish-Soviet Symposium held in Petrozavodsk 19th-27th August, 1985. Karelian Branch of the Academy of Sciences, USSR, Petrozavodsk, pp.75-103.

Kontinen, A., 1987. An early Proterozoic ophiolite - the Jormua mafic-ultramafic complex, northern Finland. Precamb. Res., 35: 313-341.

Laajoki, K., 1986a. The Precambrian supracrustal rocks of Finland and their tectono-exogenic evolution. Precamb. Res., 33: 67-85.

Laajoki, K., 1986b. The central Puolanka Group - a Precambrian regressive metasedimentary sequence in northern Finland. Bull Geol. Soc. Finland, 58: 179-193.

Laajoki, K., 1988a. Nenakangas-type conglomerates - and evidence of a major break in the sedimentation of the early Proterozoic (Karelia) quartzites in Kainuu, northern Finland. Geol. Surv. Finland, Spec. Pap., 5.

Laajoki, K., 1988b. The Pyssykulju Formation - a late Karelian (early Proterozoic) orthoquartzite phase in Kainuu, northern Finland. Geol. Surv. Finland, Spec. Pap., 5.

Laajoki, K. and Gehor, S., (in print). The Precambrian iron formations of Finland and their tectono-sedimentary settings. In "Ancient Banded Iron Formations and Deposits (Regional Presentations)". Theophrastus Publications. S.A.

Laajoki, K. and Korkiakoski, E., (in print). The Precambrian turbidite-tempestite transition as displayed by the amphibolite-facies Puolankajarvi Formation, Finland, Sediment. Geol.

Laajoki, K. and Paakkola, J. (Editors). 1988. Sedimentology of the Precambrian formations in eastern and northern Finland. Proceedings of IGCP 160 Symposium at Oulu, January 21-22, 1986. Geol. Suv. Finland, Spec. Pap., 5.

Laajoki, K. and Saikkonen, R., 1977. On the geology and geochemistry of the Precambrian iron formation of Vayrylankyla, South Puolanka area, Finland. Geol. Surv. Finland Bull., 292: 137.

Larue, D.K., 1983. Early Proterozoic tectonics of the Lake Superior region: Tectonostratigraphic terranes near the purported collision zone. Geol. Soc. Am. Mem., 160: 33-47.

Marmo, J. and Ojakangas, R.W., 1984. Lower Proterozoic glaciogenic deposits, eastern Finland. Bull. Geol. Soc. Am., 95: 1055-1062.

Marmo, J., Kohonen, J., Sarapaa, O and Aikas, O., 1988. Sedimentology and stratigraphy of the lower Proterozoic Sariola and Jatuli Groups in the Koli-Kaltimo area, eastern Finland. Geol. Surv. Finland, Spec. Pap.,5.

Morey, G.B., 1983. Animikie basin, Lake Superior region, U.S.A. In: A.F. Trendall and R.C. Morris (Editors), Iron-Formation: Facts and Problems. Elsevier, Amsterdam, pp.13-68.

Nikula, R., 1988. Palaeosedimentology of Precambrian tidal Virttiovaara and fluvial Varttiovaara quartzite formations, Sodankyla, northern Finland. Geol. Surv. Finland, Spec. Pap., 5.

Ohlander,B., Skiold, T., Hamilton, P.J. and Claesson, L.A., 1987. The western border of the Archaean province of the Baltic Shield: Evidence from northern Sweden. Contr. Min. Pet., 95: 437-450.

Park, A.F., Bowes, D.R., Halden, N.M. and Koistinen, T.J., 1984. Tectonic evolution at an early Proterozoic continental margin: the Svecokarelides of eastern Finland. J. Geodynam., 1: 359-386.

Pekkarinen, L.J.,1979. The Karelian formations and their depositional basement in the Kiihtelysvaara - Vartsila area, East Finland. Geol. Surv. Finland Bull., 301: 141pp.

Perttunen, V., 1985. On the Proterozoic stratigraphy and exogenic evolution of the Perapohja area. In: K.Laajoki and J. Paakkola (Editors), Proterozoic exogenic processes and related metallogeny. Geol. Surv. Finland Bull., 330, pp.131-142.

Piirainen, T., 1975. The Svecokarelian orogenic cycle and related metallogenesis in Finland. Bull. Geol. Soc. Finland, 47: 139-153.

Rasanen, J. and Makela, M., 1988. Early Proterozoic fluvial deposits in the Pyhatunturi area, northern Finland, Geol. Surv. Finland, Spec. Pap., 5.

Reading, H.I.G., 1980. Characteristics and recognition of strike-slip fault systems. Spec. Publ. Int. Assoc. Sedimentologists, 4: 7-26.

Ricketts, B.D. and Donaldson, J.A., 1981. Sedimentary history of the Belcher Group of Hudson Bay. Geol. Surv. Canada, Pap. 81-10: 235-254.

Simonen, A., 1980. The Precambrian of Finland. Geol. Surv. Finland Bull., 304: 58pp.

Sims, P.K., Card, K.D. and Lumbers, S.B., 1981. Evolution of early Proterozoic basins of the Great Lake Region. Geol. Surv. Canada, Pap., 81-10: 379-397.

Sokolov, V.A. and Heiskanen, K.L., 1985. Evolution of Precambrian volcanogenic-sedimentary lithogenesis in the south-eastern part of the Baltic Shield. In: K.Laajoki and J.Paakkola (Editors), Proterozoic exogenic processes and related metallogeny. Geol. Surv. Finland Bull., 331, pp.91-106.

Stauffer, M.R., 1984. Manikewan: An early Proterozoic ocean in central Canada, its igneous history and orogenic closure. Precamb. Res., 25: 257-281.

Strand, K., 1988. Alluvial sedimentation and tectonic setting of the lower Proterozoic Kurkikyla and Kainuu Groups in Northern Finland. Geol. Surv. Finland, Spec. Pap., 5.

Tankard, A.J., Jackson, M.P.A., Erikson, K.A., Hobday, D.K., Hunter, D.R. and Minter, N.E.L., 1982. Crustal Evolution of Southern Africa. 3.8 Billion Years of Earth History. Springer-Verlag, New York, 523pp.

Vayrynen, H., 1933. Uber die Stratigraphie der karelischen Formationen. C.R.Soc.Geol. Finlande 6: 54-78. Also Bull. Comm. Geol. Finlande, 6: 54-78. 101.

Ward, P., 1987. Early Proterozoic deposition and deformation at the Karelian craton margin in southeastern Finland. Precamb. Res., 35: 71-93.

Wardle, R.J. and Bailey, D.G., 1981. Early Proterozoic sequences in Labrador. Geol. Surv. Canada Pap., 81-10:331-359.

Welin, E., 1987. The depositional evolution of the Svecofennian supracrustal sequences in Finland and Sweden. Precamb. Res., 35: 95-113.

Young, G.M. (Editor), 1973. Huronian stratigraphy and sedimentation. Geol. Soc. Canada, Spec. Pap., 12: 271pp.

CARBON ISOTOPE VARIATIONS IN CAMBRIAN - PROTEROZOIC ROCKS -- A CASE FOR SECULAR GLOBAL TREND

D.M.BANERJEE

ABSTRACT

$\delta^{13}C$ values of Lower Cambrian and Proterozoic carbonates of India, Pakistan and Mongolia show a systematic variation through time. Depletion in the Lower Cambrian, highly positive excursions in the Upper Proterozoic and near-normal distributions in the Middle Proterozoic seem to follow a global pattern as depicted by isotopic distribution data from other parts of the world. Environmental and interregional implications of these geochemical perturbations are discussed.

INTRODUCTION

It is generally believed that C^{13}/C^{12} ratios of carbonate rocks do not show any definite age trend (Craig, 1957; Galimov et al., 1968; Keith and Weber, 1964; Becker and Clayton, 1972; Schidlowski et al., 1975; Veizer and Hoefs, 1976; Schidlowski, 1986) and that the isotopic distribution shows a maximum scatter of $\sim 3^{o}/oo$ relative to PDB standard. Some workers, however, are of the opinion that the small range of $\delta^{13}C$ variation actually followed well-defined periodic perturbations and reflected systematic changes in the carbon-isotopic composition of the contemporaneous sea-water (Weber, 1967; Compston, 1960). In recent years, with enlarged data bases for the Phanerozoic carbonates and elemental carbon (organic carbon = kerogen in mature rocks), it has been possible to show secular trends in the carbon-isotopic composition and the plaeoenvironment has been largely interpreted on these evidences (Schidlowski, 1983; 1986 and Hayes et al., 1983). A reinterpretation of earlier records of carbon-isotopic compositions of Proterozoic carbonate shows more or less the same variability as that of the Phanerozoic (Schidlowski et al., 1983; Schidlowski, 1986). Due to poor sample density, paucity of well-defined age markers and resultant inadequate stratigraphic controls on the analysed samples, Precambrian secular curves generally suffer from lack of precision. Although Veizer and Hoefs

(1976) indicated a lack of a definite age trend in the $\delta^{13}C$ values of either limestones or contemporaneous primary dolomites, they certainly recorded a tendency of $\delta^{13}C$ becoming heavier in the Late Precambrian carbonates as compared to those of Phanerzoic times. It was also realized that carbonates of the early Palaeozoic era show a tendency to reflect lighter C^{13}/C^{12} ratios and it is now widely believed that this depletion is real and reflects the chemistry of the contemporaneous seawater (Eichmann and Schidlowski, 1975).

The geological sections which have been sampled and analysed for the present report belong to various levels in the Proterozoic and lower Cambrian. Conceding the facts that sample density is low, age constraints are controversial, post-depositional modifications are variable in different samples and bacterial and bacterio-diagenetic changes have played their role in some sample locations, an attempt has been made to delineate a secular tend in $\delta^{13}C$ variations of carbonates (dolomite and limestone) and carbonate associated with phosphorites of Proterozoic and Lower Cambrian rocks of India and to compare the results with the variations shown by carbonate rocks of similar ages from NW Pakistan and the Khubsugal Basin of Mongolia and other regions of the world (cf.Schidlowski et al., 1975; Knoll et al., 1986 and references therein).

The investigated geological sections were assigned different positions in the Proterozoic stratigraphy on the basis of stromatolite taxonomy, microbiota and organic-matter characteristics and temporal correlations with reference to better known sedimentary basins and their counterparts in other sectors of the world. Until recently, serious age controversies existed as to the stratigraphic position of the Krol-Tal sediments of Lower Himalaya and Aravalli rocks of Rajasthan (Banerjee, 1986). Recent studies on the skeletal microfaunas in the Tal Formation and systematic Pb-isotopic studies on syngenetic basemetal sulphides of Rajasthan, are likely to settle this age controversy in the near future.

SAMPLE LOCATION

The present report consists of carbon isotopic data from the carbonate and phosphate-carbonate rocks belonging to geological groups and formations informally designated as Tal, Krol, Khubsugal, Abbotabad, Chattisgarh, Kaladgi, Bhima-Badami,Cuddapah,

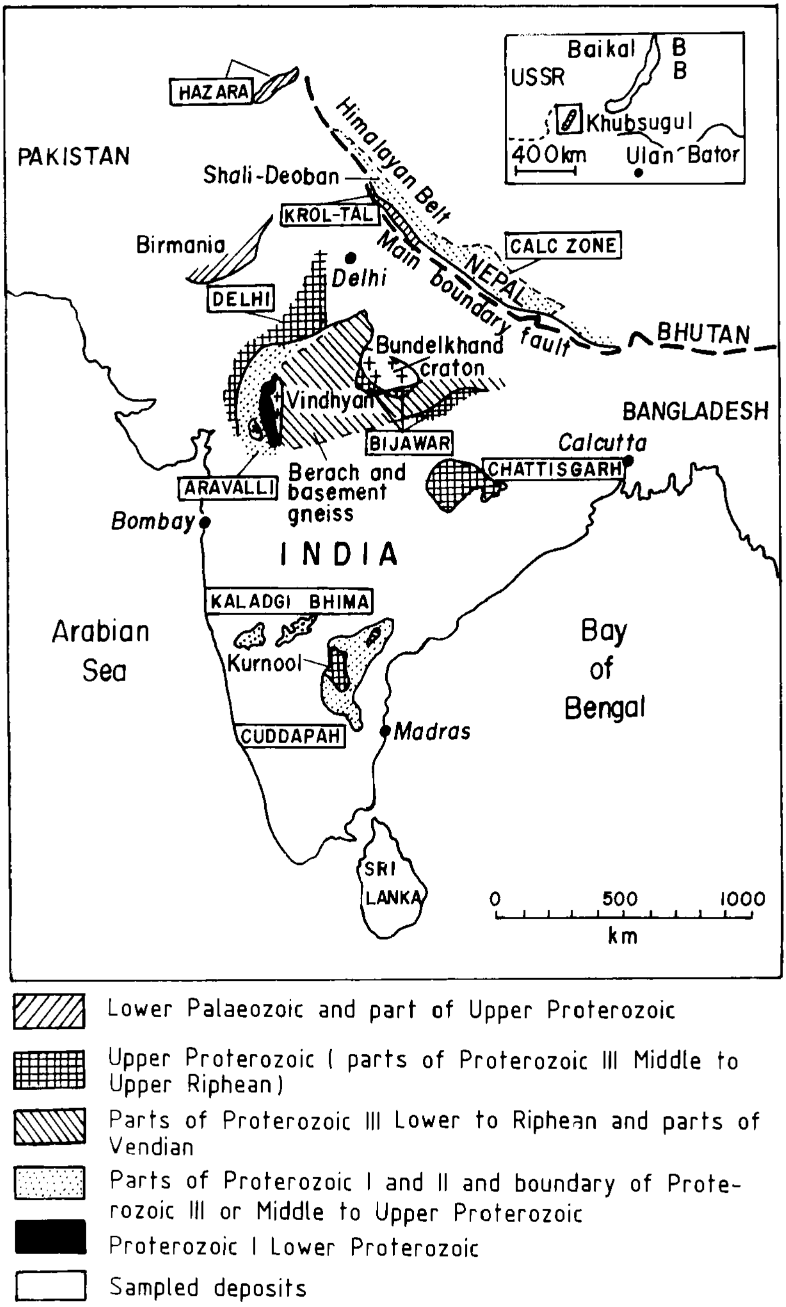
Baikal
B
B
USSR
Khubsugul
400 km
Ulan Bator
HAZARA
Himalayan Belt
PAKISTAN
Shali-Deoban
KROL-TAL
Main boundary fault
NEPAL
CALC ZONE
Birmania
Delhi
DELHI
BHUTAN
Bundelkhand craton
Vindhyan
BANGLADESH
BIJAWAR
Calcutta
CHATTISGARH
ARAVALLI
Berach and basement gneiss
Bombay
INDIA
KALADGI BHIMA
Arabian Sea
Bay of Bengal
Kurnool
CUDDAPAH
Madras
SRI LANKA
0
500
1000
km
Lower Palaeozoic and part of Upper Proterozoic
Upper Proterozoic (parts of Proterozoic III Middle to Upper Riphean)
Parts of Proterozoic III Lower to Riphean and parts of Vendian
Parts of Proterozoic I and II and boundary of Proterozoic III or Middle to Upper Proterozoic
Proterozoic I Lower Proterozoic
Sampled deposits

Figure 1. Proterozoic-Lower Palaeozoic basins of India showing sample locations.

Calc-Zone and Aravalli (Fig. 1). Lithologs of each sample location and their age connotations are given in Fig.2. Several other analytical data from the Indian Proterozoic (Schidlowski et al., 1975) and recent analyses of Vendian-Riphean Krol Dolomites (Aharon et al., 1987) have been integrated with the present study in order to draw a time-trend curve. Some of the locations mentioned in Schidlowski et al. (1975) have been assigned revised stratigraphic levels.

SAMPLE PREPARATION AND ISOTOPIC ANALYSIS

Cleanly chipped carbonates (sometimes carbonate-phosphate admixtures) were pulverized to fine powders in an agate ball mill and were treated with 100% H_2PO_4 at 35°C following McCrea (1950) and Craig (1953). The resultant CO_2 gas was collected in sealed glass tubes and subjected to mass-spectrometric analysis. Isotope ratios of both carbon and oxygen were determined for the CO_2 obtained by the phosphoric-acid treatment and measurements were performed on a Varian- Mat CHS mass spectrometer. Results are reported as values in permil relative to the conventional PDB standard. All isotope ratios are corrected for the contribution of $\delta^{17}O$ to mass 45 according to Craig (1957). The precision of the measurements is better than ± 0.15 $^o/oo$. Assays of total carbon and organic carbon were performed in an automated carbon analyzer, Strohlein Coulomat 701.

GEOLOGY AND ISOTOPE DATA

Lower Cambrian - Upper Proterozoic Sections

Krol-Tal. The discovery of trace fossils, trilobites and well-documented skeletal microfauna indicates a Tommotian age (Lower Cambrian) for the Lower Tal Formation of Lower Himalaya. This formation, with chert, phosphorite, black shale and carbonate (Fig. 2), overlies a dominantly dolomitic Upper Krol Formation. The Proterozoic-Cambrian boundary lies within a few meters below the Krol-Tal junction, within the uppermost part of the Krol-E Unit of the Upper Krol Dolomite (Aharon et al., 1987). The Upper Krol dolomitic formation with minor shales, limestone and sandstones, is Vendian to Uppermost Riphean in age in view of the sporadic occurrence of a typical Conophyton and many other palaeogeographic constraints, such as the stratigraphic position of these beds in relation to Proterozoic Blaini glacial beds at the base (Banerjee, 1986).

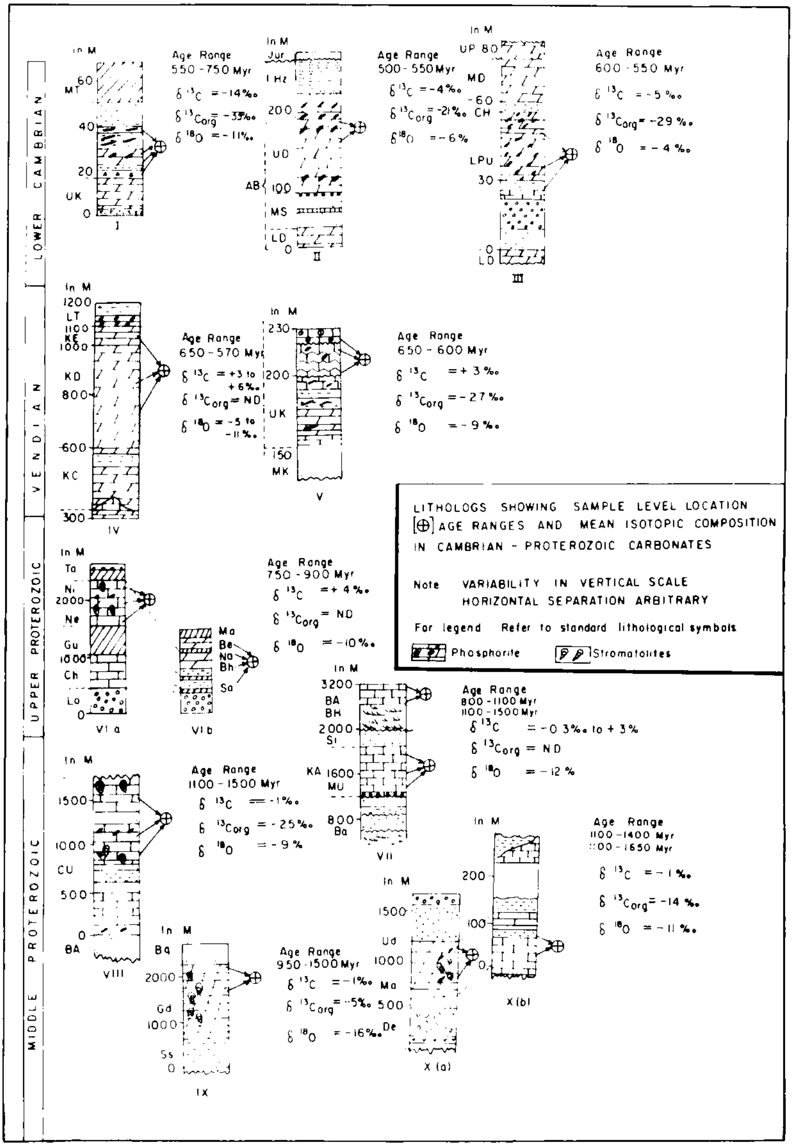

Figure 2. Lithologs with relevant geological and geochemical data arranged on a Proterozoic-Cambrian time scale, depending on $\delta\ ^{13}C$ variation through time.

(i) Tal Formation in Mussorrie Hills, Lower Himalaya, (ii) Abbotabad Formation, N.W. Pakistan, (iii) Dolomite-Phosphate Unit, Khubsugul, Mongolia, (iv) Upper Krol Formation in Mussoorie Hills, (v) Upper Krol Formation in Nainital Hills, (vi) Raipur Formation in Chattisgarh Basin, central India, (vii) Bhima (Badami)-Kaladgi Groups of South India, (viii) Cuddapah Group of South Central India, (ix) Calc Zone of Pithoragarh, Lesser Himalaya, (xa) Aravalli Group at Udaipur, Western India and (xb) Aravalli Group at Jhabua in Central India.

Carbonates of the Lower Tal Formation, frequently associated with dark-grey phosphorites, have yielded a markedly negative $\delta^{13}C$ with average values of -14 ± 4.8 ^{o}/oo with the heaviest value of -6.3^{o}/oo. A $\delta^{18}O$ value of -11.4±0.9^{o}/oo for the carbonates is apparently normal and belongs to a 'normal' marine carbonate regime.

The Krol dolomite (Krol E) of the Mussoorie hills of Garhwal Himalaya, underlying the Tal Formation, shows a marked shift of $\delta^{13}C$ values in the positive direction. The gradual change of $\delta^{13}C$ values to ≈+2^{o}/oo in the Krol E is attended by a record shift in the upper parts of Krol D (See Fig. 2 for stratigraphic position, where the $\delta^{13}C$ value goes upto + 6^{o}/oo, showing a remarkable excursion to a highly positive value from extremely low carbonate values of the Lower Tal Formation. There is a slight decline in the isotope value for the carbonates of the lower parts of Krol D and Krol C (3.5^{o}/oo) which fluctuates within a range of 0.3 to 3^{o}/oo. These positive $\delta^{13}C$ records of the Krol carbonates have been discussed by Aharon et al., (1987).

The overall lithological association in the Upper Krol dolomite of Nainital hills in Kumaun Himalaya (Fig. 2) indicates an euxinic facies within a carbonate-bank environment. Oolitic dolomites and pelletal carbonates (and minor phosphates) have yielded $\delta^{13}C$ values very close to + 3.2^{o}/oo, consistent with positive $\delta^{13}C$ values shown by the dolomitic rocks of the same age from the Mussoorie hills. The overlying phosphate-bearing Tal Formation is not documented in the Nainital hills.

Abbotabad. In NW Pakistan, overlying the Proterozoic Tanakki boulder bed and also the Hazara and Tanawal formations, there lies a thick sequence of unmetamorphosed shale, sandstone, and dolomite. Some of these dolomites contain phosphate. On the basis of faunal evidence, Abbotabad dolomites are placed in the Lower Cambrian. Phosphate-bearing dolomite samples from the upper 10 meters of the Upper Dolomite unit yielded a mean $\delta^{13}C$ value of -4^{o}/oo and a $\delta^{18}O$ value of -6.5^{o}/oo (Banerjee, 1986). In spite of being similar in age to that of the Tal Formation of Mussoorie hills, the low C_{org} values (~0.16%) of the Abbotabad dolomites (as compared to the Tal carbonate mean, 1.1%) and the virtual absence of any evidence for the euxinic facies assemblage seem to govern the isotopic fractionation and limit the $\delta^{13}C$ excursion to within -3 to -4^{o}/oo.

Khubsugul. Extensive phosphate-carbonate deposits overlying the Vendian dolomites of this Mongolian deposit (Fig. 2), have yielded some Lower Cambrian microfauna. The carbonates, associated with pelletal and massive phosphorites (Ilyin et al., 1986), have been collected from various exploratory trenches, particularly trenches 12 and 6. Dolomite in the Lower Phosphate Member has yielded $\delta^{13}C$ values of -4 to $-5^{o}/oo$ and imitates the Vendian-Lower Cambrian boundary situation. High C_{org} values (0.5 to 0.7 % maximum 1.1%) are indicative of a high productivity zone in the ancient sea bottom. Heavy $\delta^{18}O$ values ($-3.7^{o}/oo$) are somewhat intriguing.

Upper Proterozoic

Chattisgarh. The stratigraphy of the carbonate rocks from the undisturbed limestone-dolomite sequence near Raipur in Madhya Pradesh has been established and reinterpreted a number of times. Schnitzerd's (1969) facies-based stratigraphy (Fig.2, VIb) formed the basis of sample locations for Schidlowski et al., (1975). Recently, Murthy (1987) has reconstructed a new stratigraphic column (Fig. 2 Vl (a)) for these same rocks. Stromatolite biostratigraphy favours an Upper Proterozoic (Riphean) age for this formation. The discussion of these samples includes five analyses from Schidlowski et al., (1975) and two new analyses of the uppermost dolomitic formation (Fig. VI(a)). $\delta^{13}C$ values lie between + 3-4% while $\delta^{18}O$ values are ≈-14%.

Bhima, Badami and Kaladgi. The Bhima Formation, coeval with the Badami Formation in Karnataka State of South India, is made up of light-coloured flaggy dolomites with basal sandstone and conglomerate (Satyanarayana et al., 1987; Jayapraksh et al., 1987). These rock seqeuences have been assigned a tentative Upper-Proterozoic to Vendian age. Cyclic clastics and carbonate rocks of the Kaladgi Group with stromatolite assemblages underlie Bhima Formations. Upper to Middle Proteozoic (1000-1260 Ma) ages have been suggested for the Kaladgi.

Flaggy carbonates of Bhima (=Badami) are poor in organic matter (0.04%) and display heavy carbonate contents in the range of $+ 3.4 \pm 0.5^{o}/oo$, atypical of a 'normal'marine carbonate but consistent with the pattern shown by the Upper Proterozoic carbonates of other basins. $\delta^{18}O$ values of $- 9.4 \pm 1.2^{o}/oo$ are decidedly normal for the rocks of this age. The Kaladgi carbonates have yielded

$\delta^{13}C$ values in the range of 0.3 ± 1.2^{o}/oo, which shows a very limited scatter away from the typical 'marine' water carbonate (0 ^{o}/oo). These values are in marked contrast to positive $\delta^{13}C$ values for the overlying Badami and Bhima carbonates.

Cuddapah. Overlying a shallow-water quartz-arenite unit, the Cumbum Formation of Cuddapah (Fig. 2, VIII) contains stromatolitic dolomite with minor phosphorites and is extensively developed in parts of Andhra Pradesh. Based on several lines of evidence-radiometric, biostratigraphic (stromatolite based), spatial and temporal correlations, the Cuddapah Group as a whole is placed in Middle Proterozoic (1100-1500 Ma). Samples for the isotopic analysis have been taken from lower parts of the Cumbum Formation. One analysis from Schidlowski et al., (1975) ($\delta^{13}C$ = 0.9^{o}/oo) has also been used in this report. Phosphate-bearing dolomite has yielded a $\delta^{13}C$ value of + 1.1^{o}/oo and $\delta^{18}O$ values of - 8 to $1\text{-}10^{o}$/oo.

Calc zone. The Calc zone of Pithoragarh in Kumaun Himalaya bordering Nepal in the east, is made up of lower-slate, middle--carbonate and upper-arenaceous facies. The carbonate unit contains stromatolite, phosphorite and magnesite. Stromatolite biostratigraphy indicates a Middle-Proterozoic age for these rocks. $\delta^{13}C$ values for the carbonates are close to - 1^{o}/oo, very similar to the ideal marine-water value of 0^{o}/oo. $\delta^{13}C_{org}$ values are exceptionally high, and since the metamorphic effects on the rocks are negligible, the heavy kerogen apparently represents the primary organic matter.

Aravalli. The Aravalli Supergroup of rocks, with basal conglomerate and quartzite, grades upward into carbonaceous phyllite and dolomite which are occasionally rich in stromatolitic phosphorites (Banerjee, 1985). The carbonate samples used in this study occur with stromatolitic phosphorite. The exact age of the Aravalli carbonate is disputed and no consensus exists. Recent views suggest 1700 Ma for the type Aravalli sediment of the Udaipur region. Geological and stromatolite morphometric correlation of the type Aravalli of the Udaipur Valley with that of Aravalli carbonates from Jhabua indicates a possibly younger time frame for the latter (Fig. 2 Xa,b). $\delta^{13}C$ values of - 0.7 ± 0.8^{o}/oo and $\delta^{18}O$ values of - 12.1 ± 2^{o}/oo are well within the range of variation shown by the marine carbonates. Only $\delta^{13}C_{crg}$ is exceptionally heavy (- 14^{o}/oo).

Except for Aravalli dolomite and some sections of Calc Zone carbonates, none of the Proteozoic or Cambrian samples have suffered metamorphism. The Aravalli and Calc Zone samples in particular have been collected from areas showing a maximum of greenschist facies of metamorphism. Sections affected by higher than greenschist facies transformation have been excluded from the study.

DISCUSSION

In all earlier studies related to isotopic variations (Veizer and Hoefs, 1976; Schidlowski et al., 1976, 1983; Banerjee et al., 1986 and many others), $\delta^{13}C$ values (often in conjuction with $\delta^{13}C_{org}$ and $\delta^{18}O$) have been evaluated as being pristine or reflecting primary modifications in the carbon-isotopic ratio during biologically mediated synthesis. The present analysis of the available carbon isotopic data from the Indian Proterozoic and Cambrian carbonates is also aimed at establishing the primary nature of the C^{13}/C^{12} ratio and evaluating its significance as against $\delta^{13}C$ shifts caused by isotopic exchange in response to biological activities, diagenesis and/or metamorphism. Comparison of $\delta^{13}C$ isotopic data from various Proterozoic-Cambrian sequences of the world with those from India, Pakistan and Mongolia, is directed toward understanding the changes in global environment through the Proterozoic and Early Phanerozoic and assess the possible effects of changing oxygen and carbon budgets on the sedimentation in the contemporaneous Proteozoic-Cambrian sea.

$\delta^{13}C$ values plotted against geological formations were arranged in increasing order of age (Fig. 3) and a scatter diagram (Fig. 4) was made depicting the range of $\delta^{13}C$ variation through time. The most important aspect of these depictions is that they show a more or less well-defined time-trend in $\delta^{13}C$ ratios between Middle Proterozoic and Cambrian. Most of the early investigators have found a relative constancy in Phanerozoic $\delta^{13}C$ carbonate values transgressing well into the Precambrian, with the exception of some excursions into the positive field (Schidlowski et al., 1975; Keith and Weber, 1964; Becker and Clayton, 1972 and many others). The relative constancy of carbon values through geological times is quite outstanding and it perhaps indicates that sedimentary carbon was almost always partitioned between C_{org} and δC_{carb} in the ratio of 20:80 (Schidlowski et al., 1983; Hayes et al.,

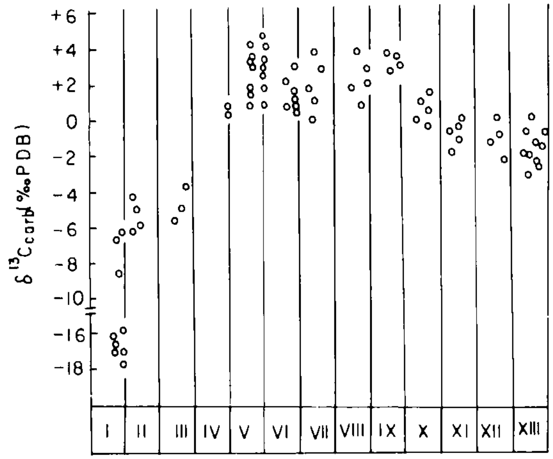

Figure 3. $\delta^{13}C$ plot against various geological units. A low isotopic value on the left half of the figure is followed by a major spurt in the central part and tapering down to normal level in the right side of the figure.

I-Lower-Cambrian Tal, II, Lower-Cambrian Abbotabad, III. Khubsugul Vendo-Cambrian, IV, Vendian Krol-E-Member V. Vendian Krol, D Member, VI Riphean Krol -C, VII-Vendian-Riphean Krol-D (Nainital), VIII-Upper-Proterozoic Chattisgarh, IX. Upper-Proterozoic-Bhima and Badami, X Upper to Middle-Proterozoic Kaladgi, XI. Middle--Proterozoic Calc zone, XII, Middle-Proterozoic to Upper--Proterozoic Cuddapah, XIII Middle-Proterozoic Aravalli (Udaipur and Jhabua). Open Circles are carbonates.

1983). However, some investigators have recorded that isotopic age curves for carbonate carbon show displacement towards heavier $\delta^{13}C$ around the Precambrian-Cambrian boundary (Veizer and Hoefs, 1976). Such variations have also been recorded recently by Banerjee et al. (1986), Knoll et al. (1985), Aharon et al. (1987), Lambert et al. (1987), but the interpretations are varied and controversial.

Carbonate constituents of the Tal Formation immediately overlying the Proterozoic-Cambrian boundary, clearly demonstrate highly anomalous isotopic signatures. $\delta^{13}C_{carb}$ values of 14 ± 4.8 ^{o}/oo (heaviest recorded being - 6.3^{o}/oo) for the dolomite (associated with organic-rich pelletal phosphorite) are considerably below the value for normal marine carbonates which is close to zero permil (Schidlowski et al., 1983). In line with ideas of Becker and Clayton (1972) and Bauer et al., (1985), it can be suggested that such unusual organic-rich carbonates have incorporated a large quantity of isotopically light bicarbonate whose CO_2

precursor was apparently generated at the sites of extensive organo-sedimentary mineralization. Such large-scale production of biologically mediated bicarbonate ion could have suppressed the low seawater influence and favoured preferential precipitation of light carbonates. Such carbonates would therefore display an inheritance of the isotopic characters of the biological source material. Anaerobic decomposition of organic matter with simultaneous release of δC^{13}-depleted carbon dioxide was apparently widespread during Tal sedimentation, primarily due to the euxinic environment of the primary depositional basin. Ubiquitous pyrite in the dolomites (and also in phosphorites) suggests that a major portion of the isotopically light CO_2 which ultimately generated CO_3^{-2} component of the newly formed carbonate, was made available by the bacterial sulphate reducers proliferating in anoxic bottom mud. The associated apatite-bound carbonate shows fairly negative $\delta^{13}C$ values (-7.3 ± 4.8) although much heavier than the host carbonates. It has been tentatively interpreted that the carbon of apatite-bound CO_3^{-2} and that of host carbonate originated in the same bicarbonate pool, which remained consistently buffered by biological contributions. Preferential concentration of lighter bicarbonate (although much lower than the average marine carbonate) in the host-rock dolomites, compared to phosphorite, was apparently due to hitherto unknown reasons (Banerjee et al., 1986). It is possible that such a highly unusual and negative excursion of $\delta^{13}C$ values marks the early phase of Proterozoic--Cambrian (or Vendian-Cambrian) to the precise transition (see Knoll et al., 1986; Awramik, 1986). These negative excursions appear to represent the responses of the oceans to changes caused by widespread biomineralization and rapid diversification and proliferation of phytoplankton. It may be possible in the future to document that such geochemical perturbations were linked to the generation of external stimuli resulting in the early evolution of metazoans, thereby unbalancing the near-steady C_{org} and C_{carb} ratio during the Early Cambrian. Hsu et al., (1985) found similar negative values for $\delta^{13}C$ in some Lower Cambrian beds of China which are accompanied by increased iridium, osmium and gold contents. Such deviations from the normal concentration values possibly reflected a fertility crisis (Hsu et al., 1985) caused by mass mortality, phosphate removal from the seawater and its extensive precipitation during this period, widespread increase in the organic-matter fixation in the sediments and total unbalance in the carbon budget of the sedimentary pool.

In the Abbotabad Formation of NW Pakistan and the Khubsugual phosphate deposits of Mongolia, the negative character of $\delta^{13}C$ persists ($-4^{o}/oo$ to $-6^{o}/oo$) and compares with $\delta^{13}C$ values of apatite-bound carbonates of the Tal formation. These values are also comparable to Lower-Cambrian-Vendian carbonates from China (Hsu et al., 1985; Awarmik, 1986).

Immediately underlying the Lower Cambrian formation in the Mussoorie hills, the Krol-E marks the latest Vendian stage. It reflects a new normal $\delta^{13}C$ value ($+ 0.3^{o}/oo$). This is followed by a definitive excursion (explosive or progressive?) of $\delta^{13}C$ within + 2 to $5^{o}/oo$. That these isotopic values are pristine and reliable is indicated by petrographic data, paucity or organic matter in the carbonate matrix, $^{87}Sr/^{86}Sr$ data of textural variants and undisturbed biological markers in the rocks(Aharon et al., 1987). However, establishing a truely uncontaminated isotopic composition of old sediments and identification of all secondary modification processes is an onerous task (Brand and Veizer, 1981). Knoll et al., (1986) have further emphasized that no secondary processes are known which would religiously shift the isotopic composition of carbonate carbon and organic carbon in the same direction and at the same rate. Oxygen isotopic signatures are insignificant in such interpretations, since it is well established that in geologically older rocks, post-depositional $O^{18}/^{16}O$ exchange with the isotopically light meteoric and surface waters results in $\delta^{18}O$ depletion. In contrast, only one of the carbons (carbonate carbon or organic carbon) is affected at a time (Hayes, 1983) when secondary processes modify the carbon-isotopic signature. In the present study, relatively few organic-carbon isotopes could be measured, primarily due to paucity of organic matter in most Proterozoic carbonates. Wherever $\delta^{13}C_{org}$ values are available, they show similar orders of depletion or enrichment as demonstrated by $\delta^{13}C_{carb}$. Due to such close parallelism of organic- and carbonate-carbon distribution patterns, the potentiality of using these geochemical perturbations as chemochronostratigraphic signals for long-range intrabasinal correlation increases. Such a viewpoint lends weight to the observations of Hsu et al., (1985), Knoll et al., (1986) and Morris and Bengtson (1986).

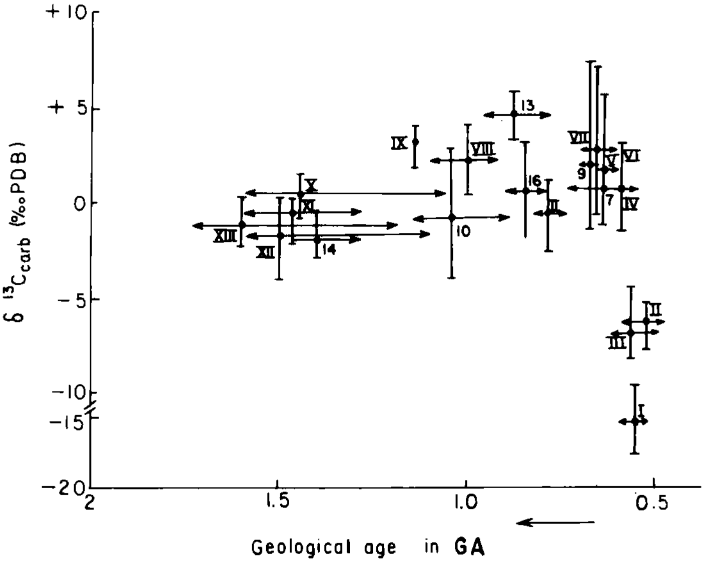

Figure 4. Carbon-isotope compositions of unaltered and slightly altered carbonates as a function of time. Mean $\delta^{13}C$ values are indicated by circles. Horizontal arrow shows possible time range. Vertical lines indicate standard deviation.

Arabic numbers refer to Table Nos. in Schidlowski et al., (1975) and roman numbers follow the legend in Fig.3.

The most significant features depicted by Figs. 3 and 4 are a strong depletion of carbonate isotope in the lowermost Cambrian (with fairly light $\delta^{13}C_{org}$ values), gradual excursion into the positive field during the Late Vendian (still showing a fairly low negative range with respect to 'normal' marine carbonates) and a strong enrichment during the Lower Vendian and Riphean (Upper Proterozoic). This Upper-Proterozoic enrichment level is more or less maintained within ± 2^{o}/oo , until a negative excursion commences at the beginning of the Middle-Proteozoic which ultimately reaches a level of near stabilization at zero permil. Following the explanations presented by Schidlowski et al., (1975, 1983) and many others, it can be stated that the Mid-Proterozoic $\delta^{13}C$ trend remained more or less constant during the Lower Proterozoic and Archaean, and the episodes of carbon-isotopic excursions remained close to near 'normal' values.

Some unusual $\delta^{13}C_{org}$ values in Middle-Proterozoic carbonates associated with stromatolitic phosphorites of the Aravalli Supergroup warrants special mention. While $\delta^{13}C$ values of the carbonates have a near 'normal' to slightly negative trend, organic carbon ($\delta^{13}C_{org}$= -15.1 ± 2.9^o/oo) shows a markedly heavier excursion compared to the mainstream of fossil $\delta^{13}C_{org}$ records (-25 to -27^o/oo). Metamorphism within the lower ranges of green-schist facies and occurrences as vertically standing columnar stromatolites support the contention that $\delta^{13}C_{org}$ values shown by these carbonates are original isotopic signatures of the kerogen fraction.

These stromatolite-related heavy-organic carbons seem to imply a derivation from cyanobacterial progenitor material which, in turn, points towards a modern cyanobacteria-controlled diffusion limited assimilatory pathway. Such an assimilatory route of organic carbon is known to cause a marked enrichment in ^{13}C compared to other autotrophs and the degree of enrichment is apparently linked to the salinity of the medium (Schidlowski et al., 1985). As reported by Banerjee et al. (1986), these stromatolitic carbonates constitute the first record of organic contents whose $\delta^{13}C_{org}$ values are identical to the contemporary benthic microbial ecosystems of "stromatolitic type". Another case of exceptionally heavy organic carbon (≈5^o/oo) is found in the Middle-Cambrian carbonates of the Calc Zone in the Himalaya. This indicates their derivation from 'super heavy' organic progenitor materials (Banerjee et al., 1986). Super heavy biomass of such type was apparently derived from saline sabkha and near-coastal environments (Schidlowski et al., 1985). The association of synsedimentary magnesite points towards an evaporitic condition.

The highly positive trend of $\delta^{13}C_{carb}$ shown by the Krol dolomites of Nainital was originally interpreted as due to hyper-saline evaporitic conditions of deposition (Banerjee et al., 1986). This interpretation appears superfluous in view of the Upper-Proterozoic age of the Krol dolomite and a commonality of positive trends in all Vendian Riphean (Upper Proterozoic) carbonates (Figs.2,3 and 4). Alternatively, it can be argued that all Vendian-Upper Riphean carbonates were formed in widespread and persistent evaporitic situations. This phenomenon is possibly global, as is evident from the studies carried out by Knoll et al., (1986). It can be further argued that peculiar isotopic excursions to very negative and very positive $\delta^{13}C$ values between the Lower-Cambrian and Upper-Proterozoic were caused by locally restricted basinal conditions, where they were generated either due to preferential fixation and accumulation or bacteriogenic removal of organic carbon. These processes could have caused enrichment of the carbonates in heavy isotopes during the Upper--Proterozoic and depletion in the Lower Cambrian, especially when atmospheric diffusion and local circulation patterns failed to maintain isotopic equilibrium with the open ocean. It is also possible that such short-term excursions of $\delta^{13}C$ to the heavy realm are due to an unusual isotopic composition of the sea water in the Upper-Proterozoic caused by global transfer of $\delta^{12}C$ into organic matter. This point is further amplified by the synchroneity of these geochemical anomalies with an increased phosphogenic episode during the Upper-Proterozoic, reaching its zenith at the Precambrian/Cambrian boundary (Cook and McElhinny, 1979) and coinciding with the 'Fifth Cycle' of global Proterozoic-Cambrian phosphogenesis (Banerjee, 1985).

The suggestion that these isotopic perturbations are regional or even global is stimulated by the consistency in the isotopic distribution pattern shown by the data points from Cambrian carbonates of India, Pakistan and Mongolia, of all major Upper--Proterozoic and Mid-Proterozoic carbonates of India, and of several continents, as cited in Knoll et al. (1986); Schidlowski et al., (1975) and Aharon et al., (1987). The present study and the regional survey of available isotopic data demonstrates their utility not only as a tool for inter-regional correlation, but also for significant interpretations of palaeoclimates, phosphogenesis, organochemical base-metal sulphide fixation and palaeoweathering processes. It has to be conceded at this juncture that the secular trends demarcated in the present study suffer from a lack of precise age data and a very small $\delta^{13}C_{org}$ data base. In order to produce a more definitive evolutionary model, more detailed profile-wise sampling, $\delta^{13}C_{carb}$ and $\delta^{13}C_{org}$ estimations and simultaneous sulphur-isotopic measurements would be required.

ACKNOWLEDGEMENTS

Analyses were carried out at the Max Planck Institut fur Chemie, Mainz, West Germany, during the tenure of an Alexander von Humboldt Foundation Fellowship in 1982-84. Discussions with Manfred Schidlowski, Paul Aharon, Indrabir Singh, Mihir Deb during the last few years provided the stimulus for writing this paper.

REFERENCES

Aharon, P., Schidlowski, M. and Singh, I.B., 1987. Chronostratigraphic markers in the End-Precambrian Carbon Isotope Record of the Lesser Himalaya. Nature, 327, 6124 : 699-702.

Awaramik, S.M., 1986. The Precambrian-Cambrian boundary and geochemical perturbations. Nature, 319, 6055: 696-697.

Banerjee, D.M., 1985. Proterozoic stratigraphy of the Indian Platform and the Concept of Phosphogenic cycles - A Proposal. Bull. Geol. Surv. Finland, 331: 73-89.

Banerjee, D.M., 1986. Proterozoic and Cambrian Phosphorites - Regional Review: Indian Subcontinent, In P.J.Cook and J.H.Shergold, (Editors), Phosphate Deposits of the World, v.1, Proterozoic - Cambrian Phosphorites, Cambridge University Press, pp.70-90.

Banerjee, D.M., Schidlowdki, M. and Arneth, J.D., 1986. Genesis of Upper Proterozoic - Cambrian Phosphorite Deposits of India: Isotopic inferences from carbonate fluorapatites, carbonate and organic carbon, Precamb. Res., 33: 239-253.

Bauer, M.E., Hayes, J.M. Studley, S. and Walter, M.R., 1985. Millimeter scale variations of stable isotope abundances in carbonates from banded iron-formation in the Hamersley Group of Western Australia, Econ. Geol., 80: 270-282.

Becker, R.H. and Clayton, R.N., 1972. Carbon isotope evidence for the origin of banded iron formation in Western Australia, Geochim, Cosmochim. Acta, 36: 577-597.

Brand, U. and Veizer, J., 1981. Chemical diagenesis of multicomponent carbonate system- 2.Stable Isotopes, J. Sed. Petrol., 51: 987-997.

Compston, W., 1960. The carbon isotopic composition of certain marine invertebrates and coals from the Australian Permian, Geochim. Cosmochim. Acta, 18: 1-22.

Cook, P.J. and McElhinny, M.W., 1979. A revaluation of the spatial and temporal distribution of Sedimentary Phosphate deposits in the light of Plate tectonics, Econ. Geol., 74: 315-330.

Craig, H., 1953. The geochemistry of stable carbon isotopes, Geochim. Cosmochim. Acta, 3: 53-92.

Craig, H., 1957. Isotopic standards for carbon and oxygen and correlation factors for mass spectrometric analyses of carbon dioxide, Geochim. Cosmochim. Acta, 12: 133-149.

Eichmann, R. and Schidlowski, M., 1975. Isotopic fractionation between coexisting organic carbon - carbonate pairs in Precambrain sediments, Geochim. Cosmochim. Acta, 39: 585-595.

Galimov, E.M., Kuznetsova, N.G. and Prokhorov, V.S., 1968. The composition of the former atmosphere of the Earth as indicated by isotope analysis of Precambrian carbonates, Geochem. Internat., 5: 1126-1131.

Hayes, J.M., 1983. Geochemical evidence bearing on the origin of aerobiosis A speculative hypothesis, In: J.W.Schopf (Editor), Earth's Earliest Biosphere: Its origin and Evolution, Princeton University Press, Princeton, N.J., pp.291-301.

Hayes, J.M., Kaplan, I.R. and Wedeking, K.W., 1983. Precambrian organic geochemistry: Preservation of the record, In: J.W.Schopf (Editor), Earth's Earliest Biosphere: Its origin and Evolution, Princeton University Press, Princeton, N.J., pp.93-134.

Hsu, K.J., Oberhansli, H., Gao, J.Y. Sun Shu, Chen Haihong and Krahenbuhl, U., 1985.'Strangelov' Ocean before the Cambrian exploitation, Nature, 316: 809-811.

Ilyin, A.V. Zaitsev, N.S. and Bjamba, Z., 1986. Proterozoic and Cambrian phosphorite Deposits: Khubsugul, Mongolian People's Republic, In P.J.Cook and J.H.Shergold (Editors), Phosphate Deposits of the World, v.1, Proterozoic and Cambrian Phosphorites, Cambridge University Press, pp.162-174.

Jayaprakash, A.V., Sundaram, V., Hans, S.K. and Mishra, R.N., 1987. Geology of the Kaladgi - Badami Basin, Karnataka. In: Purana Basins of Peninsular India. Mem. Geol. Soc. India. Mem. 6: 201-225.

Keith, M.L. and Weber, J.M. 1964. Carbon and oxygen isotopic composition of selected limestones and fossils, Geochim. Cosmochim. Acta, 28: 1787-1816.

Knoll, A.H., Hayes, J.M., Kaufman, A.J., Sweet, K. and Lambert, I.B., 1986. Secular variation in carbon isotope ratios from Upper Proterozoic successions of Svalbard and East Greenland, Nature, 6073: 832-838.

Lambert, I.B., Walter, M.R., Wenlong, Z., Songnian, L. and Guogan, M., 1987. Plaeoenvironment and Upper Proterozoic Carbonates of the Yangtze Platform, Nature, 328: 140-142.

McCrea, J.M., 1950. On the Isotopic chemistry of carbonates and a palaeotemperature scale, Jour. Chem. Phys., 18: 849-857.

Morris, S.C. and Bengtson, S., 1986. The Precambrian-Cambrian boundary and geochemical perturbations, Nature, 319, 6055: 696-697.

Murthy, K.S., 1987. Stratigraphy and Sedimentation in Chattisgarh Basin. In: Purana Basins of Peninsular India, Geol. Soc. India, Mem.6: 239-260.

Satyanarayana, S., Schidlowski, M. and Arneth, J.D. 1987. Stable Isotope geochemistry of sedimentary carbonates from the Proterozoic Kaladgi, Badami and Bhima Groups, Karnataka, India, Precamb. Res., 37: 147-156.

Schidlowski, M., Hayes, J.M. and Kaplan, I.R., 1983. Isotopic inferences of ancient biochemistries: carbon, sulfur, hydrogen and nitrogen, In: J.W. Schopf (Editor), Earth's Earliest Biosphere: Its Origin and Evolution. Princeton University Press, Princeton, N.J, pp.149-186.

Schidlowski, M., 1984. Biological modulation of the terrestrial carbon cycle: isotope clues to early organic evolution, Adv. Space Res., 4(12): 183-193.

Schidlowski, M., Matzigkeit, U., Mook, W.G. and Krumbein, W.E. 1985. Carbon isotope geochemistry and ^{14}C ages of microbial mats from the Gavish Sabkha and the Solar Lake, In: G.M. Friedman and W.E. Krumbein (Editors), Hypersaline Ecosystems: Ecological Studies, 53, Springer Verlag, Berlin: 381-401.

Schidlowski, M., 1986. $\delta^{13}C/^{12}C$ Ratios as Indicators of Biogenecity, In: R.B.Johns (Editor), Biological Markers in the Sedimentary Record. Methods in Geochemistry and Geophysics, Elsevier, Netherlands, 24, pp.347-361.

Schidlowski, M., Eichmann, R. and Junge, C.E., 1975. Precambrian sedimentary carbonates: carbon and oxygen geochemistry and implication for the terrestrial oxygen budget, Precamb. Res., 2: 1-69.

Schnitzer, W.A., 1969. Zur stratigraphic and Lithologie des nordichen Chattisgarh - Becken (Zentral Indien) Unter besonderer Berucksichtigung von Algenriff Komplexenzdt. Geol. Ges.: 290-295.

Veizer, J. and Hoefs, J., 1976. The nature of $\delta^{18}O/^{16}O$ and $\delta^{13}C/^{12}C$ secular trends in sedimentary carbonate rocks; Geochim. Cosmochim. Acta, 40: 1387-1395.

Weber, J.N., 1967. Possible changes in the isotopic composition of the oceanic and atmospheric carbon resevoir over geologic time, Geochim. Cosmochim. Acta, 31: 2343-2351.

MIDDLE-PROTEROZOIC MICROFOSSILS FROM THE NAUHATTA LIMESTONE (LOWER VINDHYAN), ROHTASGARH, INDIA

B.S.VENKATACHALA, V.K.YADAV AND MANOJ SHUKLA

ABSTRACT

A well-preserved assemblage dominated by coccoid cyanobacteria associated with a few filamentous forms is reported from the Lower-Vindhyan black cherts associated with the Nauhatta Limestone (1400-1000 Ma) exposed in the easternmost margin of the Vindhayan Basin. The taxa described include *Myxococcoides reticulata* Schopf; *Palaeoanacystis vulgaris* Schopf; *Sphaerophycus parvum* Schopf; *Eosynechococcus medius* Hofmann; *Tetraphycus major* Oehler; *Diplococcus* sp.; *Bigeminococcus* sp.; *Huroniospora* sp.; *Glenobotrydion* sp.; *Eoentophysalis belcherensis* Hofmann; *Eomycetopsis robusta* Schopf; *Siphonophycus kestron* Schopf; *Biocatenoides* sp. The biota is interpreted as having inhabited a shallow intertidal environment.

INTRODUCTION

The Vindhyan Supergroup (ca. 1400-700 Ma) represents a large sedimentary sequence surrounding the Bundelkhand massif extending from Dehri-on-Sone to Hoshangabad and from Chittorgarh to Agra and Gwalior. It contains diversified stromatolitic bioherms which are a testimony to extensive biological activity. Significant microfossils represented by acritarchs and coccoid and filamentous cyanobacteria have been reported by Maithy and Shukla (1977); McMenamin et al., (1983) and others. *Hyoliths* (Rode, 1946), *Misracyathus* an *Archaeocyathid* (Misra, 1949, see also Volgdin, 1957) and circular algal carbonaceous structures (Misra and Bhatnagar, 1950) are known from the Rohtasgarh area.

A distinctive filamentous and coccoid cyanobacterial assemblage from the Nauhatta limestone (Semri Group) is described from a study of petrographic thin sections.

GEOLOGICAL SETTING

The Vindhyan Supergroup is divided into two lithostratigraphic units viz., Lower and Upper Vindhyan (Auden, 1933). The

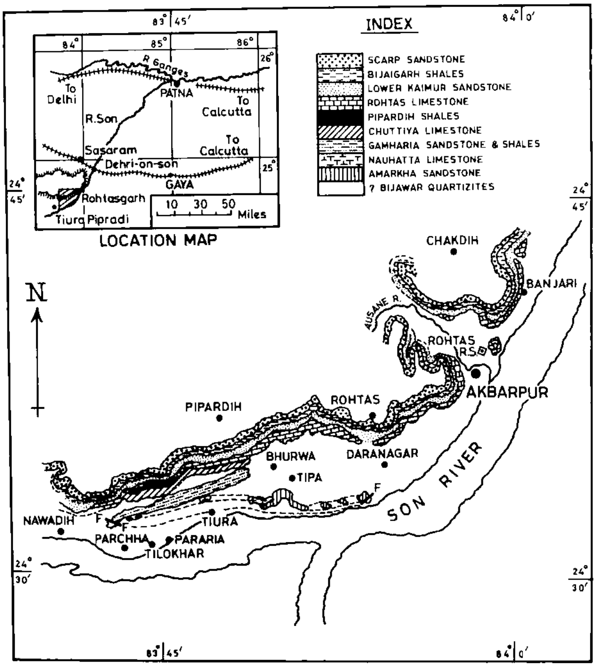

Figure 1. Geological map of the eastern part of the Vindhyan Basin.

Lower-Vindhyan (Semri Group) is unconformably overlain by the Upper-Vindhyan composed of the Kaimur, Rewa and Bhander Groups in lithochronological order from base to top.

The Semri and Kaimur Groups are exposed at Rohtasgarh, Bihar and constitute the easternmost fringe of the Vindhyan Basin (Fig. 1). The Semri Group mainly consists of calcareous facies while the Kaimur Group is mainly arenaceous (Table 1). These rocks are not tectonically affected, with the result the dips are low (5^{o} to 20^{o}) predominantly in the northward direction. Semri and Kaimur rocks trend in a NE-SW direction and show variable thickness. Lahiri (1964) studied a part of this area and named different litho-units. The Amarkha Sandstone, the basalmost litho-unit, has faulted contact with the Pre-Vindhyan rocks comprising the Bijawar Quartzites (Yadav et al., 1986). The Narmada-Sone lineament, a significant tectonic structure of central India, marks the southern limit of the Vindhyan at Rohtasgarh. The Nauhatta limestone forming a part of the basal subgroup contains fossiliferous cherts. This limestone is exposed in isolated small hillocks

TABLE 1.
Geological succession of the area.

Supergroup	Group	Subgroup		Thickness
VINDHYAN	Kaimur	Upper Kaimur	Scarp Sandstone	150 m
		Lower Kaimur	Bijaigarh Shale	15-45 m
			Lower Kaimur Sandstone	90 m
	Semri	Rohtas	Rohtas Limestone with alternating shales	230 m
		Kheinjua	Pipardih Shale	20 m
			Chuttiya Limestone	30 m
			Gamharia Shale and Sandstone	30 m
		Basal	Nauhatta Limestone	15-20 m
			Amarkha Sandstone	25 m

---------------------------Faulted Contact------------------------

Pre-Vindhyan rocks, Bijawar Quartzites (?)

conformably overlying the Amarkha Sandstone. The limestone is stromatolitic and shows large bioherms of Stratifera and Irregularia types. Columnar and conical stromatolites are absent. This litho-unit is equivalent to the Kajrahat Limestone. The position of different litho-units is shown in Table 1. The biota described in this paper are embedded in this chert.

AGE

The Bijawar Group underlying the Vindhyan has been dated by the Rb-Sr method at 2500 Ma (Crawford and Compston, 1970). The Vindhyan Supergroup occupies a time span of 700 Ma (1400-700 Ma) (Vinogradov et al.,1964; Mathur, 1982). On the basis of K-Ar dating, Vinogradov et al.(1964) place the age of the Semri Group between 1100 and 1400 Ma. No direct radiometric dates are available for the Semri Group exposed around Rohtasgarh. Fossil-bearing black chert of the Nauhatta limestone, which represents a part of the basal portion of the Semri Group (Lower-Vindhyan) is lithologically correlated with the Kajrahat limestone of Son Valley. Thus, the age of the fossiliferous black chert in the basal part of the Nauhatta Limestone may be taken to range between 1400 and 1000 Ma.

FOSSILIFEROUS CHERT

The fossiliferous chert occurs as lenses and nodules, usually flattened in the plane of bedding, and is thinly laminated measuring less than ten centimeters in thickness. Fresh surface appears waxy and the broken surface shows conchoidal fractures. In thin sections, finely disseminated amorphous organic matter imparts an amber to dark-brown colour to the chert. The chalacedony grains form an interlocking mosaic pattern. The chert often consists of fibrous chalcedonic quartz which exhibits radial structures. Microfossils are absent in these radial structures and secondary void fillings. They are also absent in secondary locally recrystallized chert. Well-preserved microbiota are concentrated in the form of dark-brown, continuous wavy laminae in association with abundant amorphous organic matter. (Pl. I, Fig. 10). The chert matrix contains microscopic specks of carbonate rhombs, sometimes stained with iron oxides which are interpreted as evidence of incomplete replacement of the host rock by silica. These scattered rhombs in the chert matrix have well-defined outlines. They occur either as solitary rhombohedra or as interlocking mosaics. Quartz grains, commonly more than 100 µm in diameter, are locally present as fracture fillings.

PRESERVATION OF BIOTA

The microbiota is three-dimensionally preserved within the black chert, affording a detailed study. The spheroidal unicells are abundant and dominate the assemblage, sometimes showing different patterns of cell division. *Eoentophysalis* Hoffman (1976), a coccoidal mat builder, is the major component of the assemblage. They form a characteristic billowy fabric and palmelloid clusters. Thread-like filamentous sheaths of *Eomycetopsis* Schopf (1968) are rare in the assemblage. Other chroococcacean unicells are distributed in pockets and are not sufficiently densely packed to be considered as mat forming.

The microbiota represents the degradation-resistant residue of microbial communities inhabiting a carbonate tidal flat at the easternmost margin of the Vindhyan platform. The preserved cells possibly survived bacterial destruction and were later permineralized. Compaction of the limestone resulted in the transformation of simple spherical unicells into ellipsoidal forms

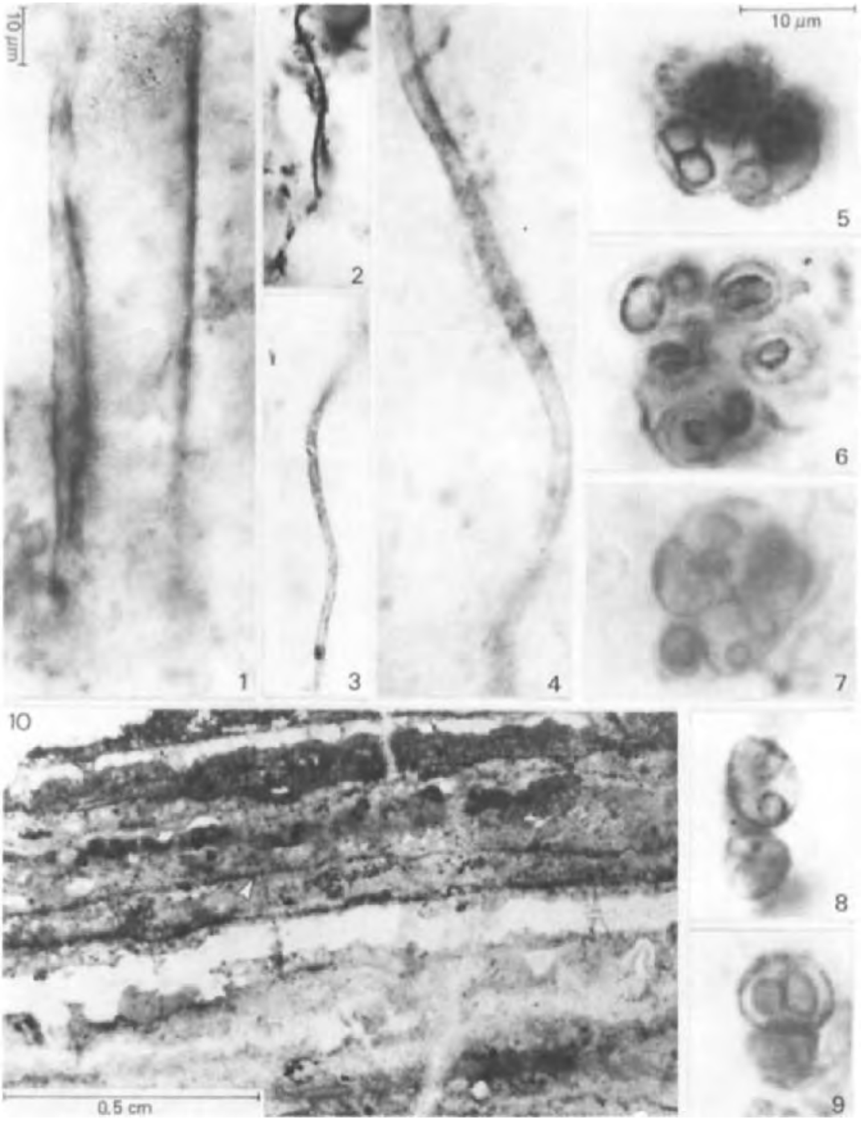

Plate No. 1

Microfossils from petrographic thin sections of Nauhatta chert, Lower-Vindhyans, near Rohtasgarh, India. Magnifications for Figs. 1-4 are given in Fig. 1 and for Figs. 5-9 in Fig. 5.

Fig. 1. *Siphonophycus kestron* Schopf (1968)

Fig. 2. *Biocatenoides* sp.

Figs. 3,4 *Eomycetopsis robusta* Schopf (1968)

Figs. 5-9 *Eoentophysalis belcherensis* Hofmann (1976)

Fig. 10 Thin section of fossiferous black chert. The arrow indicates a concentration of microfossils.

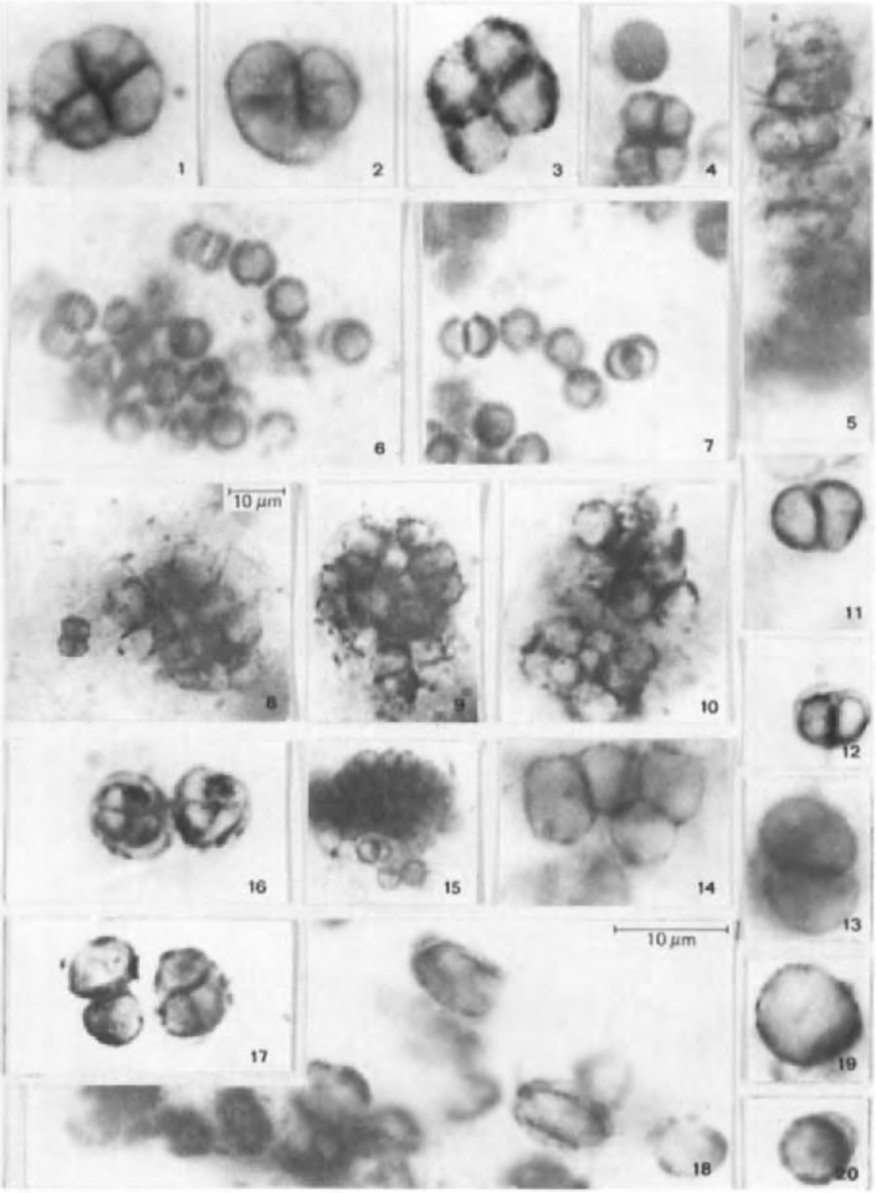

Plate No.II

Coccoid cyanobacteria from petrographic thin sections of Nauhatta Chert, Lower-Vindhyan, near Rohtasgarh, India. Magnification for Figs. 5 and 8-10 are indicated in Fig. 8; for rest of the figures magnifications given in Fig. 18.

Figs. 1-4 *Tetraphycus major* Oehler (1978)
Fig. 5 ?*Glenobotrydion* sp.
Figs. 6,7 *Sphaerophycus paryum* Schopf (1968)
Figs. 8-10 *Myxococcoides reticulate* Schopf (1968)
Figs. 11-14 *Diplococcus* sp.
Fig. 15 *Palaeoanacystis vulgaris* Schopf (1968)
Figs. 16,17 *Bigeminococcus* sp.
Fig. 18 *Eosynechococcus medius* Hofmann (1976)
Figs. 19,20 *Huroniospora* sp.

(Pl. II, Fig. 18), occasionally showing a filamentous appearance (Pl. II, Fig. 5).

The preservation of the microbial community within the Nauhatta chert is similar to that of other well-known Proterozoic localities, e.g., Gunflint Iron Formation (Barghoorn and Tyler, 1965); Bitter Springs Formation (Schopf, 1968; Schopf and Blacic, 1971);
Belcher Islands (Hofmann, 1976) and others.

TAXONOMY

The assemblage comprises tubular sheaths, thread-like filaments, detached spherical unicells, dyads, tetrads, loose clusters and globular colonies. Sheaths encompassing individual cells or colonies are occasionally present. These fossils show morphological affinities to extant cyanobacteria.

The taxonomy of Precambrian microfossils is difficult and there is no general agreement on their classification. The fossil microorganisms in the Nauhatta chert are taxonomically grouped on the basis of their gross morphology, ie., size, shape, pattern of cell division and clustering habits. Cells assume different shapes and sizes during diagenetic processes and add to the variability of characters. This has been conclusively shown through experimental studies on modern biota(Golubic and Hofmann, 1976; Knoll and Barghoorn, 1975; Awramik et al., 1972). The forms described here have been placed in the existing genera for purposes of reference and comparision, though they could be diagenetic variants.

The present study is based on studies of petrographic thin sections under transmitted light. The slides have been deposited in the museum of the Birbal Sahni Institute of Palaeobotany.

Genus *Eomycetopsis* Schopf, 1968
Eomycetopsis robusta Schopf, 1968,
amended Knoll and Golubic, 1979.
Plate - I, Figs. 3 and 4

Description

Filaments unbranched, cylindrical, nonseptate, sinuous, tubular, partially flattened, circular to elliptical in cross section, 2 - 5 µm in diameter and up to 200 µm long, surface coarsely to irregularly granular.

Remarks

Forms described here do not form characteristic mesh networks. The genus was interpreted by Hofmann (1976) as sheaths of either a cyanophyte or *Leptothrix* type of filamentous bacteria. Knoll and Golubic (1979) considered it as sheaths of oscillatorian cyanophytes of the *Phormidium* - *Lyngbya* type.

Genus *Sphonophycus* Schopf, 1968

Siphonophycus kestron Schopf, 1968

Plate - I, Fig. 1

Description

Tubular, nonseptate, cylindrical, unbranched sheaths measuring 18-20 µm in diameter and up to 150 µm long, surface texture uneven.

Remarks

These forms have been compared with the empty sheaths of *Lyngbya* and *Oscillatoria*. The forms described here have larger diameters than those recorded from the Bitter Springs Formation.

Genus *Biocatenoides* Schopf, 1968

Biocatenoides sp.

Plate - I, Fig. 2

Description

Filamentous, slender, unbranched, slightly curved colonies of submicron-sized closely spaced rods, diameter varies from 0.5 - 1 µm and up to 60 µm long.

Remarks

These forms have been compared with filamentous colonies of streptococcus-like bacteria (Hofmann, 1976). In the assemblage described here, individual component of the colony are not distinct.

Genus *Myxococcoides* Schopf, 1968

Myxococcoides retriculata Schopf, 1968

Plate - II, Figs. 8-10

Description

Globular colonies, cells spherical to subspherical, occasionally flattened due to mutual compression, cell diameter 8-10 µm, colonies having up to 50 cells, surface psilate to finely textured, sheath absent but embedded in well developed amorphous non-lamellar organic matrix.

Remarks

These forms are considered to be members of the family Chroococcaceae and identified on the basis of cell size, colonial habit and encompassing amorphous organic matrix.

Genus *Palaeoanacystis* Schopf, 1968

Palaeoanacystis vulgaris Schopf, 1968

Plate - II, Fig. 15

Description

Cells spheroidal to ellipsoidal, rarely solitary, commonly clumped forming small colonies, up to 30 cells in a colony, cell diameter 2-7 µm, sheaths of individual cells absent, colony embedded in a non-lamellar organic matrix.

Remarks

This genus is similar to the extant genus Anacystis of the family chroococcaceae in its colonial habit, cell shape and size.

Genus *Sphaerophycus* Schopf, 1968

Sphaerophycus parvum Schopf, 1968

Plate - II, Figs. 6 and 7

Description

Cell spheroidal to ellipsoidal, solitary or in pairs or forming small colonies, size 2.5 - 3 µm, surface granular or rarely psilate, sheath generally absent, if present non-lamellated.

Remarks

This form is refered to the family Chroococcaceae and is identified by spherical shape and small cell size. Stages of binary fission are common.

Genus *Diplococcus* Oehler, 1978

Diplococcus sp.

Plate - II, Figs. 11-14

Description

Spherical to hemispherical cells occurring in pairs, occasionally forming planar colonies, surface smooth to slightly granular, cell 2.5 - 3 µm wide and 3 - 5 µm long.

Remarks

These forms resemble dividing Chroococcacean cells representing binary fission.

Genus *Tetraphycus* Oehler, 1978

Tetraphycus major Oehler, 1978

Plate - II, Figs. 1-4

Description

Cells spherical to slightly ellipsoidal, forming planar tetrads or rarely dyads, individual cells 3 - 5 µm in diameter, surface smooth to faintly granular, sheath absent.

Remarks

This form shows morphological affinities with Chroococcaceae and dyads and tetrads found in the assemblage possibly represent stages of division. (Oehler, 1978).

Genus *Eosynechococcus* Hofmann, 1976

Eosynechococcus medius Hofmann, 1976

Plate - II, Fig. 18

Description

Cells oblong, rod shaped or ellipsoidal, without distinct envelope and intracellular bodies, 3 - 7 µm long and 1.5- 3.5 µm across, solitary or in loosely aggregated irregular clumps, division apparently by transverse fission.

Remarks

The fossil genus is similar to modern cyanobacteria *Synechococcus* Nageli. *E. medius* may also be possibly a diagenetic variant of spherical cells of chroococcaceae.

Genus *Bigeminococcus* Schopf and Blacic, 1971

Bigeminococcus sp.

Plate - II, Figs. 16 and 17

Description

Cells spheroidal to ellipsoidal, flattened by mutual compression, occurring as cross tetrads encompassed in a common sheath, cell diameter 2.5 - 3 µm, smooth to coarsely granular, individual cell sheath absent.

Remarks

This form is also referred to Chroococcaceae. It shows small cell dimensions as compared to *B.lamellosus* and *B.mucidus* described from the Bitter Springs Formation (Schopf and Blacic, 1971).

Genus *Huroniospora* Barghoorn, 1965

Huroniospora sp.

Plate - II, Figs. 19 and 20

Description

Spheroidal, solitary, thick walled, psilate, cells 3 - 7 µm in diameter.

Remarks

These forms may represent detached cells of a colony. The form described here differs from *H. psilata* Barghoorn in having a thick wall and from *H. microreticulata* and *H. macroreticulata* Barghoorn in having psilate nature.

Genus *Eoentophysalis* Hofmann, 1976

Eoentophysalis belcherensis Hofmann., 1976

Plate - I, Figs. 5-9

Description

Cells spherical to ellipsoidal 2.5 - 9 µm in diameter, forming irregular clusters of solitary or paired cells. Individual cells show distinct organic envelope. The total colony shows distinct mucilaginous sheath.

Remarks

These forms are comparable to extant genera *Entophysalis major* and show a wide morphological variability which has been attributed to degradational processes by Golubic and Hofmann (1976). They represent coccoidal mat builders and dominate the assemblage. The forms described here lack intracellular black bodies unlike *E. belcherensis* Hofmann (1976). The absence may be due to difference in preservation.

Genus *Glenobotrydion* Schopf, 1968

Glenobotrydion sp.

Plate - II, Fig. 5

Description

Cells spherical to ellipsoidal, distorted due to mutual compression, surface texture punctate or reticulate, cell diameter 10 - 12 μm, solitary or in loosely assocated linear groups giving pseudofilamentous structure non-lamellated sheath covers the total colony.

Remarks

G. aenigmatis described from the Bitter Springs Formation (Schopf, 1968) contains distinct central black bodies. *G.*sp. described here contains a central body only in some cells of the colony. These intracellular black bodies have been interpreted as pyrenoid-like structures (Schopf, 1968). Later studies suggest that these bodies represent cytoplasmic degradation products (Awramik et al., 1972; Knoll and Barghoorn, 1975; Knoll and Barghoorn, 1979).

PALAEOENVIRONMENT AND PALAEOECOLOGY

The Vindhyan Supergroup was deposited on a shallow, tectonically stable platform (Auden, 1933). The lithological assemblage and the associated sedimentary structures at Rohtasgarh are suggestive of a shallow marine environment for the Nauhatta limestone. In this area, the basal subgroup comprises Amarkha sandstone and stromatolitic Nauhatta limestone. The common sedimentary structures present in Amarkha sandstone are ripple marks, current laminations and mud cracks. The Nauhatta limestone contains patchy and poorly developed stromatolites, indicative of incoming tides which could have caused an agitational environment not conducive to profuse development of stromatolite. Such environments are common features of tidal flats (Hardie, 1986).

Eoentophysalis, a colonial mat-builder, occurs in large populations forming a thin zone along the bedding plane reflecting "algal blooming". The other mat-builders, *Eoentophysalis,* include filamentous tubular sheaths assignable to *Eomycetopsis robusta* and *Siphonophycus kestron*. These taxa are poorly preserved and occur as isolated sheaths instead of forming meshworks of filaments. However, in the Bitter Springs Chert, *E. robusta* is the major mat builder (Barghoorn and Schopf, 1975; Schopf, 1968; Schopf and Blacic, 1971). The mat dwellers (benthics) present in the Nauhatta biota are small coccoidal cyanobacteria represented by *Eosynechococcus, Sphaerophycus, Tetraphycus, Bigemniococcus* and *Diplococcus*.

Planktonic forms are absent in Nauhatta chert. The absence of open-shelf planktonic acritarchs and dominance of benthos suggests that sediments accumulated in a restricted shallow marine environment. Dominance of a coccoidal mat-builder, *Eoentophysalis,* indicates an intertidal environment with occasional subaerial exposure. Extant *Entophysalis* build coherent mamilllate mats, dominantly in the lower intertidal zone, such as are evident in the lagoons of Abu Dhabi, the Persian Gulf and Shark Bay and on the tidal flats of the Bahamas. They are cosmopoliton in distribution, inhabiting warmer seas (Golubic and Hofmann, 1976). The fossil taxa assignable to *Eoentophysalis* (Pl.1 Fig.5-9) from Nauhatta chert show encapsulated envelopes. They represent microorganisms which have evolved additional mechanisms to cope with a periodical exposure to a subaerial environment. The gelatinous sheath helped them tolerate periods of desiccation and protected them from harmful solar radiations. According to Golubic (1976), all intertidal mat-building blue-green algae produce gels which encapsulate and protect them during periods of desiccation.

ACKNOWLEDGEMENT

We thank our colleagues Mr. Mukund Sharma and Mr. Rajendra Bansal for useful discussions. The work has been supported by DST grant No. SP/12/PCO/86. We also thank Mr.P.C.Roy for assistance in photography and Mr. Madhukar Arvind for secretarial support.

REFERENCE

Auden, J.B., 1933. Vindhyan sedimentation in Son Valley, Mirzapur District. Mem. Geol. Surv. India., 62: 141-250.

Awramik, S.M., Golubic, S. and Barghoorn, E.S., 1972. Blue-green algal cell degradation and its implication for the fossil record. Geol. Soc. Am. Abs. with programs, 4: 438.

Barghoorn, E.S. and Schopf, J.W., 1965. Microorganisms from the Late Precambrian of Central Australia. Science, 150: 337-339.

Barghoorn, E.S. and Tyler, S.A., 1965. Microorganisms from the Gunflint Chert. Science, 147: 563-577.

Crawford, A.R. and Compston, W., 1970. The age of the Vindhyan System of Peninsular India. Q. J. Geol. Soc. London, 125: 351-371.

Golubic, S., 1976a. Organisms that build stromatolites. In: M.R. Walter (Editor), Stromatolites. Elsevier, Amsterdam, pp.113-129.

Golubic, S. and Hofmann, H.J., 1976. Comparison of Holocene and mid-Precambrian Entophysalidaceae (Cyanophyta) in stromatolitic algal mats: Cell division and degradation. J. Palaeont., 50: 1074-1082.

Hardie, L.A., 1986. Carbonate Tidal Flat deposition: Ten basic facts. Colorado School of Mines Quaterly: 3-6.

Hofmann, H.J., 1976. Precambrian microflora, Belcher Islands, Canada: Significance and systematics. J. Palaeont., 50: 1040-1073.

Knoll, A.H. and Barghoorn, E.S., 1975. Precambrian eucaryotic organisms: a reassessment of the evidence. Science, 190: 52-54.

Knoll, A.H. and Golubic, S., 1979. Anatomy and taphonomy of a Precambrian algal stromatolite. Precamb. Res., 10: 115-151.

Lahiri, D., 1964. Petrology of the Vindhyan rocks around Rohtasgarh, India. J. Petroleum Geol., 34(2): 270-280.

Maithy, P.K. and Shukla, M., 1977. Microbiota from the Suket shales, Rampura, Vindhyan system (Late Precambrian), Madhya Pradesh. Palaeobotanist, 23: 176-188.

Mathur, S.M., 1982. Precambrian sedimentary sequences of India: their geochronology and correlation. Precamb. Res., 18: 139-144.

McMenamin, D.S., Kumar, S. and Awramik, S.M., 1983. Microbial fossils from the Kheinjua Formation. Middle Proterozoic Semri Group (Lower Vindhyan), Son Valley area, Central India. Precamb. Res., 21: 247-271.

Misra, R.C., 1949. On organic remains from Vindhyan (Precambrian). Curr. Sci., 18: 438-439.

Misra, R.C. and Bhatnagar, G.S., 1950. On carbonaceous discs and algal dust from the Vindhyans Precambrian. Curr. Sci., 19: 88-89.

Oehler, D.J., 1978. Microflora of the Middle Proterozoic Balbirini Dolomite (McArthur Group) of Australia. Alcheringa, 2: 269-309.

Rode, K.P., 1946. A new find of fossils in Vindhyan rocks of Rohtas hill in Bihar. Curr. Sci., 15: 247-248.

Schopf, J.W., 1968. Microflora of the Bitter Springs Formation, Late Precambrian, Central Australia, J. Paleont., 42: 651-688.

Schopf, J.W. and Blacic, J.M., 1971. New microorganisms from the Bitter Springs Formation (Late Precambrian) of the north central Amadeus Basin, Australia. J. Paleont., 45: 925-960.

Vinogradov, A.P., Tugarinov, A.I., Zhikov, C.I., Stupnikova, N.I., Bibikova, E.V. and Khorre, K., 1964. Geochronology of Indian Precambrian. Rep. 22nd Int. Geol. Cong. New Delhi, 10: 553-567.

Volgdin, B.N., 1957. On the ontogeny of Archaeocyatha. Dokl. Acad. Nauk. USSR, 116: 493-496.

Yadav, V.K., Narain, K. and Maithy, P.K., 1986. Lower Vindhyan Tectonism and Sedimentation around Rohtas, Bihar. VIth Convention, Indian Assoc. Sedimentologists, (abst.), 130pp.

PRECAMBRIAN RIFTS AND ASSOCIATED TECTONICS OF PENINSULAR INDIA

D.C.MISHRA

ABSTRACT

Geophysical data from the Archaean schist belt and granulite terrains of South India are studied. The Bouguer anomaly of the region suggests a thickening of the crust by approximately 6 km in the central part and a NNW-SSE structural trend for the schist belts. The eastern margin of the Chitradurga schist belt depicts sharp gradients in Bouguer anomaly and airborne total magnetic intensity profiles, suggesting deep-seated faults. Airborne magnetic data record high-amplitude magnetic anomalies for the mafic and ultramafic units of the schist belt, like metabasalts and magnetite quartzites with susceptibilities of the order of 15.1 x 10^{-3} CGS units associated with NW-SE magnetic trends for the schist belts. The granulite terrain is characterized by a large Bouguer'low' acompanied by sharp gradients on either side, suggesting deep faults and thrusts with a thick crust in the center. The airborne magnetic map of this region shows high-amplitude magnetic anomalies over the known charnockite rocks and suggests a predominant NE-SW magnetic trend conforming with the general structural trend of the region. These data have been incorporated to suggest a model in which some form of underplating of the Indian crust has taken place towards the south, creating a compressional regime over the granulites, and farther north an extensional regime in which rifted basins were formed for the greenstones to deposit, as is observed in the present-day back-arc regions of the Himalayas and the Alps.

The geophysical signatures of one of the Lower Proterozoic rift basins (Pakhal Basin) are described. Though the Bouguer anomaly of the region primarily reflects the effects of Gondwana (Permian--Jurassic) tectonics in the region, its linear nature, indications of basic intrusions along the marginal faults and the presence of high-density material along the Moho suggest that the Pakhal sediments were deposited in rifted basins which might have influenced an even later orogeny during Gondwana time to form a typical continental graben in the region.

INTRODUCTION

Rifts are one of the most fundamental structures on the surface of the earth responsible for the development of the large-scale regional tectonic features. They are basically the products of extensional stresses and associated phenomena.Depending on their tectonic setting, they are broadly classified under two groups- active and passive (Kazmin, 1987). The rifts associated with extension, caused by subsurface plume-generated asthenospheric upwelling and large-scale uplift and volcanism, are termed active rifts, whereas those caused by regional stresses originating from plate motions, for example, in the back-arc regions, are termed passive rifts. However, subsequent signatures of rift activity in the form of their linear occurrence, uplift and magmatism at various levels, etc., may be the same in both the cases, making it difficult to distinguish one from the other, especially in the case of those which have been formed during past geological times and now no longer active. This is specially true for the Precambrian rifts as most of these regions have been affected subsequently by several orogenic activities that obliterated the known signatures of rifting, rendering it extremely difficult to identify them during present-day field investigations. Therefore, delineation of the rifts in Precambrian terrains requires multi-parametric investigations of the region and in this context geophysical surveys assume special significance. It is reasonable to assume that the modern plate-tectonics-type activities must have taken place from the Middle-Late Proterozoic onwards (Windley, 1984). Radhakrishna and Naqvi (1986) have advocated the start of modern-type plate tectonics almost from the same period in the Indian peninsula. However, its counterpart during the Archaean is difficult to visualize. This difficulty may be largely due to our poor understanding of the activities during that period and to preconceived notions about the evolution of the Archaean crust. As the formation of rifts is related to plate tectonics, their investigation during the Archaean and Proterozoic assumes special significance. The existence of a typical rift type of activity during the Archaean may be difficult to visualize; however, a somewhat modified version might have been operative, as suggested by Milanovysky (1987) and Blake and Groves (1987). Due to high heat production and consequently high losses during the Archaean, an even higher state of plate-tectonic activities has been postulated by some workers (Bickle, 1984). We shall describe the Precambrian rifts of India in two groups: the first belonging to the Archaean and the second to the Proterozoic.

ARCHAEAN RIFTS

The two important geological provinces recognised during the Archaean are low-grade greenstone belts and the high-grade granulite terrains. The greenstone belts, representing volcano-sedimentary sequences, are found in sedimentary basins which are faulted with reference to the surrounding rock formations and which represent the early crustal conditions. They are usually surrounded by later granitic intrusions. The granulites-highly metamorphosed supracrustal rocks- are exposed in the early mobile belts of the world. In South India both these Archaean provinces occur, side by side, separated by a transition zone almost along 11^{o}-12^{o}N latitude. South of this zone are the granulite rocks represented by charnockites and khondalites, while north of it are the greenstone belts of the Dharwar craton.

Dharwar schist belts

Bouguer Anomaly. Fig. 1 presents the Bouguer anomaly map (NGRI., 1978) on which the schist belts of the Dharwar craton (Karnataka, India) are superimposed. It clearly suggests their linear pattern, largely oriented NNW-SSE, depicting the bands of 'lows' and 'highs' in the Bouguer anomaly. The density distributions of various rock types of this region suggest a higher density for mafic and ultramafic sequences of the schist belt and 'low density' for granitic plutons. The other sedimentary units of the schist belt depict almost the same density as surrounding granites and gneisses. The 'highs' and 'lows' are therefore largely attributed to the high-density volcano-sedimentary sequences of schist belts and exposed or subsurface granitic intrusions (Subrahmanyam and Verma, 1982).

However, a close examination of Fig.1 clearly suggests a broad Bouguer 'low' over the large schist belt between Hubli and Shimoga over which the short-wavelength anomalies such as L1-L5 and H1-H6 are superimposed. As has been explained above, the short-wavelength, high-amplitude anomalies are attributed to the mafic and ultramafic units of the schist belt and the 'lows' to the granitic plutons. However, the broad 'low' referred to above cannot be attributed to any of the exposed geological units or some shallow

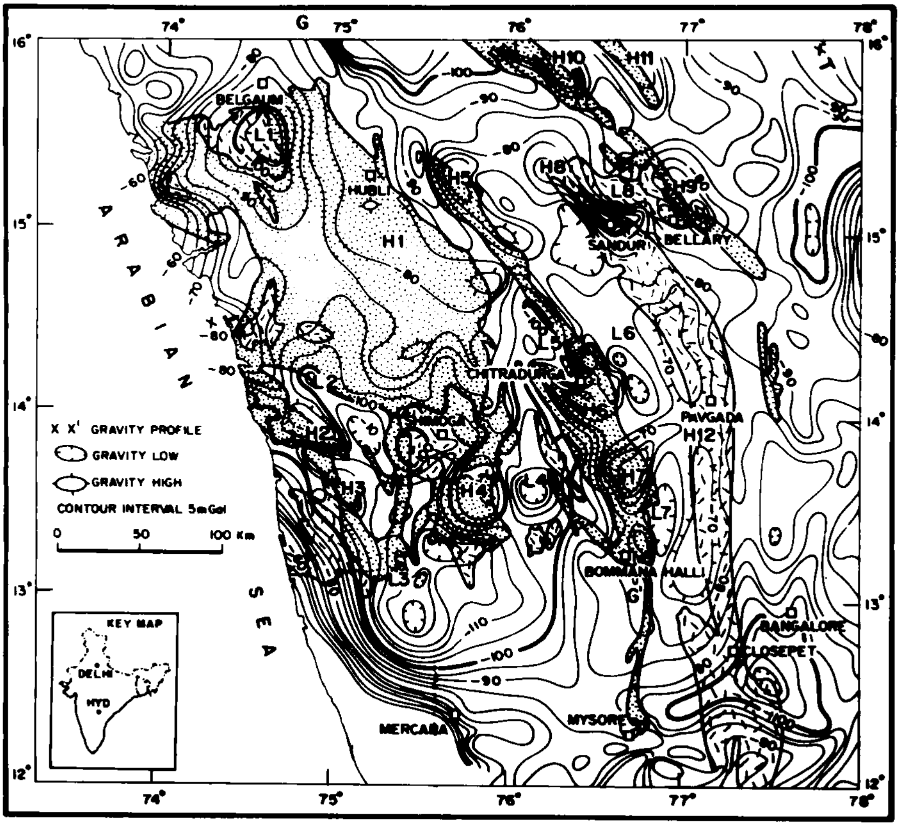

Figure 1. Bouguer anomaly map of the Dharwar schist belts, Karnataka, India with superimposed geology (NGRI., 1978; Subhrahmanyam and Verma, 1982).

structures. This broad 'low' is characteristic of the entire region whose sources must be at considerable depth. A high-altitude airborne magnetic profile along 13^{o} latitude also suggested faulted margins for the eastern contact of the Chitradurga schist belt (Hari Narain et al., 1969). Deep seismic sounding (DSS) along a profile passing from Chitradurga (Kaila et al., 1979) suggested deep-seated faults along which the depth of the Moho varies from approximately 35 km to 40 km under this schist belt.

The Bouguer anomaly map of the region (Fig.1) depicts a sharp gradient along GG', taking a turn around Chitradurga almost

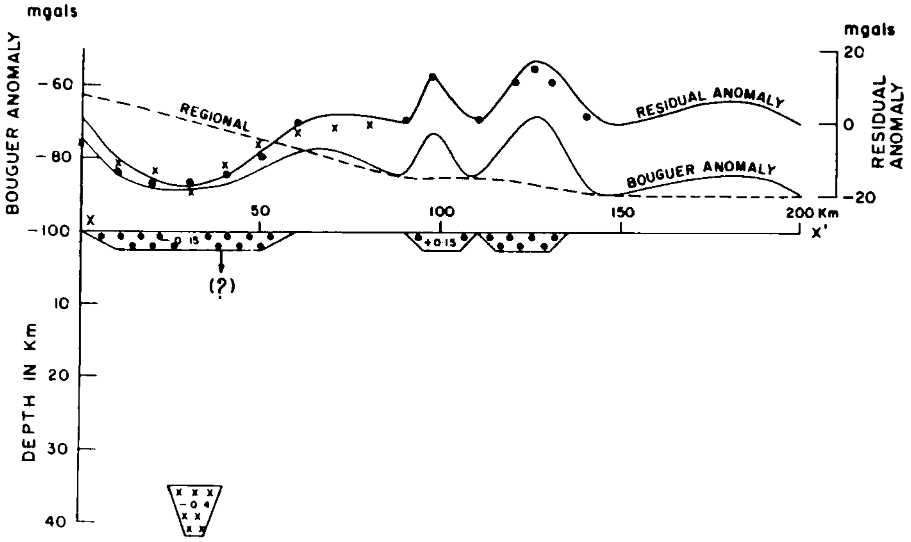

Figure 2. Profile XX and interpreted cross-section of the causative sources. The broad low towards X can be interpreted both by a surface density contrast or increase in crustal thickness. Based on the densities of exposed rocks, the latter alternative - the increase in crustal thickness is preferred.

extending from the top of the map to Bommana Halli, suggesting a deep-seated fault west of which the broad Bouguer low referred to above is located. A profile XX' (Fig.2), adopted from the Bouguer anomaly map representing mainly the long-wavelength anomalies, is modelled using the surface geology and known density contrasts.

As shown in the diagram, the broad lows can be modelled to be a result of either a 2.5 km-thick lighter metasedimentary cover of a density of 2.5 g/cm^3 or thickening of the crust from 36 km to 42 km. However, the existence of boundary faults affecting the entire crust and the absence of any rock unit of low density in the schist belt, suggests the latter alternative to be more plausible. The two highs along this profile (Fig.2) appear to be caused by the 2.5 km-thick mafic and ultramfic units of a density of 2.8 g/cm^3. Similarly to what is referred to above, the short--wavelength lows (L1-L5) of Fig.1 can be attributed to shallow granitic intrusions. Therefore, the Bouguer anomaly gradient GG' passing from Chitradurga and the broad low west of it suggest a faulted block in which these large schist belts are located and under which the crust has thickened by 6 kms.

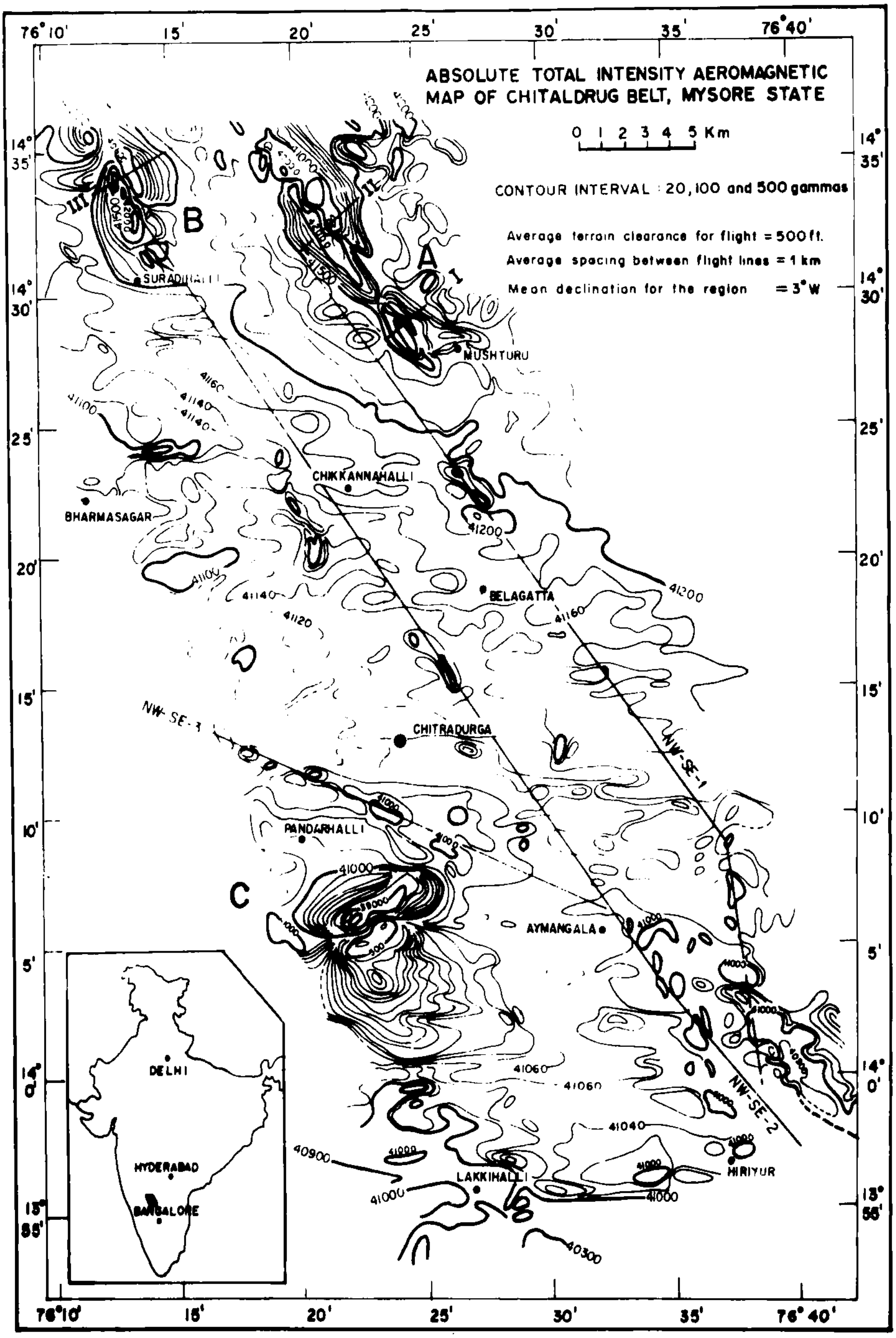

Figure 3. Airborne total-intensity map of a part of the Chitradurga Schist Belt (NGRI., 1967).

Airborne Magnetic Data. The association of magmatism with the rifts has rendered magnetic surveys extremely useful for delineating rifted structures, specially from older terrains (Hinze et al., 1982). An airborne magnetic survey of a part of the Chitradurga schist belt (Fig. 3, NGRI, 1967) delineated several high-amplitude magnetic anomalies, corresponding to the mafic and ultramafic units, and the general structural trend in the form of alignment of contours and small-magnitude anomalies. There are three large magnetic anomalies, A,B and C. A and B are linear magnetic anomalies and may correspond to the exposed metabasalts in the schist belt. They coincide with large magnetic trends (NW-SE, Fig.3) suggesting that these may be structurally controlled. Quantitative interpretation along profiles I and III suggests that these are caused by dyke-like features of higher susceptibility (of the order of 15.1 x 10^{-3} emu, Fig.4a), suggesting the presence of a relatively high percentage of ferromagnetic minerals in the entire bulk of these rock units. The magnetite anomaly (C) appears to be caused by a three-dimensional body and coincides with the metavolcanics and metasediments including magnetic quartzites and cherts of Chitradurga schist belt. A three-dimensional interpretation for this anomaly using the principle of harmonic inversion (Mishra, 1984) suggests a hillock of magnetic material of a maximum height of 250 m above the surface with a magnetization of 600 nT (Fig.4b), providing a susceptibility of approximately 15 x 10^{-3} CGS units, suggesting large percentage of ferromagnesian minerals (specially magnetite) which are unaltered.

This interpretation suggests that metavolcanics of the Dharwar schist belt consist of basic volcanic rocks which are structurally controlled by large faults and might represent magmatism associated with rift tectonics.

Granulite Terrain

South of the Dharwar schist belt terrain, granulite rocks represented by charnockites and khondalites are exposed. There are high-pressure and high-temperature mineral assemblages in these rocks, suggesting that they represent the lower crustal continental rocks. Besides the granulite rocks occupying the high land area, amphibolite-facies gneisses are found in low lands separated by major shears or lineaments.

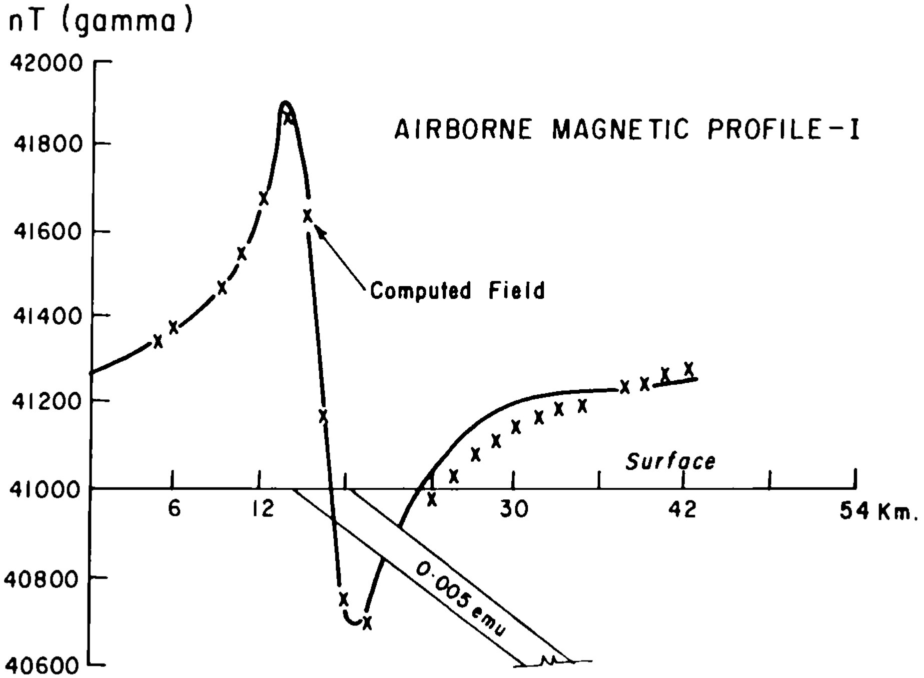

Figure 4a. Profile I and interpreted cross-section of the causative sources.

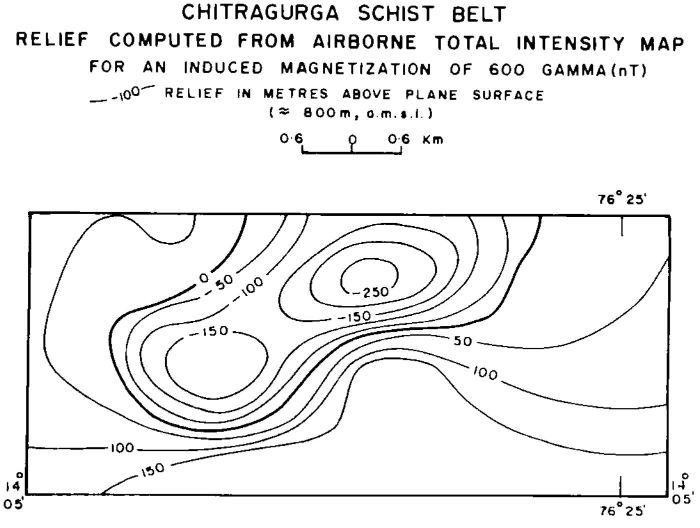
CHITRAGURGA SCHIST BELT
RELIEF COMPUTED FROM AIRBORNE TOTAL INTENSITY MAP
FOR AN INDUCED MAGNETIZATION OF 600 GAMMA(nT)
-100 RELIEF IN METRES ABOVE PLANE SURFACE
(≈ 800m, a.m.s.l.)
0·6 0 0·6 Km
76° 25'
0
50
100
-250
-150
-150
50
100
100
150
14° 05'
14° 05'
76° 25'

Figure 4b. Three-dimensional configuration of the airborne magnetic anomaly C of Figure 3.

It is generally understood that the granulites represent the lower parts of the thickened crust which has been uplifted and is now exposed at the surface. The thickening of the crust can take place either at the active plate margins or by underplating of the normal crust (Ellis, 1987) and suggests isostatic adjustments inferred from a combined study of gravity and seismic soundings (Taylor and McLennan, 1985). That granulite-facies metamorphism was the result of widespread rifting within the continental lithosphere has been suggested by Weber (1984). Fountain and Salisbury (1981) have analysed the Bouguer anomaly pattern over different granulite terrains of the world and suggested that they are similar to those expected when two continents collide and one is subducted under the other, resulting in crustal thickening. They further concluded that the complexity of the crust is the result of continuous evolution by recycling and metamorphism through time in a variety of tectonic environments.

Bouguer anomaly. The Bouguer anomaly map of this region (NGRI.,1978) with superimposed geology (Verma., 1985; Fig.5) depicts a large gravity 'low' coinciding with the high lands of

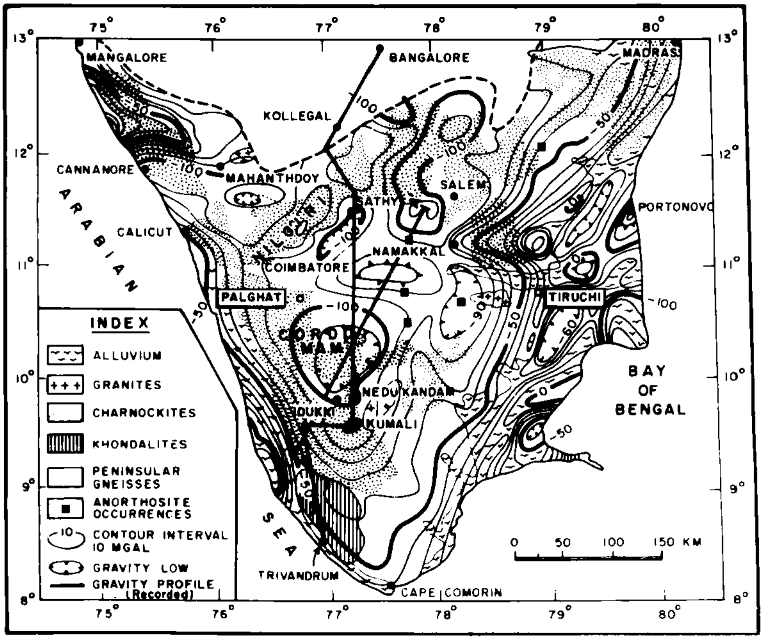

Figure 5. Bouguer anomaly of the granulite terrain of South India with superimposed geology (NGRI., 1978; Verma, 1985).

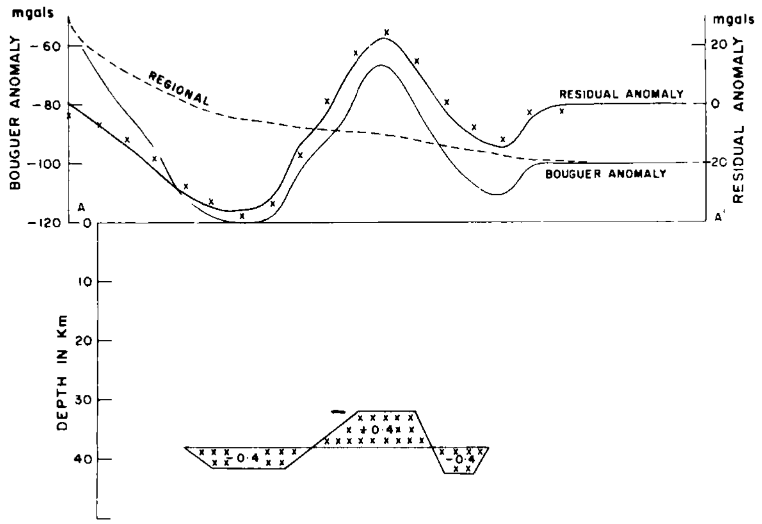

Figure 6. Profile AA' and interpreted cross-section along this profile depicting variations in Moho from 32 km to 42 km.

the Cardomom hills, comprising charnockites which form almost the highest ranges of the Western Ghats located south of the physiographic gap known as the Palghat Gap. As is apparent from this figure, the Palghat-Tiruchi line is located over a gradient in the Bouguer anomaly, suggesting a deep-seated fault which may be related to the general tectonic development of this region. Comparison of Deep Seismic Sounding studies along different profiles in the country and modelling the Bouguer anomaly along them (Mishra, 1988; Mishra et al., 1987; Kaila and Bhatia, 1981) suggest that most of the long-wavelength Bouguer anomalies observed on the Bouguer anomaly map of the southern peninsula (NGRI.,1978) are caused by variations in the Moho. Further, in the absence of any exposed rock units of lower density, the large 'low' and accompanying northern 'high' along the profile (AA', Fig.5) are interpreted using variations in Moho, i.e.,thickness of the crust. The resulting model (Fig.6) provides a maximum thickness of crust of 42 km under the observed low and a minimum thickness of 32 km north of Palghat-Tiruchi line, suggesting it to be a deep-seated fault.

Airborne magnetic map of south India. Airborne magnetic data of south India up to 12°N flown at altitudes of 5,000'-9,000' with profiles spaced 5 km apart, has been described by Suryanarayana and Bhan (1985) and Ramachandran et al., (1986) and Reddi et al., (1988). Suryanarayan and Bhan have presented a map of Kerala State and the adjoining offshore region which shows high-amplitude magnetic anomalies along the coast on the continental shelf. Similar large-amplitude magnetic anomalies were also recorded by Hari Narain et al., (1969) along the west coast of India in a high-altitude airborne magnetic profile along the 13th parallel. This anomaly that is well on the continental shelf appears to be caused by a dyke-like feature running almost along the coast. The other significant part of this map is the concentration of anomalies south of the Palghat-Tiruchi gap, almost coinciding with the large Bouguer-anomaly `low' referred to above. Ramachandran et al., (1986) and Reddi et al. (1988) have described an airborne total-intensity magnetic map which mainly depicts E-W and NE-SW trends, suggesting the general structural magnetic trend of the region. These trends, which are primarily E-W towards the South, become NE-SW towards the east coast, implying that the entire region is subjected to stress from its southern and SE side.

An evolutionary model

Thickening of the crust below the granulite terrain of S.India and east-west striking magnetic trends throughout the south of the 12°N parallel, along with the nature of the Bouguer anomaly suggest that underplating of the crust has taken place in this region from the surrounding region and this might be either in the form of slippage along low-angle nappes or some form of subduction during that period. That the, Dharwar schist belts in Karnataka occur in the form of linear belts controlled by deep-seated faults, and the associated magmatism suggests that they possibly represent rift-type tectonics which were formed as back-arc rifted basins similar to those observed at present in the case of the Himalayas and the Alps. Subsequent to the deposition of greenstones in the rifted basins, a compressional regime has probably set in, resulting in large-scale granitic intrusions along the margins of the Karnataka craton comprising these basins (Radhakrishna and Naqvi, 1986). Tarney has suggested a similar model for the development of Archaean greenstone belts in back arc marginal basins (Windley, 1984). The occurrence of large linear dykes on the continental shelf off the west coast in this region, similar to those observed in the case of the Red Sea rift, requires detailed investigation regarding the nature of the western margin of Peninsular India.

PROTEROZOIC RIFTS

There may be several Proterozoic rifts in this country, but the Pakhal-Sullavai basin on either side of the Gondwana sediments of the Godavari Basin stand out conspicuously due to their linear nature. Their faulted margins on either side have led several workers (Raju, 1986; Subba Raju et al., 1978) to postulate that these sediments were deposited in a rift-type basin (Fig.7). Dar and Viswanathan (1964) even attributed a Precambrian ancestry to the Gondwana rift valley in the region which is of much later period (Permian to Jurassic). The Bouguer anomaly and the total intensity magnetic map of the entire region covering both the Gondwanas and the Pakahls is described by Mishra et al., (1987). Accordingly, the Bouguer anomaly map is characterised by a large central 'low'corresponding to Gondwana sediments flanked by 'highs' on either side covering the Pakhals and the Sullavais (Fig. 7). A profile CC' is shown in Fig.8a in which the central 'low'is modelled as being caused by approximately 5 km of Gondwana sediments of a density of 2.35 g/cm^3. In spite of assuming a high

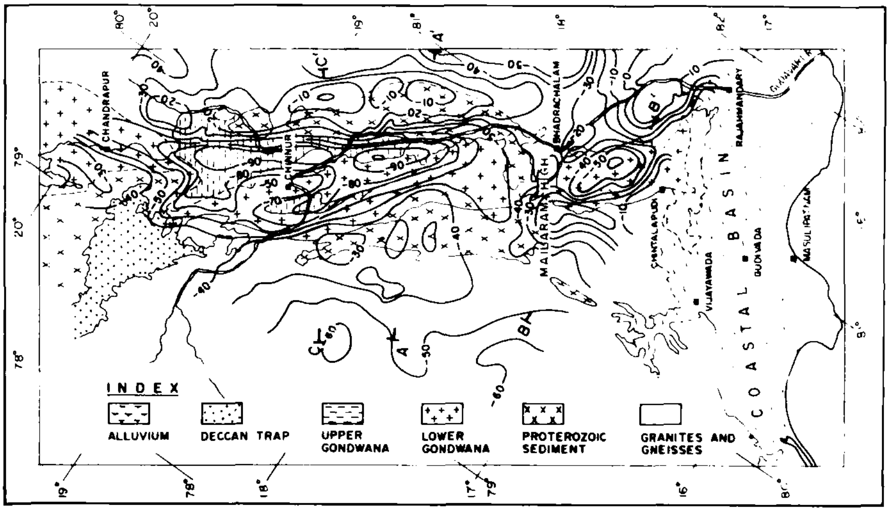

Figure 7. Bouguer anomaly of the Pakhal Basin with superimposed geology. The central 'low' is occupied by Gondwana sediments with flanking 'highs' coinciding with Proterozoic sediments.

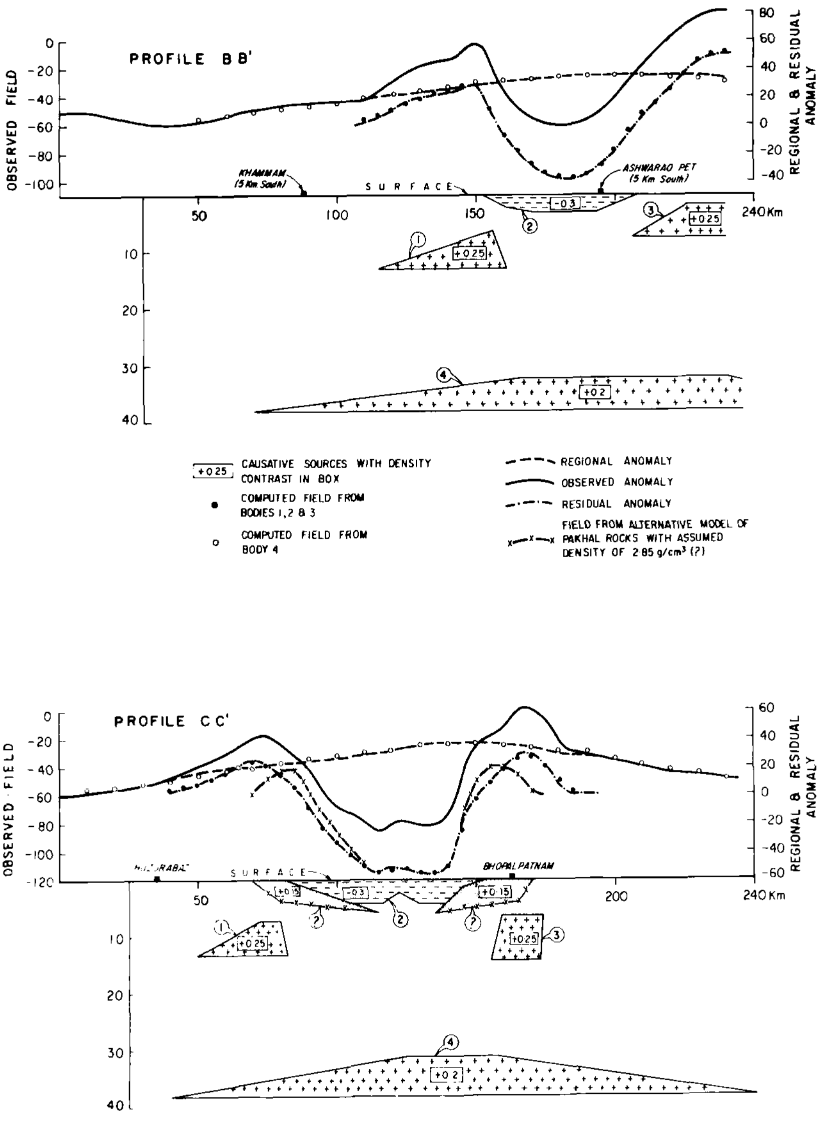

Figure 8. Bouguer anomaly profiles and interpreted cross -sections across the Godavari Basin, covering Pakhal and Gondwana sediments. The central 'low' represents the Gondwana sediments while flanking 'highs' are due to high-density material in the upper part of the crust. a) Profile CC'demonstrating that even an assumed high--density contrast for the Pakhals does not explain the observed Bouguer anomaly; b) Profile BB' along which no Pakhal rocks are exposed and which still depicts a similar anomaly pattern.

density for the Pakhals and computing the field due to it, it has been demonstrated that the flanking 'highs' of the Bouguer anomaly cannot be accounted for by them and therefore they are attributed to high-density material of a density of 2.9 g/cm^3 along the shoulders of the Gondwana rift valley. Figure 8 also presents another profile BB' along which the Pakhals are absent. The presence of flanking 'highs' along this profile further suggests that these highs are unrelated to them and represent sub-surface high-density material. However, the regional field extrapolated from the observed field is attributed to high-density material from 32km to 38km which covers the entire region of both the Pakhals and the Gondwanas. The total-intensity magnetic map presented by Mishra et al. (1987) depicts several high-amplitude magnetic anomalies along the marginal faults defining the Pakhal Basin, suggesting the presence of basic intrusions associated with the rift formation during Pakhals (Lower-Middle Proterozoic) time. From the surrounding region of Archaean gneisses, several basic intrusions have also been reported, which may also be related to the formation of the Proterozoic rifts in this region. The high-density material inferred from the Bouguer anomaly and basic intrusions along marginal faults and in adjacent regions suggest that the Pakhals and the Sullavais of this region have been deposited in a typical rift valley whose other signatures might have become obliterated with time.

ACKNOWLEDGEMENT

Thanks are due to the Director, N.G.R.I. for his kind permission to publish this work.

REFERENCES

Bickle, M.J., 1984. Variation in tectonic style with time: Alpine and Archaean systems. In: H.D. Holland and A.F. Trendall (Editors), Patterns of change in Earth evolution. Dahlem Conference - Springer Verlag, Berlin, pp.357-370.

Blake, T.S. and Groves, D.I., 1987. Continental rifting and the Archaean-Proterozoic transition. J. Geology, 15: 229-232.

Dar, K. and Viswanathan, S., 1964. On the possibility of the existence of Cuddapah rift valley in the Penganga Godavari Basin. Bull. Geol. Soc. India, 1: 1-5.

Ellis, D.J., 1987. Origin and evolution of granulites in normal and thickened crust. Geology, 15: 167-170.

Fountain, D.M. and Salisbury, M.H., 1981. Exposed cross-section through the continental crust: implications for crustal structure, Petrology and Evolution. Earth Planet. Sci. Lett., 56: 263-277.

Hari Narain, Sanker Narayana, P.V., Mishra, D.C. and Rao, D.A. 1969. Results of airborne magnetometer profiles from offshore Mangalore to offshore Madras (India) along 13th degree parallel. Pure and Applied Geophysics, 75: 133-139.

Hinze, W.F., Wold, R.J. and O'Hara, N.W., 1982. Gravity and magnetic anomaly studies of Lake Superior. Geol. Soc. Am. Mem., 156: 203-221.

Kaila, K.L. and Bhatia, S.C., 1981. Gravity study along the Kavali-Udipi Deep Seismic Sounding Profile in the Indian peninsular shield. Some inferences about the origin of anorthosites and the Eastern Ghat orogeny. Tectonophysics, 79: 129-143.

Kaila, K.L., Roy Choudhury, K.R., Reddy, P.R., Krishna, V.G., Hari Narain, Subbotin, S.I., Sollogub, V.B., Chekunov, A.V., Kharetchko, G.E., Lazarenko, M.A. and Ilchenko, T.V., 1979. Crustal structure along Kavali-Udipi profile in the Indian Peninsular Shield from Deep Seismic Sounding, J. Geol. Soc. Ind., 120: 307-333.

Kazmin, V., 1987. Two types of rifting: dependence on the condition of extension. Tectonophysics, 143: 85-92.

Milanovasky, E.E., 1987. Rifting evolution in geological history, Tectonophysics, 143: 103-118.

Mishra, D.C., 1984. Magnetic anomalies-India and Antarctica. J. Earth and Planet. Sci. Lett., 71: 173-180.

Mishra, D.C., 1988. On deciphering two scales of the Regional Bouguer anomaly of the Deccan Trap and Crust-Mantle Inhomogeneities. J. Geol. Soc. Ind., 33: 48-54.

Mishra, D.C., Gupta, S.B., Rao, M.B.S.V., Venkatarayudu, M. and Laxman, G., 1987. Godavari Basin - A Geophysical Study, J. Geol. Soc. Ind., 30: 469-476.

N.G.R.I., 1967. Report on airborne magnetometer and scintillometer surveys over parts of Chitaldurg Schist belt - A technical report, Dept. of Mines and Geology, Karnataka, 1.

N.G.R.I., 1978. Gravity Series map of India. NGRI, GPH-2.

Radhakrishna, B.P. and Naqvi, S.M., 1986. Precambrian Continental Crust of India and its Evolution. J. Geol., 94: 145-166.

Raju, P.S.R., 1986. Geology and hydrocarbon prospects of Pranhita -Godavari graben, J. Assoc. Expl. Geophysics, 7: 131-146.

Ramachandran, T.V., Mishra, A., Mishra, R.S., 1986. Geological Evaluation of Absolute Total Intensity Aeromagnetic Data of Tamil Nadu. J. Assoc. Expl. Geophys., 7: 151-162.

Subba Raju, M., Sreenivas Rao, T., Setti, D.N. and Reddi, B.S.R., 1978. Recent advances in our knowledge of the Pakhal Supergroup with special reference to the central part of Godavari valley. Rec. Geol. Surv. India, 110: 39-59.

Subrahmanyam, C. and Verma, R.K., 1982. Gravity interpretation of the Dharwar greenstone, gneiss - granite terrain in the southern Indian shield and its geological implications. Tectonophysics, 84: 225-245.

Suryanarayana, M. and Bhan, S.K., 1985. Aeromagnetic survey over parts of Kerala and the adjoining offshore region, India. Geophys. Res. Bull., 23: 105-114.

Taylor, S.R. and McLennan, S.M., 1985. The continental crust: Its composition and evolution, Blackwell Scientific Publications, pp.1-312.

Reddi, A.G.B., Mathew, M.P., Singh, B. and Naidu, P.S., 1988. Aeromagnetic evidence of crustal structure in the Granulite Terrane of Tamil Nadu, Kerala, J. Geol. Soc. Ind., 32: 368-381.

Verma, R.K., 1985. Gravity field, seismicity and tectonics of the Indian peninsula and the Himalayas, D.Reidel Publishing Co., Holland, pp.1-213.

Weber, R.K., 1985. Variations in tectonic style with time (Variscan and Proterozoic System). In: H.D. Holland and A.F. Trendall (Editors), Patterns of change in Earth evolution, Dahlem Conference 1984. Springer Verlag, Berlin, pp.371-386.

Windley, B.F., 1984. The Evolving Continents, John Wiley and Sons Ltd., 2nd Edition, pp.1-399.

TECTONIC EVOLUTION OF THE PROTEROZOIC IN THE NORTH CHINA PLATFORM

SUN DAZHONG AND LU SONGNIAN

ABSTRACT

The Precambrian of the North China platform, based on orogenic movements, is divided into three tectonic megastages: the formation of the Archaean Craton, the early Proterozoic protoplatform, and the middle to late Proterozoic platform. Each division has a distinct tectonic history.

The Fupingian orogeny (ca. 2.50 Ga) at the end of the Archaean was an intensive tectono-thermal event that metamorphosed Archaean rocks and deformed them to form an extensive basement, called the North China Craton.

Some ensialic basins and troughs, varying in scale, were formed by rifting and sagging within the primary consolidated craton during the early Proterozoic. The depth, nature and activity of faults and the features of the sialic crust gave rise to the differences between calc-alkaline and subalkaline volcanics, poorly sorted turbidites in deep water and well-sorted sediments in shallow water, as well as BIF of Algoma and Superior type in different basins and troughs, at the early stage of the early Proterozoic. After the Wutai Orogeny (ca. 2.3 Ga) in the middle of the early Proterozoic, molasse accumulation first occurred, followed by the deposition of neritic and lagoon sediments with minor mafic volcanic rocks.

The Luliangian-Zhongtiao Orogeny (ca. 1.9-1.8 Ga) was another important tectonothermal event at the end of the early Proterozoic. During the panorogenic period, terminal consolidation of the protoplatform was achieved, as the principal tectonic framework of the North China Platform acquired its pattern.

Three main tectonic basins occurred in different portions of the platform during the middle-late Proterozoic. The largest intracontinental basin was located within the central part of the platform. At an early graben stage, fluvial facies were deposited and these were followed by quartz-arenite, shale and dolomite

sedimentation in shallow water. The anorogenic magmatic events were represented by ultrapotassic volcanics and rapakivi granites (ca. 1.6-1.5 Ga), respectively. The widest transgression took place and produced thick carbonate sediments. After frequent elevation and subsidence in the Late Proterozoic, the main parts of the intracontinental basin were uplifted. However, a few small taphrogenic basins located in the eastern part of the basin continued to receive sediments. A proto-platform marginal basin was formed at the sourthern border of the North China Platform. Its tectonic evolutionary characteristics and stages are very similar to those of the above-mentioned intracontinental basins. Another continental marginal basin, extending in an E-W direction, evolved on the northern border of the platform during the middle Proterozoic. Subsequently, only smaller basins were formed in the Late Proterozoic.

INTRODUCTION

The North China Platform, i.e., the Sino-Korean paraplatform (Huang, 1980), is referred to as that region on which the cover strata were formed after the Luliangian or Zhongtiaon Orogeny. Its border is defined by a Late-Precambrian sedimentary basin and its southern limit is bounded by the Lushi-Queshan fault (Fig. 1b). However, for the North China protoplatform (1800-2500 Ma), the southern boundary extended farther south to the southern limit of the Huaiyang Shield (Cheng Yuqi et al., 1984) or the northern limit of the glaucophane-schist belt within the Huaiyang region (Fig. 1a, Dong Shenbao et al., 1985).

Precambrian rocks are extensively exposed, and they have been studied for several decades. Recently, Cheng Yuqi et al. (1982a, b, 1984); Ma Xingyuan et al. (1981, 1984); Chen Jinbiao et al. (1980) and Wang Hongzhen et al. (1984) have provided a synthesis of the Archaean and the Early-Proterozoic stratigraphy and petrology, the Precambrian tectonics, the Late-Precambrian stratigraphy and the tectonic framework of the Proterozoic.

The North China platform has undergone at least three tectonic megastages, namely the formation of the craton (>2500 Ma), the protoplatform, and the platform stage, respectively having distinctive characteristics of petrology, stratigraphy, geochemistry and tectonic environment (Wang and Qiao, 1984; Ma et al.,

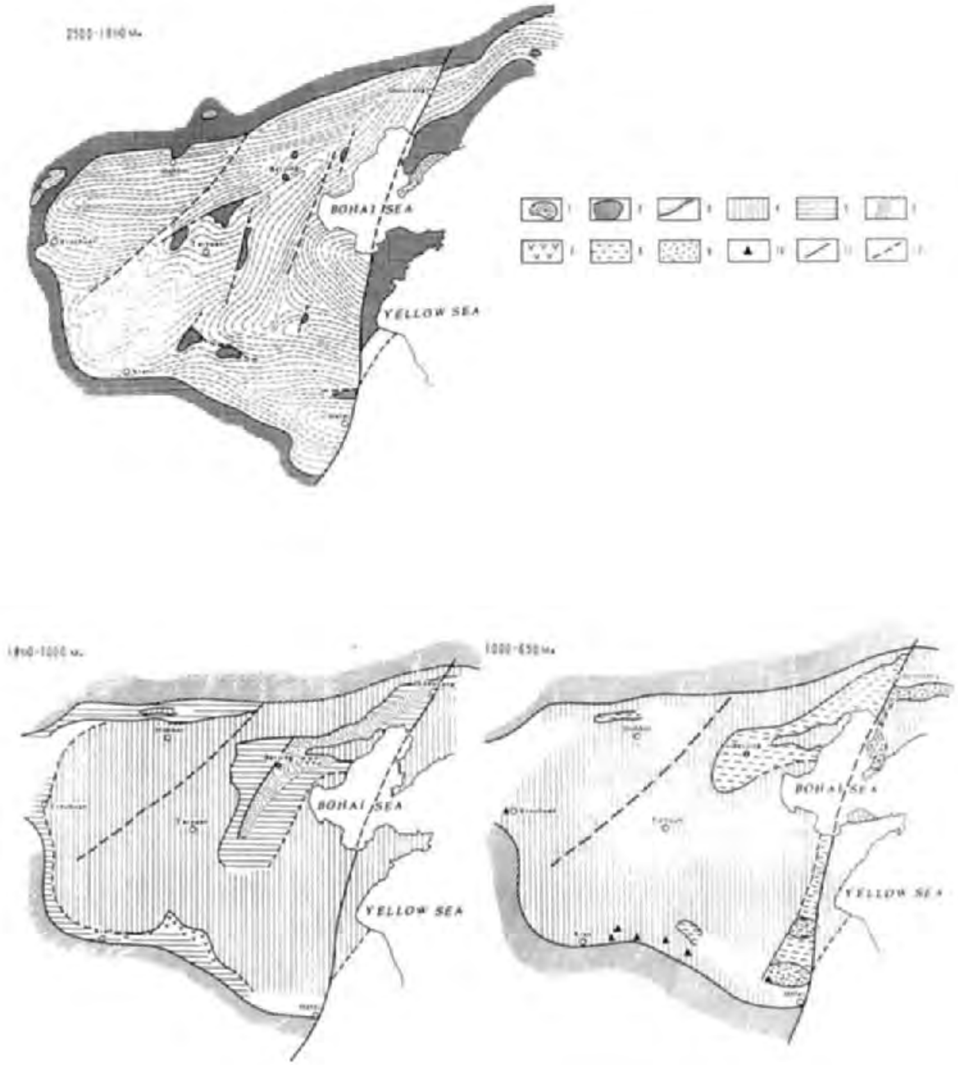

Figure 1. Tectonic evolutionary stages of the Proterozoic in the North China platform. a.2500-1800 Ma-Early Proterozoic; b. 1800-1000 Ma-Middle Proterozoic; and c.1000-650 Ma-Late Proterozoic. 1. Archaean craton; 2. Early Proterozoic basins or troughs; 3. Border of platform; 4. Upwarped district; 5. Mid-Proterozoic tectonic basin; 6. Fluvial deposit; 7. Volcanics; 8. Early basin of the Late Proterozoic; 9. Late basin of Late Proterozoic (Sinian); 10. Tillite; 11. Fault; 12. Inferred fault.

1984). The evolutionary process from the craton to the platform is the history of the Proterozoic tectonic evolution of the North China platform.

THREE TECTONIC MEGASTAGES OF THE NORTH CHINA PLATFORM

Cheng Yuqi et al. (1984) divided the Early Precambrian of the North China platform into four evolutionary stages on the basis of volcano-sedimentary and/or sedimentary mega-cycles, two for the Archaean and two for the Early Proterozoic. Petrological and geochemical characteristics of the rocks of the Archaean basement of the North China platform, which are older than at least 2500-3000 Ma according to reliable ages have been described by Sun Dazhong and Wu Changhua (1981) and Cheng Yuqi et al. (1984).

The Archaean craton of North China is the product of preliminary cratonization. The craton is made up of medium- to high-grade metamorphic rocks. This has led to some controversy as to whether a typical greenstone belt does exist in the Archean of China. Secondly, in the Archaean, the North China craton was less stable. The tectonic movement at the end of the Archaean is a protopanorogeny named the Fupingian. As a result of the cratonization, the basement of the North China platform, along with the adjacent region, began consolidating. But subsequent crustal movements caused the basement to yield due to brittle faulting and uplift which gave rise to the North China protoplatform, and successively some taphrogenic basins on the craton.

During the Early Proterozoic, in the basins and troughs surrounding the craton, there were less extensive volcano--sedimentary cover rocks. This was the time of the development of most of the North China protoplatform. In this period, tectonic activity was still frequent. There are differences in volcanic activity and the nature of the sediments in different parts of the protoplatform. On the protoplatform, the lower part of the ensialic basins consists dominantly of eugeosynclinal volcano--sedimentary rocks, while the upper part is comprised mainly of miogeosynclinal, well-differentiated epicontinental sediments. This sequence shows a tendency for the evolution of the protocrust from activity to stability with time. Since then, the whole North China protoplatform was in a para-stable stage. At the end of the Early Proterozoic, panorogeny again took place, finally resulting in the cratonization of the North China protoplatform. This orogeny, named the Luliangian or Zhongytiaoan, has the same significance as that at the end of the Archaean. It is so important that the North China platform, from then on, records a new stage of development.

After attaining a relatively stable tectonic setting, the North China platform, which is bounded by faults, was as large as the present North China platform terrain. On its basement and surrounding it, the accumulation of a well-differentiated sedimentary cover occurred. In spite of recurring transgression and regression, as well as sinking and uplift, the North China platform has remained relatively stable.

In the present paper, the Proterozoic is divided into three tectonic stages i.e., the Early Proterozoic (2500-1800 Ma), the Middle Proterozoic (1800-1000 Ma) and Late Proterozoic (1000-610 Ma) (Fig. 1).

THE EARLY PROTEROZOIC TECTONIC STAGE (2500-1800 Ma)

In the North China Protoplatform (Fig.1a), during the Early Proterozoic, the volcano-sedimentary basin developed principally as intracratonic basins and also as marginal basins. The intracratonic basins were well developed in Wutaishan north of Taiyuan, Luliangshan in the West, Taihangohan in the east, Zhongtiaoshan in the south and Songshan in the southeast, and also east of Beijing in the eastern Hebei. The marginal cratonic basins are distributed in eastern Shangdong, eastern Liaoning and in the northern marginal zone of the platform. These volcano-sedimentary basins and/or troughs have a basement of high-grade metamorphic and granitic rocks of the Archaean, so they are characteristically ensialic. The Early-Proterozoic rocks show unconformable contacts with the Archaean in some places (a few distinct basal conglomerates occur). Elsewhere, contacts between them are fault contacts. Whether a contact is an unconformity or a fault, we cannot rule out the possibility that the formation of the original volcano-sedimentary basins of the Early-Proterozoic was a result of faulting. Dislocation was the predominant factor leading to the formation of these basins or troughs. These faults are mainly NNE, subordinately ENE-WNW, and were generated in the basement of the Archaean craton.

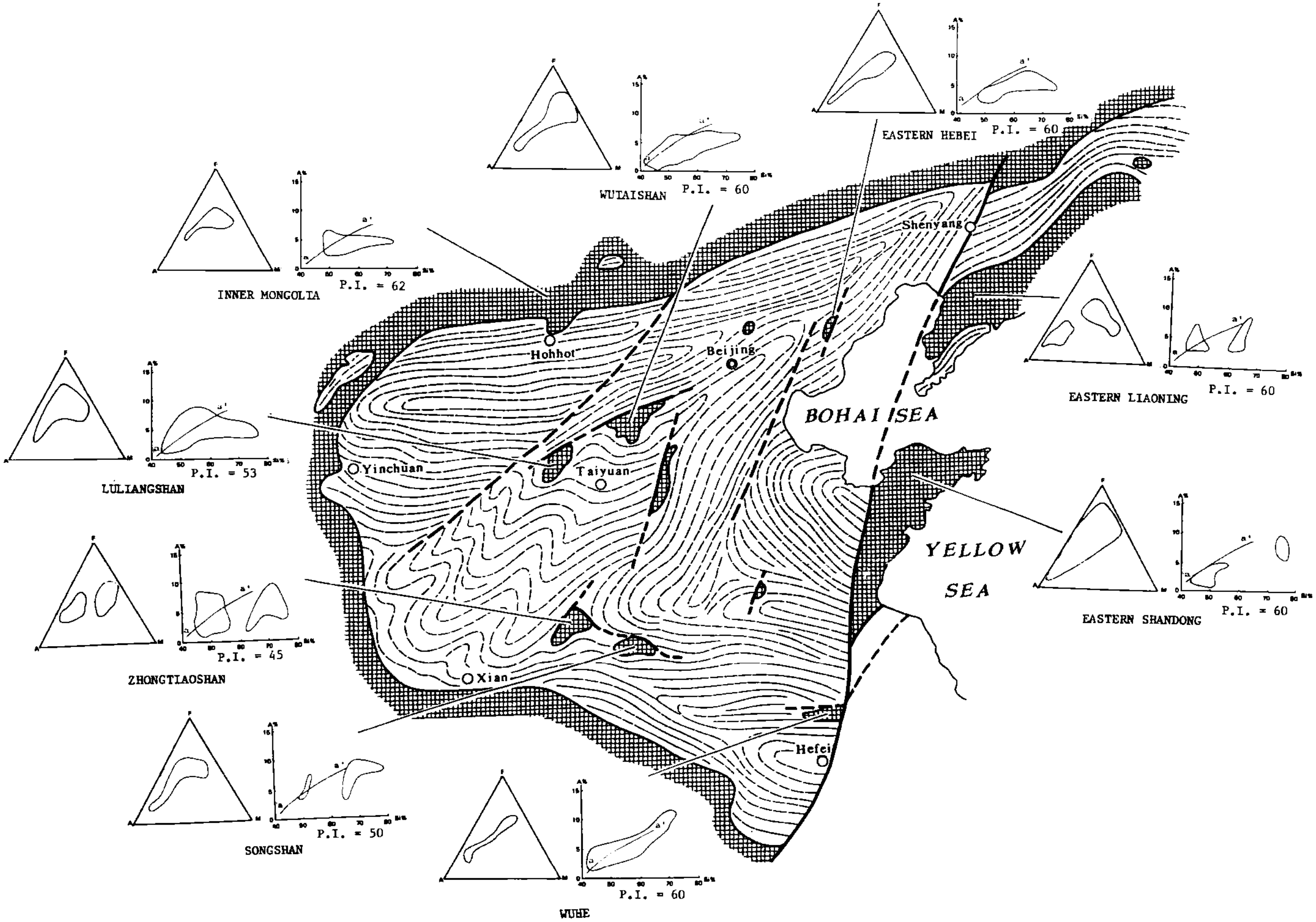
WUTAISHAN
P.I. = 60
EASTERN HEBEI
P.I. = 60
INNER MONGOLIA
P.I. = 62
EASTERN LIAONING
P.I. = 60
LULIANGSHAN
P.I. = 53
EASTERN SHANDONG
P.I. = 60
ZHONGTIAOSHAN
P.I. = 45
SONGSHAN
P.I. = 50
WUHE
P.I. = 60
Shenyang
Hohhot
Beijing
BOHAI SEA
Yinchuan
Taiyuan
YELLOW SEA
Xian
Hefei
F
A
M
A%
Si%
a
a'

In the early stage of the Early-Proterozoic, these basins or troughs were of different shapes and sizes, and were made up of different volcano-sedimentary products. According to the difference in tectonic setting, the features of volcanics and sedimentary rocks can be divided into two types: (1) The bimodal volcanic rocks of the cratonic marginal basins, located in eastern Shandong and eastern Luiaoning Province, to the east of the Tan-Lu fault; they are composed of predominantly boron-rich volcanic rocks which have been described by Cheng Yuqi et al., (1984). On the AFM diagram (Fig.2a), they conform to the volcanic rocks of tensional type according to the criterion of Petro et al., (1979). The Peacock's index for them is about 60, similar to calc-alkaline suites. But the nature of the volcanics and their geochemical charcteristics are still unique (Zhang Quesheng et al., 1985). (2) The calc-alkaline or bimodal volcanics, which filled in the intracratonic basin; often basic rocks are dominant in the succession as compared to those in greenstone belts of the Proterozoic. On the craton, in the separated intracratonic basins, the volcanic rocks changed from calc-alkaline to a calc-alkaline plus tholeiite series from north to south (Fig. 2) and the Peacock's index from 60 to 50 and even 45, which indicates alkaline basalt and trachytic basalt in Zhongtiaoshan. In fact (as for example, in Wutaishan in a very typical sequence) we can find that more than one volcanic suite accumulated in one basin. There are two volcanic suites with distinctive petrological, geochronological and geochemical characteristics (Cheng Yuqi et al., 1984). In particular, on the basis of their REE composition, the basic volcanic rocks of the lower part with a REE pattern enriched in LREE and those of the upper with a flat REE pattern can be distingushed; these probably reflect the difference in the tectonic stages. But it was noticed that parts of the flat REE patterns are not always considered as representative of oceanic basic volcanics. The envelope of the REE pattern of continental basalt could include flat REE patterns, even for some basalts with depleted LREE

Figure 2. AFM and A-Si diagrams for the trends of the early stage of the Early-Proterozoic volcanics within the basins or troughs of the North China protoplatform (ca. 2500-2300 Ma). On the A-Si diagram, curve a-a' represents the boundary between the alkaline and subalkaline series after Irvine and Baragar (1971); A=K_2O+Na_2O; F=FeO^*; M=MgO; Si=SiO_2, P.I.= Peacock's Index.

(Culler and Graf, 1984). In practice, the REE patterns of metabasic volcanic rocks of the eastern Hebei show a gradual transformation from LREE enriched into a flat REE pattern within a distance of 30 m upwards in the sequence, but with no indication of any new tectonic change. In the light of the observable geological conditions, it can be considered that the cause of the REE change could be explained by tensional and compressional environments, as suggested by Wood (1979). Ma Xingyuan et al. (1984) proposed the evolutionary stages of the Wutaishan Basin, showing the formation of the lower Wutai (Shizhuei subgroup) within an attenuated environment and the accumulation of the upper Wutai (Taihuai subgroup) following recumbent folding and low-angle thrusting.

In most of the basins (e.g., Eastern Liaoning, Eastern Heibei, Luliang Shan, Zhongtioshan and Songshan, etc.), epicontinental coarse clastic rocks appear in the lower portion; semipelitic sediments are common towards the upper part. Thick carbonate rocks are found only in eastern Liaoning, turbidites and BIF of Algoma type were deposited in the Heibei and Wutaishan. They also show differences between intra-cratonic and cratonic marginal basins. It should be pointed out that a thick BIF similar to the Superior type occurs in the Luliangshan intra-cratonic basin which is located to the west of Wutaishan Basin, indicating the distinction between the sedimentation conditions in the two neighbouring basins on the protoplatform.

The time range and tectonic stages of the above-mentioned basins and troughs are varied. Detailed geochronological studies of the early stage of the Wutaishan Basin suggest that accumulation of volcano-sedimentary rocks should have occurred within a limited time range betweeen 2560 and 2520 Ma ago. But Bai Jin et al.(1982) consider that the rocks may be of Archaean age. Neverthless, the Wutai greenstone belt has undergone at least three phases of deformation and this has been accepted by many geologists, because there are two unconformities that could be distinctly recognised. A case like this, i.e., of two unconformities in one basin, has not yet been found elsewhere in the early stage of the Early-Proterozoic.

In general, the metamorphic grade of these rocks in cratonic marginal basins, particularly in the eastern Shandong and eastern Liaoning, is higher than in intra-cratonic basins. Metamorphic zones of from greenschist to amphibolite facies in eastern Liaoning and granulite facies in eastern Shandong are shown to be regional progressive metamorphism (Dong Shenbao et al., 1985). By comparison, in most intracratonic basins, the volcano-sedimentary rocks were merely metamorphosed to greenschist facies, except in the lower part of the Wutai and Zhongtiao sequences which have been affected by amphibolite facies. At the end of Wutaian Orogeny, closure of these basins took place owing to horizontal shortening, giving rise to fan-shaped complex folds (Ma Xiangyaun et al., 1984) or tight isoclinal folds (Sun Dazhong et al., 1984). In addition, during the early stage of the orogeny, granitic and/ or tonalitic-trondhjemitic rocks were emplaced by way of intrusion or migmatization.

In the late stage of the Early-Proterozoic, after the Wutaian Orogeny, all of the basins, both large or small in size, overlie the early-stage orogenic belts or occur adjoining them.

In this period (ca. 2300-1800 Ma), the succession in the basins consists predominantly of neritic-terrestrial clastic sediments, semipelitic and carbonate rocks and minor basic volcanics with continental features. The succession resembles the sedimentary products of intracratonic basins or lagoon-shaped semi-enclosed basins which have favoured the formation of magnesite. Moreover, close to the stromatolite-bearing metacarbonate strata and meta-black shale, strata-bound copper deposits could be found, either in cratonic marginal basins or in intracratonic basins.

To sum up, the environments were like miogeosynclines, which represent a transition from mobile to relatively stable conditions. Final cratonization or panorogeny of the North China protoplatform was accompanied by inversion folding and greenschist-facies metamorphism, as well as intrusion of granites.

THE MIDDLE-PROTEROZOIC TECTONIC STAGE (1800-1000 Ma)

The Middle-Proterozoic, ranging from about 1800-1000 Ma, is the period when the Changcheng and Jixian systems, which represent typical platform cover, were deposited. The terminal consolidation of the North China platform was achieved and the major tectonic framework of the North China platform had been formed by the close of the Luliangian-Zhongtiaoan Orogeny (cs. 1900-1800 Ma). Three main tectonic basins (Fig. 1b) occurred in different portions of the North China platform. The largest intracontinental basin was developed within the central part of the platform. A protoplatform marginal basin was formed at the southern border and a tectonic basin evolved on the northern border of the North China platform. Although the basins are comparatively stable, there are still some differences among them in their tectonic nature, sedimentary environments, magmatism, and mineralization.

The intracontinental basin

This basin mainly extends along the Yanshan and Tihang ranges. From its sedimentary-volcanic nature and tectonic evolution, this intracontinental basin can be separated into two tectonic stages.

In the first stage (ca. 1800 to 1400 Ma), a fault-bounded rift-like graben was formed in the central part of the rigid protoplatform. The initial fluvial deposits were strongly controlled by the graben which was filled by terrestrial coarse-grained clastic rocks belonging to the lower Changzhougou Formation. According to palaeo-current data (Wang Changyao, 1983), the main channel of the palaeo-river is consistent with the axis of the graben, and the palaeo-river ran into the sea from SW to NE (Fig.3). Then the first transgression took place with the graben development, and sedimentary deposits were distributed in a wider region outside the graben (Fig. 1b). Above the fluvial deposits, fine-grained, pinkish and white quartzitic sandstones of the upper Changzhougou Formation formed in a littoral environment. These are overlain by intratidal black shales of the Chauanlinggou Formation. Muddy and silty dolomicrites of the Tuanshanzi Formation overlying the black shales accumulated below the wave base. The overlying Dahongyu Formation, which consists chiefly of quartzitic sandstone and ultrapotassium alkaline volcanics, terminated the first tectonic stage.

It is noted that the sedimentary deposits from the Changzhougou Formation to the Dahongyu Formation had been controlled by a fault-bounded graben. Some differences in stratigraphic thickness and sedimentary facies within and outside the graben can easily be observed (Fig.4). A remarkable anorogenic magmatic event, represented by Rapakivi granite and alkaline volcanics, occurred at the end of the first stage. A 1644 Ma old Rapakivi granite situated in Miyun County of Beijing has been found. The date falls in the interval 1500-1800 Ma during which Rapakivi granites

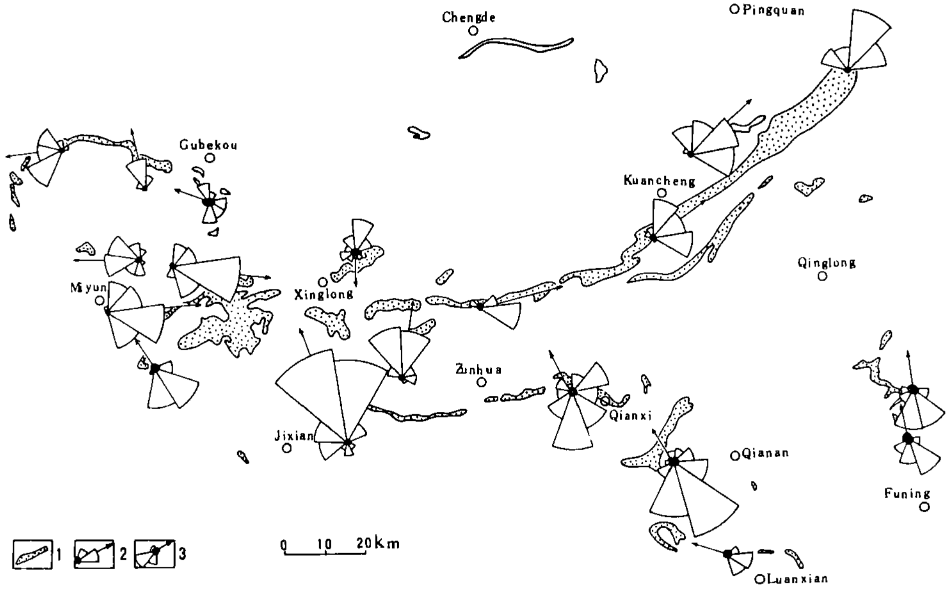

Figure 3. Paleocurrent map of the early Changzhougou epoch (after Wang Changyao, 1983). 1. outcrop of the Lower Changzhougou Formation. 2.Paleocurrent shown by cross-bedding. 3. Paleocurrent shown by gravels.

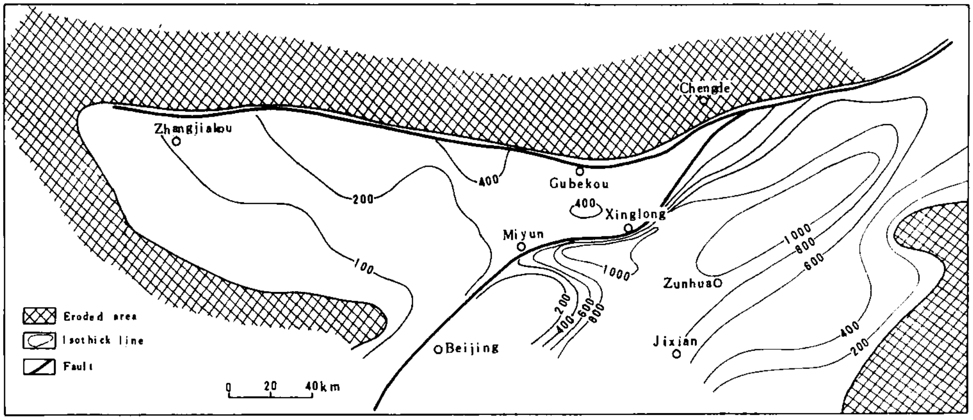

Figure 4. Sketch map showing isothickness line of the Changzhougou Formation in the Yanshan Range.

in other parts of the world were emplaced (Salop, 1983). The alkaline volcanic rocks of the Dahoungyu Formation are K-rich. They mainly include ultrapotassic tephriphonolite and phonotephrite (Fig.5). A potassium content of up to 10% is common and K_2O/Na_2O ratios range from about 10 to more than 100; in this respect, they differ from other potassic volcanic rocks of the world. Generally, the ultrapotassic volcanic rocks of the Dahongyu Formation are quite similar in chemical composition to the Wyomingite from Wyoming (Table 1). In mineral composition, however, there is a distinct difference between them. The main potassium-bearing mineral of the Dahongyu volcanics is potash feldspar, but those of Wyomingite comprise phlogopite and leucite.It is considered that such ultrapotassic volanic rocks are related to the rift-type basins. It is well known that some high-potassium volcanic rocks have been found in rift-basins in other basins in other places (Hughes, 1982).

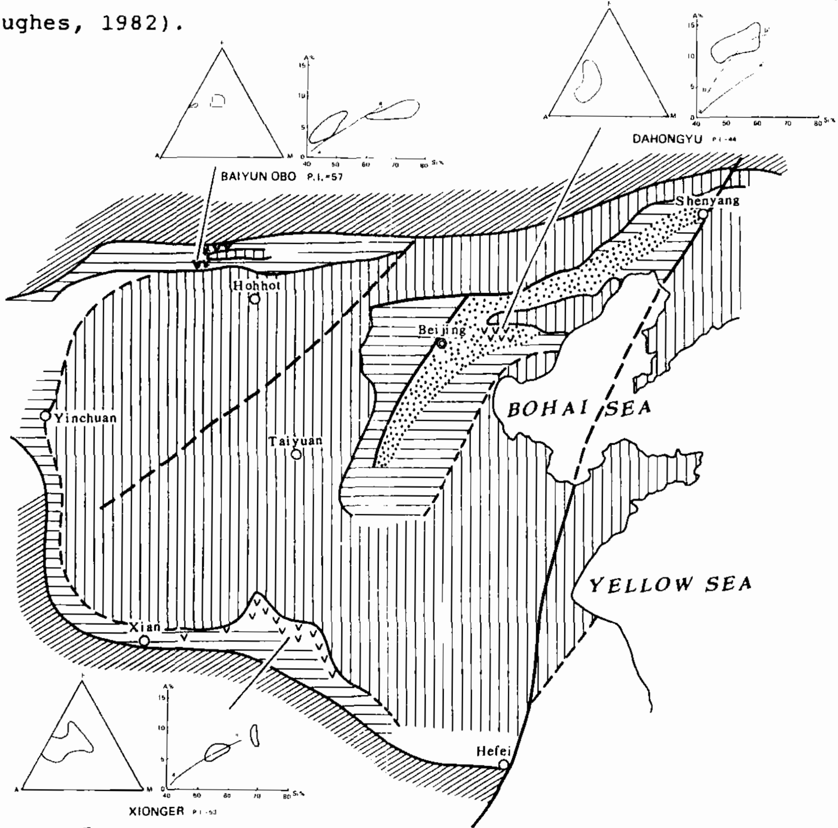

Figure 5. AFM and A-Si diagram of the volcanic rocks of the Middle-Proterozoic (1800-1000 Ma) on the North China Platform. On the A-Si diagram, curve a-a' represents the boundary between the alkaline and subalkaline series, Curve b-b'is the boundary between ultra-alkaline and alkaline series (after Irvine and Baragar, 1971); P.I.= Peacock's Index; $A=K_2O+Na_2O$, $F=FeO^*$, $M=MgO$, $Si=SiO_2$.

Table 1.
Comparison of chemical composition between Dahongyu volanic rocks and Wyomingite

	Dahongyu volcanic rock	Wyomingite*
SiO_2	51.29	50.23
Al_2O_3	16.27	10.15
Fe_2O_3	5.86	3.65
FeO	4.37	1.21
MnO	0.08	0.09
MgO	3.12	7.48
CaO	1.58	6.12
Na_2O	0.18	1.29
K_2O	11.08	10.48
TiO_2	1.55	2.30
Number of analyses	14	4

* After I.S.E. Carmichael (1967).

During the second tectonic stage (ca. 1400-1000 Ma), subsidence of the basin was predominant. The widest marine transgression took place, which brought about carbonate deposition of a large thicknesses in a widespread region. Above the Dahongyu Formation, with a break,comes the Gaoyuzhuang Formation, which is composed of dolomite, dolomitic limestone, silty shale and manganiferous dolomite. The K-Ar age of glauconite from the Gaoyuzhuang Formation is 1387 ± 37 Ma. Therefore, the time boundary between the first and the second stage is inferred to be at about 1400 Ma. The overlying Yangzhuang Formation, which consists of red and white silt-bearing muddy dolomite, rests conformably upon the Gaoyuzhuang Formation. The boundary between both the formations has been regarded as separating the Jixian system from the Changchenge system. It is preferable to place the boundary between these two systems at the base of the Gaoyuzhuang Formation. Higher up, comes the Wumishan Formation, which is composed of dolomite and cherty dolomite. This is followed by shale and silty shale of the Hongahuizhuang Formation. The uppermost strata of Jixian system is the Tieling Formation comprising dolomite, shale and stromatolitic limestone.

In the second stage, the tectonic basin lost the distinct linear extension of the graben, and became a shallow tectonic basin, which is characterized by greater stability and areal extent. Almost all contact relations of the strata are continuous, apart from the regional unconformity between the upper and lower members of the Tieling Formation. Carbonates formed in a tidal platform environment are predominant, deep facies rare, and changes of regional lithofacies not clear. All these features together demonstrate that during the second stage the nature of the palaeo-sea was similar to that of an epeiric sea. In addition, magmatism was also quite weak; large-scale intrusions and volcanism have not been found. Only mafic dyke swarms which have isotopic ages of around 1200 Ma have been recognised.

The protoplatform marginal basin

This tectonic basin is developed at the southern border of the North China Platform and is separated from the Qinling geosyncline by faults. The tectonic nature and evolution of the basin are identical to those of the intracontinental basin described in the foregoing. It is believed that during the initial tectonic stage the basin was a rift or aulacogen (Ma Xingyuan et al., 1984; Wang Hongzhen et al., 1984). The Xionger Group, which is composed of terrestrial, coarse-grained clastic rocks and volcanic rocks, filled the triangle-shaped basin. The sequence approximately corresponds to the sequence from the Changzhougou to Dahongyu formations.

Volcanic rocks of the Xionger Group consist of basalt, andesite, dacite and rhyolite (Li Dazhou and Ye Danian, 1980). According to the chemical classification of volcanic rocks (Le Maitre, 1984), shoshonite and dacite are predominant. The volcanic rocks seem to belong to the calc-alkaline series (Fig. 4). However, it is obvious that their potassium content is quite high, and it is higher than the sodium content. In addition, SiO_2 ranges from 52 to 70 percent, the FeO(t)/MgO ratio is generally more than 2. Judging from the afore-mentioned features, the volcanics of the Xionger Group probably resemble those of Andean-type continental margins. It is believed that at the first stage the tectonic basin may be regarded as an arm of a triple rift system whose other arms continued to develop into the Qinling geosyncline. But the arm filled by the Xionger Group quickly failed.

The overlying Ruyang Group rests unconformably upon the Xionger Group, and marks the beginning of the next stage. The Ruyang Group is composed of terrestrial clastic rocks and littoral sandstone. Higher up, comes the Luoyu Group which comprises chiefly sandstone, shale and carbonate. Both groups have greater spread than the Xionger Group and have a clear E-W extension which differs from the near N-S direction of the initial failed arm (Fig. 1c).

The continental marginal basin

This tectonic basin borders the Mongolia geosyncline with abyssal faults. The Middle-Proterozoic Baiyun Obo and Chaertai groups occupy the middle part of inner Mongolia, located at the northern border of the North China platform. Recently, the tectonic nature and evolution of the basin have been studied by Liu Renfu (personal communication) and Wang Hongzhen and Quiaoxiufu (1984).

The basin is separated into two belts by a long and narrow uplifted, Early-Precambrian basement. The Baiyun Obo Group is developed in the northern belt, and the Chaertali Group in the

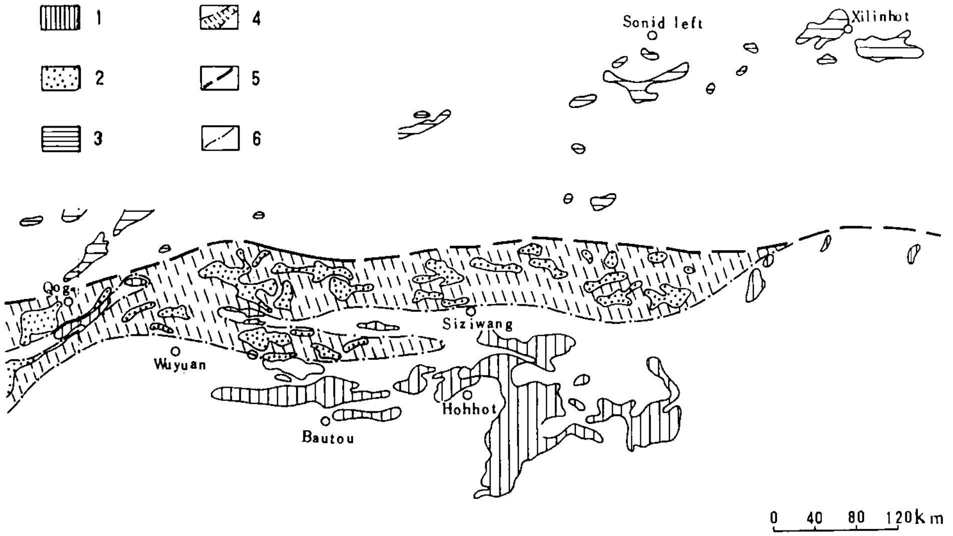

Figure 6. Tectonic sketch map of the continental marginal basin during the Middle-Proterozoic. 1. Early-Precambrian, 2. Middle--Proterozoic outcrop, 3. Deposits of Paleozoic geosyncline, 4. Middle-Proterozoic basin, 5. Fault, 6. Border of the basin.

southern belt (Fig. 6). Both groups are of flysch association, and are made up of two sedimentary cycles. The lower part of each cycle contains metamorphosed gravel-bearing coarse clastic rocks, and the upper part carbonaceous slate, phyllite and crystalline carbonates, which were mainly deposited in fluvial and intertidal environments. However, the products of slumping and turbidity currents have been observed in the northern belt (Li Jiliang, 1981), which exhibits greater slope and depth for the northern belt as compared to that of the southern belt.

Volcanics can be found at different levels, but are more concentrated in the lower part of each cycle. Bimodal series consisting of basalt/trachy-basalt and rhyolite are the predominant types (Fig.5). Potassium in the rhyolites is commonly higher than sodium.

Pb-Pb ages of 1600 Ma, 1520 Ma and 1310 Ma for the Baiyun Obo Group have been reported (Tu Guangzhi, 1984). The Baiyun Obo Group and its analogues approximately correspond to the Changcheng and Jixian systems. It has been well known that among the three basins of the North China Platform, the continental marginal basin is the most important for the Middle Proterozoic mineralization. Rare--earth iron formation has been found in Baiyun Obo. Copper and lead-zinc deposits which are located in the western part of the basin may be contemporaneous with the rare-earth iron formation.

The movement between the Middle and the Late-Proterozoic in the intracontinental basin is named the Qinyu uplift. It separates the Qingbaikou from the Jixian systems. The former includes the Xiuamaling and Jingeryu formations. The Xiamaling Formation consists of shaly siltstone and lenticular sandstone; higher up, arkosic sandstone, gluconite-bearing arkosic sandstone, shale and limestone. It is unconformably overlain by the middle part of the Early Cambrian in the Yanshan Range.

In the eastern region of the Late Proterozoic basin, the Yongning and Xinhe groups are equivalent to the Qingbaikou System. The Yongning Group, which rests unconformably upon Archaean migmatized granite, comprises fluvial conglomerate, alternations of littoral conglomerate and coarse sandstone, and tidal coarse sandstone with a total thickness of 4500 m. The Yongning Group seems to be the initial accumulation in a new rift-type graben. The overlying Xihe Group is made up of littoral sandstone,

Table 2.
Major events of the Proterozoic in the North China platform

	Tectonic stages	Stratigraphic subdivision	Lithology	Sedimentary Tectonic environment*	Magmatism
	Palaeozoic platform		Shale, limestone,	Transgressive marine,	
Platform	Late-Proterozoic platform (650-1000 Ma)	Jixianian (800 Ma?)	Predominant carbonates. Littoral sandstone, shale and neritic limestone.	Intracontinental taphrogenic basins.	Anorthosite (750 Ma).
	Middle-Proterozoic platform (1000-1800 Ma)	(Qinyu uplift) (1000 Ma) (Qinglong uplift) (1400 Ma)	Epeiric carbonates-predominant, dolomite. Littoral, neritic shale & dolostone, potassic volcanics orthoquartzitic sandstone, fluvial deposits.	Intra-protoplatform tectonic basins.	Basic dyke swarm (1200 Ma) Rapakivi granite (~1600 Ma)
Protoplatform	Early-Proterozoic protoplatform (2500-1800 Ma)	Luliangian (Zhongtiaoan) (1800 Ma)	Dolomite, slate, meta-arkose, and minor basic lava.	(Terminal cratonization) Intracratonic sedimentary basins.	Granite (1800 Ma),
		Wutai-an (2300 Ma)	Phyllite and metamorphosed silt (turbidite),chlorite schist, BIF, Amphibolite, mica schist.	Intracratonic troughs and basins.	Granite and minor TTG (2200-2300 Ma)
	Archaean (>2500 Ma)	Fupingian (2500 Ma)	High-grade metamorphic rocks.	(Primary cratonization)	Granite and TTG (2500 Ma).

* For intracontinental, intraprotoplatform and intracratonic basins.

glauconite-bearing arkosic sandstone, shale and limestone. A K-Ar age of 818 Ma for glauconite of the lower Xihe Group has been obtained (Lin Weixing et al., 1983).

During the Sinian Period, when the western part of the tectonic basin had been uplifted, the eastern basin continued to subside, resulting in sedimentary deposits thousands of metres thick.

The Liaonan Group, belonging to the Sinian System, located in the northeast part of the North China platform, consists chiefly of fine clastic rocks and carbonates. It is conformably underlain by the Xihe Group, but para-unconformably overlain by the middle Early Cambrian. The Rb-Sr isochron age of the lower Liaonan Group is 723±43 Ma, and that of the upper Liaonan Group is 649.5±20 Ma (Lin Weixing et al., 1983).

The Sinian System in the southeastern part of the platform is very similar to the Liaonan Group in stratigraphic sequence and lithology. The K-Ar dates for the lower, middle and upper parts of the Sinian System are respectively 749.8, 681 and 647 Ma (Wang Gluixiang, personal communication). In addition, abundant remains of worm traces have been reported (Wang Guixiang et al., 1983).

Two problems should be pointed out. The first one is the migration of the basins. It is obvious that the basin migrated gradually from the west to the east throughout the Late Proteozoic. It is uncertain whether the migration was related to the development of a fault in NE-SW direction (See Fig. 1C). The second problem is about the tectonic nature of the intracontinental basin in the Sinian Period. The tectonic nature at that time was very similar to that of the second stage of the Middle--Proterozoic, shallow-marine deposition, stable lithofacies in the region, and weak magmatism. All of them show the platform nature.

CONCLUSION

The proterozoic tectonic evolution of the North China Platform represents a long span of geological history developed on the extensive Archeaean high-grade metamorphosed basement. The Proterozoic of the North China Platform (Table 2), consists of two tectonic stages - the protoplatform stage and the platform stage. The two stages are separated by the Luliangian-Zhongtian Orogeny. During the protoplatform stage, controlled by faults, several ensialic mobile belts, varying in size, were formed within or around the craton. Eugeosyncline-type basins or troughs, which are similar to the greenstone belts in tectonic features, were predominant in the first stage (2500-2300 Ma), but miogeosyncline--type basins in the later stage (2300-1800 Ma). All of them show that the protoplatform evolved from a more active to more stable state through the Early-Proterozoic. Then, the Luliangian-Zhongtiaon Orogeny resulted in the final cratonisation of the North China Platform. The platform of the Middle-Late Proterozoic is characterised by rift-type basins with mainly vertical movements, well-sorted sedimentary deposits, and potassium-rich volcanic rocks, which shows that the platform at that time had stable tectonic features.

The North China Platform is somewhat similar to the Proterozoic Platform in many respects, indicating the similarity of major parts of Asia during the Proterozoic tectonic evolution.

ACKNOWLEDGEMENTS

The authors wish to thank the anonymous reviewer for critical reading and correction of the manuscript and valuable suggestion. Thanks also are due to Mr. Yang Chunliang and Tang Min who assisted in the preparation of the manuscript.

REFERENCES

Carmichael, I.S.E., 1967. The mineralogy and petrology of the volcanic rocks from the Leucite Hills, Wyoming. Contr. Min Pet., 15: 24-66.

Chen Jinbiao, Zhang Huimin, Xing Yusheng and Ma Guogan., 1981. On the Upper Precambrian (Sinian Suberathem) in China. Precamb. Res., 15: 207-228.

Chen Yuqi, Bai Jin and Sun Dazhong., 1982a. The lower and Middle Precambrian of China. In: An outline of the stratigraphy in China. Geology Publishing House, Beijing (in Chinese with English summary), pp.1-46.

Cheng Yuqi, Bai Jin and Sun Dazhong., 1982b. The Lower Precambrian of China. Revista Brasileira de Geociencias, Sao Paulo, 12(1-3): 65-73.

Cheng Yuqi, Sun Dazhong and Wu Jiashan., 1984. Evolutionary megacycles of the early Precambrian proto-North China platform. Geodynamics, 1: 251-277.

Cullers, R.L. and Graf, J.L., 1984. Rare earth elements in igneous rocks of the continental crust: Predominantly basic and ultrabasic rocks. In: P.Henderson (Editor), Rare Earth Element Geochemistry. Elsevier, Amsterdam, pp.237-274.

Dong Shenbao, Shen Qihan, Sun Dazhong and Lu Liangzhao (Editor), 1985. "Metamorphic Map of China", Geology Publishing House, Beijing (in print).

Huang, T.K., 1980. An outline of the tectonic characteristics of China. In "Continental Tectonics", Natl. Acad. Sci., Washington: 184-197.

Hughes, C.J., 1982. Igneous Petrology. Elsevier Scientific Publishing Company, 552pp.

Irvine, T.N. and Baragar, W.R.A., 1971. A guide to the chemical classification of the common volcanic rocks. Can. J. Earth Sci., 8: 523-548.

Le Maitre, R.W., 1984. A proposal by the IUGS Subcommission on the systemstics of igneous rocks for a chemical classification of volcanic rocks based on the total alkali silica (TAS) diagram. Australian J. Earth Sci., 31:243-255.

Li Dazhou and Ye Danian., 1980. A preliminary recognition of metamorphism and volcanism along the southern margin of the North China Block Region. In: Formation and Development of the North China Fault Block Region. Sci. Press. Beijing: 133-142 (in Chinese).

Li Jiliang and Hu Fuyou., 1981. The serpentinitic olistostrome in Bayun Obo Group. Scientia Geologica Sinica, 3: 269-272 (in Chinese with English abstract).

Lin Weixing, Pu Dean, Yang Sen, Gao Rongfan, Fan Yiqing, Ma Junxiao, Wu Zhenwen, Bo Qing., 1983. Late Precambrian in Southern Liaodong Peninsula (in print).

Ma Xingyuan and Wu Zhengwen., 1981. Early tectonic evolution of China. Precamb. Res., 14: 185-202.

Ma Xingyuan, Zhang Jiasheng, Bai Jin and Suo Shutian., 1984. Variations in tectonic style through the Precambrian history of China. J. Geodynamics, 1: 221-249.

Petro, W.I., Vogel, T.A. and Wilban, J.T., 1979. Major-element chemistry of plutonic rock suites from compressional and extensional plate boundaries. Chem. Geol., 26: 217-235.

Salop, L.J., 1977. Precambrian of the Northern Hemisphere. Elsevier, Amsterdam, 378pp.

Salop, L., 1983. Geological Evolution of the Earth During the Precambrian. Springer-Verlag, Berlin, Heidelberg, 459pp.

Sun Dazhong and Lu Songnian., 1985. A subdivision of the Precambrian of China. Precamb. Res., 28: 137-162.

Sun Dazhong and Wu Changhua., 1981. The principal geological and geochemical characteristics of the Archaean greenstone-gneiss sequences in North China. Spec. Publ. Geol. Soc. Aust., 7: 121-132.

Sun Dazhong, Bai Jin, Jin Wenshan, Jiang Yongnian, Gao Fan, Wang Wuyun, Wang Junlian, Gao yadong and Yang Chunliang., 1984. The Early Precambrian Geology of the Eastern Hebei. Tianjin Sciences and Technology press, Tianjin, 274pp.

Tu Guangzhi., 1984. Some characteristics of Proterozoic strato-bound ore deposits in China. In "Developments in geoscience", Science Press, Beijing, pp.263-269.

Wang Changyao., 1983. Recognition of palaeoalluvial facies, characteristics and evolution of palaeogeography of the Changzhougou stage in Yanshan Range (in print).

Wang Guixiang, Zhou Benhe and Xiao Ligong., 1983. Late Precambrian Megascopic fossils from Huainan, Anhui Province and their significance (in print).

Wang Hongzhen and Qiao Xiufu., 1984. Proterozoic stratigraphy and tectonic framework of China. Geol. Mag., 121(6): 599-614.

Wood, D.A., 1979. Dynamic partial melting: its application to the petrogenesis of basalt lava series from Iceland, the Faeroe Island, the Isle of Skye (Scotland) and Troodos Massif (Cyprus). Geochim. Cosmochim Acta, 43: 1031-1046.

PRECAMBRIAN ROCKS OF THE HIMALAYA

K.S. VALDIYA

ABSTRACT

The Himadri (Great Himalaya) ranges are made up of Precambrian high-grade metamorphic rocks evolved at temperatures of 600-650°C and pressures of 5-7 Kb. The early Precambrian rocks which formed the basement of the Tethys basin to the north, have been uplifted from great depths (15-30 km) by the Main Central Thrust.

The metamorphic rocks of Himadri are overlain in the discontinuous Tethys basin by a great succession of sediments of the later Proterozoic and Phanerozoic time span. The lower part is uniformly argillo-arenaceous flysch, characterized locally by intraformational lenses of diamictites. These are followed upwards by an argillo-calcareous succession with large lenticular horizons of stromatolitic dolomites. Significantly, the Cambrian strata are altogether missing in the central and eastern sectors.

South of the Himadri, the larger part of the Lesser Himalaya comprises Riphean to Vendian sedimentary rocks, lithologically similar to and homotaxial with the Proterozoic succession of the Tethys province. The flysch formation possibly rests upon a basement of 1900 ± 100 Ma. old porphyritic granite of middle crustal origin, now found tectonically implanted in the sedimentaries in some places. The lower part of the succession is of argillo-arenaceous facies, characterized locally by turbidites, diamictite lenses and very prominent penecontemporaneous basic volcanic rocks of Lower Riphean (1350 ± 50 Ma.) age.

This assemblage grades upwards into a calc-argillaceous succession, characterized by stromatolite-bearing dolomites, lenticular deposits of coarsely crystalline magnesite associated with talc and base-metals and carbonaceous shale-marble rhythmites in the upper part. While the columnar-branching stromatolites indicate an age from Middle Riphean to Vendian for the dolomites of the inner sedimentary belt, the conodonts, primitive brachiopods and trilobites in a horizon of the youngest (terminal) formation of the outer sedimentary belt point to a Lower Cambrian age.

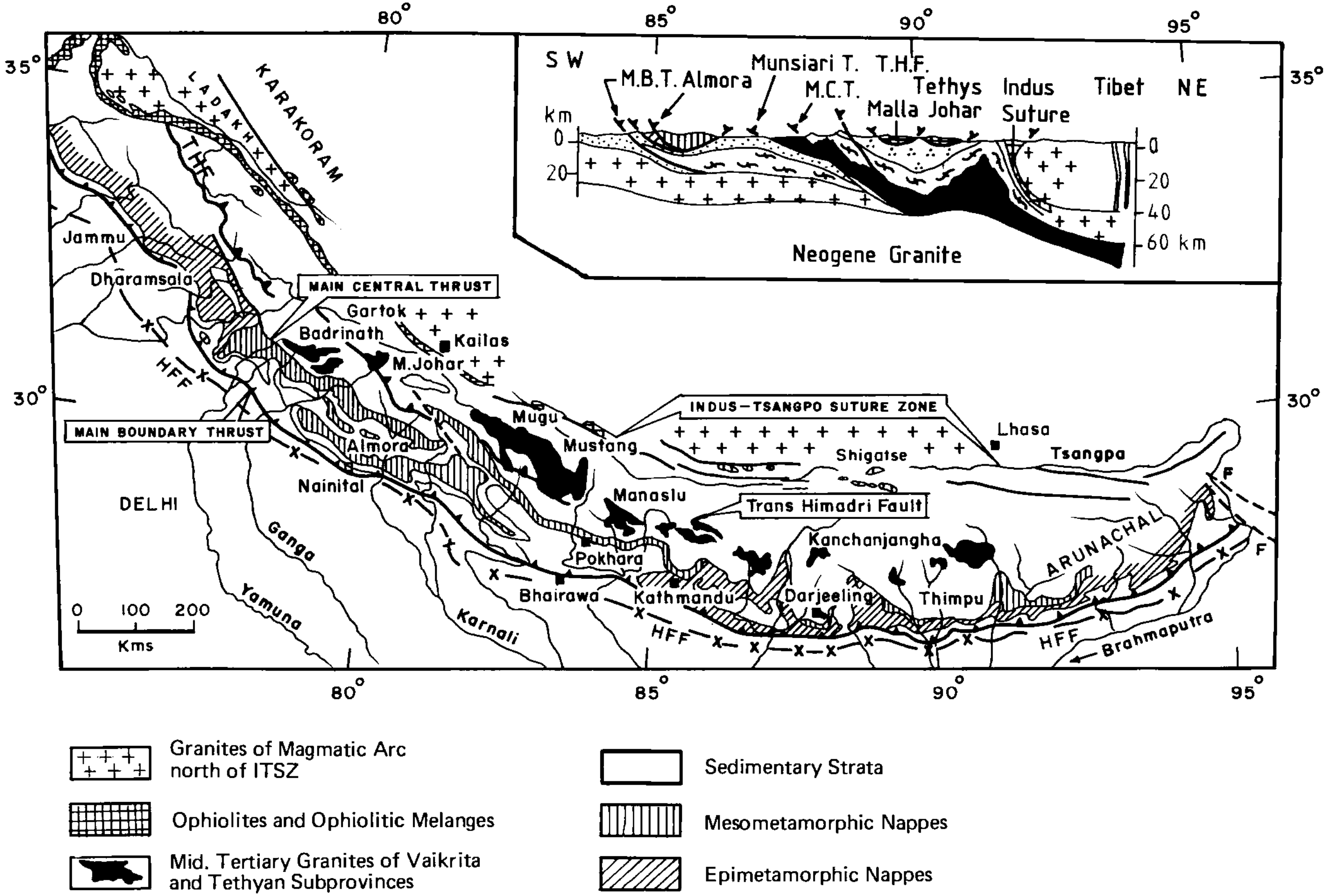
80°
85°
90°
95°
35°
30°
S W
M.B.T. Almora
Munsiari T.
T.H.F.
M.C.T.
Tethys
Malla Johar
Indus
Suture
Tibet
N E
km
0
20
40
60 km
Neogene Granite
KARAKORAM
LADAKH
THE
Jammu
Dharamsala
MAIN CENTRAL THRUST
Gartok
Badrinath
Kailas
M.Johar
HFF
MAIN BOUNDARY THRUST
Almora
Mugu
Mustang
INDUS–TSANGPO SUTURE ZONE
Lhasa
Shigatse
Tsangpo
Nainital
DELHI
Manaslu
Trans Himadri Fault
Kanchanjangha
Pokhara
ARUNACHAL
F
Ganga
Yamuna
Bhairawa
Kathmandu
Darjeeling
Thimpu
Karnali
Brahmaputra
0 100 200
Kms
Granites of Magmatic Arc north of ITSZ
Ophiolites and Ophiolitic Melanges
Mid. Tertiary Granites of Vaikrita and Tethyan Subprovinces
Sedimentary Strata
Mesometamorphic Nappes
Epimetamorphic Nappes

The sedimentary rocks are thrust over by a succession of two sheets of complexly folded metamorphic rocks injected by highly tectonized granites. The lower sheet of epimetamorphics represents a flysch-facies thrust up along with the 1900 ± 100, Ma. basement of porphyritic granite, now in a much mylonitized state. The upper sheet consists of mesograde metamorphics representing the shallower facies sedimentary rocks resting on the basement granite and intruded by Lower Caledonian (550 ± 50 Ma.) granodiorite-granite bodies.

GENERAL SET UP

The 2400 km-long arcuate Himalayan province is divisible into five longitudinal domains, each with its distinctive stratigraphic sequence, sedimentation pattern, and igneous and tectonic histories (Fig. 1).

The Himadri or the Great Himalaya, comprises higher-grade Precambrian metamorphics, which constitute the basement on which the Proterozoic-Phanerozoic sediments of the Tethyan subprovince were laid down. The Precambrian metamorphic rocks are invaded extensively by Cambro-Ordovician and Miocene granites

The Himadri metamorphics are tectonically separated from the sediments of the Tethyan domain above by the recently recognized Trans-Hamadri Fault (T-HF). The dominant part of the sedimentary pile of the Lesser Himalaya is assigned to the Lower Riphean to Vendian time span, and a relatively smaller fraction in the southern belt belongs to the upper Palaeozoic. These latter accumulated in narrow basins resulting from Hercynian movements. The Riphean-Vendian sedimentary strata bear a considerable lithological similarity and seem to be homotaxial with the Proterozoic sediments of the Tethys Basin across the Himadri. The basal flysch either rests upon the basement of porphyritic granite (1900 ± 100 Ma. old), or more likely, the granite is tectonically emplaced in the lower part of the lower sedimentary assemblage.

Figure 1. The sketch map of the Himalaya shows major lithotectonic subdivisions delimited by intracrustal boundary thrusts. In the Great Himalayan (Himadri) domain, the katazonal metamorphic complex of the Vaikrita (blank) is intruded by dominantly Miocene granite (black). In the Lesser Himalaya, the autochthonous-parautochthonous Proterozoic sedimentary rocks (blank) are overthrust successively by sheets of epi- and mesograde metamorphic rocks, incorporating granite bodies 1900 ± 100 Ma. as well as 550 ± 50 Ma. old.

Along the delimiting boundary thrusts-- Main Boundary Thrust (MBT) and Main Central Thrust (MCT)-- the sedimentary succession is involved in the duplex tectonics of the intracrustal thrusts which has given rise to structural imbrications throughout the expanse of the thrust zones.

The complexly folded Precambrian sediments have been thrust over by a succession of two allochthonous sheets. The lower one, constituted of epimetamorphics, strongly resembles the basal flysch sediments of the autochthon and is intimately associated with the 1900 ± 100 Ma. old mylonitized porphyritic granites. The upper sheet, of mesograde metamorphics, intruded commonly by Lower Caledonian (550 ± 50 m.y.old) granodiorite-granite bodies.

HIMADRI DOMAIN : BASEMENT COMPLEX

Tectonic Design

The extremely rugged and geomorphologically youthful mountain rampart, rising to heights of 3000 to 8000 m, is made up of Precambrian high-grade metamorphic rocks intruded by Miocene and older granites. The 10-20 km-thick metamorphic complex of the Himadri domain served as the basement for the Tethyan sediments lying above in the north.

At the base, the Himadri complex is sharply defined by the Main Central Thrust (MCT), and recent investigations in Nepal, Kumaun and Zanskar have demonstrated that the boundary between the basement complex and the Tethys sedimentary cover is demarcated by a large detachment fault of regional dimension (>1600km in length), and named the Trans-Himadri Fault (Valdiya, 1988b).

Pronounced domal upwarp of the northern edge of the drifting Indian plate in the proximity of the subduction zone in the Sindhu-Tsangpo valleys has exposed the high-grade metamorphic rocks of the Vaikrita basement. The Gurla Mandhata-Rakshas Tal High of the Kailas-Mansarovar region, and the doubly-plunging Tso-Morari-Nimaling anticline in Ladakh represent this frontal upwarp of the basement (Valdiya, 1988b).

Lithology and Metamorphic Evolution in Kumaun

What has been described as the "Central Crystalline Zone" or "Central Gneisses" really consists of two distinctly different lithotectonic units, the bulk of the Great Himalaya being constituted of *Vaikrita* (Griesbach, 1891). The lower part of the

10-20 km-thick "Central Crystalline Zone" of Heim and Gansser (1939), named *Munsiari Formation*, has been separated by the MCT from the Vaikrita Group (Fig. 2) and assigned to the Lesser Himalayan ensemble (Valdiya, 1981).

Mineral assemblages of the Vaikrita Group (Valdiya and Goel, 1983) demonstrate Barrovian-type regional metamorphism reaching upper amphibolite to lower granulite facies locally in the Pindari Formation. This early metamorphism probably occurred in the period 70-50 Ma., as is indicated by the concentration of isotopic mineral dates (K-Ar and Rb-Sr) and fission-track studies (Mehta,

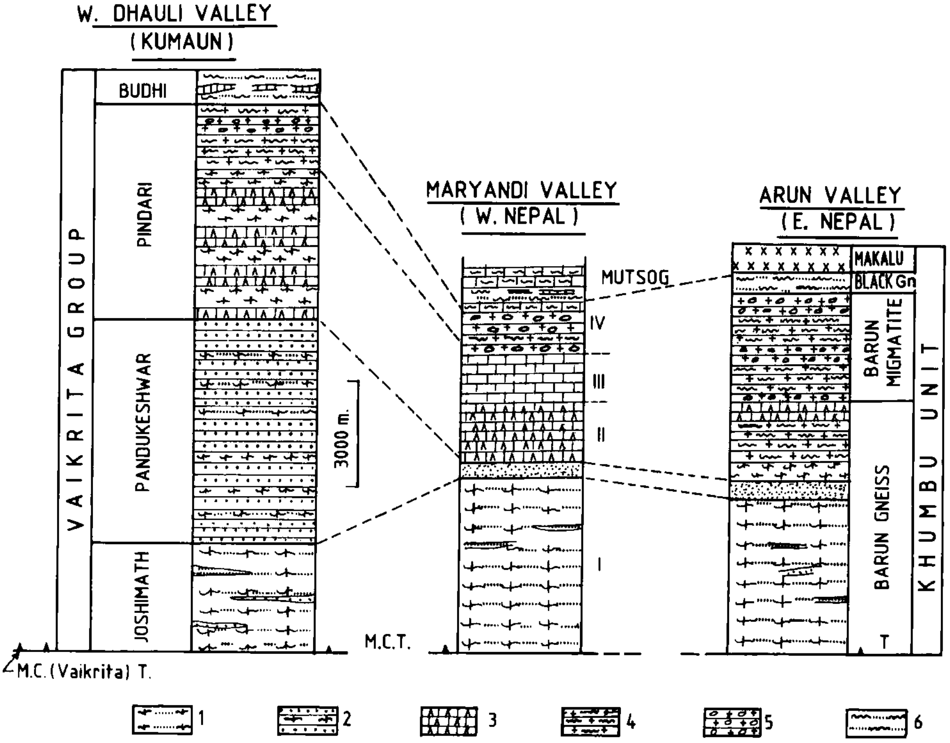

Figure 2. Columns showing lithological successions of the Great Himalayan groups (A) Vaikrita in Western Dhauli valley-Nanda Devi massif, Kumaun (Valdiya and Goel, 1983), (B) "Tibetan Slab" in Marsyandi valley-Annapurna Range, Nepal (Bordet et al, 1971), (C) Barun Group in Arun Valley-Sagarmatha massif in eastern Nepal (Jaros and Kalvoda, 1976).

1. Kyanite-sillimanite-garnet psammitic gneiss and subordinate schist; 2. kyanite-garnet schist interbedded with gneissic biotite-quartzite; 3. marble and calc-silicate fels, rich in pyroxenes and amphiboles; 4. migmatite and related gneisses; 5. augen gneisses; 6. biotite-porphyroblastic calc-schist.

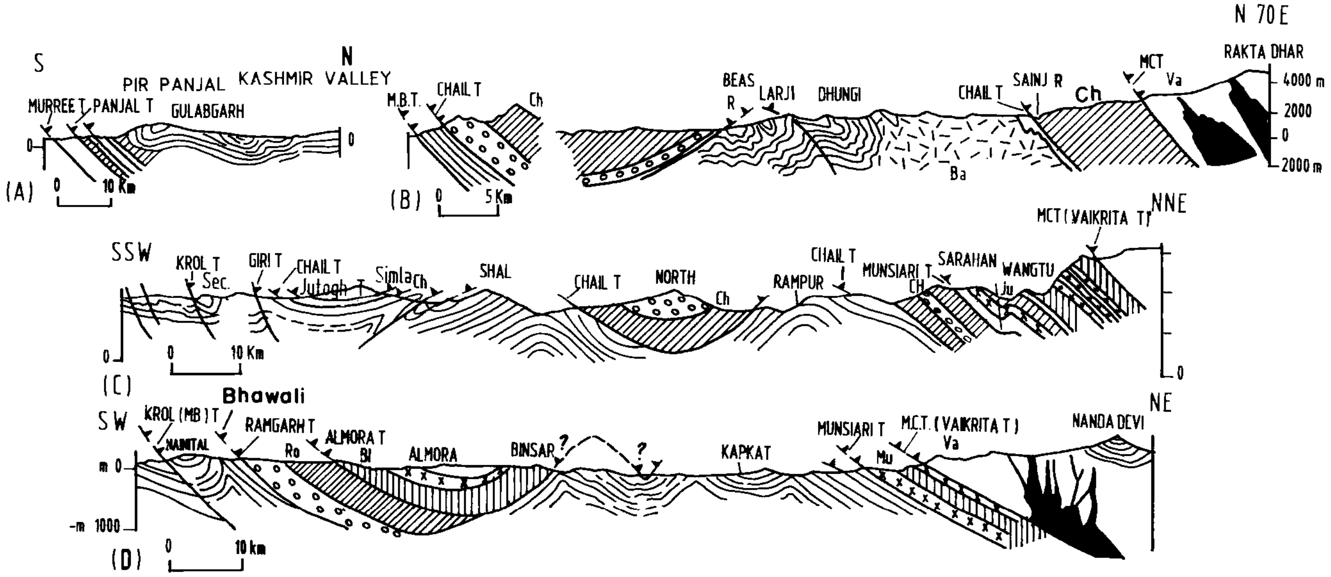
S
PIR PANJAL
KASHMIR VALLEY
N
MURREE T
PANJAL T
GULABGARH
0
(A)
0
10 Km
M.B.T.
CHAIL T
Ch
(B)
0
5 Km
BEAS R
LARJI
DHUNGI
Ba
CHAIL T
SAINJ R
Ch
MCT
Va
N 70 E
RAKTA DHAR
4000 m
2000
0
2000 m
SSW
KROL T
Sec.
GIRI T
CHAIL T
Jutogh T
Simla
Ch
SHAL
CHAIL T
NORTH
Ch
RAMPUR
CHAIL T
MUNSIARI T
CH
SARAHAN
WANGTU
Ju
MCT (VAIKRITA T)
NNE
0
0
10 Km
0
(C)
Bhawali
SW
KROL (MB) T
NAINITAL
RAMGARH T
Ro
ALMORA T
Bl
ALMORA
BINSAR
?
?
KAPKAT
MUNSIARI T
Mu
M.C.T. (VAIKRITA T)
Va
NANDA DEVI
NE
m 0
-m 1000
0
10 km
(D)

1980). The sillimanite-kyanite-garnet-biotite-quartz-feldspar (± muscovite) assemblage in the metapelites and metapsammites, and the associations of calcite-hornblende-labradorite (An_{50-65})-grossularite, and hornblende-diopside-andesine-quartz in the calc-gneisses and calc-silicate rocks suggest metamorphism of the Vaikrita Group under upper amphibolite facies conditions within P-T ranges of 5 - 5.7 kb and 600 - 650/700°C (Valdiya and Goel, 1983). The presence of cordierite and sapphire in the sillimanite-biotite-plagioclase subfacies in the Badarinath area, and the occurrence of diopside and a variety of corona structures in pegmatites indicate the rise of the metamorphic grade even up to pyroxene granulite facies (Gupta, 1980).

The granitic bodies are of batholithic dimension, such as the *Badrinath Granite*, dated 28 Ma. by the K-Ar method (Seitz et al., 1976). They have thrown up a network of dykes and veins of leucogranites, adamellite, aplite and pegmatite. There was large--scale permissive injection of granitic melt (Powar, 1972) formed at depths of 15-30 km by anatexis of the metapelites and metapsammites. This resulted in the development of migmatites of various kinds and granitic gneiss on a large scale (Valdiya and Goel, 1983). The anatectic origin is borne out by high initial strontium ratios (0.743-0.789), and by the presence in granites and migmatites of such minerals as cordierite, sillimanite, garnet and locally kyanite. The great variability of the strontium ratio implies involvement of a variety of metasediments in the differential melting. The appreciably high concentration of mineral dates (K-Ar, Rb-Sr, fission-track) in the periods 40-25 and 20-10 Ma. (Mehta, 1980) is suggestive of dynamothermal events leading to anatexis, genesis of granites and attendant late-kinematic thermal metamorphism during these two periods.

In the upper part of the Vaikrita (Fig. 2) succession (Pindari Formation) around larger bodies of granites, the effects of

---

Figure 3. Cross-sections across Northwestern Himalaya elucidating the structural positions of the various lithotectonic units;
A. Kashmir Himalaya (after Fuchs, 1977).
B. Western Himachal Pradesh (based on Frank et al., 1973 and V.P. Sharma, 1977).
C. Eastern Himachal (after Auden, 1934; and Valdiya, 1981).
D. Eastern Kumaun Himalaya (modified after Gansser, 1964 and Valdiya, 1981) (Sa = Salkhala; Ch = Chail; Va = Vaikrita; Ju = Jutogh; Al = Almora; Mu = Munsiari).

contact metamorphism are superimposed on the regional metamorphic rocks, thus accentuating the grade of metamorphism. On the other hand, at the base of the Vaikrita, the high-grade (progressive) metamorphism is overprinted by retrograde metamorphism related to movements on the thrust planes of the MCT zone.

The Basement in the Northwestern Sector

The Vaikrita Group is traceable northwestward to the Zanskar Range in Ladakah. In the Bapsa Valley, the Joshimath-Pindari-Budhi succession is well developed, and succeeded by carbonaceous phyllites, slates and greywackes with calc-silicate bands forming the Haimanta sequence. The Haimanta sequence has been intruded by the Leo Pargial Granite and associated veins and dykes (Figs. 3 & 4).

In the Doda district, the Padar Group (Jangpangi et al., 1978) represents the Vaikrita. Further north and northwest in the Zanskar Range, the 10 to 12 km thick Vaikrita has been described as the Giumbal Group (Srikantia et al., 1978), and as the Higher Himalayan Crystallines (Fuchs, 1982; Baud et al., 1984; and Thakur, 1987). The lithology of these units strikingly resembles that of the Joshimath, Pindari and Budhi formations of Kumaun. The leucocratic granites that constitute 30-50% of the Himadri domain, characterized by extremely high and variable initial strontium ratios (0.755-0.769) and low REE, were produced by partial melting of a wide variety of metasedimentary rocks rich in H_2O, B, P, Li and F (Searle and Fryer, 1986). The heat required for melting is attributed to crustal shortening and structural thickening due to duplexing of thrust sheets.

"Tibetan Slab" and Eastward Extension

In the Annapurna-Dhaulagiri massifs of western central Nepal the Vaikrita is known as the "Tibetan Slab" (Pecher and Le Fort, 1986) "Higher Himalayan Crystallines" (Fuchs, 1980), "Annapura Gneiss Complex" (Bodenhausen and Egeler, 1971) and "Himalayan Gneiss (Hashimoto et al., 1973). Le Fort (in Bordet et al., 1971) recognizes three formations in the Tibetan Slab (Fig. 2), which are analogues of the Joshimath and Pindari formations. The Pandukeshwar and Budhi are possibly undeveloped.

The fibrolite-bearing granites of the Mugu-Makalu-Manaslu belt, with their remarkably constant mineralogy, have been dated by Krummenacher (in Bordet et al., 1971). They return very young dates 18.7 - 13.4 Ma. and the average age of cooling of the high-grade metamorphics is placed at about 9 Ma. These granites are related to the tectonics of the MCT (Le Fort et al., 1986). The faster rate of slippage (5 cm/year) along the multiplicity of shear planes of the MCT must have generated the heat necessary for differential melting. A hot Tibetan Slab was thrust over the sedimentary rocks of the Lesser Himalaya, which provided the fluid necessary to induce partial melting in the overheated slab (Le Fort, 1981).

In the Darjeeling-Sikkim Hills (Fig. 4C) the *Darjeeling Gneiss* (=Lower Vaikrita) is made up of kyanite-sillimanite-garnet psammitic gneisses and schists, associated with calc-silicate rocks in larger and minor bands (Acharyya, 1975). There is widespread migmatization in the upper part. The lithology is very similar to that of the *Barun Group* (Jaros and Kalvoda, 1976) in the adjoining Sagarmatha (Everest) region. The Darjeeling Gneiss records P-T conditions of 6.5 - 7.0 (± 0.5) kb and 570 ± 10^{o}C (Lal et al., 1981).

In Bhutan, the extension of the Darjeeling is known as the *Thimpu* (Nautiyal et al., 1964). Gansser (1964) described the southern and northern flanks of the folded thrust sheet of the Thimpu as Chasilakha and Takhtasand gneisses, respectively (Fig. 4D). It is overlain by the *Chekha*, the lithological constitution of which strongly recalls the combined Budhi and Martoli of the Kumaun Tethys Himalaya. The *Sela* of Kameng District (Das et al., 1976), made up of garnetiferous sillimanite gneiss, hornblende-gneiss, fine-grained biotite-plagioclase gneiss, migmatite and intrusive granites and pegmatites, represents the easterly extension of the Vaikrita.

TETHYS BASINS

Tectonic Setting

The Tethys domain is represented by several basins, partially truncated in the north by the Indus-Tsangpo Suture (Fig.1). Even though not continuous, there is a remarkable lithological and faunal uniformity throughout the extent of the domain. With minor and local interruptions, the succession spans a long period of time from Proterozoic to Early Eocene.

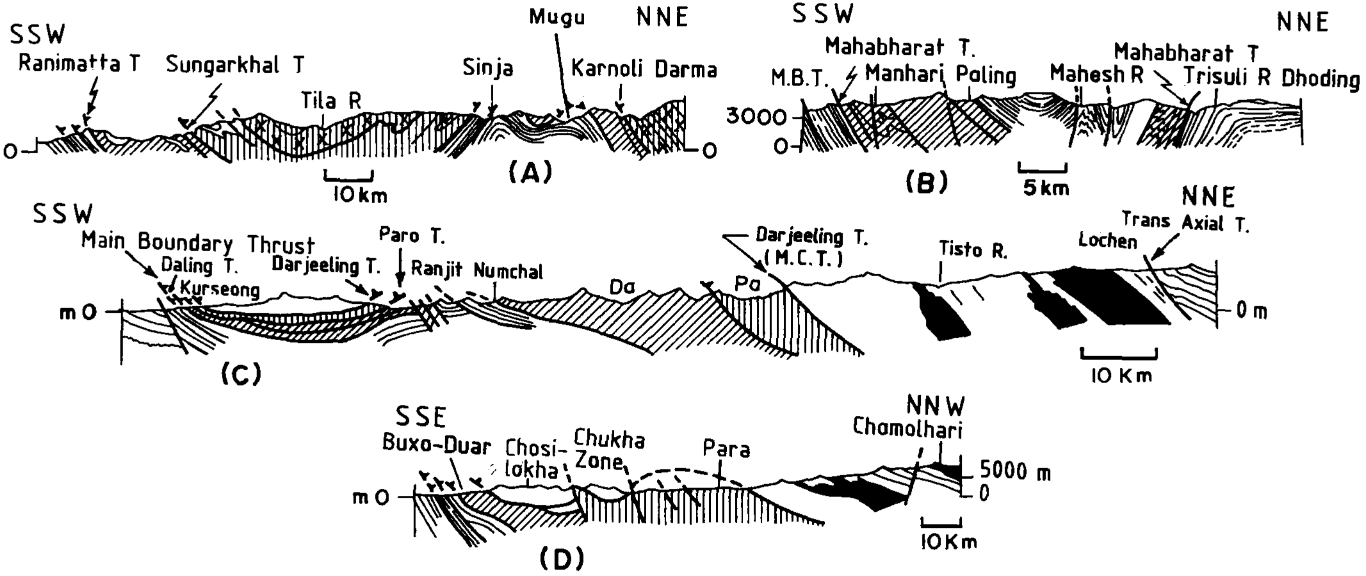
SSW
Ranimatta T
Sungarkhal T
Tila R
Sinja
Mugu
NNE
Karnoli Darma
0
0
10 km
(A)
SSW
Mahabharat T.
M.B.T.
Manhari
Poling
Mahesh R
Mahabharat T
Trisuli R
Dhoding
NNE
3000
0
5 km
(B)
SSW
Main Boundary Thrust
Daling T.
Kurseong
Darjeeling T.
Paro T.
Ranjit
Numchal
Da
Pa
Darjeeling T.
(M.C.T.)
Tisto R.
Trans
Lochen
Axial T.
NNE
m 0
0 m
10 Km
(C)
SSE
Buxo-Duar
Chosi-lokha
Chukha Zone
Para
NNW
Chomolhari
5000 m
0
m 0
10 Km
(D)

The boundary between the Great Himalayan domain and the Tethys zone is demarcated by a detachment fault of regional dimension (>1600 km in length), designated as the Trans-Himadri Fault (Valdiya, 1988b). The fault has caused attenuation and elimination of quite a few lithological horizons of both the basement and the cover succession, including the absence of the Cambrian fossil-bearing sediments in the Kumaun and Nepal.

Another very significant feature of great tectonic importance is the fact that in the Kashmir-Chamba Basin in the northwest, the Phulchauki Basin in south-central Nepal, and the Tangchu Basin in Bhutan, the fossiliferous formations rest apparently concordantly upon the epimetamorphic rocks of the Salkhala-Bhimpedi-Daling formations. The occurrence of Tethyan sediments in the physiographic Lesser Himalayan domains is presumably due to the gentle folding and southward thrusting of the crystalline basement. This is in sharp contrast to the situation in the main basins across the Himadri, where the Tethyan sediments rest on the high-grade metamorphic rocks of the Vaikrita, Barun Gneiss, Darjeeling Gneiss, etc.

Main Tethys Basin Across Himadri

In the Nanda Devi massif in Kumaun, the Budhi schist of the Vaikrita Group transitionally gives way upward to the rhythmic alternation of greywackes, siltstones and slates of the *Martoli* flysch. Elsewhere, the Malari Fault (local name for the Trans-Himadri Fault) cuts the Vaikrita sharply from the sedimentary sequence, attenuating and eliminating the Martoli and the succeeding *Ralam*. The Ralam consists of oligomictic conglomerate interbedded with dominant quartz-arenite. The Ralam gives way to the *Garbyang*, made up of alternations of yellow dolomitic limestone, calcilutite and gypseous marl in the lower part and sandstone and shale in the upper. It is succeeded by fossiliferous Lower-

---

Figure 4. Cross-sections across central and eastern Himalaya, showing structural disposition of the main lithotectonic units.
A.Western Nepal (Appreciably modified after Fuchs, 1980)
B.Central Nepal (Stocklin, 1980).
C.Darjeeling-Sikkim Himalaya (After Acharyya, 1975).
D.Bhutan Himalaya (after Gansser, 1964) (Ram = Ranimata, Ku = Kutti, Ch = Chail 1-2, LrC = Lower Crystallines, Bh = Bhimpedi, Dar = Darjeeling, Pa = Paro, Da = Daling, Th = Thaktasang; Sh = Shumar (Samchi); Ch = Chasilakha.

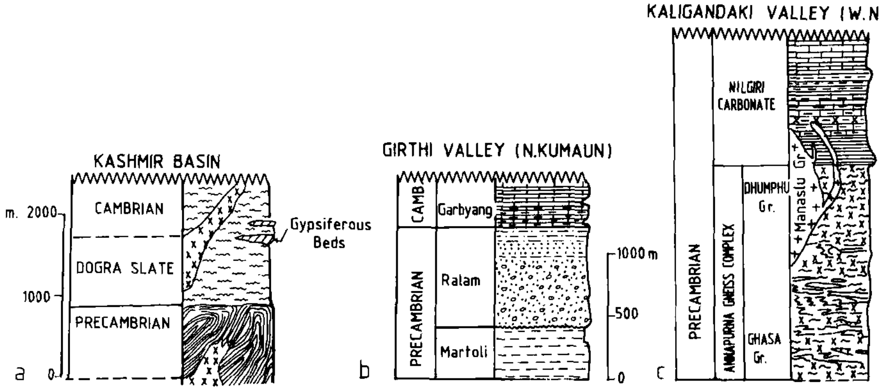

Figure 5. Lithostratigraphic columns of the Precambrian sediments of Tethyan zone in the Girthi valley in Kumaun (after Shah and Sinha, 1974), Kali Gandaki valley in central Nepal (Bodenhausen and Egeler, 1971), and Kashmir basin in the west (After Gansser, 1964).

-Ordovician strata. The Martoli flysch-Ralam quartz-arenites--Garbyang carbonates sequence is comparable (Fig. 5) with the Damtha-Tejam succession of the Lesser Himalaya (Fig. 6). Possibly the two successions are homotaxial.

To the northeast, the Vaikrita crystallines are separated by a fault from the Haimanta flysch in the Spiti-Lahaul region and from the *Phe* in the Zanskar region (Nanda and Singh, 1976; Baud et al., 1984). The *Haimanta* (Griesbach., 1891) is a succession of variegated slates, greywackes and quartzites. The upper part (Parahio) contains Cambrian fossils, including *Redlichia*, *Ptychoparia* and *Olenus*. The Phe of the Pugthal tectonic unit comprises, like the Martoli, greywackes, sublithicarenites and shales which are locally pyritic. The lithology of the *Karsha* underlying the fossiliferous Late-Cambrian rocks, comprising yellow dolomites interbedded with slates (dolomites being characterised by stromatolites), is very similar to that of the Lower Garbyang.

In north-central Nepal, the Tibetan Slab is succeeded with a recognizable disharmony by the Dhaulagiri Limestone (Fuchs, 1977), comprising marble and dolomites interbedded towards the upper part with siltstone and calcilutites which have yielded Ordovician brachiopods and gastropods. The Dhaulagiri is lithotectonically similar to the Garbyang, but there are no analogues of the Martoli and Ralam.

In northeastern Nepal, the Barun Gneiss of the Himadri is conformably succeeded by the Everest Pelites (Wager, 1939), made up of slates, which are sandy, quartzose, sericitic, feldspathic and calcareous. The formation is succeeded by the Everest Limestone ---a formation of yellow schistose limestone, arenaceous dolomitic limestone and dolomites. The Everest is overlain by the Permian Lachi Formation in the Sagarmatha area and by the Ordovician Chaatsun Group on the Tibetan side (Mu et al., 1973). In the adjoining Lingshi Basin in Bhutan, the basement is tectonically overlain (Nautiyal et al., 1964) by diamictites and the greywacke-slate alternation of the Shodun Formation. The upper part has yield distorted remains of corals.

Isolated Basins South of Himadri

In the small "Tangchu Basin" (central Bhutan), the Chekha phyllites are overlain by limestone and shales bearing Devonian fossils (Termier and Gansser, 1974). In the Mahabharat Range, the Bhimpedhi (Chail) is overlain transitionally (Stocklin, 1980) or unconformably (Kumar et al., 1978) by the 5-6 km-thick *Phulchauki Group*, which comprises *Tistang Sandstone*, *Sopyang Slate*, *Chandragiri Limestone*, *Chitlang Shale* and *Phulchauki Limestone*. The Chandragiri has yielded Cambro-Ordovician fossils and the Tistang-Sopyang recalls the lithologies of the Ralam-Garbyang succession.

In the Chamba-Kashmir Basin, the basement is made up of *Salkhala* epimetamorphics. The contact is tectonic (Wadia, 1934; Shah, 1980) in the north, but gradational in the southeast. The *Dogra__Slate* is a succession of dominant phyllites and slates interbedded with subordinate greywackes in the lower part. These give way in the northwestern part to shales characterized by redlichid trilobites of the oldest Cambrian (Shah et al., 1980).

In the Chamba Basin, the analogue of the Dogra Slates is termed the *Bhadarwah-Sunbain* (Sharma, 1977), representing essentially a flysch succession. This group is overlain by the Manjir Conglomerate of probable upper Carboniferous to Permian age.

LESSER HIMALAYAN SEDIMENTARY SUCCESSION

Pattern and Sequence

A very large part of the central sector of the Himalaya is made up of sedimentary rocks exhibiting a uniform pattern and sequence

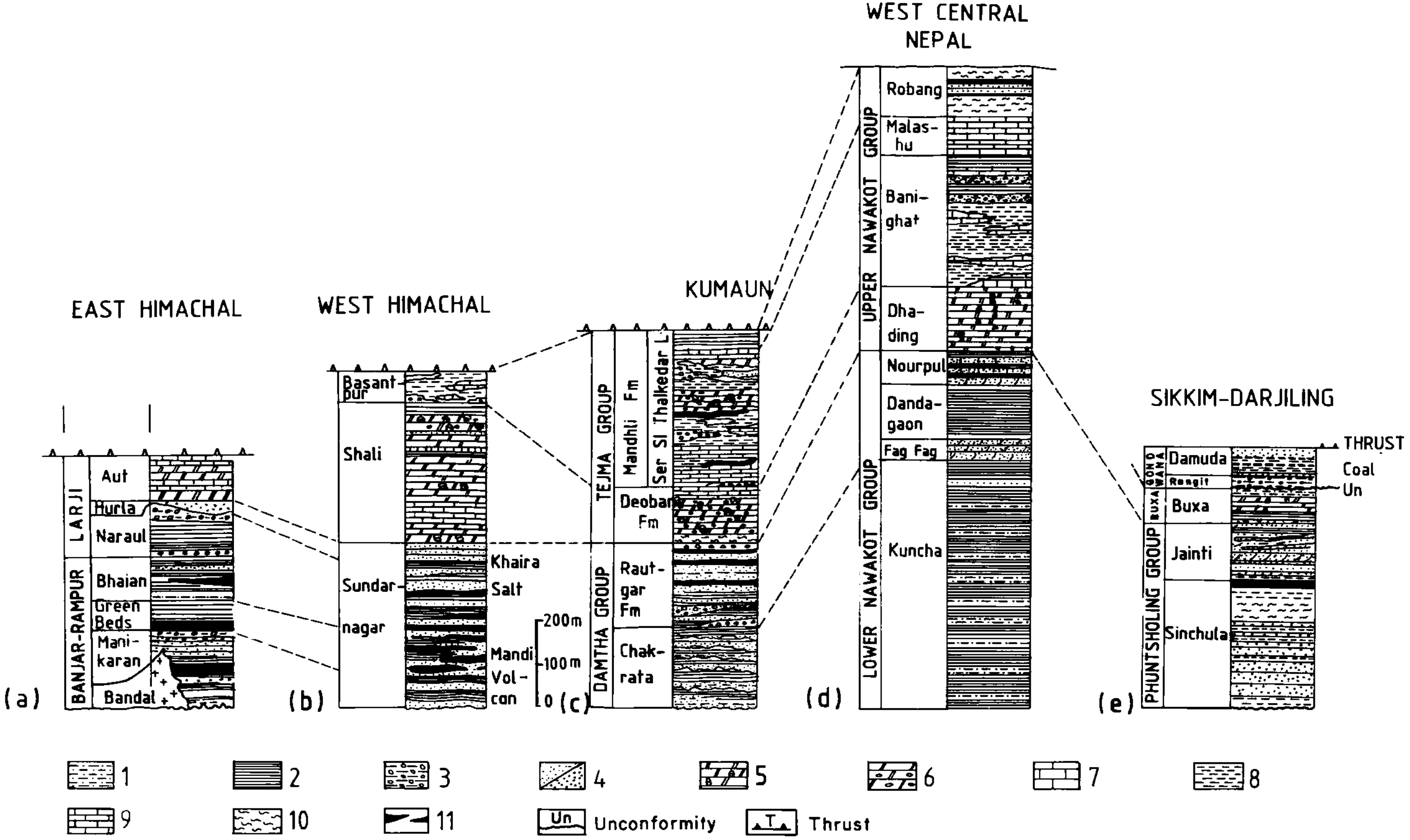
EAST HIMACHAL
WEST HIMACHAL
KUMAUN
WEST CENTRAL NEPAL
SIKKIM-DARJILING
(a)
LARJI
BANJAR-RAMPUR
Aut
Hurla
Naraul
Bhaian
Green Beds
Mani-karan
Bandal
(b)
Basant-pur
Shali
Sundar-nagar
Khaira Salt
Mandi Vol-can
200m
100m
0
(c)
TEJMA GROUP
DAMTHA GROUP
Mandhli Fm
Ser Sl Thalkedar L
Deoban Fm
Raut-gar Fm
Chak-rata
(d)
UPPER NAWAKOT GROUP
LOWER NAWAKOT GROUP
Robang
Malas-hu
Bani-ghat
Dha-ding
Nourpul
Danda-gaon
Fag Fag
Kuncha
(e)
GONDWANA
BUXA
PHUNTSHOLING GROUP
Damuda
Rangit
Buxa
Jainti
Sinchula
THRUST
Coal
Un
1
2
3
4
5
6
7
8
9
10
11
Un Unconformity
T Thrust

of sedimentation. Discoveries in recent years of rare fossils in the Mussoorie Hills in the outermost belt has necessitated drastic modification of earlier age-assignments of the rock-formations of the Krol Belt, and revival of the two-fold subdivision model (Valdiya, 1964). The sedimentary succession (Figs. 6 and 7) encompasses four lithological assemblages put into two groups---the lower argillo-arenaceous *Damtha-Jaunsar Groups* and the upper calc-argillaceous *Tejam-Mussoorie Groups* (Valdiya, 1988 a). The four lithological facies (Table 1) include (i) a turbiditic flysch assemblage *(Chakrata)* at the base in the autochthonous inner zone and the non-turbiditic *Chandpur* in the parautochthonous Krol Belt in the southern part, (ii) the predominantly quartzite-slate succession of the *Rantgara* (with penecontem poraneous spilitic basic volcanic rocks) that gradationally succeeds and laterally interfingers with the Chakrata flysch--the *Sundernagar, Banjar, Phuntsholing, Sinchula-Jainti* and *Miri* in the autochthon, as well as Nagthat and Berinag of the parautochthonous Krol Belt, (iii) the carbonate-rock assemblage comprising the *Jammu* (Great), *Shali, Deoban, Gangolihat, Krol, Dhading, Buxa* and *Dedza* of the autochthonous to paraautochthonous zone (Table 1) and (iv) predominantly argillo-calcareous, carbonaceous-pyritic units with lentiform horizons of carbonate formations (including the *Raipur, Basantpur, Mandhali, Benighat-Malekhu-Robang,* and *Saleri*). Admittedly, this is too simplified a picture of a much more complicated situation.

These sedimentary rocks have been overthrust by two groups of metamorphics, both intimately associated with granitic bodies.

Figure 6. Lithological columns of the Lesser Himalayan sedimentary succession in (A) Larji window in Beas valley and Dhamladhan Range (combined), (B) Sirmaur-Shali section in eastern Himachal, (c) Yamuna and Kali sections (combined) in Kumaun Himalaya, (D) Trishuli-Mahabharat section in west central Nepal (Stocklin, 1980 and original by the author).(E) Sikkim-Bhutan in the east.
1. Turbidite greywacke; 2. slate; 3. diamictite and other conglomerates; 4. sublitharenite arenite; 5. dolomite with stromatolites; 6. cherty dolomite; 7. dolomitic limestone; 8. carbonaceous and calcareous slates and marble; 9. calcian limestone; 10. phyllitic slate; 11 penecontemporaneous basic lavas and tuffs.

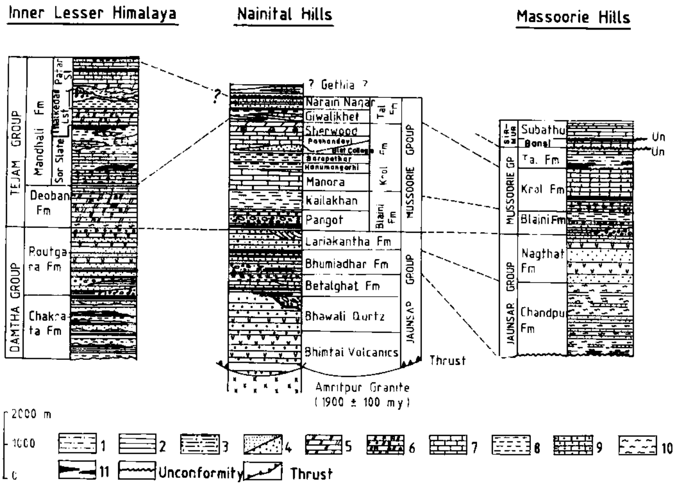

Figure 7. Correlation of the Riphean sedimentary formations of the autochthonous inner Lesser Himalaya with those of the para-autochthonous Krol Belt in the outer Lesser Himalaya in Kumaun (Valdiya, 1988 a), (Index as in Fig. 6).

Argillo-arenaceous Group

The argillo-arenaceous *Damtha Group* (Fig. 6) is exposed in deeply dissected antecedent valleys. The base is nowhere exposed. But there is a reason to believe that 1900 ± 100 Ma-old porphyritic granites underlie the flysch assemblage. For, in the Gori valley in northeastern Kumaun the flyschoid rocks are intimately involved with a tectonized body of 1900 ± 100 Ma-old porphyritic granite-quartz porphyry.

The Damtha is divisible into two formations. In the valleys of the Tons and Yamuna in western Kumaun, a thick succession of greywackes and siltstones alternating rhythmically with slates is known as the *Chakrata* (Valdiya, 1980). Originally described as the Morar-Chakrata beds by Auden (1934), it has been correlated with---and seems to be an extension of ---the *Simla Slates* of Himachal Pradesh (Pilgrim and West, 1928). The Simla Slates, like the Chakrata, are a turbidite suite characterized by such features as graded bedding, flute casts, etc. (Valdiya, 1970), representing a fan-deposit, distal turbidity current shaly flysch that discharged from the northeasterly prolongation of presumably the pristine Aravalli.

Laterally grading or transitionally succeeding the Chakrata flysch in the Tons-Yamuna valleys and occupying the lowermost

TABLE 1

Tectonic succession in the Himalaya

Kashmir	Himachal	Kumaun	Nepal (Fuchs/ French)	Darjeeling	Bhutan	Kameng
Tethys sediments	Tethys sediments	Tethys sediments	Tethys sediments		Tethys sediments	
? ?	"Central Gneiss"	Vaikrita	Up Cryst / Tibetan Slab	Darjeeling	Thimpu (Chasilakha)	Sela
	MC (Vaikrita) T	MC (Vaikrita) T	MCT	T	T	T
Salkhala	Jutogh	Munsiari (+Almora)	Lr Cryst/UP Midland	Paro	Paro	Bomdila
Panjal T	Jutogh T	Munsiari T	Thrust	T	T	T
Ramsu	Chail	Ramgarh (Bhatwari Unit)	Chail-2/Lr Midland	Daling	Samchi (Shumar)	Tenga
Duldhar T	Chail T	Bhatwari-Ramgarh T	Thrust	T	T	T
	Jaunsar	Berinag	Chail-3/ Birethanti			
	Jaunsar T	Berinag T	Thrust			
Parautochthon	Parautochthon-autochthon	Autotochthon	Parautochthon-autochthon	Parautochthon	Parautochthon	Autochthon
	Tons T	Shrinagar T				
	Krol	Krol		Tansen		
Murree T	Krol T	Korl T	K-Thrust-MBT	MBT	MBT	MBT (Garu)
Murree	Dharmsala	Siwalik	Siwalik	Siwalik	Siwalik	Siwalik

level in the vast belt throughout Himachal and Kumaun Himalaya, is the *Rautgara*, made up of fine-to medium-grained sublithic arenites and subgreywackes interbedded with slates. The lentiform horizons of diamictite within the flyschoid succession at various levels, and the basic lavas and intrusive dolerites of spilitic composition, occurring as integral parts of the formation within the sediments, are important features. K-Ar dating (Sinha and Bagdarsian, 1976) shows that the older volcanics (1190 ± Ma.) are indistinguishably associated with the younger (720 ± 10, 414 ± 7, 410 ± 10 Ma.) intrusives.

The Khaira Quartzite in the middle reaches of the Satluj Valley in the Rampur area, the Sundernagar (Srikantia and Sharma, 1971) in the outer central Himachal Himalaya and the *Larji* or Banjar (Sharma, 1977) in the Beas and its tributary valleys represent the northwestward extension of the Rautgara. The Sundernagar Quartzites intimately associated with spilitic *Mandi Volcanics* are dated at 1487 ± 45 Ma. by the Rb-Sr method (Kakar, 1986). They are apparently "intruded" by the porphyritic Bandal Granite (Fig. 3B) which has a whole-rock Rb-Sr age of 1860 ± 150 Ma. (Frank, 1975). The *Bandal Granite* most probably represents the basement that has been thrust up and involved in the complex tectonics of the Larji rocks, which doubtless belong broadly to the Lower Riphean period (1600-1350 ± 50 Ma.).

In Nepal (Figs. 4A, 4B, 6), the Damtha is represented by the *Kunchha* (Bordet et al., 1971) comprising *Fagfog Quartzite, Dandagaon Phyllite* and *Nourpul Limestone* and their variously named local equivalents in different parts of Nepal (Stocklin, 1980; Maruo and Kizaki, 1981; Arita et al., 1982). Fuchs (1980) recognizes these units as Chandpur and Nagthat. Significantly, the whole-rock K-Ar age of the sediments in the valley of Tamba Khola in the Janakpur region was determined at 1150 Ma. (Talalov, 1972).

In the foothills of the Eastern Himalaya, the *Sinchula-Jainti Quartzite* of Sikkim (Gansser, 1964), the *Phuntsholing* of Bhutan (Nautiyal et al., 1964), the *Bichom* of western Arunachal (Das et al., 1976) and the *Miri* of the Subansiri and Siang districts (Jain et al., 1974), are the Lower-Riphean formations at the base of the succession. The Miri is intimately associated with the *Abor Volcanics*, which also embraces intrusives as young as Permian.

Calc-argillaceous Group

The Damtha Group is transitionally succeeded by a sequence of carbonate rocks interbedded with slates. The lower unit described as the *Great Limestone* in the Jammu region, *Aut Limestone* Dhauladhar Limestone in western Himachal Pradesh, *Shali* in eastern Himachal *Deoban* in western Kumaun, *Dhading* in Nepal, *Buxa* in Bhutan, and *Dedza* in western Arunachal Pradesh (Table 1) consists of dolomites and dolomitic limestones locally incorporating synsedimentary intraformational flat-pebble conglomerates. They exhibit prolific development of columnar-branching stromatolites identified as *Baicalia, Masloviella, Kussiella* and *Minjaria* in the Gangolihat-Deoban (Valdiya, 1969); *Conophyton, Tungussia, Colonella, Newlandia, Baicalia* and *Kussiella* in the Shali (Sinha, 1977); *Colonella, Kussiella, Conophyton* and *Baicalia* in the Jammu Limestone of Vaishnodevi (Raha, 1980) and also in the Buxa. The stromatolite assemblages place the carbonate formations in the Middle-Riphean period (1350 ± 50 --- 950 ± 50 Ma.), possibly towards the later part (Valdiya, 1969). Filamentous spheroidal cyanophycean algae of Algonkian affinity recovered from the Gangolihat (Nautiyal, 1980) and the 967 Ma-old galena in the quartzite at the top of the Jammu Limestone (Raha, 1980) tend to corroborate this age assignment.

A very significant feature noticed in the carbonate group is its mineralization. Chains of lentiform deposits of very coarsely crystalline magnesite, intimately associated with soapstone and disseminated sulphide minerals occur in Jammu, Kumaun and Nepal (Valdiya., 1980). These carbonate sediments were deposited on a sublittoral to eulittoral inner shelf, in which biohermal barriers were created by algal growths.

The dolomites and limestones of the Gangolihat-Deoban give way upward to a thick succession of calc slates, marl, carbonaceous pyritic slates interbedded and interbanded with marble and limestone, and locally with lentiform horizons of intraformational synsedimentary conglomerates at various levels. Designated as the *Mandhali* in the Deoban mountain, this formation in eastern Kumaun comprises *Sor Slate, Thalkedar Limestone* and *Patet Slate* (Valdiya, 1980). In eastern Himachal Pradesh the Shali, likewise, is succeeded by the *Basantpur* (Srikantia and Sharma, 1971) with its prime horizon the *Naldera Limestone* (Pilgrim and West, 1928) analoguous to the Thalkedar. These two carbonate horizons are characterized by Upper-Riphean to Vendian (<1000 to 570 Ma. old) columnar stromatolites, *Jurusania* and *Irregularia* (Valdiya, 1969; Sinha, 1977). This is borne out by the K-Ar whole-rock dates of black slates of the Sirkang unit at Purtighat and Ramdighat in Nepal, respectively 559 ± 18 and 540 ± 17 Ma. (Khan and Tater, 1969). The Sirkaghat is a local name for the lowermost member of the *Benighat Slate-Malekhu Limestone-Robang Phyllite* (upper Nawakot) or their equivalents (Sakai, 1984) representing the easterly extension of the Mandhali. Fuchs (1980) has described these units as "Tal". In western Arunachal Pradesh, the Mandhali is represented by the *Saleri* (Das et al., 1976).

The Deoban-Mandhali succession has been designated as the *Tejam Group* (Heim and Gansser, 1939; Valdiya, 1980). In Nepal, it is called the *Upper Nawakot*. It is assigned to the period Middle Riphean to Vendian or possibly stretching to the lower Cambrian.

The Mandhali sediments were deposited in a poorly ventilated euxinic environment possibly under a humid climate, created by semi isolation of the basin of deposition due to the luxurious growth of algae which impeded water circulation. The conglomeratic horizons indicate intervals of disquiet and interrupted sedimentation, generated presumably by tectonic instability presaging events which caused the retreat of the sea water from a vast part, and restricted the sedimentation to a narrow belt in the Krol Basin in outer Lesser Himalaya (Valdiya, 1980).

Krol Belt Stratigraphy

Despite comprehensive studies (Srikantia and Bhargava, 1974; Valdiya, 1980, 1988a), the stratigraphy of the Krol Belt on the outer fringe of the Lesser Himalaya in Kumaun and Himachal remains complicated. The recent discoveries of fossils at the base of the uppermost formation has necessitated revision of the old stratigraphic scheme. The thick pile has been thrust 4 to 23 Km southwards over the Outer Himalayan Cenozoic domain, thus forming the autochthonous Krol Nappe (Bhargava, 1972, 1979). It comprises the *Jaunsar* and *Mussoorie* Groups (Valdiya, 1988 a) made up of the *Betalghat* (not Mandhali), *Chandpur, Nagthat, Blaini, Krol* and *Tal formations* (Fig.7). What Auden (1934) had described as Mandhali at the base of the Krol succession, has now been distinguished as an entirely different stratigraphic unit---an expanded lenticular facies at the base of the Chandpur---and designated the *Betalghat Formation* (Valdiya, 1988a). The Betalghat comprises variegated marble, rhythmically alternating with black carbonaceous phyllite, conglomeratic quartzite intercalated with carbonaceous phyllite, talcose phyllite and marlite, grey phyllite-siltstone rhythmite, and ferruginous sideritic limestone.

In the zone of intracrustal MBT in the southeastern sector of the Nainital Hills, a thick body of extremely tectonized spectacularly porphyritic, granite-quartz porphyry association--- the *Amritpur Granite* --- occurs within the argillo-arenaceous Jaunsar succession which is characterised by high (0.748 to 0.741) initial strontium ratios, and whole-rock ages of 1584 ± 192 to 1010 ± 131 Ma. (Singh et al., 1986). It seems to represent a huge slice of the basement brought up by the MBT.

The northern flank and eastward-plunging extremity of the Krol synclinorium are formed exclusively of the Jaunsar Group (Betalghat-Chandpur-Nagthat) and the southern flank of the Mussoorie Group (Blaini-Krol-Tal). The argillo-arenaceous *Bhawali Formation* is overlain successively by the *Chandpur* and *Nagthat*. The Chandpur consists of phyllites, siltstones and greywackes, with local lentiform horizons of diamictite of non-turbidite origin, and the transitionally overlying Nagthat is a succession of quartzarenites and sublithicarenite with red slates and locally developed shoestring oligomictic conglomerate. The Naghtat is integrally associated with penecontemporaneous lavas and tuffs--- the *Bhimtal Volcanics*. The spilitic volcanic rocks exhibit zeolite-facies metamorphism, resulting from deeper burial (Varadarjan, 1974). The Bhawali-Chandpur-Nagthat successions (Jaunsar Group), sediments deposited on the unstable to stable shelf, represent the southern prolongation in the Krol Belt of the Damtha Group (Valdiya, 1988 a).

The formation that rests upon the Nagthat, and is made up of polymictic conglomerate with green sandstones, and purple red cherty dolomite, limestone and purple shales, overlain by a thick succession of carbonaceous shale, is known as the *Blaini*. The diamictite is believed to be glaciogenic, but this has been questioned. The conglomerates are integrally associated with characteristically pink dolomite, and red shales and siltstone showing flute casts, prod casts or cross-bedding (Rupke, 1974;

Valdiya, 1980, 1988a), together with slump structures and erosional channels in the underlying Naghtat, indicating an environment in which currents were active. The following *Infrakrol*, comprising shales suggests mildly unstable and reducing conditions prevailing in the lagoonal parts.

The *Krol* consists of calc slates, marls, ferruginous-gypsiferous as well as carbonaceous black shales, limestones and dolomites. The dolomites at the top of the horizon are characterized by short, stunted columnar and domal stromatolites. The phosphatic bed at the uppermost part of the formation in the Mussoorie hills yielded a rich suite of conodonts of the earliest Cambrian (Azmi and Pancholi, 1983).

The *Tal* comprises black, pyritic and phosphatic shales, chert and limestone in the lower part and a variety of white, pale--yellow, deep-brown and black sandstones, characterized by felspars and/or pyrite or limonite and mudstone in the upper part. The newly defined Tal excludes the coarse-grained, cross-bedded orthoquartzite, grading upwards into sandy oolitic and shelly limestone of the so-called Upper Tal. The lithology and sedimentary structures such as ripple-marks, mud-cracks, rain prints, foam marks and phosphatic nodules in carbonaceous sediments indicate a shallow basin with rather restricted circulation of water. The upper member indicates shallow lagoonal basins in intertidal to supratidal conditions.

While the rich assemblage of conodonts, hyolithids, etc., in the phosphorite in the Mussoorie Hills indicates a Cambro-Ordovician age (Azmi and Pancholi, 1983), the brachiopod *Diandogia* cf *pista*, and the gastropod *Palagiella* suggest a Lower-Cambrian age (Kumar et al, 1983). The overlying sandstone horizon in the Mussoorie Hills has yielded Early Cambrian (Botomian) primitive brachipods, including *Obolella, Lingulella* and *Obolus* (Tripathi et al., 1986). In the Nigalidhar Hills in southeastern Himachal Pradesh, the trilobite identified as *Redlichia* confirms the Early Cambrian (Botomian) age of the Upper Tal (Kumar et al., 1987).

If indeed the Bhawali-Betalghat-Chandpur-Naghtat succession of the Jaunsar Group, comparable with the Damtha Group of the inner Lesser Himalaya, is of Lower-Riphean age (1600-1350 ± 50 Ma.) and the Mussoorie Group of the Blaini-Krol-Tal formations extends up to the Early Cambrian, the Mussoorie Group becomes homotaxial with or rather a prolongation of the Tejam Group, the upper formations of which (Mandhali) are of Upper-Riphean to Vendian (950 ± 50 to 570 Ma.) age (Valdiya, 1988a). As a matter of fact, Fuchs (1980) has been consistent in correlating the Deoban-Shali with the Krol. However, he placed them in the Permo-Triassic period. Difficulties arise particularly when it comes to the Tejam Group. Even though the Deoban carbonates bear some lithological resemb- lance to those of the Krol, there is no analogue of the Blaini conglomerates and the associated Infrakrol slates and turbidities in the Tejam Group. Likewise, there is no exact equivalent of the Mandhali in the Krol unit, even though the Lower Tal, like the Mandhali, contains carbonaceous-pyritic slates and conglomeratic horizons.

It is obvious that the beginning of the Cambrian period witnessed the termination of sedimentation throughout the Lesser Himalaya subprovince, with the rare exception of several basins. The cessation of sedimentation throughout the Lesser Himalaya, and concomitant widespread interruption in the Tethys domain across the Himadri, are related to a tectonic event that was accompanied by the large-scale intrusion of granite of Cambro-Ordovician (550 ± 50 Ma.) age throughout the Himalayan province--in all the three domains.

Lesser Himalayan Nappes of Metamorphic Rocks

The Precambrian sedimentary rocks are tectonically overlain by and concordantly folded with a succession of two imbricate and discontinuous sheets of metamorphic rocks (Figs.3 and 4). The lower sheets are made up of epimetamorphics integrally associated with sheared and mylonitized (1900 ± 100 Ma-old) porphyritic granite and the upper sheet of mesograde metamorphic rocks intruded by granodiorite and granite, commonly 550 ± 50 Ma. old.

Epimetamorphic Rock-formations. The sedimentary rocks are tectonically succeeded by an assemblage of low-grade metamorphics, known as the *Ramgarh*. The slates, phyllites, sericite quartzite, quartz-schist, marble and talcose phyllite are associated with remarkably porphyritic and pronouncedly sheared and mylonitized granite and quartz-porphyry, representing tectonically emplaced slabs sliced off from the basement. Recent work in the Nainital Hills in Kumaun has shown that the steeply-inclined Ramgarh Thrust has brought up from great depth a voluminous body of highly tectonized granites of the basement along with metamorphosed basal flysch---the *Nathuakhan* (=Rautgara of Damtha Group)--- to form the northern limb of a west-plunging overturned anticline over the southern limb which is also the northern flank of the synclinorial Krol nappe (Valdiya, 1988a). The porphyritic granite quartz-porphyry of the Ramgarh gives Rb-Sr isochron ages of 1765 ± 60 to 1875 ± 90 Ma, with a strontium-isotopic ratio equal to 0.7335 ± 0.0046, indicating an upper-crustal origin (Trivedi et al., 1984).

The northern part of the sedimentary belt is involved in the duplex tectonics of the MCT. The lithotectonic sheets of the schuppen zone comprise sedimentary formations, epimetamorphics, and basement gneisses dated 1900 ± 100 Ma. (and even as old as 2120 ± 60 Ma; Bhanot et al., 1980; Raju et al., 1982). One of the sheets--the *Bhatwari* nappe (Valdiya, 1981)--extends westward and joins with the Chail in Himachal Pradesh. The other sheet, made up predominantly of sericite-rich quartz arenite that is interbedded with penecontemporaneous basic lava flows and tuffs, covers a vast stretch of the inner Lesser Himalaya in the form of the *Berinag nappe*. These sheets represent the uprooted overthrust and metamorphosed argillo-arenaceous and arenaceous parts of the Damtha Group. It turns out that while the Krol Nappe is the dislocated frontal part of the Riphean sedimentary pile, the Berinag-Bhatwari (Chail) sheets represent the overfolded and uprooted back-part of the same pile.

The *Chail,* lithotectonically indistinguishable from the Ramgarh, covers a vast area in Himachal Pradesh including the Simla Hills, (Virdi, 1976) the Dhauladhar Range (Gupta and Thakur, 1974) and the Kulu region in the Beas valley. (Sharma, 1977; Frank et al., 1973) (Fig. 3). The Chail of western Himachal Pradesh is intruded by spectacularly porphyritic granites (550±50 Ma.) with younger (362-322 Ma.) adamellite and pegmatite dykes. Everywhere these porphyritic granites (interbedded with phyllites and quartz-schist) have ultramylonitic margins.

The Chail extends northwestward through Chamba and Kishtwar to Kashmir where it is known as the *Salkhala* (Wadia, 1934; Srikantia and Bhargava, 1974b). The mineral assemblages of the Salkhala in the Kishtwar region indicate temperatures over 100°C and pressure around 5.5 kb (Das, 1978). In the Bhadarwah region of Kashmir, the *Seawa Gneiss* is intimately associated with slates, conglomerate and quartzite and with the *Kund Kaplas Granite* (Shah., 1980).

Turning east, in Western Nepal the easterly extension of the Chail-Ramgarh has been described as *Daling* and *Bhimpedhi* (Stocklin, 1980). In the northern and northwestern flanks of Mahabharat Range, the Bhimpedhi is intruded by multiple bodies of porphyritic granite, occurring in streaky banded and mylonitized conditions. Immediately under the MCT in the duplex zone, there is a horizon at the base of epimetamorphic rocks, conspicuously porphyritic *Ulleri Gneiss*.

A large part of the Darjeeling Hills, Sikkim, southern Bhutan (Figs. 4C-D) and Arunachal Pradesh is covered with the *Daling*, locally described as *Shumar* or *Samchi* in Bhutan, as *Bomdilla* in the Kameng district and as *Siang* and *Tenga* in central and eastern Arunachal. The *Lingtse Gneiss* within the Daling is a sheared, mylonitized porphyroid representing a thrust-up basement ridge.

It may be emphasised again that just as the Chail is lithologically indistinguishable from the undifferentiated Jaunsar of the autochthon (Srikantia and Bhargava, 1974a), and the Ramgarh bears uncanny resemblance with the Rautgara of the Damtha Group (Valdiya, 1980), the Daling-Shumar-Siang also bears remarkably strong lithological similarity with the Phuntsholing-Sinchula-Miri of the underlying sedimentary succession. It seems that the epimetamorphic formations characterized by tectonized porphyroids represent the mildly metamorphosed argillo-arenaceous group of the sedimentary succession which has been thrust up and southward along with the basement, made up of porphyritic granite--quartzporphyry (1900 ± 10 Ma. old), intruded in some belts by Cambro- Ordovician granite (550 ± 50 Ma).

Medium-grade Metamorphics. In the central sector between the Satluj and Trishuli rivers, large nappes constituted of metamorphic rocks of lower amphibolite facies and intruded by granodiorite-granite occur towards the upper part of the succession (except in the Jaljaladhura and Mahabharat ranges where Tethyan sediments form the summits). In the inner belt, these mesometamorphic rocks occur as thin, impersistent bands or slices sandwiched between the Great Himalayan Vaikrita above and the Chail (=Daling) below. The sheets comprise garnetiferous biotite-sericite schist interbedded with carbonaceous phyllite, graphitic schists, marble and amphibolite. Named *Jutogh* in the Simla Hills and Chaur Mountain (Pilgrim and West, 1928), the formation is intruded by a porphyroblastic *Chaur Granite*, the analogue of which at Wangtu in the Satluj valley has given a whole-rock isochron age of 2025 ± 86 Ma. with an initial strontium ratio of 0.1074 ± 0.0100 (Kwatra et al., 1986). The Jutogh extends southeastward into Kumaun where it has been recognized as the *Munsiari* (Valdiya, 1980), delimited by the MCT above the Munsiari Thrust below. The sericite-chlorite-quartz and muscovite-chlorite-chloritoid-garnet-quartz assemblages in meta-pelites and epidote-actinolite-oligoclase (An_{20})-quartz and epidote-hornblende-andesine (An_{29})-quartz in the metabasites of the Munsiari suggest upper-greenschist-facies metamorphism taking place at 450^{o} - 500^{o}C and 4 kb (Valdiya and Goel, 1983). The Munsiari is dominated by augen gneisses of granite-granodiorite composition whose age is 1900 ± 100 Ma. with a low strontium ratio varying from 0.703 to 0.725 (Singh et al., 1986). The Munsiari appears to be the root of the vast Almora Nappe and its many klippen in the inner Lesser Himalaya. It is intruded by 560 ± 20 Ma--old granite granodiorite bodies with initial strontium ratios of 0.7109 ± 0.0013 (Trivedi et al., 1984) and they show little deformation, but grade marginally into augen gneiss. The basal part of the Almora Nappe and the larger part of the klippen consist of 1820 ± 130 Ma-old (with strontium ratios of 0.7114 ± 0.118 Ma.) augen gneisses much like those of the Baijnath and Askot klippen and the Munsiari root. The composite batholithic body of the *Champawat Granodiorite* within the Almora Nappe grades on the one hand into quartz diorite, and on the other into adamellite, and is a synkinematic plutonic body intruded into moist sediment by late-tectonic or post-kinematic undeformed leucocratic adamellite, granite and pegmatite (Valdiya, 1980).

In western Nepal it has been described as the *Lower crystalline nappe* (Fuchs, 1977), in central Nepal as the *Upper Midland Formation* (Hashimoto et al., 1973), in eastern Nepal as the *Arun Group* (Jaros and Kalvoda, 1976), in Sikkim and Bhutan as the *Paro* (Acharyya, 1975) and in Arunachal Pradesh as the *Bomdilla* (Das et al., 1976).

Like the Chail, the Jutogh-Munsiari and their equivalents seem to be metamorphosed parts of the shallower facies of the underlying sedimentary succession resting on the basement granites and intruded by Cambro-Ordovician granite. The intrusion of the younger granite has locally caused contact metamorphism leading to development of situations not much different from that of the Vaikrita domain.

ACKNOWLEDGEMENT

Financial assistance from the Council of Scientific and Industrial Research and the University Grants Commission (under the COSIST Programme) is gratefully acknowledged.

REFERENCES

Acharyya, S.K., 1975. Structure and stratigraphy of the Darjeeling frontal zone, Eastern Himalaya. Geol. Sur. Ind. Misc. Pub., 24: 71-90.

Arita, K., Hayashi, D. and Yoshida, M., 1982. Geology and structure of the Pokhara-Piuthan area, central Nepal. J. Nepal Geol. Soc., 2: 51-58.

Auden, J.B., 1934. The geology of the Krol belt. Rec. Geol. Surv. Ind., 69: 123-167.

Azmi, R.J. and Pancholi, V.P., 1983. Early Cambrian (Tomatian) conodonts and other shelly microfauna from the Upper Krol of Mussoorie syncline, Garhwal Lesser Himalaya, with remarks on the Precambrian boundary. Himalayan Geology, 11: 360-372.

Baud, A., Geetani, M., Garzanti, E., Fois, E., Nicora, A., and Tintoria, A, 1984. Geological observations in south-eastern Zanskar and adjacent Lahul area (northwestern Himalaya). Eclogae. Geol. Helvet., 77(1) : 171-197.

Bhanot, V.B., Pandey, B.K., Singh, V.P. and Kansal, A.K., 1980. Rb-Sr ages for some granitic and gneissic rocks of Kumaun and Himachal Himalaya. In: K.S. Valdiya and S.B. Bhatia (Editors), Stratigraphy and Correlations of the Lesser Himalayan Formations, Hindustan Pub. Corp., Delhi, pp.139-144.

Bhargava, O.N., 1972. A reinterpretation of the Krol Belt. Himalayan Geology, 2: 47-81.

Bhargava, O.N., 1979. Outline of the stratigraphy of Eastern Himachal Pradesh and Uttar Pradesh, with special reference to the Jutogh Group. In: K.S. Valdiya and S.B. Bhatia (Editors), Stratigraphy and Correlation of the Lesser Himalayan Formations, Hindustan Pub. Corp., Delhi, pp.117-125.

Bodenhousen, J.W.A. and Egeler, C.G., 1971. On the geology of the Upper Kali Gandaki valley, Nepalese Himalayas, Konikl. Nederl. Akad. Weten., 74: 526-546.

Bordet, P. Colchen, M., Krummenacher, D., Le Fort, P., Mouterde, R. and Remy, M., 1971. Recherches Geologigues dans l' Himalaya du Nepal Region de la Thakkola. Centre National Recher. Scientifiques, Paris, 279pp.

Das, A.K., Bakliwal, P.C. and Dhoundial, D.P., 1976. A brief outline of the geology of parts of Kameng District. N.E.F.A., Misc. Publ. Geol. Surv. Ind., 24(1) : 115-127.

Das, B.K., 1978. Polyphase medium to high-pressure regional metamorphism of the pelitic rocks around Kishtwar, J and K, India, J. Miner. Abh., 132: 73-90.

Frank, W., 1975. Daten und gedanken zur Entwicklungageschichet des Himalaya. Mitteil. Geol. Gesell., 66-67: 1-7.

Frank, W., Hoinkes, G., Milter, C., Purtschellere, F., Richter, W. and Thoni, M., 1973. Relations between metamorphism and orogeny in a typical section of the Indian Himalayas, Tschermark. Min. Petr. Mitt., 20: 303-332.

Fuchs, G.R., 1977. The geology of the Karnali and Dolpho regions, western Nepal. Jahrb. Geol. Bundesanst, 120: 165-217.

Fuchs, G., 1980. The Lesser Himalayan geology of the West Nepal and its regional importance, In : K.S. Valdiya and S.B. Bhatia (Editors), Stratigraphy and Correlation of the Lesser Himalayan Formations, Hindustan Publishing Corp., Delhi, pp.163-173.

Fuchs, G., 1982. The geology of Western Zanskar. Jb. Geol., B.A. 125/1-2: 1-50.

Gansser, A., 1964. Geology of the Himalaya. Interscience Publishers, London, 289pp.

Griesbach, C.L., 1891. Geology of the Central Himalaya. Mem. Geol. Surv. Ind., 23: 1-232.

Gupta, L.N., 1980. On the field aspects of the root zone of the Badrinath and Mana Pass Area, Central Himalaya, In: P.S. Saklani (Editor), Structural Geology of the Himalaya, Today and Tomorrows Publishers, New Delhi, pp.59-74.

Gupta, V.J. and Thakur, V.C., 1974. Geology of the area around Dharmasala, Kangra District, H.P. Geol. Rundschau, 63: 548-558.

Hashimoto, S., Ohta, Y. and Akiba, C., 1973. Geology of the Nepal Himalayas. Himalayan Committee of Hokaido Univ., Sapporo, Japan, 248pp.

Heim, A. and Gansser, A., 1939. Central Himalaya, Denks. Schweiz. Nat. Gessel., 73: 1-245.

Jain, A.K., Thakur, V.C. and Tandon, S.K., 1974. Stratigraphy and structure of the Siang District Arunachal (NEFA) Himalaya, Himalayan Geology, 4: 28-60.

Jangapangi, B.S., Dhaundial, D.P., Kumar, G., and Dhaundiyal, J.N., 1978. On the geology of Sumcham Sapphire Mines area, Doda District, J & K, Himalayan Geology, 8(III): 837-849.

Jaros, J. and Kalvoda, J., 1976. Geological Structure of the Himalayas, Mt. Everest - Makalu Section. Acad. Naladaelstvi Cosk. Akad. Ved. Prahs: 69pp.

Kakar, R.K., 1986. Rb-Sr radiometric ages of the Darla Volcanics and amphibolites from Jutogh rocks near Simla, H.P., Bull. Ind. Geol. Assoc., 19: 97-101.

Khan, R.H. and Tater, J.M., 1969. Radiometric dates of some Nepalese rocks. Unpubl. Report of H.M.G. Nepal Geol. Surv., Kathamandu, 15pp.

Kumar, R., Shah, A.N. and Bingham, D.K., 1978. Positive evidence of a Precambrian tectonic phase in Central Nepal Himalaya, J. Geol. Soc. Ind., 19: 519-522.

Kumar, G., Raina, B.K., Bhatt, D.K. and Jangapangi, B.S., 1983. Lower Cambrian body and trace fossils from the Tal formation, Garhwal synform, Uttar Pradesh, India. J. Paleontol. Soc. Ind., 28: 106-111.

Kumar, G., Joshi, A. and Mathur, V.K., 1987. Redlichid trilobites from the Tal formation, lesser Himalaya, Curr. Science, 13: 659-663.

Kwatra, S.K., Bhanot, V.B., Kakar, R.K. and Kansal, A.K., 1986. Rb-Sr radiometric ages of the Wangtu Gneissic Complex, Kinnaur district, Himachal Himalaya. Bull. Ind. Geol. Assoc., 19: 127-130.

Lal, T.K., Mukherji, S. and Ackermand, D., 1981. Deformation and Barrovian metamorphism at Takadah, Eastern Himalaya, In: P.S. Saklani (Editor), Metamorphic Tectonites of the Himalaya, Today and Tomorrow's Publishers, New Delhi, pp.231-278.

LeFort, P., 1981. Manaslu leucogranite: a collision signature of the Himalaya: A model for its genesis and emplacement, J. Geophys. Res., 86: 10545-10568.

LeFort, P., Debon, F., Pecher, A. Sonet, J., and Vidal, P., 1986. The 500 Ma magmatic event in Alpine southern Asia, a thermal episode at Gondwana scale, In: Orogenic Evolution of Southern Asia, (Mem. Sci. Terre.), C.N.R.S., Paris: 191-209.

Maruo, Y. and Kizaki, K., 1981. Structure and metamorphism in eastern Nepal, In: P.S. Saklani (Editor), Metamorphic Tectonites of the Himalaya, Today and Tomorrow's Publishers, New Delhi, pp.175-230.

Mehta, P.K., 1980. Tectonic significance of the young mineral dates and the rates of cooling and uplift in the Himalaya, Tectonophysics, 62: 205-217.

Mu, A.T. Wen, S., Wang, Y., Chang, P. and Yin, C., 1973. Stratigraphy of the Mount Jolmo-Lungma region in southern Tibet, China. Scientia Sinica, 16 (1): 96-111.

Nanda, M.M. and Singh, M.P., 1976. Stratigraphy and sedimentation of the Zanskar area, Ladakh and adjoining parts of the Lahaul region of Himachal Pradesh, Himalayan Geology, 6: 365-388.

Nautiyal, A.C., 1980. Cynophycean algal remains and palaeoecology of the Precambrian Gangolihat Dolomite Formation of the Kumaun Himalaya. Ind. J. Earth Sci., 7: 1-11.

Nautiyal, S.P., Jangapangi, B.S., Singh, P., Guha Sarkar, T.K., Bhate, V.D., Raghavan, M.R. and Sahai, T.N., 1964. A preliminary note on the geology of Bhutan Himalaya. Rep. 22nd Int. Geol. Cong., 11: 1-14.

Pecher, A. and LeFort, P., 1986. The metamorphism in Central Himalaya, its relations with the thrust tectonics, In: P. LeFort, M. Colchen and C. Montenat (Editors), Orogenic Evolution of Southern Asia (Mem. Sci. Terre.) C.N.R.S., Paris, pp.285-309.

Pilgrim, G.E. and West, W.D., 1928. The structure and correlation of the Simla rocks. Mem. Geol. Surv. Ind., 53: 1-140.

Powar, K.B., 1972. Petrology and structure of the Central Crystalline zone, Northeastern Kumaun. Himalayan Geology, 2: 34-46.

Raha, P.K., 1980. Stratigraphy and depositional environment of the Jammu Limestone, Udhampur District, Jammu, In: K.S. Valdiya, and S.B. Bhatia (Editors), Stratigraphy Correlations of the Lesser Himalayan Formations, Hindustan Pub. Corp., Delhi, pp.145-151.

Raju, B.N.V., Bhabria, T., Prasad, R.N., Mahadevan, T.M. and Bhalla, N.S., 1982. Early Proterozoic Rb-Sr isochron age for the Central Crystalline rocks, Bhilangana valley, Garhwal Himalaya. Himalayan Geology, 12: 196-205.

Rupke, J., 1974. Stratigraphic and structural evolution of the Kumaun Lesser Himalaya. Sedimentary Geology, 11: 81-265.

Sakai,H., 1984. Stratigraphy of Tansen area in the Nepal Lesser Himalaya. J. Nepal Geol. Soc., 4: 41-52.

Seitz, J.F., Tewari, A.P. and Obradovich, J., 1976. A note on the absolute age of the tourmaline-granite, Arwa Valley, Garhwal Himalaya. Misc. Publ. Geol. Surv. Ind., Calcutta, 24(2): 332-337.

Searle, M.P. and Fryer, B.J., 1986. Garnet, tourmaline and muscovite-bearing granites of the Higher Himalayas from Zanskar, Kulu, Lahaul and Kashmir, In: M.P. Coward and A.C. Ries, (Editors), Collision Tectonics, Geol. Soc. London, pp.185-201.

Shah, S.K., 1980. Stratigraphic and tectonic setting of the Lesser Himalayan belt of Jammu, In: K.S. Valdiya, and S.B. Bhatia, (Editors), Stratigraphy and Correlation of the Lesser Himalayan Formations, Hindustan Pub. Corp., Delhi, pp.152-162.

Shah, S.K. and Sinha, Anshu, K., 1974. Stratigraphy and tectonics of the "Tethyan" zone in a part of western Kumaun Himalaya. Himlayan Geology, 4: 1-27.

Shah, S.K., Raina, B.K. and Razdan, M.L., 1980. Redlichid fauna from the Cambrian Kashmir. J. Geol. Soc. Ind., 21(10): 511-517.

Sharma, V.P., 1977. Geology of the Kulu-Rampur belt, Himachal Pradesh. Mem. Geol. Surv. Ind., 106: 235-407.

Sinha, A.K., 1977. Riphean stromatolites from western Lower Himalaya, Himachal Pradesh, India. In: E. Flugel (Editor), Fossil Algae, Springer-Verlag, Berlin, pp.86-100.

Sinha, A.K. and Bagdasarian, G.P., 1976. Potassium-argon dating of some magmatic and metamorphic rocks from Tethyan and Lesser Himalayan zones of Kumaun and Garhwal Himalaya and its implication in the Himalayan tectogenesis. In: Himalaya, Sciences de la Terre, C.N.R.S., Paris, Mem. 268: 374-387.

Singh, R.P., Singh, V.P., Bhanot, V.B., and Mehta, P.K., 1986. Rb-Sr ages of the gneissic rocks of Rihee-Gangi, Bhatwari, Hanumanchatti and Naitwar areas of the Central Crystalline zone of Kumaun Himalaya. Ind. J. Earth Sci., 13: 197-208.

Singh, V.P., Singh, R.P. and Bhanot, V.B., 1986. Rb-Sr isotopic studies for the granitic rocks of Amritpur area of the outer Lesser Himalaya of Kumaun, U.P. Ind. J. Earth Sci., 13: 189-196.

Srikantia, S.V. and Sharma, R.P. 1971. Simla Group - a reclassification of "Chail Series", "Jaunsar Series" and "Simla Slates" in the Simla Himalaya. J. Geol. Soc. Ind., 12: 234-240.

Srikantia, S.V. and Bhargava, O.N., 1974 a. The Jaunsar problem in the Himalaya - a critical analysis and elucidation. J. Geol. Soc. Ind., 15: 115-136.

Srikantia, S.V. and Bhargava, O.N., 1974b. The Salkhala and the Jutogh relationship in the Kashmir and Himachal Himalaya - A reappraisal. Himalayan Geology, 4: 396-413.

Srikantia, S.V., Ganesan, T.M., Rao, P.N., Sinha, P.K. and Tirkey, B., 1978. Geology of Zanskar area, Ladakh Himalaya. Himalayan Geology, 8: 73-78.

Stocklin, J., 1980. Geology of Nepal and its regional frame. J. Geol. Soc. London, 137: 1-34.

Talalov, V.A., 1972. Geology and ores of Nepal. Unpubl. Rep., Dep. of Mines and Geology, Khatmandu.

Termier, G. and Gansser, A., 1974. Les series Devoniennes du Teng Chu (Himalaya du Bhoutan). Ecol. Geol. Helv., 67(3): 587-596.

Thakur, V.C., 1987. Development of major structure across the northwestern Himalaya, India. Tectonophysics, 135: 1-13.

Trivedi, J.R., Gopalan, K. and Valdiya, K.S., 1984. Rb-Sr ages of granites within the Lesser Himalayan Nappes, Kumaun Himalaya. J. Geol. Soc. Ind., 25: 641-654.

Tripathi, C., Jangapangi, B.S., Bhatt, D.K., Mathur, V.K., Joshi, A. and Jangapangi, B.S., 1986. Additional early Cambrian (Botomian) brachiopod fossil localities in Tal Formation, Lesser Himalaya, and their significance. Curr. Science. 55 (12): 585-586.

Valdiya, K.S., 1964. The unfossiliferous formations of the Lesser Himalaya and their correlation. Rep. 22nd Int. Geol. Cong., 11: 15-56.

Valdiya, K.S., 1969. Stromatolites of the Lesser Himalayan Carbonate formations and the Vindhyan. J. Geol. Soc. Ind., 10: 1-25.

Valdiya, K.S., 1970. Simla Slates, the Precambrian flysch of Lesser Himalaya; its turbidities, sedimentary structures and palaeocurrents. Geol. Soc. Amer. Bull., 81: 451-468.

Validya, K.S., 1980. Geology of the Kumaun Lesser Himalaya, Wadia Institute of Himalayan Geology, Dehradun, 291pp.

Valdiya, K.S., 1981. The tectonics of the central sector of the Himalaya. In: H.K. Gupta and F.M. Delany (Editors), Zagros-Hindukush-Himalaya: Geodynamic Evolution, Amer. Geophys. Union, Washington, pp.87-110.

Valdiya, K.S., 1988a. Geology and Natural Environment of Nainital Hills, Gyanodaya Prakashan, Nainital, 155pp.

Validya, K.S., 1988b. Trans-Himadri Intracrustal Fault and basement upwarps south of Indus-Tsangpo suture zone, In: L.L. Malinconico, and R.J. Liuic (Editors), Tectonics of Western Himalaya. Geol. Soc., America, Boulder.

Valdiya, K.S. and Goel, O.P., 1983. Lithological subdivision and petrology of the Great Himalayan Vaikrita Group in Kumaun. Proc. Indian Acad. Sci., (Earth and Planetary Science), 92: 141-774.

Varadarajan, S., 1974. Prehnite-Pumpellyte metagraywacke, Facies of metamorphism of the metabasites of Bhimtal Bhawali area, Nainital District, Kumaun Himalaya, India. Himalayan Geology 4: 581-599.

Virdi, N.S., 1976. Migmatization of the Jutogh metasediments of Narkanda area, District Simla, H.P., India. Bull. Ind. Geol. Assoc., 9: 1-16.

Wadia, D.N., 1934. The Cambrian-Trias sequence of northwestern Kashmir (Parts of Muzaffarabad and Darmula Districts). Rec. Geol. Surv. Ind., 68: 121-176.

Wager, L.R., 1939. The Lachi Series of N. Sikkim and the age of the rocks forming Mount Everest. Rec. Geol. Surv. Ind., 74(2): 171-188.

THE NATURE AND OCCURRENCE OF MINERALISATION IN THE EARLY PRECAMBRIAN CRUST OF ZIMBABWE

J.F.WILSON AND T.H.C.NUTT

ABSTRACT

A review of the early Precambrian geological record (approximately 3500 - 2500 Ma) of Zimbabwe shows that the distribution of mineralisation pertaining to gold, nickel, chromite, chrysotile asbestos and pegmatites is, for a variety of reasons, not random either in time or space and that most relate to events spanning the Archaean-Proterozoic transition.

The major chromite ores are restricted to the earliest Archaean (*c.* 3500 Ma) Sebakwian Group; and to the earliest Proterozoic (2461 Ma) Great Dyke. The most important Sebakwian deposits occur at Shurugwi but smaller deposits occur farther east in other parts of the Tokwe crustal segment (of pre *c.* 2700 Ma rocks) and also extend into the north marginal zone of the Limpopo mobile belt. The podiform nature of the Sebakwian ores results largely from deformation of originally stratiform chromitites. The remarkable continuity of the Great Dyke's thin stratiform chromite seams reflects the stability of the then recently formed Zimbabwe craton and the retention of this stability until the present day.

Nearly all the other mineralisation occurs on the craton and relates to major igneous and tectonic events in the *c.* 2700-2600 Ma timespan, which culminated in this cratonisation.

Nickel mineralisation is confined to the *c.* 2700 Ma Upper Greenstones of the Bulawayan Group and ultramafic-hosted deposits to the early volcanic and intrusive activity of these greenstones. Two major layered sills, also part of this same igneous activity, host the main chrysotile asbestos deposits at Zvishavane and Mashava. These intrusions cut the dominantly gneissic terrain of the Tokwe segment. The late phases of main deformation provided the structural control of the asbestos formation, and the restriction of the major deposits to the region is a partial reflection of the pre-Upper Greenstones minicraton stability of this segment.

Gold mineralisation occurs in Archaean rocks of all ages but can be regarded as a late Archaean event. Various deformation zones related to block movements within the emerging craton during the late phases of the main deformation were important controls in the gold mineralisation. The gold deposits and asbestos formation are thus different manifestations of the same regional structural control and in this sense are broadly contemporaneous. The western succession of Upper Greenstones contains more gold than the eastern succession and this is partly related to the intrusion of the tonalitic to granodioritic Sesombi Suite of late granites.

Beryllium-lithium pegmatites are associated with the more potassic, c. 2600 Ma Chilimanzi Suite of late granites, with a major deposit of lithium minerals at Bikita. These granites are post-tectonic to the main deformation.

An unusual occurrence of gold mineralisation in high-grade terrain occurs at Renco in the north marginal zone of the Limpopo belt. The occurrence seems related to the post-Chilimanzi Suite, but pre-Great Dyke, overthrusting of the north marginal zone granulites over the craton: the mineralisation may thus be early Proterozoic.

INTRODUCTION

Most of Zimbabwe's mineral wealth is found in rocks of Precambrian age with a major contribution coming from the Zimbabwe craton, a low-grade Archaean granite-greenstone terrain which forms the geological foundation of the country (Fig.1). It is part of the larger crystalline shield of southern Africa and extends SW into Botswana where it is mostly obscured by younger cover rocks. Stabilisation to form a large block of continental lithosphere took place in late Archaean times and had been achieved by c. 2500 Ma ago. Since then it has remained a coherent geological entity; it has been fractured to different degrees and has been intruded by various dykes and sills, but internally it has not been otherwise deformed. In contrast, its margins have been tectonically active at various times since c. 2500 Ma to form mobile belts. Marginal instability has also been a controlling factor in the dominantly sedimentary Proterozoic and Phanerozoic basins that ring Zimbabwe and whose infillings in places extend well onto the craton.

Flanking the Zimbabwe craton on the south and separating it from the Kaapvaal craton of South Africa is the high-grade terrain of the Limpopo mobile belt. This can be divided into the north marginal zone (NMZ) wholly within Zimbabwe, a central zone (CZ) partly in Zimbabwe and a south marginal zone (SMZ) which lies completely outside Zimbabwe. The marginal zones consist of rocks of the adjacent cratons at high metamorphic grade, whereas the CZ contains some lithologies unrepresented within the cratons. While the rocks of the Limpopo belt are of Archaean age, deformation and metamorphism are not confined to the Archaean but extend into the early Proterozoic (Wilson, 1987). The Great Dyke intruded at 2461 ±16 Ma (Hamilton, 1977) is the first major igneous event after the cratonic stabilisation and has been variously described as late Archaean (Wilson, 1981; Nisbet, 1982) and early Proterozoic (Wilson et al., 1987). It is here regarded as early Proterozoic: almost bisecting Zimbabwe, its satellites extend into the NMZ.

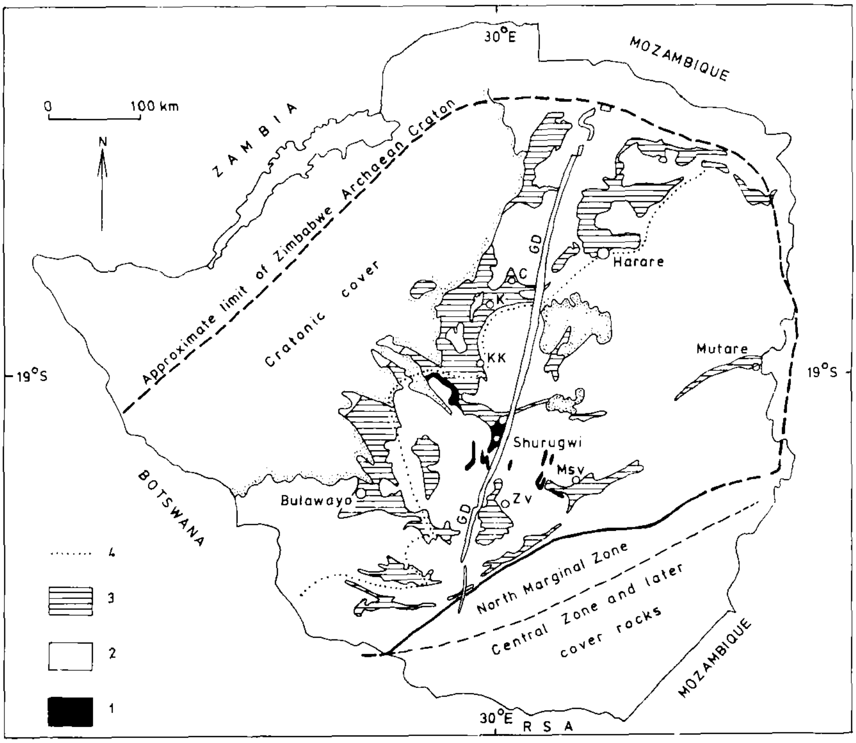

Figure 1. Simplified geological map of the Zimbabwe craton and part of the Limpopo Mobile Belt. 1) Sebakwian Group; 2) Granites and gneisses of various ages; 3) Bulawayan and Shamvaian Groups; 4) Approximate boundary between eastern and western succession of the Upper Greenstones of the Bulawayan Group; GD-Great Dyke; C-Chegutu; K-Kadoma; KK-Kwekwe; Zv-Zvishavane; Msv-Masvingo.

In this paper we review the nature and occurrence of the early Precambrian mineralisation of Zimbabwe and some of the controlling factors. We confine ourselves to gold, asbestos, nickel (including copper and platinum-group metals where associated) chromite and pegmatite minerals; and pay particular attention to their distribution in time and space from the earliest Archaean to the Great Dyke.

OUTLINE OF THE GEOLOGICAL HISTORY

Archaean continental crustal growth is a subject of considerable debate. As interpreted by Moorbath (1984), it occurred in a number of "accretionary super-events" which were episodic on a regional scale but perhaps diachronous world wide. Such crustal growth was accompanied by volcanism and orogeny, and embraced low-grade and high-grade terrains. In the Zimbabwean context, two such "super-events" seem recognisable (cf. Wilson, 1981). The first was at c. 3500 - 3300 Ma, although the existence of even older rocks is implied by the occurrence of *c*. 3800 Ma detrital zircons in certain of the ancient sediments of the craton (M. Dodson *pers.* comm. 1987); the second was at *c*. 2900 - 2600 Ma and culminated in cratonisation.

The first saw the formation of the *c*. 3500 Ma Sebakwian Group greenstone belts now occurring largely as remnants tightly infolded with tonalitic gneisses (Fig. 2). Rocks of this "super-event" are now of limited preservation and have been recognised only in the south and central parts of the craton. They probably extend into the NMZ of the Limpopo belt (Cotterill, 1979). The roughly triangular Tokwe segment (J.F.Wilson in preparation), from Shurugwi southwards to Masvingo and Zvishavane and beyond, contains the largest recognised development of *c*. 3500 Ma rocks. This crustal segment is cut by various later granites (Fig. 2) but still preserves the northerly trend of the *c*. 3500 Ma deformation over much of its area.

The second "super-event" is of much more widespread preservation and on surface saw the accumulation of extensive volcano-sedimentary piles whose deformed remains now constitute the Bulawayan and Shamvaian Groups (Figs. 1 and 2) which make up the main greenstone belts. Within the Bulawayan Group, two ages of greenstone belt development can be recognised in the south and central parts of the craton where a stratigraphic break in most of

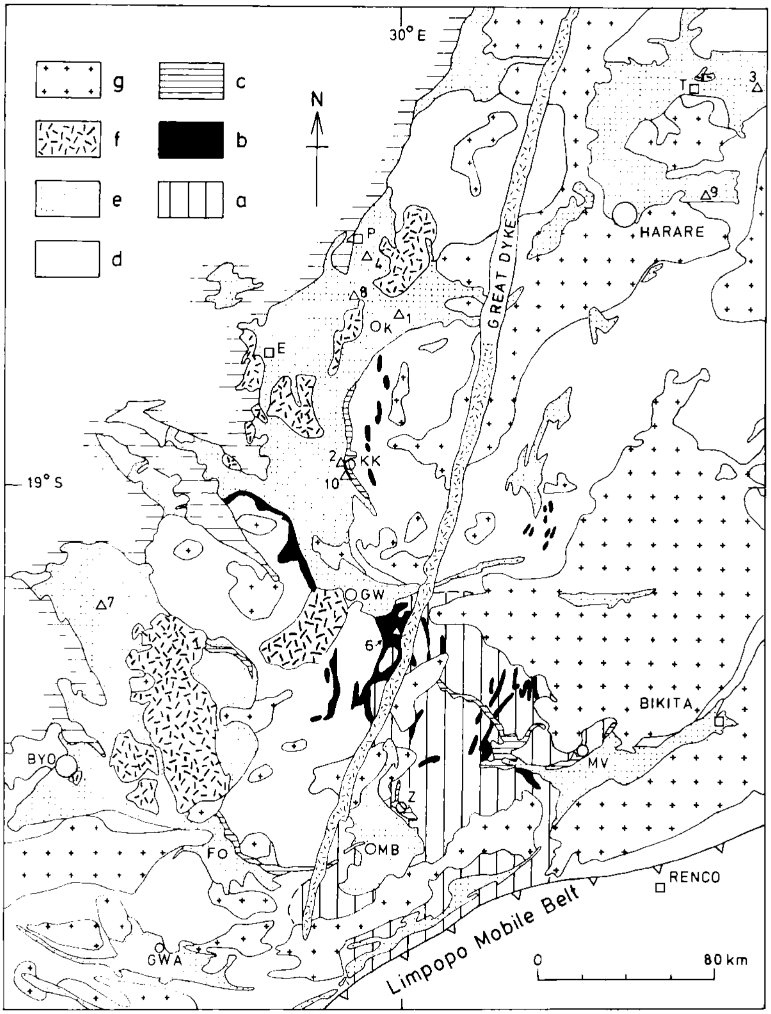

Figure 2. Geological map of part of south-central Zimbabwe; a) Tokwe segment; b) Sebakwian Group; c) Mashaba Ultramafic Suite; d) Granites and gneisses of various ages; e) Bulawayan and Shamvaian Groups; f) Sesombi Suite granites; g) Chilimanzi Suite granites. Open circles are towns and cities mentioned in the text BYO-Bulawayo; GWA-Gwanda; F-Filabusi; MB-Mberengwa; Z-Zvishavane; MV-Masvingo; GW-Gweru; KK-Kwekwe; K-Kadoma. Open triangles show positions of most of the major gold mines numbered 1-10 in Table 2. Open squares are other mines mentioned in text; E-Empress; P-Perseverance; T-Trojan. (Modified after Foster et al., 1986).

the larger greenstone belts allows division of the Bulawayan Group into two sequences. Above this break the major lithostratigraphic units which constitute the upper sequence can be correlated across greenstone belts (Wilson et al., 1978; Wilson, 1979). In the Belingwe greenstone belt west of Zvishavane, where the break was first recognised, the upper sequence transgresses the lower to rest directly on *c*. 3500 Ma gneisses. To the east, near Masvingo, the upper sequence rests unconformably on the the *c*. 2900 Ma Mushandike granite (Orpen and Wilson, 1981; Moorbath et al.,1987) The two sequences have been termed the Lower and Upper Greenstones (Wilson, 1979, 1981) or the Lower and Upper Bulawayan (Stagman, 1978) and their correlation, within Zimbabwe, has been tentatively extended across the whole craton (Foster and Wilson, 1984; Foster et al., 1986). The time span represented by the stratigraphic break is unknown and may not everywhere be the same, but the Lower Greenstones are tentatively taken as *c*. 2900 Ma old. They appear to consist largely of the remains of cyclic alternations of felsic and ultramafic-mafic volcanics which were folded and eroded before the advent of the Upper Greenstones. The Upper Greenstones are *c*.2700 Ma old, possibly 2800 Ma in their basal sediments (Moorbath et al., 1987).

The succession of the Upper Greenstones in the west of the craton differs from that in the east (Fig. 1 and Table 1) and allows speculation on the tectonic setting of the sequence. The lower parts in each are the same and dominated by an extensive "platform-type" basaltic unit (cf. Groves and Batt, 1984). The upper part of the western succession, however, consists of a bimodal unit of mafic-felsic volcanic cycles overlain by an andesite-dominated calc-alkaline unit; the linear distribution of each suggests perhaps the incoming of major rift control possibly followed by a magmatic arc (see also Nisbet et al., 1981; Wilson, 1981).

Intruding the basement on which the Upper Greenstones were deposited and best developed in the southern half of the craton, is the Mashaba Ultramafic Suite of predominantly peridotitic sills some of which show distinct igneous layering. They probably represent the remains of the system of magma chambers that fed the thick basaltic unit of the lower part of the Upper Greenstones.

Table 1.

Western succession	Eastern succession
CALC-ALKALINE unit Andesite-dominated volcanics; pyroclasts and flows: mafic sills (± 4 km thick)	Not developed
BIMODAL unit Alternations of mafic (± ultramafic) and felsic flows; felsic pyroclasts and volcaniclastic sediments; BIF (± 4km thick)	MIXED unit Pillowed and massive mafic flows (1-2 km) in part interbedded with underlying pelite--dominated sediments and BIF, some limestones (up to 2 km thick).
BASALTIC unit As for eastern succession	BASALTIC unit Pillowed and massive flows; subsidiary sills; very minor pyroclastics (4-6 km thick).
KOMATIITIC unit As for eastern succession.	KOMATIITIC unit Ultramafic and mafic pillowed and massive flows (0-2 km thick).
BASAL SEDIMENTARY unit As for eastern succession	BASAL SEDIMENTARY unit BIF, clastic sediments; minor limestones (0-0.25 km thick).

The various mafic dyke swarms of the Mashaba-Chibi dykes, which intrude the Tokwe segment of pre-2700 Ma rocks and largely define its extent, are also considered to be part of the feeder system to the Upper Greenstones (Wilson, 1979; Wilson et al., 1987).

The predominantly sedimentary Shamvaian Group overlies the Upper Greenstones and appears to have been deposited in a number of isolated basins from a provenance which in places included granitic terrain.

The history of granite intrusion during the second "super-event" is not understood. Dates cover the whole time span *c.* 2900 - 2600 Ma (Wilson, 1981) and whereas the felsic volcanics of the Lower Greenstones may equate with certain of *c.* 2900 - 2800 Ma granites and gneisses, it is not clear to what extent granite plutonism was episodic, nor whether the time break evident in the Bulawayan Group also applies to the granites. Two major suites of late granites intrude the Upper Greenstones. The *c.* 2700 Ma tonalite-granodiorite Sesombi Suite occurs in the west on a line parallel to the western succession of Upper Greenstones and may represent a late plutonic expression of the upper parts of this succession. The later. *c.* 2600 Ma Chilimanzi Suite of more potassium-rich granites (adamellites) in contrast, is more craton wide (Fig. 2).

The structural history of the craton is long and complex and early ideas explaining the granite-greenstone belt pattern simply in terms of vertical movements are no longer adequate; horizontal tectonics have played a major part (cf. Wilson, 1981). A recent synthesis (J.F. Wilson in preparation) expands the ideas of Coward et al., (1976). The main deformation, which in essence produced the present greenstone-belt pattern, is explained as a progressive "main" deformation sequence involving SW movement of the Zimbabwe block relative to crustal masses to the north and south as envisaged by Coward, but is considered to have begun near the end of Upper Greenstones volcanism to produce an early cross-folded, dome and basin pattern which was progressively deformed with time. Deformation increased towards the SW with the development of thrusts and strike faults near the block margins; it finally passed into the intrablock "billiard ball" tectonics of Coward, involving jostling of smaller blocks to produce major shear zones and intense flattening and the separation of once continuous structures. The early stages of the main deformation, initiated erosion which produced the Shamvaian Group. In the later stages the Upper Greenstones and Shamvaian Group were deformed together.

The intrusion of the Sesombi Suite may have started before the end of the Upper Greenstones volcanism and continued in time to cut the folded Bulawayan and Shamvaian rocks, whereas the Chilimanzi Suite granites are essentially post-tectonic to the main deformation although a few intrusions are affected by its waning stages. Crustal shortening involved in the main deformation contributed to the crustal thickening, the Chilimanzi Suite of late granites being the last major event in the cratonisation. The restriction of undeformed Mashaba-Chibi dyke swarms to the Tokwe segment indicates that by *c.* 2700 Ma this segment had achieved stability such that it might be considered a mini-craton (Coward, 1984; Wilson, 1979) and emphasises the diachronous and progressive nature of the late Archaean cratonisation process.

In the south after the emplacement of the Chilimanzi granites, granulites of what is now the NMZ were thrust NNW onto lower grade cratonic rocks. This overthrusting, subsequent major fracturing of the craton and NMZ, and emplacement of the Great Dyke into part of this fracture pattern have been explained by some kind of "megajostling" between the Zimbabwe and Kaapvaal cratons perhaps involving a protracted collision event (Wilson, 1987 and in preparation; Wilson et al., 1987).

MINERALISATION IN THE CRATON

Gold

Modern gold production began in Zimbabwe in 1892 and up to the end of 1986 has been estimated at 1500 tonnes, of which 1450 tonnes had been derived from the craton; the 1986 annual production amounted to 14.86 tonnes. Production prior to the British colonisation in 1890 has been estimated by Summers (1969)to have reached a total of 150 tonnes. Most of the modern mines were sited on these ancient workings which mined supergene ores (Fig.3).

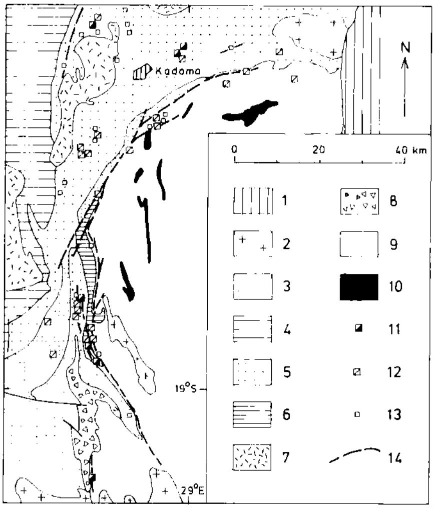

Figure 3. Northwest margin of the Rhodesdale batholith and adjacent greenstone belt rocks 1) Great Dyke; 2) Chilimanzi Suite granites; 3) Shamvaian Group; 4) Calc-alkaline unit of Upper Greenstones; 5) Bimodal and Basaltic units of Upper Greenstones; 6) Kwekwe Ultramafic Complex; 7) Sesombi Suite tonalites; 8) Lower Greenstones 9) Rhodesdale batholith; 10) Sebakwian Group; 11-13) Gold mines with (11) production greater than 15 tonnes gold (500 000 ozs); (12) 1-15 tonnes and 13) 0.3-1.0 tonnes; 14) Shear zones.

The most detailed reviews of the cratonic deposits are by Foster and various co-workers (Foster, 1985; Foster and Wilson, 1984; Foster et al., 1986). On the basis of mineralisation style, these authors classify the gold occurrences into *non-stratabound* comprising vein and shear zone deposits; and *stratabound*, of which banded iron formations (BIF) are the most important, but which also include clastic- and volcaniclastic-hosted deposits.

The *vein type* deposits are tabular or planar quartz and quartz-carbonate filled fractures with minor sulphides and may contain "free-milling" gold. Vein widths range from a few millimetres up to 20 metres and the veins can be traced continuously along strike for tens and even hundreds of metres. A number are continuous for more than a kilometre but economic gold is generally confined to distinct "shoots". Associated alteration is often weak and confined to the immediate wallrocks. Sulphide assemblages have ubiquitous pyrite with other iron-rich sulphides, but many also include various copper, lead, arsenic and antimony sulphides and sulphosalts.

The *shear zone types* are ductile deformation zones with discontinuous dilation veins surrounded by highly altered schistose wall rocks. Visible alteration may extend up to tens of metres and the cryptic alteration haloes may extend for a further few hundred metres. These deposits are dominated by iron-rich sulphides, notably pyrite, pyrrhotite, and arsenopyrite. Shear zone type orebodies are generally wider than the vein type. There is really, however, no sharp transition between the ductile and brittle ore-forming regimes and the subdivision is somewhat arbitrary.

Economic gold mineralisation in BIF is often associated with zones of fracturing and accompanying iron-rich sulphides (Foster et al., 1986; Gilligan and Foster, 1987; Macgregor, 1932; Nutt, 1985; Phillips et al., 1984). In general, the higher gold values are associated with one or more of the sulphides pyrite, pyrrhotite, or arsenopyrite: sulphide abundances decrease rapidly with distance from fractures. The host rock BIF can be oxide, hematite (Nutt, 1985; Macgregor, 1932); or magnetite (Foster et al., 1986; Gilligan and Foster, 1987); silicate (Foster et al., 1986); or carbonate (Fripp, 1974; 1976) facies. The known major sulphide-facies BIF, e.g., at Mphoengs, near the Botswana border in the extreme SW of Zimbabwe (Anhaeusser and Ryan, 1979) and at

Iron Duke Mine, north of Harare (Foster, 1984), contain only minor gold with concentrations at ppb levels. The role of sulphide-facies BIF in hosting gold is unclear, with banded sulphides previously being described by Fripp (1974, 1976) as sulphide facies but later considered as replacement of iron oxides (Fuchter and Hodgson, 1986; Phillips et al., 1984).

The origin of gold in BIF deposits is problematical and controversial. Gold ores confined to BIF are largely stratabound but this does not necessarily imply a syngenetic origin. Some authors, however, have argued for such a mode of formation and advocate a primary volcanic exhalative model (Fripp, 1974; 1976); others have proposed an epigenetic style with ore-bearing fluids related to subsequent Archaean events (Fuchter and Hodgson, 1986; Nutt, 1985). Foster (1985), Foster and Wilson (1984) and Foster et al., (1986) have acknowledged both syngenetic and epigenetic styles but favour, both for BIF and other stratabound deposits, a primary syn-sedimentary enrichment of gold related to exhalative and sub-sea floor hydrothermal activity followed by a second-stage mobilisation in response to late Archaean metamorphic and magmatic activity. Whether such early syngenetic enrichment is essential and did occur is difficult to evaluate since no large database on gold contents of Zimbabwean BIF exists, but high gold contents certainly seem related to enrichment during metamorphism and deformation when "cracked" BIF acted as gold sinks (Nutt, 1985a).

Foster et al., (1986) included under their stratabound ores a number of clastic and volcaniclastic hosted deposits. The most important of these is the Shamva Mine, NE of Harare. The mine has been considered hosted by arkoses (Lockett, 1968) and felsic volcaniclastic units (Stidolph, 1979; Foster et al., 1987). The economic mineralisation, however is confined to southwesterly trending zones of intense potassic metasomatism (Foster et al., 1987) in which original rock features have been largely obliterated. Ore genesis has been attributed to sea-floor hydrothermal activity related to downward percolating sea water being heated by underlying large dacitic porphyry intrusions. Subsequent metamorphism and deformation "remobilised" the gold and minor Mo and As into the southwesterly ore zones (Foster et al., 1987).

The nature of alteration in gold deposits is largely dependent upon the host rock involved but fluid-rock interactions are controlled by three chemical phenomena:

1. Hydrolysis of silicates to produce a range of micas, largely muscovitic (P.J. Treloar and T.H.C. Nutt in preparation), chlorite and amphiboles.

2. Carbonatisation to form a range of carbonate minerals, dominated by ankerite in mafic and felsic lithologies, and magnesite or dolomite in ultramafic hosts (Foster et al., 1986).

3. Redox reactions that produce sulphidised wallrocks in most iron-rich rocks. The most obvious redox alteration reactions occur during the reduction of magnetite to pyrite (Gilligan and Foster, 1987; Phillips et al., 1984) and hematite (Nutt, 1985a).

A considerable number of Zimbabwe's gold mines lie within a few km of granite-greenstone contacts, occurring both in the greenstone belt rocks and the granitoids; these contacts can be either tectonic or intrusive. The tectonic contacts relate to the late intra-block movements of the main deformation and an important example is the broad arcuate deformation zone north and south of Kwekwe (Mann, 1984). The greenstone belt rocks to the west are largely Upper Greenstones with some Shamvaian Group sediments; the granitoids to the east form the western margin of the Rhodesdale "batholith" and are probably mostly basement to the Upper Greenstones. Around Kwekwe and extending northwards to 25 km SE of Chegutu, are numerous mines forming distinct clusters (Fig.3). Stowe (1979) recognised four major groups on the basis of mineralogy and tectonic setting. He found most to occur along dislocations which he termed "master shears" and emphasized the regional nature of the shear system. Mineralisation occurs within older tonalitic gneisses and in a variety of greenstone belt lithologies. The more competent gneisses host numerous vein deposits (Wiles, 1957; Bliss, 1970) whereas mineralisation in the greenstone belt rocks occurs in more ductile zones (Stowe, 1979). In the Globe and Phoenix Mine, at Kwekwe, the orebodies occur as veins in the tonalitic gneiss and as more diffuse sulphide impregnated zones in carbonated ultramafic schists (Stowe, 1979; Macgregor, 1932).

Intrusive granite contacts near which gold mineralisation occurs generally involve tonalitic to granodioritic plutons related to the *c.* 2700 Ma Sesombi Suite, but not all Sesombi Suite intrusions are so associated. Gold-bearing veins occur both within the intrusions and in haloes around them: in many instances the veins also contain scheelite. Examples are known from the Whitewaters tonalite pluton west of Kadoma (Foster et al., 1979; Foster, 1981); the Mazowe granodiorite, northwest of Harare (Tomschi et al., 1986); north of Harare at Bindura (Kalbskopf, 1985) and southeast of Bulawayo (Foster et al., 1977). The later more widespread and more potassic Chilimanzi Suite granites have only very minor associated gold mineralisation.

Over 80 percent of modern production has come from vein and shear deposits with most of these (60 percent) hosted in mafic rocks, followed by ultramafic lithologies and granites (including gneisses). While gold occurs in Archaean rocks of all ages, on a space-time basis, there is a clear bias towards certain major

Table 2

	Output (tonnes)	Grade (g/t)	Host lithology	Ore characteristics
1. Cam and Motor	147.17	12.4	Mafic lavas and greywackes.	Mixed vein-shear system.
2. Globe and Phoenix	121.19	27.6	Globe section: granite;Phoenix section: magnesite rock and serpentinite.	Veins within major shear zone.
3. Shamva	55.86	5.2	Metasomatised volcaniclastic sediments.	Disseminated sulphides and minor stringers.
4. Dalny	53.36	7.8	Andesitic and basaltic lavas.	Shear zone.
5. Rezende	37.78	10.4	Mafic lavas and quartz-diorite.	Vein.
6. Wanderer	36.47	4.1	Conglomerate and BIF.	Shears and replacement of BIF.
7. Lonely	34.77	17.5	Mafic lavas and serpentinite.	Vein.
8. Golden Valley	31.06	22.3	Mafic lavas and felsic sill.	Vein.
9. Arcturus	27.58	10.2	Mafic schists.	Shear zone.
10. Gaika	22.23	8.6	Magnesite schist.	Vein within major shear zone.

stratigraphic units, especially those in the Upper Greenstones (Foster and Wilson, 1984). About 55 percent of the country's non-stratabound gold has come from the western succession of the Upper Greenstones, in particular from deposits hosted in the Basaltic unit and to a lesser extent in the Bimodal unit. This is not merely a reflection of areal extent and is in sharp contrast to their relatively barren counterparts in the eastern succession, which have produced very little. The Calc-alkaline unit in the western succession has also proved a poor producer.

The production disparity between the eastern and western successions is also reflected in the BIF-hosted deposits. Those of the western Bimodal unit have yielded considerably more gold than those of the eastern Mixed unit although in the latter the BIF are more extensively developed.

Table 2 lists the characteristics of the ten largest gold producers in Zimbabwe: their locations, with the exception of the Rezende which occurs near Mutare, are given in Fig. 2.

Chrysotile asbestos

Although blue sodic amphiboles are known from BIF in greenstone belts in two areas of the country (Swift, 1956; Wilson, 1964), no amphibole asbestos occurrences have been recorded and all asbestos production from Zimbabwe has been of the chrysotile variety. At its simplest the formation of chrysotile fibre veins can be viewed as follows; the necessary olivine-bearing host rocks are fractured; suitable fluids penetrate the cracks producing serpentinisation of the olivine and effecting a simultaneous increase in volume; the excess material is removed in solution and crystallises in the cracks as chrysotile fibre.

Economic deposits require not only the most favourable large--scale interplay of host rocks, solutions and fractures, but the host rock must be olivine-rich and not just olivine-bearing. In the larger mines in Zimbabwe, the host rocks are serpentinised dunites and peridotites which originally contained not less than 85 percent olivine by volume. The fluids involved were hydrothermal; late-stage alteration of the host rock, involving also an increase in CO_2 content of the solutions, produced talc and talc-carbonate rocks and in places early silky fibre has become brittle and even pseudomorphed by talc. Zimbabwe's deposits are dominated by cross-fibre veins, i.e., dilation fracture-fillings, where the fibre has grown during extension; slip-fibre is developed only locally in some shear planes.

While all serpentinised olivine-rich rocks of any age are potential asbestos hosts, economic deposits are limited to the south of the craton with the Zvishavane and Mashava areas (formerly Shabani and Mashaba, respectively) being responsible for the great bulk of the production, most having been obtained from three mines; Shabani, Gaths and King. Smaller amounts have come from the Filabusi, Mberengwa (formerly Belingwe) and Gwanda areas. The deposits occur in thick ultramafic sills consisting predominantly of dunite and harzburgites with some intrusions also containing olivine bronzitites and bronzitites; mafic rocks in most cases are minimal but if present locally cap the sills. Macro-layering is developed in some intrusions giving units similar to those of the ultramafic sequences of the Great Dyke (see later) but lacking the chromitite layers. On present knowledge most, if not all, of the sills can be explained as intrusions related to the komatiitic and basaltic volcanism of the lower part of the Upper Greenstones of the Bulawayan Group, the larger intrusions constituting the Mashaba Ultramafic Suite (Wilson, 1979, 1981a) and representing the remains of the magma chamber system that fed the thick Basaltic unit. In most cases the magmas involved were probably komatiitic.

The Shabani and Mashaba igneous complexes (Figs. 2 and 4), intruding the Tokwe segment, are the two most important and best documented members of the Mashaba Ultramafic Suite (Laubscher, 1968, 1986; Wilson, 1968, 1968a, and 1981a). The Shabani complex occurs east of the Belingwe greenstone belt as a sill intruding c.3500 Ma gneisses. It shows an apparently simple differentiation sequence from thick dunite passing upwards into harzburgite and pyroxenite, the latter partially capped by gabbros. The structure is one of a near NW-trending, elongated anticline plunging gently to the NW and SE (Martin, 1978; Tinofirei, 1984). The SW limb dips SW towards the greenstone belt whereas the remnants of the NE limb are relatively flat. Movement has taken place between the base of the intrusion and the gneiss with relative upward displacement of the SW limb to the NE.

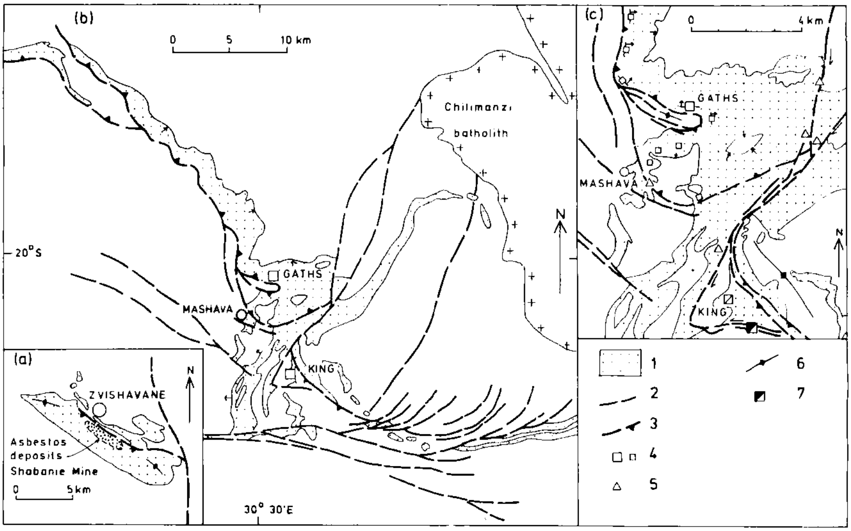

Figure 4. The Shabani (a) and Mashaba (b) and (c) complexes, and their asbestos deposits in relation to major thrusts and faults. 1) Igneous complexes; 2) faults; 3) thrust showing dip direction; 4) Gaths type orebodies; 5) other orebodies near faults or steeply-dipping thrusts; 6) anticlinal axes; 7) Prince chromite mine. (Modified after Martin, 1978; Tinofirei, 1984; Wilson, 1968).

The various sections of the Shabani Mine, the biggest asbestos mine in Africa, occur in part of the SW limb above the thick talc and talc-carbonate zones associated with the basal thrust. The deposits are large irregular pod-like bodies separated along strike and down dip by narrow talc zones which splay from the main basal development, and by mafic dykes, orebody size being determined by the spacing of talc zones and dykes. A zone of carbonated serpentinite with brittle fibre separates the orebodies from the basal talcose zone. The bodies consist of concentrations of cross-fibre seams separated by partially serpentinised dunite. The dykes belong to the Mashaba-Chibi swarms and pre-date the fibre-producing deformation.

The Mashaba igneous complex is the result of multiple intrusions with major recognisable "units", numbered 1-4 downwards. Unit 1 is of limited extent and chromitite-bearing (see later). Units 2 and 3 together form the extensive main sill, the top of unit 3 in places being marked by a bronzitite layer occurring some one third of the way up the sill; the upper margin of unit 2 is generally capped only by a thin zone of poikilitic harzburgite. The relatively small Unit 4 was emplaced under the main sill as a separate intrusion and unlike other parts of the complex shows a full differentiation sequence from dunites through pyroxenites to quartz gabbro, with a major development of mafic rocks.

The main sill extends from the central area of the complex for over 40 km as a NW-trending, gently NE-dipping composite intrusion cutting at a high angle across the strike of the *c.* 3500 Ma gneisses, with their infolded Sebakwian remnants, and c. 2900 Ma tonalite. SW movement of the large masses of overlying gneiss and tonalite has produced a thrust along the base of the sill, the upper contact of the sill and gneisses remaining intact. Sill and thrust have been gently cross-folded. In the central area of the complex, the basal thrust steepens and transgresses the main sill. To the east there has been later SW movement of a huge contiguous block of granite and gneiss with which deformation of the complex is also associated. King Mine, the largest mine in the Mashaba complex is developed in this latter area in the south; Gaths Mine, the second largest, typifies major fibre body development in the main sill (Fig. 4).

The Gaths type deposits are similar to those of Shabani Mine in their position relative to the basal thrust, but are much more regular and approximately parallel to it; splays from the main thrust and pre-fibre formation dykes in the ultramafics are few and their overall influence minimal. A simplified cross-section is a) sheared footwall gneiss, b) talc-carbonate zone associated with the basal thrust, c) barren carbonated zone usually with some brittle fibre, d) economic fibre zone, e) partially serpentinised dunite or olivine-rich harzburgite. The contacts between c), d) and e) are gradational. The fibre bodies are "banded lodes" with the asbestos occurring in more or less parallel seams, which occur in groups in serpentinite separated by less serpentinised areas. The strike and dip of the seams often does not conform to the attitude of the overall fibre body, and the various groups themselves converge and intersect.

Small deposits of asbestos also occur in places near the roof of the main sill, especially in the NW arm of the complex, immediately below the narrow pyroxene-rich roof rock zone. These are probably related to shearing contemporaneous with the main thrust, their position near the roof having been controlled by the difference in competency between the roof rocks and underlying more olivine-rich peridotites.

The King Mine deposit is quite different. It occurs in what we presume to be the main sill some distance below the chromitite-bearing unit 1. The host rock shows a much higher degree of overall serpentinisation than that found in the Gaths type deposits and the asbestos of the two King Mine orebodies occurs as stockwork - an interlacing network of fibre seams. The pattern results from the intersection of major shear zones forming an apparent conjugate set in response to the SW directed maximum compressive stress, produced by the SW block movement. Slips and minor shears sympathetic to the major zones are found throughout the mine area. Fibre development is confined to lenticular masses between shears and the ore bodies consist of a series of closely-spaced, steeply-plunging, structurally-controlled, economic units (cf. Laubscher, 1986).

Nickel

On present knowledge, all of Zimbabwe's nickel deposits, with the exception of Madziwa Mine, 110 km NNE of Harare, are of Archaean age. The Madziwa Mine occurs in a differentiated mafic intrusion dated at c.1870 Ma (Birch and Buchanan, 1987) and as such appears to form part of the widespread, post-Great Dyke, Mashonaland Igneous Event (see Wilson et al., 1987). The Archaean occurrences fall into two major types: nickel ores with high Ni:Cu ratios hosted by ultramafic rocks; nickel-copper ores with much lower Ni:Cu ratios occurring in mafic rocks. The ultramafic-hosted ores can be subdivided into those in komatiite flows and those within ultramafic intrusions (Williams, 1979; Clutten et al., 1981). There is a clear time-stratigraphic distribution on the scale of major lithostratigraphic units, and all the deposits are associated with volcanism and intrusion of Upper (Bulawayan) Greenstones age (cf. Wilson, 1979 and 1981). Most of the production has come from four mines - Trojan, Shangani, Epoch and Empress.

The Trojan Mine (Fig. 2) and the Damba orebodies (Fig. 5) occur in komatiite flows in the lower part of the Komatiitic unit basal to the Upper Greenstones volcanic succession. The rocks have

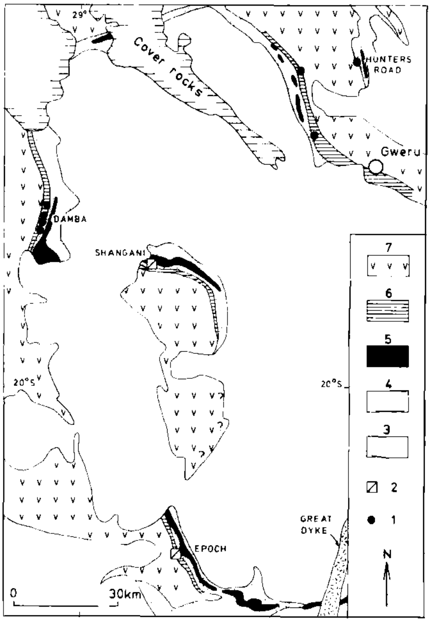

Figure 5. Distribution of nickel ore deposits in the region surrounding Shangani nickel mine. 1) Nickel occurrences; 2) Producing nickel mines; 3) Granites, gneisses and Sebakwian remnants; 4) Lower Greenstones; 5) Mashaba Ultramafic Suite; 6) Ultramafic lavas of the Upper Greenstones; 7) Mafic lavas and other volcano-sedimentary portions of the Upper Greenstones.

undergone greenschist to lower amphibolite metamorphism but some relict spinifex textures are preserved. At Trojan the mineralisation occurs as five orebodies within different flows comprising several ore-types. A full ore sequence comprises up to 1 m thick massive sulphides at the base of the flow with an overlying net-textured ore grading upwards into more disseminated ore. Subsequent tectonism has resulted in some sulphide injection downwards into underlying tholeiitic lavas and cherty sediments (Chimimba and Ncube, 1986; Maiden et al., 1986). The five Damba orebodies lack the massive sulphide development of Trojan and are relatively small disseminated bodies. They occur in regions of increased flow thickness where local depressions appear to have trapped the heavier immiscible sulphide liquid after separation from the high-magnesium silicate melt (Killick, 1986; and cf. Naldrett, 1981). The Trojan ore is dominated by pyrrhotite, with minor pentlandite, and rarer chalcopyrite, pyrite and millerite (Chimimba and Ncube, 1986). The Damba orebodies are characterised by varying amounts of pentlandite, millerite and pyrite, with rare pyrrhotite (Killick, 1986; Williams, 1979).

The Shangani and Epoch Mines (Fig. 5) are associated with the Shangani and Filabusi layered intrusions respectively. These are major sills which intrude the volcanic rocks of the Lower Greenstones a short distance below the overlying Upper Greenstones in each of the greenstone belts concerned; they form part of the Mashaba Ultramafic Suite (Wilson, 1979 and 1981). The orebody development in both instances is somewhat similar and associated with an unusual protruberance, which apparently extends upwards from the top of the main sills.

At Shangani this extension is "mushroom-shaped" and largely serpentinitic. Massive sulphides occur on the foot-wall margin of the underside of each of the "lobes" of the mushroom with disseminated sulphides occurring higher up. The massive sulphide ore consists of mainly pyrrhotite with lesser amounts of pentlandite; the disseminated ore of pentlandite with lesser amounts of pyrrhotite. Pyrite and chalcopyrite are minor constituents of both types. Deformation has resulted in extensive remobilisation of the primary disseminated ore into talc-carbonate alteration zones (Viljoen et al., 1979; Viljoen and Bernasconi, 1979). At Epoch the ore mineralogy is dominated by millerite, pyrite, pentlandite, violarite and rare chalcopyrite. Pyrrhotite is much less common than at Shangani (Baglow, 1986; Ncube, 1981).

The Empress Mine, 40 km WSW of Kadoma (Fig. 2), is the one example of Ni-Cu ores related to mafic rocks. It occurs in a differentiated sill cutting lavas of the calc-alkaline unit of the western succession of Upper Greenstone and a small granodiorite stock which we presume is related to the Sesombi Suite. The host rock is a metagabbro with altered peridotite lenses representing primary igneous layering; relict cumulate textures can be recognised. The ore takes the form of disseminated sulphides occurring in both rock types. The ore mineralogy comprises pyrrhotite, pentlandite, chalcopyrite and pyrite, in descending order of frequency. Semi-massive vein ore, the product of tectonic redistribution, has a similar ore assemblage (Anderson, 1986).

The problematic Hunters Road nickel occurrence (Fig. 5), which has been only partially explored, is situated within a poorly exposed serpentinite mass which appears to transgress the boundary between the Lower and Upper Greenstones (Cheshire et al., 1980). Relict olivine spinifex textures, however, have been described from the ore-bearing serpentinite (Mowbray et al., 1979). The major ore minerals are pyrite, pentlandite, chalcopyrite and pyrrhotite with violarite and millerite occurring as supergene minerals near the surface.

The small, but enigmatic, Perseverance Mine occurs 60 km NW of Kadoma, in the Bimodal unit of the Upper Greenstones. The general country rock consists of felsic metavolcanics described locally as "dacites and andesites". The main orebody occurs as a number of massive sulphide lenses in a highly sheared talc-antigorite rock near its contacts with the altered "andesite". Disseminated sulphides occur within the talc-antigorite rock and the altered andesite. The sulphide mineralogy is pyrrhotite, pentlandite, chalcopyrite and pyrite. A further orebody occurs near the base of a serpentinised dunite which appears to form part of an intrusion cutting the metavolcanics. The Ni:Cu ratio in all the orebodies is low, even in the dunite-hosted ore (Anderson et al., 1979).

Chromite

Chromite ore on the craton is associated with ultramafic rocks of two vastly different ages: the older and much more important with those of the c. 3500 Ma Sebakwian Group; the younger with those of the *c*. 2700 Ma Mashaba Ultramafic Suite. The two major producers, the Railway Block and Selukwe Peak mines, occur in the Sebakwian rocks near Shurugwi (formerly Selukwe) in the Selukwe ultramafic complex (Cotterill, 1969, 1976, 1979; Stowe, 1968, 1974, 1984, 1987). Small masses of Sebakwian chromitite-bearing ultramafic rocks also occur east of the Great Dyke, tightly infolded with the ancient gneisses of the Tokwe segment and extend to the Mashava area (Cotterill, 1979; Wilson, 1968).

Cotterill (op. cit.) and Stowe (op.cit.) describe the Selukwe Ultramafic Complex as the remains of a large layered intrusion (or intrusions) emplaced into high-magnesium basalts and subsequently disrupted into a number of partially overlapping sheets up to 1km thick. The original rock types were dunite, harzburgite and pyroxenite, but have been extensively altered and variously serpentinised, steatised, carbonated and silicified such that talc-carbonate rock is now the dominant lithology. Some relict cumulate textures are, however, still preserved. The host rocks to the chromite bodies are altered dunites, and economic chromitite is restricted to a 70-120m wide zone. This zone is within a few hundred metres of the contact of the dunite with pyroxenite.

The ore zone commonly occurs near the Wanderer erosion surface which marks a major unconformity between the complex and the stratigraphically overlying sedimentary Wanderer Formation which contain clasts derived from the complex, including chromitite pebbles. The complex underwent considerable deformation and alteration before the deposition of the Wanderer sediments. Post-Wanderer tectonism produced the imbrication of the complex and inversion of the strata referred to as the "Selukwe nappe" by Cotterill and Stowe and generally regarded as part of the *c.* 3500 Ma events (Wilson, 1981).

Cotterill (op. cit.) distinguished two distinct forms of chromite within the ore zone; he termed these main crop and second crop crystals respectively. His main crop chromites form over 80 percent of the major orebodies which are mostly massive-type ore (with bulk Cr:Fe ratios of 3.8-4.3). These bodies are extremely elongate lenticular pods up to 25m thick, 120 m wide and 1000m long, but average about half these dimensions. They occur in discrete groups within the ore zone. The sub-economic second crop chromites (with a Cr:Fe ratio of 2.6-3.8) occur as disseminations or centimetre-scale cumulate layers throughout much of the ore zone. In places these layers were deposited over, and even banked against, aggregates of main crop crystals.

Chromitite in the Mashaba Ultramafic Suite of intrusions has been recorded from the Filabusi (Ferguson, 1934) and Mashava areas (Wilson, 1968; 1981a) but has been mined only from SE of Mashava, from the topmost layered unit (Unit 1) of the Mashaba igneous complex near King asbestos mine (see earlier). A number of mines have been worked with the largest production having come from the Prince Mine (Fig. 4). Here a chromite-rich zone occurs in serpentinised dunite. The zone lies between two major shears related to the regional deformation associated with asbestos development at King Mine. In spite of the tectonic disruption, a 30 metre layered sequence can be recognised: a basal 3 m zone of coarse-grained cumulus chromite passes into a 15 m "banded zone" comprising hundreds of layers of chromitite and serpentinite derived from dunite in an alternating fine-scale sequence with layer thicknesses ranging from 5 - 50mm. Above this are three thinner but similarly banded sub-zones separated by dunite-serpentinite rich in disseminated cumulus chromite. Only the basal coarse-grained chromitite layer was mined as ore (Cr:Fe 3.23-3.52). Cotterill (1976, 1979) noted similarities between the Shurugwi and Prince Mine deposits and proposed that the chromitite-bearing unit 1 might not be part of the Mashaba igneous complex *per se* but might belong to the Sebakwian Group. We consider this highly unlikely.

Pegmatite minerals

Early Precambrian pegmatites are widely distributed throughout the craton. The great majority are small quartzo-feldspathic bodies barren of mineralisation. These simple pegmatites are of various ages and occur in greenstone-belt rocks, granites and gneisses alike. In contrast, the mineralised "complex" pegmatites are large and usually show some degree of mineral zoning: tabular in shape and of variable dip, they are mainly confined to the greenstone belts and transgress regional structures in Bulawayan and, to a lesser extent, Shamvaian rocks. Their intrusion is thus a late Archaean event, and their source appears to be restricted to the *c.* 2600 Ma Chilimanzi Suite granites: in some instances, e.g., north of Masvingo, they can be traced directly into such granites (Wilson, 1968).

The important minerals are beryl, columbite-tantalite, microlite, pollucite, cassiterite and lithium minerals, dominantly petalite and lepidolite but also including spodumene, amblygonite and eucryptite. Many of the pegmatite areas were first exploited on a small scale for tin, and were somewhat euphemistically known as "Tinfields". Today lithium ores are the most valuable minerals produced and tin production comes from the younger *c.* 1000 Ma Kamativi-type pegmatites in the extreme NW of Zimbabwe.

Zimbabwe's early Precambrian pegmatites have all species of lithium minerals but, apart from lepidolite, which is ubiquitous and predominantly an end-stage product, the paragenesis of the other lithium minerals is problematical. This applies particularly to the distribution of petalite and spodumene (Grubb, 1973). In most of the world's major lithium pegmatites these two minerals are antipathetic and essentially mutually exclusive; in Zimbabwe spodumene and petalite are often closely associated. The spodumene occurrence, however, at least in Zimbabwe's Archaean pegmatites, is not one of coarse-bladed crystals, common in other parts of the world, but of quartz-spodumene intergrowths.

Although mineralised pegmatites occur in the NE portion of the craton the main concentration is in the SE, the most important being the Bikita "Tinfield" at the eastern end of the Masvingo greenstone belt (Cooper, 1964; Martin, 1964; Wilson, 1964). The largest intrusion and one which has produced most of Zimbabwe's lithium ore, in the form of petalite and lepidolite, is the Bikita main pegmatite. This is a sill-like body dipping eastward at 15-40 degrees in Upper Greenstones volcanics with minor intercalated sediments. It has a strike length of about 2000m, a maximum true width of about 65m and displays a pronounced asymmetric internal zoning. Broadly speaking, this zoning embraces: a) a massive lepidolite core over 300m long at surface; b) various intermediate zones of albite, spodumene and huge masses of petalite and pollucite; c) wall zones of albite-oligoclase, quartz and mica with varying amounts of beryl; d) border zones of mica selvedge and quartz-albite (Martin, 1964). Grubb (1973) divides Zimbabwe's lithium pegmatites into two types of which his Bikita type is much more common. He sees this type with its petalite, quartz-spodumene assemblages, eucryptite and lepidolite, as the product of open-system crystallisation, probably above 600° C, involving successive injection and intense late-stage replacement.

A further important product of the late Archaean pegmatite intrusion has been the development of *emerald*. In several areas in the south of the craton this chromiferous variety of beryl has resulted from the intrusion of beryllium-bearing pegmatite fluids into ultramafic rocks, the gemstones generally occurring in metasomatically altered ultramafic rock immediately adjacent to the resultant pegmatite. This alteration usually takes the form of a phlogopite-or magnesium-biotite-rich selvedge. Emeralds of exceptionally high quality have been produced from the Zeus claims, about 65km south of Zvishavane, and marketed under the name "Sandawana". The host rocks are pale-green tremolite schists of presumed Lower Greenstones age. Some emeralds have also been produced from the Filabusi area. Northeast of Masvingo, chrysoberyl and alexandrite have been found along with emerald in altered peridotites of the Mashaba igneous complex (Wilson, 1964; Anderson, 1976).

MINERALISATION IN THE LIMPOPO MOBILE BELT

Gold

The Renco Mine, SE of Masvingo (Fig. 2), is the largest of several known occurrences of gold mineralisation that constitute the Nyajena goldfield in the Limpopo belt. Odell (1975) showed the area, which is part of the NMZ, to be dominated by leucocratic gneisses, showing retrogression from granulite to amphibolite facies. Enclosed by the gneisses are a number of ENE elongated relict enderbite granulite "pods". Renco mine lies near the approximate geographic centre of what seems to constitute one such pod, some 15km long and 4km wide; the other occurrences are all east of the mine but are apparently confined to the same enderbite mass.

About 10 km to the north of Renco is the ENE-striking, southerly-dipping cataclastic zone which marks the northern limit of the NMZ and along which the high-grade terrain has been thrust northwards onto the craton. A second parallel thrust occurs about 2km S of the mine along the southern margin of the Renco enderbite mass. The mass itself in the goldfield area has been deformed by an asymmetric antiform plunging ENE at 15-30 degrees (Tabeart, 1987).

The ore mineralogy at Renco is characterised by pyrrhotite-chalcopyrite assemblages with or without pyrite, some traces of gold, bismuth and maldonite (Au_2 Bi). The origin of the deposits is controversial. Bohmke and Varndell (1986) recognise four "reefs". These are relatively siliceous mineralised zones ranging from a few centimetres to approximately 3 metres in thickness. Their overall structure is one of a northerly striking, easterly dipping series transgressing the regional foliation and folded about axial planes parallel to this foliation. Most of the other occurrences in the goldfield are nearly parallel to this foliation. In the highly contorted areas the Renco reefs also contain pegmatite. The authors describe the reefs as being associated with well-laminated quartz-magnetite granulites. Their model is one in which original cherty sediments containing syngenetic exhalative gold and bismuth, having survived deformation and granulite facies metamorphism, were overprinted by a late retrogressive phase involving erratic pegmatite formation and sulphide mineralisation.

Tabeart (1987), on the other hand, considers the mineralisation wholly epigenetic and structure as the major controlling factor. He sees all the Renco "reefs" as shear zones which may have originated as a wrench fault system, with the folds being possible sheath folds. He describes a range of reef lithologies based on texture and mineralogy, and recognises an abundance of mylonitic fabrics. He suggests that the bulk of the mineralisation was introduced during the late brittle deformation phase recognised in the mylonites, and relates the structural control to the overthrusting of the granulites onto the craton.

Chromitite

In the NMZ, 100-110 km WSW of Renco, irregular bodies of chromitite occur in tectonically disrupted and metamorphosed mafic-ultramafic intrusions infolded with greenstone-belt remnants in the high-grade gneisses (Worst, 1962; Robertson, 1973; 1974). Production has been small and has come mainly from the Rhonda and Spinel mines. Ore from the various sections of the Rhonda workings shows a Cr_2O_3 range from 32-54%, and Cr:Fe ratios range from 1.23-3.03 (Worst, 1962). Cotterill (1979) has made the likely suggestion that the chromitites and their host rocks are part of the Sebakwian Group of the craton and equate with the Shurugwi and other early chromitite occurrences of the Tokwe segment.

MINERALISATION IN THE GREAT DYKE

The Geology of the Great Dyke

The Great Dyke is a linear mass of mafic and ultramafic rocks which cuts NNE across Zimbabwe for over 500km. Its width ranges from about 4 to 11km. At its present level of exposure it is not a true dyke in the sense of a steep-walled intrusion, but the remains of a number of contiguous, extremely elongate, layered intrusive complexes whose layers dip inwards from the margins. Gravity studies indicate that the overall structure is funnel or trumpet shaped in cross-section with a true feeder dyke-like feature at depth along most of the length (Podmore and Wilson., 1987).

Worst (1960) recognised four complexes each consisting of an ultramafic sequence overlain by a mafic sequence. Each ultramafic succession can be divided into a number of macro-rhythmic or cyclic units, an ideal unit consisting of a thin chromitite layer at or near the base followed by, in sequence, a thick dunite and thick bronzitite (Wilson and Wilson, 1981; Wilson, 1982). In the lower part of each ultramafic sequence the units lack the bronzitite layer. The bronzitite of the uppermost unit in all four complexes is overlain by a 10 - 15m thick websterite marking the incoming of cumulus augite; within a short vertical distance cumulus plagioclase becomes important, heralding the passage into the mafic unit, which consists largely of various gabbros and norites.

Chromite

The most important mineral produced from the Great Dyke is chromite. The "chromite seams" are best developed and have been most extensively mined in the Hartley Complex, the largest of the four complexes. The upper three seams each consist of one or more layers of massive chromitite or disseminated olivine and chromite, each 5 to 100cm thick, separated by harzburgite layers giving a total thickness of up to 4m. The seams show lateral variations in many areas and generally only the massive chromitites are mined. The lowermost seams usually consist of a single massive, relatively uniform chromitite layer 100 - 150 mm thick. The upper group of chromitites are relatively low grade, 36-49% Cr_2O_3 with bulk Cr:Fe ratios of 1.9-2.5:1, whereas the lower group are of higher grade with 43-54% Cr_2O_3 and bulk Cr:Fe of 2.6-3.5:1. (Wilson and Prendergast, 1987).

Wilson's (1982) detailed studies of mineral compositions in the Hartley Complex indicate that repeated influxes of parental magma (komatiitic basalt) gave rise to the macro-units. The chromitites basal to these units appear to have been formed near the chamber floor after the mixing of old and new magmas, following each replenishment.

The Main Sulphide Zone (MSZ)

The MSZ is a persistent, 1 - 2m thick tabular zone of disseminated sulphide minerals in pyroxenite found near the boundary of the mafic and ultramafic sequences in all of the complexes. It occurs in the uppermost macro-unit of the ultramafic sequence directly underlying, or up to a few metres below the base of the websterite which caps this unit. The main sulphide minerals are pyrrhotite, chalcopyrite, pentlandite and pyrite with a strong concentration of platinum group elements (PGE) in the lower half of the zone. The principal precious metals are platinum and palladium (Pt:Pd ratio is 1:1.3) with important quantities of gold nickel and rhenium. There are systematic lateral variations in metal content and thickness, especially between the walls and axis of the Dyke. The MSZ comprises several billion tonnes of mineralised rock, within which have been proved large tonnages of potential ore (Wilson and Prendergast, 1987).

Chrysotile Asbestos

Surface serpentinisation is a feature of the dunites and olivine-rich harzburgites of the Dyke. This, however, is unrelated to the development of chrysotile asbestos in such rocks where serpentinised adjacent to major faults. Production has been from only one small mine, the Ethel Mine, situated in the northen part of the Hartley Complex near its western margin. The asbestos occurs south of a near easterly trending fault which dextrally displaces the western margin for about 1200m. Dolerite dykes sub-parallel to the fault cut the fibre zones. The ages of the faulting and dolerite intrusion are not known (Keep, 1930; Worst, 1960).

DISCUSSION AND CONCLUSIONS

The factors controlling early Precambrian gold mineralisation in Zimbabwe are numerous and complex and any detailed evaluation is quite beyond the scope of this paper. Except for Renco Mine and associated deposits, the mineralisation is confined to the craton. The gold occurs in Archaean rocks of all ages but most workers agree that most of it, if not all, is a late Archaean phenomenon (Foster, 1985, 1987; Fuchter and Hodgson, 1986; Nutt, 1985; Stowe, 1979; Twemlow, 1984). The economic concentration appears to have been a result of the c. 2700 Ma tectonic and magmatic activity. On the craton the late stages of the main deformation, especially major shear zones marginal to and within the greenstone belts, constitute a vitally important controlling factor, as also does the Sesombi Suite of late granites. The source of the large volumes of hydrothermal fluids involved in the mineralisation process is unknown: workers have variously invoked a magmatic origin (Foster et al., 1977, 1979); a metamorphic origin (Foster, 1985; Nutt, 1985); and downward percolating seawater (Fripp, 1974; Foster et al., 1986). The ultimate source of the gold is unknown although Foster (1985) has postulated inter-pillow zones and syn-sedimentary enrichments in BIF.

The disparity of distribution of cratonic gold mineralisation between the western and eastern succession of the Upper Greenstones is real. It emphasises the active role of the Sesombi Suite and supports the suggestions of Foster and coworkers (op cit) of early syngenetic enrichment in the west. On the other hand, if the Bimodal unit of the western succession and its linear distribution are to be explained by the incoming of a rift-controlled environment, involving major fractures in this region and not in the east, then such major fractures might well have had a decisive influence on the subsequent intrablock movements of the main deformation, and in the positioning of major deformation zones and other possible fluid conduits.

Gold mineralisation is a feature uncommon in high-grade terrains in general and the origin of the Renco and nearby deposits, unique in the context of Zimbabwe, is not yet understood. If the ore concentration is tectonically induced, as seems likely, and related to the northerly translation of the NMZ, then this mineralisation is younger than the gold mineralisation of the craton, since this overthrusting deforms the southern members of the Chilimanzi Suite late granites; on this basis it might even be very early Proterozoic. Dewatering of the low-grade mass underlying the overthrust granulites, consequent on the increased temperature gradient, provides a mechanism for the retrograde metamorphism in the gneisses surrounding the enderbite pods and a ready transport medium for ore formation, but other controls are required to explain the apparent localisation of the Renco-type orebodies to one enderbite mass.

Fluid movement in large volumes has also occurred on the craton away from the western succession of Upper Greenstones as is evident from the major asbestos deposits in the Tokwe segment.As with the gold mineralisation, the origin of the fluids is not known but a common source seems possible. Both sets of fluids involve some CO_2 metasomatism; and localised small gold occurrences are known along the basal thrust of the NW arm of the Mashaba complex.

Chrysotile asbestos mineralisation, however, is a stress--related mineral and given the necessary olivine-rich host rock and fluid availability, it is the stress pattern and extent of this stress that controls fibre development. In the Zvishavane and Mashava areas, this control is related to the regional deformation. Earlier, dealing with the Mashava area, Wilson (1968, 1968a) attributed the control to deformation caused by the emplacement of the Chilimanzi Suite granites (and saw these granites as the source of the hydrothermal fluids) but later (Wilson, 1979, 1981a) refuted these ideas. The structural control in both areas results from the behaviour of the Tokwe segment during the intrablock movements of the pre-Chilimanzi Suite main deformation: thus, the cratonic gold mineralisation and asbestos formation are broadly synchronous.

The confinement of the major long-lived producers to the Tokwe segment probably reflects in part the relatively higher stability of this minicraton compared with the rest of the emergent Zimbabwe craton at this stage. Within the segment, however, the Shabani-Gaths-type deposits are restricted to large sills that are, a) intruded into the gneissic terrain and b) now oriented such that their strike (approximately NW) is at a high angle to the maximum compressive stress vector during deformation. While factors such as dykes and possibly cross-folding (cf Anhaeusser, 1976; 1986) are locally involved in delineation of fibre deposits, the combination of the two regional factors seem more important on the large scale. The maximum competency difference between granitoids and ultramafic sill so achieved has favoured sliding along the base of the sill. In the Gaths type of orebodies this also marks the "leading edge" of one of the SW moving blocks within the segment. Where sill strike, inside or outside the Tokwe segment (Wilson, 1979), is more easterly or north easterly oriented, shearing has been too intense for major cross-fibre development. In other parts of Zimbabwe, e.g., in the Shangani and Filabusi intrusions, where sill strike is NW, the country rocks are greenstones and fibre development is minimal. The uniqueness of the Zvishavane-Mashava thus seems a combination of optimum conditions, as well as their host rock occurrences, within the minicraton of the Tokwe segment.

With the syngenetic magmatic ores of nickel and PGE mineralisation and chromitite, magma composition and crystallisation history are of paramount importance. The major economic developments of chromitite, although geographically remarkably close, are separated by about one billion years in time - from the *c.* 3500 Ma Sebakwian Group in the southern part of the craton and extending into the NMZ, to the *c*. 2500 Ma Great Dyke. In spite of the considerable areal distribution of the *c*. 2700 Mashaba Ultramafic Suite, only one small unit of the Mashaba igneous complex has yielded mineable chromitite. Accessory chromite, however, is present in most of the ultramafic rocks of the rest of the Mashaba complex, and in many of the komatiites of the Lower and Upper Greenstones of the Belingwe greenstone belt. Thus chromiferous magmas seem to have been available throughout the early Precambrian record in Zimbabwe. The restriction of the major deposits to the earliest Archaean and earliest Proterozoic emphasises the importance of physico-chemical controls in the formation of chromitite layers. The early and late Archaean deposits were originally stratiform and their present "podiform" nature arises from the intense deformation(s) to which they have been subjected, although for Shurugwi, Cotterill (1979) has suggested that some thickening of the main crop ore may be an original "sedimentary" feature due to current action in the magma. Alteration during deformation has also affected ore grades.

While Zimbabwe's Archaean komatiitic magmas were apparently chromiferous, it is not known whether they were all equally nickeliferous. The time-space restriction of ultramafic-hosted nickel mineralisation, not only to the late Archaean but specifically to the early part of the *c*. 2700 Ma Upper Greenstones volcanic and intrusive activity might suggest not. However, the sulphur content of the magma and the concentration of immiscible sulphide melt are among the factors controlling such ore formation.

The last act in the cratonisation process was the emplacement of the Chilimanzi Suite of granites and its related Be-Li pegmatites, but whether their source is restricted to a particular chemical type in this suite is not known.

The obvious stratiform nature of the chromitites of the Great Dyke and continuity of the thin seams over many tens of kilometres reflect the rigid stability of the newly formed craton, as does the paucity of chrysotile asbestos. The PGE mineralisation is unique to the Great Dyke. It has not been recognised in the intrusions of the Mashaba Ultramafic Suite and its controls are not yet understood.

In summary, for a variety of reasons, mineralisation in the early *c.* 3500-2500 Ma crust of Zimbabwe is not random either in space or time: except for important *c.* 3500 Ma chromite ores, most of it can be related to events in the approximate 2700-2500 Ma time range which spans the Archaean-Proterozoic transition and marks the passage of Zimbabwe into a stable craton.

ACKNOWLEDGEMENTS

We gratefully acknowledge the painstaking reviewing of this paper by Drs. J.D.Kramers and M.S.Garson. We wish also to thank R.Wheeler and D. Burton, both of the Department of Geography, University of Zimbabwe, for the reduction of the diagrams.

REFERENCES

Anderson, I.G., 1986. The Empress Nickel Deposit, Zimbabwe, In: C.R. Anhaeusser and Maske S. (Editors), Mineral Deposits of Southern Africa. Geol. Soc. S. Afr., 1, pp.231-236.

Anderson, I.G., Varndell., B.J. and Westner, G.J., 1979. Some geological aspects of the Perseverance Nickel Mine, Rhodesia. Spec. Publ. Geol. Soc. S. Afr., 5: 67-98.

Anderson, S.M., 1976. Notes on the mineralogy and occurrence of Emeralds in Rhodesia. Annals. Rhod. Geol. Surv., 2: 50-55.

Anhaeusser, C.R., 1976. Archaean metallogeny in southern Africa. Econ. Geol., 71: 16-43.

Anhaeusser, C.R., 1986. The geological setting of chrysotile asbestos in southern Africa. In: C.R.Anhaeusser and S.Maske. (Editors), Mineral Deposits of Southern Africa. Geol. Soc. S.Afr., 1, pp.359-376.

Anhaeusser, C.R. and Ryan, P.J., 1979. "Barren" Massive Sulphide Deposits in the Mphoengs Schist Belt, Rhodesia: A Case History. Spec. Publ. Geol. Soc. S. Afr., 5: 181-204.

Baglow, N., 1986. The Epoch Nickel Deposit, Zimbabwe. In: C.R.Anhaeusser and S. Maske, (Editors), Mineral Deposits of Southern Africa. Geol. Soc. S. Afr., 1, pp.255-262.

Birch, G. and Buchanan, D.L., 1987. Petrology of the Madziwa Mafic Intrusion, Zimbabwe. In: A Campbell (Editor), 5th Magmatic Sulphides Field Conference: Abstracts and Field Guide volume Geol. Soc. Zimb. 13pp.

Bliss, N.W., 1970. The geology of the country around Gatooma. Bull. Geol. Surv. Rhod. 64, 240pp.

Bohmke, F.C. and Varndell, B.J., 1986. Gold in granulites at Renco Mine, Zimbabwe. In: C.R. Anhaeusser and S. Maske (Editors), Mineral Deposits of Southern Africa. Geol. Soc. S. Afr., 1, pp.221-230.

Cheshire, P.E., Leach, A. and Milner, S.A., 1980. The Geology of the country between Gwelo and Redcliff. Bull. Geol. Surv. Zim. 86, 300pp.

Chimimba, L.R. and Ncube, S.M.N., 1986. Nickel Sulphide Mineralisation at the Trojan Mine, Zimbabwe. In: C.R. Anhaeusser ans S.Maske (Editors), Mineral Deposits of Southern Africa. Geol. Soc. S. Afr., 1, pp.249-254.

Clutten, J. M., Foster, R.P. and Martin, A., 1981. Nickel mineralisation in Zimbabwe. Episodes, 2: 10-15.

Cooper, D.G., 1964. The geology of the Bikita pegmatite. In: S.H.Haughton (Editor), The geology of some ore deposits of Southern Africa. Geol. Soc. S. Afr., 1, pp.441-463.

Cotterill, P., 1969. The chromite deposits of Selukwe, Rhodesia. Econ. Geol. Monogr., 4: 154-186.

Cotterill, P., 1976. The geology of the chromitite deposits of Selukwe, Rhodesia. Unpubl. D.Phil. thesis. Univ. of Rhodesia: 205pp.

Cotterill, P., 1979. The Selukwe schist belt and its chromitite deposits. Spec. Publ. Geol. Soc. S. Afr., 5: 229-246.

Coward, M.P., 1984. Major shear zones in the Precambrian crust: examples from NW Scotland and southern Africa and their significance. In: A. Kroner and R. Greiling (Editors), Precambrian Tectonics Illustrated. Stuttgart Schweizerbart' -sche Verlagsbuchhandlung, pp.207-236.

Coward, M.P., James, P.R. and Wright, L., 1976. Northern margin of the Limpopo Mobile Belt, southern Africa. Bull Geol. Soc. Am. 87: 601-611.

Ferguson, J.C., 1934. The geology of the country around Filabusi, Insiza District. Bull. Geol. Surv. S. Rhod., 27: 179pp.

Foster, R.P., 1981. The genesis of Archaean gold deposits-Golden Valley Mine. 12th Ann. Rep. Inst. Mining Res. Univ. Zimbabwe: 16-18.

Foster, R.P., 1984. Gold in banded iron formations, 15th Ann. Rep. Inst. Mining Res. Univ. Zimbabwe: 66-70.

Foster, R.P., 1985. Major controls of Archaean Gold Mineralisation in Zimbabwe. Trans. Geol. Soc. S. Afr., 88: 109-133.

Foster, R.P., 1987. Archaean gold metallogenesis and exploration in Zimbabwe. In: African Mining, Institute of Mining and Metallurgy, London, pp.103-126.

Foster, R.P. and Wilson, J.F., 1984. Geological setting of Archaean gold deposits in Zimbabwe. In: R.P.Foster (Editor) GOLD '82: The Geology, Geochemistry and Genesis of Gold Deposits. A.A.Balkema, Rotterdam, pp.521-551.

Foster, R.P., Mann, A.G., Armin, T. and Burmeister, B.B., 1977. Richardson's Kop Wolframite Deposit: a Geochemical Model for the Hydrothermal Behaviour of Tungsten. Spec. Publ. Geol. Soc. S. Afr., 4: 107-128.

Foster, R.P., Mann, A.G., Miller, R.G. and Smith, P.J.R., 1979. Genesis of gold mineralisation in the Gatooma area, Rhodesia. Spec. Publ. Geol. Soc. S. Afr., 5: 25-38.

Foster, R.P., Mann, A.G., Stowe, C.W. and Wilson, J.F., 1986. Archaean gold mineralisation in Zimbabwe. In: C.R.Anhaeusser and S. Maske (Editors), Mineral Deposits of Southern Africa. Geol. Soc. S. Afr., 1, pp.43-112.

Foster, R.P., Furber, F.M.W., Gilligan, J.M. and Green, D., 1987. Shamva Gold Mine, Zimbabwe: a product of calc-alkaline linked exhalative, volcaniclastic, and epiclastic sedimentation in the late Archaean. In: J.D. Keepie, R.W. Boyle and S.J.Haynes (Editors), Turbidite-hosted Gold Deposits. Geol. Assoc. Can., Spec. Paper, 32, pp.41-65.

Fripp, R.E.P., 1974. The Distribution and Significance of Stratabound Mineral Deposits in Archaean Banded Iron Formation in Rhodesia. Unpubl. M.Phil. thesis. Univ. Rhod., 147pp.

Fripp, R.E.P., 1976. Stratabound gold deposits in Archaean banded iron-formation, Rhodesia. Econ. Geol., 71: 58-75.

Fuchter, W.A.H. and Hodgson, C.J., 1986. Gold Deposits of the North Western Mining Camp, Gwanda Greenstone Belt, Zimbabwe. In: A.J.Macdonald (Editor), GOLD '86: An International Symp. on the Geology of Gold Deposits, pp.255-269.

Gilligan, J.M. and Foster, R.P., 1987. Gold mineralisation in iron formations: the importance of contrasting modes of deformation at Lennox mine, Zimbabwe. In: African Mining, Institute of Mining and Metallurgy, London, pp.127-138.

Groves, D.I. and Batt, W.D., 1984. Spatial and temporal variations of Archaean metallogenic associations in terms of evolution of granitoid-greenstone terrains with particular reference on the Western Australian Shield. In: A.Kroner (Editor), Archaean Geochemistry, Springer-Verlag, Berlin, pp.73-98.

Grubb, P.L.C., 1973. Paragenesis of Spodumene and other Lithium minerals in some Rhodesian pegmatites. Geol. Soc. S.Afr. Spec. Publ., 3: 201-216.

Hamilton, P.J., 1977. Sr isotope and trace element studies of the Great Dyke and Bushveld Mafic Phase and their relation to early Proterozoic magma genesis in southern Africa. J. Petrol., 18: 24-52.

Kalbskopf, S.K., 1985. Gold mineralisation around the Bindura granite stock. Zim. Chamber of Mines J., 27:9: 29-35.

Keep, F.E., 1930. The geology of the chromite and asbestos deposits of the Umvukwes Range, Lomagundi and Mazoe districts. Bull. Geol. Surv. S. Rhod., 105pp.

Killick. A.M., 1986. The Damba Sulphide Nickel Deposits, Zimbabwe. In: C.R.Anhaeusser and S. Maske (Editors), Mineral Deposits of Southern Africa. Geol. Soc. S. Afr., 1, pp.263-274.

Laubscher, D.H., 1968. The origin and occurrence of chrysotile asbestos in the Shabani and Mashaba areas, Rhodesia. In: D.J.L. Visser (Editor), Symposium on the Rhodesian Basement Complex. Geol. Soc. S. Afr. Annexure to LXXI, pp.175-188.

Laubscher, D.H., 1986. Chrysotile Asbestos in the Zvishavane (Shabani) and Mashava (Mashaba) Areas, Zimbabwe. In: C.R. Anhaeusser and S. Maske, (Editors), Mineral Deposits of Southern Africa. Geol. Soc. S. Afr., 1, pp.377-395.

Lockett, N.J., 1968. The Geology of the Cymric Section of the Shamva Mine. Unpubl. Hons. Proj. Univ. Rhod., 50pp.

Macgregor, A.M., 1932. The geology of the country around Que Que, Gwelo District, Bull. Geol. Surv. Rhod., 20: 113.

Maiden, K.J., Chimimba, L. and Smalley, T.J., 1986. Cuspate Ore-wall Rock Interfaces, Piercement Structures and the Localization of Some Sulfide Ores in Deformed Sulfide Deposits. Econ. Geol., 81: 1464-1472.

Mann, A.G., 1984. Gold mines in Archaean granitic rocks in Zimbabwe. In: R.P.Foster, (Editor), GOLD '82: The Geology, Geochemistry and Genesis of Gold Deposits. A.A.Balkema, Rotterdam, pp.553-568.

Martin, A., 1978. The geology of the Belingwe-Shabani schist belt. Bull. Geol. Surv. Rhod., 83: 220pp.

Martin, H.J., 1964. The Bikita Tinfield. In: Wilson, J.F., 1964. The geology of the country around Fort Victoria. Bull. Geol. Surv. S. Rhod., 58, 147pp.

Moorbath, S.M., 1984. Patterns and geological significance of age determinations in continental blocks. In: H.D.Holland and A.F. Trendall (Editors), Patterns of change in earth evolution. Dahlem Konferenzen. Berlin Heidelberg, New York, Tokyo: Springer Verlag, pp.207-220.

Moorbath, S.M., Taylor, P.N. Orpen, J.L., Treloar, P.J. and Wilson, J.F., 1987. First direct dating of Archaean stromatolitic limestone. Nature, 326: 865-867.

Mowbray, R.J., Brand, E.L., Hofmeyr, P.K. and Potter, M., 1979. The Hunters Road Nickel Prospect. Spec. Geol. Soc. S. Afr., 5: 109-116.

Naldrett, A.J., 1981. Nickel sulphide deposits: classification, composition and genesis. 75th Anniv. Vol. Econ. Geol., 628-685.

Ncube, S.M.N., 1981. The mineralogy of the North Orebody, Epoch Mine, Filabusi. Inst. Min. Res. Univ. Zimbabwe., Rep. C223. (Unpubl.)

Nisbet, E.G., 1982. Definition of "Archaean" - comment and a proposal on the recommendation of the International Subcommission on Precambrian Stratigraphy. Precamb. Res., 19: 111-118.

Nisbet, E.G., Wilson, J.F. and Bickle, M.J., 1981. The evolution of the Rhodesian craton and adjacent Archaean terrain: tectonic models. In: A. Kroner (Editor), Precambrian Plate Tectonics. Elsevier, Amsterdam, pp.161-183.

Nutt, T.H.C., 1984. Archaean gold mineralisation in the Nando and Pinkun mines, Kadoma district, Zimbabwe. In: R.P.Foster (Editor), GOLD '82: The Geology, Geochemistry and Genesis of Gold Deposits. A.A. Balkema, Rotterdam, pp.261-284.

Nutt, T.H.C., 1985. The geology and geochemistry of the Nando and Pinkun mines, and their bearing on the genesis of the Venice-What Cheer goldfield, Zimbabwe. Unpubl. M.Phil. thesis, Univ. Zimbabwe, 266pp.

Nutt, T.H.C., 1985a. The geology of the Broomstock and Indarama gold mines, In: T.J.Broderick (Editor), Ann. Zim. Geol. Surv., 10(1984), pp.107-120.

Odell, J., 1975. Explanation of the geological map of the country around Bangala Dam. Short Rep. of Geol. Surv. Rhod., 42: 46.

Orpen, J.L. and Wilson, J.F., 1981. Stromatolites of 3500 Myr and a greenstone-granite unconformity in the Zimbabwe Archaean. Nature, 291: 218-220.

Phillips, G.N., Groves, D.I. and Martyn, J.E., 1984. An epigenetic origin for Archaean banded iron-formation hosted gold deposits. Econ. Geol., 79: 162-171.

Podmore, F. and Wilson, A.H., 1987. A reappraisal of the structure and geology of the Great Dyke, Zimbabwe. In: H.C. Halls and W.F.Fahrig (Editors), Mafic Dyke Swarms: Geol. Assoc. Canada Spec. Paper 33.

Robertson, I.D.M., 1973. Potash granites of the southern edge of the Rhodesian Craton and North Marginal Zone of the Limpopo Mobile Belt. Spec. Publ. Geol. Soc. S. Afr., 3: 265-276.

Robertson, I.D.M., 1974. Explanation of the geological map of the country south of Chibi. Short Rep. Geol. Surv. Rhod., 41: 40.

Stagman, J.G., 1978. An outline of the geology of Rhodesia. Bull. Geol. Surv. Rhod., 80: 126.

Stidolph, P.A., 1979. The distribution of gold in the Shamva greenstone belt. Spec. Publ. Geol. Soc. S.Afr., 5: 49-54.

Stowe, C.W., 1968. The geology of the country south and west of Selukwe. Bull. Geol. Surv. Rhod., 59: 209.

Stowe, C.W., 1974. Alpine-type structures in the Rhodesian basement complex at Selukwe, J. Geol. Soc. Lond., 130: 411-425.

Stowe, C.W., 1979. Gold and Associated Mineralization in the Que Que District, Rhodesia. Spec. Publ. Geol. Soc. S. Afr., 5: 39-48.

Stowe, C.W., 1984. The early Archaean Selukwe nappe, Zimbabwe, In: A. Kroner and R.Greiling (Editors), Precambrian Tectonics Illustrated: Stuttgart Schweizerbart'sche Verlagsbuchhandlung, pp.41-56.

Stowe, C.W., 1987. Chromite deposits of the Shurugwi greenstone belt, Zimbabwe. In: C.W. Stowe (Editor), Evolution of Chromium orefields. Van Nostrand Reinhold. New York, pp.71-87.

Summers, R., 1969. Ancient Mining in Rhodesia. Mem. Natn. Mus. Rhod., 3. Salisbury: 236pp.

Swift, W.H., 1956. The geology of the Odzi gold belt. Bull. Geol. Surv. Rhod., 45: 44.

Tabeart, F., 1987. Controls to the deposition of gold, copper and bismuth at Renco mine, Zimbabwe. In: African Mining, IMM, London: 347-363.

Tinofirei, J., 1984. The geology of the Zvishavane Ultramafic Complex. Hons. Proj. Univ. Zimbabwe, (unpubl).

Treloar, P.J. and Nutt, T.H.C., in prep. Cr-muscovites in auriferous shear zones, Zimbabwe.

Twemlow, S.G., 1984. Archaean gold-telluride mineralisation of the Commoner Mine, Zimbabwe. In: R.P. Foster (Editor), GOLD '82: The Geology, Geochemistry and Genesis of Gold Deposits. A.A.Balkema, Rotterdam, pp.469-492.

Tomschi, H,P., Oberthur, T., Saager, R. and Kramers, J.D., 1986. Geochemical and mineralogical data on the genesis of the Mazowe goldfield in the Harare-Bindura greenstone belt, Zimbabwe. Extended Abst. Geocongress '86, Geol. Soc. S. Afr. Johannesburg: July 1986, pp.345-348.

Viljoen, M.J. and Bernasconi, A.,1979. The geochemistry, regional setting and genesis of the Shangani-Damba Nickel deposits Rhodesia. Spec. Publ. Geol. Soc. S. Afr., 5: 67-98.

Viljoen, M.J., Bernasconi, A., Van Coller, N., Kinloch, E., and Viljoen, R.P., 1979. The geology of the Shangani nickel deposit, Rhodesia. Econ. Geol., 71: 76-95.

Wiles, J.W., 1957. The geology of the eastern portion of the Hartley gold belt, Part 1, 128pp. Gold Deposits and mines, Part 2, 180pp. Bull. Geol. Surv. Rhod., 44.

Williams, D.A.C., 1979. The association of some nickel sulphide deposits with komatiite volcanism in Rhodesia. Can. Mineral., 17: 337-349.

Wilson, A.H., 1982. The geology of the Great "Dyke", Zimbabwe: The ultramafic rocks. J.Petrology, 23: 240-292.

Wilson, A.H. and Wilson, J.F., 1981. The Great "Dyke". In: D.R. Hunter (Editor), Precambrian of the Southern Hemisphere. Elsevier, Amsterdam, pp.472-578.

Wilson, A.H. and Prendergast, M.D., 1987. The Great Dyke of Zimbabwe. 1: A review and overview. In: A. Campbell (Editor), 5th Magmatic Sulphides Field Conference: Abstracts and Field Guide volume. Zim. Geol. Soc., pp.9-10.

Wilson, J.F., Jones, D.L. and Kramers, J.D., 1987. Mafic Dyke swarms in Zimbabwe. In: H.C.Halls and W.F. Fahrig (Editors) Mafic Dyke Swarms: Geol. Assoc. Canada Spec. Paper, 33pp.

Wilson, J.F., 1964. The geology of the country around Fort Victoria. Bull. Geol. Surv. S. Rhod., 58, 147pp.

Wilson, J.F., 1968. The geology of the country around Mashaba. Bull. Geol. Surv. Rhod., 62: 239pp.

Wilson, J.F., 1968a. The Mashaba igneous complex and its subsequent deformation. In: D.J.L Visser (Editor), Symposium on the Rhodesian Basement complex. Geol. Soc. S. Afr. Annexure to Vol. LXXI, pp.175-188.

Wilson, J.F., 1979. A preliminary re-appraisal of the Rhodesian basement complex. Spec. Publ. Geol. Soc. S. Afr., 5: 1-23.

Wilson, J.F., 1981. The granitic-gneiss greenstone shield, Zimbabwe. In: D.R.Hunter, (Editor), Precambrian of the Southern Hemisphere. Elsevier, Amsterdam, pp.454-488.

Wilson, J.F., 1981a. Mashaba Igneous Complex. In: D.R.Hunter, (Editor), Precambrian of the Southern Hemisphere. Elsevier, Amsterdam, pp.570-572.

Wilson, J.F., 1987. The tectonic settings of the Great Dyke of Zimbabwe and the Mashonaland Igneous Event. Abstracts 14th Colloquium of African Geology, Berlin, pp.140-141.

Wilson, J.F., (in prep). A craton and its cracks: some of the behaviour of the Zimbabwe block from the late Archaean to the Mesozoic in response to horizontal movements, and the significance of its mafic dyke fracture patterns.

Wilson, J.F., Bickle, M.J., Hawkesworth, C.J., Martin, A. Nisbet, E.G. and Orpen, J.L., 1978. Granite-greenstone terrains in the Rhodesian Archaean craton. Nature, 271: 23-27.

Worst, B.G., 1962. The geology of the Buhwa Iron Ore Deposits and Adjoining Country, Belingwe District. S. Rhod. Geol. Surv. Bull., 53.

Worst, B.G., 1960. The Great Dyke of Southern Rhodesia. S. Rhod. Geol. Surv. Bull., 47.

This Page Intentionally Left Blank

MINERAL OCCURRENCES IN THE 3.6 Ga OLD ISUA SUPRACRUSTAL BELT, WEST GREENLAND

PETER W.UITTERDIJK APPEL

ABSTRACT

In the early Archaean Isua supracrustal belt, West Greenland, a banded iron-formation is closely associated with stratabound copper sulphides. In banded amphibolites of the supracrustal sequence, scheelite occurrences are known. The scheelite, which occurs as tiny grains arranged parallel to the banding of the amphibolites, is clearly stratabound. The scheelite is of submarine exhalative origin and was chemically precipitated contemporaneously with the deposition of the host mafic volcanic rocks.

INTRODUCTION

The Isua supracrustal belt in West Greenland is the oldest known supracrustal sequence. Numerous age determinations have been carried out on these supracrustal rocks, the first by Moorbath et al. (1973), and the latest by Compston et al., (1986) on single zircons by ion probe that have yielded an age of 3807 ± 1 Ma. But for its unique age, the Isua belt resembles younger Archaean supracrustal belts found elsewhere, and has the same rock types, even mafic and acid volcanics, minor intercalations of metasediments and chemical precipitates such as iron-formation and stratabound sulphides.

GENERAL GEOLOGY

The Isua supracrustal belt has recently been described by Nutman (1986) and the reader is referred to that paper for details. In the present article only a brief account is given.

The supracrustal rocks occur in an arcuate belt up to 4 km wide and 30 km long which is enclosed in the Amitsoq gneisses (Fig. 1). The rocks comprise metasediments and metavolcanics together with intrusive ultrabasic rocks and a major intrusive garbenschiefer unit. Metavolcanic rocks comprise massive and banded amphibolites, presumably derived from basic lavas, tuffs

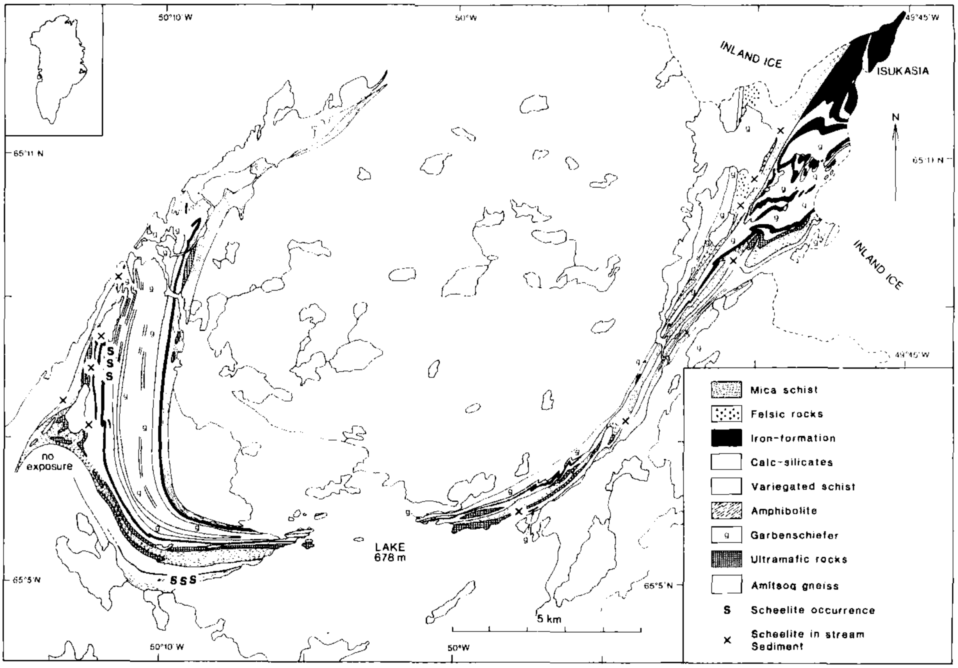

Figure 1. Simplified geological map of the Isua supracrustal belt. (Modified slightly from Nutman et al., 1984). S = scheelite occurrences. X = streams in which grains of scheelite have been found in heavy mineral concentrates.

and intrusives, with chemical similarities to Archaean tholeiites (Nutman et al., 1984). Felsic rocks, which locally display graded bedding, consist of layers of plagioclase, quartz, biotite and muscovite. Variegated schists comprise a mixed sequence of banded hornblende-plagioclase amphibolite with small amounts of biotite and garnet-amphibolite, interlayered with biotite-rich metapelites and layered felsic rocks.

A calc-silicate formation (Fig. 1) is composed of hornblende-rich rocks containing minor clinopyroxene, plagioclase and biotite with stringers and irregular bands of carbonate and quartz. Mica schists (Fig. 1) display a regular layering and consist of biotite, garnet and quartz together with small amounts of staurolite, kyanite and carbonates.

Few sedimentary structures have been preserved. Graded bedding has been recognised locally. In the iron-formation several thin bands with intraformational breccias are seen. A conglomerate layer up to 5 m thick, traceable at intervals for several hundred metres along strike, contains elongated metachert pebbles up to 10 cm long in a matrix consisting mainly of quartz, scapolite, mica, garnet, carbonate with small amounts of magnetite, sulphides and tourmaline. Appel (1984) suggested that the conglomerate was formed in an evaporitic or sabkha-like environment.

After deposition, the volcano-sedimentary pile was repeatedly deformed and metamorphosed. The first deformation and amphibolite facies metamorphism took place 3.8 to 3.6 Ga ago (Nutman et al., 1984). During the 3.1 to 2.6 Ga period, the supracrustal rocks were again deformed and metamorphosed under amphibolite facies conditions.

MINERAL OCCURRENCES

In the Isua supracrustal belt several different types of mineralization have been found of which the most prominent is a banded iron-formation. Stratabound copper sulphides, as well as stratabound scheelite, are seen associated with the iron-formation. Of minor importance are scattered molybdenite occurrences and a few galena showings.

The iron-formation is mainly found in the amphibolitic sequence, where it forms layers up to several tens of metres thick which can be traced up to several hundred metres along strike. However, most iron-formation occurrences are considerably smaller.

The iron-formation occurs as different facies which can be classified according to the terminology suggested by James (1954), for descriptive purposes without any connotation on proximity to shore lines.

Oxide-facies iron-formation is the most widespread facies of the Isua supracrustal belt. It is a classical oxide facies and consists of magnetite-rich layers alternating with quartz (metachert) layers. The layers range in width from millimetres to about 30 cm. In the quartz layers a very fine "dusting" with magnetite is seen. Minor components in oxide facies are actinolite and pyrite. Actinolite occurs as tiny needles, mostly developed on the border between magnetite and quartz layers. Pyrite crystals up to one centimetre are irregularly distributed.

The hematitic oxide facies is very rare. It consists of hematite layers alternating with hematite-stained quartz layers. Microscopic investigations of the hematitic iron-formation reveal that the hematite was formed at the expense of magnetite, and is thus not primary. However, it is not known at which stage of the metamorphic history hematite was formed.

Oxide-facies horizons are generally a few tens of metres across the strike and up to a few hundred metres along the strike. An exception is seen in the extreme north-eastern part of the supracrustal belt, where tectonic thickening has produced a major iron-ore body (Fig. 1) with an estimated 2×10^9 tonnes of ore with an average grade of 32% Fe.

Carbonate-facies iron-formation is not frequently found in the Isua supracrustal belt. Most layers of this facies are only a few centimetres wide and a few metres long. One layer, however, is up to five metres wide and can be traced for a few hundred metres along strike. This facies consists of alternating bands of magnetite and siderite. The magnetite bands range from a few millimetres to one centimetre in width whereas the siderite bands may be up to 10 centimetres wide. The siderite contains up to a few percent manganese and magnesium. Graphite, as tiny flakes and up to 0.2 millimetre round aggregates, is common and evenly distributed in the magnetite and siderite bands. The total graphite content is in the order of 5 vol. percent. Iron-silicates, mainly actinolite but also rarely grunerite, occur in minor amounts in the carbonate facies. Sulphides are evenly distributed as small grains and in irregular veinlets. Pyrrhotite is the dominating sulphide whereas chalcopyrite is more sparse. The total amount of sulphides rarely exceeds a few percent.

Silicate-facies iron-formation can be subdivided into 3 types: 1. Grunerite facies, 2. Actinolite facies, and 3. Shaly iron--formation.

1. The grunerite facies is well banded, consisting of alternating bands of magnetite and grunerite. The bands range from half a centimetre to a couple of centimeteres thick. This facies occurs in layers up to several tens of metres wide and up to a few hundred metres long. Trace amounts of pyrrhotite and chalcopyrite are found.

2. The actinolite facies consists of weakly banded actinolite with scattered millimetre-sized magnetite grains. Locally, small amounts of chalcopyrite and pyrrhotite are seen as scattered grains.

3. Shaly iron-formation is not common. It occurs in up to one metre wide layers which can be traced for a few tens of metres along the strike. This facies is only slightly layered. It consists of magnetite, grunerite, graphite and minor amounts of pyrrhotite and chalcopyrite. The graphite content is up to about 5 vol. percent. Quartz is characteristically absent.

The sulphide facies is uncommon in the Isua supracrustal belt. It occurs as layers up to a few metres wide and a few tens of metres long, consisting mostly of pyrite and quartz. Another variety of sulphide facies consists of actinolite, magnetite with well over ten percent chalcopyrite.

The different facies of iron-formation occur as inextensive layers and there appears to be no regular distribution pattern of these facies types throughout the supracrustal belt. This feature could be due to the strong deformation which could have obliterated a regular distribution pattern of the facies. Perhaps a more likely explanation is that no regular distribution ever existed, and the different facies of iron-formation were precipitated in isolated small basins on the sea floor with slightly different Eh-pH conditions (Appel, 1980).

CHEMISTRY OF THE IRON-FORMATION

A large number of samples of different facies of the iron-formation have been analysed by various techniques including XRF, atomic absorption and neutron activation. The results will be published elsewhere (Appel, in press). In Table 1 the average chemical compositions for selected elements in the different facies are presented.

The major-element composition of the iron-formation agrees well with that of younger iron-formations. Trace-element geochemistry shows some interesting features and most of the elements display a strong correlation with facies of iron-formation. Barium contents are very low in oxide facies compared with silicate facies. Copper shows a strong increase from oxide facies through carbonate facies and silicate facies to shaly iron-formation; and zinc shows the

Table 1.

Average chemical composition of different facies of the Isua iron-formations, West Greenland.

	Oxide	Carbonate	Silicate	Shaly
SiO_2 %	48.51	0.75	49.05	4.30
TiO_2 %	0.04	0.01	0.08	0.14
Al_2O_3 %	0.11	0.42	0.47	1.87
FeO^* %	46.50	62.06	36.86	66.60
MnO %	0.08	3.54	0.30	3.32
CaO %	1.27	0.94	1.46	0.60
P_2O_5 %	0.03	0.49	0.15	0.12
Volat %	1.55	22.15	4.22	15.53
Na ppm	306	23	522	68
K ppm	123	17	248	49
Ba ppm	4	n.a	18	6
Cr ppm	16	25	32	58
W ppm	0	6	31	1
Mo ppm	2	n.a	1	6
Cu ppm	8	42	94	154
Zn ppm	92	74	238	116

Oxide= oxide facies; Carbonate= carbonate facies; Silicate= silicate facies; Shaly= shaly iron-formation. n.a.= not analysed.

same distribution pattern. This indicates that these trace elements were in solution in the brines which carried the iron and silica. These trace elements were then chemically precipitated under the appropriate Eh - pH conditions and/or scavenged by clay minerals.

The tungsten content is very low in oxide facies and shaly iron-formation, but the element shows considerable enrichment in the other facies, especially silicate facies (Table 1). This is also an indication that tungsten was in solution in the brines which supplied the material for the iron-formation.

SULPHIDE OCCURRENCES

Copper sulphides are quite abundant in the Isua supracrustal belt (Appel, 1979). The most common mode of occurrence is as tiny disseminated grains and stringers in banded amphibolites arranged parallel to the banding. Copper sulphides are also seen concentrated into discordant veinlets and veins. The copper sulphides are mostly found together with pyrrhotite and the relative proportion between the iron and copper sulphides varies. The total amount of sulphides rarely exceeds 10 vol. percent. The two most important copper sulphides, chalcopyrite and cubanite, occur as lamellar intergrowths as a result of unmixing. Chalcopyrite is normally the dominant phase but the relative proportions of the two sulphides vary within wide limits. In some samples unmixing of chalcopyrite and cubanite was accompanied by unmixing of coarse spindles of pyrrhotite. Sulphide-bearing banded amphibolites are up to several tens of metres wide and can be traced for several hundred metres along strike. Field relationships clearly show that copper sulphides are stratabound and that only minor mobilisation took place during amphibolite-facies metamorphism and deformation (Appel, 1979).

Stratabound galena is found only in two horizons of banded amphibolite. The galena is very fine grained and amounts to less than one percent. Small amounts of sphalerite, chalcopyrite and complex sulphides of Ni, Sb, Cd and Ag are seen associated with galena (Appel, 1982). Locally, galena has been mobilised into a fuchsite-stained quartzite where it occurs as up to 5 mm grains.

Molybdenite has been found as tiny flakes and as centimetre-sized porphyroblasts in all major rock types. It is particularly abundant in some of the carbonate layers where it locally amounts to a couple of percent.

SCHEELITE OCCURRENCES

Scheelite has been discovered only recently in the Isua supracrustal rocks. The first indication of its presence was found in a stream sediment sampling programme carried out in 1983. Subsequent search for scheelite occurrences was carried out during 1984 and 1986 (Appel, 1985).

Search for *in situ* scheelite by ultraviolet light in central West Greenland is quite difficult. During the summer time there is 24 hours daylight, and it is only towards the end of the field season in late August and beginning of September that the nights get dark enough for field work with ultraviolet light. At the same time, winter is approaching with frequent snow storms. Thus the search for *in situ* scheelite can be carried out only during a short period.

The stream sediment sampling programme suggested that scheelite is widespread in the Isua supracrustal belt (Fig. 1). However, for reasons mentioned above, only two small areas have been investigated so far for *in situ* scheelite (Fig. 1).

Scheelite is found in banded amphibolites, hornblendites and calc-silicate rocks. The most common host is a grey banded amphibolite in which scheelite occurs as tiny grains arranged parallel to the banding. These amphibolites are up to a few metres wide and can be traced for a couple of hundred metres along strike. In hornblenditic rocks, sheelite occurs as disseminated grains and these occurrences are about 10 cm wide and traceable for a few tens of metres along strike. In the basic rocks, scheelite also occurs as joint coatings and as centimetre-sized porphyroblasts. Scheelite in calc-silicate rocks is found exclusively as scattered porphyroblasts.

The fluorescence colour of scheelite is mostly bluish, indicating very low contents of molybdenum. Some of the scheelite porphyroblasts, however, display white fluorescence colours indicating molybdenum contents of about one percent. Rare cases of yellowish molybdenum-rich fluorescent scheelite were found on joints and in veinlets.

SUMMARY AND CONCLUSIONS

The most abundant type of mineral occurrence in the Isua supracrustal belt is banded iron-formation, which occurs in different facies types. The different facies do not exhibit any regular distribution pattern. The layers of iron-formation are not extensive and mainly associated with banded amphibolites.

Copper occurrences are common in the supracrustal rocks, and are seen as stratabound mineralization in banded amphibolites. Copper sulphides are locally abundant in sulphide-facies iron--formation.

Galena has been found stratabound in amphibolites and mobilised into late fault zones.

Scheelite is apparently quite abundant within the supracrustal belt; most of it is clearly stratabound in banded amphibolite. Scheelite, occurring as grains arranged parallel to the amphibolite banding, displays a bluish fluorescence, whereas scheelite as porphyroblasts and on joints is molybdenum bearing, as is witnessed by the white to yellowish fluorescence colours. Tungsten anomalies have been encountered in some facies of the iron-formation.

Previous investigations (Appel, 1979, 1980) have suggested that the banded iron-formation and the stratabound copper sulphides are of submarine exhalative origin, and that the different facies of iron-formation were chemically precipitated on the sea floor in restricted basins with slightly different Eh and pH conditions. The sulphides were chemically precipitated over fairly large areas on the sea floor contemporaneously with the deposition of basic tuffaceous rocks (Appel, 1979). It has been shown that the banded iron-formation and the stratabound copper sulphides are cogenetic (Appel, 1979, 1980).

The genesis of the scheelite mineralisation has been debated since Maucher (1965) and Holl and Maucher (1967) demonstrated the existence of stratabound scheelite of submarine-exhalative origin in Felbertal, Austria. Prior to this discovery, the majority of scheelite occurrences were ascribed to a granitic origin. Since 1965, several syngenetic scheelite occurrences have been found, e.g.. Broken Hill, Australia (Plimer, 1980) and the Malene supracrustal belt, Nuuk, West Greenland (Appel, 1986). The stratabound scheelite occurrences at Felbertal, Broken Hill and Nuuk have, in spite of their difference in age, many characteristics in common. They are intimately associated with metamorphosed mafic volcanic and calc-silicate rocks and scheelite occurs as grains arranged parallel to the banding of the amphibolites.

The scheelite occurrences in the Isua supracrustal rocks display many of the features characteristic for amphibolite-hosted stratabound scheelite deposits elsewhere.

Another important feature in this context is the high content of tungsten found in some facies of the Isua iron-formation. This shows that tungsten was in solution in the sea water during precipitation of the iron-formation. The elevated tungsten contents also indicate that tungsten, iron and silica are likely to be of common heritage.

It is concluded that the stratabound scheelite in the Isua supracrustal belt is of submarine exhalative origin, being precipitated contemporaneously with the precipitation of the host mafic volcanic tuffs. Further it can be concluded that the first precipitated scheelite contained virtually no molybdenum. During metamorphism and deformation of the volcanic pile, some of the scheelite was mobilised and migrated into veinlets and joints.

During this process the scheelite incorporated small amounts of molybdenum.

ACKNOWLEDGEMENTS

This article is written in honour of Dr.B.P.Radhakrishna, Bangalore, India, whom I met during my stay at the Universities of Bangalore and Mysore. My trip to India was financed by the Danish Natural Science Research Council. My stay at Bangalore was financed by the University of Bangalore. This article is published with the permission of the Director, Geological Survey of Greenland.

REFERENCES

Appel, P.W.U., 1979. Strata bound copper sulfides in a banded iron-formation and in basaltic tuffs in the Early Precambrian Isua supracrustal belt, West Greenland, Econ. Geol., 74: 45-52.

Appel, P.W.U., 1980. On the Early Archaean Isua iron-formation, West Greenland, Precamb. Res., 11: 73-87.

Appel, P.W.U., 1982. Strata bound sulphides in the Early Archaean Isua supracrustal belt, West Greenland. In: G.C. Amstutz, A. A. Goresy, G. Frenzel, C. Kluth, G. Moh, Wauschkuhn and R.A. Zimmermann (Editors), Ore Genesis - The state of art. Springer-Verlag, Berlin, Heidelberg ,New York, pp.405-413.

Appel, P.W.U., 1984. Tourmaline in the early Archaean Isua supracrustal belt, West Greenland. J. Geol., 92: 599-605.

Appel, P.W.U., 1985. On the occurrence of scheelite in the Early Archaean Isua supracrustal belt, West Greenland. Rapp. Gronl. Geol. Unders., 125: 45-47.

Appel, P.W.U., 1986. Strata bound scheelite in the Archaean Malene supracrustals, West Greenland. Mineral. Deposita, 21: 207-215.

Appel, P.W.U. in press: Geochemistry of the Early Archaean Isua iron-formation, West Greenland. In: P.W.U. Appel and G. LaBerge, (Editors), Precambrian iron-formations. Theophrastus Publications, Athens.

Compston, W., Kinny, P.D., Williams, I.S. and Foster, J.J., 1986. The age and Pb loss behaviour of zircons from the Isua supracrustal belt as determined by ion microprobe. Earth Planet. Science Lett., 80: 71-81.

Holl, R. and Maucher, A., 1967. Genese und Alter der Scheelit-Magnesit-Lagerstatte. Tux. Bayer. Akad. Wiss. Mathem. Naturw: 1-11.

James, H.L., 1954. Sedimentary facies of iron-formation. Econ. Geol., 49: 235-293.

Maucher, A., 1965. Die Antimon-Wolfram-Quecksilber-Formation und ihre Beziehungen zu Magmatismus und Geotektonik. Freiberg Forsch. H.C., 186: 161-176.

Moorbath, S., O'Nions, R.K. and Pankhurst, R.J., 1973. Early Archaean age for the Isua iron formation, West Greenland, Nature, 245: 138-139.

Nutman, A.D., 1986. The early Archaean to Proterozoic history of the Isukasia area, southern West Greenland. Bull. Gronl. Geol. Unders., 154: 80pp.

Nutman, A.P., Allaart, J.H., Bridgwater, D., Dimroth, E. and Rosing, M., 1984. Stratigraphic and geochemical evidence for the depositional environment of the Early Archaean Isua supracrustal belt, southern West Greenland. Precamb. Res., 25: 356-396.

Plimer, I.R., 1980. Exhalative Sn and W deposits associated with mafic volcanism as precursors to Sn and W deposits associated with granites. Mineral. Deposita, 15: 275-289.

This Page Intentionally Left Blank

EARLY EVOLUTION OF LIFE AND ECONOMIC MINERAL AND HYDROCARBON RESOURCES

MANFRED SCHIDLOWSKI

ABSTRACT

Life processes - notably the introduction during early biological evolution of major bioenergetic innovations - have caused changes in the chemical regime of the Earth's surface that have profoundly affected geochemical transformations in the exogenic cycle (including those responsible for the formation of commercial mineral and energy deposits). In particular, progressive oxygenation of terrestrial (aquatic and subaeric) near-surface environments by O_2-evolving photosynthesis, and large-scale release of H_2S following the emergence of dissimilatory (bacterial) sulfate reduction, entrained formidable metallogenetic potential that gave rise to time-and/or facies- bound lithologies such as Precambrian banded iron-formation and stratiform sulfides. This paper reviews some principal processes of Precambrian metallogeny that are believed to have been largely biologically mediated, as well as problems and questions related to the genesis of the oldest (Late Proterozoic) petroleum and gas deposits.

INTRODUCTION

Since the publication of Vernadsky's (1924, 1930) seminal concept of the catalytic function of the terrestrial biosphere in global geochemical transformations, various lines of evidence have confirmed that life is a most powerful geochemical agent operative at the interface of lithosphere, hydrosphere and atmosphere from where it exercises a profound impact on the exogenic rock cycle. As from its first appearance on Earth, life has demonstrably modulated and, in part, determined the chemical regime on the surface of the planet. This influence ultimately derives from the fact that living systems represent dynamic states maintaining themelves removed from thermodynamic equilibrium at relatively low entropy levels at the expense of their non-living environment. All processes leading to the formation and proliferation of life have been shown to absorb both *matter* (mostly the elements C, O, H, N, S and P) and *energy* (primarily in the form of electromagnetic radiation) from their surroundings and to build up enclaves of higher order within a largely unordered environment, thus apparently defying the second law of thermodynamics and the universal trend towards increasing entropy; in fact, life itself may be defined in terms of its entropy-deferring properties. The negative entropy accumulated in the biosphere consequently pervades all terrestrial near-surface environments, giving rise to a pronounced thermodynamic gradient that serves, in turn, as a driving force for several geochemically important reactions in the exogenic cycle (notably during processes of weathering and sedimentation). Altogether, a stationary sedimentary mass of some 2.4×10^{24} g had been exposed to the influence of the biosphere during its formation; this quantity corresponds to almost one-tenth of the mass of crust. With a mass half-age of the average

Table 1.

Reduction of carbon dioxide to the carbohydrate level (CH_2O) by the most common carbon-fixing reactions utilizing inorganic reductants (H_2, H_2S, H_2O). Reaction 1 would proceed of its own accord ("chemosynthesis"), while 2-4 need to be powered by radiant energy ("photosynthesis"). Note that the anoxygenic forms of bacterial photosynthesis (Nos. 2 and 3) that have preceded the O_2-evolving variant (No.4) in the evolution of photoautotrophy release oxidized species other than free oxygen (sulfate and elemental sulfur). The markedly increased energy demand of oxygenic photosynthesis (operated by cyanobacteria, eukaryotic algae and green plants) is due to the energetically expensive splitting of the hydrogen-oxygen bonds of the water molecule that serve as reductant in this reaction. Standard free energy changes recalculated from Broda (1975, p.75).

$$2H_2 + CO_2 \longrightarrow CH_2O + H_2O \qquad \Delta G_0' = -1 \text{ kcal} \quad (1)$$

$$0.5\,H_2S + H_2O + CO_2 \xrightarrow{h\nu} CH_2O + H^+ + 0.5\,SO_4^{2-} \qquad \Delta G_0' = +28 \text{ kcal} \quad (2)$$

$$2H_2S + CO_2 \xrightarrow{h\nu} CH_2O + H_2O + 2S \qquad \Delta G_0' = +12 \text{ kcal} \quad (3)$$

$$2H_2O^* + CO_2 \xrightarrow{h\nu} CH_2O + H_2O + O_2^* \qquad \Delta G_0' = +112.5 \text{ kcal} \quad (4)$$

sediment on the order of 0.6 Ga (Garrels and MacKenzie, 1971), at least 6 to 7 equivalents of the extant sedimentary shell can be expected to have been processed under the same conditions since the start of the sedimentary record 3.8 Ga ago.

The most exemplary of the life-imposed thermodynamic imbalances is the redox gradient caused by photosynthetic oxygen and its oxidation equivalents (cf. Table 1) that powers oxidation weathering and a host of other oxidation processes on the Earth's surface (the universal character of this gradient is demonstrated by the fact that there is no place on Earth where one cannot light a fire). Another, though less conspicuous, process is the release of large quantities of hydrogen sulfide by sulfate-reducing bacteria in the marine realm which holds considerable metallogenetic potential because bacteriogenic H_2S tends to scavenge iron and base metals from the surrounding seawater giving, under favourable circumstances, rise to stratiform sulfide deposits (cf. Trudinger et al., 1972). Also, the reducing quality of biogenic matter ultimately stemming from the reduction of carbon dioxide to the carbohydrate level during photosynthesis (Table 1) has proved to be a geochemical agent of paramount importance. Sedimentary basins accumulating organic debris represent the most reducing natural environments, with redox potentials between -0.1 and -0.5 volt ("black shale facies"). Under such conditions, a host of metal ions that are soluble (and thus mobile) will undergo precipitation at higher oxidation states.

Reactions of the above type illustrate the crucial role played by the biosphere in the establishment of geochemical differentiation patterns in the Earth's crust. As sediment-forming processes represent the quantitatively most important geochemical differentiation process, it has even been argued that biologically mediated "sorting" of crustal material in the exogenic cycle (and specifically in the black shale facies) is ultimately to be credited with the origin of metallogenic provinces (Knight, 1957; Tugarinov, 1963).

ANTIQUITY OF LIFE AND ESTABLISHMENT OF BIOGEOCHEMICAL ELEMENT CYCLES

Since the products of biologically affected transformations of crustal material have come to be preserved in the sedimentary record, it is possible to trace the underlying biological processes back into the geological past. Such an approach may potentially help to identify the time when life itself or the advent of major bioenergetic innovations had started to exercise an impact on the global rock cycle, thereby providing us with an approximate time-table of early organic evolution. It may be reasonably expected that important quantum steps, notably in bioenegetic evolution (such as the emergence of oxygenic photosynthesis and bacterial sulfate reduction), have caused profound changes in the chemical regimes of substantial parts of the Earth's surface which should have necessarily affected weathering and sedimentation processes (including those responsible for the formation of exogenic mineral deposits). Specifically, the redox-

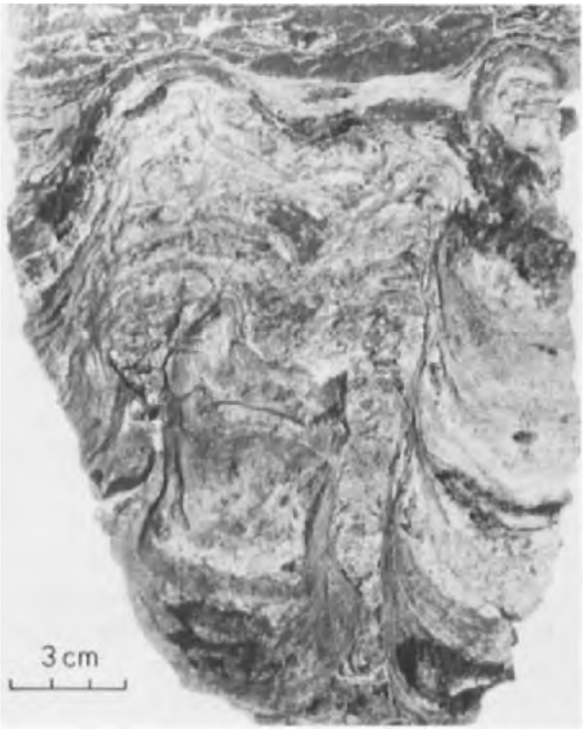

Figure 1. Stromatolite from the Transvaal Dolomite Series, South Africa (~2.3 Ga), giving a typical example of a lithified set of superimposed bacterial and algal mats. The bun-shaped, partially interfering laminae represent successive growth stages of the primary microbial ecosystem. The mat-building microbenthos was commonly dominated by cyanobacteria which were the first photoautotrophs to carry out the water-splitting variant of the photosynthetic process (Table 1, No 4) and thus responsible for the oxygenation of the Earth's surface.

coupled geochemical cycles of the elements carbon, sulfur, oxygen and iron should have been largely governed by the biosphere since the establishment of life on Earth.

During the last decade, disparate lines of evidence have merged to indicate that the Earth was indeed covered by a veneer of microbial life as from almost 4 Ga ago. It is firmly established today that fossil organosedimentary structures of the "stromatolitic" type (Fig. 1) that have preserved the matting behaviour of benthic prokaryotes (mostly photosynthetic bacteria including O_2-evolving cyanobacteria) make their appearance in sedimentary rocks as from ~3.5 Ga ago (cf. Dunlop et al., 1978; Lowe, 1980; Walter et al., 1980). There is, moreover, evidence that the Archaean microbial mat-builders were capable of photic responses in general and of photoautotrophy in particular; in their general morphology, the most ancient stromatolites do not differ significantly from those of geologically younger formations (Walter, 1983). Accordingly, there is a continuous fossil record of benthic microbial ecosystems over 3.5 Ga of Earth history (see also Schopf and coworkers, 1983). Considering the high degree of morphological and functional differentiation characteristic already of the prokaryotic cell, we may reasonably infer that the ancestral lines of the oldest microbial mat-builders must extend much further back in time, i.e., almost certainly to Isua times (3.76 Ga; cf. Moorbath et al., 1973, 1975) and possibly beyond.

Presumed cellular morphologies of prokaryotic affinity reported from various early Archaean sediments (Dunlop et al., 1978; Awrawik et al., 1983), and notably from the ~3.7 Ga-old Isua supracrustals (Pflug and Jaeschke-Boyer, 1979; Robbins, 1987), have been objects of considerable attention and dispute (Bridgwater et al., 1981; Roedder, 1981; Buick, 1984; and others). It seems, however, safe to say that at least part of this micropaleontological evidence cannot be readily dismissed, calling rather for further scrutiny and confirmation by more sophisticated diagnostic approaches.

The paleontological evidence hitherto available is decidedly in concert with straightforward implications of the isotope age curve of sedimentary carbon (Fig. 2). Since both carbonate carbon (C_{carb}) and organic carbon (C_{org}) are preserved in the sedimentary record, we can readily trace the isotopic fractionation between

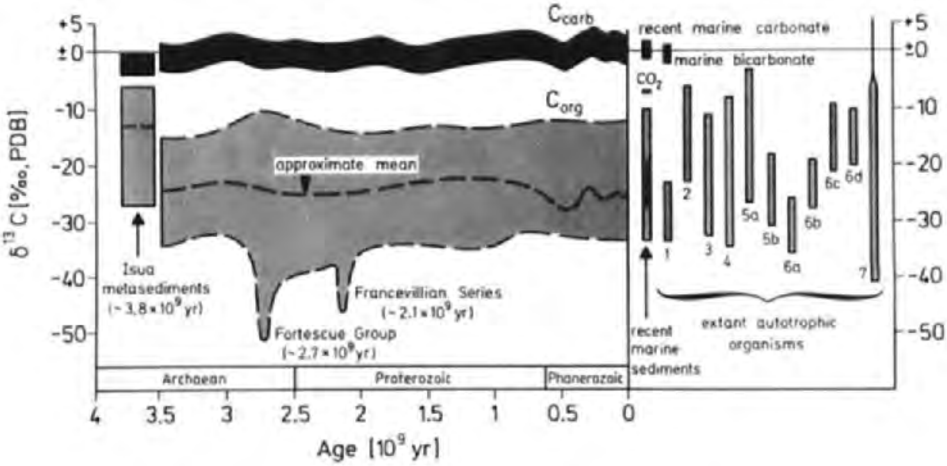

Figure 2. Isotope age functions of carbonate (C_{carb}) and organic carbon (C_{org}) over 3.8 Ga of recorded geological history as compared with the isotopic compositions of their progenitor materials in the contemporary environment (marine bicarbonate and biogenic matter, see right box). Isotopic compositions are given as $\delta^{13}C$ values indicating either an increase (+) or a decrease (-) in the ^{13}C content of the respective sample (in permil) relative to the PDB standard [as organic carbon gives consistently negative readings of $\delta^{13}C$, it is correspondingly enriched in light carbon (^{12}C)]. Numbered groups of extant autotrophic organisms are (1) C3 plants, (2) C4 plant, (3) CAM plants, (4) eukaryotic algae, (5) cyanobacteria (Natural and cultured), (6) photosynthetic bacteria other than cyanobacteria, (7) methanogenic bacteria. The envelope shown for fossil organic carbon covers an update of the data base originally presented by Schidlowski et al., (1983); conspicuous negative offshoots such as at 2.7 and 2.1 Ga indicate the involvement of methane-utilizing pathways in the formation of the respective kerogen precursors. Note that the isotope spreads of extant primary producers have been propagated into the record with just the extremes eliminated, the resulting isotope age function thus representing an index line of autotrophic carbon fixation over almost 4 Ga of Earth history.

these two carbon species back in time (which is further facilitated by the fact that secondary effects linked to their diagenesis and related postdepositional alterations are well understood and amenable to quantitative assessment). The fairly constant average fractionation through time between carbonate and so-called "kerogen", the highly polymerized, acid-insoluble end-product of the postdepositional reconstitution of sedimentary organic matter, clearly reflects respective fractionations between their precursor substances as observed in the present environment (marine bicarbonate and average biomass) and, henceforth, can be best interpreted as an isotopic signature of biological (autotrophic) carbon fixation. Since the characteristic negative shift of $\delta^{13}C$ in ancient kerogens is obviously due to the process that gave rise to the biological precursor materials, the conclusion seems hard to challenge that the organic carbon record as a whole gives a remarkably consistent signal of photoautotrophy on Earth as from 3.5, if not 3.8 Ga ago (Schidlowski, 1982, 1987a; Schidlowski et al., 1979, 1983; Hayes et al., 1983). The mainstream of the broad envelope for $\delta^{13}C_{org}$ depicted in Fig.2 is, in fact, the geochemical manifestation of the isotope discriminating properties of the key enzyme of the Calvin cycle (Ribulose-1,5-bisphosphate carboxylase) that catalyzes most of the carbon transfer from the inorganic to the living world. Since the isotope shifts displayed by both carbon species in the oldest (t>3.5 Ga) sedimentary rocks are almost certainly due to the amphibolite-grade metamorphism of the Isua supracrustals, there is little doubt that the primary biological signature had originally extended to the very beginning of the record ~3.8 Ga ago.

The implications of the carbon isotope age curve are fully substantiated by the observation that the reduced carbon content of Precambrian sediments (inclusive of the Isua suite) scatters within the range of Phanerozoic rocks, with the means of well-investigated series lying between 0.2 and 0.7% (cf. Dungworth and Schwartz, 1974; Nagy et al., 1974; Reimer et al., 1979; Cameron and Garrels, 1980; Ronov, 1980) and an overall average in the range of perhaps 0.4-0.6% (Schidlowski, 1982). Such approximate constancy of the organic carbon content of the average sedimentary rock through time would stand out as a necessary consequence of the largely time-invariant isotope age functions since the $\delta^{13}C$ values of both sedimentary carbon species are coupled to their relative proportions by the isotope mass balance.

$$\delta^{13}C_{prim} = R\delta^{13}C_{org}+(1-R)\delta^{13}C_{carb}.$$

Here, $R=C_{org}/(C_{org}+C_{carb})$ would equal 0.2 if we accept $\delta^{13}C_{org}=25^{o}/oo$ and $\delta^{13}C_{carb}=0^{o}/oo$ as long-term averages for organic and carbonate carbon, and $\delta^{13}C_{prim}=\delta 5^{o}/oo$ as a reasonable approximation for the primordial carbon originally released from the Earth's mantle; R = 0.2 would, in turn, imply a ratio $C_{org}/C_{carb}=0.2/0.8$, indicating that the relative proportions of both carbon species were always close to 20% and 80% of total sedimentary carbon, respectively.

Moreover, it may be reasonably argued that the presence of kerogen constituents and their metamorphic derivatives like graphite in Precambrian sediments constitutes, *per se*, evidence of contemporaneous biological activity as no other process has as yet been demonstrated to introduce sizable quantities of reduced carbon into sedimentary rocks [processes such as the production of kerogen-like substances by photochemical reactions in methane-rich atmospheres (Lasaga et al., 1971) remain a theoretical possibility whose actual involvement in the formation of ancient kerogens still remains to be shown]. In view of the prodigious rates of primary production sustained by extant microbial benthos of predominantly cyanobacterial composition (around 10 g Cm^{-2} day^{-1}, cf. Krumbein and Cohen, 1977; Cohen et al., 1980), the astoundingly modern organic carbon content of Precambrian rocks should not be surprising at all. It is well known that the Precambrian was the "Golden Age" of microbial life and notably of prokaryotic ecosystems of both the benthic and planktonic type (cf. Cloud, 1976; Schopf, 1983). If such impressive rates of primary production can be sustained by microbial photoautotrophs operating on the prokaryotic level, photosynthesis may have gained little in quantitative importance on a global scale ever since the oldest microbial communities had established dominion on the Archaean Earth.

Considering the above evidence, we may reasonably conclude that autotrophic carbon fixation - and notably photoautotrophy as the quantitatively most important process of CO_2 assimilation - had been extant as both a biochemical process and as a geochemical agent since at least 3.8 Ga ago.

BIOLOGICALLY MEDIATED ROCK TRANSFORMATIONS AND PRECAMBRIAN MINERAL DEPOSITS

Direct or indirect involvement of biological processes had been invoked since long for the origin of several types of economically important mineral deposits of Precambrian age. The formation of the respective deposits is commonly linked to the introduction of major innovations in biological (notably bioenergetic) evolution. Specifically, early metallogenetic processes appear to have been extremely sensitive to (a) the biologically imposed change of the redox regime during the early history of the Earth resulting from the progressive oxygenation of terrestrial near-surface environments and, (b) the emergence and subsequent proliferation of bacterial sulfate reducers. Moreover, the increasing chances of preservation of fossil biomass during successively younger cycles of sedimentation and reworking have given rise to the first accumulations of oil and gas in sedimentary sequences of the latest Precambrian.

In the following, a brief overview will be given of some economically relevant mineral-forming processes during the Earth's early history that appear to be related to ancient biological activity.

PRECAMBRIAN BANDED IRON-FORMATION

Finely laminated sequences of ferruginous cherts and iron minerals of so-called "banded iron-formation" (BIF) have, since long, come to be regarded as the prototype of a time-bound lithology characteristic of Archaean to Early Proterozoic times (cf. Gole and Klein, 1981; James and Trendall, 1982; Walker et al., 1983). This sedimentary rock type hosts the bulk of the World's economically recoverable iron resources and provides the source material for $\geq$90% of the contemporary iron production; its major occurrences disappear from the record at a relatively sharp time boundary close to 1.8 Ga ago.

The pronounced time-specificity of Precambrian banded iron-formation had invited speculations about special conditions during their deposition (inclusive of a possible biological connection) already in the early stages of their investigation. As had been postulated by MacGregor (1927) and subsequently re-emphasized by others (e.g., Urey, 1959; Lepp and Goldich, 1964; Cloud, 1973), a transfer to the marine realm of such vast amounts of iron as subsequently piled up in major BIF provinces (notably of the Superior or Hamersley types) was almost certainly contingent on the participation of this element in the continental weathering cycle in the bivalent state, implying that early Precambrian weathering processes had operated under anoxygenic conditions. Assuming that the atmosphere in those times was basically devoid of free oxygen, a large-scale solubility of iron would be a necessary corollary of such a scenario, with hydrated ferrous ions (Fe^{2+})washed out from the ancient continents in amounts comparable

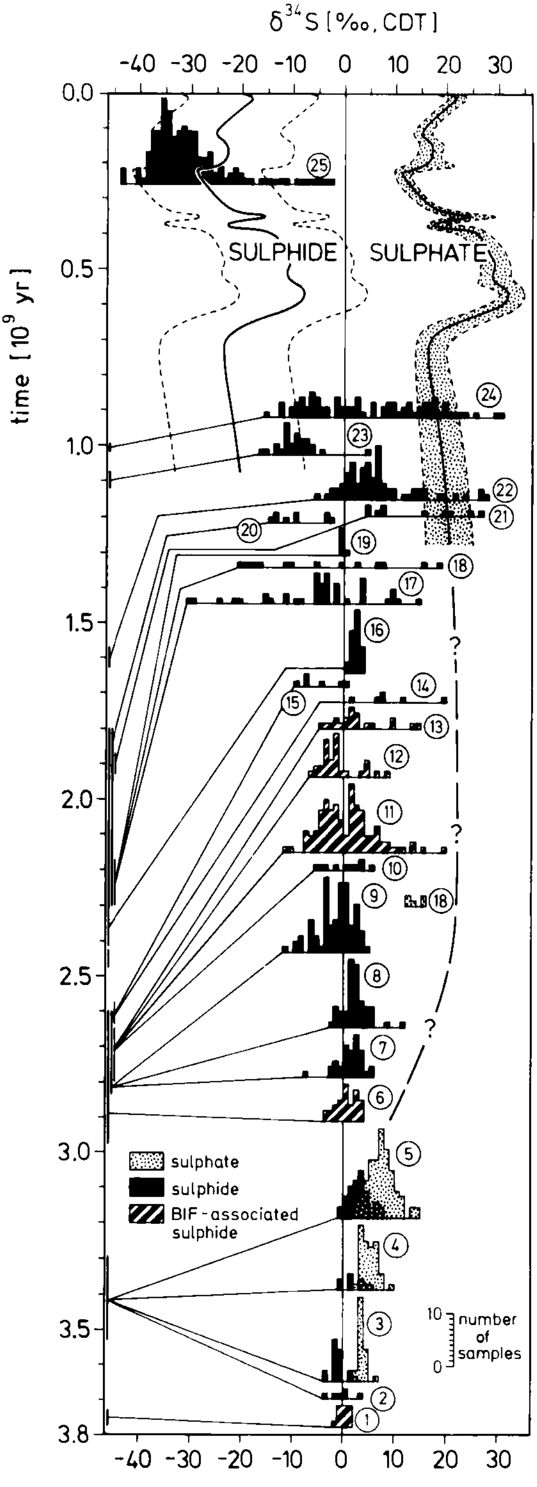

$\delta^{34}S$ [‰, CDT]
-40
-30
-20
-10
0
10
20
30
time [10^9 yr]
0.0
0.5
1.0
1.5
2.0
2.5
3.0
3.5
3.8
SULPHIDE
SULPHATE
?
▨ sulphate
■ sulphide
▨ BIF-associated sulphide
10
0
number of samples
①
②
③
④
⑤
⑥
⑦
⑧
⑨
⑩
⑪
⑫
⑬
⑭
⑮
⑯
⑰
⑱
⑲
⑳
㉑
㉒
㉓
㉔
㉕

to present weathering rates of calcium (or alkaline earths in general), and competing with the latter for the same depositional sites in the contemporaneous marine environment. (Incidentally, this might account for some of the more conspicuous lithological similarities between BIF and common carbonate series).

With dissolved iron thus abundantly present, notably in the miogeosynclinal and shelf regions of the ancient seas, it has become customary to view the deposition of banded iron-formation as the principal oxygen-eliminating process when ancient communities of microbial photoautotrophs widespread in these

---

Figure 3. Isotopic composition of sedimentary sulfide and sulfate through time, with special reference to the evolution of the isotope distribution patterns of sediment-hosted sulfides during the Precambrian (from Schidlowski, 1987b). The negative displacement of the $\delta^{34}S$ values for sulfide relative to sulfate indicates a derivation of these sulfides (mostly pyrite) from ^{34}S-depleted bacteriogenic H_2S. Note that the oldest presumably bacteriogenic patterns of sedimentary sulfides (Nos. 8, 11, 12) date back to ~2.7 Ga. All older sulfide occurrences hitherto investigated are isotopically "undifferentiated", with $\delta^{34}S$ values close to primordial sulfur (about zero permil). This holds specifically for the sulfide fraction of the Earth's oldest sediments from Isua, West Greenland (No. 1). Numbered occurrences: (1) Banded iron-formation from Isua, West Greenland (Monster et al., 1979). (2) Onverwacht Group, South Africa (Schidlowski et al., 1983). (3) Warrawoona Group of Pilbara Block, Western Australia (Lambert et al., 1978). (4) Fig Tree Group, South Africa (Lambert et al., 1978; Perry et al., 1971; Vinogradov et al., 1976). (5) Iengra Series of Aldan Shield, Siberia (Vinogradov et al., 1976). (6) Banded iron-formation from Archaean schist belts, Zimbabwe (Fripp et al., 1979). (7) Black shales from Yilgarn Block, Western Australia (Donnelly et al., 1977). (8) Deer Lake greenstone belt, Minnesota, U.S.A. (Ripley and Nicol, 1981). (9) Birch-Uchi greenstone belt, Canada (Seccombe, 1977). (10) Fortescue Group of Hamersley Basin, Australia (Schidlowski et al., 1983). (11), (12),(13) Michipicoten, Woman River and Lumby-Finlayson Lakes banded iron formations, Canada (Goodwin et al., 1976; Thode and Goodwin, 1983). (14) Steeprock Lake Series, Canada (Veizer and Nielsen, unpublished data). (15) Ventersdorp Supergroup, South Africa (Veizer and Nielsen, unpublished data). (16) Cahill Formation of Pine Creek Geosyncline, Australia (Donnelly and Ferguson, 1980). (17) Transvaal Supergroup, South Africa (Cameron, 1982). (18) Lorraine and Gordon Lake Formations of the Cobalt Group (Upper Huronian Supergroup), Canada (Cameron, 1983; Hattori et al., 1983). (19) Frood Series of Sudbury Distict, Canada (Thode et al., 1962). (20) Black Shales from Outokumpu, Finland (Makela., 1974, and pers. comm., 1978). (21) Onwatin Slate of Sudbury Basin, Canada (Thode et al., 1962). (22) Sediments of McArthur Basin, Australia (Smith and Croxford, 1973, 1975). (23) Adirondack sedimentary sulfides, Canada (Buddington et al., 1969).(24) Nonesuch Shale, Canada (Burnie et al., 1972). (25) Kupferschiefer (Permian), Central Europe (Marowsky, 1969).

environments released molecular oxygen as a by-product of their metabolism (Table 1, No. 4). There is no doubt that the ubiquitous bivalent iron ions must have constituted oxygen acceptors *par excellence* that efficiently absorbed free oxygen from the marine realm, allowing just negligible quantities to escape to the atmosphere where these latter were apt to be rapidly scavenged by photochemical reactions involving a host of reduced atmospheric gas species. The fact that the pre-Silurian continents were virtually barren of life, and that the biological cycle was largely submerged below the ocean level during Precambrian times, has certainly enhanced the effectivity of this oxygen sink. In this way, the ferrous iron burden of the ancient seas would have sequestered the bulk of photosynthetically released oxygen and consequently precipitated as a ferric (Fe^{3+}) oxide slime which, by diagenetic and metamorphic reconstitution (cf. Klein, 1983), was transformed to the present banded iron-formation in the fullness of time. Possible implications of the assumed process of O_2-removal for the ecology of early life and subsequent biological evolution have been set out in detail by Cloud (1973).

Only after successive episodes of intense BIF deposition had overwhelmed this ferrous iron buffer about 2 Ga ago and BIF faded from the record, photosynthetic oxygen could have accumulated as a gaseous species with a concomitant build-up of appreciable partial pressures in the atmosphere. Ever since then, oxidation of bivalent iron from primary rocks took place, mainly in continental weathering crusts, thus drying up its supply to the seas and reducing the dissolved iron content of modern seawater to the ppb-level (10^{-9}). As a consequence, major formations of continental (terrigenous) red beds make up for the disappearance of BIF from the record at $t<1.8$ Ga. As subaerial oxidation processes proceed in a rather sluggish way as compared to the kinetics of the previously operating marine Fe^{2+} buffer, the residence time of molecular oxygen in the near-surface environment was substantially increased, and atmospheric Po_2 was bound to rise until the photosynthetic source and the principal sinks finally reached a state of dynamic equilibrium at a markedly elevated environmental O_2-level.

If this model envisaged for the origin of Precambrian BIF is basically correct (for an alternative view see Holland, 1973), the obvious restriction of this lithology to the Archaean and Early Proterozoic would stand out as a direct consequence of the progressive oxygenation of the Earth's surface by the oldest microbial(prokaryotic) photoautotrophs. Due to the submersion below ocean levels of the bulk of the early microbial ecosystems, this oxygenation had apparently proceeded from the aquatic (marine) to the atmospheric realm, reaching the latter with a conspicuous delay due to the operation of the marine iron buffer that had unfolded its full O_2-absorbing (and thereby metallogenetic) potential between 3.8 and 1.8 Ga ago, with a probable climax during the Early Proterozoic (2.5 - 2.0 Ga). Accordingly,the appearance in the record of BIF as a specific sedimentary rock type would be directly related to a biologically induced differential modulation of marine and continental environments during the early Precambrian.

An essential corollary of the ferrous iron buffer model for the early oceans would be that the rise of free oxygen in the atmosphere was not necessarily linked to the process of photosynthetic oxygen production as such (which had already started long before the build-up of an atmospheric O_2-reservoir), but was rather a function of the partitioning of oxygen among the principal geochemical reservoirs. There is little doubt that the 4% of the total photosynthetic budget that is at present stored in the atmosphere would, in principle, be quickly eliminated by abundant reductants present in both the environment and the crust if it were not for a kinetic lag in the currently operating oxygen-consuming reactions (cf. Schidlowski, 1984). In any case, the small size and ephemeral character of the atmospheric O_2-burden is likely to make this reservoir particularly responsive (and vulnerable) to different modes of operation of the global oxygen cycle. Since the marine Fe^{2+} buffer assumed for the early Precambrian had constituted an exogenic scenario in which the geochemically most relevant O_2-consuming reaction was not subject to kinetic inhibition, modern turnover rates and a modern-size total reservoir of photosynthetic oxygen could have been readily coupled with negligible partial pressures in the atmosphere (which would have resulted in a marked disproportionation between the "bound" and "free" reservoirs as compared to contemporary standards). In other words, the operation of this iron buffer was probably the prime factor retarding the oxygenation of the Earth's surface--and notably of the early atmosphere--for more than 1.5 Ga after microbial photoautotrophs had started releasing photosynthetic oxygen to their aquatic habitats (Schidlowski, 1984). Hence, the process of BIF deposition may be viewed as one of the principal biologically mediated geochemical reactions that has extensively modulated terrestrial near-surface environments during the Earth's early history.

BACTERIAL SULFATE REDUCTION AND STRATIFORM SULFIDE DEPOSITS

A major proportion of the World's copper reserves and considerable accumulations of lead, zinc and silver occur as strata-bound sulfide bodies within Precambrian sediments and metasediments, notably of Proterozoic age (for an overview see Schidlowski, 1973). Although the origin of vast quantities of base metal sulfides such as are accumulated, for instance, in the Zambian Copper Belt had posed a puzzle to generations of geologists, the rigid stratigraphic control of the mineralization left little doubt that the ore-forming processes in this and related cases were largely contemporaneous or "syngenetic" with the formation of the host sediment, and that hydrogen sulfide released to the primary depositional environment by bacterial sulfate reducers was most probably instrumental in the precipitation of these stratiform sulfide assemblages. Such observations were bound to focus attention on the metallogenetic potential of bacterial sulfate reduction as a specific bioenergetic process that primarily affects sedimentation and diagenesis in the near-coastal marine facies.

Since bacterial photosynthesis (Table I, Eqs.2 anb 3) had almost certainly preceded the energetically more demanding water-splitting variant of the photosynthetic process (Eq. 4), sulfate as a mild oxidant should have appeared in the early environment long before the advent of free oxygen. Thereby, the stage was set for the emergence of dissimilatory sulfate reduction, an energy-yielding process that couples the reduction of sulfate to hydrogen sulfide with the oxidation of organic substances, i.e.,

$$2CH_2O + SO_4^{2-} \rightarrow 2HCO_3^- + H_2S$$

Because sulfate serves as an oxidant in this reaction instead of free oxygen, this process may be regarded as a form of anaerobic respiration ("sulfate respiration"). Although utilized by only few genera of strictly anaerobic bacteria (Pfennig et al., 1981) which mostly thrive in the deeper anaerobic layers of the littoral sea floor, the above reaction is of paramount importance from the geochemical viewpoint as it catalyzes a large-scale conversion of sulfate to sulfide under the low-temperature regime of the Earth's surface. Constituting a pivotal link in the global sulfur cycle, this reduction of sulfate to sulfide is, for energetic reasons, fully dependent on biological mediation at temperatures below 150°C (Trudinger et al., 1985). Incidentally, a combination of photosynthetic oxidation and dissimilatory reduction of sulfur would give rise to a closed biological sulfur cycle powered by radiant energy ("sulfuretum", cf. Truper, 1982) in which the dissimilatory process may be viewed as an adaptive reversal of a primary assimilatory pathway relying on H_2S as a reductant (cf. Table 1, Eq. 2). An abstracted version of these cyclic transformations may be presented as

$$H_2S + 2HCO_3^- \underset{\text{dissimilation}}{\overset{\text{assimilation}}{\rightleftarrows}} 2CH_2O + SO_4^{2-} .$$

The H_2S released in large quantities to the marine environment by bacterial sulfate reducers commonly bears a characteristic isotopic signature in that its $\delta^{34}S$ values are shifted by an average of 30-40°/oo in negative direction as compared to the seawater sulfate source (Thode et al., 1949; Nielsen, 1965; Thode and Monster, 1965; Chambers and Trudinger, 1979). When this isotopically light (^{32}S-enriched) bacteriogenic hydrogen sulfide is precipitated in the form of metal sulfides (preferentially as pyrite), its isotopic composition is essentially transcribed into the newly-formed sulfide minerals. Accordingly, sedimentary sulfides basically preserve the $^{34}S/^{32}S$ ratio of their bacteriogenic H_2S precursor, thus propagating the isotopic signature of dissimilatory sulfate reduction into the rock section of the sulfur cycle.

Bringing about a large-scale removal of dissolved iron and base metals from seawater in the form of sedimentary sulfides, this process possesses a prodigious metallogenetic potential (Trudinger et al., 1972; Trudinger, 1979). Therefore, the time of emergence of the underlying bioenergetic process would provide an important temporal constraint on the distribution of strata-bound sulfide deposits in the geological past. Leaving their isotopic fingerprints in sedimentary rocks, sulfate-reducing bacteria can be best tracked down in the record by the characteristic $\delta^{34}S$ patterns bequeathed to the sulfides precipitated in their primary sedimentary habitats. The prototype of such a bacteriogenic pattern is exemplified by the frequency distribution of $\delta^{34}S$ values of the Permian Kupferschiefer of central Europe (Fig. 3, No. 25), an euxinic facies for which an impressive data base has been assembled (Marowsky, 1969). Characteristic features of such bacteriogenic sulfide patterns are (a) a general shift of $\delta^{34}S$ towards negative values as compared to the parent seawater sulfate, and (b) a considerable scatter of the values, with a broad peak and an elongated tailing towards the $\delta^{34}S$ of the marine sulfate source (indicating that part of the fractionation had been achieved in a Rayleigh process operating in semi-closed compartments of the depositional basin).

Accepting these characteristics as evidence of bacteriogenic sulfide formation, the presumably oldest isotope patterns meeting the criteria of biogenicity are those presented by Nos. 8, 11 and 12 of Fig.3, all of which fall into the time span 2.6 - 2.8 Ga ago (Schidlowski, 1979, 1987). The earlier record depicted in Fig. 3 and notably the oldest stratiform sulfides from the Isua metasediments of West Greenland (No.1) - seem to lack bacteriogenic features. If we were to rely on the isotopic evidence alone, the above 2.6 - 2.8 Ga interval would, accordingly, define the time of appearance of sulfate-reducing bacteria, implying that dissimilatory sulfate reduction had emerged much later than photoautotrophy (an inference consistent with its interpretation as an adaptive reversal of bacterial photosynthesis).

However, with photoautotrophy certainly dating back to 3.5 Ga and most probably to 3.8 Ga ago, it is difficult to understand why bacterial sulfate reduction should have followed photosynthesis with a time lag of about one billion years. The fact that the build-up of a marine sulfate reservoir (as attested to by the occurrence of sulfate evaporites; cf. Fig. 3, Nos. 3-5) had likewise commenced 3.5 Ga ago or earlier, would make such a lag even more enigmatic. Hence, the question seems justified whether the earliest biogenic sulfur isotope patterns might have been obliterated in the record so that their first manifestations some 2.7 Ga ago just give a *minimum age* for the emergence of dissimilatory sulfate reduction. We certainly cannot exclude that the isotopic differentiation of the marine sulfur reservoir was both retarded and camouflaged by the high-temperature regime of a mantle-dominated Archaean ocean. Since the disappearance of the biogenic signature in the $\delta^{34}S$ record roughly coincides with the Archaean-Proterozoic boundary, this might indeed hint at peculiarities of Archaean seawater chemistry. With vast areas of newly formed oceanic crust exposed to the sea and a substantially higher heat flow, basalt-seawater interactions can be expected to have been at a peak during Archaean (t<2.5 Ga) times (Veizer et al., 1982). Due to a correspondingly enhanced seawater circulation through ocean floor hydrothermal systems, the chemistry of the early ocean may indeed have been mantle-dominated, with marine sulfate continuously undergoing isotopic re-equilibration with the primordial sulfur of the basaltic sea floor. As a result of such re-equilibration, $\delta^{34}S$ values of marine sulfur could have been closely tethered to the value of mantle sulfur (about zero per mil). It is in keeping with such conjectures that isotopic fractionations between sulfide and sulfate in the oldest record are relatively small (Fig.4, Nos. 3-5), with particularly the sulfide fraction bearing the isotopic signature of sulfur from mantle rocks.

Since the quantitative impact of basalt-seawater interaction on the sulfur isotope geochemistry of the present ocean is still under debate, the potential influence of the assumed mantle--buffering on the Archaean sulfur cycle and the suspected obliteration of the oldest biogenic isotopic signatures is still difficult to assess. It should be noted in this context that Ohmoto and Felder (1987) have, for different reasons, also argued for a considerbly earlier onset of dissimilatory sulfate reduction.

On the other hand, it seems well established that bacterial sulfate reduction did not develop its full metallogenetic potential prior to Proterozoic times because strata-bound sulfide deposits of economic grade have invariably proved to be younger than 2 Ga (Jacobsen, 1975). Proterozoic sequences, however, have been shown to host a fair quantity of sedimentary sulfide deposits which either represent, or are among, the World's largest producers of copper, lead, zinc and silver (e.g., Copper Belt, Zambia; Mount Isa and Broken Hill, Australia). Although the isotopic link of some of these ore deposits to bacterial sulfate reduction appears to be weak or even equivocal, generally a good case can be made for their syngenetic origin and the probable involvement of biogenic H_2O as precipitant for the primary sulfides on account of other evidence. In several other sediment-hosted sulfide accumulations of Proterozoic age the isotopic evidence linking these deposits to the activity of sulfate reducers is, however, straightforward. Notably, the stratiform sulfides from Outokumpu (Finland), the McArthur Basin (Australia), the Adirondack deposits and the Nonesuch Shale (Canada) display fairly unequivocal bacteriogenic $\delta^{34}S$ patterns (Fig. 3, Nos. 20, 22, 23, 24). Altogether, it is safe to say that the currently available geological and geochemical evidence gives eloquent testimony to large scale involvement of bacterial sulfate reducers in the formation of economically important stratiform base metal sulfides as from at least Proterozoic times.

FOSSIL FUELS OF PRECAMBRIAN AGE

As in geologically younger formations, the organic fraction of Precambrian sediments exists almost exclusively in the form of kerogenous materials which, with increasing metamorphic grade, are being progressively transformed into graphite. Since the average C_{org}-content of Precambrian rocks has been shown not to differ basically from younger ones (see above), the conspicuous absence of accumulations of both coaly material and hydrocarbons must appear outright enigmatic. Whereas the absence of coal measures (except algal coals) can be explained by the non-existence of higher plants in those times, it is difficult to accept why an early microbial biosphere should not be entertained as a formidable hydrocarbon-generating potential. This is the more puzzling as paleontological and organic geochemical studies have shown that many unmetamorphosed Precambrian rocks are rich in kerogens of algal and bacterial derivation that are not yet over-mature and thus potential indicators of petroleum (e.g., McKirdy, 1974; Oehler and Logan, 1977; Peat et al., 1978; McKirdy and Hahn, 1982). There is, accordingly, good reason to believe that the extreme scarcity of fossil fuel deposits in the early record is due to secondary causes, mainly a reduced geological half-life during crustal evolution of potentially oil and gas-hosting geological terranes (cf. Veizer et al., 1988). Incidentally, the apparent lack of commercial energy deposits in older geological formations had nurtured the long-standing dogma of a coincidence of the lower boundary of the Cambrian with the economic basement for hydrocarbon accumulations.

However, investigations carried out during the last decade (mostly as part of IGCP Project 157; see Oehler and Schidlowski, 1980; Schidlowski, 1985) have demonstrated that this base line was outright arbitrary. Prospecting conducted on a world-wide scale has proved the existence of a large number of hydrocarbon reservoirs (inclusive of some commercial deposits) within the Proterozoic sedimentary covers of several ancient shield regions such as Siberia, Canada, Australia and Africa (Vassoyevich et al., 1971; McKirdy, 1974). There is, meanwhile, ample evidence that the respective petroleum and gas occurrences are indeed indigenous to these Proterozoic sequences irrespective of the fact that migration (even into fractured igneous and metamorphc rocks) is a widespread phenomenon also in Precambrian oil-bearing terranes.

One of the best explored Proterozoic hydrocarbon provinces with the largest known reserves of gas and oil is the Lena-Tunguska region situated on the Central Siberian Platform (Meyerhoff, 1980). Since large-scale prospecting had commenced in this area during the early sixties, more than 20 separate gas and oil fields were discovered of which about a dozen are rated commercial. The Precambrian gas and oil-bearing sequence consists of several thousand meters of mostly marine, flat-lying shelf sediments, with Riphean and Vendian sandstones acting as principal reservoir rocks. The fact that the arenaceous reservoirs are tightly sealed by shales constitutes the strongest proof that the petroleum is indigenous to the Proterozoic sequence. The overlying Cambrian oil reservoirs hosted by fractured carbonate rocks appears to be genetically unrelated to the Riphean and Vendian deposits. A bemusing aside of the exploration history of this Siberian hydrocarbon province is that the first Precambrian oil and gas discoveries were made accidently when single drill holes went astray and inadvertently transected Cambrian structural traps to penetrate part of the underlying Proterozoic sequence.

The Siberian discoveries were instrumental in sparking off similar exploration efforts in other Proterozoic-Early Paleozoic terranes, notably from Australia (Amadeus, Georgina and Officer Basins), North America (Williston, Michigan and Appalachian Basins), Southern Africa (Damara Belt) and China. These exploration programs were, in part, substantially assisted by sophisticated geochemical techniques utilizing, inter alia, the biomarker geochemistry of the potential hydrocarbon-bearing sequence. Biological markers or "chemofossils", respectively (Mackenzie, 1982; Johns, 1986) are molecules or molecule fragments of the biogenic progenitor materials that are capable of withstanding humification and subsequent diagenetic transformations in the sediment with little or no change. Prior to the appearance of vascular plants around the Silurian/Devonian boundary, sedimentary organic matter was almost solely derived from bacteria, algae and marine invertebrates all of which have bequeathed specific sets of biological marker compounds to the record. These markers constitute source indicators as they transcribe selected biochemical characteristics of the early marine biomass into pre-Devonian kerogens, bitumens and oils, thus providing powerful exploration tools in the search for the oldest petroleum and gas deposits. As a by-product of current exploration programs, remarkable insight has been gained into the biomarker geochemistry of pre-Devonian organic matter. Specifically, these investigations have revealed an unexpectedly diverse array of marker hydrocarbons in a large collection of Proterozoic and Cambro-Ordovician crude oils which, as "molecular fossils", furnish crucial clues as to the nature of the parent biomass (cf. McKirdy et al., 1980, 1981; McKirdy and Kantsler, 1980; Zumberge, 1981).

In sum, this work has firmly established the oil-and gas-generating potential of Precambrian source rocks which, in turn, derives from the fossil remains of the Earth's oldest microbial (largely prokaryotic) biomass. It is a reasonable conjecture that the apparent lack of petroleum accumulations in lower Proterozoic and older sediments is not primarily due to any inherent hydrocarbon-generating deficiency of a microbially dominated early terrestrial biosphere, but rather is caused by the preferential destruction of ancient oil-bearing terranes as a result of tectonism and sedimentary recycling.

REFERENCES

Awramik, S.M., Schopf, J.W. and Walter, M.R., 1983. Filamentous fossil bacteria from the Archaean of Western Australia. In: B.Nagy, R. Weber, J.C. Guerrero and M. Schidlowski (Editors), Developments and Interactions of the Precambrian Atmosphere, Lithosphere and Biosphere, (Developments in Precambrian Geology 7), Elsevier, Amsterdam, pp.249-266.

Bridgwater, D., Allaart, J.H., Schopf, J.W., Klein, C., Walter, M.R., Barghoorn, E.S., Strother, P., Knoll, A.H. and Gorman, B.E., 1981. Microfossil-like objects from the Archaean of Greenland: a cautionary note. Nature, 289: 51-53.

Broda, E., 1975. The Evolution of the Bioenergetic Processes. Pergamon, Oxford, 220pp.

Buddington, A.F., Jensen, M.L. and Mauger, R.L., 1969. Sulfur isotopes and origin of northwest Adirondack sulfide deposits. Geol. Soc. Am. Mem., 115: 423-451.

Buick, R., 1984. Carbonaceous filaments from North Pole, Western Australia; are they fossil bacteria in Archaean stromatolites? Precamb. Res., 24: 157-172.

Burnie, S.W., Schwarcz, H.P. and Crocket, J.H., 1972. A sulfur isotopic study of the White Pine Mine, Michigan, Econ. Geol., 67: 895-914.

Cameron, E.M., 1982. Sulphate and sulphate reduction in early Precambrian oceans. Nature, 296: 145-148.

Cameron, E.M., 1983. Evidence from early Proterozoic anhydrite for sulphur isotopic partitioning in Precambrian oceans. Nature, 304: 54-56.

Cameron, E.M. and Garrels, R.M., 1980. Geochemical compositions of some Precambrian shales from the Canadian Shield. Chem. Geol., 28: 181-197.

Chambers, L.A. and Trudinger, P.A., 1979. Microbiological fractionation of stable sulfur isotopes: a review and critique. J. Geomicrobiol., 1: 249-293.

Cloud, P.E., 1973. Paleoecological significances of the banded iron formation. Econ. Geol., 68: 1135-1143.

Cloud, P.E., 1976. Beginnings of biospheric evolution and their biogeochemical consequences. Paleobiology, 2: 351-387.

Cohen, Y., Aizenshtat, Z., Stoler, A. and Jorgensen, B.B., 1980. The microbial geochemistry of Solar Lake, Sinai. In: J.B.Ralph, P.A. Trudinger and M.R. Walter (Editors), Biogeochemistry of Ancient and Modern Environments. Springer, Berlin, pp.167-172.

Donnelly, T.H. and Ferguson, J., 1980. A stable isotope study of three deposits in the Alligator Rivers uranium field, N.T. In: J.Ferguson and A.B. Goleby (Editors), Uranium in the Pine Creek Geosyncline: International Atomic Energy Agency, Vienna, pp.397-407.

Donnelly, T.H., Lambert, I.B., Oehler, D.Z., Hallberg, J.A., Hudson, D.R., Smith, J.W., Bavinton, O.A., and Golding, L., 1977. A reconnaissance study of stable isotope ratios in Archaean rocks from the Yilgarn Block, Western Australia. J. Geol. Soc. Austr., 24: 409-420.

Dungworth, G. and Schwartz, A.W., 1974. Organic matter and trace elements in Precambrian rocks from South Africa. Chem. Geol., 14: 167-172.

Dunlop, J.S.R., Muir, M.D., Milne, V.A. and Groves, D.I., 1978. A new microfossil assemblage from the Archaean of Western Australia. Nature, 274: 676-678.

Fripp, R.E.P., Donnelly, T.H. and Lambert, I.B. 1979. Sulphur isotope results from Archaean banded iron formation, Rhodesia. Spec. Publ. Geol. Soc. S. Afr., 5: 205-208.

Garrels, R.M. and Mackenzie, F.T., 1971. Evolution of Sedimentary Rocks. Norton, New York, 397pp.

Gole, M.J. and Klein, C., 1981. Banded iron-formations through much of Precambrian time. J. Geol., 89: 169-183.

Goodwin, A.M., Monster, J. and Thode, H.G., 1976. Carbon and sulfur isotope abundances in Archaean iron formations and early Precambrian life. Econ. Geol., 71: 870-891.

Hattori, K., Krouse, H.R. and Campbell, F.A., 1983. The start of sulfur oxidation in continental environments: about $2.2x10^9$ years ago. Science, 221: 549-551.

Hayes, J.M., Kaplan, I.R. and Wedeking, K.W., 1983. Precambrian organic geochemistry: preservation of the record. In: J.W.Schopf (Editor), Earth's Earliest Biosphere: Its Origin and Evolution: Princeton University Press, Princeton, N.J., pp.93-134.

Holland, H.D., 1973. The oceans: a possible source of iron in iron-formations. Econ. Geol., 68: 1169-1172.

Jacobsen, J.B.E., 1975. Copper deposits in time and space. Miner, Sci. Eng., 7: 337-371.

James, H.L. and Trendall, A.F., 1982. Banded iron formation: Distribution in time and paleoenvironmental significance. In: H.D. Holland and M.Schidlowski (Editors), Mineral Deposits and the Evolution of the Biosphere.Springer, Berlin, pp.199-218.

Johns, R.B. (Editor) 1986. Biological Markers in the Sedimentary Record (Methods in Geochemistry and Geophysics, 24). Elsevier, Amsterdam, 364pp.

Klein, C., 1983. Diagenesis and metamorphism of Precambrian banded iron formations. In: A.F. Trendall and R.C. Morris (Editors), Iron-Formation: Facts and Problems. Elsevier, Amsterdam, pp. 417-469.

Knight, C.L., 1957. Ore genesis - the source bed concept. Econ. Geol., 52: 808-817.

Krumbein, W.E. and Cohen, Y., 1977. Primary production, mat formation and lithification chances of oxygenic and facultative anoxygenic cyanophytes (cyanobacteria). In: E.Flugel (Editor), Fossil Algae.Springer, Berlin, pp.37-56.

Lambert, I.B., Donnelly, T.H., Dunlop, J.S.R. and Groves, D.I., 1978. Stable isotopic compositions of Early Archaean sulphate deposits of probable evaporitic and volcanogenic origins. Nature, 276: 808-811.

Lasaga, A.C., Holland, H.D. and Dwyer, M.J., 1971. Primordial oil slick. Science, 174: 53-55.

Lepp, H. and Goldich, S.S., 1964. Origin of Precambrian Iron Formation. Econ. Geol., 59: 1025-1060.

Lowe, D.R., 1980. Stromatolites 3,400-Myr old from the Archaean of Western Australia. Nature, 284: 441-443.

MacGregor, A.M., 1927. The problem of the Precambrian atmosphere. S. Afr. J. Sci., 24: 155-172.

Mackenzie, A.S., 1982. Molecular organic geochemistry,. Terra cognita, 2: 99-107.

Makela, M., 1974. A study of sulfur isotopes in the Outokumpu ore deposits, Finland. Geol. Surv. Finl. Bull., 267: 45pp.

Marowsky, G., 1969. Schwefel-,Kohlenstoff-und Sauerstoff -Isotope nuntersuchungen am Kupferschiefer als Beitrag zur genetischen Deutung. Contr. Min. Pet., 22: 290-334.

McKirdy, D.M., 1974. Organic geochemistry in Precambrian research. Precamb. Res., 1: 75-137.

McKirdy, D.M., Aldridge, A.K. and Ypma, P.J.M., 1981. A geochemical comparison of some crude oils from pre-Ordovician carbonate rocks. In: M. Bjoroy et al. (Editors), Advances in Organic Geochemistry 1981, Wiley, Chichester, pp.99-107.

McKirdy, D.M. and Hahn, J., 1982. The composition of kerogen and hydrocarbons in Precambrian rocks. In: H.D. Holland and M. Schidlowski (Editors), Mineral Deposits and the Evolution of the Biosphere, Springer, Berlin, pp.123-154.

McKirdy, D.M. and Kantsler, A.J., 1980. Oil geochemistry and potential source rocks of the Officer Basin, South Australia. Austr. Petr. Explor. Assoc. J., 20: 68-86.

McKirdy, D.M., McHugh, D.J. and Tardif, J.W., 1980. Comparative analysis of stromatolitic and other microbial kerogens by pyrolysis-hydrogenation-gas chromatography. In: B.J. Ralph, P.A. Trudinger and M.R. Walter (Editors), Biogeochemistry of Ancient and Modern Environments. Springer, Berlin, pp.187-200.

Meyerhoff, A.A., 1980. Geology and petroleum fields in Proterozoic and Lower Cambrian strata, Lena-Tunguska petroleum province, eastern Siberia. In: M.T. Halbouty (Editor), Giant Oil and Gas Fields of the Decade 1968-1978. Am. Ass. Petrol. Geol. Mem., 30, pp.225-252.

Monster, J., Appel, P.W.U., Thode, H.G., Schidlowski, M., Carmichael, C.M., and Bridgwater, D., 1979. Sulfur isotope studies in Early Archaean sediments from Isua, West Greenland: implications for the antiquity of bacterial sulfate reduction. Geochim. Cosmochim. Acta, 43: 405-413.

Moorbath, S., O'Nions, R.K. and Pankhurst, R.J., 1973. Early Archaean age for the Isua iron-formation, West Greenland. Nature, 245: 138-139.

Moorbath, S., O'Nions, R.K. and Pankhurst, R.J., 1975. The evolution of Early Precambrian crustal rocks at Isua, West Greenland-geochemical and isotopic evidence. Earth Planet. Sci. Lett., 27: 229-239.

Nagy, B., Kunen, S.M., Zumberge, J.E., Long, A., Moore, C.B., Lewis, C.F., Anhaeusser, C.R. and Pretorius, D.A., 1974. Carbon content and carbonate ^{13}C abundances in the Early Precambrian Swaziland sediments of South Africa. Precamb. Res., 1: 43-48.

Nielsen, H., 1965. Schwefelisotope im marinen Kreislauf und das $\delta^{34}S$ der fruheren Meere. Geol. Rundschau., 55: 160-172.

Oehler, J.H. and Logan, R.G., 1977. Microfossils, cherts, and associated mineralisation in the Proterozoic McArthur (HYC) lead-zinc-silver deposit. Econ. Geol., 72: 1393-1409.

Oehler, J.H. and Schidlowski, M., 1980. Early biological evolution in relation to mineral and energy resources: IGCP Project 157. Rev. Inst. Franc. Petrol., 35: 319-324.

Ohmoto, H. and Felder, R.P., 1987. Bacterial activity in the warmer, sulphate bearing, Archaean oceans. Nature, 328: 244-246.

Peat, C.J., Muir, M.D., Plumb, K.A., McKirdy, D.M. and Norvick, M.S., 1978. Proterozoic microfossils from the Roper Group, Northern Territory, Australia, BMR J. Austr. Geol. Geophys., 3: 1-17.

Perry, E.C., Monster, J. and Reimer, T., 1971. Sulfur Isotopes in Swaziland System barites and the evolution of the Earth's atmosphere. Science, 171: 1015-1016.

Pfennig, N., Widdel, F. and Truper, H.G., 1981. The Dissimilatory sulfate reducing bacteria. In: M.P. Starr, H.Stolp, H.G., Truper, A. Balows and H.G. Schlegel (Editors), The Prokaryotes Springer, Berlin, 1, pp.926-940.

Pflug, H.D. and Jaeschke-Boyer, H., 1979. Combined structural and chemical analysis of 3,800-Myr-old microfossils. Nature, 280: 483-486.

Reimer, T.O., Barghoorn, E.S. and Margulis, L., 1979. Primary productivity in an Early Archaean microbial ecosystem. Precamb. Res., 9: 93-104.

Ripley, E.M. and Nicol, D.L., 1981. Sulfur isotopic studies of Archaean slate and graywacke from northern Minnesota: evidence for the existence of sulfate reducing bacteria. Geochim. Cosmochim. Acta, 45: 839-846.

Robbins, E.I., 1987. Appelella ferrifera, a possible new iron-coated microfossil in the Isua iron-formation, southwestern Greenland. In: P.W.U. Appel and G.L. LaBerge (Editors), Precambrian Iron-Formations, Theophrastus Publications, Athens, pp.141-154.

Roedder, E., 1981. Are the 3.800-Myr-old lsua objects microfossils, limonite stained fluid inclusions, or neither? Nature, 293: 459-462.

Ronov, A.B., 1980. Osadochnaya Obolochka Zemli (Earth's Sedimentary Shell). 20th Vernadsky Lecture. Moscow, Izdatel'stvo Nauka, 97pp.

Schidlowski, M., 1973. Sulfur in the Precambrian metallogeny. Geol. Rundschau., 62: 840-863.

Schidlowski, M., 1979. Antiquity and evolutionary status of bacterial sulfate reduction: sulfur isotope evidence. Origins of Life, 9: 299-311.

Schidlowski, M., 1982. Content and isotopic composition of reduced carbon in sediments. In: H.D. Holland and M.Schidlowski (Editors), Mineral Deposits and the Evolution of the Biosphere, Springer, Berlin, pp.103-122.

Schidlowski, M., 1984. Early atmospheric oxygen levels: constraints from Archaean photoautotrophy, J. Geol. Soc. London, 141: 243-250.

Schidlowski, M., 1985. Early life and mineral resources. Nature and Resources, 21, (2): 11-17.

Schidlowski, M., 1987a. Application of stable carbon isotopes to early biochemical evolution on Earth. Ann. Rev. Earth Planet. Sci., 15: 47-72.

Schidlowski, M., 1987b. Evolution of the early sulphur cycle. In: R.Rodriguez-Clemente and Y. Tardy (Editors), Geochemistry and Mineral Formation in the Earth Surface Consejo Superior de Investigaciones Cientificas, Madrid, pp.29-49.

Schidlowski, M., Appel, P.W.U., Eichmann, R. and Junge, C.E., 1979. Carbon isotope geochemistry of the 3.7x10^9 yr old Isua sediments, West Greenland: implications for the Archaean carbon and oxygen cycles. Geochim. Cosmochim. Acta, 43: 189-199.

Schidlowski, M., Hayes, J.M. and Kaplan, I.R., 1983. Isotopic inferences of ancient biochemistries: carbon, sulfur, hydrogen and nitrogen. In: J.W. Schopf (Editor), Earth's Earliest Biosphere: Its Origin and Evolution: Princeton University Press, Princeton, N.J., pp.149-186.

Schopf, J.W. (Editor) 1983. Earth's Earliest Biosphere: Its Origin and Evolution: Princeton University Press, Princeton, N.J: XXV + 543pp.

Seccombe, P.K., 1977. Sulphur isotope and trace metal composition of stratiform sulphide as an ore guide in the Canadian Shield. J. Geochem. Explor., 8: 117-137.

Smith, J.W. and Croxford, N.J.W., 1973. Sulphur isotope ratios in the McArthur lead-zinc-silver deposit. Nature, Phys. Sci., 245: 10-12.

Smith, J.W. and Croxford, N.J.W., 1975. An isotopic investigation of the environment of deposition of the McArthur mineralization. Mineral. Deposita, 10: 269-276.

Thode, H.G., Dunford, H.B. and Shima, M., 1962. Sulfur isotope abundances in rocks of the Sudbury District and their geological significance. Econ. Geol., 57: 565-578.

Thode, H.G. and Goodwin, A.M., 1983. Further sulfur and carbon isotope studies of Late Archaean iron-formations of the Canadian Shield and the rise of sulfate-reducing bacteria. In: B.Nagy, R.Weber, J.C. Guerrero and M.Schidlowski (Editors), Developments and Interactions of the Precambrian Atmosphere, Lithosphere and Biosphere (Developments in Precambrian Geology 7), Elsevier, Amsterdam, pp.229-248.

Thode, H.G., MacNamara, J. and Collins, C.B., 1949. Natural variations in the isotopic content of sulphur and their significance. Can. J. Res., B-27: 361-373.

Thode, H.G. and Monster, J., 1965. Sulfur isotope geochemistry of petroleum, evaporites, and ancient seas. Am. Assoc. Petr. Geol. Mem., 4: 367-377.

Trudinger, P.A.,1979. The biological sulfur cycle. In: D.J. Swaine and P.A. Trudinger (Editors), Biogeochemical Cycling of Mineral Forming Elements, Elsevier, Amsterdam, pp.293-313.

Trudinger, P.A. Chambers, L.A. and Smith, J.W., 1985. Low- tempera ture sulphate reduction: biological vs abiological. Can. J. Earth Sci., 22: 1910-1918.

Trudinger, P.A., Lambert, I.B. and Skyring, G.W., 1972. Biogenic sulfide ores: a feasibility study. Econ. Geol., 67: 1114-1127.

Truper, H.G., 1982. Microbial processes in the sulfur cycle through time. In: H.D.Holland and M.Schidlowski (Editors), Mineral Deposits and the Evolution of the Biosphere, Springer, Berlin, pp.5-30.

Tugarinov, A.I., 1963. Causes of the formation of metallogenic provinces. In: A.P.Vinogradov (Editor), Chemistry of the Earth's Crust, Israel Progr. f.Scient. Transl., Jerusalem, pp. 160-185.

Urey, H., 1959. The atmospheres of the planets. In: S.Flugge (Editor), Handbuch der Physik, LII Springer, Berlin, pp. 363-418.

Vassoyevich, N.B., Vysotskiy, I.V., Sokolov, B.A. and Tartarenko, Y.I., 1971. Oil-gas potential of Late Precambrian. Internat. Geol. Rev., 13: 407-418.

Veizer, J., Compston, W., Hoefs, J. and Nielsen, H., 1982. Mantle buffering of the early oceans. Naturwissenschaften, 69: 173-180.

Veizer, J., Laznicka, P. and Jansen, S.L., 1988. Mineralization through geologic time: recycling perspective. Am. J. Sci. (in press).

Vernadsky, V.I., 1924. La Geochimie. Felix Alcan, Paris, 404pp.

Vernadsky, V.I., 1930. Geochemie in ausgewahlten Kapiteln. Akademische Verlagsgesellschaft, Leipzig, 370pp.

Vinogradov, V.I., Reimer, T.O., Leites, A.M. and Smelov, S.B., 1976. The oldest sulfates in Archaean formations of the South African and Aldan Shields and the evolution of the Earth's oxygenic atmosphere. Lithology and Mineral Resources, 11: 407-420.

Walker, J.C.G., Klein,C., Schidlowski, M., Schopf, J.W., Stevenson, D.J. and Walter, M.R., 1983. Environmental evolution of the Archaean-Early Proterozoic Earth. In: J.W.Schopf (Editor), Earth's Earliest Biosphere: Its Origin and Evolution. Princeton University Press, Princeton, N.J., pp.260-290.

Walter, M.R., 1983. Archaean stromatolites: evidence of the Earth's earliest benthos. In: J.W.Schopf (Editor), Earth's Earliest Biosphere: Its Origin and Evolution. Princeton University Press, Princeton, N.J., pp.187-213.

Walter, M.R., Buick, R. and Dunlop, J.S.R., 1980. Stromatolites 3400-3500 Myr old from the North Pole area, Western Australia. Nature, 284: 443-445.

Zumberge, J., 1981. Tricyclic diterpane distributions in the correlation of Paleozoic crude oils from the Williston Basin. In: M.Bjoroy et al., (Editors), Advances in Organic Geochemistry 1981 Wiley, Chichester, pp.738-745.

ISOTOPIC CONSTITUTION OF SULFUR IN THE CONFORMABLE BASE-METAL SULFIDE DEPOSITS IN THE PROTEROZOIC ARAVALLI-DELHI OROGENIC BELT, NW INDIA

M.DEB

ABSTRACT

The isotopic compositions of sulfur in 220 sulfide-mineral separates from 14 conformable Zn-Pb-Cu, Zn-Pb and Cu sulfide-ore deposits/prospects in the Proterozoic Aravalli-Delhi orogenic belt in NW India, are presented. The deposits occur in successive linear belts - Bhilwara, Aravalli and Delhi (from east to west), and are conformable, sediment-hosted and isofacially metamorphosed with their host rocks.

Within the Bhilwara belt, the mean $\delta^{34}S$ is 9.1^{o}/oo in sphalerites from Rampura-Agucha, while in the zoned Dariba deposit $\delta^{34}S$ increases stratigraphically upwards from 1.8^{o}/oo in the foot-wall Cu zone through 2.3^{o}/oo in the Pb-Zn (Ag-As) zone to 7.7^{o}/oo in the hanging-wall Fe zone. The northward extension of this pyrite-pyrrhotite zone at Sindeswar Kalan has a mean value of 2.5^{o}/oo. The ore zone in the Zawar field, within the Aravalli belt, shows sharp variations from an average of 2.2^{o}/oo at Balaria to 6.2^{o}/oo at Mochia Magra and from 0.5^{o}/oo at Baroi Magra to 10.9^{o}/oo at Zawar Mala. In the southern half of the Delhi belt, Ambaji-Deri ores have the heaviest sulfur compositions with an average $\delta^{34}S$ of 18.4^{o}/oo, while Basantgarh ores have an average of 7.2^{o}/oo. In the northern half, along the Khetri Cu belt, there is continuous depletion of ^{34}S southwards: the average $\delta^{34}S$ is 11^{o}/oo at Madan Kudan, through 9.4^{o}/oo at Kolihan to 8^{o}/oo at Chandmari. 50 Km further south at Saladipura the average is 46^{o}/oo.

Sulfur-isotope geothermometry indicates that small-scale (in mm) equilibration/re-equilibration has occurred during metamorphism but primary isotopic variations (in mm-scale) have remained by and large undisturbed. Temperature estimates in the range $64^{o}C$ - $383^{o}C$ probably represent primary equilibration in the exhalative fluids during ore generation. Small and restricted $\Delta^{34}S_{SW-Sulf}$ values between -2.1 and 17.5^{o}/oo in all but one deposit suggest that the ores incorporated mainly reduced sulfur of hydrothermal,

rather than bacteriogenic origin. Contribution from basaltic sulfides to the inorganically reduced seawater sulfate is envisaged for Rampura-Agucha, Rajpura-Dariba and Basantgarh ores, while a bacteriogenic sulfur contribution is apparent in the hanging-wall part of the Dariba deposit and its northward extension at Sindeswar Kalan, in the Zawar ore field, the southern part of the Khetri belt, and particularly at Saladipura. The heaviest sulfur at Ambaji-Deri, with $\delta^{34}S$ > contemporary seawater sulfate, can be best explained by high temperatures (>250°C), near-complete reduction of marine sulfates and a partial contribution from evaporitic sulfates.

INTRODUCTION

The Proterozoic Aravalli-Delhi orogenic belt in NW India is the repository of a considerable number of major base metal sulfide deposits and many occurrences and partially explored prospects. The deposits are generally conformable, sediment-hosted types and are hosted by the supracrustal linear belts of Bhilwara, Aravalli and Delhi. Their locations and regional geologic settings figure in the paper by Sugden et al., (this volume). Several other aspects are discussed by Sharma and A.B.Roy in this volume.

The present contribution reports the isotopic composition of sulfur in 220 mineral separates from 14 ore deposits/prospects in this orogenic belt, evaluates the possible equilibration effects on the original isotopic compositions of these ores during metamorphism, and attempts to trace the probable sources of sulfur in the deposits under consideration and, also, to comment on the depositional environments of these ores. Previous contributions in this direction are that by Deb (1986) dealing with the Rajpura-Dariba deposits in Udaipur district of Rajasthan and by Jaireth (1986) on the Madan Kudan and Kolihan deposits of the Khetri copper belt.

CONFORMABLE BASE-METAL SULFIDE DEPOSITS

Some of the main characteristics of the major base-metal deposits in the region considered in this study are summarised in Table 1. The deposits are generally Zn-Pb-Cu, Zn-Pb and Cu types with ubiquitous Fe, although the Saladipura deposit consists mainly of pyrite-pyrrhotite-rich orebodies (22.5% S) with varying and localised concentrations of Zn. These deposits generally occur

Table 1. Summary of the characteristics of conformable Proterozoic Zn, Pb, Cu deposits in the Aravalli-Delhi orogenic belt, NW India.

Deposit	Host sequence/ belt	Host rocks	Morphology	Associated volcanics	Metamorphic grade	Tectonic setting
Rampura Agucha	Bhilwara belt	Graphite-mica-sillimanite schist within garnet-biotite-sillimanite gneiss; amphibolite, calc-silicate rocks, pegmatite in ore zone; granite gneiss & mylonite.	Long lensoid body, doubly plunging synform	Amphibolites (mafic volcanics)	Upper Amphibolite - granulite 650°C/6Kb	Incipient divergent plate boundary
Rajpura-Dariba	Aravalli equivalent, Bhilwara belt	Impure dolomitic marble, chert, kyanite-staurolite-bearing graphite-mica schist.	Conformable layers inter-bedded with the host rocks; Dariba lode stratiform, lensoid.	Amphibolites (mafic volcanics?) in footwall argillite; tuffaceous layers in graphite mica schist.	Amphibolite 550°/5.4 Kb	-"-
Zawar	Aravalli	Fine-grained dolomite, carbonaceous phyllite	Conformable layers, fracture fillings; massive replacement bodies	None represented	Greenschist	Rifted Aravalli continental margin
Ambaji-Deri	Ajabgarh group Delhi belt	Cordierite-anthophyllite rocks, quartz-chlorite-tremolite schist, diopside-forsterite marble	Lenses and tabular bodies pene-concordant with bedding; minor discordance in massive quartzite	Amphibolites (mafic volcanics); felsic to intermediate plutons.	Greenschist superimposed by hornblende hornfels; 3.4Kb/ 575°C.	Back arc spreading zones
Basantgarh	-"-	Chlorite-muscovite-quartz schists, actinolite-biotite-quartz schist, amphibolite, cordierite-garnet-mica schist, metamorphosed carbonates	Conformable discontinuous bands.	Mafic volcanics	Greenschist facies(?)	Convergent plate boundary
Saladipura	Ajabgarh group Delhi belt.	Massive amphibolite, cordierite amphibolite rock, phyllite, biotite quartzite, carbonaceous phyllite, marble.	Conformable synformal layers with parabolic outcrop.	Amphibolite (basalt tuff ?)	Low P int. facies sr. culminating at 5.5 Kb/ 600°C.	Convergent plate boundary setting
Khetri	Ajabgarh/ Alwar group	Garnetiferous chlorite schist, banded amphibole quartzite, andalusite mica schist, cordierite-anthophyllite rocks.	Conformable lensoid, stratabound	Nearest 50 km S - at Saladipura - amphibolite.	Low P int. facies series 550° - 600°C/ 5.5 kb.	-"-(?+

in close association with mafic metavolcanic rocks and have all been deformed and isofacially metamorphosed along with their enclosing rocks. Except for the Ambaji, Deri and Basantgarh deposits, carbonaceous matter of biogenic derivation (Deb unpubl. data) is present in the ore zone of all deposits. More details of the deposits, considered to be syn-sedimentary in origin, are available in Deb (1982).

SAMPLING AND ANALYTICAL PROCEDURES

All the samples were chosen from the author's collections, built up during his studies in the region since 1970. The Rampura-Agucha samples came mostly from the exploratory adit, while the Dariba main lode samples were all from the underground workings at the 400 mRL (cf. Deb, 1986 for exact locations). Sindeswar Kalan, Ambaji, Deri and Basantgarh samples were all from cores of bore-holes drilled in the prospects by the exploration agencies. In the Khetri belt, the samples from Madan Kudan and Kolihan were collected from underground workings; those of Chandmari from the open-cast mine and the ones from Saladipura, from the exploratory adit.

Separation of sulfide minerals from the samples was carried out by conventional techniques (heavy liquid and Franz isodynamic separator). The separates were further purified by repeated hand picking under a binocular microscope. The purity of the separates was generally greater than 95% as checked in some polished sections. The SO_2 samples for the isotopic analyses were produced in evacuated silica tubes by reaction of the minerals with V_2O_5 at 1000^oC, following the procedure described in Ricke (1964), modified considerably at the isotope laboratories of the Geochemisches Institut at Gottingen.

The isotopic analyses on SO_2 were performed by means of a Finnigan Mat 251 mass spectrometer with a typical accuracy of 0.2%. The isotopic compositions are given in the usual δ notation, the $\delta^{34}S$ relative to the Canon Diablo troilite.

SULFUR ISOTOPE COMPOSITIONS

The $\delta^{34}S$ values of sulfide minerals from the deposits in Bhilwara, Aravalli and Delhi belts, mentioned above, are presented in Table 2, and as histograms in Fig. 1. The mean of sulphur-isotope values for each mineral from a deposit or metal zone, as

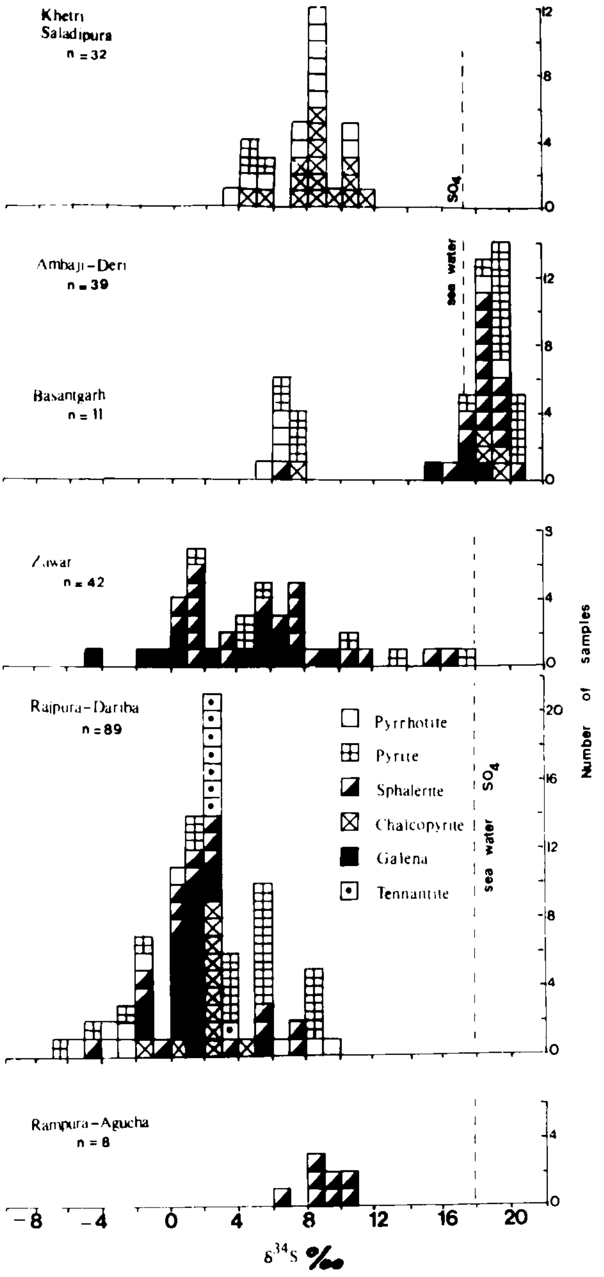

Figure 1. Frequency distribution of sulfur ratios from different mineralized zones in the Aravalli - Delhi orogenic belt, NW India. $\delta^{34}S$ values of seawater sulfate for mid-Proterozoic (18.0°/oo) and upper Proterozoic (17.4°/oo), based on Claypool et al. (1980), are shown as dashed lines.

also the 'weighted' averages for each sample are also indicated in the table. The weighted mean $\delta^{34}S$ of total sulfides in a sample has been calculated starting from a modal volume of sulfides converted to a proportional weight per cent of total weight of sulfides. From this, the proportion of total weight of sulfur in each phase is computed and multiplied by the measured $\delta^{34}S$ to obtain the proportional value in each phase. Their sum is the weighted mean of total sulfides in the sample in question. The average $\delta^{34}S$ of a deposit/zone is based on this weighted mean for multi-phase samples. The isotopic data from the Dariba main lode is presented zone-wise from foot wall to hanging wall. The borehole samples from Sindeswar Kalan, Ambaji and Deri are ordered depthwise. Since all the ores under study are recrystallized and annealed to various degrees, the phases have been chosen not on the basis of any mineral paragenesis, but on their co-existence in the scale of a polished section, lack of fine inclusions and also, the geologic setting of the deposit.

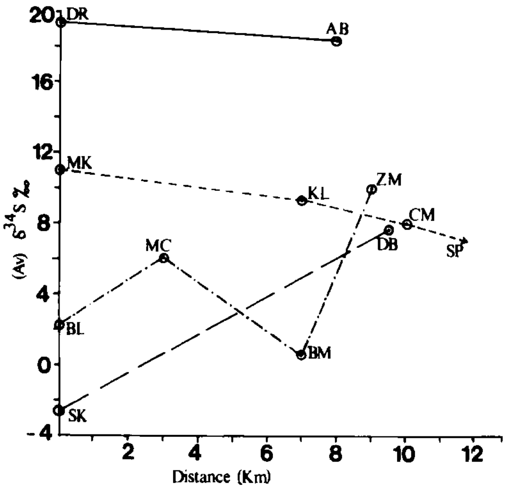

Figure 2. Average $\delta^{34}S$ from deposits in different mineralized zones plotted against distance between them to show lateral variation of sulfur-isotope ratios. Abbreviations: DR=Deri; Ab=Ambaji; MK=Madan Kudan; KL=Kolihan; CM=Chandmari; SP=Saladipura; BL=Balaria; MC=Mochia Magra; BM=Baroi Magra; ZM=Zawar Mala; SK=Sindeswar Kalan; DB=Dariba.

The range of $\delta^{34}S$ values and their mean for each deposit/belt, along with other details of isotopic data, are presented in Table 3. Within the Bhilwara belt, the mean $\delta^{34}S$ of sphalerites from the Rampura-Agucha massive sulfide orebody is $9.1^{o}/oo$. In the Rajpura-Dariba mineralized zone, $\delta^{34}S$ ranges from $9.1^{o}/oo$ to $-6.7^{o}/oo$, with the lighter sulfur compositions (0.9 to $-5.5^{o}/oo$; $x=-2.5^{o}/oo$) concentrated preferentially in the pyrite-pyrrhotite ores in the Sindeswar Kalan prospect to the north (cf. Fig. 2). In the zoned Dariba main lode, mean $\delta^{34}S$ values increase from $1.8^{o}/oo$ in the Cu zone in the footwall through $2.3^{o}/oo$ in the Pb-Zn zone, $4.3^{o}/oo$ in the Ag-As patch to $7.7^{o}/oo$ in the Fe zone in the hanging wall. This picture of stratigraphic dependence of sulfur-isotope compositions is more marked in pyrite, which undergoes a sharp increase in ^{34}S from the Pb-Zn to the Fe zone, than in the other sulfides (Deb., 1986). Similar trends are also apparent in the Sindeswar Kalan ores when $\delta^{34}S$ in pyrrhotite is plotted against borehole depths (Deb, op. cit.). In banded samples from the Dariba mine, monomineralic pyrite and sphalerite separates generally showed maximum variations of only $0.3^{o}/oo$ and $0.5^{o}/oo$, respectively, in $\delta^{34}S$ values. However, in a banded cherty recrystallized siliceous dolostone from the Pb-Zn zone (no. 42, Table 2), with bands of differently coloured sphalerites, a large variation of $10^{o}/oo$ was noted between brown and lemon-yellow sphalerite.

In the Zawar ore field, located within the Aravalli continental margin sediments, the widest range of $\delta^{34}S$ values has been noted from $-4.2^{o}/oo$ in galena at Baroi Magra to $17.2^{o}/oo$ in pyrite at Zawar Mala. Mineralization in dolomite in the four deposits of this field is probably restricted to a single intricately folded band, about 16 km in length. Sulfur-isotopic compositions vary almost periodically from an average $\delta^{34}S$ of $2.2^{o}/oo$ at Balaria to $6.2^{o}/oo$ at Mochia Magra and again from $0.5^{o}/oo$ at Baroi Magra to $10.9^{o}/oo$ at Zawar Mala (Fig. 2). There is no clear picture of stratigraphic dependence of $\delta^{34}S$ values in this field.

In the southern half of the Delhi belt, the polymetallic Ambaji-Deri ores have the heaviest sulfur compositions with an average $\delta^{34}S$ of $18.4^{o}/oo$. In contrast, Basantgarh sulfides in the same region have much lighter sulfur ($\bar{x} = 7.2^{o}/oo$). A faint lateral variation is discernible along the 8 km-long Ambaji-Deri zone (Fig.2) from an average $\delta^{34}S$ value of $17.2^{o}/oo$ at Ambaji to

Table 2. Sulfur-isotope data

Deposit/ zone/ Depth(m)	Sample No.	Remarks	^{34}S(%.)					
			gn	cp	sph	po	py	tn
Rampura-Agucha	SMG1	GS;sph			8.6			
	SMG2	GS;sph			6.9			
	SMG4	GS;sph			8.8			
	DC	GS;sph-gn-aspy			10.1			
	OD 1	GS;sph			8.3			
	OD 2	GS;sph			10.0			
	OD10	GS;sph			9.8			
	OD12	GS;sph			$\bar{x}$=9.1			
Dariba main lode	104	RSD;cp-gn		2.4				
	266	RSD;cp-gn-sph	1.1	2.3				
	259	RSD;cp-gn		0.8				
	26	RSD;orange sph-gn	-1.1		2.3			
Cu	305	Remobilised vein in RSD;coarse cp-gn	1.8	2.8				
	8	RSD;cp-gn	1.2					
	232	RSD;cp-gn-sph	1.6	2.1				
			$\bar{x}$=0.5	$\bar{x}$=2.1				
pb-zn	44	RSD;orange sph-gn-py			0.0		-4.7	
	98	RSD;gn-sph-tn	0.2					2.2
	32	RSD;gn-sph-tn	1.3					2.3
	15	RSD;orange sph-gn			2.8			
	263	RSD;gn-sph-tn	1.6					2.6
	4	RSD;gn-cp-tn-py	0.6	2.5			1.9	2.4
	28	RSD;gn-sph-py	1.4					
	13	RSD;tn-sph-gn						2.3
	52	RSD;tn-gn	0.5					2.3
	27	RSD;gn-sph	1.4					
	30A	RSD;sph-py					-6.7	
	247	RSD;gn-sph	2.7					
	245	RSD;orange sph-gn-py	0.6		1.7		2.0	
	23	Ch rh;orange sph			0.0			
	236	Ch rh;gn-cp-sph	1.3	2.3				
	22	Ch rh;gn-tn-sph	2.4					3.6
	239	RSD;orange sph-gn-cp	0.8	2.1	1.4			
	237	RSD;gn-cp-sph-py	1.7	2.1				
	401/1	Bl ch;sph-py					3.4	
	401/2						3.4	
	401/3						3.4	
	402/1	Bl ch;lemon sph-py			-1.0			
	402/2				-1.0			
	402/3				-1.5			
	409/1	Bl ch;sph-gn-py					5.5	
	409/2						5.6	
	411/1	Bl ch;sph-gn-py					5.5	
	411/2						5.6	
	411/3						5.9	
	413/1	Bl ch;brown sph-py			5.2			
	413/2						5.8	
	414	Bl ch;brown sph-py			3.8		5.6	
	42	RSD-ch;brown sph-py			5.4			
		orange sph-gn	-1.3		0.1			
		lemon sph-py			-4.6			

	231	RSD;gn-cp-sph	0.4	2.1				
	34	RSD;sph-py					3.5	
			$\bar{x}$=1.0	$\bar{x}$=2.3	$\bar{x}$=0.6		$\bar{x}$=2.0	$\bar{x}$=2.5
Ag-As	14	RSD;orange sph-gn			2.3			
	29	Diop.rk;lemon sph-gn			7.1			2.5
Fe	2	GS;brown sph-py			7.6		8.5	
	3	GS;sph-py				6.5		
	202	GS;cp-py		4.7				
	224	GS;gn-py	5.8					
	28A	GS;sph-py					8.5	
	270/1	GS-Bl ch rh;sph-py					8.5	
	270/2						8.8	
	RPD6/5	GS;po				8.9		
	RPD22/8	GS;po				9.1		
						$\bar{x}$=8.2	$\bar{x}$=8.6	
Sindeswar Kalan								
151.2	6/1	GS;banded ore;po-py		-1.8		-2.4		
219	7/1	GS; do ;py-po-sph				-2.1		
280	8/1	GS; do ;py-po-sph				-2.0		
293	8/2	GS; do ;py-po-sph				-3.0	-2.9	
306.9	8/3	GS; do ;py-po-sph				-5.5		
200.8	10/1	GS; do ;po				0.9		
286.8	10/2	GS; do ;po				-3.8		
						x=-2.5		
Mochia	ZMC 2	Dol;gn	2.8					
Magra	ZMC 6	Dol;gn-sph	5.6		7.8			
	ZMC 7	Dol;gn	5.6					
	ZMC 9	Dol;gn	7.1					
	ZMC 17A	Dol;gn	5.4					
	ZMC 18	Dol;sph	4.8		8.4			
	ZMC 20	Dol;gn-sph	6.0		7.7			
			$\bar{x}$=5.3		$\bar{x}$=8.0			
Balaria	BL 2	Dol;sph-py			3.5		4.1	
	BL 4	Dol;sph-gn	0.9		1.3			
	BL 5	Dol;sph-py			0.9			
	BL 6	-do-			0.1		1.7	
	BL 7	-do-			7.1		10.6	
	BL 8	-do-			1.3			
	BL 9	Dol;sph-gn	-0.0		1.7			
	BL 10	-do-	-1.1		1.3			
	BL 11	-do-	0.7		1.3			
			$\bar{x}$=0.1		$\bar{x}$=2.1		$\bar{x}$=5.4	
Zawar-	ZM 4	Dol;sph-py			6.5		6.0	
Mala	ZM 5	Dol;sph-gn-py	9.3		10.7		13.4	
	ZM 12	Dol;sph-py			15.7		17.2	
	ZM 22	Dol;sph-py-gn			16.4			
	ZM 25	Dol;sph-py			7.3		4.4	
	ZM 26	Dol;sph			11.9			
	ZM 27	Dol;sph-gn	6.7		5.1			
			$\bar{x}$=8.0		$\bar{x}$=10.5		$\bar{x}$=10.3	
Baroi	BM 3	Quartzite;sph			2.0			
Magra	BM 6	Quartzite;sph			3.8			
	BM 7	Quartzite;gn banded	-4.2					
					$\bar{x}$=2.9			

Ambaji							
44.5	BH 21/5	imp.marble;sph	15.7		17.1		
45.5	BH 21/6	do			16.6		17.8
74.0	BH 21/7	Qtzite;sph-cp	17.1		18.6		
76.0	BH 21/9	Qtzite;cp		19.3			
93.0	BH 21/10	imp.marble;sph-cp-gn			17.9		
95.5	BH 21/11	do			18.5		19.3
185	BH 21/13	trem.qtz.sch;cp		19.8			
165	BH 87/3	bt.qtz.sch;sph-py	18.2		18.9		19.5
167	BH 87/7	imp.marble;sph-py			18.6		19.7
113.3	BH 22/10	do ;sph-cp-py			18.5		
113.9	BH 22/11	do					18.9
114.7	BH 22/14	do			18.4		
230	BH 22/22	talc trem sch;cp-py					20.0
			$\bar{x}$=17.0	$\bar{x}$=19.5	$\bar{x}$=18.1		$\bar{x}$=19.2
Deri							
54.5	DR 6/5	trem.qtz.sch;sph-py			20.4		20.8
105.0	DR 6/13	amph;cp-po		18.6		18.0	
110.0	DR 6/21	amph;po-cp		18.3			
116.0	DR 6/22	amph;sph-py-po	17.9		18.9	19.2	19.9
29.0	DR 18/7	chl rock;sph-py			20.0		20.6
53.7	DR 18/11	amph;sph-py			19.7		20.0
60.2	DR 18/12	chl rock;sph-py			19.0		19.8
66.7	DR 18/13	chl rock;sph-py			19.3		19.7
73.0	DR 18/14	chl rock;sph-py			19.0		19.8
				$\bar{x}$=18.4	$\bar{x}$=19.5	$\bar{x}$=18.6	$\bar{x}$=20.1
Basant-garh	BG 1/1	bt.qtz.sch;cp-py-po		7.1		6.6	7.6
	BG 1/11	-do- ;py-po				6.4	7.4
	BG 2/1	-do- ;sph-py-po			6.3	6.5	7.6
	BG 2/11	-do- ;py-po					6.9
	BG 2/111	-do-				5.5	6.8
						$\bar{x}$=6.2	$\bar{x}$=7.3
Khetri belt							
Madan	MK 2	amph.chl.qtz.sch;cp-po		11.1		10.9	
Kudan	MK 4	amph.qtz.sch;cp-po		10.9 $\bar{x}$=11.0		10.8 $\bar{x}$=10.85	
Kolihan	KL 1	gar.chl.sch;cp-po		10.2			
	KLB 1	gar.chl.sch;cp-po		8.9			
	KL 2	amph.qtz;cp-po		10.4			
	KLB 1	vq;cp-po		8.8			
	KLB 11	-do-		9.0			
	KLD	amph.qtzite;gar-cp-po				9.0	
				$\bar{x}$=9.5			
Chand-mari	CM 1	amph;cp-po		7.6		7.9	
	CM 3	amph;qtzite;cp-po		7.8		8.6	
	CM 4	-do- ;cp		8.3		8.3	
	CM 5	gar.chl.sch;cp-po		8.1		8.0	
	CM 6	amph;cp-po		8.2		7.4	
	CM 9	-do-		7.6		8.0	
	CM 11	amph.qtzite;cp-po		8.3		8.2	
				$\bar{x}$=8.0		$\bar{x}$=8.1	
Saladi-pura	SP 1	amph;py-po				3.0	4.3
	SP 11	-do-		5.1		4.0	4.2
	SP 111	-do		5.5		5.1	5.7
				$\bar{x}$=5.3		$\bar{x}$=4.1	$\bar{x}$=4.7

Abbreviations: RSD=recrystallised silliceous dolostone; Ch rh=cherty rhythmite; Bl ch=black chert; GS=graphite schist; Dol=dolomite; amph=amphibolite; chl=chlorite; trem=tremolite; gar=garnet; sch=schist; vq=vein quartz; gn=galena; sph=sphalerite; cp=chalcopyrite; po=pyrrhotite; py=pyrite; tn=tennantite.

$19.5^{o}/oo$ at Deri in the north. The trend of stratigraphic variation of isotopic ratios, though not quite so conspicuous, appears dissimilar at Ambaji and Deri. While in boreholes DR 18 and DR 6 at Deri there is a faint increase in $\delta^{34}S$ of the separated sulfides towards the top of the sequence, i.e., at shallower depths, in boreholes BH 21 and 22 at Ambaji, the trend is exactly reversed (cf. Table 2). In the northern half of the Delhis, along the Khetri Cu belt, there is continuous depletion of ^{34}S southwards (Fig.2); average $\delta^{34}S$ is $11^{o}/oo$ at Madan Kudan, through $9.4^{o}/oo$ at Kolihan to $8^{o}/oo$ at Chandmari in the South. 50 km further south at Saladipura, even larger depletions are noted, with average $\delta^{34}S$ of $4.6^{o}/oo$.

METAMORPHIC RE-EQUILIBRATION AND SULFUR ISOTOPE GEOTHERMOMETRY

Since thoroughly metamorphosed sulfides are being considered in this study, it is imperative to ascertain how much redistribution and re-equilibration of sulfur isotopes have taken place during metamorphism. It is possible that in certain cases isotopic variations related to the original source and equilibrium processes may become totally obscured or severely modified by metamorphism, thus invalidating any interpretation regarding the primary process. Indications on the extent of such redistribution/ re-equilibration may be obtained through sulfur isotope geothermometry.

The $\delta^{34}S$ values of sulfide pairs analyzed from different deposits were corrected for the estimated amounts of impurities. However, in the event of undetected fine sulfide impurities in the separates, the fractionation value would give a maximum isotopic temperature. The temperature estimates and uncertainties for sphalerite-galena, pyrite-sphalerite, pyrite-galena and pyrite-pyrrhotite pairs are based on the equations presented by Ohmoto and Rye (1979). Chalcopyrite-galena temperatures were estimated from the curve presented by Nielsen (1979). The spread of the estimated temperatures for the ore zones, along with the range of metamorphic temperatures derived from other sources, are presented graphically in Fig.3. Interestingly, the expected order of enrichment in ^{34}S under equilibrium conditions (Bachinski, 1969): pyrite > pyrrhotite = sphalerite > chalcopyrite > galena, has been observed in all samples with more than one analyzed sulfide, except for two samples each from Dariba main lode and Zawar Mala.

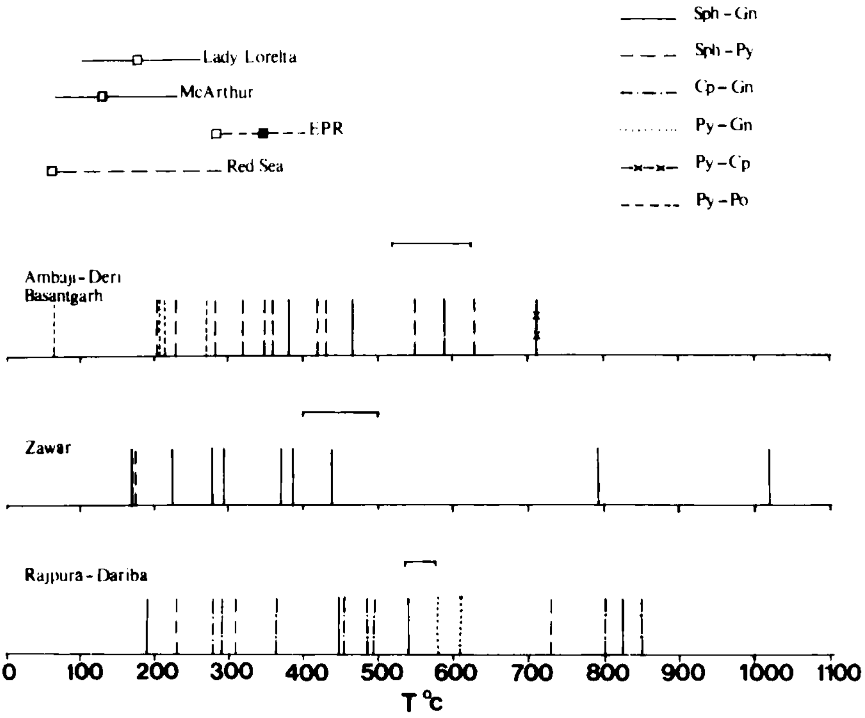

Figure 3. Distribution of temperatures indicated by sulfur-isotope fractionation in samples from Dariba main lode (Rajpura-Dariba belt), Zawar group of deposits and Ambaji-Deri-Basantgarh deposits. For comparison, estimated temperatures of metamorphism of these deposts (see text) are also shown as bars, along with estimated temperatures in two ancient deposits based on sphalerite -galena fractionation (mean as square and range)-McArthur (Smith and Croxford, 1973) and Lady Loretta (Carr and Smith, 1977), as well as temperatures found in modern hydrothermal systems-East Pacific Rise (McDonald et al., 1980) and Red Sea (Shanks and Bischoff, 1980). In these last two locations, black square = vent temperature in sulfide-depositing system and white square = vent temperature in barite + silica-depositing system.

A perusal of the temperature estimates (Fig.3) shows three broadly defined clusters in each of the three ore zones. A low-temperature group ranging from 190°C to 365°C (n=6; $\bar{x}$=278°C) at Rajpura-Dariba; 171°C to 294°C (n=5; $\bar{x}$=229°C) for the Zawar deposits and 64°C to 383°C (n=11; $\bar{x}$=262°C) for the Ambaji-Deri and Basantgarh zones, may represent primary equilibration in the hot hydrothermal fluids, during exhalation. A comparison with the temperature estimates for the two ancient deposits and two modern hydrothermal systems (Fig.3) supports this possibility. The middle range of temperatures at Rajpura-Dariba is represented by 7 sulfide pairs between 447^{o}C and 610^{o}C ($\bar{x}$=516^{o}C) in which at least two pyrite-galena pairs and one sphalerite-galena pair gave temperatures concordant with other estimates of amphibolite-facies temperatures in the zone (Deb and Bhattacharya, 1980). This range at Zawar is between 371^{o}C and 438^{o}C (n=3; $\bar{x}$=398^{o}C), consistent with the conditions of lower greenschist facies metamorphism of the enclosing rocks. In the Ambaji-Deri zone, two sphalerite--galena and 4 sphalerite-pyrite pairs represent the middle range between 423^{o}C and 629^{o}C ($\bar{x}$=515^{o}C). No sample from Basantgarh falls in this range. At least three temperature estimates are concordant with conditions of low-pressure thermal metamorphism (525^{o} - 575^{o}C), worked out for this zone (Deb., 1980). This picture of concordance of some isotopic temperatures with estimates of metamorphic peak temperatures and a spread of values of up to 100^{o}C towards lower temperatures, may indicate incomplete prograde equilibration or partial re-equilibration during metamorphic cooling (cf. Whelan et al., 1984). Unrealistically high temperature estimates were obtained for 4 sulfide pairs at Rajpura-Dariba (730^{o} - 850^{o}C), 2 from Balaria (793^{o}C and 1023^{o}C) in the Zawar ore field and one from Basantgarh (712^{o}C). Along with these temperature estimates, two negative δ^{34}S values each in Rajpura-Dariba and Zawar Mala deposits obviously represent disequilibrium. Further, 10^{o}/oo variations in δ^{34}S between sphalerites of different colours and probably compositions, in different bands of a rhythmite sample in the Dariba main lode, as mentioned earlier, indicate that primary isotopic variations have survived in cm-scale, even under the amphibolite-facies metamorphism of the Rajpura-Dariba ore zone.

These results suggest that small-scale (in mm) equilibration/ re-equilibration of sulfur-isotopic ratios has occurred in all the sulfide deposits in response to metamorphism, but such equilibration has had limited effect on primary isotopic distributions. Therefore, large-scale spatial variations, as well as stratigraphic variations in, sulfur-isotopic compositions described earlier, may be related to kinetic/equilibrium processes in the mineralizing systems and varying sources of sulfur.

SOURCE(S) OF SULFUR AND DEPOSITIONAL ENVIRONMENTS

The foregoing sulfur isotope data and the discussion on metamorphic equilibration, summarised in Table 2, warrant interpretation of the macroscopic variations in isotopic ratios in terms of the source(s) of sulfur in the ore deposits and/or fractionation processes operating in the feeder system or on the sea floor, related to their depositional environments. These two aspects are considered in the following paragraphs in the light of the geological setting of each of the deposits (cf. Table 1). It must, however, be pointed out here that all these stratiform ore deposits are considered to be of exhalative sedimentary origin (Deb, 1982), with the metals derived from upper-crustal sources through seawater hydrothermal circulation. Mixing of the exhaled fluid with marine sulfate would occur at the sea floor, but rapid cooling, dilution and more or less instantaneous precipitation would tend to inhibit significant sulfur-isotope exchange. It is also very likely that substantial mixing of connate or marine waters with the hydrothermal fluid would take place below the sediment-water interface due to percolation of the former, brought about by permeability of the sediments in the vertical direction, into the vent system (cf. Hutchinson et al., 1980). The physico-chemical conditions expected in the simplest mixing situation would include bulk composition, equilibrium temperature and redox conditions. The effects of these conditions in determining the isotopic compositions of sulfur compounds in the vent system may be assessed by mass-balance calculations, proposed by Lusk (1972), and will be considered later in a separate publication.

The two major terrestrial reservoirs of sulfur are the lithosphere (mantle or homogenized crust) and the ocean (seawater sulfate). The sulfur from these reservoirs could be incorporated in sulfide-ore deposits by (1) reduction of seawater sulfate by bacterial action or during geothermal circulation and (2) by mobilization of sulfides contained within basaltic material ($\delta^{34}S=0.01^{o}/oo$; Hubberton, 1983) or evaporitic sediments ($\delta^{34}S >$ seawater sulfate) and (3) by a combination of these processes. The spectrum of $\delta^{34}S$ values observed in ore deposits (cf. Nielsen, 1979), in addition to the source composition and the process of incorporation, is also affected by (1) equilibrium fractionation, involving the partitioning of the minor isotope relative to the major as a function primarily of temperature, along with fS_2, fO_2, pH, salt concentration of fluids, etc. (Ohmoto and Rye, 1979) and (2) kinetic fractionation, which is the result of the relatively faster rate of reaction of the lighter isotope and achieved either by sulfate-reducing bacteria or by inorganic reactions with ferrous minerals or organic-carbon compounds at elevated temperature (Ohmoto and Rye, op.cit.). The $\delta^{34}S$ distribution of biogenic H_2S and related sedimentary sulfides are also controlled by the open or closed nature of the system with respect to SO_4^{2-} and H_2S (or HS^-) (Schwarz and Burnie, 1973).

Sangster (1976) showed that the average $\delta^{34}S$ values of sulfides in a large number of stratabound deposits hosted in marine sedimentary or volcanic rocks world wide are, respectively, about 14°/oo and 17°/oo lower than the $\delta^{34}S$ of the contemporary seawater sulfate. This difference, assuming that for middle-Proterozoic seawater sulfate $\delta^{34}S$ = 18°/oo and for upper-Proterozoic, $\delta^{34}S$ = 17.4°/oo (cf. Claypool et al., 1980 and Fig. 1), is also presented for all the deposits under consideration (Table 3). Small and restricted $\delta^{34}S$ seawater sulfate-sulfide values of between - 2.1 and 17.5°/oo (except 20.5°/oo at Sindeswar Kalan) indicate that much of the mineralization in NW India incorporated reduced sulfur of hydrothermal rather than bacterial origin (cf. Willan and Coleman, 1983).

The Rampura-Agucha and Rajpura-Dariba deposits (particularly the Dariba main lode), appear to have had similar sources of metals and sulfur as well as depositional environments because of the similarity of their tectonic settings within the Bhilwara belt, their occurrence as lenticular bodies of massive sulfides in close association with graphite schists with high content of C_{org} of biogenic derivation (cf. Deb, 1986; Deb, unpubl. data) and almost identical Pb -isotope ratios and age (Deb et al., under publ.). The isotopic compositions of sulfur in the Dariba main lode have been treated exhaustively by Deb (1986) and interpreted in terms of a dual process: the footwall Cu and the overlying Pb-Zn (Ag-As) zones incorporated inorganically reduced sulfur, derived from convective seawater and partly from basaltic sulfides while the hanging-wall pyrite-pyrrhotite zone, extending northwards into the Sindeswar Kalan prospect, formed diagenetically in anoxic sediments with the sulfur supplied by bacterial reduction of marine sulfate in a system closed to SO_4^{2-}. The Rampura-Agucha

Table 3. Sulfur isotope fractionations and isotopic temperatures

Deposit/ Sample No.	$\Delta^{34}S\%$ (T°C)* cp-gn	sph-gn	py-sph	py-gn	py-po
Dariba					
266	1.2(493±20)				
26		3.4(190±15)			
305	1.1(453±15)				
232	0.5(803±25)				
44			-4.7(diseq)		
4	1.9(280±10)			1.3(610+40)	
245		1.1(540±25)	0.3(730+70)	1.4(580+35)	
236	1.0(490±15)				
239	1.4(365±15)	0.6(825±40)			
237	0.42(850±30)				
413			1.2(230+35)		
42		1.4(447±25)			
231	1.75(293±10)				
2			0.9(310+40)		
Mochia Magra					
ZMC 6		2.24(294±20)			
ZMC 18		3.58(177±15)			
ZMC 20		1.66(386±25)			
Balaria					
BL 4		0.43(1023±40)			
BL 9		1.74(371±25)			
BL 10		2.38(278±20)			
BL 11		0.64(793±35)			
Zawar Mala					
ZM 4			-0.5(diseq)		
ZM 5		1.43(438±30)		4.12(224±20)	
ZM 12			1.54(171±30)		
ZM 27		-1.64(diseq)			
Ambaji					
BH21/5		1.33(466±35)			
BH21/6			1.19(231±35)		
BH21/7		1.68(383±25)			
BH21/11			0.98(283±40)		
BH87/3		0.97(590±35)	0.61(432±50)		
BH87/7			0.86(320±40)		
Deri					
DR 18/7			0.63(423±50)		
DR 18/11			0.37(629±65)		
DR 18/12			0.80(345±40)		
DR 18/13			0.45(548±60)		
DR 18/14			0.75(360±45)		
Basantgarh					
BG1/1					1.03(271±40)
BG1/11					1.33(205±35)
BG2/1			1.28(204±30)		1.29(214±30)
BG2/111					2.66 (64±25)

Sample No. 4 py-cp = -0.6(diseq)
BG1/1 py-cp = 0.46(712±60)

* corrected for impurity wherever necessary.

mean $\delta^{34}S$ in sphalerite, though based on inadequate data, is 9.1°/oo - much heavier than the isotopic values noted in the Cu and Pb-Zn (Ag-As) zones at Dariba. The Rampura-Agucha orebody probably records the profuse influx of metalliferous fluids in a proximal palaeo-trough from which rapidly precipitated sulfides incorporated relatively 'undiluted' hydrothermal sulfur. This sulfur probably originated, at least partially, from a higher degree of inorganic reduction of seawater sulfate at similar high temperatures (~250°C). A partial contribution of basaltic sulfur from abundant tholeiitic sills in the footwall of the mineralization cannot be ruled out either.

In the Zawar ore field, the 16km-long ore-bearing horizon is characterised by strongly variable sulfur-isotopic compositions in different sectors. Sulfides in this field also show the maximum range of isotopic compositions noted in this study: from -4.2°/oo to 17.5°/oo. The $\Delta^{34}S_{SW - Sulf}$ values range from 7.1°/oo at Zawar Mala through 11.8°/oo at Mochia Magra, 15.8°/oo at Balaria to 17.5°/oo at Baroi Magra. Based on these small and restricted values of $\Delta^{34}S$, on the one hand, and the large range of $\delta^{34}S$ values, very light sulfur in sulfides from Balaria and Baroi Magra, and the biogenically derived organic carbon in ore zone phyllites (Deb, unpubl. data), on the other, a dual hydrothermal and bacteriogenic source of sulfur is envisaged. Lack of any clear picture of stratigraphic variation of $\delta^{34}S$ does not support a restricted basin model for the heavier sulfur at Zawar Mala and Mochia Magra. Instead, it is proposed that these high-grade ores formed rapidly in relatively proximal facies from considerably reduced hydrothermal solutions which failed to be diluted by basinal seawater undergoing bacterial sulfate reduction, as in the Balaria and Baroi Magra sectors.

The upper-Proterozoic polymetallic sulfide deposits at Ambaji-Deri and Basantgarh in the southernmost part of the Delhi belt show a strong bimodal distribution of $\delta^{34}S$ values (cf. Fig. 1)-an average of 18.4°/oo for Ambaji-Deri and 7.2°/oo for Basantgarh. $\Delta^{34}S_{SW - Sulf}$ values are -1.0°/oo for the former and 10.2°/oo for the latter. In both the occurrences, the stratiform sulfide ores are hosted by pockets and bands of metasediments enclosed by extensive, metamorphosed mafic volcanic flows. According to recent studies by Deb et al. (in prep.), the Ambaji-Deri volcanics show characteristics of back-arc tholeiites, while the pillowed and massive volcanics from Basantgarh display geochemical features of island-arc tholeiites. These differences and similarities suggest that the sulfur-isotopic compositions reflect a variation in source and/or evolution of the sulfur. The $\delta^{34}S$ values indicate a hydrothermal source of sulfur in both zones. At Ambaji-Deri the very high $\delta^{34}S$ of sulfides is highly suggestive of seawater sulfate having undergone a high degree of reduction of H_2S at temperatures > 250°C by reaction with ferrous components in rocks during its circulation through the hot mafic volcanics (cf. Mottl et al., 1979). Ohmoto and Rye (1979, p.543) have shown that in this temperature range, isotopic equilibrium is probably established between SO_4^{2-} and H_2S in the circulating fluid system and seawater with a $\delta^{34}S$ value of 20°/oo can produce H_2S between 20°/oo and -5°/oo, depending on the degree of reduction. $\delta^{34}S$ values of sulfides greater than that of contemporary seawater sulfate (i.e., 17.4°/oo; cf. Claypool et al., 1980) at Ambaji-Deri can be best explained by a partial contribution from evaporitic sulfate solutions in the small, rift-related back-arc basins which have undergone total reduction during high-temperature convective circulation (cf. Ripley and Ohmoto, 1977).

The lighter sulfur in Basantgarh sulfides suggests several possibilities : (a) only partial reduction of the seawater sulfate; (b) modification of highly reduced seawater by leaching of sulfur from the tholeiitic pile underneath; (c) contribution of sulfur to the ore-forming seawater from deep-seated sources. It is probable that more than one of the above possibilities provided the source of sulfur in the Basantgarh ores.

In the northern half of the Delhis, along the Khetri Cu belt and Saladipura pyrite - pyrrhotite deposit 50 km to its south, the $\Delta^{34}S_{SW-Sulf}$ values for each of the deposits (Table 3) indicate a dominant hydrothermal source of the sulfur. Jaireth (1986), on the basis of an analysis of log a_{O2} -log a_{S2} at 350°C, following the procedure of Ohmoto (1972), suggests that a hydrothermal fluid with $\delta^{34}S$ values lying between 3 and 5°/oo can best explain the sulfur-isotopic compositions noted by him in 14 chalcopyrite and 4 pyrrhotite samples from Madan Kudan and Kolihan. According to him, such fluid compositions can be largely derived from igneous sources, either as magmatic fluids or dissolution of igneous sulfides and raises doubts about the validity of the syn-sedimentary - metamorphosed model proposed for this deposit by Sarkar and Dasgupta (1980). In the first instance, the absence of pre/synchronous volcanics in the Khetri belt precludes derivation of the sulfur in the ore fluids from igneous sulfides, while the features explicitly documented by Sarkar and Dasgupta (op. cit.), makes the model of classical hydrothermal ore generation in this belt untenable. Further, the widely documented and accepted process of generation of submarine exhalative ore deposits (cf.e.g., Fryer and Hutchinson, 1976; Finlow-Bates, 1980 amongst many others), in which hydrothermal fluids emanating on the sea floor produce stratifrom, syngenetic orebodies, appears to have been overlooked. In this regard, comparable to many ancient (cf. Anger et al., 1966 amongst others) and modern hydrothermal systems (cf. Francheteau et al., 1979 amongst others), the hydrothermal fluid which deposited the syn-sedimentary ores along the Khetri belt should be viewed as complementary and *not* contradictory aspects of the total ore-forming process.

The gradual lateral variation in sulfur composition in the belt, turning lighter southward, and becoming considerably light at Saladipura, may be explained satisfactorily by an increasing contribution of bacteriogenic sulfur to the seawater hydrothermal source. Though no data on stratigraphic variation are available, the biogenic organic carbon along the belt, particularly at Saladipura (Deb, unpubl. data), may suggest a higher degree of restriction of the basin southwards.

ACKNOWLEDGEMENTS

The analytical work for this contribution was carried out in the Geochemisches Institut, Gottingen, during the tenure of an Alexander von Humboldt Stiftung Fellowship. The author thanks the Foundation for this grant. The author is indebted to Prof. K.H. Wedepohl for making all facilities at the Institute available to him and to Prof. J. Hoefs and Dr. Nielsen for their interest. Ms Uma Sehgal gave invaluable assistance during the initial stages of mineral separation. The author wishes to record his appreciation for the continued cooperation offered by Hindustan Zinc Ltd., and Hindustan Copper Ltd., both Govt. undertakings, over the years which made collection of samples from their properties possible.

REFERENCES

Anger, G., Nielsen, H., Puchelt, H. and Ricke, W., 1966. Sulfur isotopes in the Rammelsberg ore deposit (Germany). Econ. Geol., 61: 511-536.

Bachinski, D.J., 1969. Bond strength and isotopic fractionation in coexisting sulfides. Econ. Geol., 64: 56-65.

Carr, G.R. and Smith, J.W., 1977. A comparative isotopic study of the Lady Loretta zinc-lead-silver deposit. Mineral. Deposita, 12: 105-110.

Claypool., G.E., Holser, W.T., Kaplan, I.R. and Zak, 1., 1980. The age curve of sulfur and oxygen isotopes in marine sulfate and their mutual interpretation. Chem. Geol., 28: 199-260.

Deb, M., 1980. Genesis and metamorphism of two stratiform massive sulfide deposits at Ambaji and Deri in the Precambrian of western India. Econ. Geol., 75: 572-591.

Deb, M., 1982. Crustal evolution and Precambrian metallogenesis in western India. Rev. Bras. de Geol., 12: 94-104.

Deb, M., 1986. Sulfur and carbon isotope compositions in the stratiform Zn-Pb-Cu sulfide deposits of the Rajpura-Dariba belt, Rajasthan, NW India: a model of ore genesis. Mineral. Deposita, 21: 313-321.

Deb, M. and Bhattacharya, A.K., 1980. Geological setting and conditions of metamorphism of Rajpura-Dariba polymetallic ore deposits, Rajasthan, India. Proc. V. IAGOD symposium, Snowbird, U.S.A.: Schweizerbartsche Verlagsbuchhandlung, Stuttgart, 679-697.

Deb, M., Thorpe, R.I., Cumming, G.L. and Wagner, P.A., (in press) Lead isotope study of conformable sediment-hosted base metal sulfide deposits in the Proterozoic Aravalli-Delhi orogenic belt, N.W. India. Precamb. Res.

Deb. M., Sugden, T. and Windley, B.F., (in prep.). Geochemistry of meta-volcanic amphibolites in relation to tectonic setting in the Proterozoic Aravalli-Delhi orogenic belt, NW India.

Finlow-Bates, T., 1980. The chemical and physical controls on the genesis of submarine exhalative orebodies and their implications for formulating exploration concepts. A review. Geol. Jb. 40: 131-168.

Francheteau, J. et al., 1979. Massive deep sea sulfide ore deposits discovered on the East Pacific Rise. Nature, 277: 523-528.

Fryer, B.J. and Hutchinson, R.W., 1976. Generation of metal deposits on the sea floor. Canad. J. Earth Sci., 13: 126-135.

Hubberton, H.W., 1983. Sulfur content and sulfur isotopes of basalts from Costa Rica rift (Hole 504B, DSDP Legs 69 and 70). Init. Repts. DSDP 69: 629-635.

Hutchinson, R.W., Fyfe, W.S. and Kerrich, R., 1980. Deep fluid penetration and ore deposition. Minerals Sci. Eng., 12: 107-120.

Jaireth, S., 1986. Igneous source of sulfur from Madhan Kudhan and Kolihan deposits, Khetri copper belt, Rajasthan, J. Geol. Soc. India, 27: 359-368.

Lusk, J., 1972. Examination of volcanic-exhalative and biogenic origins for sulfur in the stratiform massive sulfide deposits of New Brunswick. Econ. Geol., 67: 169-183.

McDonald, K.C., Becker, K., Spiess, F.N., and Ballard, R.D., 1980. Hydrothermal heat flux of the "black smoker" vents on the East Pacific Rise. Earth Planet. Sci. Lett., 48: 1-7.

Mottl, M.J., Holland, H.D. and Corr, R.F., 1979. Chemical exchange during alteration of basalt by sea water-II. Experimental results for Fe, Mn and sulfur species. Geochim. Cosmochim. Acta, 43: 869-884.

Neilsen, H., 1979. Sulfur isotopes. In: E. Jager, and J.C. Hunzicker, (Editors), Lectures in isotope geology. Springer, Berlin-Heidelberg-New York, pp.283-312.

Ohmoto, H., 1972. Systematics of sulfur and carbon isotopes in hyderothermal ore deposits. Econ. Geol., 67: 551-578.

Ohmoto, H. and Rye, R.O., 1979. Isotopes of sulfur and carbon. In: H.L. Barnes, (Editor), Geochemistry of hydrothermal ore deposits (Barnes, 2nd Ed.), Wiley, pp.509-567.

Ricke, W., 1964. Preparation von Scwefeldioxid zur massenspektrometrischen Bestimmung des S-Isotopenverhaltnisses in natur lichen S-Verbingungen. Z. Anal. Chem., 199:401.

Ripley, E.M. and Ohmoto, H., 1977. Mineralogic, sulfur isotope, and fluid inclusion study of the stratabound copper deposits at the Raul mine Peru. Econ. Geol., 72: 1017-1041.

Sangster, D.F., 1976. Sulfur and lead isotopes in strata bound deposits. In: K.H. Wolf, (Editor), Handbook of stratabound and stratiform ore deposits , Elsevier, Amsterdam, pp.219-266.

Sarkar, S.C. and Dasgupta, S., 1980. Geologic setting, genesis and transformation of sulfide deposits in the northern part of Khetri copper belt, Rajasthan, India - an outline. Mineral. Deposita, 15: 117-137.

Schwarcz, H.P. and Burnie, S.W., 1973. Influence of sedimentary environments on sulfur isotope ratios in clastic rocks: a review. Mineral. Deposita, 8: 264-277.

Shanks, W.C. III and Bischoff, J.L., 1980. Geochemistry, sulfur isotope composition, and accumulation rates of Red Sea geothermal deposits. Econ. Geol., 75: 445-459.

Smith, J.W. and Croxford, N.J.W., 1973. Sulfur isotope ratios in the McArthur lead-zinc-silver deposit. Nature, 245: 10-12.

Whelan, J.R., Rye, R.O. and De Lorraine., 1984. The Balamat-Edwards zinc-lead deposits - syn-sedimentary ores from Missi-ssipi valley type fluids. Econ. Geol., 79: 239-265.

Willan, R.C.R. and Coleman, M.L., 1983. Sulfur isotope study of the Aberfeldy barite, zinc, lead deposit and minor sulfide mineralization in the Dalradian metamorphic terrain, Scotland. Econ. Geol., 78: 1619-1656.

This Page Intentionally Left Blank

LITHIUM PEGMATITES OF AMARESHWAR, RAICHUR DISTRICT, KARNATAKA, INDIA

T.C.DEVARAJU, N.RAJSHEKHAR, C.SRIKANTAPPA, S.D.KHANADALI AND G.SUBBA RAO.

ABSTRACT

Lithium pegmatites of Amareshwar occur as thin, tabular to lensoid discordant intrusions within Precambrian banded amphibolites in a narrow zone of 0.25X2.5 km, peripheral to granitic intrusions. They are largely unzoned composite intrusions, with units of contrasting texture and grain size, which have formed through sequential injection at two or more periods. Mineralogically, the pegmatites contain on an average 26% spodumene (Li_2O 6.95%, 1.14% Fe_2O_3), 35% quartz, 24% plagioclase (An_{2-8} and An_{25-32}),13% K-feldspar (with 6352 to 8382 ppm Rb) and 1% muscovite (~0.6% Li_2O). Garnet (52.8% alm., 44.3% spess) and gahnite (38.6% ZnO, 5.1% FeO) are the most common accessory minerals. An examination of the fluid inclusions in quartz has revealed that they are moderately to highly saline, with densities of 0.900 to 0.970 g/cm^3. Chemically, the Amareshwar Li pegmatites contain 0.13-6.42% Li_2O and are characterized by high Na_2O : K_2O ratios (3.7 : 2.12), strong enrichment in Rb (1563 ppm), Be (29 ppm), Nb (41 ppm), Ga (67 ppm) and Pb (28 ppm), a marked depletion in Sr (22 ppm), Cu (26 ppm), Ni (<1 ppm) and Zr (24 ppm) and a near absence of Ba. The pegmatites have formed from Li-rich residual fractions derived through fractional crystallization of granitic magma. The fluid-inclusion data suggest their formation at temperatures between 250° and 400°C and pressures of 4 to 5 kbar.

INTRODUCTION

India meets her requirements for Li and its compounds through imports. Although there have been a few reports of Li mineral occurrences (Bhola, 1971), the only case of possible commercial significance was described for the first time from the present study area by Sadashivaiah et al., (1980). The Amareshwar area is about 14 km west of the Hutti Gold Mines in Raichur District, Karnataka State. The area was first mapped by Mukherjee et al., (1934). Sadashivaiah et al., (1980) gave an account of the spodumene pegmatite occurrence. Narasimha and Hans (1983) have published geological and structural maps of the area.

GENERAL GEOLOGY

The main lithological units of the area comprise a sequence of schistose rocks (talc-tremolite schists, amphibolites), banded ferruginous cherts, granitoids (biotite and hornblende-bearing gneisses, pink porphyritic granites), diorites, lithium pegmatites and dolerite dykes (Table 1). These have been involved in at least two periods of folding and metamorphism. The granitoids are intrusive into schists and evidence of their interaction with the schistose rocks and amphibolites is common. The schistose rocks of the area bear evidence of metamorphism corresponding to middle amphibolite facies.

Table 1.
Stratigraphic succession and lithium contents of Amareshwar rocks

Dolerites	(17/4)*
Li Pegmatites	(2.42/26)
Diorites	(16/9)
Granites	(12/5)
Banded ferruginous quartzites	(3/6)
Amphibolites	(19/7)
Talc - tremolite schist	(4/3)

*Numbers given in parentheses refer respectively to the average lithium content (in ppm) and to the number of individual analyses of the rocks. In the case of Li pegmatites, the Li content is in Wt.%

FIELD DESCRIPTION

The Li pegmatites occur as thin tabular to lensoid and dyke-like intrusions. These are restricted to a narrow zone of about 0.25X2.5 km and are emplaced within amphibolites (Fig.1). In all, sixteen pegmatite bodies have been identified (Fig.2). These generally vary in thickness from less than 10 cm to about 4m and in strike length from 30 to 100m. However, the thickest body measures 9.5m across and the longest body is picked up continuously for 0.75 km. Tapering of the individual bodies at one or either ends is usual; pinching and swelling are also common. The bodies strike N 5^{o} to 35^{o} E, i.e., nearly parallel to the

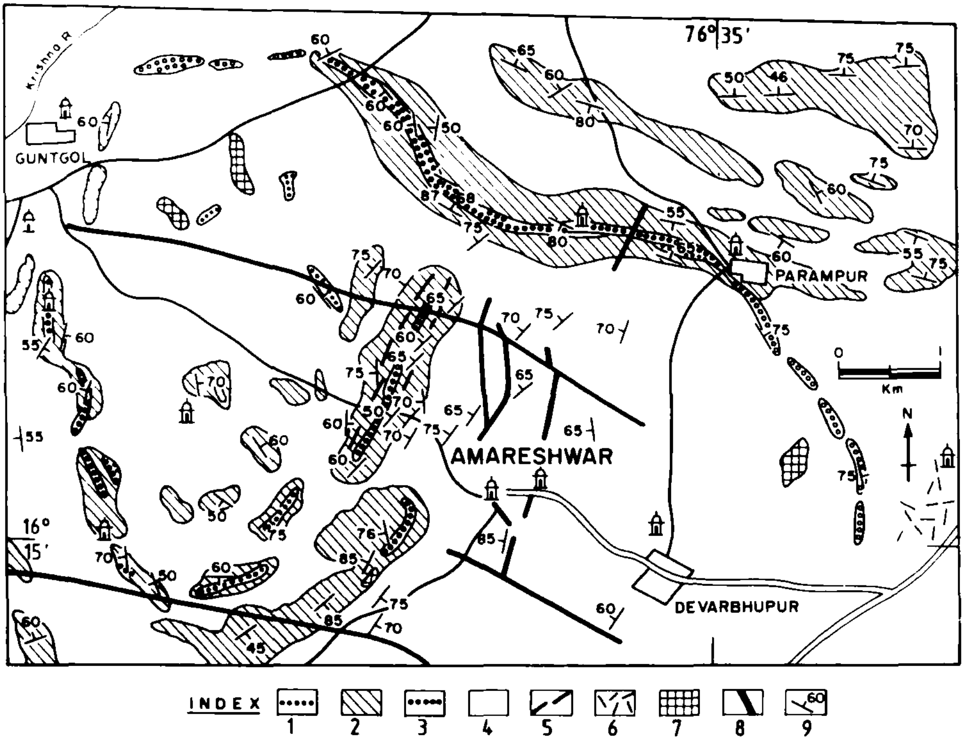

Figure 1. Geological map of Amareshwar. Note the restricted occurrence of spodumene pegmatites in the amphibolite body to the NW of Amareshwar. 1. Altered talcose ultramafics. 2. Amphibolites. 3. Banded ferruginous cherts. 4. Gneisses. 5. Spodumene pegmatite. 6. Granite. 7. Diorite. 8. Dolerite. 9. Banding/Foliation.

contact between the amphibolite and the gneiss, and dip at steep angles to the west. The said field disposition of Li pegmatites may be compared with that of the host amphibolite banding which strikes N 31° E to 43° E and dips 50 - 70° west. The contacts are sharp , no metamorphic effect or metasomatism is recognisable at the contacts of the Li-pegmatite intrusions. The amphibolite is well banded on mm to cm scale, shows whitish quartzose permeations that generally follow the banding. It is essentially composed of hornblende, epidote, plagioclase, clinopyroxene; garnet assumes importance only locally.

The Li pegmatites of Amareshwar are essentially unzoned and what looks like zoning or what earlier has been described as zoning/crude zoning structures (Rajshekhar,1983) is actually the

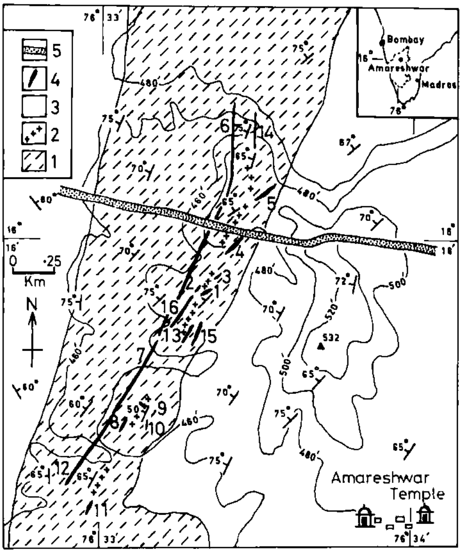

Figure 2. Geological map showing the occurrence of spodumene pegmatite intrusions. Note the location of intrusions close to the contact of amphibolite with the granitic gneiss, and parallel to sub-parallel orientation of most pegmatite intrusions with reference to the contact. 1. Banded amphibolite, 2. Banded ferruginous chert, 3. Granitic gneiss (tonalitic), 4. Spodumene pegmatite and 5. Dolerite. Numbers 1 to 16 refer to the individual lithium pegmatite bodies studied and also to the samples collected from them.

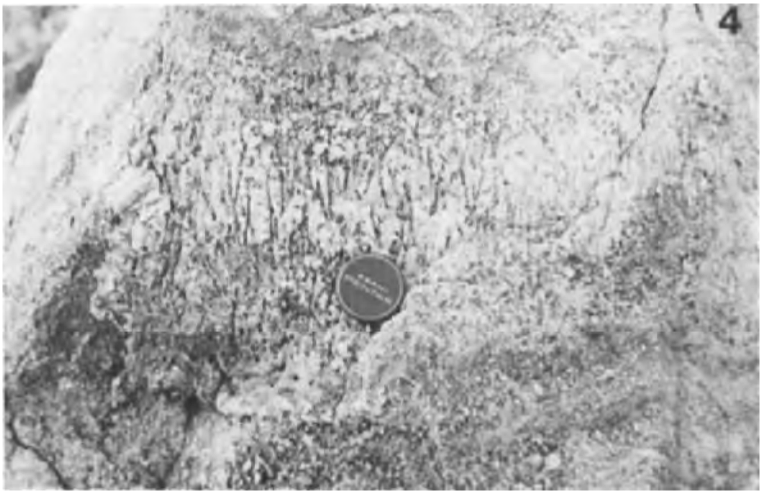

Figure 3. Comb structure exhibited by the long prisms/blades of spodumene occurring in the late-formed, coarse-grained units of the pegmatite intrusions.

composite intrusive character, which is related to the formation of these intrusions by accretion through sequential injection of pegmatitic fluid at two or more periods,separated by a time interval, which in most cases was sufficient to permit crystallization of the pre-existing intrusion. The dykes may thus be described as 'composites' consisting of non-zoned units of contrasting texture and grain size (Fig.3), but with essentially the same mineralogy; spodumene in particular being present nearly from wall to wall. In what look like zoned pegmatite bodies, there are narrow but very coarse-grained and approximately centrally located late-formed units showing near conformable field relations. These coarse--grained units display diffused and ill-defined borders with the older 'fine'-grained units and contain elongated spodumene crystals (these may measure up to 6 cm) that are oriented normal (or nearly so) to the pegmatite borders and these display 'comb' structure. The comb structure is also strongly exhibited by K--feldspar megacrysts of dyke No. 15 (Fig.2). Apart from the foregoing, a couple of dykes contain narrow core zones of white to grey massive quartz.

Based on outcrop measurement and assuming a conservative 8 meter downward extension, it is inferred that there exist in the area approximately 60,000 tonnes of Li-pegmatite analysing on average 2.42% Li_2O.

PETROGRAPHY

The Li pegmatites of Amareshwar are light-green to almost white in colour. The grain size of the minerals varies from mm to cm, even within the limits of individual units of pegmatite bodies. Except dyke No.15 (Fig.2), which contains a high proportion of K-feldspar megacrysts, all other dykes are fine- to very coarse--grained intrusions with only sporadically distributed but distinctly large megacrysts of K-feldspar. Most of the thicker dykes are, however, predominantly more fine-grained than the typical pegmatites.

In thin section, nearly all the bodies appear porphyritic with phenocrysts of spodumene (Fig.4), quartz and sometimes even plagioclase, in addition to K-feldspar. With the exception of spodumene, garnet and gahnite, which tend to form subhedral to euhedral crystals, the rest of the minerals occur as anhedral crystals; plagioclase forms typical laths. Peripheral granulation

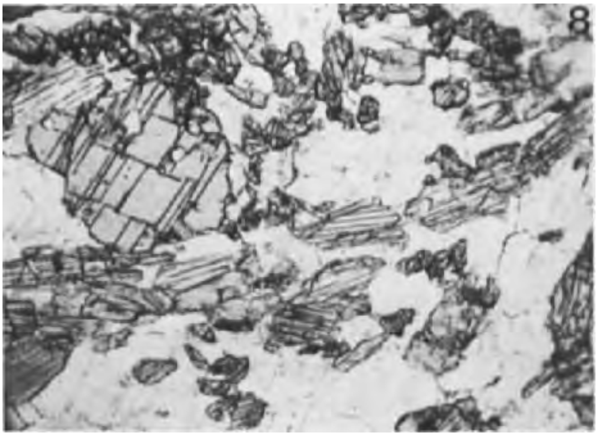

Figure 4. Photomicrograph of a spodumene-enriched pegmatite. Note the occurrence of spodumene in larger and smaller grains and also mineral lineation. Ordinary light, 32 X.

of the phenocrysts is a common feature. The K-feldspar and also quartz phenocrysts frequently bear inclusions of the matrix minerals and show evidence of having grown, pushing aside the matrix material, which was at least partly crystalline when the phenocrysts formed. The commonly observed irregular and gradational contacts between K-feldspar megacrysts and the fine-grained groundmass are consistent with either its simultaneous crystallization or its later formation by replacement of the fine-grained matrix. Plagioclase consistently forms smaller laths and it is the most abundant mineral of the matrix material. It far exceeds K-feldspar in abundance. Crushing effects and strong undulose extinction displayed by quartz and plagioclase, and the patchy/irregular twinning as well as bending/dislocation of plagioclase twin lamallae, bear evidence of post-crystallization deformation of the pegmatite formation. Reacted and resorbed borders of spodumene and muscovite are common. So also is the patchy saussuritization/sericitization of feldspars and alteration of spodumene localized to borders and fracture planes. Leaving aside portions of individual dykes displaying comb structure, a general linear orientation of matrix and phenocryst minerals parallel to pegmatite contacts is noted.

MINERALOGY

The mineralogy of Amareshwar Li pegmatites is relatively simple, with only spodumene, quartz, plagioclase, K-feldspar and muscovite making up nearly 98% or more of the individual bodies. Garnet and gahnite are common accessories. Apatite, sphene, zircon, epidote and iron oxide are occasionally recorded in traces. While beryl occurs only in Be-enriched pegmatite bodies, graphite and biotite are rare (Table 2).

Spodumene averages 24% of the mode (Table 2), although locally abnormal concentrations up to 53% are noted. It occurs as narrow prisms/laths (length to breadth ratio 13:1), ranging in size from 1.1 to 4.5 mm; as short, almost equant crystals (0.2 to .08mm) and as oriented needle/rod-like inclusions in quartz. On weathered surfaces, the mineral shows up distinctly with its rusty brown colour. Fresh surfaces appear bright semi-translucent and predominently light green in colour, comparable to hiddenite.

In thin section, spodumene is colourless to light brown and very weakly pleochroic. It is generally fresh, but border areas of individual crystals are commonly altered to a grey turbid substance, which usually consists of a very fine myrmekite-like intergrowth between spodumene and quartz and/or albite wrapped up with clayey matter. Besides, spodumene crystals are seen to contain (i) small, generally discontinuous quartz blebs, in irregular sieve-like patterns, and (ii) vermicular/graphic quartz intergrowths characteristically developed in the border areas of the individual crystals. The mineral is altered (or replaced) along grain boundaries and parting planes to fine-grained aggregates of quartz (and albite) and micaceous mineral and to a brownish chlorite-like (?) substance.

Chemically, (Table 3) the Amareshwar spodumene is characterised by a limited lithia range (6.8 to 7.15%) and high Mn, Rb and Be; it is of 'high-iron' type (see Deer et al., 1962; Heinrich, 1975; Norton, 1982)

Quartz, occurring as blebs and intergrowths in spodumene and other minerals, ranges in size from .005 to .003 mm, that filling the interstices of the matrix is 0.6 to .08 mm and that forming phenocrysts is 4.4 to 1.5 mm. The first type is glassy, clear and shows very little undulose extinction, the 2nd and 3rd types are almost always loaded with abundant grey dusty inclusions, show anhedral to subhedral boundaries, and display strong undulose extinction.

Table 2.

Modal analysis of spodumene pegmatites

	H1	RA47	H12	RA132	RA97	H7	H115	RA45	H9
	1	2	3	4	5	6	7	8	9
Spodumene	53	52	47	43	42	23	21	18	14
Quartz	30	24	40	47	36	38	44	31	39
Plagioclase	10	10	8	7	16	19	15	34	23
K-feldspar	7	12	5	2	6	20	20	17	21
Muscovite		2							3
Garnet	X	X	X	X	X	X	X	X	X
Gahnite		X		X					X
Apatite						X			
Sphene								X	
Zircon						X			
Epidote									
Biotite									
Graphite		X							
Iron oxide							X		
Beryl				X					

	RA95	RA29	RA90	RA31	H8	1	115	7	9	
	10	11	12	13	14	15	16	17	18	Average
Spodumene	8	8	3	1	1	54	30	29	15	26
Quartz	32	40	38	47	29	19	40	23	36	35
Plagioclase	32	26	34	29	48	20	22	38	40	24
K-feldspar	26	23	24	18	17	4	6	6	7	13
Muscovite		2		5		3*	2*	4*	2*	2*
Garnet	2	1	1	X	X					
Gahnite		X		X						
Apatite										
Sphene										
Zircon										
Epidote					X					
Biotite					X					
Graphite										
Iron oxide										
Beryl					X					

X = occurs as accessory mineral; AV = Average of 1 to 18
* = also includes, garnet and other accessories. Analyses 15 to 18 after Sadashivaiah et al., (1980).

Plagioclase occurs as coarse, subhedral, elongated plates forming smaller phenocrysts (1.1 to .22 mm) and as aggregates of smaller laths (.05 to .01 mm) forming the groundmass mosaic. The larger plates, essentially of oligoclase (An_{23-32}) composition, display sutured borders, strong undulose extinction, frequent bending and dislocation of twin lamellae, patchy saussuritization, antiperthitic character and evidence of replacement by K-feldspar and quartz. The smaller plagioclase laths, on the other hand, are albitic (An_{2-8}), fresh or only locally altered, either twinned or untwinned and show much less evidence of stress effects.

K-feldspar ($2V_z$= 95-107^o) occurs as interstitial patches (.1 to .02 mm) in the matrix and also as large (2.1 to .4 mm) sporadically distributed megacrysts, except in dyke No.15. While the former is more frequently cross-hatched microcline, the latter is partly microcline and partly perthitic (string type) orthoclase. The variation from orthoclase perthite to microcline is often noted within the limits of a single megacryst. The borders of the megacrysts are usually irregular and perforated with inclusions of quartz and plagioclase.

XRF analysis of 3 megacryst K-feldspar samples (Table 3) has shown that these are 91.2 to 82.5 Or and 8.8 to 17.5 Ab and are devoid of An component. A distinctive chemical feature of Amareshwar K-feldspars is their consistently high Rb content (6852 to 8352 ppm), which is much higher than the range reported for K-feldspar of Li pegmatites by Lahti (1981) and Sundelius (1963). High Pb values (av. 117 ppm) and increase in Rb, Sr, Ga and Y with K_2O are other chemical features of K-feldspar recorded (cf Heier et al., 1967; Berlin and Henderson, 1969; Higazy, 1953 and Burton and Culkin, 1972).

Muscovite has about the same light-green colour as spodumene. It is found in somewhat large plates (0.6 mm) with resorbed borders and in smaller interstitial scales (0.06 mm). It occurs closely associated with spodumene and K-feldspar and bears replacement relations with these minerals. Chemically, muscovite of Amareshwar Li-pegmatites (Table, 3) is a 'ferroan' type (comparable to phengite, Deer et al., 1963) with quite high Li_2O (0.47 to 0.6%). It is virtually devoid of Ca, Mg, Ba and Cl. Compared with the coexisting spodumene, the mica analyses 4-5 times more Fe and almost 5 times less Mn.

Garnet occurs as small (.06 to .01 mm) euhedral, almost inclusion-free crystals. It is pale purple in thin section. It occurs in the interstices in the matrix and as inclusions in larger feldspar grains. It is of the Fe-Mn variety, with 52.8%

Table 3.
Chemical analyses of minerals of lithium pegmatites.

	Spodumene		Muscovite		K-feldspar	Garnet	Gahnite
	I(4)	IA(2)	II(4)	IIA(1)	III(3)	IV(2)	V(2)
SiO_2	64.62	64.15	44.64	46.00	64.99	37.24	0.11
TiO_2	0.02		0.04		0.02	0.02	0.02
Al_2O_3	26.58	26.25	33.14	33.00	17.79	21.01	55.89
$FeO_{(t)}$	1.12	0.98	4.34		0.79	22.99	5.17
MnO	0.28	0.115	0.06	0.06	0.013	19.13	0.31
MgO			0.02	0.65	0.026		
CaO	0.01	0.10	0.01		0.003	0.99	0.02
Na_2O	0.15		0.36	0.90	1.38	0.05	
K_2O			10.14	10.80	12.76		
Li_2O	6.92	7.05	0.47	0.60	0.21		
ZnO							38.57

I, II, IV, & V : Electronprobe micro analyses (Analyst A.G. Tindle);
III : XRF analyses (Analyst J.S. Watson);
IA & IIA: AAS analyses (Analyst N. Rajshekar).
Numbers given in parentheses refer to the number of individual analyses of the minerals,
IA includes 20 ppm Cu & 47 ppm Be; II includes 0.16% F & 0.005% Cl.
IIA includes 8 ppm Cu, 29 ppm Sr and 9 ppm Be.
III includes 7582 ppm Rb, 15 ppm Cu, 83 ppm Sr, 57 ppm Y, 15 ppm Zr, 5 ppm Nb, 177 ppm Pb, < 1 ppm Th, 8 ppm Zn, 40 ppm Ga and 2 ppm Ni.

almandine and 44.3% spessartine (Table 3). Similar Fe-Mn garnets are reported from Li-rich pegmatites of other areas (e.g., Lahti, 1981; Baldwin and Von Knorring, 1983).

Gahnite also occurs as small euhedral crystals. It displays the typical octahedral and rhombic shape and has a bluish-grey tinge. Microprobe analysis (Table 3) of the mineral has indicated that it contains 38.6% ZnO (this is a little higher than the reported values, which range between 25.4 and 35.8, see Deer et al., 1963) and it is a ferroan variety (av. 5.1% FeO), almost devoid of Mg (see Tulloch, 1981). Although gahnite occurrences in granitic pegmatite have been recorded by various workers, as far as the authors are aware, there are very few reports of this mineral from the Li-rich pegmatites.

Beryl (uniaxial negative with 0.0087) is noted to occur as anhedral to subhedral grains (0.56 to 0.23 mm) only in Be-enriched pegmatite dykes (these analyse over 70 ppm Be - see Table 5 analyses 1 and 5). It is colourless and contains opaque dusty/granular inclusions which tend to be concentrated along the borders.

FLUID-INCLUSION STUDY

A fluid-inclusion study was carried out on spodumene-bearing pegmatites using a CHAIXMECA Microthermometry apparatus. The results reported have an accuracy of ± 0.5°C (Table 4).

Fluid inclusions present in quartz grains vary in size from 8 to 15 µm. They generally occur as rounded, isoloated inclusions and are presumably of primary origin. Some of the inclusions occur along healed fractures indicating their secondary (?) nature. Fluid inclusions consist of vapour (1 to 10 vol %) and liquid phases (99 to 90 vol %). Vapour+liquid±solid phase is noticed in some of the inclusions. In one sample studied (D1), the presence of highly birefringent daughter crystal (hexagonal or trigonal?) is observed, which did not melt when heated up to 300°C.

Table 4.
Microthermometric results (°C)

Sample No.	T_m	T_h	% of salinity NaCl equiv.	Density (g/cm^3) for 23 wt% NaCl
D-2A	- 4.1 to -17.5	60 to 249	7 to 20	1.000 to 0.880
D-12	- 6.0 to -19.0	57 to 110	10 to 21	0.990 to 0.970
D-29	-10.9 to -20.1	80 to 250	14 to 22	0.985 to 0.870

Biphase inclusions show temperatures of melting (T_m) from -4.1 to -20.0°C, indicating salinity values ranging from 7 to 22 wt% NaCl equivalent (Sourirajan and Kennedy, 1962). The peak T_m lie around -19°C, indicating a high salinity of 21 wt% NaCl equivalent. The inclusions in sample No.D1 show higher melting

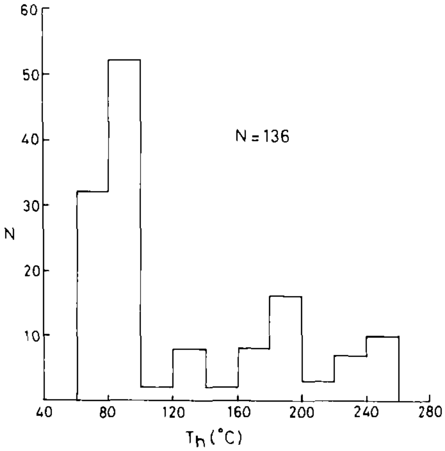

Figure 5. Plot of number of inclusions (N) against temperature of homogenization (T_h).

temperatures of -43.5, to -49.9°C, suggesting the presence of Ca in solution. Temperatures of homogenisation (T_h) of liquid + vapour to liquid phase range from 57 to 250° C with means around 90°C and 190°C (Fig.5). Using P-V-T data of Lemmlein and Klevtsov (1961) for 23 mol% NaCl in the H_2O-NaCl system, higher density values of 0.900 to 0.970 g/cm^3 are obtained.

GEOCHEMISTRY

Chemically (Table 5), Amareshwar Li pegmatites are characterised by:

1. Restricted variation in SiO_2 (71.3 - 74.4%) and Al_2O_3 (14.3 - 15.9%), as against large variation in texture and mineralogy.
2. Occurrence in traces or near absence of TiO_2, MgO, and P_2O_5.
3. A slight enrichment of MnO (av. 0.11%) and a significant depletion of CaO (av. 0.26%).
4. Near absence of S and Ba.
5. A higher average soda value compared to potash with a Na_2O/K_2O ratio of 1.74.
6. A large variation in lithia content (.05 to 6.42%), but a high average of 2.45% (Table 6) and a good positive correlation between iron and lithia (Fig.6).
7. A strong Rb enrichment (more enriched than spodumene pegmatites of Peg Claims, Sundelius, 1963), distinctly higher Be, Nb, Pb, Ga and Y values, marked depletion of Sr and Ni and significantly lower values of Zr and Cu.

TABLE 5: Chemical Analyses^{+} of Li Pegmatites.

	RA132	D1	D14	D13	H8	D2A	D7	D5	D4	D8	D6	D12	D29	D3	Av
SiO_2	71.30	72.17	72.36	72.46	72.50	72.55	72.62	72.89	72.95	73.31	73.37	73.48	74.20	74.41	72.89
Al_2O_3	15.54	15.95	15.74	15.12	15.00	15.28	15.18	15.66	15.61	14.33	15.32	15.59	14.78	14.31	15.24
TiO_2	0.04	0.00	0.00	0.01	0.04	0.00	0.00	0.00	0.00	0.00	0.00	0.02	0.00	0.00	0.01
Fe_2O_3	0.76	1.86	1.38	1.42	0.41	0.61	0.78	1.91	1.55	1.83	0.95	1.60	1.46	1.90	1.32
FeO	2.69	1.20	0.48	0.54	2.01	0.54	0.48	0.72	0.60	1.20	0.60	0.84	0.36	0.72	0.93
MnO	0.08	0.09	0.09	0.08	0.08	0.12	0.24	0.09	0.08	0.08	0.20	0.08	0.08	0.10	0.11
MgO	0.50	0.01	0.03	0.03	0.80	0.00	0.00	0.09	0.00	0.00	0.00	0.03	0.00	0.00	0.11
CaO	1.10	0.13	0.07	0.22	0.50	0.19	0.16	0.17	0.20	0.39	0.04	0.41	0.13	0.00	0.26
Na_2O	3.78	1.51	4.34	2.87	3.50	6.48	6.81	1.98	2.88	3.23	4.90	3.71	4.03	1.59	3.68
K_2O	0.80	2.12	2.32	3.45	1.50	2.38	2.53	1.60	1.95	1.20	1.94	1.89	1.77	2.21	1.97
P_2O_5	0.04	0.04	0.00	0.03	0.02	0.00	0.00	0.00	0.03	0.00	0.00	0.05	0.00	0.00	0.02
Li_2O^*	2.95	6.49	2.31	2.54	3.15	0.13	0.13	4.78	3.84	3.90	1.81	3.51	2.46	4.98	3.06
Total	99.58	101.50	99.12	98.77	99.51	98.28	98.93	99.89	99.69	99.47	99.13	101.21	99.27	100.22	99.60
Be	71	63		6	72			27	27				5		39
Rb	1527	1842	2330	1848	1527	1440	1027	1459	1633	917	1481	1363	1282	2137	1558
Sr	14	24	28	26	10	20	15	22	22	18	19	31	18	26	21
Y		34	48	39		28	40	34	34	36	27	23	42	28	34
Zr		22	23	29		22	36	17	17	17	47	16	24	19	24
Nb		45	29	49		45	58	38	42	59	40	27	47	16	41
Pb		25	22	47		27	28	20	28	20	26	22	23	31	26
Th		1	4	2		<1	3	2	<1	5	19	25	3	<1	5
Cu	64	19	93	13	64	14	16	14	13	17	18	60	13	12	30
Zn		44	115	94		86	13	93	86	38	81	23	53	46	64
Ga		80	70	61		70	46	77	69	79	63	68	61	60	67

Ni: D8-3 ppm; D3 - 2 ppm; in all other samples it is <1 ppm; U: D5, D8 & D12 - 2 ppm each, D29-0.2 ppm and other samples not analysed. + With XRF (Analyst J S Watson) * With flame photometer and AAS. U with γ-ray spectrometer Be with AAS Analyses 1 & 5 courtesy AMSE, Bangalore.

8. A fairly good positive correlation of Rb and a less well-defined negative correlation of Sr, Nb and Pb with K_2O (Fig.7); the other trace elements analysed, namely Y, Zr, Pb, Th, Cu, Zn and Ga, vary irregularly and do not follow any other trace element or major element in their distribution.

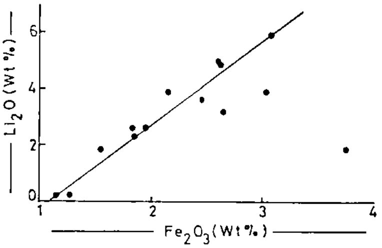

Figure 6. Linear increase of Li_2O with Fe_2O_3 of spodumene pegmatites.

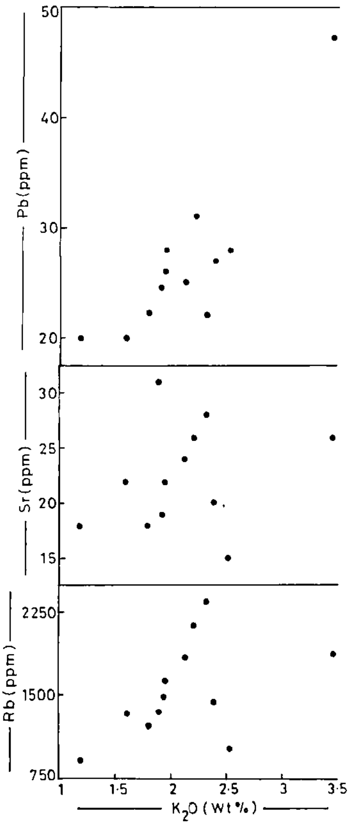

Figure 7. A general increase in Rb, Sr and Pb concentrations with K_2O in spodumene pegmatites.

DISCUSSION AND CONCLUSIONS

The anomalous location of these Li pegmatites within genetically unrelated metasedimentary/volcanic rocks instead of the genetically related granitic bodies is one of the peculiar features. It is, in fact, a feature noted with most world occurrences of Li pegmatites (see Gyongyossy and Spooner, 1979). This may be explained, as suggested by Lahti (1981), in that the markedly lower solidus temperature of the Li pegmatites possibly enables the residual Li pegmatite fractions to intrude farther away from their parent granitic melt.

The strong mineral lineation parallel to the walls of the pegmatite bodies and occurrence of angular xenolithic inclusions of the host amphibolite are evidences of forceful intrusion, the forces having operated parallel to the walls of the fractures along which the pegmatites were emplaced.

The composite character of the individual pegmatite bodies described earlier is correlated with the formation of the pegmatites by accretion through sequential injection of magma at two or more periods. The Fe-rich character of the spodumene occurring in all the units is comparable to spodumene of other unzoned composite pegmatites (Heinrich, 1975, Norton, 1982). The sharp contacts of the pegmatites indicate that the intrusions were fracture controlled and the temperature of pegmatite melt was not high enough to cause any contact metamorphic/metasomatic effects. The widespread and pervasive granulation, undulose extinction of the early formed quartz and plagioclase, and the bending, fracturing and dislocation of the twinned plagioclase crystals suggest syntectonic movements and the intrusion of pegmatite melt in largely consolidated state (Jahns, 1953). The coarser grain size of the later formed units, which generally occupy inner portions of the intrusions, may have resulted from slower cooling, a decrease in the rate of nucleation, and an increase in the rate of diffusion within the fluid.

The spodumene-quartz intergrowth is quite common, but patchy in development, being mostly limited to border areas of spodumene crystals. It appears to be due to simultaneous crystallization of the two minerals (Sundelius, 1963) and not to petalite recrystallization (Stewart, 1978). There are no petalite relics.

The fine-scale myrmekite-like intergrowth constituting the resorbed border areas of spodumene crystals, replacement of spodumene along the crystal boundaries and weak planes by albite (or K-feldspar ?) and muscovite and the resorbed borders of mica plates are all features related to the reactions between earlier formed crystals and residual fluids derived from sources within the dykes.

While the main feldspar-quartz-spodumene-bearing units of the pegmatites are most reasonably interpreted as magmatic, the massive quartz cores sometimes recorded may have formed from a gas phase that had developed in the final stages, after the magmatic crystallization of pegmatites had ended (Stewart, 1978).

The available fluid-inclusion data suggest the formation of the pegmatites under somewhat lower temperatures of 250^{o} to 400^{o}C and pressures of 4 to 5 kbars.

The high concentrations of Li, Rb, Nb, Be, Ga and Pb and distinct depletions of Sr, Ba, Ca, Mg and Ni are all chemical features which are consistent with the formation of Amareshwar Li pegmatites from moderate to highly saline residual fluids derived through fractional crystallization of differentiating granitic magma. The highly evolved magmatic crystallization of Amareshwar Li-pegmatites is also indicated by the occurrence of ferroan gahnite and a quartz-muscovite-Mn-rich garnet association (Tulloch, 1981; Baldwin and Von Knorring, 1983).

ACKNOWLEDGEMENTS

The microprobe and all but two XRF analyses (from Petrological Lab, AMSE Banglaore) presented here were obtained from the Open University, England. Dr.A.G.Tindle and J.S. Watson have carried out the respective analytical work. The 4 γ-ray spectrometric U analyses given are from AMD, Hyderabad. The early draft of the paper has been thoroughly revised in the light of the critical review by Dr.A.G.Tindle, Dr.S.A. Drury, Prof. M.Raith and Prof. P.H. Reitan. One of the authors (NR) held a UGC fellowship when most of this work was completed.

REFERENCES

Baldwin, T.A. and Von Knorring, O., 1983. Compositional range of Mn garnet in zoned granitic pegmatites. Can. Mineral, 21: 683-688.

Berlin, R. and Henderson, C.M.B., 1969. The distribution of Sr and Ba in alkali feldspar, plagioclase and ground mass phases of trachytes and phonolites. Geochim. Cosmochim. Acta, 33: 747.

Bhola, K.L., 1971. Atomic mineral deposits in Bihar mica belt. Proc. Indian National Sci. Acad., 37: 145-168.

Burton, T.D. and Culkin, F., 1970-72. Gallium: In: K.H.Wedepohl (Editor), Handbook of Geochemistry, II, 31 D,E and F.

Devaraju, T.C. and Rajshekhar, N., 1986. Diorite intrusions of Amareshwar area, Raichur dist., Karnataka. Ind. Mineral., 27: 29-40.

Gyongyossy, Z.D. and Spooner, E.T.C., 1979. Lithium: An energy element. Minerals Sci. Engg., 11: 155-176.

Heier, K.S., Palmer, P.D. and Taylor, S.R., 1967. Comment on the Pb distribution in Southern Norwegian Precambrian alkali feldspars. Norsk. Geol. Tidskr., 47: 185.

Heinrich, E.W., 1975. Economic Geology and Mineralogy of petalite and spodumene pegmatites, Ind. J. Earth. Sci., 2: 18-29.

Higazy, R.A., 1953. Observations on the distribution of trace elements in the perthite pegmatites of the Black Hills, South Dakota, Amer. Mineral., 38: 172-190.

Jahns, R.H., 1953. The genesis of pegmatites (Pt.2) - Quantitative analysis of lithium-bearing pegmatites, Mora Country, New Mexico, Amer. Mineral., 38: 1078-1112.

Lahti, S.I., 1981. On the granitic pegmatites of the Erajarvi area in Urivesi, Southern Finland. Geol. Surv. Finland Bull., 314: 1-82.

Lemmlein, G.G. and Klevtsov, P.V., 1961. Relation among the principal thermodynamic parameters in a part of the system H_2O-NaCl. Geokhimiya, 2: 133-142.

Mukherjee, S.K., Krishnamurthy, L.S., Mahadevan, C. and Krishna moorty, H.S., 1934. Geology of the western portion of Raichur Doab with special reference to the gold-bearing rocks of Dharwar bands. J. Hyderabad Geol. Surv., 2(Part I): 1-75.

Narasimha, S. and Hans, S.K., 1983. Geology of the Gurgunta Schist belt, Raichur District, Karnataka. J. Geol. Soc. India. 24: 299-302.

Norton, J.J., 1982. Iron in spodumene of different mineral assemblages in Black Hills pegmatites, S. Dakota. Econ. Geol., 77: 702-708.

Rajshekhar, N., 1983. Spodumene pegmatites and associated rocks of Amareshwar area, Raichur district, Karnataka State, India. Ph.D. Thesis (unpubl.), Karnataka University, Dharwad, 181pp.

Rama Rao, B. and Ramachandra Rao, M.B., 1939. Rec. Mysore Geol. Dept., 37.

Sadashivaiah, M.S., Devaraju, T.C., Goud Reddy, K., Machigad, B.S., Lingangoudar, V.P., Mayageri, S.K. and Kankudti, T.M., 1980. Spodumene pegmatites from Hutti, Raichur district, Karnataka State, Proc. Ind. Acad. Sci., 89: 403-411.

Sourirajan, S. and Kennedy, G.C., 1962. The system H_2O - NaCl at elevated temperatures and pressures. Am. J. Sci., 260 : 115-141.

Stewart, D.B., 1978. Petrogenesis of lithium-rich pegmatites. Amer. Mineral., 63: 970-980.

Sundelius, H.N., 1963. Peg Claims spodumene pegmatites, Maine, Econ. Geol., 58: 84-106.

Tulloch, A.J., 1981. Gahnite and columbite in an alkalie feldspar granite from New Zealand. Min. Mag., 44: 275-278.